

Study of Higher-Order Fitted Mesh Methods for Singularly Perturbed Parabolic PDEs with Smooth and Nonsmooth Data

A thesis submitted
in partial fulfillment of the requirements for the award of the degree of

Doctor of Philosophy

by

**Narendra Singh Yadav
(Identity No.: SC16D015)**



**Department of Mathematics
Indian Institute of Space Science and Technology
Thiruvananthapuram, India**

May-2022



Department of Mathematics

Indian Institute of Space Science and Technology, Thiruvananthapuram

An autonomous institute under Department of Space, Govt. of India

Certificate

This is to certify that the thesis entitled “**Study of Higher-Order Fitted Mesh Methods for Singularly Perturbed Parabolic PDEs with Smooth and Nonmooth Data**” submitted by **Narendra Singh Yadav**, to the Indian Institute of Space Science and Technology, Thiruvananthapuram, in partial fulfillment of the requirements for the award of the degree of Doctor of Philosophy, is a bonafide record of the research work carried out by him under my supervision. The contents of this report, in full or in parts, have not been submitted to any other Institute or University for the award of any degree or diploma.

Dr. Anil Kumar C.V.

Professor and Head of the
Department Mathematics
Indian Institute of Space Science and Technology
Thiruvananthapuram, India

Dr. Kaushik Mukherjee

Associate Professor
(Ph.D Advisor)

Department Mathematics
Indian Institute of Space Science and Technology
Thiruvananthapuram, India

Place: Thiruvananthapuram
May-2022



Department of Mathematics

Indian Institute of Space Science and Technology, Thiruvananthapuram, India
An autonomous institute under Department of Space, Govt. of India

Declaration

It is certified that the work contained in this thesis entitled “**Study of Higher-Order Fitted Mesh Methods for Singularly Perturbed Parabolic PDEs with Smooth and Nonsmooth Data**” submitted in partial fulfillment of the requirements for the award of the degree of **Doctor of Philosophy** is a record of the original work carried out by me under the supervision of **Dr. Kaushik Mukherjee**, and has not formed the basis for the award of any degree, diploma, associate-ship, fellowship, or other titles in this or any other Institution or University of higher learning. In accordance with the ethical practice of reporting scientific information, proper acknowledgment has been made wherever the findings of others have been cited.

Place: Thiruvananthapuram

Date: May-2022

Narendra Singh Yadav

(Identity No.: SC16D015)

Department of Mathematics

Indian Institute of Space Science and Technology

Thiruvananthapuram, India

This thesis is dedicated to my parents.
For their endless love, support and encouragement

Acknowledgements

First and foremost, I would like to express my heartfelt gratitude to my thesis supervisor, Dr. Kaushik Mukherjee, for guiding me through every step of my research; his careful guidance, constructive criticism, and valuable suggestions proved very stimulating and helpful. I have been benefited greatly from your wealth of knowledge and meticulous editing. Your professional knowledge and meticulous editing have been extremely beneficial to me. This thesis would not have been possible without the guidance of Dr. Kaushik Mukherjee, who have been trained me from the beginning of my research and helped me develop an understanding of the subject. I am extremely thankful for the extraordinary experiences he arranged for me, as well as the opportunities he provided for me to progress professionally. Thank you to his family for allowing him to respond to phone call and emails late at night and early in the morning.

I am grateful to the members of my doctoral committee, Prof. Natesan Srinivasan and Dr. Jugal Mohapatra, and the head of the department of mathematics at IIST and Prof. Raju K. George, as well as Dr. Prosenjit Das and Dr. Basudeb Ghosh, for their constructive criticism and for overseeing the progress of my work. I would like to take this opportunity to thank all of the faculty members in the Department of Mathematics who have assisted me, directly or indirectly, at various stages of my research.

A special thanks to Dr. Prosenjit Das for his professional and technical advice and support throughout my Ph.D.

I would also like to thank the entire Department of Mathematics, both students and office staff, for providing an energising environment in which to pursue this work.

I am extremely thankful to the Indian Institute of Space Science and Technology Thiruvananthapuram for funding my Ph.D. program.

My love and thanks to having friends like Rattan Lal, Navneet, Surya, Mahesh, Krishna, Raman, Jogender, Shiyaj, Promod, Akshay, and all other friends. I acknowledge their company for making my life at IIST is a great pleasure.

Further, yet importantly, a sense of respect goes to my father Mr. Shivpal Yadav, my mother Mrs. Kalawati Yadav, and my family for their strong support economically as well as regular encouragement in every step to make me in the present stage. Similarly, other relatives are also subjects to special thanks for their inspiration and cooperation in my study.

Last but not least, my heartfelt gratitude goes to my Phupha, Mr. Ganga Narayan Yadav, and my Bua, Mrs. Ramdevi for their strong financial support as well as regular encouragement in every step that has brought me to this point. Thank you all for your support and encouragement.

May-2022

With Regards
Narendra Singh Yadav

Abstract

This thesis addresses various higher-order accurate fitted mesh methods (FMMs) for solving singularly perturbed linear and nonlinear parabolic partial differential equations (PDEs) with smooth and nonsmooth data. The diffusion coefficient of those PDEs is generally considered as a small parameter ε , called “singular perturbation parameter”. Depending on the smooth and nonsmooth data, generally singularly perturbed differential equations (SPDEs) exhibit boundary or/and interior layers. These are thin regions in the vicinity of the boundary line of the given domain or/and the line of discontinuity of the given data where the gradients of the solution change rapidly as the perturbation parameter ε gets smaller; and hereby, the analytical solution of SPDEs inherently adapts to the multi-scale character.

Several real-life problems are often modeled as linear and nonlinear PDEs involving space and time variables, which can be viewed as SPDEs with smooth and nonsmooth data. Indeed, computational analysis of those PDEs that appeared, particularly in mathematical biology, has become incredibly significant for an understanding of the various biological processes and also for the application of such models to the medical sciences. As a prominent example in the context of mathematical biology, one can consider the chemo-taxis model, which arises in the mathematical modeling of tumor angiogenesis. On the other hand, the drift-diffusion equations are the most widely used mathematical models for describing semiconductor devices, which usually represent SPDEs with discontinuous source term. Henceforth, from the application point of view as well as for the multi-scale character of the analytical solution, the construction of effective numerical techniques are essential and challenging for analyzing SPDEs. It is well-known that devising FMMs constituted on appropriate layer-resolving non-uniform meshes is of natural and prime interest to the scientific community so as to achieve “parameter-robust”(also familiar as “ ε -uniformly convergent”) numerical solution that converges independent of the parameter ε .

The major objective of the thesis is to devise, analyze, and compute parameter-robust, cost-effective high-order numerical approximations for a class of singularly perturbed linear parabolic PDEs of the convection-diffusion type with smooth and nonsmooth data; and their extensions to the semilinear parabolic PDEs.

Our investigation in this thesis begins with developing an ε -uniformly convergent robust numerical algorithm for solving a class of singularly perturbed one-dimensional linear parabolic convection-diffusion initial-boundary-value problems (IBVPs) with time-dependent convection coefficient and possessing a regular boundary layer. The current numerical algorithm consists of two parts. The first one is the development of a new hybrid FMM for higher-order numerical approximation in the spatial variable; the other one is the implementation of the Richardson extrapolation technique solely in the temporal direction (called temporal Richardson extrapolation) for enhancing the temporal accuracy. The idea behind the newly developed algorithm is further extended for the cost-effective higher-order numerical approximation of two-dimensional singularly perturbed linear parabolic problems with time-dependent boundary conditions by proposing a new fractional-step fitted mesh method (FSFMM) and, later, by the temporal Richardson extrapolation. Next, a complete convergence analysis is provided towards higher-order numerical approximations for a class of singularly perturbed one-dimensional semilinear parabolic convection-diffusion IBVPs exhibiting a regular boundary layer

by proposing two novels FMMs (the fully-implicit FMM and the implicit-explicit (IMEX) FMM) followed by the extrapolation technique. Our further investigation involves cost-effective higher-order numerical approximations of two-dimensional semilinear singularly perturbed parabolic convection-diffusion problem with non-homogeneous boundary data by developing two new fractional-step fitted mesh methods (FSFMMs) (the fully-implicit FSFMM and the IMEX-FSFMM); and later, by the extrapolation technique. Next, we turn our attention to investigating singularly perturbed PDEs with nonsmooth data. In this regard, efficient numerical methods are proposed and analyzed for two different classes of model problems with nonsmooth data. The first one is the singularly perturbed parabolic PDEs exhibiting strong interior layers, and the other one is the singularly perturbed parabolic PDEs exhibiting both boundary and weak interior layers. Finally, we focus our attention on devising and analyzing a higher-order time-accurate FMM for a class of singularly perturbed semilinear parabolic convection-diffusion IBVPs exhibiting both boundary and weak interior layers.

Contents

List of Figures	xv
List of Tables	xvii
Nomenclature	xxi
1 Introduction	1
1.1 Introduction to SPPs and brief history	1
1.2 Applications of SPDEs to specific models	2
1.3 Computational challenges and opportunities in SPDEs	3
1.4 Motivation and objectives	4
1.5 Preliminaries	8
1.6 List of model problems	10
1.7 Structure of the thesis	14
2 On ε-Uniform Higher-Order Accuracy of New Efficient Numerical Method for Singularly Perturbed 1D Linear Parabolic PDEs with Smooth Data	17
2.1 Introduction	17
2.2 The analytical solution of continuous problem	19
2.3 The discrete solution of continuous problem	20
2.4 Convergence analysis	22
2.5 Error related to temporal Richardson extrapolation	38
2.6 Singularly perturbed semilinear parabolic problem	41
2.7 Numerical experiments	42
2.8 Conclusion	46
3 Higher-Order Efficient Numerical Method for Singularly Perturbed 2D Linear Parabolic PDEs with Non-homogeneous Boundary Data : ε-Uniform Convergence and Order Reduction Analysis	66
3.1 Introduction	66
3.2 Asymptotic behavior for the analytical solution	68
3.3 The time semidiscrete problem	68
3.4 The fully discrete problem	72
3.5 Error analysis for temporal Richardson extrapolation	92

3.6	Numerical experiments	95
3.7	Conclusion	102
4	Convergence Analysis of Higher-Order Parameter Uniform Numerical Methods for Singularly Perturbed 1D Semilinear Parabolic PDEs with Smooth Data	112
4.1	Introduction	113
4.2	Properties of the analytical solution	114
4.3	Formulation of the discrete problems	120
4.4	Convergence analysis for the IMEX-FMM	122
4.5	Convergence analysis for the fully-implicit FMM	132
4.6	The temporal Richardson extrapolation	140
4.7	Numerical experiments	147
4.8	Conclusion	152
5	Higher-order Efficient Numerical Methods for Singularly Perturbed 2D Semilinear Parabolic PDEs with Non-homogeneous Boundary Data: ε-Uniform Convergence and Order Reduction Analysis	167
5.1	Introduction	168
5.2	Properties of the analytical solution	169
5.3	The discrete problem-I	172
5.4	The discrete problem-II	190
5.5	The temporal Richardson extrapolation	216
5.6	Numerical experiments	218
5.7	Conclusion	220
6	Convergence Analysis of New Efficient Numerical Methods for Singularly Perturbed Linear Parabolic PDEs with Nonsmooth Data	228
6.1	Introduction	228
6.2	The analytical solution of model problem-I	230
6.3	The discrete solution of model problem-I	232
6.4	Auxiliary results	241
6.5	Error analysis	243
6.6	Semilinear singularly perturbed parabolic problem	251
6.7	Numerical experiments	252
6.8	The analytical solution of model-II	267
6.9	The discrete solution and stability analysis of the model problem-II	271
6.10	Error analysis	282
6.11	Numerical experiments	288
6.12	Conclusion	300

7	Parameter-Uniform Higher-Order Time-Accurate Numerical Method for Singularly Perturbed Semilinear Parabolic PDEs with Nonsmooth Data	301
7.1	Introduction	301
7.2	The analytical solution of continuous problem	303
7.3	The discrete solution of continuous problem	309
7.4	Error analysis	312
7.5	Numerical experiment	320
7.6	Conclusion	321
8	Conclusions	326
8.1	Outcomes of the research works	326
8.2	Future scopes	328
	Bibliography	330
	List of Publications	339
	Appendices	341
A	Monotonicity of the proposed FMM on the standard Shishkin mesh for singularly perturbed linear parabolic PDEs exhibiting both boundary and weak interior layers	341
B	Verification of compatibility conditions: test examples for 2D liner and semilinear parabolic PDEs	343

List of Figures

2.1	Shishkin mesh	20
2.2	Numerical solutions computed at $t = 1$ for $N = 128$	48
2.4	Surface plots of the numerical solutions of Example 2.2	49
2.3	Surface plots of the numerical solutions of Example 2.1	49
2.5	Surface plots of the numerical solutions of Example 2.3	49
2.6	Loglog plot for comparison of ε -uniform maximum point-wise errors before and after the extrapolation for Example 2.1.	50
2.7	Loglog plot for comparison of ε -uniform maximum point-wise errors before and after the extrapolation for Example 2.2.	51
2.8	Loglog plot for comparison of ε -uniform maximum point-wise errors before and after the extrapolation for Example 2.3.	52
2.9	Loglog plot for compariosn of the temporal order of convergence for Example 2.1	53
2.10	Loglog plot for compariosn of the temporal order of convergence for Example 2.2	54
2.11	Loglog plot for comparison of the temporal order of convergence for Example 2.3	55
2.12	Loglog plot for comparison of the spatial order of convergence for Example 2.1	57
2.13	Loglog plot for comparison of the spatial order of convergence for Example 2.2	59
2.14	Loglog plot for comparison of the spatial order of convergence for Example 2.3	61
2.15	Loglog plot for comparison of the ε -uniform order of convergence computed using extrapolation with $\Delta t = \frac{1}{N}$ for Example 2.1	63
2.16	Loglog plot for comparison of the ε -uniform order of convergence computed using extrapolation with $\Delta t = \frac{1}{N}$ for Example 2.2	63
2.17	Loglog plot for comparison of the ε -uniform order of convergence computed using extrapolation with $\Delta t = \frac{1}{N}$ for Example 2.3	63
3.1	Shishkin mesh in the spatial direction	73
3.2	Graphs of numerical solution for Example 3.1 $N = 64$, $M = 32$ at $t = 1$	96
3.3	Graphs of numerical solution for Example 3.2 $N = 64$, $M = 32$ at $t = 1$	98
3.4	Graphs of error $ U^{N,\Delta t} - u $ corresponding to Example 3.1 for $\varepsilon = 2^{-6}$ using (a) natural b.c (b) alternative b.c and for $\varepsilon = 2^{-14}$ using (c) natural b.c (d) alternative b.c at $t = 1$	100
3.5	Graphs of error $ U^{N,\Delta t} - U^{2N,\Delta t/2} $ corresponding to Example 3.2 for $\varepsilon = 2^{-6}$ using (a) natural b.c (b) alternative b.c and for $\varepsilon = 2^{-14}$ using (c) natural b.c (d) alternative b.c at $t = 1$	101
3.6	Loglog plot for comparison of the ε -uniform errors $e^{N,\Delta t}$ for Example 3.1	103

3.7	Loglog plot for comparison of the ε -uniform errors $\widehat{e}^{N,\Delta t}$ for Example 3.2.	104
3.8	Loglog plot for comparison of the local temporal errors without extrapolation using the proposed scheme (3.22) for Example 3.1	106
3.9	Loglog plot for comparison of the local temporal errors without extrapolation using the proposed scheme (3.22) for Example 3.2	108
4.1	Plots of Example 4.1 for $\varepsilon = 2^{-20}$, $N = 128$	149
4.2	Plots of Example 4.2 for $\varepsilon = 2^{-20}$, $N = 128$	150
4.3	Loglog plot for comparison of the ε -uniform errors for Example 4.1.	155
4.4	Loglog plot for comparison of the ε -uniform errors for Example 4.1.	155
4.5	Loglog plot for comparison of the temporal order of convergence for Example 4.1	157
4.6	Loglog plot for comparison of the temporal order of convergence for Example 4.2	159
4.7	Loglog plot for comparison of the spatial order of convergence for Example 4.1	162
4.8	Loglog plot for comparison of the spatial order of convergence for Example 4.2	165
5.1	Loglog plot for comparison of the ε -uniform errors for Example 5.1.	222
5.2	Loglog plot for comparison of the ε -uniform errors for Example 5.1.	223
6.1	Shishkin mesh in spatial direction	233
6.2	Numerical solutions computed at $t = 1$ for $N = 128$	256
6.3	Surface plots of the numerical solutions of Example 6.1	257
6.4	Surface plots of the numerical solutions of Example 6.2	257
6.5	Surface plots of the numerical solutions of Example 6.3	257
6.6	Loglog plot of ε -uniform maximum point-wise errors computed with $\Delta t = 0.8/N$ and $1.6/N$	259
6.7	Loglog plot for comparison of the spatial order of convergence for Example 6.1	261
6.8	Loglog plot for comparison of the spatial order of convergence for Example 6.2	263
6.9	Loglog plot for comparison of the spatial order of convergence for Example 6.3	265
6.10	Modified layer-adapted mesh in the spatial direction	272
6.11	Standard Shishkin mesh in the spatial direction	272
6.12	Numerical solutions obtain using the proposed method at $t = 1$ for $N = 128$	292
6.13	Surface plot of the numerical solutions obtained using the proposed method	293
6.14	Loglog plot for comparison of ε -uniform maximum point-wise errors of Example 6.4	294
6.15	Loglog plot for comparison of ε -uniform maximum point-wise errors of Example 6.5	295
6.16	Loglog plot for comparison of ε -uniform maximum point-wise errors of Example 6.6	296
7.1	Standard Shishkin mesh in the spatial direction	309
7.2	Surface plots of numerical solution for Example 7.1	323

List of Tables

2.1	ε -uniform maximum point-wise errors and order of convergence for Example 2.1 computed before temporal extrapolation.	50
2.2	ε -uniform maximum point-wise errors and order of convergence for Example 2.1 computed after temporal extrapolation with $\Delta t = 0.8/N$	50
2.3	ε -uniform maximum point-wise errors and order of convergence for Example 2.2 computed before temporal extrapolation.	51
2.4	ε -uniform maximum point-wise errors and order of convergence for Example 2.2 computed after temporal extrapolation with $\Delta t = 0.8/N$	51
2.5	ε -uniform maximum point-wise errors and order of convergence for Example 2.3 computed before temporal extrapolation.	52
2.6	ε -uniform maximum point-wise errors and order of convergence for Example 2.3 computed after temporal extrapolation with $\Delta t = 0.8/N$	52
2.7	Comparison of the temporal accuracy for Example 2.1 computed before and after the extrapolation.	53
2.8	Comparison of the temporal accuracy for Example 2.2 computed before and after the extrapolation.	54
2.9	Comparison of the temporal accuracy for Example 2.3 computed before and after the extrapolation.	55
2.10	Comparison (region-wise) of the spatial accuracy for Example 2.1 computed using extrapolation with $\Delta t = 1/N$	56
2.11	Comparison (region-wise) of the spatial accuracy for Example 2.2 computed using extrapolation with $\Delta t = 1/N$	58
2.12	Comparison (region-wise) of the spatial accuracy for Example 2.3 computed using extrapolation with $\Delta t = 1/N$	60
2.13	Comparison of ε -uniform maximum point-wise errors and order of convergence for Example 2.1 computed using extrapolation with $\Delta t = \frac{1}{N}$	62
2.14	Comparison of ε -uniform maximum point-wise errors and order of convergence for Example 2.2 computed using extrapolation with $\Delta t = \frac{1}{N}$	62
2.15	Comparison of ε -uniform maximum point-wise errors and order of convergence for Example 2.3 computed using extrapolation with $\Delta t = 1/N$	62
2.16	Comparison of computational time (in seconds) for Example 2.1.	64

2.17	Comparison of computational time (in seconds) for Example 2.2.	64
2.18	Comparison of computational time (in seconds) for Example 2.3.	65
3.1	Comparison of ε -uniform errors and order of convergence for Example 3.1 computed using $\Delta t = 1.6/N$ without temporal extrapolation	103
3.2	Comparison of ε -uniform errors and order of convergence for Example 3.2 computed using $\Delta t = 1.6/N$ without temporal extrapolation	104
3.3	Maximum point-wise local errors $e_{loc}^{N,\Delta t}$ and order of convergence $r_{loc}^{N,\Delta t}$ for Example 3.1 with natural boundary conditions (3.12)	105
3.4	Maximum point-wise local errors $e_{loc}^{N,\Delta t}$ and order of convergence $r_{loc}^{N,\Delta t}$ for Example 3.1 with alternative boundary conditions (3.13)	105
3.5	Maximum point-wise local errors $\hat{e}_{loc}^{N,\Delta t}$ and order of convergence $\hat{r}_{loc}^{N,\Delta t}$ for Example 3.2 with natural boundary conditions (3.12)	107
3.6	Maximum point-wise local errors $\hat{e}_{loc}^{N,\Delta t}$ and order of convergence $\hat{r}_{loc}^{N,\Delta t}$ for Example 3.2 with alternative boundary conditions (3.13)	107
3.7	Comparison of temporal accuracy with natural and alternative boundary conditions after temporal Richardson extrapolation for Example 3.1	109
3.8	Comparison of temporal accuracy with natural and alternative boundary conditions after temporal Richardson extrapolation for Example 3.2	109
3.9	Comparison (region wise) of maximum point-wise errors and order of convergence for Example 3.1, with alternative boundary data and using temporal Richardson extrapolation with $\Delta t = \frac{1}{N}$.	110
3.10	Comparison (region wise) of maximum point-wise errors and order of convergence for Example 3.2, with alternative boundary data and using temporal Richardson extrapolation with $\Delta t = \frac{1}{N}$.	111
4.1	Comparison of ε -uniform maximum point-wise errors for Example 4.1	154
4.2	Comparison of ε -uniform maximum point-wise errors for Example 4.2	154
4.3	Comparison of the temporal accuracy for Example 4.1 computed using the IMEX-FMM (4.30)	156
4.4	Comparison of the temporal accuracy for Example 4.1 computed using the fully-implicit FMM (4.29)	156
4.5	Comparison of the temporal accuracy for Example 4.2 computed using the IMEX-FMM (4.30)	158
4.6	Comparison of the temporal accuracy for Example 4.2 using the fully-implicit FMM (4.29) . .	158
4.7	Comparison of the spatial accuracy in the outer region, i.e., $[0, 1 - \eta]$ for Example 4.1	160
4.8	Comparison of the spatial accuracy in the layer region, i.e., $(\eta, 1]$ for Example 4.1	161
4.9	Comparison of the spatial accuracy in the outer region, i.e., $[0, 1 - \eta]$ for Example 4.2	163
4.10	Comparison of the spatial accuracy in the layer region, i.e., $(\eta, 1]$ for Example 4.2	164
4.11	Comparison of computational time (in seconds), taking $\Delta t = \frac{1}{N}$	166
5.1	Comparison of ε -uniform errors and order of convergence for Example 5.1 using the IMEX-FSMM (5.37) computed with $\Delta t = 1.6/N$ without using Richardson extrapolation in time	222

5.2	Comparison of ε -uniform errors and order of convergence for Example 5.1 using the fully-implicit FSFMM (5.102) computed with $\Delta t = 1.6/N$ without using Richardson extrapolation in time	223
5.3	Maximum point-wise local errors $e_{loc}^{N,\Delta t}$ and order of convergence $r_{loc}^{N,\Delta t}$ for Example 5.1 using the IMEX-FSFMM (5.37) for natural boundary conditions (5.21) and without using Richardson extrapolation in time	224
5.4	Maximum point-wise local errors $e_{loc}^{N,\Delta t}$ and order of convergence $r_{loc}^{N,\Delta t}$ for Example 5.1 using the IMEX-FSFMM (5.37) for alternative boundary conditions (5.22) and without using Richardson extrapolation in time	224
5.5	Maximum point-wise local errors $e_{loc}^{N,\Delta t}$ and order of convergence $r_{loc}^{N,\Delta t}$ for Example 5.1 using the fully-implicit FSFMM (5.102) for natural boundary conditions (5.82) and without using Richardson extrapolation in time	225
5.6	Maximum point-wise local errors $e_{loc}^{N,\Delta t}$ and order of convergence $r_{loc}^{N,\Delta t}$ for Example 5.1 using the fully-implicit FSFMM (5.102) for alternative boundary conditions (5.83) and without using Richardson extrapolation in time	225
5.7	Comparison (region-wise) of maximum point-wise errors and order of convergence for Example 5.1, with alternative boundary conditions (5.22) and (5.83)	226
5.8	Comparison of temporal accuracy for IMEX-FSFMM (5.37) with natural and alternative boundary conditions after Richardson extrapolation for the time variable for Example 5.1	227
5.9	Comparison of temporal accuracy for fully-implicit FSFMM (5.102) with natural and alternative boundary conditions after Richardson extrapolation for the time variable for Example 5.1	227
6.1	ε -uniform maximum point-wise errors and order of convergence for Example 6.1	258
6.2	ε -uniform maximum point-wise errors and order of convergence for Example 6.2	258
6.3	ε -uniform maximum point-wise errors and order of convergence for Example 6.3	258
6.4	Comparison (regionwise) of maximum point-wise errors and order of convergence for Example 6.1, taking $\Delta t = \frac{1}{N^2}$	260
6.5	Comparison (regionwise) of maximum point-wise errors and order of convergence for Example 6.2, taking $\Delta t = \frac{1}{N^2}$	262
6.6	Comparison (region wise) of maximum point-wise errors and order of convergence for Example 6.3, taking $\Delta t = \frac{1}{N^2}$	264
6.7	Comparison of computational time (in seconds) for Example 6.1, taking $\Delta t = \frac{1}{N^2}$	266
6.8	Comparison of computational time (in seconds) for Example 6.2, taking $\Delta t = \frac{1}{N^2}$	266
6.9	Comparison of computational time (in seconds) for Example 6.3, taking $\Delta t = \frac{1}{N^2}$	266
6.10	ε -uniform maximum point-wise errors and order of convergence for Example 6.4	294
6.11	ε -uniform maximum point-wise errors and order of convergence for Example 6.4 computed with $\Delta t = 0.8/N$ using classical upwind scheme.	294
6.12	ε -uniform maximum point-wise errors and order of convergence for Example 6.5	295
6.13	ε -uniform maximum point-wise errors and order of convergence for Example 6.5 computed with $\Delta t = 0.8/N$ using classical upwind scheme.	295

6.14	ε -uniform maximum point-wise errors and order of convergence for Example 6.6	296
6.15	ε -uniform maximum point-wise errors and order of convergence for Example 6.6 computed with $\Delta t = 0.8/N$ using classical upwind scheme.	296
6.16	Comparison of spatial errors for Example 6.4 computed in the region i.e., in $[0, d + \eta]$, using $\Delta t = 1/N^2$	297
6.17	Comparison of spatial errors for Example 6.4 computed in the region i.e., in $(d + \eta, 1]$, using $\Delta t = 1/N^2$	297
6.18	Comparison of spatial errors for Example 6.5 computed in the region i.e., in $[0, d + \eta]$, using $\Delta t = 1/N^2$	298
6.19	Comparison of spatial errors for Example 6.5 computed in the region i.e., in $(d + \eta, 1]$, using $\Delta t = 1/N^2$	298
6.20	Comparison of spatial errors for Example 6.6 computed in the region i.e., in $[0, d + \eta]$, using $\Delta t = 1/N^2$	299
6.21	Comparison of errors for Example 6.6 computed in the region i.e., in $(d + \eta, 1]$, using $\Delta t = 1/N^2$	299
7.1	ε -uniform maximum point-wise errors and order of convergence for Example 7.1 computed with $\Delta t = 1/N$ using the proposed nonlinear scheme (7.29)	324
7.2	Comparison of the temporal accuracy for Example 7.1 computed using the FMMs (7.29) and (7.59)	325

Nomenclature

SPPs	Singular perturbation problems
SPDEs	Singularly perturbed differential equations
BVP, IBVP	Boundary value problem, initial-boundary value problem
ODE	Ordinary differential equation
FOM, FMMs	Fitted operator method, fitted mesh methods
FSFMM, IMEX	Fractional-step fitted mesh method, implicit-explicit
ε, \mathbb{R}	Singular perturbation parameter, set of real numbers
N, M	Discretization parameters
C	Generic positive constant independent of ε, N, M
$ \cdot $ or $\ \cdot\ $	Supremum norm over the domain \mathfrak{D} and \mathbb{D}
$O(\cdot), o(\cdot)$	Landau order symbols
$\Omega, \bar{\Omega}, \Omega^-, \Omega^+$	$(0, 1), [0, 1], (0, \mathfrak{d}), (\mathfrak{d}, 1), \quad 0 < \mathfrak{d} < 1$
$\mathfrak{D}, \bar{\mathfrak{D}}$ and $\tilde{\mathfrak{D}}$	$\Omega \times (0, T], \bar{\Omega} \times [0, T]$ and $(0, \frac{1}{\varepsilon}) \times (0, T]$
\mathfrak{D}^- and \mathfrak{D}^+	$\Omega^- \times (0, T]$ and $\Omega^+ \times (0, T]$
$\bar{\Omega}^N$ and $\hat{\Omega}^{2N}$	Piecewise-uniform layer-adapted meshes in the spatial direction
$\Lambda^{\Delta t}, \Lambda^{\Delta t/2}, \Lambda^{\Delta t}$	Equidistant meshes in the temporal direction
$\bar{\mathfrak{D}}^{N, \Delta t}, \bar{\mathfrak{D}}^{N, M}, \hat{\mathfrak{D}}^{2N, \Delta t/2}, \hat{\mathfrak{D}}^{2N, 2M}$	$\bar{\Omega}^N \times \Lambda^{\Delta t}, \bar{\Omega}^N \times \Lambda^M, \hat{\Omega}^{2N} \times \Lambda^{\Delta t/2}, \hat{\Omega}^{2N} \times \Lambda^{2M}$
$\mathbb{G}, \bar{\mathbb{G}}, \mathbb{D}, \bar{\mathbb{D}}$	$(0, 1)^2, [0, 1]^2, \mathbb{G} \times (0, T], \bar{\mathbb{G}} \times [0, T]$
$\bar{\mathbb{G}}_x^N$ and $\bar{\mathbb{G}}_y^N$	Piecewise-uniform layer-adapted meshes in the x and y directions
$\bar{\mathbb{G}}^N, \bar{\mathbb{D}}^{N, \Delta t}$	$\bar{\mathbb{G}}_x^N \times \bar{\mathbb{G}}_y^N, \bar{\mathbb{G}}^N \times \Lambda^{\Delta t}$
$\eta, \hat{\eta}, \eta_1, \eta_2, \hat{\eta}_1, \hat{\eta}_2$	Transition parameters

$y(x, t), u(x, y, t)$	Solution of the continuous problem
$y^{n+1}(x), u^{n+1}(x, y)$	Solutions of the time semidiscrete problem
$Y_j^{n+1}, U_{i,j}^{n+1}$	Solution of the fully discrete problem
$\tilde{y}^{n+1}(x), \tilde{u}^{n+1}(x, y)$	Solution of the auxiliary BVP
$\tilde{Y}_j^{n+1}, \tilde{U}_{i,j}^{n+1}$	Solution of the spatial discrete problem
$y^{\Delta t}(x, t_{n+1})$	Solution of the semidiscrete problem on the mesh $\bar{\Omega} \times \Lambda^{\Delta t}$
$u^{\Delta t}(x, y, t_{n+1})$	Solution of the semidiscrete problem on the mesh $\bar{G} \times \Lambda^{\Delta t}$
$z^{\Delta t}(x, \tilde{t}_{n+1})$	Solution of the semidiscrete problem on the mesh $\bar{\Omega} \times \Lambda^{\Delta t/2}$
$u^{\Delta t/2}(x, y, \tilde{t}_{n+1})$	Solution of the semidiscrete problem on the mesh $\bar{G} \times \Lambda^{\Delta t/2}$
$Y^{N,\Delta t}(x_j, t_{n+1})$	Solution of the fully discrete problem on the mesh $\bar{\Omega}^N \times \Lambda^{\Delta t}$
$Z^{N,\Delta t}(x_j, \tilde{t}_{n+1})$	Solution of the fully discrete problem on the mesh $\bar{\Omega}^N \times \Lambda^{\Delta t/2}$
$U^{N,\Delta t}(x_i, y_j, t_{n+1})$	Solution of the fully discrete problem on the mesh $\bar{G}^N \times \Lambda^{\Delta t}$
$U^{N,\Delta t/2}(x_i, y_j, \tilde{t}_{n+1})$	Solution of the fully discrete problem on the mesh $\bar{G}^N \times \Lambda^{\Delta t/2}$
$y_{exp}^{\Delta t}(x, t_{n+1})$	Extrapolated solution of the semidiscrete problem on the mesh $\bar{\Omega} \times \Lambda^{\Delta t}$
$u_{exp}^{\Delta t}(x, y, t_{n+1})$	Extrapolated solution of the semidiscrete problem on the mesh $\bar{G} \times \Lambda^{\Delta t}$
$Y_{exp}^{N,\Delta t}(x_j, t_n)$	Extrapolated solution of the fully discrete problem on the mesh $\bar{\Omega}^N \times \Lambda^{\Delta t}$
$U_{exp}^{N,\Delta t}(x_i, y_j, t_n)$	Extrapolated solution of the fully discrete problem on the mesh $\bar{G}^N \times \Lambda^{\Delta t}$
e^{n+1}	Global error related to the semidiscrete scheme at the time t_{n+1}
\tilde{e}^{n+1}	Local error related to the semidiscrete scheme at the time t_{n+1}
E^{n+1}	Global error related to the fully discrete problem at the time t_{n+1}
\tilde{E}^{n+1}	Local error related to the spatial discretization of at the time t_{n+1}
$e_{\varepsilon}^{N,\Delta t}, e_{\varepsilon}^{N,M}, \hat{e}_{\varepsilon}^{N,\Delta t}, \hat{e}_{\varepsilon}^{N,M}$	Maximum point-wise errors
$e^{N,\Delta t}, e^{N,M}, \hat{e}^{N,\Delta t}, \hat{e}^{N,M}$	ε -uniform maximum point-wise errors
$r_{\varepsilon}^{N,\Delta t}, r_{\varepsilon}^{N,M}, \hat{r}_{\varepsilon}^{N,\Delta t}, \hat{r}_{\varepsilon}^{N,M}$	Order of convergence
$r^{N,\Delta t}, r^{N,M}, \hat{r}^{N,\Delta t}, \hat{r}^{N,M}$	ε -uniform order of convergence
$e_{loc}^{N,\Delta t}, \hat{e}_{loc}^{N,\Delta t}$	Maximum point-wise local errors
$r_{loc}^{N,\Delta t}, \hat{r}_{loc}^{N,\Delta t}$	Local order of convergence

Chapter 1

Introduction

This chapter begins with the general introduction and historical perspective to singularly perturbed problems (SPPs). It further highlights specific applications of singularly perturbed differential equations (SPDEs) to the real life problems which are relevant to the model problems considered in this thesis. Apart from this, it consists of review of the related literature emphasizing computational difficulties and several numerical methods as well as motivation and objectives of the research works carried out in this thesis, and also contains some preliminaries followed by a brief description of the model problems and the structure of the thesis.

1.1 Introduction to SPPs and brief history

Mathematical and numerical aspects of the model problems consisting of partial differential equations (PDEs) with the highest order spatial derivative multiplied by a small parameter ε , known as SPPs, are always being the subject of interest to many researchers because of the application of SPPs in the various fields of engineering and applied sciences; and also due to the occurrence of the interior and boundary layers in the solutions of SPDEs. Interior or/and boundary layers, which are thin regions in the vicinity of the boundary line of the given domain or/and the line of discontinuity of the given data where the gradient of the solution changes rapidly as the perturbation parameter ε gets smaller, are usually common features of the solutions of SPDEs.

SPDEs can be classified into two subcategories: SPDEs with smooth data and SPDEs with nonsmooth data. We call the problems with smooth data when the coefficients and the right-side term of the differential equation are continuous in the domain under consideration. However, if the coefficients and the right-side term of the differential equation are not continuous in the domain, we call them SPDEs with nonsmooth data. Note that the problems with nonsmooth data can sometimes consist of discontinuous initial or boundary conditions (see [46, 47, 51]).

In 1904, at the Third International Congress of Mathematicians in Heidelberg, Prandtl's seven-pages report, which was published in that conference proceedings [93], introduced the *boundary layer theory* as the fundamental building block of fluid dynamics; and subsequently laid the foundations of SPPs. Prandtl highlighted the significance of viscous flow demonstrating how a quantity as small as the viscosity of common fluids like water and air may play a significant role in determining their flow. The key factor behind his analysis was that any flow over a surface can be separated into two regions: a thin region close to the surface (called the boundary layer) where the effect of viscosity is strong; and a region outside the boundary layer where the effect viscosity is negligible. In 1964, Friedrichs and Wasow used the term *singular perturbation* for the first time in their paper [42] while studying nonlinear vibration theory at New York University. Even though Prandtl initiated work on

boundary layer theory; but Wasow's contribution in [117] and his other works for next few decades on asymptotic theory of solution of SPDEs gave it considerably more generality to SPPs from theoretical perspective.

1.2 Applications of SPDEs to specific models

Several real-life problems are modeled in linear and nonlinear PDEs involving space and time variables which can be viewed as SPDEs with smooth and nonsmooth data. One can explore and analyze such PDEs for understanding the physical significance of SPDEs; and some of them are cited below in relevance with of the model problems discussed in this thesis.

As a prominent example, one can consider the advection-dispersion equation which governs many physical process including advective transport, molecular diffusion, and hydrodynamic dispersion, chemical reaction in the liquid phase, contaminant decay or production with the solid phase. This model equation appears often in geology, hydrology, environmental engineering, chemical and petroleum engineering (see [64]). Even for the understanding of biological processes, one can study the advection-dispersion equation used for modeling oral drug absorption phenomena (see [40]).

In the context of application of SPDEs to the mathematical biology, particularly to the medical sciences, we cite an interesting model, known as chemo-taxis model [54], which arises in mathematical modeling of tumor angiogenesis [38], spatial and temporal evolution of chemotactic bacterial bands [8] etc. As an illustration of the tumor angiogenesis, we consider the one-dimensional model equations which essentially describe the growth of solid tumors from the dormant avascular state to the vascular state. In that case, the tumour cells stimulate angiogenesis, the process whereby tumour secretes a diffusible chemical substance, known as tumour angiogenesis factor (TAF), that induces neighboring endothelial cells to migrate towards the tumor through a chemotaxis phenomena; and further continues to spread to the other organs of the body. The model is therefore composed of two phenomenon: the diffusion of TAF into the surrounding tissue, and its effect on the neighboring endothelial cells; and thus consists of two coupled equations: one for the concentration of TAF, denoted by $c(x, t)$; and the other for the the endothelial cell density, denoted by $\rho(x, t)$. After normalizing the PDEs, the population diffusion chemotaxis equation for the endothelial cells, and the diffusion equation for the TAF are respectively given as follows:

$$\begin{cases} \frac{\partial \rho}{\partial t} = \varepsilon \frac{\partial^2 \rho}{\partial x^2} - \frac{\partial}{\partial x} \left(k \frac{\partial c}{\partial x} \rho \right) + \mu \rho (1 - \rho) \max(0, c - c^*) - \beta \rho, \\ \frac{\partial c}{\partial t} = \delta \frac{\partial^2 c}{\partial x^2} - \lambda c - \frac{\alpha \rho c}{\gamma + c}, \end{cases}$$

subject to appropriate initial and boundary conditions. When the diffusion coefficient ε of the endothelial cells in the population equation is substantially smaller than the speed of migration caused by the taxis term, the corresponding model behaves like SPDEs. For more details, we refer [13] and the references therein.

On the other hand, the drift-diffusion equations, the most widely used mathematical model for describing semiconductor devices, can be considered as a significant application of SPDEs with nonsmooth data. The drift-diffusion equations govern the evolution of the flow of electrons and holes in semiconductor devices on the dielectrical relaxation time scale. In this regard, the one-dimensional model equations subject to suitable

initial and boundary conditions are mentioned below:

$$\begin{cases} \frac{\partial n}{\partial t} = \varepsilon \frac{\partial^2 n}{\partial x^2} - \frac{\partial}{\partial x} \left(n \frac{\partial \Phi}{\partial x} \right), \\ \frac{\partial p}{\partial t} = \varepsilon \frac{\partial^2 p}{\partial x^2} + \frac{\partial}{\partial x} \left(p \frac{\partial \Phi}{\partial x} \right), \\ \frac{\partial^2 \Phi}{\partial x^2} = n - p - C(x), \end{cases}$$

where $x \in (0, 1)$ and $t > 0$ with suitable initial-boundary conditions. The functions (n, p, Φ) represents the electron concentration, the hole concentration, and the electric potential, respectively. The function $C(x)$ models the doping concentration and the preconcentration of electrons and holes in the semiconductor; and treated as discontinuous function. Due the small diffusion coefficient ε , the above equations behave like SPDEs. For more details, see [74] and the references therein.

1.3 Computational challenges and opportunities in SPDEs

It is well-known that the investigation and construction of the asymptotic approximation as well as the numerical approximation to the solutions of SPPs are of great importance in applied mathematics. One can construct an asymptotic approximation to the analytical solution by employing the perturbation technique which consists at least two asymptotic expansions, called the inner-expansion and the outer-expansion, which are respectively valid inside and outside the boundary layer. To know more about the perturbation techniques, we refer to the books of Bush [10], Eckhaus [31], Kevorkian and Cole [62], Lagerstrom [66], O'Malley [87], Van Dyke [30] and the review article [67] of Lagerstrom and Casten.

From computational point of view, finding efficient numerical solutions of SPDEs are of extreme importance. Classical numerical techniques which are appropriate when ε is $O(1)$; and are often inappropriate when $\varepsilon \rightarrow 0$, unless the number of mesh intervals, N , satisfies the condition $N = O(\varepsilon^{-1})$. Failing to satisfy this condition, the classical numerical techniques are not adequate on the uniform meshes for small ε , as they may not able to capture the gradient of the solution accurately inside the layers generally, the region of most interest. This goes against the natural expectation that error of a numerical method can decrease when the mesh is refined. In this regard, one can refer to the books [77, 99] and the article [76] of Miller et al. This disadvantage motivates researchers to develop and analyze numerical methods that are robust to the perturbation parameter ε ; and it has become a very active field of study since past few decades. Such "parameter robust" (also known as " ε -uniformly convergent") numerical methods play a key role to achieve accurate numerical results without much resolving the boundary layer, whether $\varepsilon = 10^{-2}$ or $\varepsilon = 10^{-6}$.

There are two basic numerical approaches in the literature in connection with parameter robust numerical methods: One is called the fitted operator method (FOM) and the other is called the fitted mesh method (FMM). The FOMs approximate the differential operator by a specified difference operator by introducing an artificial diffusion parameter, called exponential fitting factor, and the methods utilize uniform meshes (see the book [29]). Despite the fact that the FOM, such as the Π' -in Allen-Southwell method, performs well when applied to one dimensional SPDEs; but the extension of FOMs to 2D SPDEs are difficult and even impossible in the case of characteristic boundary layers (see [39, Example 2.2]). On the other hand, FMMs utilize a specified difference operator on special layer-resolving meshes (which is fine inside the layer region and coarse outside

the layer region) adapted to the nature of the differential operator (see the book [77]). Because of their easy implementation and extension to address higher dimensional and nonlinear problems, FMMs offer an advantage over FOMs and often considered as a well-known methodology for solving SPPs to overcome the limitations of the traditional methods. In the context of FMMs, Shishkin [102] is the first person to introduce a special nonuniform mesh fitted accurately to capture the layer phenomena, known as the Shishkin mesh. This well-known layer-resolving mesh can be constructed easily if the location and the width of the boundary/interior layers are known a-priori. There is also a growing interest recently in the generation of layer-adapted meshes other than Shishkin meshes that not only allow layer structure resolution, but also provide ε -uniform convergence of the numerical solutions for different FMMs. To know about construction of different layer-resolving meshes and associated FMMs, we refer to the books [32, 77, 99, 105, 113], the survey articles of Kadalbajoo and Gupta [56], and kadalbajoo and Patidar [57], the latest survey article [98] of Roos as well as to the monographs [68, 110]. Further, one can refer the articles of Hemkar et al. [52] and Clavero et al. [15, 16] for dealing with high-order FMMs for singularly perturbed parabolic PDEs. Apart from this, the further development of FMMs based on the equidistribution principle, one can look into the research work of Beckett in [3]; and couple of recent research findings of Natesan with his co-authors in [2, 28, 43, 78].

As the thesis mainly focuses on computational and theoretical aspects of various classes of linear and nonlinear parabolic PDEs which are singularly perturbed in nature; a quick review of the literature in connection with numerical approximations of general class of parabolic PDEs is also furnished below.

In this regard, we want to highlight contributions of Kadalbajoo with his co-authors in [49, 50, 59]; and recently, by Gowrisankar and Natesan in [44] for efficient numerical approximation of Burgers' equation. To cite a few, we refer the standard books [14, 53, 79, 107, 112] which address various numerical techniques including finite difference and finite element methods for solving parabolic PDEs. In addition to these, one can also recall contributions of Wade et al. in [63, 1, 114, 115, 116] and that of Gracia et al. in [48, 108], respectively towards advancement of numerical techniques for the non-homogeneous parabolic evolution problems and for the time-fractional evolution problems.

1.4 Motivation and objectives

The major objective of the thesis is to devise, analyze, and compute parameter-robust cost-effective high-order numerical approximations for a class of singularly perturbed linear parabolic PDEs of convection-diffusion type with smooth and nonsmooth data; and their extensions to the semilinear parabolic PDEs. In the following, we cite a brief survey of research works which significantly contributed towards parameter-robust numerical techniques for solving SPDEs with smooth and nonsmooth data; and pose the possible relevant questions investigated in this thesis.

Construction of parameter-uniform higher-order FMMs for SPDEs is always a difficult undertaking. Notable among them is the hybrid numerical scheme which in the recent years has become popular as an efficient FMM for solving numerous stationary and non-stationary convection-diffusion SPPs. In the context of SPDEs with smooth data, the hybrid scheme is proposed for solving singularly perturbed convection-diffusion BVP by Stynes and Roos in [109]. The similar method is also investigated by kadalbajoo and Ramesh in [58] for singularly perturbed second-order differential-difference equation of convection-diffusion type; and for system of singularly perturbed convection-diffusion BVPs by Priyadharshini et al. in [94]. Further, Mukherjee and Nate-

san in [81] proposed the similar hybrid scheme for singularly perturbed parabolic convection-diffusion IBVP; and Das and Natesan in [26] investigated the same for singularly perturbed parabolic convection-diffusion IBVP with time delay. The above literature shows that the hybrid scheme converges with almost second-order accuracy in the spatial variable on a piecewise-uniform Shishkin mesh, unless the condition $\varepsilon \ll N^{-1}$ is satisfied. On the contrary, it can be demonstrated through the numerical experiments that whenever $\varepsilon \gg N^{-1}$, the spatial accuracy reduces to $O(N^{-1})$, specifically outside the boundary layer. On the other hand, it is noticed that the numerical scheme in [26, 81] produces first-order accurate numerical solution of the parabolic IBVP with respect to the temporal discretization; and thus, the corresponding fully discrete approximation yields globally first-order convergent numerical solution (considering both the spatial and temporal accuracy). However, achieving globally higher-order convergent numerical solutions to SPDEs are always a desirable and challenging task. In view of the above observations, we pose the following natural question:

- *“Is it possible to construct and analyze a new FMM followed by a post-processing technique to obtain ε -uniformly convergent globally higher-order accurate numerical solution (with respect to both space and time) for a class of singularly perturbed 1D parabolic IBVPs with time-dependent convection coefficient so as to overcome the drawback of the existing method?”*

In this context, we want to mention that there are couples of research works on the post-processing technique found in the literature for obtaining better approximation to the numerical solutions of SPDEs. For instance, the articles [27, 82] can be referred to the Richardson extrapolation technique for non-stationary convection-diffusion SPPs. However, these cited articles mostly focus on the convergence analysis of the extrapolated solution with respect to the spatial variable apart from enhancing the temporal order of convergence. We now discuss about couple of research outcomes related to fractional-step fitted mesh methods (FSFMMs), which play vital role for solving singularly perturbed multidimensional evolutionary PDEs. The advantage of using the fractional-step method is that it reduces the computational cost remarkably because only tridiagonal linear systems need to be solved at each time level instead of solving the block tridiagonal linear system to compute the numerical solution. In connection with the fractional implicit Euler methods, for instance, one can refer [25, 69] for singularly perturbed 2D parabolic reaction-diffusion IBVPs; and [24] for singularly perturbed 2D parabolic convection-diffusion IBVPs. These methods are uniformly convergent with first-order accurate in time. Further, we refer contributions of Clavero et al. in [17], Mukherjee and Natesan in [84] and Bujanda et al. in [9] to develop higher-order (with respect to both space and time) FSFMMs for singularly perturbed 2D parabolic IBVPs by using the Peaceman-Rachford fraction-step method. Note that most the above cited articles consider homogeneous boundary conditions.

It is observed that in the case of fully discrete numerical approximation of evolutionary PDEs with non-homogeneous (in particular, time-dependent) boundary conditions; the classical evaluation of the boundary data causes the order reduction in time. In the literature there are relatively few research articles which deal with numerical approximation of singularly perturbed 2D parabolic PDEs with time-dependent boundary conditions. In the recent past, Clavero and Jorge implement the fractional implicit Euler method in the time variable and the classical finite difference schemes in the spatial variables to develop and analyze FSFMMs for solving singularly perturbed 2D parabolic reaction-diffusion problems in [21] and convection-diffusion problems in [22] with time-dependent boundary conditions. In both the cases, order reduction in time is observed if the natural evaluation of the boundary data is used; and a suitable modification to the natural evaluation is suggested

to eliminate such order reduction. Nevertheless, development and convergence analysis of higher-order ε -uniform numerical approaches for singularly perturbed 2D parabolic convection-diffusion problems with time-dependent boundary conditions are still in the early stages and challenging too. Here, we ask the following relevant question:

- “Can we construct and analyze a new FSFMM followed by a post-processing technique to obtain ε -uniformly convergent globally higher-order accurate numerical solution (with respect to both space and time) for a class of singularly perturbed 2D linear parabolic IBVPs with time-dependent boundary condition; and propose a suitable evaluation of the boundary data to avoid the order reduction phenomena before and after extrapolation ? ”

Over the last few decades, the construction of parameter-robust numerical methods (on uniform or special non-uniform meshes) for solving stationary and non-stationary semilinear SPPs has also drawn attention to the several researchers due to various reasons such as modeling of real life problems via semilinear SPDEs, the computational difficulty in tackling the nonlinearity etc. In this regard, we cite few articles which significantly contributed to numerical approximation of singularly perturbed semilinear BVPs at the initial stage of development. Farrell et al. in [35] prove that it is not possible to attain parameter-uniform convergence of exponentially fitted finite difference method in the discrete supremum norm on uniform meshes. Contrary to this, the fitted mesh methods (FMMs) (see the book [77]) which utilize a specified difference operator on special layer-adapted meshes are quite successful to achieve accurate numerical results with much resolving the boundary layer, whether $\varepsilon = 10^{-2}$ or $\varepsilon = 10^{-6}$. Farrell et al. in [34] construct such uniformly convergent finite difference methods on special piecewise-uniform meshes for solving singularly perturbed semilinear elliptic BVPs; and they prove that the methods are first-order accurate in the discrete supremum norm. Further, Gracia et al. in [45] analyze a first-order FMM for a system of semilinear SPDEs of reaction-diffusion type; and recently, Mariappan and Tamilselvan in [72] analyze a higher-order FMM for a system of semilinear SPDEs of reaction-diffusion type.

On the other hand, computational investigation of FMMs for solving semilinear parabolic SPDEs is still in its growing phase. In this context, couple of research articles which deal with numerical approximation of semilinear parabolic IBVPs are cited here. For instance, one can recall the contributions of Shishkina and Shishkin in [106]; and Clavero and Jorge in [19] for efficient numerical solution of system of 1D singularly perturbed semilinear parabolic reaction-diffusion IBVPs on layer-adapted non-uniform meshes. Recently, Rao and Chaturvedi in [95] analyze a parameter-uniform second-order spatially accurate FMM for a system of semilinear parabolic reaction-diffusion IBVPs. In addition to this, we recall contributions of Boglaev to propose and analyze first-order uniformly convergent monotone iterative method in [6] and in [7] on layer resolving non-uniform meshes for solving singularly perturbed 2D semilinear parabolic PDEs of reaction-diffusion and convection-diffusion type with homogeneous boundary conditions. However, up to our knowledge, hardly any research work is done towards ε -uniform higher-order numerical techniques in combination with a post-processing technique for solving singularly perturbed semilinear parabolic PDEs of convection-diffusion type. In connection with the above, we pose the following relevant questions:

- “Can we construct and analyze a new fully-implicit FMM followed by a post-processing technique to obtain ε -uniformly convergent globally higher-order accurate numerical solution (with respect to both

space and time) for singularly perturbed 1D semilinear parabolic PDEs of convection-diffusion type? ”

- *“Is it possible to extend investigation of ε -uniformly convergent globally higher-order accurate numerical solution (with respect to both space and time) for singularly perturbed 2D semilinear parabolic PDEs of convection-diffusion type with time-dependent boundary condition by developing a new fully-implicit FSFMM followed by a post-processing technique? ”*
- *“Note that the fully implicit method results in nonlinear systems and henceforth, it increases the computational cost due to the solvability of the nonlinear systems via iterative methods. We further ask regarding possible formulation of fully discrete linearized FMM and FSFMM, respectively for singularly perturbed 1D semilinear parabolic PDEs and 2D semilinear parabolic PDEs of convection-diffusion type so that we can avoid solving the nonlinear systems associated with the fully implicit method. ”*

So far we discuss about various computational aspects and challenges related to singularly perturbed convection-diffusion PDEs with smooth data. We now proceed further to look into various scopes for efficient numerical approximation of convection-diffusion SPDEs with nonsmooth data. Firstly, we focus on SPDEs having discontinuous convection coefficient with alternating sign pattern. This type of problem can be viewed as the linearized version of the time dependent viscous Burger’s equation exhibiting shock layer (see [88]). In the recent years, the development of FMMs for solving such SPDEs has received significant attention by the several authors. Likewise the smooth data case, the hybrid numerical scheme is also analyzed by Cen in [11] for singularly perturbed BVPs with discontinuous data. Afterwards, Mukherjee and Natesan in [80, 83] analyze a similar hybrid scheme for a class of singularly perturbed IBVPs possessing strong interior layers. They construct the method on a piecewise-uniform Shishkin mesh resolving interior layers and prove that the method is at least second-order (up to the logarithmic factor) accurate in space measured in the discrete supremum norm, provided the parameter ε satisfies $\varepsilon \ll N^{-1}$. However, one can observe from the numerical experiments that whenever $\varepsilon \gg N^{-1}$, the spatial order of convergence reduces to first-order, particularly outside the interior layers. In view of this observations, the following typical question naturally arises:

- *“Is it possible to design a new FMM which is at least second-order accurate in the spatial variable both outside and inside the interior layers, regardless of the parameter ε , for a class of singularly perturbed 1D linear parabolic IBVPs having strong interior layers? ”*

Next, we consider convection-diffusion SPDEs whose right-hand side source term has a jump discontinuity at the interior of the domain. Here, the convection coefficient has the same sign pattern through out the domain and is possibly discontinuous at the same point. This type of problem appears in the semiconductor device modeling (see, e.g., [73]); and the solution of which possesses a layer at the boundary in addition to an interior layer. In this context, we recall contribution of Farrell et al. in [33], and Shishkin in [103], respectively for singularly perturbed convection-diffusion BVPs and singularly perturbed parabolic IBVPs with discontinuous right-hand side source term. Furthermore, differential equations with discontinuous data have been discussed in [100]. It is to be noted that the structure of the Shishkin mesh near the point of discontinuity in case of convection-diffusion SPDEs with weak interior layer is substantially different from that of convection-diffusion SPDEs with strong interior layers. Due to the occurrence of weak interior layer in one side of the point of discontinuity, the Shishkin mesh becomes finer on one side and coarser on other side of the interface point. Our current investigation in

[119] reveals that this mesh structure indeed causes great difficulty while establishing inverse-monotonicity of the higher-order FMM, a possible extension of the new FMM proposed for singularly perturbed parabolic IBVPs with boundary and weak interior layers. Here, we pose the following objectives which are challenging tasks from theoretical as well as computational point of view:

- “Can we construct a higher-order FMM for singularly perturbed 1D linear parabolic convection-diffusion IBVPs having both boundary and weak interior layers, by suitable modification of the standard Shishkin mesh fitted to both the layers, so that we can overcome the theoretical difficulty in proving inverse-monotonicity property of the method and also, achieve at least second-order accuracy across the different regions, regardless of the parameter ε ? ”

On the other hand, theoretical and numerical investigations of efficient FMMs for solving nonlinear SPDEs with discontinuous data are still in its growing stage. In this regard, we highlight couple of research articles that made significant contributions towards numerical approximation of stationary nonlinear SPDEs with discontinuous data. To cite a few, Farrell et al. propose and analyze uniformly convergent nonlinear finite difference methods on appropriate layer-adapted meshes, respectively for singularly perturbed semilinear reaction-diffusion BVPs in [36] and for quasilinear convection-diffusion BVPs in [37] with discontinuous data. They also study existence of the solution of the continuous nonlinear problem by means of the upper and lower solution approach; and also discuss about existence of the solution of the discrete nonlinear problem. In addition to this, we recall contribution of Rao et al. in [96] for parameter uniform numerical solution of singularly perturbed system of semilinear reaction-diffusion BVPs and IBVPs on non-uniform Shishkin mesh. However, to the best of our knowledge, hardly any attempt has been made to investigate theoretical and computational aspects of singularly perturbed nonlinear parabolic PDEs of convection-diffusion type with discontinuous data. In light of the foregoing, we raise the following pertinent question:

- “Is it possible to analyze parameter-robust higher-order accurate numerical approximation of a class of singularly perturbed 1D semilinear parabolic PDEs of convection-diffusion type with discontinuous data; and to study existence of the solution of the continuous as well as the discrete nonlinear problems ? ”

1.5 Preliminaries

This part presents some important definitions, frequently used notations, and conventions that will be utilized throughout the thesis.

We consider the following definition to call a numerical method “ ε -uniform” or “parameter-robust” in the thesis.

Definition 1.1 ([32]). Consider a family of mathematical problems parameterized by a perturbation parameter ε , such that $\varepsilon \in (0, 1]$. Assume that u_ε be the unique solution of each problem in that family and U_ε be the numerical approximation of each u_ε obtained by a numerical method, where U_ε is defined on the discrete domain $\bar{D}^{N, \Delta t}$ with the discretization parameters N and M , respectively in the spatial and temporal directions such that $\Delta t = T/M$. Then, the numerical method is said to converge ε -uniformly in the norm $\|\cdot\|$, if there exist some positive integers N_0 and M_0 (independent of ε) such that for some all $N \geq N_0$ and $M \geq M_0$, one

gets

$$\max_{0 < \varepsilon \leq 1} \|U_\varepsilon - u_\varepsilon\| \leq C(N^{-p} + (\Delta t)^q),$$

where C , p and q are positive numbers and are independent of ε , N , M .

Here, p and q are called ε -uniform order of convergence of the numerical method in the spatial and temporal variables, respectively, and C is called the ε -uniform error constant.

To define how a function behaves as $\delta \rightarrow 0$, we introduce **Landau's order symbols** O (big-oh) and o (little-oh) used in the thesis. For further details, see the books [62, 85]. Let $f = f(x, \delta)$ and $g = g(x, \delta)$ be two real valued functions with x lying in some domain D , where $\delta > 0$.

Definition 1.2. We can write $f(x, \delta) = O(g(x, \delta))$, as $\delta \rightarrow 0$, if there exists positive numbers M and δ_0 independent of ε such that

$$|f(x, \delta)| \leq M|g(x, \delta)|, \quad \text{for all } \delta \leq \delta_0.$$

Definition 1.3. We can write $f(x, \delta) = o(g(x, \delta))$, as $\delta \rightarrow 0$, if

$$\lim_{\delta \rightarrow 0} \frac{f(x, \delta)}{g(x, \delta)} = 0.$$

Let us introduce the well-known function spaces considered in the thesis, particularly, for one-dimensional parabolic problem. Let $D \subset \mathbb{R} \times [0, T]$. For each integer $\ell \geq 0$, $\mathcal{C}^\ell(D)$ denotes the set of functions which are continuously differentiable up to order ℓ in D . Let $\gamma \in (0, 1)$. Then, $\mathcal{C}^\gamma(D)$ denotes the set of Hölder continuous functions in D . Below, we define the Hölder continuous function.

Definition 1.4 ([41, 92]). A function $f : D \rightarrow \mathbb{R}$ is said to be Hölder continuous of exponent γ if there exist a constant M such that

$$|f(X, t) - f(Y, \tau)| \leq M(|X - Y|^2 + |t - \tau|)^{\gamma/2}, \quad \text{for all } (X, t), (Y, \tau) \in D.$$

Then, for each integer $\ell \geq 1$, $\mathcal{C}^{\ell+\gamma}(D)$ is denoted as the parabolic Hölder space and is defined as

$$\mathcal{C}^{\ell+\gamma}(D) := \left\{ f : \frac{\partial^{j+k} f}{\partial x^j \partial t^k} \in \mathcal{C}^\gamma(D), \quad \forall j, k \in \mathbb{N} \cup \{0\} \text{ and with } 0 \leq j + 2k \leq \ell \right\}.$$

Note that the above definitions and notations are often used with \bar{D} , ∂D .

We use the standard supremum norm throughout the thesis, which is denoted by $\|\cdot\|_{\bar{D}}$, and for a function $f : D \rightarrow \mathbb{R}$ defined by

$$\|f\|_D = \max_{(X, t) \in D} |f(X, t)|.$$

When the domain is obvious, we sometimes omit “ D ” from the above notation.

Next, we furnish the following definition of M-matrix used in the thesis.

Definition 1.5. [32, 91] A matrix $A \in \mathbb{R}^{N, N}$ is called an M-matrix if A is invertible, $A^{-1} \geq 0$, and $a_{i,j} \leq 0$ for all $i, j = 1, \dots, N$, $i \neq j$.

In the following, we introduce the difference operators which are used frequently to describe the finite difference schemes in the subsequent chapters. For this purpose, for one-dimensional parabolic problem, we consider arbitrary meshes respectively in the spatial and the temporal domains as $\bar{D}^N = \{x_j\}_{j=0}^N$ and $\Lambda^{\Delta t} = \{t_n\}_{n=0}^M$, where N and M are positive integers. Let us denote $\Delta t = t_n - t_{n-1}$, $n = 1, \dots, M$; and $h_j = x_j - x_{j-1}$, $j = 1, 2, \dots, N$ and $\hat{h}_j = h_j + h_{j+1}$, $j = 1, 2, \dots, N-1$.

For a given mesh function $\psi_j^n = \psi(x_j, t_n)$, we then define the forward difference, backward difference, modified-central difference, second-order central operators in space, respectively denoted by $D_x^+, D_x^-, D_x^*, \delta_x^2$ (or $D_x^+ D_x^-$) and the backward difference operator in time, denoted by D_t^- , as follows:

$$\begin{cases} D_x^- \psi_j^n = \frac{\psi_j^n - \psi_{j-1}^n}{h_j}, & D_x^+ \psi_j^n = \frac{\psi_{j+1}^n - \psi_j^n}{h_j}, & D_x^* \psi_j^n = \frac{h_j}{\hat{h}_j} D_x^+ \psi_j^n + \frac{h_{j+1}}{\hat{h}_j} D_x^- \psi_j^n, \\ D_x^+ D_x^- \psi_j^n = \delta_x^2 \psi_j^n = \frac{2}{\hat{h}_j} (D_x^+ \psi_j^n - D_x^- \psi_j^n), & \text{and} & D_t^- \psi_j^n = \frac{\psi_j^n - \psi_j^{n-1}}{\Delta t}. \end{cases}$$

Further, for two-dimensional parabolic problem, we consider arbitrary mesh in the spatial domain as $\bar{D}^N = \{x_i, y_j\}_{i/j=0}^{i/j=N}$. and we denote $h_{x_i} = x_i - x_{i-1}$, $1, 2, \dots, N$ and $\hat{h}_{x_i} = h_{x_i} + h_{x_{i+1}}$, $1, 2, \dots, N-1$. in the x -direction.

For a given mesh function $\psi_{i,j}^n = \psi(x_i, y_j, t_n)$, the difference operators denoted by $D_x^+, D_x^-, D_x^*, \delta_x^2$ in the x -direction and the backward difference operator denoted by D_t^- in the t -direction, are defined as follows:

$$\begin{cases} D_x^+ \psi_{i,j}^n = \frac{\psi_{i+1,j}^n - \psi_{i,j}^n}{h_{x_i}}, & D_x^- \psi_{i,j}^n = \frac{\psi_{i,j}^n - \psi_{i-1,j}^n}{h_{x_i}}, & D_x^* \psi_{i,j}^n = \frac{h_{x_i}}{\hat{h}_{x_i}} D_x^+ \psi_{i,j}^n + \frac{h_{i+1}}{\hat{h}_{x_i}} D_x^- \psi_{i,j}^n, \\ \delta_x^2 \psi_{i,j}^n = \frac{2}{\hat{h}_{x_i}} (D_x^+ \psi_{i,j}^n - D_x^- \psi_{i,j}^n), & \delta_x^2 \psi_{i,j}^n = \frac{2}{\hat{h}_{x_i}} (D_x^+ \psi_{i,j}^n - D_x^- \psi_{i,j}^n), \\ \text{and} & D_t^- \psi_{i,j}^n = \frac{\psi_{i,j}^n - \psi_{i,j}^{n-1}}{\Delta t}. \end{cases}$$

Similarly for the y -direction, we define the difference operators denoted by $D_y^+, D_y^-, D_y^*, \delta_y^2$. Throughout the thesis, C (sometimes subscripted) denotes a positive constant that is independent of the perturbation parameter ε , N and M (number of mesh-intervals in the spatial and the temporal directions, respectively). Note that an unsubscripted C may take a generic value but whenever a subscripted C is used, we treat it as a fixed constant for that particular position. However, for clarity of our presentation, we also use the notations $\mathfrak{M}_0, \mathfrak{M}_1, \mathfrak{K}_0, \mathfrak{K}_1$ which are fixed constants and independent of perturbation parameter and discretization parameters.

1.6 List of model problems

In this section, we describe model problems briefly that are considered in this thesis.

1.6.1 Singularly perturbed 1D linear parabolic PDE with smooth data

Here, we consider the following class of singularly perturbed parabolic convection-diffusion initial-boundary value problems (IBVPs) posed on the domain $\mathfrak{D} = \Omega \times (0, T] = (0, 1) \times (0, T]$:

$$\begin{cases} \left(\frac{\partial}{\partial t} + \mathcal{L}_{x,\varepsilon} \right) y(x, t) = g(x, t), & (x, t) \in \mathfrak{D}, \\ y(x, 0) = q_0(x), & \text{on } \bar{\Omega} = [0, 1], \\ y(0, t) = s_l(t), \quad y(1, t) = s_r(t), & t \in [0, T], \end{cases} \quad (1.1)$$

where

$$\mathcal{L}_{x,\varepsilon} y = -\varepsilon \frac{\partial^2 y}{\partial x^2} + a(x, t) \frac{\partial y}{\partial x} + b(x, t) y, \quad (1.2)$$

and ε is a small parameter such that $\varepsilon \in (0, 1]$. The coefficients $a(x, t)$, $b(x, t)$ and the source term $g(x, t)$ are considered to be sufficiently smooth with

$$a(x, t) \geq m > 0, \quad b(x, t) \geq \beta \geq 0, \quad \text{on } \bar{\mathfrak{D}} = \bar{\Omega} \times [0, T]. \quad (1.3)$$

The boundary and the initial data, *i.e.*, s_l , s_r and q_0 are also assumed to be sufficiently smooth. The solution of the IBVP (1.1)-(1.3) generally possesses boundary layer at $x = 1$ of width $O(\varepsilon)$.

1.6.2 Singularly perturbed 2D linear parabolic PDE with smooth data

Here, we consider the following class of singularly perturbed parabolic convection diffusion IBVPs posed on the domain $\mathfrak{D} = \mathbb{G} \times (0, T]$; $\mathbb{G} = (0, 1) \times (0, 1)$:

$$\begin{cases} \left(\frac{\partial}{\partial t} + \mathbb{L}_\varepsilon \right) u(x, y, t) = g(x, y, t), & (x, y, t) \in \mathfrak{D}, \\ u(x, y, 0) = q_0(x, y), & (x, y) \in \bar{\mathbb{G}} = [0, 1] \times [0, 1], \\ u(x, y, t) = s(x, y, t), & \text{in } \partial \mathbb{G} \times (0, T], \end{cases} \quad (1.4)$$

where

$$\begin{cases} \mathbb{L}_\varepsilon u = -\varepsilon \Delta u + \vec{v}(x, y, t) \cdot \vec{\nabla} u + b(x, y, t) u, \\ \vec{v}(x, y, t) = (v_1(x, y, t), v_2(x, y, t)), \end{cases} \quad (1.5)$$

and ε is a small parameter such that $\varepsilon \in (0, 1]$. The coefficients $\vec{v}(x, y, t)$, $b(x, y, t)$ and the source term $g(x, y, t)$ are considered to be sufficiently smooth with

$$v_1(x, y, t) \geq m_1 > 0, \quad v_2(x, y, t) \geq m_2 > 0, \quad b(x, y, t) \geq 0, \quad \text{on } \bar{\mathfrak{D}}. \quad (1.6)$$

The boundary and the initial data, *i.e.*, s and q_0 are also assumed to be sufficiently smooth. The solution of the IBVP (1.4)-(1.6) generally possesses exponential layers of width $O(\varepsilon)$ at the outflow boundaries $x = 1$ and $y = 1$.

1.6.3 Singularly perturbed 1D semilinear parabolic PDE with smooth data

Here, we consider the following class of singularly perturbed semilinear 1D parabolic convection-diffusion IBVPs posed on the domain $\mathfrak{D} = \Omega \times (0, T] = (0, 1) \times (0, T]$:

$$\begin{cases} \frac{\partial y(x, t)}{\partial t} + \mathbb{L}_{x, \varepsilon} y(x, t) + b(x, t, y(x, t)) = g(x, t), & (x, t) \in \mathfrak{D}, \\ y(x, 0) = \mathbf{q}_0(x), & x \in \bar{\Omega} = [0, 1], \\ y(0, t) = \mathbf{s}_l(t), \quad y(1, t) = \mathbf{s}_r(t), & t \in (0, T], \end{cases} \quad (1.7)$$

where

$$\mathbb{L}_{x, \varepsilon} y = -\varepsilon \frac{\partial^2 y}{\partial x^2} + a(x) \frac{\partial y}{\partial x},$$

and ε is a small parameter such that $\varepsilon \in (0, 1]$. The coefficient $a(x)$, the source term $g(x, t)$ are considered to be sufficiently smooth with

$$a(x) \geq \mathfrak{m} > 0, \quad \text{on } \bar{\Omega}. \quad (1.8)$$

In addition, it is assumed that the function $b(x, t, y)$ satisfies that

$$\frac{\partial b(x, t, y)}{\partial y} \geq \beta > 0, \quad (x, t, y) \in \bar{\mathfrak{D}} \times \mathbb{R}. \quad (1.9)$$

The boundary and the initial data, *i.e.*, $\mathbf{s}_l, \mathbf{s}_r$ and \mathbf{q}_0 are also assumed to be sufficiently smooth. The solution of the IBVP (1.7)-(1.9) generally possess boundary layer of width $O(\varepsilon)$ at $x = 1$.

1.6.4 Singularly perturbed 2D semilinear parabolic PDE with smooth data

Here, we consider the following class of singularly perturbed parabolic convection-diffusion IBVPs posed on the domain $\mathfrak{D} = \mathbb{G} \times (0, T]$:

$$\begin{cases} \frac{\partial u(x, y, t)}{\partial t} + \mathbb{L}_{\varepsilon} u(x, y, t) + b(x, y, t, u(x, y, t)) = g(x, y, t), & (x, y, t) \in \mathfrak{D}, \\ u(x, y, 0) = \mathbf{q}_0(x, y), & (x, y) \in \bar{\mathbb{G}} = [0, 1] \times [0, 1], \\ u(x, y, t) = \mathbf{s}(x, y, t), & \text{in } \partial \mathbb{G} \times (0, T], \end{cases} \quad (1.10)$$

where

$$\begin{cases} \mathbb{L}_{\varepsilon} u = -\varepsilon \Delta u + \vec{v}(x, y, t) \cdot \vec{\nabla} u, \\ \vec{v}(x, y, t) = (v_1(x, y, t), v_2(x, y, t)), \end{cases} \quad (1.11)$$

and ε is a small parameter such that $\varepsilon \in (0, 1]$. The coefficients $\vec{v}(x, y, t)$ and the source term $g(x, y, t)$ are considered to be sufficiently smooth with

$$v_1(x, y, t) \geq \mathfrak{m}_1 > 0, \quad v_2(x, y, t) \geq \mathfrak{m}_2 > 0, \quad \text{on } \bar{\mathbb{D}}. \quad (1.12)$$

In addition, it is assumed that the function $b(x, y, t, u)$ satisfies that

$$\frac{\partial b(x, y, t, u)}{\partial u} \geq \beta > 0, \quad (x, y, t, u) \in \bar{D} \times \mathbb{R}. \quad (1.13)$$

The boundary and the initial data, *i.e.*, \mathbf{s} and \mathbf{q}_0 are also assumed to be sufficiently smooth. The solution of the IBVP (1.10)-(1.13) generally possesses exponential layers of width $O(\varepsilon)$ at the outflow boundaries $x = 1$ and $y = 1$.

1.6.5 Singularly perturbed linear parabolic PDE with nonsmooth data

In the beginning, for describing the model problem, we introduce the following notations:

$$\begin{cases} \mathfrak{D}^- = \Omega^- \times (0, T] = (0, \mathfrak{d}) \times (0, T], & \mathfrak{D}^+ = \Omega^+ \times (0, T] = (\mathfrak{d}, 1) \times (0, T], & 0 < \mathfrak{d} < 1, \\ \mathfrak{D} = \Omega \times (0, T] = (0, 1) \times (0, T], & \bar{\mathfrak{D}} = \bar{\Omega} \times [0, T] = [0, 1] \times (0, T]. \end{cases}$$

Here, we consider the following class of singularly perturbed parabolic IBVPs:

$$\begin{cases} \left(\mathcal{L}_{x,\varepsilon} - \frac{\partial}{\partial t} \right) y(x, t) = g(x, t), & (x, t) \in \mathfrak{D}^- \cup \mathfrak{D}^+, \\ y(x, 0) = \mathbf{q}_0(x), & x \in \bar{\Omega}, \\ y(0, t) = \mathbf{s}_l(t), \quad y(1, t) = \mathbf{s}_r(t), & t \in (0, T], \end{cases} \quad (1.14)$$

where

$$\mathcal{L}_{x,\varepsilon} y = \varepsilon \frac{\partial^2 y}{\partial x^2} + a(x) \frac{\partial y}{\partial x} - b(x, t) y,$$

together with the following interface conditions:

$$[y](\mathfrak{d}, t) = 0, \quad \left[\frac{\partial y}{\partial x} \right](\mathfrak{d}, t) = 0, \quad t \in (0, T]. \quad (1.15)$$

Here, ε is a small parameter such that $\varepsilon \in (0, 1]$; and we assume that the convection coefficient $a(x)$, the reaction term $b(x, t)$, and the source term $g(x, t)$ are sufficiently smooth on $\Omega^- \cup \Omega^+$, $\bar{\mathfrak{D}}$ and $\mathfrak{D}^- \cup \mathfrak{D}^+$, respectively; such that

$$\begin{cases} |[a](\mathfrak{d})| \leq C, & |[g](\mathfrak{d}, t)| \leq C, \\ b(x, t) \geq \beta \geq 0, & \text{on } \bar{\mathfrak{D}}. \end{cases} \quad (1.16)$$

We consider two cases for the convection coefficient:

$$\textbf{Case I} : -\mathfrak{m}_1^* < a(x) < -\mathfrak{m}_1 < 0, \quad x < \mathfrak{d}, \quad \mathfrak{m}_2^* > a(x) > \mathfrak{m}_2 > 0, \quad x > \mathfrak{d}, \quad (1.17)$$

$$\textbf{Case II} : a(x) \geq \mathfrak{m}_0 > 0, \quad \bar{\Omega}^- \cup \bar{\Omega}^+. \quad (1.18)$$

The boundary and the initial data, *i.e.*, *i.e.*, $\mathbf{s}_l, \mathbf{s}_r$ and \mathbf{q}_0 are also assumed to be sufficiently smooth. Here, $[g](\mathfrak{d}, t) = g(\mathfrak{d}^+, t) - g(\mathfrak{d}^-, t)$, where $g(\mathfrak{d}^\pm, t) = \lim_{x \rightarrow \mathfrak{d}^\pm 0} g(x, t)$. In **Case I**, the solution of the IBVP (1.14)-(1.16) with (1.17) generally possess strong interior layers of width $O(\varepsilon)$ in the vicinity of the point $x = \mathfrak{d}$; and in **Case II**, the solution of the IBVP (1.14)-(1.16) with (1.18) generally possess a boundary layer at

left boundary $x = 0$ and a weak interior layer in the right side of the point $x = d$ of width $O(\varepsilon)$.

1.6.6 Singularly perturbed semilinear parabolic PDE with nonsmooth data

Here, we consider the following class of singularly perturbed parabolic IBVPs of the form:

$$\begin{cases} \mathbb{L}_{x,\varepsilon}y(x,t) - b(x,t,y(x,t)) - \frac{\partial y}{\partial t} = g(x,t), & (x,t) \in \mathfrak{D}^- \cup \mathfrak{D}^+, \\ y(x,0) = q_0(x), & x \in \bar{\Omega} = [0,1], \\ y(0,t) = s_l(t), \quad y(1,t) = s_r(t), & t \in (0,T], \end{cases} \quad (1.19)$$

where

$$\mathbb{L}_{x,\varepsilon}y = \varepsilon \frac{\partial^2 y}{\partial x^2} + a(x) \frac{\partial y}{\partial x},$$

together with the interface conditions

$$[y](d,t) = 0, \quad \left[\frac{\partial y}{\partial x} \right](d,t) = 0, \quad t \in (0,T]. \quad (1.20)$$

Here, ε is a small parameter such that $\varepsilon \in (0,1]$; and it is assumed that the convection coefficient $a(x)$ is smooth on $\bar{\Omega}^-$ and $\bar{\Omega}^+$, and the source term $g(x,t)$ is smooth enough on $\bar{\mathfrak{D}}^-$ and $\bar{\mathfrak{D}}^+$ such that

$$a(x) > m > 0, \quad \forall x \in \Omega^- \cup \Omega^+, \quad |[a](d)| \leq C, \quad |[g](d,t)| \leq C. \quad (1.21)$$

In addition, it is assumed that the function $b(x,t,y)$ satisfies that

$$\frac{\partial b(x,t,y)}{\partial y} \geq \beta > 0, \quad (x,t,y) \in \bar{\mathfrak{D}} \times \mathbb{R}. \quad (1.22)$$

The boundary and the initial data, *i.e.*, s and q_0 are also assumed to be sufficiently smooth. The solution of the IBVP (1.19)-(1.22) generally possesses a weak interior layer to the right side of $x = d$, in addition to the boundary layer at $x = 0$ of width $O(\varepsilon)$.

1.7 Structure of the thesis

The thesis is composed of eight chapters and the rest of the chapters are structured as follows:

The major research contributions are presented in **Chapters 2-7**; out of which the first four chapters are devoted to investigation of robust numerical methods for time-dependent SPDEs with smooth data; and the remaining two chapters are for time-dependent SPDEs with nonsmooth data. A concise description of research works in those chapters are sequentially unveiled below.

In **Chapter 2**, we propose and examine a robust numerical method for one-dimensional singularly perturbed linear parabolic IBVPs of the form (1.1)-(1.3), which can consist of the time-dependent convection coefficient. At the beginning, we discuss about the analytical properties which include stability and asymptotic behavior of the solution of the continuous problem. We then analyze a new FMM together with the Richardson extrapolation technique (solely in the temporal direction) for achieving higher-order numerical approximation (with respect to both space and time) of the IBVP (1.1)-(1.3). To constitute the fully discrete scheme associated with the new FMM, firstly we discretize the governing PDE using the backward-Euler method in the temporal direction;

and afterwards, the resulting semidiscrete problem is approximated by proposing a new hybrid finite difference scheme in the spatial direction. To achieve this, the spatial domain is discretized by means of a piecewise-uniform Shishkin mesh accumulated near the boundary at $x = 1$, and the time domain by an equidistant mesh. At the end, numerous numerical results are presented to corroborate the theoretical findings; and also to demonstrate the computational efficiency (in terms of computational time) and the accuracy of the present numerical method in comparison with the existing numerical method given in [81]. Further, we carry out numerical experiments for the semi-linear parabolic problems using the Newton's linearization technique.

In **Chapter 3**, we extend our study for cost-effective higher-order numerical approximation of two-dimensional singularly perturbed linear parabolic IBVPs of the form (1.4)-(1.6) consisting of the time-dependent boundary conditions. Firstly, we present the analytical properties of the solution of the continuous problem; and thereafter, we study computational aspects of the IBVP (1.4)-(1.6) by proposing a new FSFMM, followed by the Richardson extrapolation technique solely in the temporal direction. The proposed FSFMM combines the fractional implicit Euler method to discretize in time and a new hybrid finite difference scheme to discretize in space. To constitute this method, we discretize the spatial domain using a non-uniform rectangular mesh (tensor-product of 1D piecewise-uniform Shishkin meshes with N mesh-intervals in each spatial direction), and the time domain by an equidistant mesh. In addition to this, we discuss the order reduction phenomena in connection with the classical evaluation of the time-dependent boundary conditions. Finally, numerous numerical experiments demonstrate that the theoretical findings match well with the numerical results. We also compare the accuracy of the proposed method with the FSFMM proposed in [22] to show the robustness of the current algorithm.

Chapter 4 is devoted to the study of two novel computational methods for one dimensional singularly perturbed semilinear parabolic IBVPs of the form (1.7)-(1.9). The study begins with stability analysis and derivation of asymptotic behavior of the analytical solution of the governing semilinear problem. We approximate the IBVP (1.7)-(1.9) by proposing two new FMMs followed by the extrapolation technique; and provide convergence analysis of those methods. The first one is the fully-implicit method which utilizes the implicit Euler method for the temporal discretizing; and the other one is the implicit-explicit (IMEX) method which utilizes the IMEX-Euler method for the temporal discretizing. The spatial discretization for both the numerical methods is based on a new finite difference scheme. To accomplish this, the spatial domain is discretized by means of a piecewise-uniform Shishkin mesh accumulated near the boundary at $x = 1$, and the time domain by an equidistant mesh. Finally, numerous numerical results are presented to validate the theoretical findings, and a comparative study is made among the proposed methods along with the standard implicit upwind finite difference scheme to test the effectiveness of the newly developed methods with regard to the order of accuracy and the computational cost.

In **Chapter 5**, we extend our study of analyzing different computational methods for two-dimensional singularly perturbed semilinear parabolic IBVPs of the form (1.10)-(1.13). At first, the analytical properties of the solution of the continuous problem is discussed. At first, two new FSFMMs are developed and analyzed for cost-effective numerical approximations of the IBVP (1.10)-(1.13), and later on, the extrapolation technique is applied solely in the temporal direction to achieve globally higher-order accurate numerical solution. The proposed methods are the fully-implicit fractional-step method, which utilizes the fractional implicit Euler method for the temporal discretizing; and the IMEX fractional-step method, which utilizes the fractional IMEX-Euler method for the temporal discretizing. The spatial discretization for both the numerical methods is based

on a new finite difference scheme. To constitute this method, we discretize the spatial domain using a non-uniform rectangular mesh (tensor-product of 1D piecewise-uniform Shishkin meshes with N mesh-intervals in each spatial direction), and the time domain by an equidistant mesh. In addition to this, we analyze the order reduction phenomena in connection with the classical evaluation of the time-dependent boundary conditions. Finally, we carry out extensive numerical experiments to validate the theoretical findings. Moreover, the numerical results of the proposed methods are compared with the fractional-step implicit upwind finite difference scheme to examine the robustness of the newly developed methods.

Chapter 6 deals with two different class of singularly perturbed linear parabolic convection-diffusion IBVPs of the form (1.14)-(1.16) with nonsmooth data. At first we focus our attention on the IBVP (1.14)-(1.16) together with the condition (1.17), whose solution possesses strong interior layers. Here, we devise and analyze a new efficient FMM, which is constituted utilizing a suitable layer-resolving Shishkin mesh in the spatial direction. Next, we turn our attention to the IBVP (1.14)-(1.16) together with the condition (1.18), whose solution exhibits both boundary and weak interior layers. Here, we propose and analyze a new efficient FMM, which is constituted utilizing a modified layer-adapted mesh in the spatial direction. The modified layer-adapted mesh is a modification of the standard Shishkin mesh adapted to both boundary and weak interior layers. In the both cases, we use an equidistant mesh in the temporal direction. Finally, extensive numerical experiments are conducted in both the cases to support the theoretical findings and also to show the improvement in terms of spatial order of convergence in comparison with the existing numerical method. Further, we carry out numerical experiments for the semi-linear parabolic problems using the Newton's linearization technique.

In **Chapter 7**, we focus on robust numerical approximation of a class of singularly perturbed semilinear parabolic IBVPs of the form (1.19)-(1.22) with nonsmooth data. Here, the solution exhibits both boundary and weak interior layers. At first, we study existence, stability of the analytical solution of the governing semilinear problem and derive asymptotic behavior of the analytical solution. We then propose and analyze a higher-order time accurate FMM utilizing a suitable layer-adapted Shishkin mesh in the spatial direction and an equidistant mesh in the temporal direction. Finally, The theoretical error estimates are finally verified by numerical experiments, which also include comparison of the proposed numerical method with the implicit upwind method in terms of order of accuracy.

The thesis ends with a summary of the research contributions in **Chapter 8**; and also provides intuitive ideas for possible future scopes of the current research works. It is to be noted that the examples considered in the thesis satisfy the required compatibility conditions. In this context, one can see Appendix B which verifies the compatibility conditions for examples considered in Chapter 3 and 5.

Chapter 2

On ε -Uniform Higher-Order Accuracy of New Efficient Numerical Method for Singularly Perturbed 1D Linear Parabolic PDEs with Smooth Data

This chapter aims to achieve higher-order numerical approximation to the solutions of a class of singularly perturbed parabolic problems which can consist of the time-dependent convection coefficient and generally possess regular boundary layer. In order to fulfill the aim, at first we develop and analyze an efficient numerical method by discretizing the model problem using a new finite difference scheme on an appropriate layer-adapted mesh in the spatial direction, and the time derivative using the backward-Euler method on an equidistant mesh. We adopt the two-stage discretization process to establish the parameter-uniform estimate in the discrete supremum norm; and provide stability analysis in both the temporal and spatial discretization cases. Afterwards, we apply the Richardson extrapolation technique solely in the temporal direction for enhancing the temporal accuracy. We finally show that the resulting numerical solution is globally second-order convergent with respect to both the spatial and temporal variables. At the end, numerous numerical results are presented to corroborate the theoretical findings; and also to demonstrate the computational efficiency and the accuracy of the present numerical method in comparison with the existing numerical method. Besides this, we extend the computational experiment by solving the singularly perturbed semi-linear parabolic problem.

2.1 Introduction

In this chapter, we study the following class of singularly perturbed parabolic convection-diffusion initial-boundary value problems (IBVP) posed on the domain $\mathfrak{D} = \Omega \times (0, T] = (0, 1) \times (0, T]$:

$$\left\{ \begin{array}{l} \left(\frac{\partial}{\partial t} + \mathcal{L}_{x,\varepsilon} \right) y(x, t) = g(x, t), \quad \text{in } \mathfrak{D}, \\ y(x, 0) = q_0(x), \quad \text{on } \bar{\Omega} = [0, 1], \\ y(0, t) = s_l(t), \quad y(1, t) = s_r(t), \quad t \in [0, T], \end{array} \right. \quad (2.1)$$

where

$$\mathcal{L}_{x,\varepsilon} y = -\varepsilon \frac{\partial^2 y}{\partial x^2} + a(x, t) \frac{\partial y}{\partial x} + b(x, t) y,$$

$\varepsilon \in (0, 1]$ is a small parameter, and the coefficients $a(x, t)$, $b(x, t)$ and the source term $g(x, t)$ are considered to be sufficiently smooth with

$$a(x, t) \geq m > 0, \quad b(x, t) \geq \beta \geq 0, \quad \text{on } \overline{\mathcal{D}} = \overline{\Omega} \times [0, T]. \quad (2.2)$$

The existence of the solution $y(x, t)$ of the IBVP (2.1)-(2.2) follows from [Chapter IV, §5] of the book [65] by Ladyzenskaja et al. The solution of the IBVP (2.1)-(2.2) generally possesses boundary layer at $x = 1$ of width $O(\varepsilon)$. In the model problem, apart from imposing the smoothness criterion on a, b and g , the boundary and the initial data, *i.e.*, s_l, s_r and q_0 are assumed to be sufficiently smooth. Besides this, the following compatibility conditions are imposed at the corner points $(0, 0)$ and $(1, 0)$:

$$q_0(0) = s_l(0), \quad q_0(1) = s_r(0), \quad (2.3)$$

and

$$\begin{cases} \frac{ds_l(0)}{dt} = g(0, 0) + \varepsilon \frac{d^2 q_0(0)}{dx^2} - a(0, 0) \frac{dq_0(0)}{dx} - b(0, 0) q_0(0), \\ \frac{ds_r(0)}{dt} = g(1, 0) + \varepsilon \frac{d^2 q_0(1)}{dx^2} - a(1, 0) \frac{dq_0(1)}{dx} - b(1, 0) q_0(1). \end{cases} \quad (2.4)$$

Under these hypothesis the IBVP (2.1)-(2.2) exhibits a unique solution $y \in \mathcal{C}^{2+\gamma}(\overline{\mathcal{D}})$. Further, in order to derive the bounds of the derivatives up to fourth-order in space and second-order in time in Lemma 2.3, we require the solution $y \in \mathcal{C}^{4+\gamma}(\overline{\mathcal{D}})$, which is ensured by the assumption of the compatibility conditions in (2.3)-(2.4) together with the following compatibility conditions at the corner points $(0, 0)$ and $(1, 0)$:

$$\begin{cases} \frac{d^2 s_l(0)}{dt^2} = \frac{\partial g(0, 0)}{\partial t} - q_0(0) \frac{\partial b(0, 0)}{\partial t} - q'_0(0) \frac{\partial a(0, 0)}{\partial t} - \mathcal{L}_{x, \varepsilon} (g - \mathcal{L}_{x, \varepsilon} q_0)(0, 0), \\ \frac{d^2 s_r(0)}{dt^2} = \frac{\partial g(1, 0)}{\partial t} - q_0(1) \frac{\partial b(1, 0)}{\partial t} - q'_0(1) \frac{\partial a(1, 0)}{\partial t} - \mathcal{L}_{x, \varepsilon} (g - \mathcal{L}_{x, \varepsilon} q_0)(1, 0). \end{cases} \quad (2.5)$$

Here, it is important to note that papers [26, 81] assume the convection coefficient ' a ' as the function of x only, *i.e.*, $a = a(x)$. However, we consider time dependent convection coefficient in the considered PDE in (2.1) which makes the theoretical and computational analysis more interesting and challenging.

The layout of this chapter is structured as follows: The properties of the analytical solution consisting of the stability and the asymptotic behavior are discussed in Section 2.2. Section 2.3 provides an appropriate layer-adapted mesh and describes the newly proposed numerical method. In Section 2.4, we perform the convergence analysis by adopting the two-stage discretization process. Firstly, we estimate the error related to the time semidiscretization and later, we estimate the error related to the spatial discretization of the resulting stationary problem (2.15). Finally, we prove the main convergence result related to the ε -uniform error estimate of the proposed method. In Section 2.5, we discuss about the temporal Richardson extrapolation. Further, Section 2.6 presents the Newton's linearization method for solving the singularly perturbed semi-linear parabolic problem. Finally, the numerical results are presented in Section 2.7 for several test examples to validate the theoretical results; and the computational efficiency accuracy as well as the accuracy of the present method are also

compared with the existing scheme. The chapter is ended up with a brief summary in Section 2.8.

2.2 The analytical solution of continuous problem

In this section, we discuss properties of the analytical solution of the IBVP (2.1)-(2.2) and its derivatives. These properties are essential for convergence analysis related to the numerical approximation of the IBVP (2.1)-(2.2). At first, we show that the differential operator $\left(\frac{\partial}{\partial t} + \mathcal{L}_{x,\varepsilon}\right)$ corresponding to our model problem (2.1) satisfies the maximum principle in Lemma 2.1 and consequently, we obtain the stability result in Lemma 2.2. A concise proof of Lemma 2.1 is furnished below for clarity of the presentation. Let $\partial\mathfrak{D} = \overline{\mathfrak{D}} \setminus \mathfrak{D}$.

Lemma 2.1. *Let the function $\phi \in \mathcal{C}^0(\overline{\mathfrak{D}}) \cap \mathcal{C}^2(\mathfrak{D})$ be such that $\phi \leq 0$, on $\partial\mathfrak{D}$ and $\left(\frac{\partial}{\partial t} + \mathcal{L}_{x,\varepsilon}\right)\phi \leq 0$, in \mathfrak{D} , then it implies that $\phi \leq 0$ on $\overline{\mathfrak{D}}$.*

Proof: Here, we use method of contradiction. Firstly, $\phi \in \mathcal{C}^0(\overline{\mathfrak{D}}) \implies$ there exists $(s, \tau) \in \overline{\mathfrak{D}}$ such that

$$\phi(s, \tau) = \max_{(x,t) \in \overline{\mathfrak{D}}} \phi(x, t),$$

and without loss of generality, we assume that $\phi(s, \tau) > 0$. Now, in conformity with the hypothesis of the maximum principle, $\phi(x, t) \leq 0$ on $\partial\mathfrak{D} \implies (s, \tau) \in \mathfrak{D}$. Therefore, under the above assumption, we have $\left(\frac{\partial}{\partial t} + \mathcal{L}_{x,\varepsilon}\right)\phi(s, \tau) > 0$, and this contradicts the hypothesis that $\left(\frac{\partial}{\partial t} + \mathcal{L}_{x,\varepsilon}\right)\phi(x, t) \leq 0$ for all $(x, t) \in \mathfrak{D}$. Hereby, we complete the proof. ■

The following ε -uniform stability result is deduced by applying Lemma 2.1.

Lemma 2.2. *The solution $y(x, t)$ of the IBVP (2.1)-(2.2) satisfies that $\|y\|_{\overline{\mathfrak{D}}} \leq \|y\|_{\partial\mathfrak{D}} + \frac{1}{m}\|g\|_{\overline{\mathfrak{D}}}$.*

Now, according to the result stated in [[90], Lemma 2.2], without loss of generality, we assume that $y \equiv 0$ on $\partial\mathfrak{D}$. Hence, the first-order compatibility conditions in (2.4) and the second-order compatibility conditions in (2.5), respectively imply that

$$g(0, 0) = 0 = g(1, 0), \quad \text{and} \quad \frac{\partial g(0, 0)}{\partial t} - \mathcal{L}_{x,\varepsilon}g(0, 0) = 0 = \frac{\partial g(1, 0)}{\partial t} - \mathcal{L}_{x,\varepsilon}g(1, 0). \quad (2.6)$$

Now, apart from assuming the conditions on the function g at the corner points $(0, 0)$ and $(1, 0)$, we further assume the following conditions:

$$\frac{\partial^{j+k}g(0, 0)}{\partial x^j \partial t^k} = 0, \quad \text{for } 0 \leq j + 2k \leq 3, \quad (2.7)$$

which are required to show that the reduced solution $\mathcal{U}(x, t)$ of the IBVP (2.1)-(2.2) is sufficiently smooth. Afterwards, we decompose the solution $y(x, t)$ as

$$y(x, t) = \mathcal{U}(x, t) + \mathcal{V}(x, t) + \mathcal{W}(x, t),$$

where \mathcal{V} is a boundary layer type function and \mathcal{W} is the remainder term which is of $O(\varepsilon)$; and derive the bounds of the derivatives given in (2.8) by adopting the approach given in [90], as mentioned in [99, Part II, Section 2.2, Remark 2.8].

Lemma 2.3. *The derivatives of the solution $y(x, t)$ of the IBVP (2.1)-(2.2) satisfy the following estimate*

$$\left| \frac{\partial^{j+k} y(x, t)}{\partial x^j \partial t^k} \right| \leq C \left(1 + \varepsilon^{-j} \exp(-m(1-x)/\varepsilon) \right), \quad (x, t) \in \overline{\mathcal{D}}, \quad (2.8)$$

$\forall j, k \in \mathbb{N} \cup \{0\}$ satisfying $0 \leq j + 2k \leq 4$.

2.3 The discrete solution of continuous problem

This section provides the description of the layer-adapted mesh for discretizing the domain $\overline{\mathcal{D}}$ and the proposed numerical method for discretizing the IBVP (2.1)-(2.2).

2.3.1 Discretization of the domain

Let $N(\geq 4)$ be an even positive integer. Now, to discretize the domain $\overline{\mathcal{D}}$, we construct a mesh $\overline{\mathcal{D}}^{N, \Delta t} = \overline{\Omega}^N \times \Lambda^{\Delta t}$. Here, $\overline{\Omega}^N$ is denoted as the piecewise-uniform Shishkin mesh on the spatial domain $\overline{\Omega}$ as depicted in Fig 2.1. To construct the mesh, we partition $\overline{\Omega}$ into two sub-intervals $[0, 1 - \eta]$ and $[1 - \eta, 1]$, where the transition parameter η is defined by

$$\eta = \min \left\{ \frac{1}{2}, \eta_0 \varepsilon \ln N \right\}, \quad \eta_0 = 2/\theta,$$

where θ is a positive constant to be determined later. We consider non-uniform mesh in the analysis and for that we consider $\eta = \eta_0 \varepsilon \ln N$.

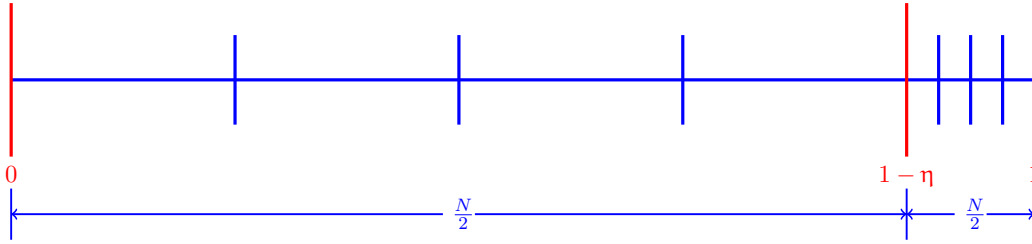


Figure 2.1: Shishkin mesh

Now, on each sub-interval we place equidistant mesh with $N/2$ mesh-intervals such that $\overline{\Omega}^N = \{x_j\}_{j=0}^N$, where

$$x_j = \begin{cases} \frac{2(1-\eta)j}{N}, & \text{for } 0 \leq j \leq N/2, \\ (1-\eta) + \left(j - \frac{N}{2}\right) \frac{2\eta}{N}, & \text{for } N/2 < j \leq N. \end{cases}$$

On the other hand, we construct an equidistant mesh, denoted by $\Lambda^{\Delta t} := \{t_n\}_{n=0}^M$, with M mesh-intervals in the temporal direction having the step-size $\Delta t = T/M$. Next, $h_j = x_j - x_{j-1}$, $1 \leq j \leq N$, is denoted as the step-size in the spatial direction such that $\hat{h}_j = h_j + h_{j+1}$, $1 \leq j \leq N - 1$; and it follows from the definition of x_j 's that

$$h_j = \begin{cases} H = 2(1-\eta)/N, & \text{for } 1 \leq j \leq \frac{N}{2}, \\ h = 2\eta/N, & \text{for } \frac{N}{2} < j \leq N. \end{cases}$$

2.3.2 Proposed numerical method

Firstly, we discretize (2.1) by using the backward-Euler method with respect to the temporal variable and it yields the following semidiscrete scheme:

$$\begin{cases} y^0(x) = q_0(x), & x \in \bar{\Omega}, \\ (I + \Delta t \mathcal{L}_{x,\varepsilon}^{n+1})y^{n+1}(x) = y^n(x) + \Delta t g(x, t_{n+1}), & x \in \Omega, \\ y^{n+1}(0) = s_l(t_{n+1}), & y^{n+1}(1) = s_r(t_{n+1}), \end{cases} \quad (2.9)$$

where

$$\mathcal{L}_{x,\varepsilon}^{n+1} \equiv -\varepsilon \frac{\partial^2}{\partial x^2} + a(x, t_{n+1}) \frac{\partial}{\partial x} + b(x, t_{n+1}).$$

Here, $y^n(x)$ denotes the semidiscrete approximation to the exact solution $y(x, t)$ of the IBVP (2.1)-(2.2) at the time level $t_n = n \Delta t$.

Afterwards, in order to constitute the fully discrete scheme, we discretize (2.9) in the spatial direction by proposing a new hybrid finite difference scheme. The scheme consists of a modified central difference scheme whenever $\varepsilon > \|a\|N^{-1}$; and whenever $\varepsilon \leq \|a\|N^{-1}$, the scheme is constituted by combining the midpoint upwind scheme in the outer region $(0, 1 - \eta]$ and the modified central difference scheme in the boundary layer region $(1 - \eta, 1)$.

Thus, to get the numerical solution of the IBVP (2.1)-(2.2) on $\bar{\mathcal{D}}^{N,\Delta t}$, we use the fully discrete finite difference scheme of the following form:

$$\left\{ \begin{array}{l} Y_j^0 = q_0(x_j), \quad 0 \leq j \leq N, \\ \left\{ \begin{array}{l} Y_j^{n+1} + \Delta t \mathcal{L}_{N,mcd}^{n+1} Y_j^{n+1} = Y_j^n + \Delta t g_j^{n+1}, \\ \text{for } 1 \leq j \leq N/2, \text{ and when } \varepsilon > \|a\|N^{-1}, \\ Y_{j-1/2}^{n+1} + \Delta t \mathcal{L}_{N,mup}^{n+1} Y_j^{n+1} = Y_{j-1/2}^n + \Delta t g_{j-1/2}^{n+1}, \\ \text{for } 1 \leq j \leq N/2, \text{ and when } \varepsilon \leq \|a\|N^{-1}, \\ Y_j^{n+1} + \Delta t \mathcal{L}_{N,mcd}^{n+1} Y_j^{n+1} = Y_j^n + \Delta t g_j^{n+1}, \\ \text{for } N/2 < j \leq N-1, \\ Y_0^{n+1} = s_l(t_{n+1}), \quad Y_N^{n+1} = s_r(t_{n+1}), \quad n = 0, 1, \dots, M-1, \end{array} \right. \end{array} \right. \quad (2.10)$$

where

$$\left\{ \begin{array}{l} \mathcal{L}_{N,mup}^{n+1} Y_j^{n+1} = -\varepsilon \delta_x^2 Y_j^{n+1} + a_{j-\frac{1}{2}}^{n+1} D_x^- Y_j^{n+1} + b_{j-1/2}^{n+1} Y_{j-\frac{1}{2}}^{n+1}, \\ \mathcal{L}_{N,mcd}^{n+1} Y_j^{n+1} = -\varepsilon \delta_x^2 Y_j^{n+1} + a_j^{n+1} D_x^* Y_j^{n+1} + b_j^{n+1} Y_j^{n+1}. \end{array} \right.$$

Let $\rho_j = \left(\varepsilon - \frac{a_j^{n+1}h_j}{2}\right)$. Then, we rewrite the difference scheme (2.10) in the following form:

$$\begin{cases} Y_j^0 = \mathbf{q}_0(x_j), & 0 \leq j \leq N, \\ \begin{cases} \mathbf{L}_{N,hyb}^{\Delta t} Y_j^{n+1} \equiv \mu_j^- Y_{j-1}^{n+1} + \mu_j^c Y_j^{n+1} + \mu_j^+ Y_{j+1}^{n+1} = \mathcal{G}_j^{n+1}, \\ \end{cases} & \text{for } 1 \leq j \leq N-1, \\ Y_0^{n+1} = \mathbf{s}_l(t_{n+1}), \quad Y_N^{n+1} = \mathbf{s}_r(t_{n+1}), & n = 0, 1, \dots, M-1. \end{cases} \quad (2.11)$$

Here, the coefficients $\mu_j^-, \mu_j^c, \mu_j^+$ are given by

$$\begin{cases} \mu_j^- = \Delta t \mu_{mcd,j}^-, \quad \mu_j^c = \Delta t \mu_{mcd,j}^c + 1, \quad \mu_j^+ = \Delta t \mu_{mcd,j}^+, \\ \text{for } 1 \leq j \leq N/2, \text{ and when } \varepsilon > \|a\|N^{-1}, \\ \mu_j^- = \Delta t \mu_{mup,j}^- + \frac{1}{2}, \quad \mu_j^c = \Delta t \mu_{mup,j}^c + \frac{1}{2}, \quad \mu_j^+ = \Delta t \mu_{mup,j}^+, \\ \text{for } 1 \leq j \leq N/2, \text{ and when } \varepsilon \leq \|a\|N^{-1}, \\ \mu_j^- = \Delta t \mu_{mcd,j}^-, \quad \mu_j^c = \Delta t \mu_{mcd,j}^c + 1, \quad \mu_j^+ = \Delta t \mu_{mcd,j}^+, \\ \text{for } N/2 < j \leq N-1, \end{cases} \quad (2.12)$$

where

$$\begin{cases} \mu_{mup,j}^- = -\frac{2\varepsilon}{\widehat{h}_j h_j} - \frac{a_{j-1/2}^{n+1}}{h_j} + \frac{b_{j-1/2}^{n+1}}{2}, \\ \mu_{mup,j}^c = \frac{2\varepsilon}{h_j h_{j+1}} + \frac{a_{j-1/2}^{n+1}}{h_j} + \frac{b_{j-1/2}^{n+1}}{2}, \\ \mu_{mup,j}^+ = -\frac{2\varepsilon}{\widehat{h}_j h_{j+1}}, \end{cases} \text{ and } \begin{cases} \mu_{mcd,j}^- = -\frac{2\rho_j}{\widehat{h}_j h_j} - \frac{a_j^{n+1}}{h_j}, \\ \mu_{mcd,j}^c = \frac{2\rho_j}{h_j h_{j+1}} + \frac{a_j^{n+1}}{h_j} + b_j^{n+1}, \\ \mu_{mcd,j}^+ = -\frac{2\rho_j}{\widehat{h}_j h_{j+1}}, \end{cases} \quad (2.13)$$

and the right hand side vector \mathcal{G}^{n+1} in (2.11) is given by

$$\mathcal{G}_j^{n+1} = \begin{cases} Y_j^n + \Delta t g_j^{n+1}, & \text{for } 1 \leq j \leq N/2, \text{ and when } \varepsilon > \|a\|N^{-1}, \\ \frac{1}{2}(Y_{j-1}^n + \Delta t g_{j-1}^{n+1}) + \frac{1}{2}(Y_j^n + \Delta t g_j^{n+1}), & \text{for } 1 \leq j \leq N/2, \text{ and when } \varepsilon \leq \|a\|N^{-1}, \\ Y_j^n + \Delta t g_j^{n+1}, & \text{for } N/2 < j \leq N-1. \end{cases} \quad (2.14)$$

2.4 Convergence analysis

In this section, we derive the ε -uniform error estimate associated with the fully discrete scheme (2.11)-(2.14). In order to derive the required estimate, we adopt the two-stage discretization process. Firstly, we estimate the

error related to the time semidiscretization and later, we estimate the error related to the spatial discretization of the resulting stationary problem.

2.4.1 Error related to the time semidiscretization

Here, we estimate the global temporal error related to the approximation of the exact solution $y(x, t)$ of the IBVP (2.1)-(2.2) at the time level $t = t_{n+1}$ by the semidiscrete solution $y^{n+1}(x)$. For this purpose, we perform the stability analysis and also present the consistency result of the scheme (2.9).

2.4.1.1 Stability

In the following lemma, it is shown that the operator $(I + \Delta t \mathcal{L}_{x,\varepsilon}^{n+1})$ satisfies the maximum principle.

Lemma 2.4. *Let the function $\psi \in \mathcal{C}^0(\bar{\Omega}) \cap \mathcal{C}^2(\Omega)$ be such that $\psi(0) \leq 0$, $\psi(1) \leq 0$, and $(I + \Delta t \mathcal{L}_{x,\varepsilon}^{n+1})\psi(x) \leq 0$, for all $x \in \Omega$, then it implies that $\psi(x) \leq 0$, for all $x \in \bar{\Omega}$.*

Proof: The outline of the proof is similar to that of Lemma 2.1. ■

Now, the result in Lemma 2.5 guarantees the stability of the time semidiscrete scheme (2.9) and hereby ensures that the scheme (2.9) produces a unique solution after each time step.

Lemma 2.5. *Let the function $\mathcal{Z} \in \mathcal{C}^0(\bar{\Omega}) \cap \mathcal{C}^2(\Omega)$ be such that $\mathcal{Z}(0) = 0 = \mathcal{Z}(1)$. Then we have*

$$\|\mathcal{Z}\| \leq \frac{1}{(1 + \beta \Delta t)} \|(I + \Delta t \mathcal{L}_{x,\varepsilon}^{n+1})\mathcal{Z}\|.$$

Proof: Consider the following functions

$$\psi^\pm(x) = \frac{-1}{(1 + \beta \Delta t)} \|(I + \Delta t \mathcal{L}_{x,\varepsilon}^{n+1})\mathcal{Z}\| \pm \mathcal{Z}(x), \quad x \in \bar{\Omega}.$$

It is obvious that $\psi^\pm(0) \leq 0$, $\psi^\pm(1) \leq 0$, and since,

$$\frac{(I + \Delta t \mathcal{L}_{x,\varepsilon}^{n+1})\|(I + \Delta t \mathcal{L}_{x,\varepsilon}^{n+1})\mathcal{Z}\|}{(1 + \beta \Delta t)} \geq \|(I + \Delta t \mathcal{L}_{x,\varepsilon}^{n+1})\mathcal{Z}\| \implies (I + \Delta t \mathcal{L}_{x,\varepsilon}^{n+1})\psi^\pm(x) \leq 0, \quad x \in \Omega,$$

by applying Lemma 2.4, we obtain the desired result. ■

2.4.1.2 Temporal error

We define $e^{n+1}(x) = y(x, t_{n+1}) - y^{n+1}(x)$ as the global error related to the time semidiscrete scheme (2.9) at the time level t_{n+1} . It is to be noted that for deriving the required estimate of the global error at the final time step, one needs to consider the contribution of the local error obtained at each time step. Due to this reason, we obtain estimate of the local error in Lemma 2.6.

Now, let us denote $\tilde{y}^{n+1}(x)$ as the solution of the semidiscrete scheme (2.9) obtained at the time level t_{n+1} , by choosing $y(x, t_n)$ as the initial data instead of $y^n(x)$, $x \in \Omega$; and hereby, we introduce the following auxiliary BVP:

$$\begin{cases} (I + \Delta t \mathcal{L}_{x,\varepsilon}^{n+1})\tilde{y}^{n+1}(x) = y(x, t_n) + \Delta t g(x, t_{n+1}), & x \in \Omega, \\ \tilde{y}^{n+1}(0) = \mathbf{s}_l(t_{n+1}), \tilde{y}^{n+1}(1) = \mathbf{s}_r(t_{n+1}). \end{cases} \quad (2.15)$$

Lemma 2.6. *The local error related to the time semidiscrete scheme (2.9) at the time level t_{n+1} , defined as $\tilde{e}^{n+1}(x) = y(x, t_{n+1}) - \tilde{y}^{n+1}(x)$, satisfies the following estimate:*

$$\|\tilde{e}^{n+1}\| \leq C(\Delta t)^2. \quad (2.16)$$

Proof: Applying Taylor's theorem on the analytical solution $y(x, t)$ with respect to the temporal variable, we have

$$\begin{aligned} y(x, t_n) &= y(x, t_{n+1}) - \Delta t \frac{\partial y(x, t_{n+1})}{\partial t} + \frac{(\Delta t)^2}{2} \frac{\partial^2 y(x, s)}{\partial t^2}, \quad t_n < s < t_{n+1}, \\ &= (I + \Delta t \mathcal{L}_{x, \varepsilon}^{n+1}) y(x, t_{n+1}) - \Delta t g(x, t_{n+1}) + \frac{(\Delta t)^2}{2} \frac{\partial^2 y(x, s)}{\partial t^2}. \end{aligned} \quad (2.17)$$

On the other hand, from (2.15) we have

$$y(x, t_n) = (I + \Delta t \mathcal{L}_{x, \varepsilon}^{n+1}) \tilde{y}^{n+1}(x) - \Delta t g(x, t_{n+1}). \quad (2.18)$$

Since, $\tilde{e}^{n+1}(0) = 0 = \tilde{e}^{n+1}(1)$, by using Lemma 2.5 on \tilde{e}^{n+1} , we obtain from (2.17) and (2.18) that

$$\|\tilde{e}^{n+1}\| \leq C \|(I + \Delta t \mathcal{L}_{x, \varepsilon}^{n+1}) \tilde{e}^{n+1}\| \leq C(\Delta t)^2 \left\| \frac{\partial^2 y}{\partial t^2} \right\|.$$

Thus, the proof is completed by using the bound of $\frac{\partial^2 y}{\partial t^2}$ from Lemma 2.3. ■

Now, we rewrite the global error as

$$e^{n+1}(x) = \tilde{e}^{n+1}(x) + d^{n+1}(x),$$

where the term $d^{n+1}(x) = \tilde{y}^{n+1}(x) - y^{n+1}(x)$, satisfies the following:

$$\begin{cases} (I + \Delta t \mathcal{L}_{x, \varepsilon}^{n+1}) d^{n+1}(x) = e^n(x), & x \in \Omega, \\ d^{n+1}(0) = 0, & d^{n+1}(1) = 0. \end{cases}$$

Then, by using Lemma 2.5 on $d^{n+1}(x)$, we obtain that

$$\|e^{n+1}\| \leq \|\tilde{e}^{n+1}\| + \frac{1}{(1 + \beta \Delta t)} \|e^n\|.$$

Finally, using the above relation recursively and by invoking the consistency result in Lemma 2.6, we obtain the desired estimate of the global error stated in the following Lemma.

Theorem 2.1 (Global error). *Under the hypothesis of Lemma 2.6, the global error e^{n+1} satisfies the following estimate:*

$$\sup_{(n+1)\Delta t \leq T} \|e^{n+1}\| \leq C \Delta t.$$

2.4.2 Error related to the spatial discretization

Here, we analyze the following discrete problem, which is obtained by discretizing (2.15) with respect to the spatial variable using the proposed hybrid scheme as described in Section 2.3:

$$\begin{cases} L_{N,hyb}^{\Delta t} \tilde{Y}_j^{n+1} \equiv \mu_j^- \tilde{Y}_{j-1}^{n+1} + \mu_j^c \tilde{Y}_j^{n+1} + \mu_j^+ \tilde{Y}_{j+1}^{n+1} = \tilde{g}_j^{n+1}, \\ \tilde{Y}_0^{n+1} = \mathbf{s}_l(t_{n+1}), \quad \tilde{Y}_N^{n+1} = \mathbf{s}_r(t_{n+1}), \end{cases} \quad \text{for } 1 \leq j \leq N-1, \quad (2.19)$$

where the coefficients μ_j^- , μ_j^+ , μ_j^c are described in (2.12)-(2.13) and \tilde{g}_j^{n+1} is given by

$$\tilde{g}_j^{n+1} = \begin{cases} y(x_j, t_n) + \Delta t g_j^{n+1}, & \text{for } 1 \leq j \leq N/2, \text{ and when } \varepsilon > \|a\|N^{-1}, \\ \frac{1}{2}(y(x_{j-1}, t_n) + \Delta t g_{j-1}^{n+1}) + \frac{1}{2}(y(x_j, t_n) + \Delta t g_j^{n+1}), \\ \quad \text{for } 1 \leq j \leq N/2, \text{ and when } \varepsilon \leq \|a\|N^{-1}, \\ y(x_j, t_n) + \Delta t g_j^{n+1}, & \text{for } N/2 < j \leq N-1. \end{cases} \quad (2.20)$$

In the subsequent sections, we analyze the stability and the truncation error associated with the above discrete problem; and finally, we derive the local error estimate related to the spatial discretization of (2.15).

2.4.2.1 Stability

In the following lemma, we prove that the difference operator $L_{N,hyb}^{\Delta t}$ defined in (2.11)-(2.13) satisfies the discrete maximum principle.

Lemma 2.7 (Discrete maximum principle). *Assume that the following conditions hold for $N \geq N_0$:*

$$N/\ln N > \eta_0 \|a\| \quad \text{and} \quad (2.21)$$

$$\mathfrak{m}N \geq \left(\|b\| + \frac{1}{\Delta t} \right), \quad (2.22)$$

where N_0 is some positive integer. Then, for fixed n , if any mesh function $\psi^{n+1}: \bar{\Omega}^N \rightarrow \mathbb{R}$ satisfies that $\psi_0^{n+1} \leq 0$, $\psi_N^{n+1} \leq 0$, and $L_{N,hyb}^{\Delta t} \psi_j^{n+1} \leq 0$, for $1 \leq j \leq N-1$; then it implies that $\psi_j^{n+1} \leq 0$, for all j .

Proof. In conformity with the hypothesis of the discrete maximum principle, without loss of generality we consider $\psi_j^{n+1} = \psi_j$ for fixed n ; and assume that the mesh function ψ_j satisfies the following system:

$$\begin{cases} L_{N,hyb}^{\Delta t} \psi_j = \omega_j, & \text{for } 1 \leq j \leq N-1, \\ \psi_0 = \omega_0, \quad \psi_N = \omega_N, \end{cases} \quad (2.23)$$

where $\omega_j \leq 0$, for $0 \leq j \leq N$. Now, we consider the following two cases to prove that the $(N+1) \times (N+1)$ matrix \mathcal{A} , associated with the coefficients of ψ_j in (2.23) for $0 \leq j \leq N$, is an M-matrix.

Case.1 Let $\varepsilon > \|a\|N^{-1}$. Since $H \leq 2N^{-1}$, for $1 \leq j \leq N/2$, we have

$$\rho_j \geq \left(\varepsilon - \frac{\|a\|H}{2} \right) > 0,$$

and also for $N/2 + 1 \leq j \leq N - 1$, we have

$$\rho_j \geq \left(\varepsilon - \frac{\|a\|h}{2} \right) \geq \left(\varepsilon - \frac{\|a\|H}{2} \right) > 0.$$

Hence, it follows from (2.12)-(2.13) that $\mu_j^- < 0$, $\mu_j^+ < 0$ and $|\mu_j^c| - |\mu_j^-| - |\mu_j^+| \geq 0$, for $1 \leq j \leq N - 1$.

Case 2. When $\varepsilon \leq \|a\|N^{-1}$. Here, for $N/2 + 1 \leq j \leq N - 1$, using (2.21) we obtain that

$$\rho_j \geq \left(\varepsilon - \frac{\|a\|h}{2} \right) = \varepsilon \left(1 - \|a\|\eta_0 N^{-1} \ln N \right) > 0,$$

and hence it follows from (2.12)-(2.13) that $\mu_j^- < 0$, $\mu_j^+ < 0$ and $|\mu_j^c| - |\mu_j^-| - |\mu_j^+| \geq 0$, for $N/2 + 1 \leq j \leq N - 1$. Again, for $1 \leq j \leq N/2$, we have $\mu_j^+ < 0$ and using (2.22) we obtain that

$$\begin{aligned} \mu_j^- &= \Delta t \mu_{sup,j}^- + \frac{1}{2} \\ &= -\frac{2\varepsilon \Delta t}{\tilde{h}_j h_j} - \Delta t \left[\frac{a_{j-1/2}^{n+1}}{H} - \frac{b_{j-1/2}^{n+1}}{2} - \frac{1}{2\Delta t} \right] \\ &< -\frac{\Delta t}{2} \left[\mathbf{m}N - \|b\| - \frac{1}{\Delta t} \right] \leq 0, \end{aligned}$$

and further we have

$$|\mu_j^-| + |\mu_j^+| \leq \Delta t \left(\frac{2\varepsilon}{\tilde{h}_j h_j} + \frac{a_{j-1/2}^{n+1}}{h_j} + \frac{b_{j-1/2}^{n+1}}{2} \right) + \Delta t \left(\frac{2\varepsilon}{\tilde{h}_j h_{j+1}} \right) + \frac{1}{2} < |\mu_j^c|.$$

This shows that under the assumptions (2.21) and (2.22), the matrix \mathcal{A} is an M-matrix, and since \mathcal{A} is also irreducible, $\mathcal{A}^{-1} \geq 0$. We thus obtain the desired result. ■

Remark 2.1. From Lemma 2.7, it can be concluded that the spatially discrete scheme (2.19)-(2.20) is uniformly stable under the assumption (2.21) and (2.22) in the discrete supremum norm and the corresponding system has a unique solution.

2.4.2.2 Truncation error

For the numerical scheme (2.19)-(2.20), the local truncation error is defined as

$$\begin{aligned}
\mathcal{T}_{j,\tilde{y}^{n+1}}^{N,\Delta t} &= \mathcal{L}_{N,hyb}^{\Delta t} [\tilde{y}_j^{n+1} - \tilde{Y}_j^{n+1}], \\
&= \begin{cases} \mu_j^- \tilde{y}_{j-1}^{n+1} + \mu_j^c \tilde{y}_j^{n+1} + \mu_j^+ \tilde{y}_{j+1}^{n+1} - \left(\tilde{y}_j^{n+1} + \Delta t (\mathcal{L}_{x,\varepsilon} \tilde{y}^{n+1})(x_j) \right), \\ \quad \text{for } 1 \leq j \leq N/2, \text{ and when } \varepsilon > \|a\|N^{-1}, \\ \mu_j^- \tilde{y}_{j-1}^{n+1} + \mu_j^c \tilde{y}_j^{n+1} + \mu_j^+ \tilde{y}_{j+1}^{n+1} - \frac{1}{2} \left(\tilde{y}_{j-1}^{n+1} + \Delta t (\mathcal{L}_{x,\varepsilon} \tilde{y}^{n+1})(x_{j-1}) \right) \\ \quad - \frac{1}{2} \left(\tilde{y}_j^{n+1} + \Delta t (\mathcal{L}_{x,\varepsilon} \tilde{y}^{n+1})(x_j) \right), \\ \quad \text{for } 1 \leq j \leq N/2, \text{ and when } \varepsilon \leq \|a\|N^{-1}, \\ \mu_j^- \tilde{y}_{j-1}^{n+1} + \mu_j^c \tilde{y}_j^{n+1} + \mu_j^+ \tilde{y}_{j+1}^{n+1} - \left(\tilde{y}_j^{n+1} + \Delta t (\mathcal{L}_{x,\varepsilon} \tilde{y}^{n+1})(x_j) \right), \\ \quad \text{for } N/2 < j \leq N-1, \end{cases} \\
&= \Delta t \mathcal{T}_{j,\tilde{y}^{n+1}}^N.
\end{aligned} \tag{2.24}$$

Here, for any sufficiently smooth function $\phi: \bar{\Omega} \rightarrow \mathbb{R}$, $\mathcal{T}_{j,\phi}^N$ denotes the truncation error corresponding to the stationary singularly perturbed problem and is obtained by approximating the differential operator $\mathcal{L}_{x,\varepsilon}$ with respect to the spatial variable using the newly proposed hybrid scheme. Let $\phi_j = \phi(x_j)$. Thus, it follows from (2.24) that

$$\mathcal{T}_{j,\phi}^N = \begin{cases} \mathcal{L}_{N,mcd}^{n+1} \phi_j - (\mathcal{L}_{x,\varepsilon} \phi)(x_j), & \text{for } 1 \leq j \leq N/2, \text{ and when } \varepsilon > \|a\|N^{-1}, \\ \mathcal{L}_{N,mup}^{n+1} \phi_j - (\mathcal{L}_{x,\varepsilon} \phi)_{j-1/2}, & \text{for } 1 \leq j \leq N/2, \text{ and when } \varepsilon \leq \|a\|N^{-1}, \\ \mathcal{L}_{N,mcd}^{n+1} \phi_j - (\mathcal{L}_{x,\varepsilon} \phi)(x_j), & \text{for } N/2 < j \leq N-1. \end{cases} \tag{2.25}$$

In the next lemma, the required estimates of $\mathcal{T}_{j,\phi}^N$ are derived by making use of the Taylor's theorem on the function ϕ and in this regard, we consider the remainder term in the integral form, i.e., $\frac{1}{k!} \int_{\xi}^x (x-s)^k \phi^{k+1}(s) ds$, which arises while approximating $\phi(x)$ by a Taylor polynomial of degree k around a point $\xi \in \bar{\Omega}$.

Lemma 2.8. *One can obtain the following estimates:*

(i) when $\varepsilon > \|a\|N^{-1}$,

$$\begin{cases} \left| \mathcal{L}_{N,mcd}^{n+1}(\phi_j) - (\mathcal{L}_{x,\varepsilon} \phi)(x_j) \right| \leq Ch_j \left[\varepsilon \int_{x_{j-1}}^{x_{j+1}} |\phi^{(4)}(s)| ds + \int_{x_{j-1}}^{x_{j+1}} |\phi^{(3)}(s)| ds \right], \\ \quad \text{for } 1 \leq j < N/2, \\ \left| \mathcal{L}_{N,mcd}^{n+1}(\phi_j) - (\mathcal{L}_{x,\varepsilon} \phi)(x_j) \right| \leq C \left[\varepsilon \int_{x_{j-1}}^{x_{j+1}} |\phi^{(3)}(s)| ds + h_j \int_{x_{j-1}}^{x_{j+1}} |\phi^{(3)}(s)| ds \right], \\ \quad \text{for } j = N/2, \end{cases} \tag{2.26}$$

and when $\varepsilon \leq \|a\|N^{-1}$, for $1 \leq j \leq N/2$,

$$\begin{aligned} & \left| \mathcal{L}_{N,mup}^{n+1}(\Phi_j) - (\mathcal{L}_{x,\varepsilon}\Phi)_{j-1/2} \right| \\ & \leq \left[C\varepsilon \int_{x_{j-1}}^{x_{j+1}} |\Phi^{(3)}(s)| ds + Ch_j \int_{x_{j-1}}^{x_j} \left(|\Phi^{(3)}(s)| + |\Phi^{(2)}(s)| + |\Phi^{(1)}(s)| \right) ds \right], \end{aligned} \quad (2.27)$$

(ii) for $N/2 < j \leq N-1$,

$$\left| \mathcal{L}_{N,mcd}^{n+1}(\Phi_j) - (\mathcal{L}_{x,\varepsilon}\Phi)(x_j) \right| \leq Ch_j \left[\varepsilon \int_{x_{j-1}}^{x_{j+1}} |\Phi^{(4)}(s)| ds + \int_{x_{j-1}}^{x_{j+1}} |\Phi^{(3)}(s)| ds \right]. \quad (2.28)$$

Now, to derive the bounds of the truncation error $\mathcal{T}_{j,\tilde{y}^{n+1}}^{N,\Delta t}$, one needs to know about the asymptotic behavior of the analytical solution of the auxiliary BVP (2.15) and its derivatives. For this purpose, the solution $\tilde{y}^{n+1}(x)$ is decomposed in the form (2.29) and the required bounds of its components are obtained in the following lemma.

Lemma 2.9. *The analytical solution of (2.15) is decomposed as*

$$\tilde{y}^{n+1}(x) = \tilde{p}^{n+1}(x) + \gamma \tilde{q}^{n+1}(x), \quad x \in \bar{\Omega}, \quad (2.29)$$

where the components $\tilde{p}^{n+1}(x)$ and $\tilde{q}^{n+1}(x)$ of the solution $\tilde{y}^{n+1}(x)$ satisfy the following bounds:

$$\begin{cases} \left| \frac{d^j \tilde{p}^{n+1}(x)}{dx^j} \right| \leq C \left[1 + \varepsilon^{-j+1} \exp(-\mathfrak{m}(1-x)/\varepsilon) \right], & \text{for } 0 \leq j \leq 4, \\ \tilde{q}^{n+1}(x) = \exp(-a(1, t_{n+1})(1-x)/\varepsilon), \quad \gamma = \frac{\varepsilon}{a(1, t_{n+1})} \frac{d\tilde{y}^{n+1}(1)}{dx}. \end{cases} \quad (2.30)$$

Proof: The proof follows from [18]. ■

In the following lemma, we obtain the bounds of the truncation error $\mathcal{T}_{j,\tilde{y}^{n+1}}^{N,\Delta t}$.

Lemma 2.10. *The truncation error given by (2.24) satisfies the following bounds:*

$$|\mathcal{T}_{j,\tilde{y}^{n+1}}^{N,\Delta t}| \leq \begin{cases} C\Delta t \left[H^2 + \varepsilon^{-1} \exp(-\mathfrak{m}(1-x_j)/\varepsilon) \right], & \text{for } 1 \leq j < N/2, \text{ and when } \varepsilon > \|a\|N^{-1}, \\ C\Delta t \left[\varepsilon H + H^2 + H^{-1} \exp(-\mathfrak{m}(1-x_{j+1})/\varepsilon) \right], & \text{for } 1 \leq j < N/2, \text{ and when } \varepsilon \leq \|a\|N^{-1}, \\ C\Delta t \left[\varepsilon H + H^2 + \varepsilon^{-1} \exp(-\mathfrak{m}(1-x_j)/\varepsilon) \right], & \text{for } j = N/2, \text{ and when } \varepsilon > \|a\|N^{-1}, \\ C\Delta t \left[\varepsilon H + H^2 + \varepsilon^{-1} \exp(-\mathfrak{m}(1-x_{j+1})/\varepsilon) \right], & \text{for } j = N/2, \text{ and when } \varepsilon \leq \|a\|N^{-1}, \\ C\Delta t \left[h^2 + h^2 \varepsilon^{-3} \exp(-\mathfrak{m}(1-x_j)/\varepsilon) \right], & \text{for } N/2 < j \leq N-1. \end{cases}$$

Proof: From (2.24), it is clear that in order to obtain the bound of $\mathcal{T}_{j,\tilde{y}^{n+1}}^{N,\Delta t}$, one needs to determine the appropriate bound of $\mathcal{T}_{j,\tilde{y}^{n+1}}^N$. In doing so, firstly we decompose $\mathcal{T}_{j,\tilde{y}^{n+1}}^N$ using the decomposition of \tilde{y}^{n+1} in (2.29), as

$$\mathcal{T}_{j,\tilde{y}^{n+1}}^N = \mathcal{T}_{j,\tilde{p}^{n+1}}^N + \gamma \mathcal{T}_{j,\tilde{q}^{n+1}}^N \quad (2.31)$$

where $\mathcal{T}_{j,\tilde{p}^{n+1}}^N$ and $\mathcal{T}_{j,\tilde{q}^{n+1}}^N$ denote the truncation errors corresponding to $\tilde{p}^{n+1}(x)$ and $\tilde{q}^{n+1}(x)$, respectively. Afterwards, by making use of Lemma 2.9 and 2.8 in (2.31), we obtain the required bounds of $\mathcal{T}_{j,\tilde{y}^{n+1}}^N$ by considering different cases depending on the location of mesh point $x_j \in \bar{\Omega}^N$, in the following way.

Case 1: Let $1 \leq j < N/2$. Here, two sub-cases are considered based on the relation between ε and N .

- (i) When $\varepsilon > \|a\|N^{-1}$. Using the bounds of the derivatives of \tilde{p}^{n+1} given in Lemma 2.9 and the estimate given in (2.26), we deduce that

$$\begin{aligned} |\mathcal{T}_{j,\tilde{p}^{n+1}}^N| &= |\mathcal{L}_{N,mcd}^{n+1} \tilde{p}_j^{n+1} - \mathcal{L}_{x,\varepsilon} \tilde{p}^{n+1}(x_j)| \\ &\leq C \left[h_j(h_j + h_{j+1}) + h_j \varepsilon^{-1} \left\{ \exp(-m(1 - x_{j+1})/\varepsilon) - \exp(-m(1 - x_{j-1})/\varepsilon) \right\} \right] \\ &\leq C \left[H^2 + H \varepsilon^{-1} \left\{ \exp(-m(1 - x_{j+1})/\varepsilon) - \exp(-m(1 - x_{j-1})/\varepsilon) \right\} \right] \\ &= C \left[H^2 + H \varepsilon^{-1} \exp(-m(1 - x_j)/\varepsilon) \sinh(mH/\varepsilon) \right]. \end{aligned}$$

Now, since $\varepsilon > \|a\|N^{-1}$ implies $mH/\varepsilon < 2$ and for $0 \leq \xi \leq 2$, $\sinh \xi \leq C\xi$, we obtain that

$$|\mathcal{T}_{j,\tilde{p}^{n+1}}^N| \leq C \left[H^2 + H^2 \varepsilon^{-2} \exp(-m(1 - x_j)/\varepsilon) \right].$$

Similarly, using the bounds of the derivatives of \tilde{q}^{n+1} given in Lemma 2.9 and the estimate given in (2.26), we obtain that

$$\begin{aligned} |\mathcal{T}_{j,\tilde{q}^{n+1}}^N| &= |\mathcal{L}_{N,mcd}^{n+1} \tilde{q}_j^{n+1} - \mathcal{L}_{x,\varepsilon} \tilde{q}^{n+1}(x_j)| \\ &\leq C \left[H \varepsilon^{-2} \left\{ \exp(-a(1, t_{n+1})(1 - x_{j+1})/\varepsilon) - \exp(-a(1, t_{n+1})(1 - x_{j-1})/\varepsilon) \right\} \right] \\ &\leq C \left[H^2 \varepsilon^{-3} \exp(-a(1, t_{n+1})(1 - x_j)/\varepsilon) \right]. \end{aligned}$$

Finally, using the bounds of $\mathcal{T}_{j,\tilde{p}^{n+1}}^N$ and $\mathcal{T}_{j,\tilde{q}^{n+1}}^N$ in (2.31), we have

$$\begin{aligned} |\mathcal{T}_{j,\tilde{y}^{n+1}}^N| &\leq C \left[H^2 + H^2 \varepsilon^{-3} \exp(-m(1 - x_j)/\varepsilon) \right] \\ &= C \left[H^2 + \varepsilon^{-1} \exp(-m(1 - x_j)/\varepsilon) \right]. \end{aligned}$$

- (ii) When $\varepsilon \leq \|a\|N^{-1}$. Using the bounds of the derivatives of \tilde{p}^{n+1} given in Lemma 2.9 and the estimate

given in (2.27), we deduce that

$$\begin{aligned}
|\mathcal{T}_{j,\tilde{p}^{n+1}}^N| &= |\mathcal{L}_{N,mup}^{n+1}\tilde{p}_j^{n+1} - \mathcal{L}_{x,\varepsilon}\tilde{p}^{n+1}(x_j)| \\
&\leq C \left[\varepsilon(h_j + h_{j+1}) + h_j^2 + \left\{ \exp(-\mathfrak{m}(1 - x_{j+1})/\varepsilon) - \exp(-\mathfrak{m}(1 - x_{j-1})/\varepsilon) \right\} \right. \\
&\quad \left. + h_j \varepsilon^{-1} \left\{ \exp(-\mathfrak{m}(1 - x_j)/\varepsilon) - \exp(-\mathfrak{m}(1 - x_{j-1})/\varepsilon) \right\} \right] \\
&\leq C \left[\varepsilon H + H^2 + \exp(-\mathfrak{m}(1 - x_{j+1})/\varepsilon) + H \varepsilon^{-1} \exp(-\mathfrak{m}(1 - x_j)/\varepsilon) \right].
\end{aligned}$$

Now, since $h_j = h_{j+1} = H$ and $s^k \exp(-s) \leq C$, we obtain that

$$|\mathcal{T}_{i,\tilde{p}^{n+1}}^N| \leq C \left[\varepsilon H + H^2 + \exp(-\mathfrak{m}(1 - x_{j+1})/\varepsilon) \right].$$

To find the bound of $|\mathcal{T}_{j,\tilde{q}^{n+1}}^N|$, we proceed by finding the bound for the exact expression of $\mathcal{T}_{j,\tilde{q}^{n+1}}^N = \mathcal{L}_{N,mup}^{n+1}\tilde{q}_j^{n+1} - (\mathcal{L}_{x,\varepsilon}\tilde{q}^{n+1})_{j-1/2}$. Here,

$$\mathcal{T}_{j,\tilde{q}^{n+1}}^N = \mu_{mup,j}^-(\tilde{q}_{j-1}^{n+1} - \tilde{q}_j^{n+1}) + \mu_{mup,j}^+(\tilde{q}_{j+1}^{n+1} - \tilde{q}_j^{n+1}) + \quad (2.32)$$

$$\begin{aligned}
&\frac{b_{j-1}^{n+1}}{2} (\tilde{q}_j^{n+1} - \tilde{q}_{j-1}^{n+1}) + \frac{1}{2} \varepsilon \left(\frac{d^2 \tilde{q}_j^{n+1}}{dx^2} + \frac{d^2 \tilde{q}_{j-1}^{n+1}}{dx^2} \right) \\
&\quad - \frac{1}{2} \left(a_j^{n+1} \frac{d\tilde{q}_j^{n+1}}{dx} + a_{j-1}^{n+1} \frac{d\tilde{q}_{j-1}^{n+1}}{dx} \right). \quad (2.33)
\end{aligned}$$

Now, using the expression in (2.33) and following the argument given in (2.30) for $1 \leq j < N/2$, we obtain that

$$|\mathcal{T}_{j,\tilde{q}^{n+1}}^N| \leq CH^{-1} \exp(-a(1, t_{n+1})(1 - x_{j+1})/\varepsilon).$$

Finally, using the bounds of $\mathcal{T}_{j,\tilde{p}^{n+1}}^N$ and $\mathcal{T}_{j,\tilde{q}^{n+1}}^N$ in (2.31), we have

$$|\mathcal{T}_{j,\tilde{y}^{n+1}}^N| \leq C \left[\varepsilon H + H^2 + H^{-1} \exp(-\mathfrak{m}(1 - x_{j+1})/\varepsilon) \right].$$

Case 2: Let $j = N/2$. Here, we also consider two sub-cases.

- (i) When $\varepsilon > \|a\|N^{-1}$. Using the bounds of the derivatives of \tilde{p}^{n+1} given in Lemma 2.9 and the estimate given in (2.26), we deduce that

$$\begin{aligned}
|\mathcal{T}_{j,\tilde{p}^{n+1}}^N| &= |\mathcal{L}_{N,mcd}^{n+1}\tilde{p}_j^{n+1} - \mathcal{L}_{x,\varepsilon}\tilde{p}^{n+1}(x_j)| \\
&= C \left[(\varepsilon + h_j)(h_j + h_{j+1}) + \left\{ \exp(-\mathfrak{m}(1 - x_{j+1})/\varepsilon) - \exp(-\mathfrak{m}(1 - x_{j-1})/\varepsilon) \right\} \right. \\
&\quad \left. + h_j \varepsilon^{-1} \left\{ \exp(-\mathfrak{m}(1 - x_{j+1})/\varepsilon) - \exp(-\mathfrak{m}(1 - x_{j-1})/\varepsilon) \right\} \right] \\
&\leq C \left[\varepsilon H + H^2 + \left\{ \exp(-\mathfrak{m}(1 - x_{j+1})/\varepsilon) - \exp(-\mathfrak{m}(1 - x_{j-1})/\varepsilon) \right\} \right], \\
&= C \left[\varepsilon H + H^2 + \left\{ \exp(-\mathfrak{m}(1 - x_j)/\varepsilon) (\exp(\mathfrak{m}h/\varepsilon) - \exp(\mathfrak{m}H/\varepsilon)) \right\} \right] \\
&\leq C \left[\varepsilon H + H^2 + \exp(-\mathfrak{m}(1 - x_j)/\varepsilon) \right].
\end{aligned}$$

Similarly, using the bounds of the derivatives of \tilde{q}^{n+1} given in Lemma 2.9 and the estimate given in (2.26), we obtain that

$$\begin{aligned} |\mathcal{T}_{j,\tilde{q}^{n+1}}^N| &= |\mathcal{L}_{N,mcd}^{n+1} \tilde{q}_j^{n+1} - \mathcal{L}_{x,\varepsilon} \tilde{q}^{n+1}(x_j)| \\ &\leq C \left[\varepsilon^{-1} \left\{ \exp(-a(1, t_{n+1})(1 - x_{j+1})/\varepsilon) - \exp(-a(1, t_{n+1})(1 - x_{j-1})/\varepsilon) \right\} \right] \\ &\leq C \left[\varepsilon^{-1} \exp(-a(1, t_{n+1})(1 - x_j)/\varepsilon) \right]. \end{aligned}$$

Finally, using the bounds of $\mathcal{T}_{j,\tilde{p}^{n+1}}^N$ and $\mathcal{T}_{j,\tilde{q}^{n+1}}^N$ in (2.31), we have

$$|\mathcal{T}_{j,\tilde{y}^{n+1}}^N| \leq C \left[\varepsilon H + H^2 + \varepsilon^{-1} \exp(-\mathfrak{m}(1 - x_j)/\varepsilon) \right].$$

(ii) When $\varepsilon \leq \|a\|N^{-1}$. Arguing in the same way as it is done before, we obtain that

$$\begin{aligned} |\mathcal{T}_{j,\tilde{p}^{n+1}}^N| &= |\mathcal{L}_{N,mup}^{n+1} \tilde{p}_j^{n+1} - \mathcal{L}_{x,\varepsilon} \tilde{p}^{n+1}(x_j)| \\ &\leq C \left[\varepsilon H + H^2 + \exp(-\mathfrak{m}(1 - x_{j+1})/\varepsilon) + H\varepsilon^{-1} \exp(-\mathfrak{m}(1 - x_j)/\varepsilon) \right]. \end{aligned}$$

On the other hand, using the expression in (2.33) and following the argument given in (2.30) for $j = N/2$, we obtain that

$$|\mathcal{T}_{j,\tilde{q}^{n+1}}^N| \leq C\varepsilon^{-1} \exp(-a(1, t_{n+1})(1 - x_j)/\varepsilon).$$

Finally, using the bounds of $\mathcal{T}_{j,\tilde{p}^{n+1}}^N$ and $\mathcal{T}_{j,\tilde{q}^{n+1}}^N$ in (2.31), we have

$$|\mathcal{T}_{j,\tilde{y}^{n+1}}^N| \leq C \left[\varepsilon H + H^2 + \varepsilon^{-1} \exp(-\mathfrak{m}(1 - x_{j+1})/\varepsilon) \right].$$

Case 3: When $N/2 < j \leq N - 1$. Here, we deduce that

$$\begin{aligned} |\mathcal{T}_{j,\tilde{p}^{n+1}}^N| &= |\mathcal{L}_{N,mcd}^{n+1} \tilde{p}_j^{n+1} - \mathcal{L}_{x,\varepsilon} \tilde{p}^{n+1}(x_j)| \\ &\leq C \left[h_j(h_j + h_{j+1}) + h_j\varepsilon^{-1} \left\{ \exp(-\mathfrak{m}(1 - x_{j+1})/\varepsilon) - \exp(-\mathfrak{m}(1 - x_{j-1})/\varepsilon) \right\} \right] \\ &\leq C \left[h^2 + h\varepsilon^{-1} \left\{ \exp(-\mathfrak{m}(1 - x_{j+1})/\varepsilon) - \exp(-\mathfrak{m}(1 - x_{j-1})/\varepsilon) \right\} \right] \\ &= C \left[h^2 + h\varepsilon^{-2} \exp(-\mathfrak{m}(1 - x_j)/\varepsilon) \sinh(\mathfrak{m}h/\varepsilon) \right] \\ &\leq C \left[h^2 + h^2\varepsilon^{-3} \exp(-\mathfrak{m}(1 - x_j)/\varepsilon) \right], \end{aligned}$$

since the assumption given in (2.21) yields $\mathfrak{m}h/\varepsilon < 2$ and for $0 \leq \xi \leq 2$, $\sinh \xi \leq C\xi$. Likewise

$$\begin{aligned} |\mathcal{T}_{j,\tilde{q}^{n+1}}^N| &\leq Ch\varepsilon^{-2} \left[\exp(-a(1, t_{n+1})(1 - x_{j+1})/\varepsilon) - \exp(-a(1, t_{n+1})(1 - x_{j-1})/\varepsilon) \right] \\ &\leq Ch^2\varepsilon^{-3} \exp(-a(1, t_{n+1})(1 - x_j)/\varepsilon), \end{aligned}$$

Finally, using the bounds of $\mathcal{T}_{j,\tilde{p}^{n+1}}^N$ and $\mathcal{T}_{j,\tilde{q}^{n+1}}^N$ in (2.31), we have

$$|\mathcal{T}_{j,\tilde{y}^{n+1}}^N| \leq C \left[h^2 + h^2 \varepsilon^{-3} \exp(-\mathfrak{m}(1 - x_{j+1})/\varepsilon) \right].$$

Hence, the proof. ■

2.4.2.3 Auxiliary results

This section begins with several vital results which is used in the error analysis.

Lemma 2.11. *Consider the following mesh function*

$$\mathcal{S}_j(\theta) = \begin{cases} \prod_{k=j+1}^N \left(1 + \frac{\theta h_k}{\varepsilon}\right)^{-1}, & \text{for } 0 \leq j \leq N-1, \\ 1, & \text{for } j = N, \end{cases}$$

where θ is a positive constant. Then, we get the following results:

$$(i) \quad \text{If } \theta < \mathfrak{m}/2, \text{ then } \exp(-\mathfrak{m}(1 - x_j)/\varepsilon) \leq \mathcal{S}_j(\theta), \quad \text{for } 0 \leq j \leq N-1. \quad (2.34)$$

$$(ii) \quad \mathcal{S}_{N/2}(\theta) \leq CN^{-\eta_0 \theta}. \quad (2.35)$$

Proof: See [109, Lemma 2.5] for the proof of (i) and [111, Lemma 3.1] for the proof of (ii). ■

Lemma 2.12. *If $\theta < \mathfrak{m}/2$, then under the hypothesis (2.21) of Lemma 2.7, we have*

$$\mathcal{L}_{N,hyb}^{\Delta t} \mathcal{S}_j(\theta) \geq \begin{cases} \frac{C\Delta t}{\varepsilon} \mathcal{S}_j(\theta), & \text{for } 1 \leq j \leq N/2, \text{ and when } \varepsilon > \|a\|N^{-1}, \\ \frac{C\Delta t}{H} \mathcal{S}_j(\theta), & \text{for } 1 \leq j \leq N/2, \text{ and when } \varepsilon \leq \|a\|N^{-1}, \\ \frac{C\Delta t}{\varepsilon} \mathcal{S}_j(\theta), & \text{for } N/2 < j \leq N-1. \end{cases}$$

Proof. Here, we have $\mathcal{S}_j(\theta) - \mathcal{S}_{j-1}(\theta) = \frac{\theta h_j}{\varepsilon}$. Firstly, we deduce that

$$\begin{aligned} \mathcal{L}_{N,mcd}^{n+1} \mathcal{S}_j(\theta) &\geq -\frac{2\theta h_j^2}{\varepsilon \tilde{h}_j} \mathcal{S}_{j-1}(\theta) + a_j^{n+1} \left[\frac{h_j}{\tilde{h}_j} \left(\frac{\theta}{\varepsilon} \mathcal{S}_j(\theta) \right) + \frac{h_{j+1}}{\tilde{h}_j} \left(\frac{\theta}{\varepsilon} \mathcal{S}_{j-1}(\theta) \right) \right] \\ &\geq \begin{cases} \frac{\theta}{\varepsilon + \theta h_j} \mathcal{S}_j(\theta) \left[a_j^{n+1} \frac{h_{j+1}}{\tilde{h}_j} - 2\theta \frac{h_j}{\tilde{h}_j} \right], & \text{for } j \neq N/2, \\ \frac{\theta h_j}{\varepsilon \tilde{h}_j} \mathcal{S}_j(\theta) \left[a_j^{n+1} - \frac{2\theta \varepsilon}{\varepsilon + \theta h_j} \right], & \text{for } j = N/2. \end{cases} \end{aligned} \quad (2.36)$$

and

$$\begin{aligned}
\mathcal{L}_{N,mup}^{n+1} \mathcal{S}_j(\theta) &\geq -\frac{2\theta h_j^2}{\varepsilon h_j} \mathcal{S}_{j-1}(\theta) + a_{j-1/2}^{n+1} \left[\frac{\theta}{\varepsilon} \mathcal{S}_{j-1}(\theta) \right] \\
&\geq \frac{\theta}{\varepsilon + \theta h_j} \mathcal{S}_j(\theta) \left[a_{j-1/2}^{n+1} - 2\theta \frac{h_j}{h_j} \right].
\end{aligned} \tag{2.37}$$

Next, from (2.12)-(2.13), we obtain that

$$\begin{aligned}
L_{N,hyb}^{\Delta t} \mathcal{S}_j(\theta) &= \mu_j^- \mathcal{S}_{j-1}(\theta) + \mu_j^c \mathcal{S}_j(\theta) + \mu_j^+ \mathcal{S}_{j+1}(\theta) \\
&= \begin{cases} \Delta t \mathcal{L}_{N,mcd}^{n+1} \mathcal{S}_j(\theta) + \mathcal{S}_j(\theta), & \text{for } 1 \leq j \leq N/2, \text{ and when } \varepsilon > \|a\| N^{-1} \\ \Delta t \mathcal{L}_{N,mup}^{n+1} \mathcal{S}_j(\theta) + \frac{1}{2} \left(1 + \frac{\varepsilon}{\varepsilon + \theta h_j} \right) \mathcal{S}_j(\theta), & \text{for } 1 \leq j \leq N/2, \text{ and when } \varepsilon \leq \|a\| N^{-1}, \\ \Delta t \mathcal{L}_{N,mcd}^{n+1} \mathcal{S}_j(\theta) + \mathcal{S}_j(\theta), & \text{for } N/2 < j \leq N-1. \end{cases}
\end{aligned} \tag{2.38}$$

We now split the proof into the following two cases.

Case 1: Let $1 \leq j \leq N/2$.

(i) When $\varepsilon > \|a\| N^{-1}$. From (2.36) and (2.38), we have

$$L_{N,hyb}^{\Delta t} \mathcal{S}_j(\theta) \geq \begin{cases} \Delta t \frac{\theta(\mathfrak{m}-\theta)}{\varepsilon + \theta H} \mathcal{S}_j(\theta), & \text{for } 1 \leq j < N/2, \\ \Delta t \frac{\theta(\mathfrak{m}-2\theta)}{2\varepsilon} \mathcal{S}_j(\theta), & \text{for } j = N/2. \end{cases}$$

Since $\varepsilon > \|a\| N^{-1}$ implies $\mathfrak{m}H/\varepsilon < 2$, utilizing the condition $\theta < \mathfrak{m}/2$ we obtain the desired result.

(ii) When $\varepsilon \leq \|a\| N^{-1}$. From (2.37) and (2.38), we have

$$L_{N,hyb}^{\Delta t} \mathcal{S}_j(\theta) \geq \begin{cases} \Delta t \frac{\theta(\mathfrak{m}-\theta)}{\varepsilon + \theta H} \mathcal{S}_j(\theta), & \text{for } 1 \leq j < N/2, \\ \Delta t \frac{\theta(\mathfrak{m}-2\theta)}{\varepsilon + \theta H} \mathcal{S}_j(\theta), & \text{for } j = N/2. \end{cases}$$

Since $\varepsilon \leq \|a\| N^{-1}$ implies $H/\varepsilon \leq 1/\|a\|$, we obtain the desired result utilizing the condition $\theta < \mathfrak{m}/2$.

Case 2: Let $N/2 < j \leq N-1$. From (2.36) and (2.38), we have

$$L_{N,hyb}^{\Delta t} \mathcal{S}_j(\theta) \geq \Delta t \frac{\theta(\mathfrak{m}-\theta)}{\varepsilon + \theta h} \mathcal{S}_j(\theta).$$

The desired result thus follows from the condition $\theta < \mathfrak{m}/2$ and from the inequality $\mathfrak{m}h/\varepsilon < 2$, which holds due to the assumption given in (2.21). Hence, this completes the proof. ■

Further, a straightforward calculation yields the results obtained in the following lemma.

Lemma 2.13. *Consider the following mesh function*

$$\varphi_j = \begin{cases} \frac{x_j}{1-\eta}, & \text{for } 0 \leq j < N/2, \\ 1, & \text{for } N/2 \leq j \leq N. \end{cases}$$

Then, the discrete derivatives of the function φ_j are given by

$$\delta_x^2 \varphi_j = \begin{cases} 0, & \text{for } 1 \leq j < N/2, \\ \frac{-2}{(h+H)(1-\eta)}, & \text{for } j = N/2, \\ 0, & \text{for } N/2 < j \leq N-1, \end{cases}$$

and

$$D^* \varphi_j = \begin{cases} \frac{1}{1-\eta}, & \text{for } 1 \leq j < N/2, \\ \frac{h}{(h+H)(1-\eta)}, & \text{for } j = N/2, \\ 0, & \text{for } N/2 < j \leq N-1, \end{cases}$$

and hence, we obtain that

$$\mathcal{L}_{N,mcd}^{n+1} \varphi_j \geq \begin{cases} \frac{a_j^{n+1}}{1-\eta}, & \text{for } 1 \leq j < N/2, \\ \frac{2\varepsilon N + a_j^{n+1} h N}{2(1-\eta)}, & \text{for } j = N/2, \\ 0, & \text{for } N/2 < j \leq N-1. \end{cases}$$

2.4.2.4 Local spatial error

Here, we estimate the error $|\tilde{y}_j^{n+1} - \tilde{Y}_j^{n+1}|$ in the outer region (*i.e.*, for $1 \leq j \leq N/2$) as well as in the boundary layer region (*i.e.*, for $N/2 < j < N$) separately related to the spatial discretization of the semidiscrete problem (2.15) by newly developed method (2.19).

Lemma 2.14. *Assume that $N \geq N_0$ satisfies conditions (2.21) and (2.22). Then, if $\theta < \mathfrak{m}/2$, the local error related to the spatial discretization of (2.15) satisfies the following estimate:*

$$|\tilde{y}_j^{n+1} - \tilde{Y}_j^{n+1}| \leq C \left((N^{-1} + \chi_\varepsilon) N^{-1} + N^{-\eta_0 \theta} \right), \quad \text{for } 1 \leq j \leq N/2, \quad (2.39)$$

where

$$\chi_\varepsilon = \begin{cases} \varepsilon, & \text{when } \varepsilon \leq \|a\| N^{-1}, \\ 0, & \text{when } \varepsilon > \|a\| N^{-1}. \end{cases}$$

Proof. We split up the proof into two cases.

(i) When $\varepsilon > \|a\|N^{-1}$. Consider the following discrete function

$$\Phi_j(\theta) = C \left[H^2 (1 + x_j) + H^2 \varphi_j + \mathcal{S}_j(\theta) \right], \quad \text{for } 0 \leq j \leq N,$$

where C is sufficiently large. Using the inequality (2.35) and Lemmas 2.12 and 2.13, we have

$$\mathbf{L}_{N,hyb}^{\Delta t} \Phi_j(\theta) \geq \begin{cases} C\Delta t \left[\mathfrak{m}H^2 + \frac{\mathfrak{m}H^2}{1-\eta} + \varepsilon^{-1} \exp(-\mathfrak{m}(1-x_j)/\varepsilon) \right], & \text{for } 1 \leq j < N/2, \\ C\Delta t \left[\mathfrak{m}H^2 + \frac{(2\varepsilon N + \mathfrak{m}hN)H^2}{2(1-\eta)} + \varepsilon^{-1} \exp(-\mathfrak{m}(1-x_j)/\varepsilon) \right], & \text{for } j = N/2, \\ C\Delta t \left[\mathfrak{m}H^2 + \varepsilon^{-1} \exp(-\mathfrak{m}(1-x_j)/\varepsilon) \right], & \text{for } N/2 < j \leq N-1. \end{cases}$$

Then, using Lemma 2.10, we obtain that

$$\mathbf{L}_{N,hyb}^{\Delta t} \Phi_j(\theta) \geq |\mathcal{T}_{j,\tilde{y}^{n+1}}^{N,\Delta t}|, \quad \text{for } 1 \leq j \leq N-1.$$

Thus, by employing the discrete maximum principle to $\Phi_j(\theta) \pm (\tilde{y}_j^{n+1} - \tilde{Y}_j^{n+1})$, over $\bar{\Omega}^N \cap [0, 1]$, we have

$$|\tilde{y}_j^{n+1} - \tilde{Y}_j^{n+1}| \leq \Phi_j(\theta), \quad \text{for } 1 \leq j \leq N-1.$$

Therefore, for $1 \leq j \leq N/2$,

$$|\tilde{y}_j^{n+1} - \tilde{Y}_j^{n+1}| \leq C \left[H^2 + \mathcal{S}_{N/2}(\theta) \right].$$

Now, using $H \leq 2N^{-1}$ and invoking the inequality (2.35), finally we get

$$|\tilde{y}_j^{n+1} - \tilde{Y}_j^{n+1}| \leq C \left(N^{-2} + N^{-\eta_0 \theta} \right), \quad \text{for } 1 \leq j \leq N/2.$$

(ii) When $\varepsilon \leq \|a\|N^{-1}$. Consider the following discrete function

$$\Psi_j(\theta) = \begin{cases} C \left[(\varepsilon + H)H (1 + x_j) + \mathcal{S}_{j+1}(\theta) \right], & \text{for } 0 \leq j \leq N/2, \\ C \left[(\varepsilon + H)H (1 + x_j) + \left(1 + \frac{\theta h}{\varepsilon} \right) \mathcal{S}_j(\theta) \right], & \text{for } N/2 < j \leq N, \end{cases}$$

where C is chosen sufficiently large. Using the inequality (2.35) and Lemma 2.12, we have

$$\mathbf{L}_{N,hyb}^{\Delta t} \Psi_j(\theta) \geq \begin{cases} C\Delta t \left[\mathfrak{m}(\varepsilon + H)H + H^{-1} \exp(-\mathfrak{m}(1-x_{j+1})/\varepsilon) \right], & \text{for } 1 \leq j < N/2, \\ C\Delta t \left[\mathfrak{m}(\varepsilon + H)H + \varepsilon^{-1} \exp(-\mathfrak{m}(1-x_{j+1})/\varepsilon) \right], & \text{for } j = N/2, \\ C\Delta t \left[\mathfrak{m}H^2 + \frac{\theta h}{\varepsilon^2} \exp(-\mathfrak{m}(1-x_j)/\varepsilon) \right], & \text{for } N/2 < j \leq N-1. \end{cases}$$

Afterwards, Lemma 2.10 implies that

$$\mathbf{L}_{N,hyb}^{\Delta t} \Psi_j(\theta) \geq |\mathcal{T}_{j,\tilde{y}^{n+1}}^{N,\Delta t}|, \quad \text{for } 1 \leq j \leq N-1,$$

since the assumption given in (2.21) yields $\mathfrak{m}h/\varepsilon < 2$. Thus, by employing the discrete maximum principle to $\Psi_j(\theta) \pm (\tilde{y}_j^{n+1} - \tilde{Y}_j^{n+1})$, over $\bar{\Omega}^N \cap [0, 1]$, we have

$$|\tilde{y}_j^{n+1} - \tilde{Y}_j^{n+1}| \leq \Psi_j(\theta), \quad \text{for } 1 \leq j \leq N-1.$$

Therefore, for $1 \leq j \leq N/2$, it implies that

$$|\tilde{y}_j^{n+1} - \tilde{Y}_j^{n+1}| \leq C \left[\varepsilon H + H^2 + \left(1 + \frac{\theta h}{\varepsilon}\right) \mathcal{S}_{N/2}(\theta) \right],$$

and we finally obtain the desired result using $H \leq 2N^{-1}$, (2.34) and the inequality $\mathfrak{m}h/\varepsilon < 2$. \blacksquare

Corollary 2.1. *It is straightforward from Lemma 2.14 that the estimate in (2.39) reduces to the following form:*

$$|\tilde{y}_j^{n+1} - \tilde{Y}_j^{n+1}| \leq C \left(N^{-2} + N^{-\eta_0 \theta} \right), \quad \text{for } 1 \leq j \leq N/2, \quad (2.40)$$

when $\varepsilon > \|a\|N^{-1}$ and (2.40) also holds if we select $\varepsilon \leq \|a\|N^{-1}$.

Lemma 2.15. *Assume that $N \geq N_0$ satisfies conditions (2.21) and (2.22). Then, if $\theta < \mathfrak{m}/2$, the local error related to the spatial discretization of (2.15) satisfies the following estimate:*

$$|\tilde{y}_j^{n+1} - \tilde{Y}_j^{n+1}| \leq C \left(\eta_0^2 N^{-2} \ln^2 N + N^{-\eta_0 \theta} \right), \quad \text{for } N/2 < j \leq N-1. \quad (2.41)$$

Proof: Consider the following discrete function

$$\Upsilon_j(\theta) = C \left[(N^{-2} + N^{-\eta_0 \theta}) (1 + x_j) + h^2 \varepsilon^{-2} \mathcal{S}_j(\theta) \right], \quad \text{for } N/2 \leq j \leq N,$$

where C is chosen sufficiently large. Then, it is clear that $|\tilde{y}_N^{n+1} - \tilde{Y}_N^{n+1}| \leq \Upsilon_N(\theta)$ and also from (2.40), we have $|\tilde{y}_{N/2}^{n+1} - \tilde{Y}_{N/2}^{n+1}| \leq \Upsilon_{N/2}(\theta)$. Further, using the inequality (2.34) and Lemma 2.12, we have

$$\begin{aligned} L_{N,hyb}^{\Delta t} \Upsilon_j(\theta) &\geq C \Delta t \left[(N^{-2} + N^{-\eta_0 \theta}) + h^2 \varepsilon^{-3} \mathcal{S}_j(\theta) \right], \\ &\geq C \Delta t \left[(N^{-2} + N^{-\eta_0 \theta}) + h^2 \varepsilon^{-3} \exp(-\mathfrak{m}(1 - x_j)/\varepsilon) \right]. \end{aligned}$$

Hence, it follows from Lemma 2.10 that

$$L_{N,hyb}^{\Delta t} \Upsilon_j(\theta) \geq |\mathcal{T}_{j,\tilde{y}^{n+1}}^{N,\Delta t}|, \quad \text{for } N/2 + 1 \leq j \leq N-1$$

Therefore, using $h = 2\eta_0 \varepsilon N^{-1} \ln N$ and by employing the discrete maximum principle to $\Psi_j(\theta) \pm (\tilde{y}_j^{n+1} - \tilde{Y}_j^{n+1})$, over $\bar{\Omega}^N \cap [1 - \eta, 1]$, we get

$$|\tilde{y}_j^{n+1} - \tilde{Y}_j^{n+1}| \leq \Upsilon_j(\theta) \leq C \left(\eta_0^2 N^{-2} \ln^2 N + N^{-\eta_0 \theta} \right),$$

for $N/2 < j \leq N-1$. \blacksquare

Theorem 2.2. *Assume that $N \geq N_0$ satisfies conditions (2.21) and (2.22). Then, if $\theta < \mathfrak{m}/2$ and $\eta_0 \geq 2/\theta$, the*

local error related to the spatial discretization of (2.15) satisfies the following estimate:

$$|\tilde{y}_j^{n+1} - \tilde{Y}_j^{n+1}| \leq \begin{cases} CN^{-2}, & \text{for } 1 \leq j \leq N/2, \\ CN^{-2} \ln^2 N, & \text{for } N/2 < j \leq N-1. \end{cases} \quad (2.42)$$

Proof: The proof follows from (2.40) and (2.41). ■

2.4.3 Error related to the fully discrete scheme

We define $E^{n+1}(x_j) = [y(x_j, t_{n+1}) - Y_j^{n+1}]$, for $0 \leq j \leq N$, as the global error related to the fully discrete scheme (2.11) at the time level t_{n+1} . Now, to show the ε -uniform convergence of the fully discrete scheme (2.11), we rewrite the global error in the following form:

$$E^{n+1}(x_j) = \tilde{e}^{n+1}(x_j) + \tilde{E}^{n+1}(x_j) + [\tilde{Y}_j^{n+1} - Y_j^{n+1}]. \quad (2.43)$$

Here, $\tilde{e}^{n+1}(x_j) = [y(x_j, t_{n+1}) - \tilde{y}^{n+1}(x_j)]$ and $\tilde{E}^{n+1}(x_j) = [\tilde{y}^{n+1}(x_j) - \tilde{Y}_j^{n+1}]$, respectively, denote the local error related to the time semidiscretization of the IBVP (2.1)-(2.2) and the spatial discretization of the auxiliary BVP (2.15) at time level t_{n+1} . Now, consider the fully discrete scheme after one step by taking $Y^n = E^n$ and the source term $g = 0$. Then, the term $[\tilde{Y}^{n+1} - Y^{n+1}]$ can be written as the solution of the following systems:

$$\begin{cases} L_{N,hyb}^{\Delta t} R_j^{n+1} = y(x_j, t_n) - Y_j^n, & 1 \leq j \leq N-1, \\ R_0^{n+1} = R_N^{n+1} = 0, \end{cases}$$

where $R_j^{n+1} = [\tilde{Y}_j^{n+1} - Y_j^{n+1}]$, and by employing the discrete maximum principle for the operator $L_{N,hyb}^{\Delta t}$, one can obtain that

$$\left\| \{\tilde{Y}_j^{n+1}\}_j - \{Y_j^{n+1}\}_j \right\| \leq \left\| \{y(x_j, t_n)\}_j - \{Y_j^n\}_j \right\|. \quad (2.44)$$

Afterwards, from (2.43) and (2.44), we obtain that

$$\left\| \{E^{n+1}(x_j)\}_j \right\| \leq \left\| \{\tilde{e}^{n+1}(x_j)\}_j \right\| + \left\| \{\tilde{E}^{n+1}(x_j)\}_j \right\| + \left\| \{E^n(x_j)\}_j \right\|, \quad \text{for } 1 \leq j \leq N-1. \quad (2.45)$$

Now, by invoking the estimates obtained in (2.16) and (2.42) in (2.45), with the assumption that $N^{-\delta} \leq C\Delta t$, $0 < \delta < 1$, we have

$$\left\| \{E^{n+1}(x_j)\}_j \right\| \leq \begin{cases} C(\Delta t N^{-2+\delta} + \Delta t^2) + \left\| \{E^n(x_j)\}_j \right\|, & \text{for } 1 \leq j \leq N/2, \\ C(\Delta t N^{-2+\delta} \ln^2 N + \Delta t^2) + \left\| \{E^n(x_j)\}_j \right\|, & \text{for } N/2 < j \leq N-1. \end{cases}$$

Hence, we obtain the required estimate of the global error in (2.46), which is stated in the following theorem as the main convergence result of this chapter.

Theorem 2.3 (Global error). *Assume that $N \geq N_0$ satisfies conditions (2.21) and (2.22). Then, if $\theta < m/2$ and $\eta_0 \geq 2/\theta$, the global error related to the fully discrete scheme (2.11) at the time level t_{n+1} satisfies the*

following estimate:

$$\left\| \{y(x_j, t_{n+1})\}_j - \{Y_j^{n+1}\}_j \right\| \leq \begin{cases} C(N^{-2+\delta} + \Delta t), & \text{for } 1 \leq j \leq N/2, \\ C(N^{-2+\delta} \ln^2 N + \Delta t), & \text{for } N/2 < j \leq N-1, \end{cases} \quad (2.46)$$

where N and Δt are such that $N^{-\delta} \leq C\Delta t$, $0 < \delta < 1$.

Remark 2.2. We would like point out that the error estimate (2.46) holds true for the existing hybrid scheme proposed in [81] under the restrictive condition $\varepsilon < CN^{-1}$ and we demonstrate this phenomenon in Section 2.7. Besides this, it is shown in Section 2.7 that the existing scheme converges with at least first-order accuracy in the spatial variable both outside and inside the boundary layer when $\varepsilon \gg N^{-1}$; and this observation is contrary to the computational results of the newly developed method. As consequence of this, one can see in Section 2.7 that the existing scheme after using the temporal Richardson extrapolation converges ε -uniformly with first-order global accuracy as N increases; whereas the ε -uniform global accuracy of the proposed method combined with the temporal extrapolation is of almost order two. A theoretical justification for the accuracy of the proposed method related to the temporal Richardson extrapolation is given in Section 2.5.

2.5 Error related to temporal Richardson extrapolation

On the domain $[0, T]$, we construct a fine mesh, denoted by $\Lambda^{\Delta t/2} = \{\tilde{t}_n\}_{n=0}^{2M}$, by bisecting each mesh interval of $\Lambda^{\Delta t}$. So, $\tilde{t}_{n+1} - \tilde{t}_n = T/2M = \Delta t/2$ is the step-size. Let $Y^{N, \Delta t}(x_j, t_{n+1})$ and $Z^{N, \Delta t}(x_j, \tilde{t}_{n+1})$ be the respective solutions of the fully discrete problem (2.10) on the mesh $\bar{\Omega}^N \times \Lambda^{\Delta t}$ and $\bar{\Omega}^N \times \Lambda^{\Delta t/2}$. Then, as consequence of Theorem 2.3, the global error can be expressed as

$$y(x_j, t_{n+1}) - Y^{N, \Delta t}(x_j, t_{n+1}) = C_1(\Delta t) + C_2(N^{-2+\delta} \ln^2 N) + o(\Delta t) + o(N^{-2+\delta} \ln^2 N), \quad (x_j, t_{n+1}) \in \bar{\Omega}^N \times \Lambda^{\Delta t}, \quad (2.47)$$

where C_1 and C_2 are fixed arbitrary constants. Similarly, we have

$$y(x_j, \tilde{t}_{n+1}) - Z^{N, \Delta t}(x_j, \tilde{t}_{n+1}) = C_1(\Delta t/2) + C_2(N^{-2+\delta} \ln^2 N) + o(\Delta t) + o(N^{-2+\delta} \ln^2 N), \quad (x_j, \tilde{t}_{n+1}) \in \bar{\Omega}^N \times \Lambda^{\Delta t/2}. \quad (2.48)$$

Now, from (2.47) and (2.48), we have

$$\begin{aligned} y(x_j, t_{n+1}) - \left(2Z^{N, \Delta t}(x_j, t_{n+1}) - Y^{N, \Delta t}(x_j, t_{n+1}) \right) &= o(\Delta t) + O(N^{-2+\delta} \ln^2 N) \\ &= O(\Delta t^k) + O(N^{-2+\delta} \ln^2 N), \\ &\quad (x_j, t_{n+1}) \in \bar{\Omega}^N \times \Lambda^{\Delta t}, \quad \text{for some } k > 1. \end{aligned} \quad (2.49)$$

Remark 2.3. We set $\left(2Z^{N, \Delta t}(x_j, t_{n+1}) - Y^{N, \Delta t}(x_j, t_{n+1}) \right)$ as the temporal extrapolation formula so that the temporal accuracy can be improved from $O(\Delta t)$ to $O(\Delta t^k)$, $k > 1$. However, it is clear from (2.49) that the spatial accuracy due to the temporal extrapolation remains unaltered and is of $O(N^{-2+\delta} \ln^2 N)$.

Now, let $y^{\Delta t}(x, t_{n+1})$ and $z^{\Delta t}(x, \tilde{t}_{n+1})$ be the respective solutions of the time-semidiscrete problem (2.9)

on the mesh $\bar{\Omega} \times \Lambda^{\Delta t}$ and $\bar{\Omega} \times \Lambda^{\Delta t/2}$, such that $y^{\Delta t}(x_j, t_{n+1}) \approx Y^{N, \Delta t}(x_j, t_{n+1})$ and $z^{\Delta t}(x_j, \tilde{t}_{n+1}) \approx Z^{N, \Delta t}(x_j, \tilde{t}_{n+1})$, $x_j \in \bar{\Omega}^N$, and it follows that

$$\left(2z^{\Delta t}(x_j, t_{n+1}) - y^{\Delta t}(x_j, t_{n+1})\right) \approx \left(2Z^{N, \Delta t}(x_j, t_{n+1}) - Y^{N, \Delta t}(x_j, t_{n+1})\right). \quad (2.50)$$

Again, utilizing Theorem 2.1, one can have

$$y(x_j, t_{n+1}) - \left(2z^{\Delta t}(x_j, t_{n+1}) - y^{\Delta t}(x_j, t_{n+1})\right) = O(\Delta t^k), \quad k > 1, \quad (x_j, t_{n+1}) \in \bar{\Omega}^N \times \Lambda^{\Delta t}, \quad (2.51)$$

Thus, (2.51) implies that the term $O(\Delta t^k)$ appeared in (2.49) is due to the time-semidiscrete approximation. Therefore, by analyzing the global error related to the temporal extrapolation of the solution to the time-semidiscrete problem (2.9), one can determine the temporal order of accuracy due to the extrapolation, *i.e.*, the exact value of k . Henceforth, we define the temporal extrapolation formula associated with the time-semidiscrete problem by

$$y_{exp}^{\Delta t}(x, t_{n+1}) = \left(2z^{\Delta t}(x, t_{n+1}) - y^{\Delta t}(x, t_{n+1})\right), \quad (x, t_{n+1}) \in \bar{\Omega} \times \Lambda^{\Delta t}. \quad (2.52)$$

The following expression gives the local truncation error related to the operator $(I + \Delta t \mathcal{L}_{x, \varepsilon}^{n+1})$:

$$\begin{aligned} (I + \Delta t \mathcal{L}_{x, \varepsilon}^{n+1})(y^{\Delta t}(x, t_{n+1}) - y(x, t_{n+1})) &= \left[y^{\Delta t}(x, t_n) - y(x, t_n)\right] + \\ &\quad \frac{(\Delta t)^2}{2} \frac{\partial^2 y(x, t_{n+1})}{\partial t^2} + O(\Delta t^3). \end{aligned} \quad (2.53)$$

Then, by following the approach in [60], we define a function $\phi(x, t)$ as the solution of the IBVP:

$$\begin{cases} \frac{\partial \phi(x, t)}{\partial t} + \mathcal{L}_{x, \varepsilon} \phi(x, t) = \frac{1}{2} \frac{\partial^2 y(x, t)}{\partial t^2}, & \text{in } \mathfrak{D}, \\ \phi(x, 0) = 0, & \text{on } \bar{\Omega}, \\ \phi(0, t) = \phi(1, t) = 0, & t \in (0, T], \end{cases} \quad (2.54)$$

where the coefficients associated with the operator $\mathcal{L}_{x, \varepsilon}$ satisfy the conditions given in (2.2). Since Lemma 2.3 implies that $\left\| \frac{\partial^2 y}{\partial t^2} \right\|_{\bar{\mathfrak{D}}} \leq C$, letting $g = \frac{\partial^2 y}{\partial t^2}$ in Lemma 2.2, one can derive the following ε -uniform stability result.

Lemma 2.16. *The solution $\phi(x, t)$ of the IBVP (2.54) satisfies that $\|\phi\|_{\bar{\mathfrak{D}}} \leq C$.*

Lemma 2.17. *The derivatives of the solution $\phi(x, t)$ of the IBVP (2.54) satisfies the bounds*

$$\left| \frac{\partial^{j+k} \phi(x, t)}{\partial x^j \partial t^k} \right| \leq C \varepsilon^{-j}, \quad (x, t) \in \bar{\mathfrak{D}},$$

$\forall j, k \in \mathbb{N} \cup \{0\}$ satisfying $0 \leq j + 2k \leq 4$.

Proof: By changing the independent variable x to the new variable $\tilde{x} = \frac{1-x}{\varepsilon}$ and letting $\tilde{\phi}(\tilde{x}, t) = \phi(x, t)$

with similar definitions of \tilde{a}, \tilde{b} and \tilde{y} ; the IBVP (2.54) is transformed to the following form:

$$\begin{cases} -\frac{\partial^2 \tilde{\Phi}}{\partial \tilde{x}^2} - \tilde{a} \frac{\partial \tilde{\Phi}}{\partial \tilde{x}} + \tilde{\varepsilon} \tilde{b} \tilde{\Phi} - \varepsilon \frac{\partial \tilde{\Phi}}{\partial t} = \frac{\varepsilon}{2} \frac{\partial^2 \tilde{y}}{\partial t^2}, & \text{in } \tilde{\mathcal{D}}, \\ \tilde{\Phi}(\tilde{x}, t) = 0, & \text{on } \partial \tilde{\mathcal{D}}, \end{cases}$$

where $\tilde{\mathcal{D}} = (0, \frac{1}{\varepsilon}) \times (0, T]$ and $\partial \tilde{\mathcal{D}} = \tilde{\mathcal{D}} \setminus \tilde{\mathcal{D}}$. For each $(\tilde{x}, t) \in \tilde{\mathcal{D}}$, the rectangle $R_{\tilde{x}, \delta} := (\tilde{x} - \delta, \tilde{x} + \delta) \times (0, T)$, for $\delta > 0$ is denoted as a neighbourhood of (\tilde{x}, t) such that $R_{\tilde{x}, \delta} \subset R_{\tilde{x}, 2\delta} \subset \tilde{\mathcal{D}}$. Then, by applying the result (10.5) from [65, p. 352], one can obtain that

$$\left\| \frac{\partial^{j+k} \tilde{\Phi}}{\partial \tilde{x}^j \partial t^k} \right\|_{R_{\tilde{x}, \delta}} \leq C \left[\left\| \frac{\partial^2 \tilde{y}}{\partial t^2} \right\|_{R_{\tilde{x}, 2\delta}} + \left\| \tilde{\Phi} \right\|_{R_{\tilde{x}, 2\delta}} \right], \quad \text{for } 0 \leq j + 2k \leq 4, \quad (2.55)$$

where the constant C independent of $R_{\tilde{x}, \delta}$. Hence, for each $(\tilde{x}, t) \in \tilde{\mathcal{D}}$, we apply Lemmas 2.3 and 2.16 in (2.55) to obtain that

$$\left| \frac{\partial^{j+k} \tilde{\Phi}(\tilde{x}, t)}{\partial \tilde{x}^j \partial t^k} \right| \leq C, \quad \text{for } 0 \leq j + 2k \leq 4.$$

Thus, by changing the variable \tilde{x} to the original variable x , we get the desired result. ■

Remark 2.4. In order to derive the bounds of the derivatives up to fourth-order in space and second-order in time in Lemma 2.17, we require the function $\phi \in \mathcal{C}^{4+\gamma}(\overline{\mathcal{D}})$, which is ensured by the assumption that the function $g = \frac{1}{2} \frac{\partial^2 y}{\partial t^2}$ must satisfy the compatibility conditions given in (2.6) at the corner points $(0, 0)$ and $(1, 0)$. Therefore, we require the solution $y \in \mathcal{C}^{6+\gamma}(\overline{\mathcal{D}})$, which can be guaranteed by assuming sufficient smoothness on the data associated with the IBVP (2.1)-(2.2) and the necessary compatibility conditions together with the conditions in (2.3)-(2.5) at the corner points $(0, 0)$ and $(1, 0)$ (See [[65], Chapter IV, §5]).

Remark 2.5. Note that in order to derive the expression of the local truncation error in (2.53), it is required that $\left\| \frac{\partial^3 y}{\partial t^3} \right\|_{\overline{\mathcal{D}}} \leq C$, which can be derived by applying the technique on the IBVP (2.1)-(2.2) as given in the proof of Lemma 2.17.

Again, utilizing (2.54), we obtain that

$$\begin{aligned} (I + \Delta t \mathcal{L}_{x, \varepsilon}^{n+1}) \phi(x, t_{n+1}) &= \phi(x, t_n) + \Delta t \left(\frac{\partial}{\partial t} + \mathcal{L}_{x, \varepsilon}^{n+1} \right) \phi(x, t_{n+1}) - \\ &\quad \frac{(\Delta t)^2}{2} \frac{\partial^2 \phi(x, s)}{\partial t^2}, \quad t_n < s < t_{n+1}, \\ &= \phi(x, t_n) + \frac{\Delta t}{2} \frac{\partial^2 y(x, t_{n+1})}{\partial t^2} + O(\Delta t^2). \end{aligned} \quad (2.56)$$

Therefore, (2.53) and (2.56) imply that the semidiscrete solution of problem (2.9) on the mesh $\bar{\Omega} \times \Lambda^{\Delta t}$ can be written as follows:

$$y^{\Delta t}(x, t_{n+1}) = y(x, t_{n+1}) + \Delta t \phi(x, t_{n+1}) + \mathcal{R}(x, t_{n+1}), \quad (2.57)$$

where $\mathcal{R}(x, t_{n+1})$ satisfies the following relation:

$$(I + \Delta t \mathcal{L}_{x, \varepsilon}^{n+1}) \mathcal{R}(x, t_{n+1}) = \mathcal{R}(x, t_n) + O(\Delta t^3). \quad (2.58)$$

Since, $\mathcal{R}(0, t_{n+1}) = \mathcal{R}(1, t_{n+1}) = 0$, by using Lemma 2.5 on $\mathcal{R}(x, t_{n+1})$, we have

$$\|\mathcal{R}(t_{n+1})\| \leq C\|\mathcal{R}(t_n)\| + O(\Delta t)^3. \quad (2.59)$$

Finally, using the relation in (2.59) recursively, we obtain from (2.57) that

$$y(x, t_{n+1}) = y^{\Delta t}(x, t_{n+1}) + \Delta t \phi(x, t_{n+1}) + O(\Delta t^2), \quad (x, t_{n+1}) \in \bar{\Omega} \times \Lambda^{\Delta t}. \quad (2.60)$$

Similarly, we have

$$y(x, \tilde{t}_{n+1}) = z^{\Delta t}(x, \tilde{t}_{n+1}) + \frac{\Delta t}{2} \Phi(x, \tilde{t}_{n+1}) + O(\Delta t^2), \quad (x, \tilde{t}_{n+1}) \in \bar{\Omega} \times \Lambda^{\Delta t/2}. \quad (2.61)$$

Thus, by using the extrapolation formula in (2.52), and the expressions in (2.60) and (2.61), we have

$$\begin{aligned} \left(y(x, t_{n+1}) - y_{exp}^{\Delta t}(x, t_{n+1}) \right) &= 2 \left(y(x, t_{n+1}) - z^{\Delta t}(x, t_{n+1}) \right) - \\ &\quad \left(y(x, t_{n+1}) - y^{\Delta t}(x, t_{n+1}) \right) \\ &= O(\Delta t)^2, \quad (x, t_{n+1}) \in \bar{\Omega} \times \Lambda^{\Delta t}. \end{aligned} \quad (2.62)$$

Therefore, the above analysis shows that the global temporal error due to the temporal extrapolation is uniformly convergent of second-order in time.

2.6 Singularly perturbed semilinear parabolic problem

Here, we discuss about the numerical solution of the following class of singularly perturbed semi-linear parabolic IBVPs:

$$\begin{cases} \frac{\partial y}{\partial t} - \varepsilon \frac{\partial^2 y}{\partial x^2} + a(x, t) \frac{\partial y}{\partial x} = g(x, t, y), & (x, t) \in \mathfrak{D}, \\ y(x, 0) = q_0(x), & x \in \bar{\Omega}, \\ y(0, t) = s_l(t), \quad y(1, t) = s_r(t), & t \in [0, T], \end{cases} \quad (2.63)$$

where $\varepsilon \in (0, 1]$. The convection coefficient $a(x, t)$ is smooth enough and satisfy the conditions given in (2.2). The nonlinear term $g(x, t, y)$ satisfies that

$$\mathbb{k}_1 \leq \frac{\partial g(x, t, y)}{\partial y} \leq \mathbb{k}_2, \quad \text{for } (x, t, y) \in \mathfrak{D} \times \mathbb{R}; \quad \mathbb{k}_1, \mathbb{k}_2 > 0.$$

Further, adequate smoothness on the data q_0 , s_l and s_r ; and the necessary compatibility conditions ensures that the IBVP (2.63) has a unique solution (see [65] for further details). Now, we describe the Newton's linearization technique which generates the sequence $\{y^k\}_{k=0}^{\infty}$ with the initial guess y^0 satisfying the initial and boundary

conditions of the IBVP (2.63); and y^{k+1} , for all $k \geq 0$, is the solution of the following linear IBVP:

$$\begin{cases} \frac{\partial y^{k+1}}{\partial t} - \varepsilon \frac{\partial^2 y^{k+1}}{\partial x^2} + a(x, t) \frac{\partial y^{k+1}}{\partial x} - b^k(x, t) y^{k+1} = \mathcal{G}^k(x, t), & (x, t) \in \mathfrak{D}, \\ y^{k+1}(x, 0) = q_0(x), & x \in \bar{\Omega}, \\ y^{k+1}(0, t) = s_l(t), \quad y^{k+1}(1, t) = s_r(t), & t \in [0, T], \end{cases} \quad (2.64)$$

where $b^k(x, t)$ and $\mathcal{G}^k(x, t)$ are given by

$$\begin{cases} b^k(x, t) = \frac{\partial g}{\partial y}(x, t, y^k), \\ \mathcal{G}^k(x, t) = g(x, t, y^k) - b^k(x, t) y^k. \end{cases}$$

Next, for each iteration k , we compute the numerical solution of the IBVP (2.64) by using the newly developed numerical method and apply the following condition as the stopping criterion:

$$\max_{0 \leq j \leq N, n=M} |Y^{k+1}(x_j, t_n) - Y^k(x_j, t_n)| \leq \text{TOL}, \quad (2.65)$$

where $Y^k(x_j, t_n)$ is the numerical solution at the mesh point $(x_j, t_n) \in \overline{\mathfrak{D}}^{N, \Delta t}$ and where TOL is the specified error constant. For further details, the book [29] can be referred. In the subsequent section, we present the numerical results for the semi-linear parabolic IBVP (2.63).

2.7 Numerical experiments

Here, numerous numerical results are presented to validate the theoretical findings and also to demonstrate the computational efficiency of the newly proposed numerical method. Moreover, those computational results are compared with the hybrid scheme developed in [81]. We set $\eta_0 = 4.2$, for all the experiments.

2.7.1 Test examples

Example 2.1. The first test problem is considered as the parabolic IBVP of the form:

$$\begin{cases} \frac{\partial y}{\partial t} - \varepsilon \frac{\partial^2 y}{\partial x^2} + (1 + x(1 - x)) \frac{\partial y}{\partial x} = g(x, t), & (x, t) \in (0, 1) \times (0, 1], \\ y(x, 0) = q_0(x), & x \in [0, 1], \\ y(0, t) = 0, \quad y(1, t) = 0, & t \in (0, 1], \end{cases}$$

where $g(x, t)$ and $q_0(x)$ are to be selected to fit with the exact solution given by

$$y(x, t) = \exp(-t)((1 - \exp(-(1 - x)/\varepsilon))/(1 - \exp(-1/\varepsilon)) - \cos(\pi/2x)).$$

For each ε , the maximum point-wise errors $e_\varepsilon^{N, \Delta t}$ corresponding to the proposed numerical method without and with extrapolation are respectively calculated by

$$\max_{0 \leq j \leq N, n=M} |y(x_j, t_n) - Y^{N, \Delta t}(x_j, t_n)|,$$

and

$$\max_{0 \leq j \leq N, n=M} |y(x_j, t_n) - Y_{extp}^{N, \Delta t}(x_j, t_n)|.$$

Here, $Y^{N, \Delta t}(x_j, t_n)$ and $Y_{extp}^{N, \Delta t}(x_j, t_n)$ are respectively the numerical solution and the extrapolated solution obtained at the mesh point $(x_j, t_n) \in \overline{\mathfrak{D}}^{N, \Delta t}$. From these errors, the corresponding order of convergence is computed by $r_\varepsilon^{N, \Delta t} = \log_2 \left(\frac{e_\varepsilon^{N, \Delta t}}{e_\varepsilon^{2N, \Delta t/2}} \right)$. Afterwards, for each N and Δt , the ε -uniform maximum point-wise error and the corresponding order of convergence, are respectively calculated by

$$e^{N, \Delta t} = \max_\varepsilon e_\varepsilon^{N, \Delta t} \quad \text{and} \quad r^{N, \Delta t} = \log_2 \left(\frac{e^{N, \Delta t}}{e^{2N, \Delta t/2}} \right).$$

Example 2.2. The second test problem is considered as the parabolic IBVP of the form:

$$\begin{cases} \frac{\partial y}{\partial t} - \varepsilon \frac{\partial^2 y}{\partial x^2} + (1 + xt - x^2 t^2) \frac{\partial y}{\partial x} + (1 + xt)y = 10t^2 x(1 - x), & (x, t) \in (0, 1) \times (0, 1], \\ y(x, 0) = 0, & x \in [0, 1], \\ y(0, t) = 0, \quad y(1, t) = 0, & t \in (0, 1], \end{cases}$$

The following technique is used for exhibiting the ε -uniform convergence and the accuracy of the proposed method as we are not acquainted with the exact solution of Example 2.2. We denote $\widehat{Y}^{2N, \Delta t/2}(x_j, t_n)$ and $\widehat{Y}_{extp}^{2N, \Delta t/2}(x_j, t_n)$ respectively, as the numerical solution and the extrapolated solution obtained at the mesh point $(x_j, t_n) \in \widehat{\mathfrak{D}}^{2N, \Delta t/2} = \widehat{\Omega}^{2N} \times \Lambda^{\Delta t/2}$, with $\Delta t/2 = T/2M$. Here, similar to the mesh $\overline{\Omega}^N$, we construct a piecewise-uniform Shishkin mesh $\widehat{\Omega}^N$ with the transition parameter $\widehat{\eta}$ given by

$$\widehat{\eta} = \min \left\{ \frac{1}{2}, \eta_0 \varepsilon \ln \left(\frac{N}{2} \right) \right\},$$

such that for $j = 0, 1, \dots, N$, the j^{th} point of $\overline{\Omega}^N$ becomes $2j^{\text{th}}$ point of $\widehat{\Omega}^{2N}$. For each ε , we calculate the maximum point-wise errors $\widehat{e}_\varepsilon^{N, \Delta t}$ corresponding to the proposed numerical method without and with extrapolation, respectively by

$$\max_{0 \leq j \leq N, n=M} |Y^{N, \Delta t}(x_j, t_n) - \widehat{Y}^{2N, \Delta t/2}(x_j, t_n)|,$$

and

$$\max_{0 \leq j \leq N, n=M} |Y_{extp}^{N, \Delta t}(x_j, t_n) - \widehat{Y}_{extp}^{2N, \Delta t/2}(x_j, t_n)|.$$

Then, one can compute the corresponding order of convergence by $\widehat{r}_\varepsilon^{N, \Delta t} = \log_2 \left(\frac{\widehat{e}_\varepsilon^{N, \Delta t}}{\widehat{e}_\varepsilon^{2N, \Delta t/2}} \right)$. Finally, for each N and Δt , we compute the quantities $\widehat{e}^{N, \Delta t}$ and $\widehat{r}^{N, \Delta t}$ analogously to $e^{N, \Delta t}$ and $r^{N, \Delta t}$.

Example 2.3. The third test problem is considered as the semi-linear parabolic IBVP of the form:

$$\begin{cases} \frac{\partial y}{\partial t} - \varepsilon \frac{\partial^2 y}{\partial x^2} + (1 + xt - x^2 t^2) \frac{\partial y}{\partial x} + \exp(y)y = g(x, t), & (x, t) \in (0, 1) \times (0, 1], \\ y(x, 0) = q_0(x), & x \in [0, 1], \\ y(0, t) = 0, \quad y(1, t) = 0, & t \in [0, 1], \end{cases}$$

where $g(x, t)$ and $q_0(x)$ are to be selected to fit with the exact solution as given in Example 2.1.

Now, we apply the linearization technique discussed in Section 2.6 for Example 2.3 and solve the following linear IBVP of the form (2.64) numerically for each iteration k :

$$\begin{cases} \frac{\partial y^{k+1}}{\partial t} - \varepsilon \frac{\partial^2 y^{k+1}}{\partial x^2} + (1 + xt - x^2 t^2) \frac{\partial y^{k+1}}{\partial x} + \exp(y^k)(1 + y^k)y^{k+1} = \\ g(x, t) - \exp(y^k)(1 + y^k)(1 - y^k), & (x, t) \in (0, 1) \times (0, 1], \\ y^{k+1}(x, 0) = q_0(x), & x \in [0, 1], \\ y^{k+1}(0, t) = 0, \quad y^{k+1}(1, t) = 0, & t \in [0, 1]. \end{cases}$$

We use (2.65) as the stopping criterion with $\text{TOL} = 10^{-10}$. Here, for each ε , we calculate the maximum point-wise errors $e_\varepsilon^{N, \Delta t}$ corresponding to the proposed numerical method without and with extrapolation; and the corresponding order of convergence $r_\varepsilon^{N, \Delta t}$ by using the definitions given in Example 2.1; and also compute the quantities $e^{N, \Delta t}$ and $r^{N, \Delta t}$, for each N and Δt .

2.7.2 Numerical results and observations

One can observe from Fig 2.2 that the respective numerical solutions of Examples 2.1, 2.2 and 2.3 consist of boundary layers nearest to the boundary at $x = 1$. Moreover, one can completely visualize the numerical solutions from the surface plots depicted in Figs 2.3, 2.4 and 2.5. The above figures are obtained utilizing the newly developed method with $\Delta t = 0.8/N$. In the following we discuss about the numerical results corresponding to ε -uniform convergence, effect of extrapolation on global and temporal accuracy, spatial accuracy, ε -uniform global accuracy and computational efficiency of the proposed method. Note that for computing ε -uniform errors, we select all the values of ε from $\mathbb{S}_\varepsilon = \{2^{-2}, \dots, 2^{-20}\}$.

2.7.2.1 ε -uniform convergence

In Tables 2.1, 2.3 and 2.5, for different values of ε , N and Δt , the maximum point-wise errors along with the corresponding order of convergence calculated using the proposed method with $\Delta t = 1.6/N$ and $\Delta t = 0.8/N$ are respectively presented for Examples 2.1, 2.2 and 2.3. This shows the monotonically decreasing behavior of the ε -uniform errors with increasing N and it surely reflects ε -uniform convergence of the present method. This also indicates that the rate of convergence of the ε -uniform errors increases when we select $\Delta t = 0.8/N$ instead of $\Delta t = 1.6/N$. In support of this observation, the calculated ε -uniform errors in Tables 2.1, 2.3 and 2.5 are depicted in Figs 2.6, 2.7 and 2.8; and this clearly illustrates the influence of the temporal error over the global error with the choice of the time step Δt , as we know that the temporal accuracy (which is of order one) before temporal extrapolation dominates the spatial accuracy of the proposed method according to the estimate of Theorem 2.3.

2.7.2.2 Effect of extrapolation on global and temporal accuracy

We therefore propose to implement the Richardson extrapolation technique in the temporal direction for improving the temporal accuracy of the proposed method so that the dominance of the temporal error over the global error can be reduced. For visualizing the effect of the temporal extrapolation on the global accuracy, we select $\Delta t = 0.8/N$, and further display the ε -uniform errors and the corresponding order of convergence calculated using the proposed method in Tables 2.2, 2.4 and 2.6, respectively for Examples 2.1, 2.2 and 2.3; and those numerical results are also plotted in Figs 2.6, 2.7 and 2.8, respectively. It demonstrates that the ε -uniform order of convergence of the proposed method is significantly improved after using the temporal extrapolation.

Next, for visualizing the effect of the extrapolation on the temporal accuracy, we select sufficiently large N to minimize the influence of the spatial error. In Tables 2.7, 2.8 and 2.9, for different values of ε and Δt , the maximum point-wise errors along with the corresponding order of convergence calculated before and after the temporal extrapolation using the proposed method are respectively presented for Examples 2.1, 2.2 and 2.3. For $\varepsilon = 2^{-4}, 2^{-6}$, those numerical results are also plotted in Figs 2.9, 2.10 and 2.11, respectively for Examples 2.1, 2.2 and 2.3. Henceforth, the above numerical experiment shows that the temporal accuracy of the resulting numerical solution after applying the temporal Richardson extrapolation improves from first-order to second-order, irrespective of the parameter ε , as we discussed in Section 2.5.

2.7.2.3 Spatial accuracy (region-wise)

The above numerical experiment confirms that by applying the temporal Richardson extrapolation one can also verify the spatial accuracy when selecting $\Delta t = 1/N$ in place of $\Delta t = 1/N^2$. So, the results provided in Tables 2.10, 2.11 and 2.12, respectively for Examples 2.1, 2.2 and 2.3, reflects the spatial accuracy of the proposed method. Moreover, by selecting the same discretization parameter Δt , those computational results are also compared with the existing hybrid scheme. From Tables 2.10, 2.11 and 2.12, we get a strong evidence that the spatial accuracy is at least $O(N^{-2})$ outside the boundary layer and is $O(N^{-2} \ln^2 N)$ inside the boundary layer, regardless of the smaller and the larger values of ε . This phenomenon agrees well with the theoretical output of Theorem 2.2.

Contrary to the above observation, the results of those tables related to the existing hybrid scheme reveal that the spatial accuracy is $O(N^{-1})$ outside the boundary layer and is $O(N^{-2} \ln^2 N)$ inside the boundary layer, when $\varepsilon = 2^{-6}$. In addition, when $\varepsilon = 2^{-4}$, we observe first-order spatial accuracy of the existing method and second-order spatial accuracy of the present method for both outside and inside the boundary layer; and in that case we recognize the mesh $\bar{\Omega}^N$ as the equidistant mesh. In support of this comparison, the maximum point-wise errors for $\varepsilon = 2^{-4}, 2^{-6}$ in Tables 2.10, 2.11 and 2.12 are graphically presented in Figs 2.12, 2.13 and 2.14, respectively. As a result, when $\varepsilon = 2^{-4}, 2^{-6}$ satisfying $\varepsilon \gg N^{-1}$, the newly developed method produces region-wise higher-order accurate results in comparison with the existing method. At the same time, when $\varepsilon = 2^{-14}, 2^{-20}$ satisfying $\varepsilon \ll N^{-1}$, the spatial order of accuracy of both the numerical methods remains same through out the domain.

2.7.2.4 ε -uniform global accuracy

To compare the ε -uniform global order accuracy of the proposed method with the existing hybrid scheme using the temporal extrapolation, we select $\Delta t = 1/N$, and display the ε -uniform error and the corresponding order of convergence calculated using both the proposed method and the existing method in Tables 2.13, 2.14 and 2.15, respectively, for Examples 2.1, 2.2 and 2.3; and those numerical results are also graphically presented in

Figs 2.15, 2.16 and 2.17, respectively. Here, we observe that the proposed method combined with the temporal extrapolation converges ε -uniformly with at least of $O(N^{-2} \ln^2 N)$ global accuracy which indeed matches with the spatial accuracy of the proposed method, because the temporal accuracy is of $O(\Delta t^2)$ after the extrapolation as it is discussed previously. At same-time, the existing hybrid scheme combined with the temporal extrapolation converges ε -uniformly with $O(N^{-1})$ global accuracy. This shows that there is a significant improvement in the ε -uniform global order accuracy of the proposed method over the existing method.

Remark 2.6. The numerical experiments confirm that the theoretical restriction $N^{-\delta} \leq C\Delta t$, $0 < \delta < 1$ mentioned in Theorem 2.3 is not reflected in the computed ε -uniform accuracy of the proposed numerical method. In this context, we want to point out that by following the error analysis provided in [26], one can overcome this theoretical restriction. However, the convergence analysis presented in this chapter is very much useful to extend and analyze the proposed method for solving multi-dimensional parabolic PDEs.

2.7.2.5 Computational efficiency

Finally, for the purpose of demonstrating the computational efficiency, we compare the computational time of the newly developed method with the existing hybrid scheme in Tables 2.16, 2.17 and 2.18, respectively for Examples 2.1, 2.2 and 2.3, taking $\Delta t = 1/N^2$; and those results are also compared with the computational time of the proposed method after applying the Richardson extrapolation in the temporal direction by choosing $\Delta t = 1/N$. We notice a small difference in the computational time of the present method with the existing method; and the computational times of both the numerical methods are therefore comparable in case of $\Delta t = 1/N^2$. However, we observe a significant reduction in the computational time corresponding to the newly developed method together with the temporal Richardson extrapolation which indeed produces the globally second-order convergent numerical solution with the choice of $\Delta t = 1/N$, regardless of the smaller and the larger values of ε .

2.8 Conclusion

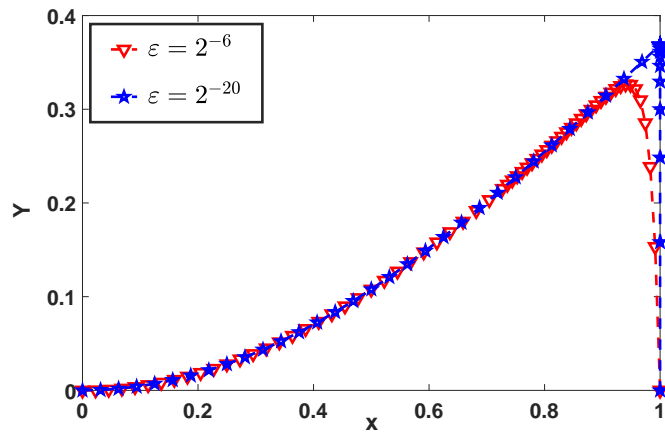
In the recent time, the existing hybrid numerical method is proven to be a useful and popular technique among various FMMs for finding efficient numerical solution of singularly perturbed convection-diffusion parabolic PDEs. While investigating about the accuracy of the method, it is found that the existing hybrid scheme converges with almost second-order accuracy in the spatial variable on a piecewise-uniform Shishkin mesh, unless the condition $\varepsilon \ll N^{-1}$ is satisfied. On the contrary, the method is not good enough to produce the numerical solution with higher-order spatial accuracy, whenever $\varepsilon \gg N^{-1}$. In this chapter, we overcome this drawback, by developing and analyzing an ε -uniformly convergent robust numerical algorithm for a class of singularly perturbed parabolic IBVPs of the form (2.1)-(2.2).

The current numerical algorithm consists of two parts. First one is the development of a new hybrid FMM, which produces at least second-order accurate numerical solution with respect to the spatial variable both in the outer region (outside the boundary layer) as well as in the boundary layer region (inside the boundary layer), irrespective of the parameter ε . This finding overshadows the drawback of the existing hybrid scheme. In this context, it is important to note that to derive the error estimate for the newly developed method, we analyze the error separately for the time semidiscretization and the spatial discretization, which finally contribute to the global error in relation with the fully discrete scheme.

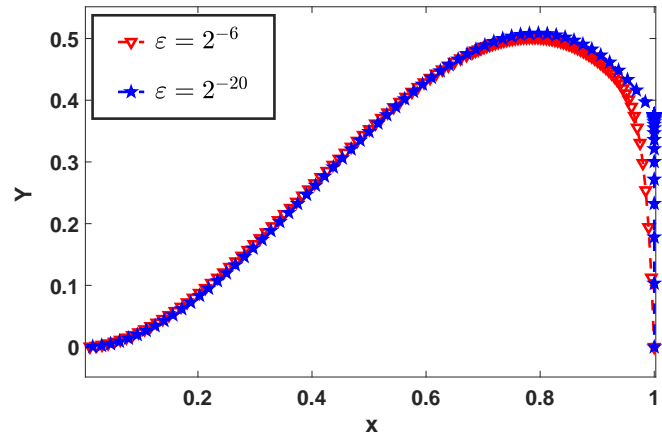
The other one is the implementation of the Richardson extrapolation technique solely in the temporal direction

for enhancing the temporal accuracy of the numerical solution from first-order to second-order. As a result of this, we show that the resulting numerical solution is not only second-order ε -uniformly convergent in the spatial variable but also in the temporal variable.

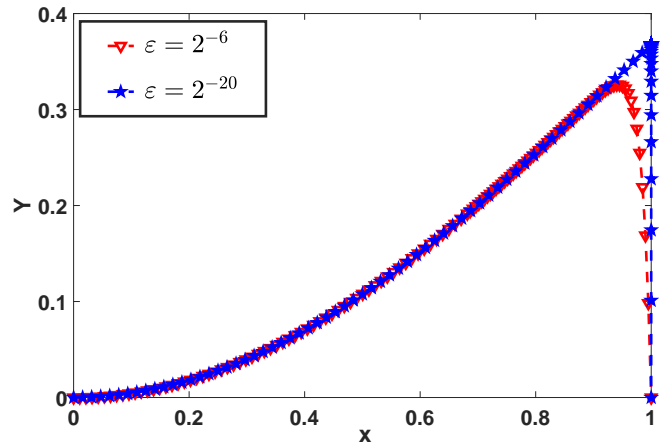
These theoretical findings are very-well supported by the several numerical experiments and also agree well with the numerical results corresponding to the singularly perturbed semi-linear parabolic problem. Moreover, one can observe a significant reduction in the computational time corresponding to the newly developed FMM together with the temporal Richardson extrapolation, regardless of the smaller and the larger values of ε . Keeping in mind the robustness of the newly proposed algorithm, we further study the computational and the theoretical aspects of the proposed numerical algorithm for solving multi-dimensional parabolic PDEs (linear and nonlinear) in the subsequent chapters.



(a) Example 2.1.

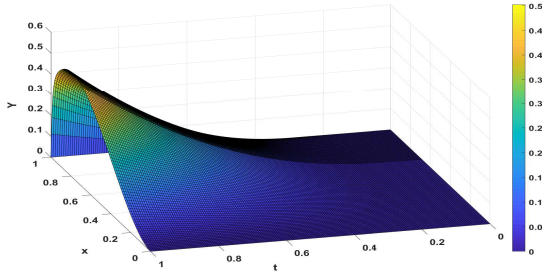


(b) Example 2.2.

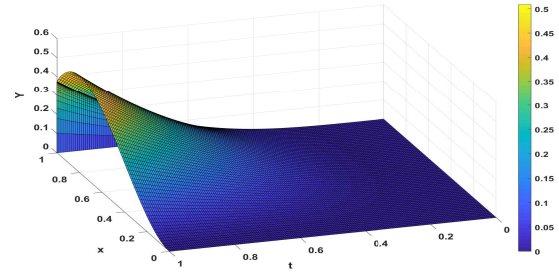


(c) Example 2.3.

Figure 2.2: Numerical solutions computed at $t = 1$ for $N = 128$

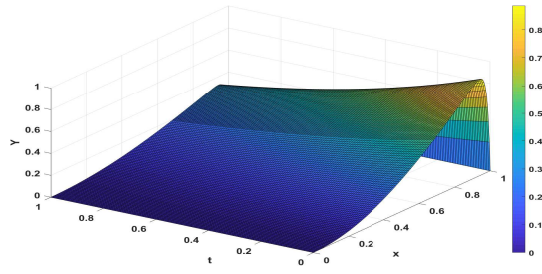


(a) for $\varepsilon = 2^{-6}$, $N = 128$

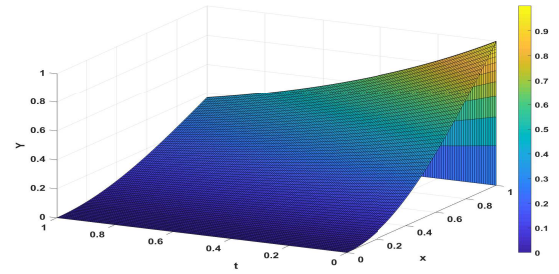


(b) for $\varepsilon = 2^{-20}$, $N = 128$

Figure 2.4: Surface plots of the numerical solutions of Example 2.2

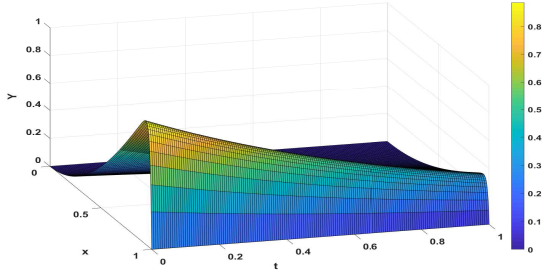


(a) for $\varepsilon = 2^{-6}$, $N = 128$

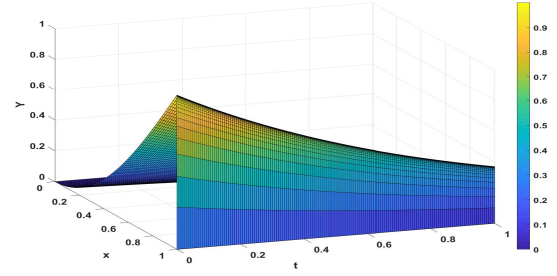


(b) for $\varepsilon = 2^{-20}$, $N = 128$

Figure 2.3: Surface plots of the numerical solutions of Example 2.1



(a) for $\varepsilon = 2^{-6}$, $N = 128$



(b) for $\varepsilon = 2^{-20}$, $N = 128$

Figure 2.5: Surface plots of the numerical solutions of Example 2.3

Table 2.1: ε -uniform maximum point-wise errors and order of convergence for Example 2.1 computed before temporal extrapolation.

$\varepsilon \in \mathbb{S}_\varepsilon$	Number of mesh intervals N / time step size Δt ($\Delta t = 1.6/N$)				
	$64 / \frac{1}{40}$	$128 / \frac{1}{80}$	$256 / \frac{1}{160}$	$512 / \frac{1}{320}$	$1024 / \frac{1}{640}$
$e^{N,\Delta t}$	4.7311e-03	1.8152e-03	6.9899e-04	2.8827e-04	1.2651e-04
$r^{N,\Delta t}$	1.3820	1.3768	1.2778	1.1882	
$\varepsilon \in \mathbb{S}_\varepsilon$	Number of mesh intervals N / time step size Δt ($\Delta t = 0.8/N$)				
	$64 / \frac{1}{80}$	$128 / \frac{1}{160}$	$256 / \frac{1}{320}$	$512 / \frac{1}{640}$	$1024 / \frac{1}{1280}$
$e^{N,\Delta t}$	4.1296e-03	1.4964e-03	5.3899e-04	1.9965e-04	7.8348e-05
$r^{N,\Delta t}$	1.4645	1.4731	1.4328	1.3540	

Table 2.2: ε -uniform maximum point-wise errors and order of convergence for Example 2.1 computed after temporal extrapolation with $\Delta t = 0.8/N$.

$\varepsilon \in \mathbb{S}_\varepsilon$	Number of mesh intervals N / time step size Δt				
	$64 / \frac{1}{80}$	$128 / \frac{1}{160}$	$256 / \frac{1}{320}$	$512 / \frac{1}{640}$	$1024 / \frac{1}{1280}$
$e^{N,\Delta t}$	3.5314e-03	1.2137e-03	3.9124e-04	1.2368e-04	3.8105e-05
$r^{N,\Delta t}$	1.5409	1.6332	1.6615	1.6985	

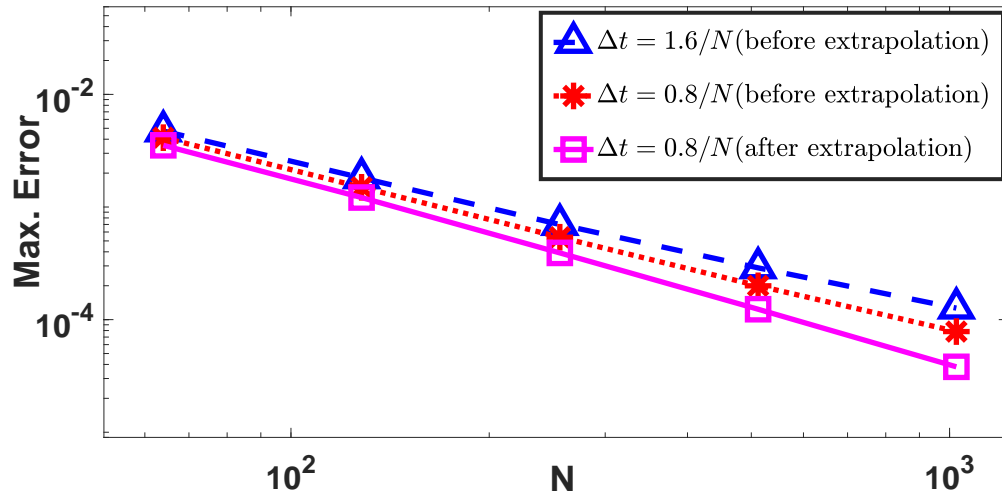


Figure 2.6: Loglog plot for comparison of ε -uniform maximum point-wise errors before and after the extrapolation for Example 2.1.

Table 2.3: ε -uniform maximum point-wise errors and order of convergence for Example 2.2 computed before temporal extrapolation.

$\varepsilon \in \mathbb{S}_\varepsilon$	Number of mesh intervals N / time step size Δt ($\Delta t = 1.6/N$)				
	$64 / \frac{1}{40}$	$128 / \frac{1}{80}$	$256 / \frac{1}{160}$	$512 / \frac{1}{320}$	$1024 / \frac{1}{640}$
$\hat{e}^{N,\Delta t}$	4.9037e-03	2.0489e-03	8.9582e-04	4.1339e-04	1.9956e-04
$\hat{r}^{N,\Delta t}$	1.2590	1.1935	1.1157	1.0507	

$\varepsilon \in \mathbb{S}_\varepsilon$	Number of mesh intervals N / time step size Δt ($\Delta t = 0.8/N$)				
	$64 / \frac{1}{80}$	$128 / \frac{1}{160}$	$256 / \frac{1}{320}$	$512 / \frac{1}{640}$	$1024 / \frac{1}{1280}$
$\hat{e}^{N,\Delta t}$	3.7560e-03	1.4350e-03	5.6899e-04	2.3827e-04	1.0637e-04
$\hat{r}^{N,\Delta t}$	1.3881	1.3346	1.2558	1.1635	

Table 2.4: ε -uniform maximum point-wise errors and order of convergence for Example 2.2 computed after temporal extrapolation with $\Delta t = 0.8/N$.

$\varepsilon \in \mathbb{S}_\varepsilon$	Number of mesh intervals N / time step size Δt				
	$64 / \frac{1}{80}$	$128 / \frac{1}{160}$	$256 / \frac{1}{320}$	$512 / \frac{1}{640}$	$1024 / \frac{1}{1280}$
$\hat{e}^{N,\Delta t}$	2.2161e-03	7.3715e-04	2.3773e-04	7.5609e-05	2.3279e-05
$\hat{r}^{N,\Delta t}$	1.5880	1.6326	1.6527	1.6995	

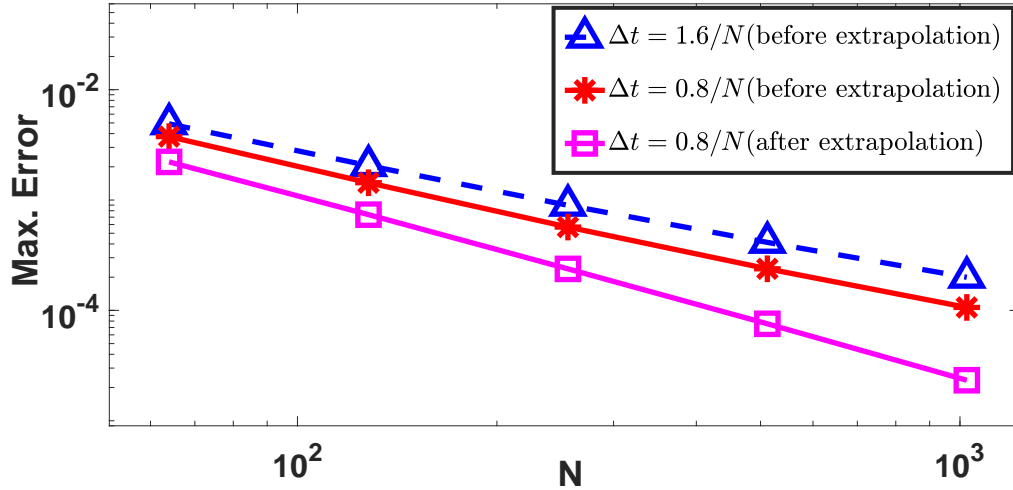


Figure 2.7: Loglog plot for comparison of ε -uniform maximum point-wise errors before and after the extrapolation for Example 2.2.

Table 2.5: ε -uniform maximum point-wise errors and order of convergence for Example 2.3 computed before temporal extrapolation.

$\varepsilon \in \mathbb{S}_\varepsilon$	Number of mesh intervals N / time step size $\Delta t(\Delta t = 1.6/N)$				
	$64 / \frac{1}{40}$	$128 / \frac{1}{80}$	$256 / \frac{1}{160}$	$512 / \frac{1}{320}$	$1024 / \frac{1}{640}$
$e^{N,\Delta t}$	4.3634e-03	1.6061e-03	6.0580e-04	2.3846e-04	9.9783e-05
$r^{N,\Delta t}$	1.4419	1.4067	1.3451	1.2569	

$\varepsilon \in \mathbb{S}_\varepsilon$	Number of mesh intervals N / time step size $\Delta t(\Delta t = 0.8/N)$				
	$64 / \frac{1}{80}$	$128 / \frac{1}{160}$	$256 / \frac{1}{320}$	$512 / \frac{1}{640}$	$1024 / \frac{1}{1280}$
$e^{N,\Delta t}$	3.9039e-03	1.3737e-03	4.8721e-04	1.7568e-04	6.6081e-05
$r^{N,\Delta t}$	1.5068	1.5014	1.4656	1.4141	

Table 2.6: ε -uniform maximum point-wise errors and order of convergence for Example 2.3 computed after temporal extrapolation with $\Delta t = 0.8/N$.

$\varepsilon \in \mathbb{S}_\varepsilon$	Number of mesh intervals N / time step size Δt				
	$64 / \frac{1}{80}$	$128 / \frac{1}{160}$	$256 / \frac{1}{320}$	$512 / \frac{1}{640}$	$1024 / \frac{1}{1280}$
$e^{N,\Delta t}$	3.4930e-03	1.1846e-03	3.8203e-04	1.2087e-04	3.7261e-05
$r^{N,\Delta t}$	1.5601	1.6327	1.6602	1.6977	

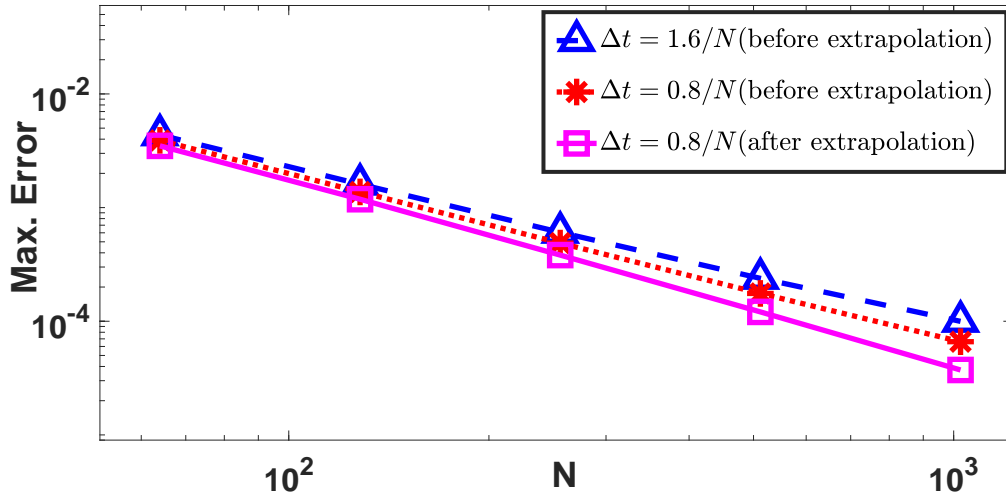


Figure 2.8: Loglog plot for comparison of ε -uniform maximum point-wise errors before and after the extrapolation for Example 2.3.

Table 2.7: Comparison of the temporal accuracy for Example 2.1 computed before and after the extrapolation.

ε	temporal extrapolation	Number of space intervals $N = 8192$				
		$\Delta t = \frac{1}{16}$	$\Delta t = \frac{1}{32}$	$\Delta t = \frac{1}{64}$	$\Delta t = \frac{1}{128}$	$\Delta t = \frac{1}{256}$
$2^{-4} \approx 10^{-1}$	before	2.9210e-03	1.4560e-03	7.2642e-04	3.6277e-04	1.8128e-04
		1.0045	1.0031	1.0018	1.0008	
	after	1.1131e-05	3.4900e-06	9.6643e-07	2.4251e-07	5.3206e-08
		1.6733	1.8525	1.9946	2.1884	
$2^{-6} \approx 10^{-2}$	before	3.9687e-03	1.9707e-03	9.8079e-04	4.8913e-04	2.4426e-04
		1.0100	1.0067	1.0037	1.0018	
	after	2.9210e-05	9.3082e-06	2.5975e-06	6.6327e-07	1.5776e-07
		1.6499	1.8414	1.9694	2.0719	
$2^{-14} \approx 10^{-4}$	before	4.6936e-03	2.3270e-03	1.1567e-03	5.7642e-04	2.8769e-04
		1.0122	1.0084	1.0049	1.0026	
	after	4.0049e-05	1.3550e-05	3.8988e-06	1.0325e-06	2.7024e-07
		1.5634	1.7972	1.9168	1.9339	
$2^{-20} \approx 10^{-6}$	before	4.7018e-03	2.3311e-03	1.1587e-03	5.7742e-04	2.8820e-04
		1.0122	1.0084	1.0049	1.0026	
	after	4.0090e-05	1.3570e-05	3.9022e-06	1.0291e-06	2.6486e-07
		1.5628	1.7981	1.9228	1.9581	

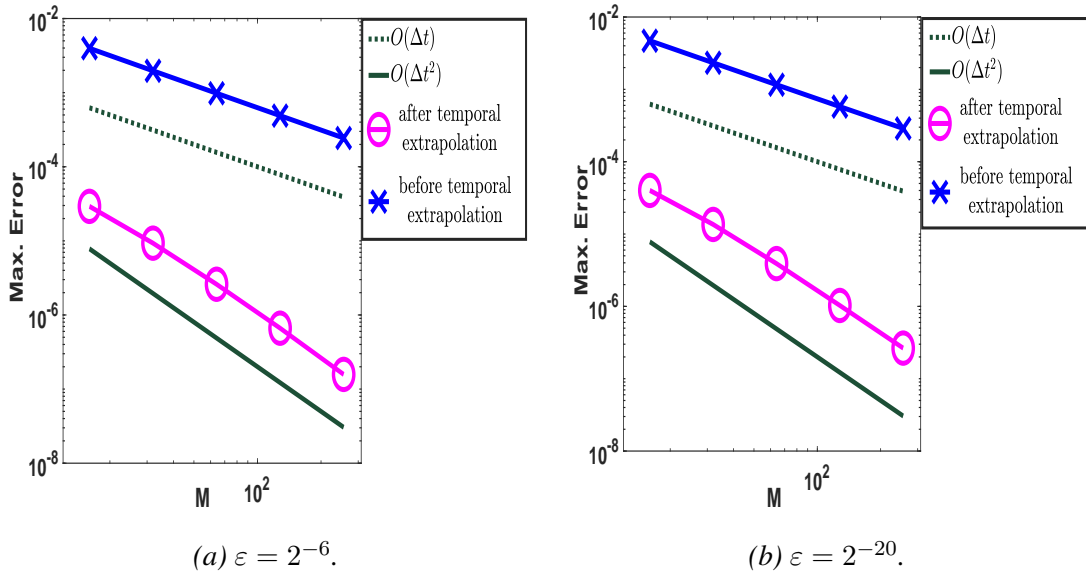


Figure 2.9: Loglog plot for comparison of the temporal order of convergence for Example 2.1

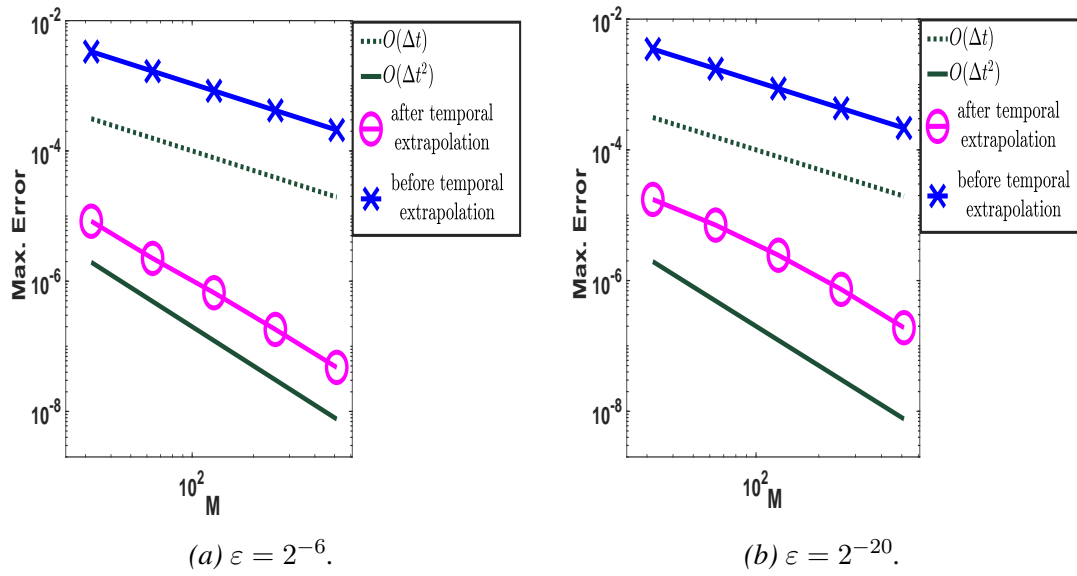


Figure 2.10: Loglog plot for compariosn of the temporal order of convergence for Example 2.2

Table 2.8: Comparison of the temporal accuracy for Example 2.2 computed before and after the extrapolation.

ε	temporal extrapolation	Number of space intervals $N = 4096$				
		$\Delta t = \frac{1}{32}$	$\Delta t = \frac{1}{64}$	$\Delta t = \frac{1}{128}$	$\Delta t = \frac{1}{256}$	$\Delta t = \frac{1}{512}$
$2^{-4} \approx 10^{-1}$	before	2.8611e-03	1.4364e-03	7.1953e-04	3.6007e-04	1.8011e-04
		0.99411	0.99736	0.99877	0.99941	
	after	1.2367e-05	2.8038e-06	6.5921e-07	1.5918e-07	3.9068e-08
		2.1410	2.0886	2.0501	2.0266	
$2^{-6} \approx 10^{-2}$	before	3.3446e-03	1.6751e-03	8.3757e-04	4.1868e-04	2.0930e-04
		0.99759	0.99995	1.0003	1.0003	
	after	8.3233e-06	2.2380e-06	6.6411e-07	1.8149e-07	4.7483e-08
		1.8949	1.7527	1.8715	1.9345	
$2^{-14} \approx 10^{-4}$	before	3.4827e-03	1.7397e-03	8.6711e-04	4.3235e-04	2.1581e-04
		1.0013	1.0046	1.0040	1.0024	
	after	1.7361e-05	7.0166e-06	2.4234e-06	7.2924e-07	1.8946e-07
		1.3070	1.5337	1.7326	1.9445	
$2^{-20} \approx 10^{-6}$	before	3.4829e-03	1.7398e-03	8.6711e-04	4.3234e-04	2.1581e-04
		1.0014	1.0046	1.0040	1.0025	
	after	1.7436e-05	7.0569e-06	2.4425e-06	7.3390e-07	1.9000e-07
		1.3050	1.5307	1.7347	1.9496	

Table 2.9: Comparison of the temporal accuracy for Example 2.3 computed before and after the extrapolation.

ε	temporal extrapolation	Number of space intervals $N = 8192$				
		$\Delta t = \frac{1}{16}$	$\Delta t = \frac{1}{32}$	$\Delta t = \frac{1}{64}$	$\Delta t = \frac{1}{128}$	$\Delta t = \frac{1}{256}$
$2^{-4} \approx 10^{-1}$	before	2.0435e-03	1.0144e-03	5.0511e-04	2.5201e-04	1.2587e-04
		1.0104	1.0060	1.0031	1.0015	
	after	1.4985e-05	4.2548e-06	1.1151e-06	2.7124e-07	5.8131e-08
		1.8163	1.9320	2.0395	2.2222	
$2^{-6} \approx 10^{-2}$	before	2.6901e-03	1.3325e-03	6.6262e-04	3.3036e-04	1.6496e-04
		1.0135	1.0079	1.0041	1.0019	
	after	2.5499e-05	7.3432e-06	1.9444e-06	4.8621e-07	1.4184e-07
		1.7960	1.9171	1.9997	1.7773	
$2^{-14} \approx 10^{-4}$	before	3.1029e-03	1.5359e-03	7.6330e-04	3.8036e-04	1.8984e-04
		1.0145	1.0088	1.0049	1.0026	
	after	3.1084e-05	9.3408e-06	2.5694e-06	6.7420e-07	1.7628e-07
		1.7345	1.8621	1.9302	1.9353	
$2^{-20} \approx 10^{-6}$	before	3.1071e-03	1.5380e-03	7.6432e-04	3.8087e-04	1.9010e-04
		1.0145	1.0088	1.0049	1.0026	
	after	3.1106e-05	9.3499e-06	2.5710e-06	6.7277e-07	1.7389e-07
		1.7342	1.8626	1.9341	1.9519	

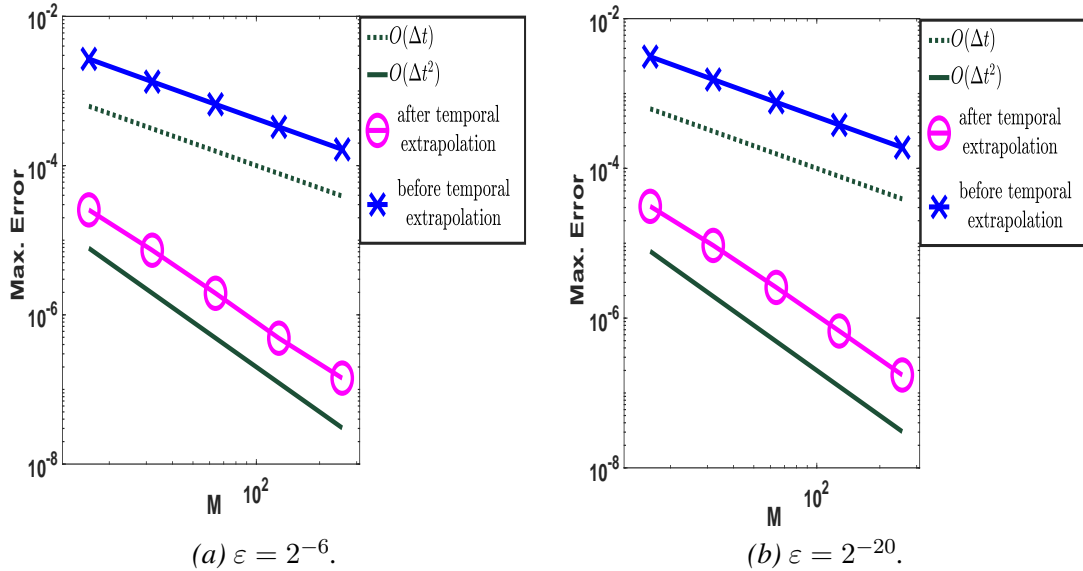
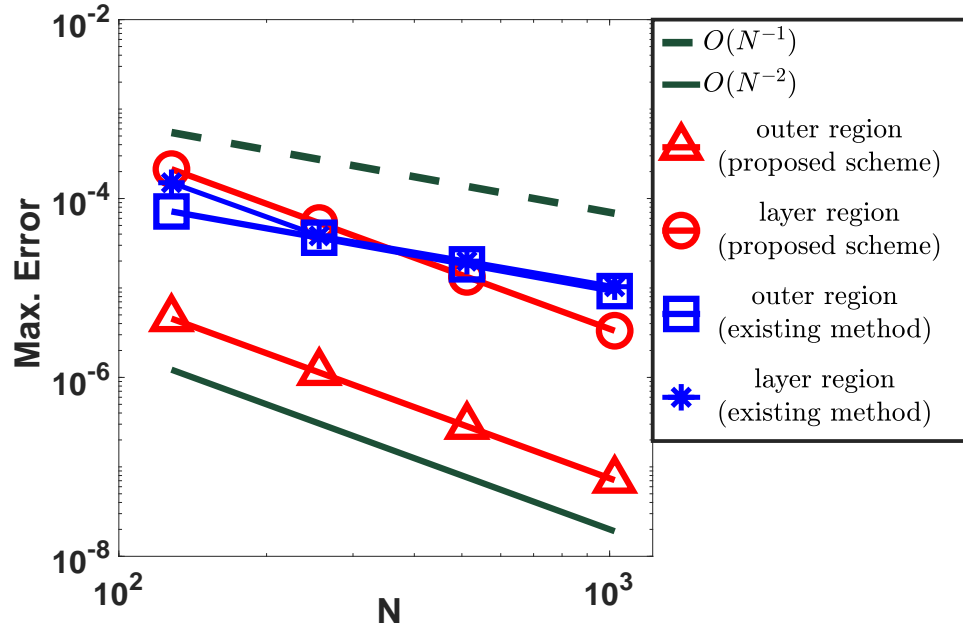


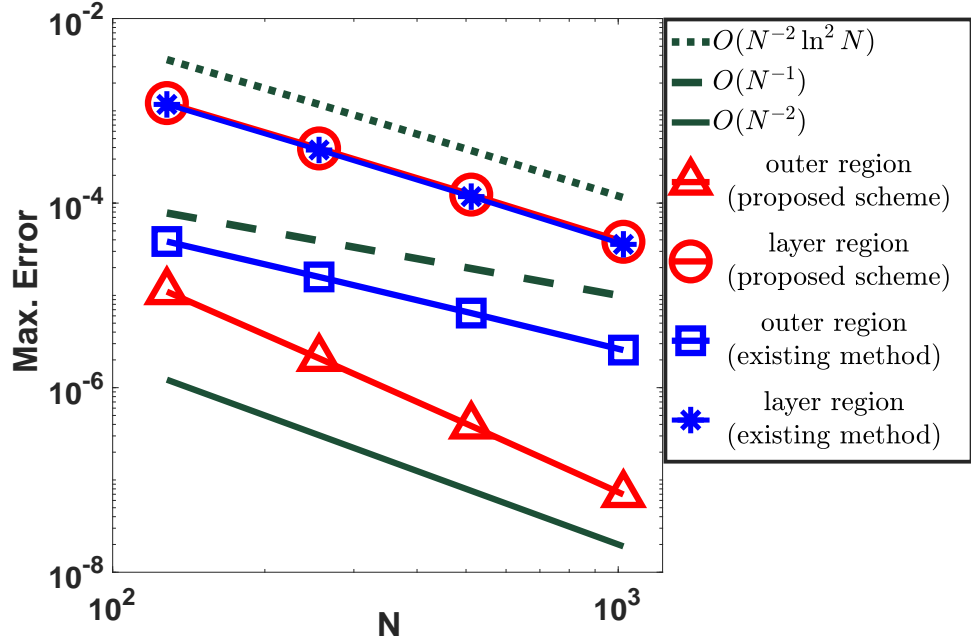
Figure 2.11: Loglog plot for comparison of the temporal order of convergence for Example 2.3

Table 2.10: Comparison (region-wise) of the spatial accuracy for Example 2.1 computed using extrapolation with $\Delta t = 1/N$.

N	proposed method		existing method [81]	
	outer region [0, 1 - η]	boundary layer region (1 - η , 1]	outer region [0, 1 - η]	boundary layer region (1 - η , 1]
$\varepsilon = 2^{-4} \approx 10^{-1}$				
128	4.5441e-06 1.9994	2.1310e-04 2.0022	7.1657e-05 0.97552	1.5010e-04 1.9721
256	1.1365e-06 2.0000	5.3195e-05 1.9999	3.6442e-05 0.98813	3.8256e-05 0.93962
512	2.8413e-07 2.0000	1.3300e-05 2.000	1.8371e-05 0.99416	1.9945e-05 0.94916
1024	7.1031e-08	3.3246e-06	9.2229e-06	1.0330e-05
$\varepsilon = 2^{-6} \approx 10^{-2}$				
128	1.0988e-05 2.4029	1.2135e-03 1.6332	3.8370e-05 1.2751	1.1735e-03 1.6418
256	2.0777e-06 2.4327	3.9119e-04 1.6614	1.5855e-05 1.3018	3.7605e-04 1.6777
512	3.8483e-07 2.4674	1.2366e-04 1.6985	6.4311e-06 1.3323	1.1755e-04 1.7185
1024	6.9583e-08	3.8102e-05	2.5540e-06	3.5719e-05
$\varepsilon = 2^{-14} \approx 10^{-4}$				
128	1.0170e-05 2.0101	1.1513e-03 1.6295	1.0170e-05 2.0101	1.1513e-03 1.6295
256	2.5248e-06 2.0204	3.7212e-04 1.6579	2.5248e-06 2.0204	3.7212e-04 1.6579
512	6.2233e-07 1.9498	1.1792e-04 1.6972	6.2233e-07 1.9498	1.1792e-04 1.6972
1024	1.6109e-07	3.6367e-05	1.6109e-07	3.6367e-05
$\varepsilon = 2^{-20} \approx 10^{-6}$				
128	1.0272e-05 1.9997	1.1514e-03 1.6293	1.0272e-05 1.9997	1.1514e-03 1.6293
256	2.5686e-06 2.0003	3.7220e-04 1.6575	2.5686e-06 2.0003	3.7220e-04 1.6575
512	6.4202e-07 2.0006	1.1798e-04 1.6965	6.4202e-07 2.0006	1.1798e-04 1.6965
1024	1.6044e-07	3.6401e-05	1.6044e-07	3.6401e-05



(a) $\varepsilon = 2^{-4}$.

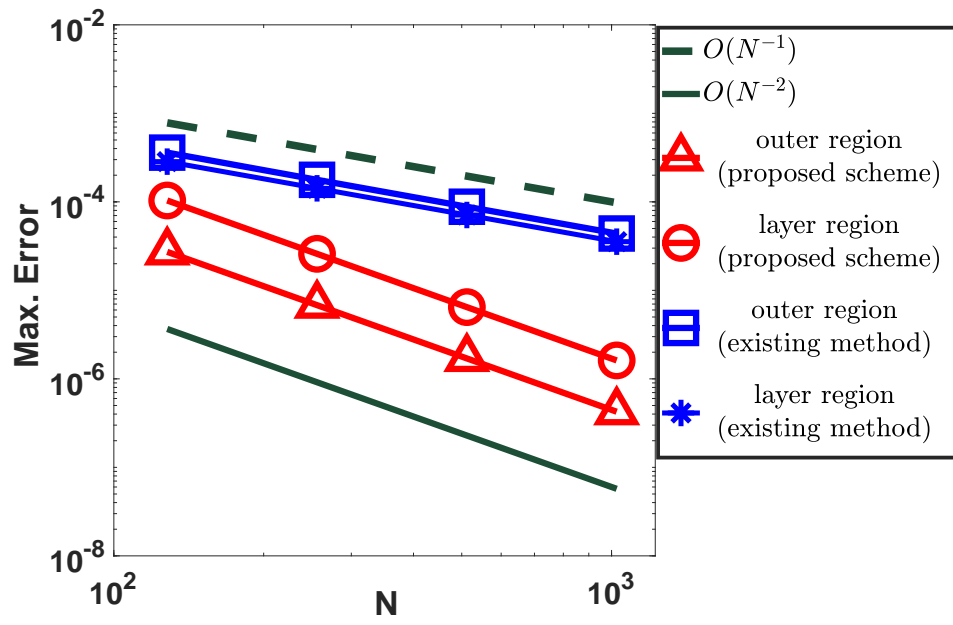


(b) $\varepsilon = 2^{-6}$.

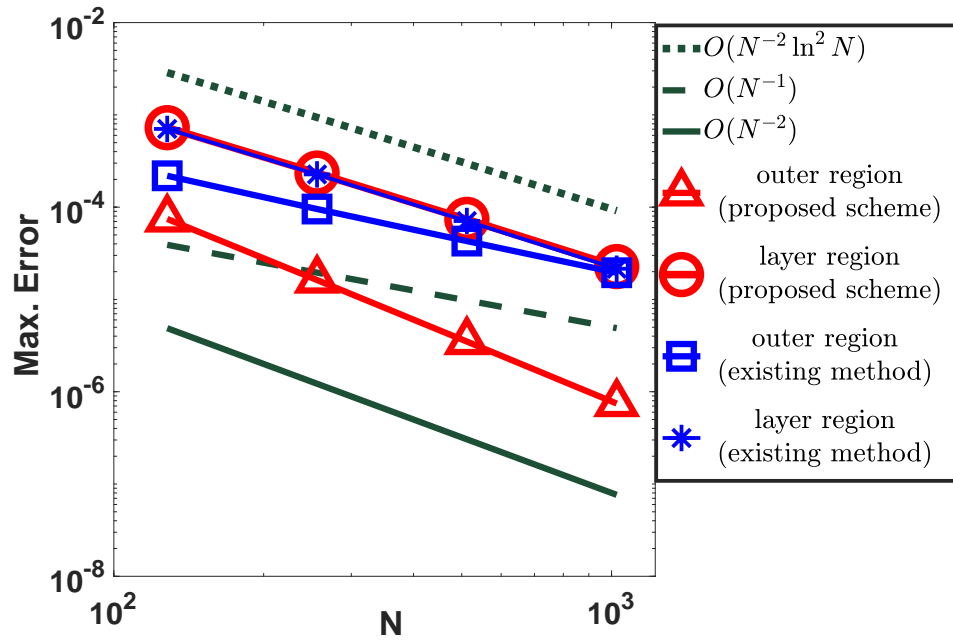
Figure 2.12: Loglog plot for comparison of the spatial order of convergence for Example 2.1

Table 2.11: Comparison (region-wise) of the spatial accuracy for Example 2.2 computed using extrapolation with $\Delta t = 1/N$.

N	proposed method		existing method [81]	
	outer region [0, 1 - η]	boundary layer region (1 - η , 1]	outer region [0, 1 - η]	boundary layer region (1 - η , 1]
$\varepsilon = 2^{-4} \approx 10^{-1}$				
128	2.7217e-05 1.9999	1.0362e-04 2.0029	3.5989e-04 1.0205	2.8470e-04 1.0019
256	6.8049e-06 2.0000	2.5853e-05 1.9999	1.7741e-04 1.0103	1.4216e-04 1.0013
512	1.7012e-06 2.0000	6.4640e-06 2.0002	8.8073e-05 1.0052	7.1015e-05 1.0007
1024	4.2530e-07	1.6157e-06	4.3879e-05	3.5489e-05
$\varepsilon = 2^{-6} \approx 10^{-2}$				
128	7.4496e-05 2.1986	7.2634e-04 1.6336	2.1879e-04 1.1966	7.0382e-04 1.6361
256	1.6229e-05 2.2141	2.3408e-04 1.6671	9.5454e-05 1.1545	2.2644e-04 1.6785
512	3.4979e-06 2.2314	7.3708e-05 1.6994	4.2880e-05 1.1382	7.0745e-05 1.7180
1024	7.4487e-07	2.2697e-05	1.9481e-05	2.1504e-05
$\varepsilon = 2^{-14} \approx 10^{-4}$				
128	7.5565e-05 1.9751	7.3649e-04 1.6328	7.5565e-05 1.9751	7.3649e-04 1.6328
256	1.9220e-05 1.9512	2.3749e-04 1.6589	1.9220e-05 1.9512	2.3749e-04 1.6589
512	4.9705e-06 1.9062	7.5210e-05 1.697	4.9705e-06 1.9062	7.5210e-05 1.6972
1024	1.3261e-06	2.3194e-05	1.3261e-06	2.3194e-05
$\varepsilon = 2^{-20} \approx 10^{-6}$				
128	7.4521e-05 1.9996	7.3674e-04 1.6327	7.4521e-05 1.9996	7.3674e-04 1.6327
256	1.8636e-05 1.9993	2.3758e-04 1.6586	1.8636e-05 1.9993	2.3758e-04 1.6586
512	4.6613e-06 1.9984	7.5254e-05 1.6968	4.6613e-06 1.9984	7.5254e-05 1.6968
1024	1.1666e-06	2.3213e-05	1.1666e-06	2.3213e-05



(a) $\varepsilon = 2^{-4}$.

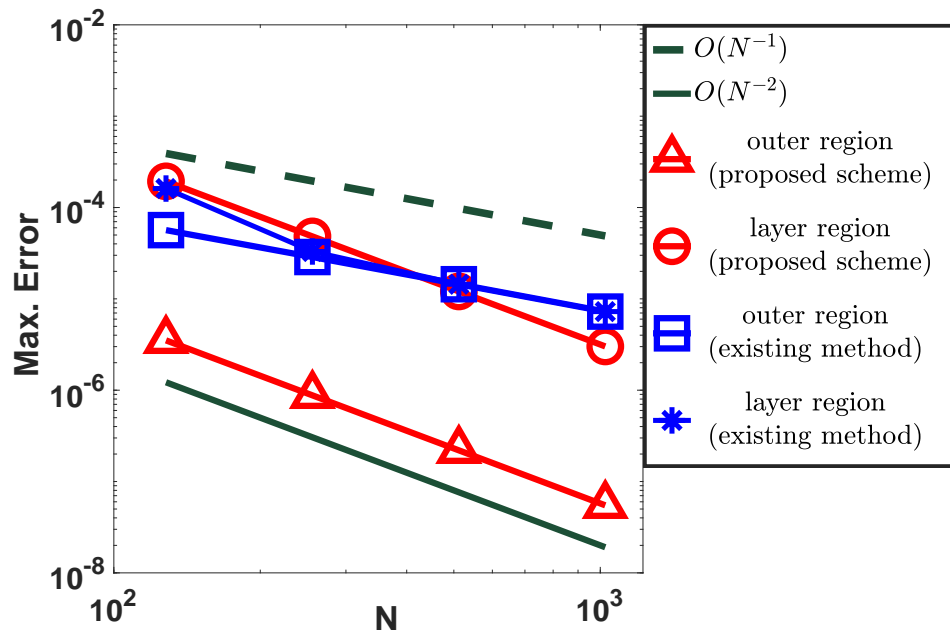


(b) $\varepsilon = 2^{-6}$.

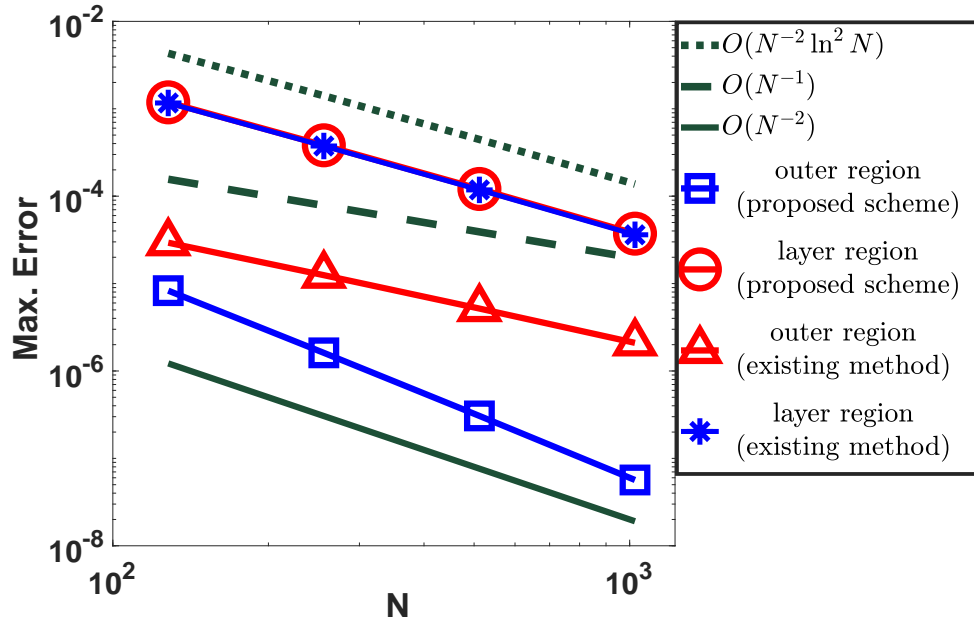
Figure 2.13: Loglog plot for comparison of the spatial order of convergence for Example 2.2

Table 2.12: Comparison (region-wise) of the spatial accuracy for Example 2.3 computed using extrapolation with $\Delta t = 1/N$.

N	proposed method		existing method [81]	
	outer region [0, 1 - η]	boundary layer region (1 - η , 1]	outer region [0, 1 - η]	boundary layer region (1 - η , 1]
$\varepsilon = 2^{-4} \approx 10^{-1}$				
128	3.5116e-06 1.9996	1.9332e-04 2.0021	5.6553e-05 0.97820	1.6133e-04 2.2891
256	8.7815e-07 2.0000	4.8257e-05 2.0005	2.8707e-05 0.98924	3.3007e-05 1.1919
512	2.1954e-07 2.0000	1.2060e-05 2.0000	1.4461e-05 0.99479	1.4449e-05 0.99428
1024	5.4884e-08	3.0149e-06	7.2566e-06	7.2530e-06
$\varepsilon = 2^{-6} \approx 10^{-2}$				
128	8.2994e-06 2.3637	1.1845e-03 1.6326	2.9347e-05 1.2338	1.1650e-03 1.6354
256	1.6126e-06 2.3971	3.8200e-04 1.6602	1.2478e-05 1.2689	3.7498e-04 1.6685
512	3.0613e-07 2.4352	1.2086e-04 1.6977	5.1781e-06 1.3031	1.1796e-04 1.7056
1024	5.6602e-08	3.7259e-05	2.0985e-06	3.6165e-05
$\varepsilon = 2^{-14} \approx 10^{-4}$				
128	7.3375e-06 2.0089	1.1562e-03 1.6306	7.3375e-06 2.0089	1.1562e-03 1.6306
256	1.8231e-06 2.0172	3.7340e-04 1.6587	1.8231e-06 2.0172	3.7340e-04 1.6587
512	4.5037e-07 2.0332	1.1827e-04 1.6976	4.5037e-07 2.0332	1.1827e-04 1.6976
1024	1.1003e-07	3.6461e-05	1.1003e-07	3.6461e-05
$\varepsilon = 2^{-20} \approx 10^{-6}$				
128	7.4022e-06 2.0002	1.1562e-03 1.6304	7.4022e-06 2.0002	1.1562e-03 1.6304
256	1.8503e-06 2.0003	3.7347e-04 1.6585	1.8503e-06 2.0003	3.7347e-04 1.6585
512	4.6249e-07 2.0005	1.1830e-04 1.6973	4.6249e-07 2.0005	1.1830e-04 1.6973
1024	1.1558e-07	3.6481e-05	1.1558e-07	3.6481e-05



(a) $\varepsilon = 2^{-4}$.



(b) $\varepsilon = 2^{-6}$.

Figure 2.14: Loglog plot for comparison of the spatial order of convergence for Example 2.3

Table 2.13: Comparison of ε -uniform maximum point-wise errors and order of convergence for Example 2.1 computed using extrapolation with $\Delta t = \frac{1}{N}$.

$\varepsilon \in \mathbb{S}_\varepsilon$	Number of mesh intervals N / time step size Δt				
	$64 / \frac{1}{64}$	$128 / \frac{1}{128}$	$256 / \frac{1}{256}$	$512 / \frac{1}{512}$	$1024 / \frac{1}{1024}$
	proposed method				
$e^{N,\Delta t}$	3.5307e-03	1.2135e-03	3.9119e-04	1.2366e-04	3.8102e-05
$r^{N,\Delta t}$	1.5408	1.6332	1.6614	1.6985	
$\varepsilon \in \mathbb{S}_\varepsilon$	existing method [81]				
$e^{N,\Delta t}$	3.5307e-03	1.1735e-03	3.7605e-04	1.7242e-04	8.6268e-05
$r^{N,\Delta t}$	1.5891	1.6418	1.1250	0.99903	

Table 2.14: Comparison of ε -uniform maximum point-wise errors and order of convergence for Example 2.2 computed using extrapolation with $\Delta t = \frac{1}{N}$.

$\varepsilon \in \mathbb{S}_\varepsilon$	Number of mesh intervals N / time step size Δt				
	$64 / \frac{1}{64}$	$128 / \frac{1}{128}$	$256 / \frac{1}{256}$	$512 / \frac{1}{512}$	$1024 / \frac{1}{1024}$
	proposed method				
$e^{N,\Delta t}$	2.2155e-03	7.3674e-04	2.3758e-04	7.5583e-05	2.3272e-05
$r^{N,\Delta t}$	1.5884	1.6327	1.6523	1.6995	
$\varepsilon \in \mathbb{S}_\varepsilon$	existing method [81]				
$e^{N,\Delta t}$	2.2155e-03	7.3674e-04	2.8181e-04	1.4051e-04	7.0160e-05
$r^{N,\Delta t}$	1.5884	1.3864	1.0040	1.0020	

Table 2.15: Comparison of ε -uniform maximum point-wise errors and order of convergence for Example 2.3 computed using extrapolation with $\Delta t = 1/N$.

$\varepsilon \in \mathbb{S}_\varepsilon$	Number of mesh intervals N / time step size Δt				
	$64 / \frac{1}{64}$	$128 / \frac{1}{128}$	$256 / \frac{1}{256}$	$512 / \frac{1}{512}$	$1024 / \frac{1}{1024}$
	proposed method				
$e^{N,\Delta t}$	3.4925e-03	1.1845e-03	3.8200e-04	1.2086e-04	3.7259e-05
$r^{N,\Delta t}$	1.5600	1.6326	1.6602	1.6977	
$\varepsilon \in \mathbb{S}_\varepsilon$	existing method [81]				
$e^{N,\Delta t}$	3.4925e-03	1.1650e-03	3.7498e-04	1.3116e-04	6.5608e-05
$r^{N,\Delta t}$	1.5840	1.6354	1.5155	0.99935	

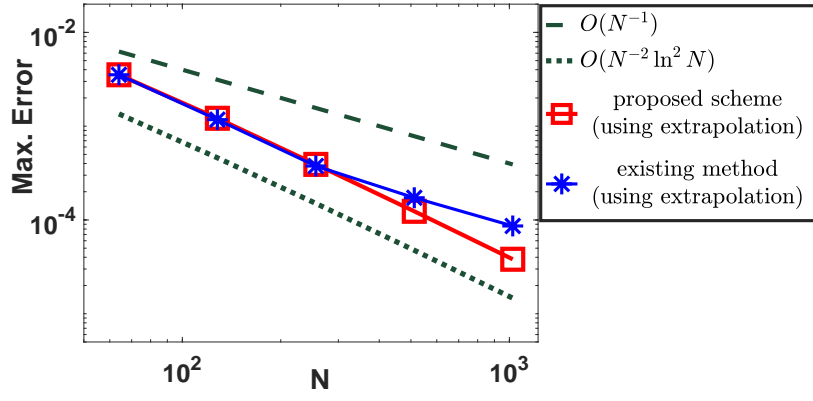


Figure 2.15: Loglog plot for comparison of the ε -uniform order of convergence computed using extrapolation with $\Delta t = \frac{1}{N}$ for Example 2.1

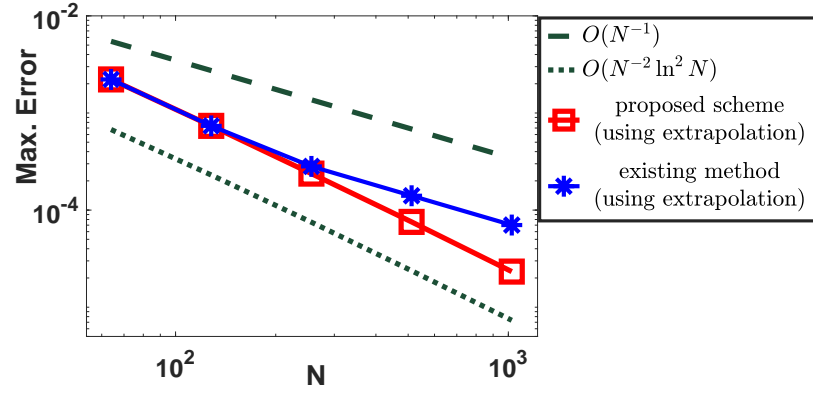


Figure 2.16: Loglog plot for comparison of the ε -uniform order of convergence computed using extrapolation with $\Delta t = \frac{1}{N}$ for Example 2.2

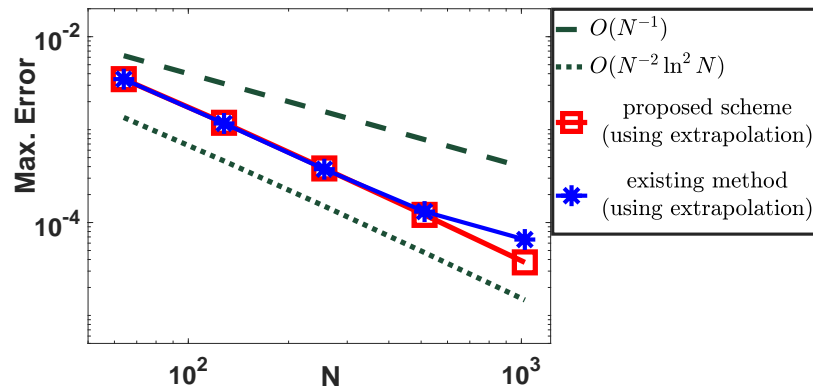


Figure 2.17: Loglog plot for comparison of the ε -uniform order of convergence computed using extrapolation with $\Delta t = \frac{1}{N}$ for Example 2.3

Table 2.16: *Comparison of computational time (in seconds) for Example 2.1.*

N	existing method [81] ($\Delta t = 1/N^2$)	proposed method ($\Delta t = 1/N^2$)	proposed method with extrapolation ($\Delta t = 1/N$)
$\varepsilon = 2^{-4} \approx 10^{-1}$			
128	2.447747	1.698225	0.082046
256	39.977219	33.678347	0.640903
512	471.538427	436.295669	5.213903
1024	6891.453204	6807.459580	40.902199
$\varepsilon = 2^{-6} \approx 10^{-2}$			
128	2.467187	1.613887	0.080390
256	39.781018	33.799365	0.689698
512	470.013505	438.211076	5.578360
1024	6881.485278	6788.904188	40.775835
$\varepsilon = 2^{-20} \approx 10^{-6}$			
128	2.366928	2.600754	0.111272
256	39.237350	43.213915	1.034624
512	463.726248	513.227230	6.906543
1024	6832.210552	7342.670128	43.881859

Table 2.17: *Comparison of computational time (in seconds) for Example 2.2.*

N	existing method [81] ($\Delta t = 1/N^2$)	proposed method ($\Delta t = 1/N^2$)	proposed method with extrapolation ($\Delta t = 1/N$)
$\varepsilon = 2^{-4} \approx 10^{-1}$			
128	21.235057	16.562923	0.638085
256	298.134008	256.980466	5.249468
512	4321.015141	4044.483856	44.559408
1024	64571.722837	62886.556371	347.377197
$\varepsilon = 2^{-6} \approx 10^{-2}$			
128	21.392572	16.693169	0.697348
256	304.132240	254.106250	6.147811
512	4411.644756	4086.152055	44.941473
1024	72732.595346	70987.220896	346.357530
$\varepsilon = 2^{-20} \approx 10^{-6}$			
128	21.916113	22.348399	1.027123
256	302.573161	306.687003	7.525740
512	4356.711021	4370.601466	49.354894
1024	64683.607333	64840.945562	357.591586

Table 2.18: *Comparison of computational time (in seconds) for Example 2.3.*

N	existing method [81] ($\Delta t = 1/N^2$)	proposed method ($\Delta t = 1/N^2$)	proposed method with extrapolation ($\Delta t = 1/N$)
$\varepsilon = 2^{-4} \approx 10^{-1}$			
128	18.543270	12.507168	0.361790
256	303.828897	232.691973	2.983254
512	3511.456426	2832.781757	22.906101
1024	40343.169721	39689.100922	166.065631
$\varepsilon = 2^{-6} \approx 10^{-2}$			
128	12.680438	9.632157	0.332569
256	195.416197	162.609039	2.905975
512	2500.498345	2147.380792	22.680907
1024	35257.318952	32977.883816	165.887013
$\varepsilon = 2^{-20} \approx 10^{-6}$			
128	10.465427	10.448180	0.541479
256	168.2466500	170.295158	3.747230
512	2120.502122	2129.276525	26.207795
1024	32790.637608	33074.209161	175.229874

Chapter 3

Higher-Order Efficient Numerical Method for Singularly Perturbed 2D Linear Parabolic PDEs with Non-homogeneous Boundary Data : ε -Uniform Convergence and Order Reduction Analysis

The aim of this chapter is to develop and analyze a cost-effective high-order efficient numerical method for a class of two-dimensional singularly perturbed linear parabolic convection-diffusion problems with non-homogeneous boundary data. To achieve the goal, we develop a new fractional-step fitted mesh method (FSFMM) that combines the fractional implicit-Euler method with an alternative evaluation of the boundary data for discretizing in time and also consists of a new finite difference method for discretizing in space. To constitute this method, we discretize the spatial domain using a non-uniform rectangular mesh (tensor-product of 1D piecewise-uniform Shishkin mesh with N mesh-intervals in each spatial direction) and the time domain by an equidistant mesh. We prove that the resulting fully discrete scheme is ε -uniformly convergent in the discrete supremum norm. We further show that the order reduction in time associated with the classical evaluation of the time-dependent boundary conditions can be eliminated by the suitable choice of the boundary data. In addition to this, we implement the Richardson extrapolation solely for the time variable in order to increase the order of convergence in the temporal direction; and as a result, we obtain a globally second-order accurate numerical solution (in both space and time). Finally, we present the numerical results with the default and alternative choices for the boundary data to validate the theoretical findings. We also compare the accuracy of the proposed method with that of the implicit upwind method to show the robustness of the current algorithm.

3.1 Introduction

We consider the following class of two-dimensional singularly perturbed parabolic convection-diffusion-reaction IBVPs posed on the domain $D = G \times (0, T] = (0, 1)^2 \times (0, T]$; $\bar{G} = [0, 1]^2$:

$$\begin{cases} \left(\frac{\partial}{\partial t} + L_\varepsilon \right) u(x, y, t) = g(x, y, t), & (x, y, t) \in D, \\ u(x, y, 0) = q_0(x, y), & (x, y) \in \bar{G}, \\ u(x, y, t) = s(x, y, t), & (x, y, t) \in \partial G \times (0, T], \end{cases} \quad (3.1)$$

where

$$\begin{cases} L_\varepsilon u = -\varepsilon \Delta u + \vec{v}(x, y, t) \cdot \vec{\nabla} u + b(x, y, t)u, \\ \vec{v}(x, y, t) = (v_1(x, y, t), v_2(x, y, t)), \end{cases}$$

and ε is a small parameter such that $\varepsilon \in (0, 1]$. The coefficients $\vec{v}(x, y, t)$, $b(x, y, t)$ and the source term $g(x, y, t)$ are considered to be sufficiently smooth with

$$v_1(x, y, t) \geq m_1 > 0, \quad v_2(x, y, t) \geq m_2 > 0, \quad b(x, y, t) \geq \beta \geq 0, \quad \text{on } \bar{D}. \quad (3.2)$$

The solution of the IBVP (3.1)-(3.2) generally possesses exponential layers of width $O(\varepsilon)$ at the outflow boundaries $x = 1$ and $y = 1$ (see [77, 99]). We set $L_\varepsilon = L_{1,\varepsilon} + L_{2,\varepsilon}$, where the differential operators $L_{1,\varepsilon}$, $L_{2,\varepsilon}$ are defined by

$$\begin{cases} L_{1,\varepsilon} u = -\varepsilon \frac{\partial^2 u}{\partial x^2} + v_1(x, y, t) \frac{\partial u}{\partial x} + b_1(x, y, t)u, \\ L_{2,\varepsilon} u = -\varepsilon \frac{\partial^2 u}{\partial y^2} + v_2(x, y, t) \frac{\partial u}{\partial y} + b_2(x, y, t)u, \end{cases}$$

with $g = g_1 + g_2$, $b = b_1 + b_2$ with $b_i \geq \beta_i \geq 0$, for $i = 1, 2$. We further assume that the initial and boundary data of the problem are sufficiently smooth functions and also assume that necessary compatibility conditions hold among them in order to $u(x, y, t) \in C^{4+\gamma}(\bar{D})$, which has continuous derivatives up to fourth-order in space and second-order in time. The existence of the solution $u(x, y, t)$ of the IBVP (3.1)-(3.2) follows from [Chapter IV, §5] of the book [65] by Ladyzenskaja et al. The compatibility conditions are given below:

$$\begin{cases} s(x, y, 0) = q_0(x, y), & \text{on } \partial G, \\ \frac{\partial s(x, y, 0)}{\partial t} = -L_\varepsilon(0)q_0(x, y) + g(x, y, 0), & \text{on } \partial G \\ \frac{\partial^2 s(x, y, 0)}{\partial t^2} = -L_\varepsilon g(x, y, 0) + L_\varepsilon^2(0)q_0(x, y) + \frac{\partial g(x, y, 0)}{\partial t}, & \text{on } \partial G, \\ \frac{\partial s(x, y, t)}{\partial t} = -L_\varepsilon s(x, y, t) + g(x, y, t), & (x, y, t) \in \{0, 1\} \times \{0, 1\} \times (0, T]. \end{cases} \quad (3.3)$$

The rest of this chapter is structured as follows: Section 3.2 presents a priori bounds for the analytical solution and its derivatives. In Section 3.3, we introduce the time semidiscrete scheme, that uses the fractional implicit-Euler method and prove its uniform convergence. In order to avoid the order reduction while considering non-homogeneous boundary conditions, an appropriate evaluation of the boundary data is suggested. The fully discrete scheme is introduced in Section 3.4 and the description of an appropriate rectangular mesh is also given. Then, by combining the errors due to the spatial and temporal discretization, we deduce parameter-uniform convergence result of the fully discrete scheme. In Section 3.5, we discuss about the temporal Richardson extrapolation. Finally, the numerical results are presented in Section 3.6 for several test examples to validate the theoretical result. Here, we compare the accuracy of the present method with the implicit-upwind method given in [22]. The conclusion of this chapter is provided in Section 3.7.

3.2 Asymptotic behavior for the analytical solution

We decompose the solution $u(x, y, t)$ such that

$$u(x, y, t) = v(x, y, t) + w(x, y, t), \quad (x, y, t) \in \bar{D},$$

where v is the regular component and w is the singular component. Again, we consider the decomposition

$$w(x, y, t) = w_1(x, y, t) + w_2(x, y, t) + w_{11}(x, y, t), \quad (x, y, t) \in \bar{D},$$

where w_1 , w_2 are the exponential layers near the sides $x = 1$ and $y = 1$ of \bar{G} , respectively; and w_{11} is the corner layer near the point $(1, 1)$. Following the approach given in [24], one can show that the components of $u(x, y, t)$ satisfy the following bounds:

$$\left| \frac{\partial^{j+k} v(x, y, t)}{\partial x^{j_1} \partial y^{j_2} \partial t^k} \right| \leq C, \quad (3.4)$$

$$\left| \frac{\partial^{j+k} w_1(x, y, t)}{\partial x^{j_1} \partial y^{j_2} \partial t^k} \right| \leq C \varepsilon^{-j_1} \exp \left(-\frac{\mathfrak{m}_1(1-x)}{\varepsilon} \right), \quad (3.5)$$

$$\left| \frac{\partial^{j+k} w_2(x, y, t)}{\partial x^{j_1} \partial y^{j_2} \partial t^k} \right| \leq C \varepsilon^{-j_2} \exp \left(-\frac{\mathfrak{m}_2(1-y)}{\varepsilon} \right), \quad (3.6)$$

$$\left| \frac{\partial^{j+k} w_{11}(x, y, t)}{\partial x^{j_1} \partial y^{j_2} \partial t^k} \right| \leq C \varepsilon^{-j} \min \left\{ \exp \left(-\frac{\mathfrak{m}_1(1-x)}{\varepsilon} \right), \exp \left(-\frac{\mathfrak{m}_2(1-y)}{\varepsilon} \right) \right\}, \quad (3.7)$$

where $\forall j_1, j_2, k \in \mathbb{N} \cup \{0\}$, $j = j_1 + j_2$, $0 \leq j + 2k \leq 4$ and $(x, y, t) \in \bar{D}$.

Lemma 3.1. *The derivatives of the solution $u(x, y, t)$ of the IBVP (3.1)-(3.2) satisfy the following bounds:*

$$\left| \frac{\partial^k u(x, y, t)}{\partial t^k} \right| \leq C, \quad (3.8)$$

$$\left| \frac{\partial^{j_1} u(x, y, t)}{\partial x^{j_1}} \right| \leq C \varepsilon^{-j_1} \exp \left(-\frac{\mathfrak{m}_1(1-x)}{\varepsilon} \right), \quad (3.9)$$

$$\left| \frac{\partial^{j_2} u(x, y, t)}{\partial y^{j_2}} \right| \leq C \varepsilon^{-j_2} \exp \left(-\frac{\mathfrak{m}_2(1-y)}{\varepsilon} \right), \quad (3.10)$$

where $j = j_1 + j_2$, $0 \leq j + 2k \leq 4$ and $(x, y, t) \in \bar{D}$.

3.3 The time semidiscrete problem

In this section, we describe the numerical method to discretize the continuous problem (3.1)-(3.2) in the temporal direction. We discuss the stability; and provide the error analysis by proposing a suitable choice of the time-dependent boundary data instead of evaluating them classically in order to avoid the order reduction phenomena.

We consider an equidistant mesh, denoted by $\Lambda^{\Delta t} := \{t_n\}_{n=0}^M$ on the temporal domain $[0, T]$ with M mesh-

intervals such that $\Delta t = t_n - t_{n-1} = T/M$, $n = 1, \dots, M$. Let $u^n(x, y) \approx u(x, y, t_n)$. Then, the semidiscrete problem obtained by utilizing the fractional-steps implicit-Euler method which can be written as two half scheme is given below:

(i) (initial condition)

$$u^0(x, y) = q_0(x, y), \quad (x, y) \in \bar{G},$$

(ii) (first half)

$$\begin{cases} (\mathbf{I} + \Delta t \mathbf{L}_{1,\varepsilon}^{n+1}) u^{n+1/2}(x, y) = u^n(x, y) + \Delta t g_1(x, y, t_{n+1}), & (x, y) \in G, \\ u^{n+1/2}(x, y) = s^{n+1/2}(x, y), & (x, y) \in \{0, 1\} \times [0, 1], \end{cases} \quad (3.11)$$

(iii) (second half)

$$\begin{cases} (\mathbf{I} + \Delta t \mathbf{L}_{2,\varepsilon}^{n+1}) u^{n+1}(x, y) = u^{n+1/2}(x, y) + \Delta t g_2(x, y, t_{n+1}), & (x, y) \in G, \\ u^{n+1}(x, y) = s^{n+1}(x, y), & (x, y) \in [0, 1] \times \{0, 1\}, \end{cases}$$

for $n = 0, \dots, M - 1$, where the operators $\mathbf{L}_{1,\varepsilon}^{n+1}$ and $\mathbf{L}_{2,\varepsilon}^{n+1}$ are defined by

$$\begin{cases} \mathbf{L}_{1,\varepsilon}^{n+1} \equiv -\varepsilon \frac{\partial^2}{\partial x^2} + v_1(x, y, t_{n+1}) \frac{\partial}{\partial x} + b_1(x, y, t_{n+1}), \\ \mathbf{L}_{2,\varepsilon}^{n+1} \equiv -\varepsilon \frac{\partial^2}{\partial y^2} + v_2(x, y, t_{n+1}) \frac{\partial}{\partial y} + b_2(x, y, t_{n+1}). \end{cases}$$

The classical choice of the boundary conditions is given by

$$\begin{cases} s^{n+1/2}(x, y) = s(x, y, t_{n+1}), & (x, y) \in \{0, 1\} \times [0, 1], \\ s^{n+1}(x, y) = s(x, y, t_{n+1}), & (x, y) \in [0, 1] \times \{0, 1\}. \end{cases} \quad (3.12)$$

Here, we propose an alternative choice of the boundary data which is given by

$$\begin{cases} s^{n+1/2}(x, y) = (\mathbf{I} + \Delta t \mathbf{L}_{2,\varepsilon}^{n+1}) s(x, y, t_{n+1}) - \Delta t g_2(x, y, t_{n+1}), & (x, y) \in \{0, 1\} \times [0, 1], \\ s^{n+1}(x, y) = s(x, y, t_{n+1}), & (x, y) \in [0, 1] \times \{0, 1\}. \end{cases} \quad (3.13)$$

We show that the operators $(\mathbf{I} + \Delta t \mathbf{L}_{1,\varepsilon}^{n+1})$ and $(\mathbf{I} + \Delta t \mathbf{L}_{2,\varepsilon}^{n+1})$ satisfy the following maximum principle.

Lemma 3.2 (Maximum principle). *Let the function $\psi \in \mathcal{C}^0(\bar{G}) \cap \mathcal{C}^2(G)$ such that $\psi(x, y) \leq 0$ on ∂G and $(\mathbf{I} + \Delta t \mathbf{L}_{k,\varepsilon}^{n+1})\psi(x, y) \leq 0$, $k = 1, 2$, for all $(x, y) \in G$. Then, it implies that $\psi(x, y) \leq 0$ for all $(x, y) \in \bar{G}$.*

Proof. For the operator $(\mathbf{I} + \Delta t \mathbf{L}_{1,\varepsilon}^{n+1})$, we first prove the maximal principle. Let us fix $y \in [0, 1]$. Let $(x^*, y) \in \bar{G}$ such that

$$\psi(x^*, y) = \max_{(x^*, y) \in \bar{G}} \psi(x, y),$$

and without loss of generality, we assume that $\psi(x^*, y) > 0$. Now, in conformity with the hypothesis of the maximum principle, $\psi(x, y) \leq 0$ on ∂G , which implies that $(x^*, y) \in G$. Since $\frac{\partial \psi}{\partial x}(x^*, y) = 0$ and

$\frac{\partial^2 \psi}{\partial x^2}(x^*, y) \leq 0$, this gives that

$$(\mathbf{I} + \Delta t \mathbf{L}_{1,\varepsilon}^{n+1})\psi(x^*, y) > 0,$$

which is a contradiction to the hypothesis $(\mathbf{I} + \Delta t \mathbf{L}_{1,\varepsilon}^{n+1})\psi(x, y) \leq 0$, for all $(x, y) \in \mathbf{G}$. Hence, we proved the result for the operator $(\mathbf{I} + \Delta t \mathbf{L}_{1,\varepsilon}^{n+1})$. Similarly, one can prove the maximum principle for the operator $(\mathbf{I} + \Delta t \mathbf{L}_{2,\varepsilon}^{n+1})$. \blacksquare

The following result ensures the stability of the time semidiscrete scheme (3.11).

Lemma 3.3. *Let the function $\mathcal{Z} \in \mathcal{C}^0(\bar{\mathbf{G}}) \cap \mathcal{C}^2(\mathbf{G})$. Then, we have*

$$\|\mathcal{Z}\|_{\bar{\mathbf{G}}} \leq \|\mathcal{Z}\|_{\partial \mathbf{G}} + \frac{1}{1 + \beta_k \Delta t} \|(\mathbf{I} + \Delta t \mathbf{L}_{k,\varepsilon}^{n+1})\mathcal{Z}\|_{\bar{\mathbf{G}}},$$

where $k = 1, 2$.

Proof. Consider the following functions

$$\Psi^\pm(x, y) = -\|\mathcal{Z}\|_{\partial \mathbf{G}} - \frac{1}{(1 + \beta_k \Delta t)} \|(\mathbf{I} + \Delta t \mathbf{L}_{k,\varepsilon}^{n+1})\mathcal{Z}\|_{\bar{\mathbf{G}}} \pm \mathcal{Z}(x, y), \quad (x, y) \in \bar{\mathbf{G}},$$

where $k = 1, 2$. It is obvious that $\Psi^\pm(x, y) \leq 0$ on $\partial \mathbf{G}$, and

$$(\mathbf{I} + \Delta t \mathbf{L}_{k,\varepsilon}^{n+1})\Psi^\pm(x, y) \leq -\frac{1 + b_k \Delta t}{1 + \beta_k \Delta t} \|(\mathbf{I} + \Delta t \mathbf{L}_{k,\varepsilon}^{n+1})\mathcal{Z}\|_{\bar{\mathbf{G}}} \pm (\mathbf{I} + \Delta t \mathbf{L}_{k,\varepsilon}^{n+1})\mathcal{Z} \leq 0, \quad (x, y) \in \mathbf{G}.$$

By applying Lemma 3.2, we obtain the desired result. \blacksquare

3.3.1 Error analysis

Let us denote \tilde{e}^{n+1} as the local truncation error of the time semidiscrete scheme (3.11) at the time t_{n+1} , i.e., $\tilde{e}^{n+1}(x, y) = \tilde{u}^{n+1}(x, y) - u(x, y, t_{n+1})$, where \tilde{u}^{n+1} is the solution of the following auxiliary problem

$$\begin{aligned} (i) \quad & u^0(x, y) = \mathbf{q}_0(x, y), \quad (x, y) \in \bar{\mathbf{G}}, \\ (ii) \quad & \begin{cases} (\mathbf{I} + \Delta t \mathbf{L}_{1,\varepsilon}^{n+1})\tilde{u}^{n+1/2}(x, y) = u(x, y, t_n) + \Delta t g_1(x, y, t_{n+1}), & (x, y) \in \mathbf{G}, \\ \tilde{u}^{n+1/2}(x, y) = \mathbf{s}^{n+1/2}(x, y), & (x, y) \in \{0, 1\} \times [0, 1], \end{cases} \\ (iii) \quad & \begin{cases} (\mathbf{I} + \Delta t \mathbf{L}_{2,\varepsilon}^{n+1})\tilde{u}^{n+1}(x, y) = \tilde{u}^{n+1/2}(x, y) + \Delta t g_2(x, y, t_{n+1}), & (x, y) \in \mathbf{G}, \\ \tilde{u}^{n+1}(x, y) = \mathbf{s}^{n+1}(x, y), & (x, y) \in [0, 1] \times \{0, 1\}, \end{cases} \end{aligned} \quad (3.14)$$

for $n = 0, \dots, M - 1$.

Lemma 3.4 (Local error). *Under the alternative boundary data of $\mathbf{s}^{n+1/2}$ and \mathbf{s}^{n+1} given in (3.13), the local error \tilde{e}^{n+1} at the time level t_{n+1} satisfies that*

$$\|\tilde{e}^{n+1}\|_{\bar{\mathbf{G}}} \leq C(\Delta t)^2. \quad (3.15)$$

Proof. From (3.14), we easily deduce that

$$(\mathbf{I} + \Delta t \mathbf{L}_{1,\varepsilon}^{n+1}) \left((\mathbf{I} + \Delta t \mathbf{L}_{2,\varepsilon}^{n+1}) \tilde{u}^{n+1}(x, y) - \Delta t g_2(x, y, t_{n+1}) \right) = u(x, y, t_n) + \Delta t g_1(x, y, t_{n+1}). \quad (3.16)$$

We expand Taylor's series expansion of the function $u(x, y, t_n)$ in the temporal variable to obtain that

$$u(x, y, t_n) = u(x, y, t_{n+1}) - \Delta t \frac{\partial u(x, y, t_{n+1})}{\partial t} + O(\Delta t)^2,$$

and using equation (3.11), we write

$$(\mathbf{I} + \Delta t \mathbf{L}_{1,\varepsilon}^{n+1}) \left((\mathbf{I} + \Delta t \mathbf{L}_{2,\varepsilon}^{n+1}) u(x, y, t_{n+1}) - \Delta t g_2(x, y, t_{n+1}) \right) = u(x, y, t_n) + \Delta t g_1(x, y, t_{n+1}) + O(\Delta t)^2. \quad (3.17)$$

Subtracting equations (3.16) and (3.17), we get

$$(\mathbf{I} + \Delta t \mathbf{L}_{1,\varepsilon}^{n+1}) (\mathbf{I} + \Delta t \mathbf{L}_{2,\varepsilon}^{n+1}) \tilde{e}^{n+1}(x, y) = O(\Delta t)^2.$$

Now, by using the alternative boundary data given in (3.13), the local error can be written as the solution of a following problem:

$$\begin{cases} (\mathbf{I} + \Delta t \mathbf{L}_{1,\varepsilon}^{n+1}) \tilde{e}^{n+1/2}(x, y) = O(\Delta t)^2, & (x, y) \in \mathbf{G}, \\ \tilde{e}^{n+1/2}(0, y) = 0, \quad \tilde{e}^{n+1/2}(1, y) = 0, & y \in [0, 1], \end{cases} \quad (3.18)$$

$$\begin{cases} (\mathbf{I} + \Delta t \mathbf{L}_{2,\varepsilon}^{n+1}) \tilde{e}^{n+1}(x, y) = \tilde{e}^{n+1/2}(x, y), & (x, y) \in \mathbf{G}, \\ \tilde{e}^{n+1}(x, 0) = 0, \quad \tilde{e}^{n+1}(x, 1) = 0, & x \in [0, 1]. \end{cases} \quad (3.19)$$

From (3.18) and (3.19), using the stability property of Lemma 3.3, we get the desired estimate of the local error. ■

Let us denote $e^{n+1}(x, y)$ as the global error of the time semidiscrete scheme (3.11) at time t_{n+1} as usual *i.e.*, $e^{n+1}(x, y) = u(x, y, t_{n+1}) - u^{n+1}(x, y)$. The following result shows that the fractional-steps implicit-Euler method converges uniformly with first-order accurate in time.

Theorem 3.1 (Global error). *Under the alternative boundary data of $\mathbf{s}^{n+1/2}$ and \mathbf{s}^{n+1} given in (3.13), the global error e^{n+1} satisfies that*

$$\sup_{(n+1)\Delta t \leq T} \|e^{n+1}\|_{\bar{\mathbf{G}}} \leq C \Delta t.$$

Proof. We rewrite the global error as

$$e^{n+1}(x, y) = \tilde{e}^{n+1}(x, y) + d^{n+1}(x, y),$$

where the term $d^{n+1}(x, y) = \tilde{u}^{n+1}(x, y) - u^{n+1}(x, y)$ can be deduced from the following problems:

$$\begin{cases} (\mathbf{I} + \Delta t \mathbf{L}_{1,\varepsilon}^{n+1}) d^{n+1/2}(x, y) = e^n(x, y), & \text{in } \mathbf{G}, \\ d^{n+1/2}(0, y) = 0, \quad d^{n+1/2}(1, y) = 0, & \text{in } [0, 1], \end{cases} \quad (3.20)$$

and

$$\begin{cases} (\mathbf{I} + \Delta t \mathbf{L}_{2,\varepsilon}^{n+1}) d^{n+1}(x, y) = d^{n+1/2}(x, y), & \text{in } \mathbf{G}, \\ d^{n+1}(x, 0) = 0, \quad d^{n+1}(x, 1) = 0, & \text{in } [0, 1]. \end{cases} \quad (3.21)$$

Then, applying Lemma 3.3 to the equations (3.20) and (3.21), we obtain that

$$\|e^{n+1}\|_{\bar{\mathbf{G}}} \leq \|\tilde{e}^{n+1}\|_{\bar{\mathbf{G}}} + \frac{1}{(\mathbf{I} + \beta_1 \Delta t)(\mathbf{I} + \beta_2 \Delta t)} \|e^n\|_{\bar{\mathbf{G}}}.$$

Finally, using the above relation recursively and by invoking the consistency result in Lemma 3.4, we obtain the desired estimate of the global error. ■

Remark 3.1. In case of non-homogeneous boundary data $\mathbf{s}(x, y, t)$, we generally see that, $\mathbf{L}_{2,\varepsilon}^{n+1} \mathbf{s}(x, y, t_{n+1}) - g_2(x, y, t_{n+1}) \neq 0$, for $(x, y) \in \{0, 1\} \times [0, 1]$. This shows that, in the first half of (3.14), a term of size $O(\Delta t)$ appears as the difference between the classical choice (3.12) and the alternative choice (3.13) of the boundary data $\mathbf{s}^{n+1/2}(x, y)$. As a result, if the the natural choice of the boundary data is used, there is an order reduction in the global error which finally becomes $O(\Delta t)^0 = O(1)$.

3.4 The fully discrete problem

On the spatial domain $\bar{\mathbf{G}} = [0, 1]^2$, we construct a rectangular mesh $\bar{\mathbf{G}}^N = \bar{\mathbf{G}}_x^N \times \bar{\mathbf{G}}_y^N \subset \bar{\mathbf{G}}$, having $(N+1)^2$ mesh point as depicted in Fig 3.1. Here, $N \geq 4$ is an even positive integer; and $\bar{\mathbf{G}}_x^N$ and $\bar{\mathbf{G}}_y^N$ denote the appropriate piecewise-uniform Shishkin meshes, respectively in the x and y directions. The detail construction of $\bar{\mathbf{G}}_x^N$ is given below. We divide the spatial domain $[0, 1]$ into two sub-intervals as $[0, 1 - \eta_1]$ and $[1 - \eta_1, 1]$, where the transition parameter η_1 is defined by

$$\eta_1 = \min \left\{ \frac{1}{2}, \eta_{1,0} \varepsilon \ln N \right\},$$

and $\eta_{1,0}$ is a positive constant. In the analysis, we consider non-uniform mesh and for that we assume that $\eta_1 = \eta_{1,0} \varepsilon \ln N$. Now, on each sub-interval we introduce equidistant mesh with $N/2$ mesh-intervals such that

$$\bar{\mathbf{G}}_x^N = \{0 = x_0, x_1, \dots, x_{N/2} = 1 - \eta_1, \dots, x_N = 1\}.$$

Analogously, we define $\bar{\mathbf{G}}_y^N$ such that

$$\bar{\mathbf{G}}_y^N = \{0 = y_0, y_1, \dots, y_{N/2} = 1 - \eta_2, \dots, y_N = 1\},$$

where

$$\eta_2 = \min \left\{ \frac{1}{2}, \eta_{2,0} \varepsilon \ln N \right\}.$$

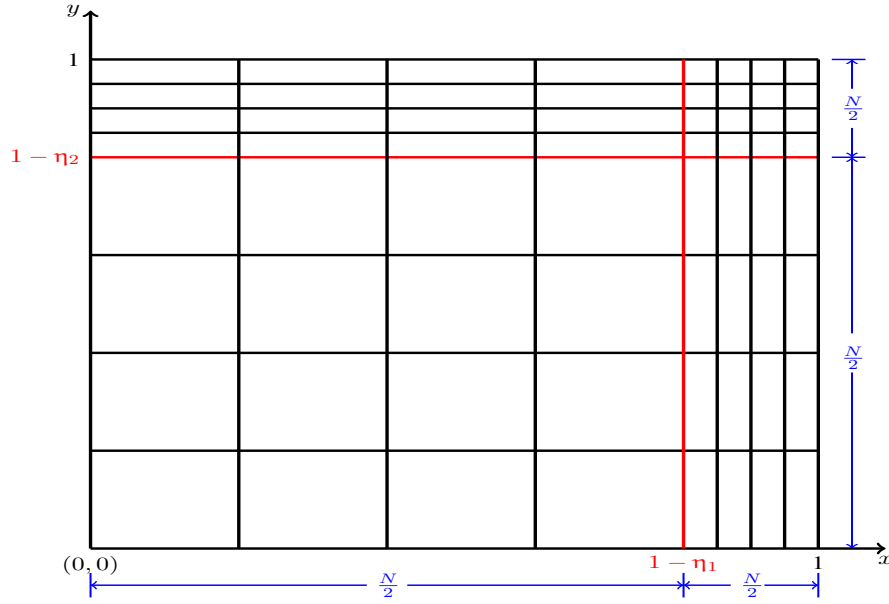


Figure 3.1: Shishkin mesh in the spatial direction

Further, the mesh widths in the spatial directions are denoted by

$$\begin{cases} h_{x_i} = x_i - x_{i-1}, & 1 \leq i \leq N, & h_{y_j} = y_j - y_{j-1}, & 1 \leq j \leq N, \\ \hat{h}_{x_i} = h_{x_i} + h_{x_{i+1}}, & 1 \leq i \leq N-1, & \hat{h}_{y_j} = h_{y_j} + h_{y_{j+1}}, & 1 \leq j \leq N-1. \end{cases}$$

Let $h_{x_i} = H_1 = \frac{2(1-\eta_1)}{N}$, $1 \leq i \leq N/2$ and $h_{y_j} = H_2 = \frac{2(1-\eta_2)}{N}$, $1 \leq j \leq N/2$. Also let $h_{x_i} = h_1 = \frac{2\eta_1}{N}$, $N/2 + 1 \leq i \leq N$ and $h_{y_j} = h_2 = \frac{2\eta_2}{N}$, $N/2 + 1 \leq j \leq N$.

3.4.1 Proposed fully discrete scheme

For a given function $\Psi_{i,j}^n = \Psi(x_i, y_j, t_n)$, defined on the mesh $\bar{D}^{N,\Delta t} = \bar{G}^N \times \Lambda^{\Delta t}$, we define $\Psi_{i-\frac{1}{2},j}^n = \frac{\Psi_{i,j}^n + \Psi_{i-1,j}^n}{2}$, $\Psi_{i,j-\frac{1}{2}}^n = \frac{\Psi_{i,j}^n + \Psi_{i,j-1}^n}{2}$. Also, we define $v_{1,i-1/2,j}^n = \frac{v_{1,i,j}^n + v_{1,i-1,j}^n}{2}$, $v_{2,i,j-1/2}^n = \frac{v_{2,i,j}^n + v_{2,i,j-1}^n}{2}$; and $b_{1,i-1/2,j}^n$, $b_{2,i,j-1/2}^n$, $g_{1,i-1/2,j}^n$, $g_{2,i,j-1/2}^n$ are defined similarly. Let us denote $G_x^N = \bar{G}_x^N \cap (0, 1)$ and $G_y^N = \bar{G}_y^N \cap (0, 1)$. In order to constitute the fully discrete scheme for the IBVP (3.1)-(3.2), we consider spatial discretization of (3.11) in each half by a new hybrid finite difference scheme. The scheme is composed of a modified central difference scheme whenever $\varepsilon > \|v_i\|N^{-1}$, $i = 1, 2$; and a combination of the midpoint upwind scheme in the outer region and the modified central difference scheme in the layer region whenever $\varepsilon \leq \|v_i\|N^{-1}$, $i = 1, 2$. On the mesh $\bar{D}^{N,\Delta t}$, the fully discrete scheme takes the

following form:

$$\begin{aligned}
(i) \quad & U_{i,j}^0 = \mathbf{q}_0(x_i, y_j), \quad \text{for } i, j = 0, 1, \dots, N, \\
(ii) \quad & \left\{ \begin{aligned}
& U_{i,j}^{n+1/2} + \Delta t L_{1,\varepsilon,mcd}^{n+1} U_{i,j}^{n+1/2} = U_{i,j}^n + \Delta t g_1(x_i, y_j, t_{n+1}), \\
& \quad \text{for } 1 \leq i \leq N/2, y_j \in \mathbb{G}_y^N \text{ and when } \varepsilon > \|v_1\| N^{-1}, \\
& U_{i-\frac{1}{2},j}^{n+1/2} + \Delta t L_{1,\varepsilon,mup}^{n+1} U_{i,j}^{n+1/2} = U_{i-\frac{1}{2},j}^n + \Delta t g_{1,i-\frac{1}{2},j}^{n+1}, \\
& \quad \text{for } 1 \leq i \leq N/2, y_j \in \mathbb{G}_y^N \text{ and when } \varepsilon \leq \|v_1\| N^{-1}, \\
& U_{i,j}^{n+1/2} + \Delta t L_{1,\varepsilon,mcd}^{n+1} U_{i,j}^{n+1/2} = U_{i,j}^n + \Delta t g_1(x_i, y_j, t_{n+1}), \\
& \quad \text{for } N/2 < i \leq N-1, y_j \in \mathbb{G}_y^N, \\
& U_{i,j}^{n+1/2} = \mathbf{s}^{n+1/2}(x_i, y_j), \quad \text{for } i = 0, N, y_j \in \bar{\mathbb{G}}_y^N,
\end{aligned} \right. \quad (3.22)
\end{aligned}$$

$$\begin{aligned}
(iii) \quad & \left\{ \begin{aligned}
& U_{i,j}^{n+1} + \Delta t L_{2,\varepsilon,mcd}^{n+1} U_{i,j}^{n+1} = U_{i,j}^{n+1/2} + \Delta t g_2(x_i, y_j, t_{n+1}), \\
& \quad \text{for } 1 \leq j \leq N/2, x_i \in \mathbb{G}_x^N \text{ and when } \varepsilon > \|v_2\| N^{-1}, \\
& U_{i,j-\frac{1}{2}}^{n+1} + \Delta t L_{2,\varepsilon,mup}^{n+1} U_{i,j}^{n+1} = U_{i,j-\frac{1}{2}}^{n+1/2} + \Delta t g_{2,i,j-\frac{1}{2}}^{n+1}, \\
& \quad \text{for } 1 \leq j \leq N/2, x_i \in \mathbb{G}_x^N \text{ and when } \varepsilon \leq \|v_2\| N^{-1}, \\
& U_{i,j}^{n+1} + \Delta t L_{2,\varepsilon,mcd}^{n+1} U_{i,j}^{n+1} = U_{i,j}^{n+1/2} + \Delta t g_2(x_i, y_j, t_{n+1}), \\
& \quad \text{for } N/2 < j \leq N-1, x_i \in \mathbb{G}_x^N, \\
& U_{i,j}^{n+1} = \mathbf{s}^{n+1}(x_i, y_j), \quad \text{for } j = 0, N, x_i \in \bar{\mathbb{G}}_x^N,
\end{aligned} \right.
\end{aligned}$$

where $\mathbf{s}^{n+1/2}, \mathbf{s}^{n+1}$ are defined in (3.13) and $L_{1,N,mcd}^{n+1}, L_{1,N,mup}^{n+1}, L_{2,N,mcd}^{n+1}, L_{2,N,mup}^{n+1}$ are given by

$$\left\{ \begin{aligned}
& L_{1,N,mcd}^{n+1} U_{i,j}^{n+1/2} = -\varepsilon \delta_x^2 U_{i,j}^{n+1/2} + v_1(x_i, y_j, t_{n+1}) D_x^* U_{i,j}^{n+1/2} + b_1(x_i, y_j, t_{n+1}) U_{i,j}^{n+1/2}, \\
& L_{1,N,mup}^{n+1} U_{i,j}^{n+1/2} = -\varepsilon \delta_x^2 U_{i,j}^{n+1/2} + v_{1,i-\frac{1}{2},j}^{n+1} D_x^- U_{i,j}^{n+1/2} + b_{1,i-\frac{1}{2},j}^{n+1} U_{i-\frac{1}{2},j}^{n+1/2}, \\
& L_{2,N,mcd}^{n+1} U_{i,j}^{n+1} = -\varepsilon \delta_y^2 U_{i,j}^{n+1} + v_2(x_i, y_j, t_{n+1}) D_y^* U_{i,j}^{n+1} + b_2(x_i, y_j, t_{n+1}) U_{i,j}^{n+1}, \\
& L_{2,N,mup}^{n+1} U_{i,j}^{n+1} = -\varepsilon \delta_y^2 U_{i,j}^{n+1} + v_{2,i,j-\frac{1}{2}}^{n+1} D_y^- U_{i,j}^{n+1} + b_{2,i,j-\frac{1}{2}}^{n+1} U_{i,j-\frac{1}{2}}^{n+1}.
\end{aligned} \right.$$

Let $\rho_{x_i} = \left(\varepsilon - \frac{v_1(x_i, y_j, t_{n+1})h_{x_i}}{2}\right)$ and $\rho_{y_j} = \left(\varepsilon - \frac{v_2(x_i, y_j, t_{n+1})h_{y_j}}{2}\right)$. Then, after rearranging the terms in (3.22), we obtain the following form of the difference scheme:

$$\left\{ \begin{array}{l} U_{i,j}^0 = \mathbf{q}_0(x_i, y_j), \quad \text{for } (x_i, y_j) \in \bar{\mathbf{G}}^N, \\ \left\{ \begin{array}{l} \mathbf{L}_{1,\varepsilon}^{N,\Delta t} U_{i,j}^{n+1/2} \equiv \mu_{x_i}^- U_{i-1,j}^{n+1/2} + \mu_{x_i}^c U_{i,j}^{n+1/2} + \mu_{x_i}^+ U_{i+1,j}^{n+1/2} = \mathbf{F}_1^{\Delta t}(x_i, y_j) \\ \text{for } 1 \leq i \leq N-1, y_j \in \mathbf{G}_y^N, \\ U_{i,j}^{n+1/2} = \mathbf{s}^{n+1/2}(x_i, y_j), \quad \text{for } i = 0, N, y_j \in \bar{\mathbf{G}}_y^N, \\ \mathbf{L}_{2,\varepsilon}^{N,\Delta t} U_{i,j}^{n+1} \equiv \mu_{y_j}^- U_{i,j-1}^{n+1} + \mu_{y_j}^c U_{i,j}^{n+1} + \mu_{y_j}^+ U_{i,j+1}^{n+1} = \mathbf{F}_2^{\Delta t}(x_i, y_j), \\ \text{for } 1 \leq j \leq N-1, x_i \in \mathbf{G}_x^N, \\ U_{i,j}^{n+1} = \mathbf{s}^{n+1}(x_i, y_j), \quad \text{for } j = 0, N, x_i \in \bar{\mathbf{G}}_x^N, \\ \text{for } n = 0, \dots, M-1, \end{array} \right. \end{array} \right. \quad (3.23)$$

where the right hand side terms $\mathbf{F}_1^{\Delta t}(x_i, y_j)$, $\mathbf{F}_2^{\Delta t}(x_i, y_j)$ in (3.23) are respectively given by

$$\mathbf{F}_1^{\Delta t}(x_i, y_j) = \left\{ \begin{array}{l} \frac{1}{2}(U_{i-1,j}^n + \Delta t \mathbf{g}_{1,i-1,j}^{n+1}) + \frac{1}{2}(U_{i,j}^n + \Delta t \mathbf{g}_{1,i,j}^{n+1}), \\ \text{for } 1 \leq i \leq N/2, \text{ and when } \varepsilon \leq \|v_1\|N^{-1}, \quad y_j \in \mathbf{G}_y^N, \\ U_{i,j}^n + \Delta t \mathbf{g}_{1,i,j}^{n+1}, \quad \text{for } 1 \leq i \leq N/2, \text{ and when } \varepsilon > \|v_1\|N^{-1}, \quad y_j \in \mathbf{G}_y^N, \\ U_{i,j}^n + \Delta t \mathbf{g}_{1,i,j}^{n+1}, \quad \text{for } N/2 < i \leq N-1, \quad y_j \in \mathbf{G}_y^N, \end{array} \right. \quad (3.24)$$

and

$$\mathbf{F}_2^{\Delta t}(x_i, y_j) = \left\{ \begin{array}{l} \frac{1}{2}(U_{i,j-1}^{n+1/2} + \Delta t \mathbf{g}_{2,i,j-1}^{n+1}) + \frac{1}{2}(U_{i,j}^{n+1/2} + \Delta t \mathbf{g}_{2,i,j}^{n+1}), \\ \text{for } 1 \leq j \leq N/2, \text{ and when } \varepsilon \leq \|v_2\|N^{-1}, \quad x_i \in \mathbf{G}_x^N, \\ U_{i,j}^{n+1/2} + \Delta t \mathbf{g}_{2,i,j}^{n+1}, \quad \text{for } 1 \leq j \leq N/2, \text{ and when } \varepsilon > \|v_2\|N^{-1}, \quad x_i \in \mathbf{G}_x^N, \\ U_{i,j}^{n+1/2} + \Delta t \mathbf{g}_{2,i,j}^{n+1}, \quad \text{for } N/2 < j \leq N-1, \quad x_i \in \mathbf{G}_x^N. \end{array} \right. \quad (3.25)$$

Here, the coefficients $\mu_{z_k}^-, \mu_{z_k}^c, \mu_{z_k}^+$ for $z_k = x_k/y_k$, $k = i$ or j and $l = 1, 2$ are given by

$$\left\{ \begin{array}{l} \mu_{z_k}^- = \Delta t \mu_{mcd, z_k}^-, \quad \mu_{z_k}^c = \Delta t \mu_{mcd, z_k}^c + 1, \quad \mu_{z_k}^+ = \Delta t \mu_{mcd, z_k}^+, \\ \text{for } 1 \leq k \leq N/2, \text{ and when } \varepsilon > \|v_l\| N^{-1}, \\ \mu_{z_k}^- = \Delta t \mu_{mup, z_k}^- + \frac{1}{2}, \quad \mu_{z_k}^c = \Delta t \mu_{mup, z_k}^c + \frac{1}{2}, \quad \mu_{z_k}^+ = \Delta t \mu_{mup, z_k}^+, \\ \text{for } 1 \leq k \leq N/2, \text{ and when } \varepsilon \leq \|v_l\| N^{-1}, \\ \mu_{z_k}^- = \Delta t \mu_{mcd, z_k}^-, \quad \mu_{z_k}^c = \Delta t \mu_{mcd, z_k}^c + 1, \quad \mu_{z_k}^+ = \Delta t \mu_{mcd, z_k}^+, \\ \text{for } N/2 < k \leq N-1, \end{array} \right. \quad (3.26)$$

where

$$\left\{ \begin{array}{l} \mu_{mup, z_k}^- = -\frac{2\varepsilon}{\tilde{h}_{z_k} h_{z_k}} - \frac{v_{1, i-\frac{1}{2}, j}^{n+1}}{h_{z_k}} + \frac{b_{1, i-\frac{1}{2}, j}^{n+1}}{2}, \\ \mu_{mup, z_k}^c = \frac{2\varepsilon}{h_{z_k} h_{z_{k+1}}} + \frac{v_{1, i-\frac{1}{2}, j}^{n+1}}{h_{z_k}} + \frac{b_{1, i-\frac{1}{2}, j}^{n+1}}{2}, \\ \mu_{mup, z_k}^+ = -\frac{2\varepsilon}{\tilde{h}_{z_k} h_{z_{k+1}}}, \end{array} \right. \text{ and } \left\{ \begin{array}{l} \mu_{mcd, z_k}^- = -\frac{2\rho_{z_k}}{\tilde{h}_{z_k} h_{z_k}} - \frac{v_{1, i, j}^{n+1}}{h_{z_k}}, \\ \mu_{mcd, z_k}^c = \frac{2\rho_{z_k}}{h_{z_k} h_{z_{k+1}}} + \frac{v_{1, i, j}^{n+1}}{h_{z_k}} + b_{1, i, j}^{n+1}, \\ \mu_{mcd, z_k}^+ = -\frac{2\rho_{z_k}}{\tilde{h}_{z_k} h_{z_{k+1}}}. \end{array} \right.$$

We show that the difference operators $L_{1, \varepsilon}^{N, \Delta t}$, $L_{2, \varepsilon}^{N, \Delta t}$ defined in (3.23) satisfy the following discrete maximum principle. Let $G^N = \bar{G}^N \cap G$ and $\partial G^N = \bar{G}^N \setminus G^N$.

Lemma 3.5 (Discrete maximum principle). *Suppose that the following conditions hold for $N \geq N_0$:*

$$\frac{N}{\ln N} > \eta_{k,0} \|v_k\| \quad \text{and} \quad m_k N \geq \left(\|b_k\| + \frac{1}{\Delta t} \right), \quad k = 1, 2, \quad (3.27)$$

where N_0 is a positive integer. If any mesh function $Z_{i,j} = Z(x_i, y_j)$ defined on \bar{G}^N satisfies that $Z_{i,j} \leq 0$ on ∂G^N and $L_{k, \varepsilon}^{N, \Delta t} Z_{i,j} \leq 0$, $k = 1, 2$, in G^N , then it implies that $Z_{i,j} \leq 0$ for all i, j .

Proof. At first, we prove the discrete maximum principle for the operator $L_{1, \varepsilon}^{N, \Delta t}$. Let us fix the index j and we denote $Z_{i,j} = Z_i$. Without loss of generality, we assume that the mesh function Z_i satisfies the following system:

$$\left\{ \begin{array}{l} L_{1, \varepsilon}^{N, \Delta t} Z_i = \omega_i, \quad \text{for } 1 \leq i \leq N-1, \\ Z_0 = \omega_0, \quad Z_N = \omega_N, \end{array} \right. \quad (3.28)$$

where $\omega_i \leq 0$, for $0 \leq i \leq N$. By adopting the approach given in [Chapter 2, Lemma 2.7], one can show that the matrix $\mathcal{A} \in \mathbb{R}^{N+1 \times N+1}$ associated with the coefficient of Z_i is an M-matrix. Since \mathcal{A} is also irreducible, $\mathcal{A}^{-1} \geq 0$. We thus obtain the desired result for the operator $L_{1, \varepsilon}^{N, \Delta t}$. Similarly, one can prove the maximum principle for the operator $L_{2, \varepsilon}^{N, \Delta t}$. ■

3.4.2 Error analysis

In the beginning, we study the asymptotic behavior of the analytical solution of the semidiscrete problem (3.14) and its derivatives. This will be used later to derive the bounds of the truncation errors $\mathcal{T}_{x_i, \tilde{u}^{n+1/2}}^{N, \Delta t}$ and $\mathcal{T}_{y_j, \tilde{u}^{n+1}}^{N, \Delta t}$. From Lemma 3.3, it is clear that $\|\tilde{u}^{n+1/2}\| \leq C$ and $\|\tilde{u}^{n+1}\| \leq C$, since $u(x, y, t_n), g_1, g_2, \mathbf{s}^{n+1/2}$ and \mathbf{s}^{n+1} are ε -uniformly bounded. At first, we deduce a priori bounds for $\tilde{u}^{n+1/2}(x, y)$ and its derivatives in the x -direction and also for $\tilde{u}^{n+1}(x, y)$ and its derivatives in the y -direction. For the proof of Lemma 3.6, apart from the requirement of ε -uniform boundedness and smoothness criteria on the given data, we also need certain compatibility conditions at $(0, t_n)$ and $(1, t_n)$ as mentioned in (3.38). Note that, we also take care of the presence of the non-homogeneous boundary data $\mathbf{s}^{n+1/2}, \mathbf{s}^{n+1}$, in the following derivations.

Lemma 3.6. *The solutions $\tilde{u}^{n+1/2}(x, y)$ and $\tilde{u}^{n+1}(x, y)$ of the time semidiscrete scheme (3.14) and their derivatives satisfy that*

$$\left| \frac{\partial^j \tilde{u}^{n+1/2}(x, y)}{\partial x^j} \right| \leq C(1 + \varepsilon^{-j} \exp(-\mathfrak{m}_1(1-x)/\varepsilon)), \quad j = 0, 1, 2, 3, 4, \quad (3.29)$$

and

$$\left| \frac{\partial^j \tilde{u}^{n+1}(x, y)}{\partial y^j} \right| \leq C(1 + \varepsilon^{-j} \exp(-\mathfrak{m}_2(1-y)/\varepsilon)), \quad j = 0, 1, 2, 3, 4, \quad (3.30)$$

for all $(x, y) \in \bar{\mathcal{G}}$.

Proof. We split up the proof into two parts. In the first part, we derive the result (3.29) for $\tilde{u}^{n+1/2}(x, y)$ and in the second part, the result (3.30) is established for $\tilde{u}^{n+1}(x, y)$.

Part-I: Consider the auxiliary BVP

$$(\mathbf{I} + \Delta t \mathbf{L}_{1, \varepsilon}^{n+1}) \zeta(x, y) = -\mathbf{L}_{1, \varepsilon}^{n+1} u(x, y, t_n) + g_1(x, y, t_{n+1}) \equiv \mathcal{H}_1(x, y), \quad (3.31)$$

where

$$\zeta(x, y) = \frac{\tilde{u}^{n+1/2}(x, y) - u(x, y, t_n)}{\Delta t},$$

with boundary conditions:

$$\begin{aligned} \zeta(0, y) &= \frac{\tilde{u}^{n+1/2}(0, y) - u(0, y, t_n)}{\Delta t}, \\ &= \frac{(\mathbf{I} + \Delta t \mathbf{L}_{2, \varepsilon}^{n+1}) \mathbf{s}(0, y, t_{n+1}) - \Delta t g_2(0, y, t_{n+1}) - \mathbf{s}(0, y, t_n)}{\Delta t}, \\ &= \mathbf{L}_{2, \varepsilon}^{n+1} \mathbf{s}(0, y, t_{n+1}) - g_2(0, y, t_{n+1}) + \frac{d\mathbf{s}(0, y, t_n)}{dt} + O(\Delta t), \end{aligned} \quad (3.32)$$

$$\zeta(1, y) = \mathbf{L}_{2, \varepsilon}^{n+1} \mathbf{s}(1, y, t_{n+1}) - g_2(1, y, t_{n+1}) + \frac{d\mathbf{s}(1, y, t_n)}{dt} + O(\Delta t). \quad (3.33)$$

Therefore, (3.31)-(3.33) reduces to the following form:

$$\begin{cases} (\mathbf{I} + \Delta t \mathbf{L}_{1,\varepsilon}^{n+1}) \zeta(x, y) = \mathcal{H}_1(x, y), \\ \zeta(0, y) = \mathbf{L}_{2,\varepsilon}^{n+1} \mathbf{s}(0, y, t_{n+1}) - g_2(0, y, t_{n+1}) + \frac{ds(0, y, t_n)}{dt} + O(\Delta t), \\ \zeta(1, y) = \mathbf{L}_{2,\varepsilon}^{n+1} \mathbf{s}(1, y, t_{n+1}) - g_2(1, y, t_{n+1}) + \frac{ds(1, y, t_n)}{dt} + O(\Delta t). \end{cases} \quad (3.34)$$

We see boundary conditions of problem (3.34) are $(\varepsilon, \Delta t)$ -uniformly bounded. Let $|\mathbf{L}_{1,\varepsilon}^{n+1} u(x, y, t_n)| \leq C$, then $|\mathcal{H}_1(x, y)| \leq C$. Hence, applying Lemma 3.3, we obtain that $|\zeta(x, y)| \leq C$. We have

$$\begin{cases} \mathbf{L}_{1,\varepsilon}^{n+1} \tilde{u}^{n+1/2}(x, y) = -\zeta(x, y) + g_1(x, y, t_{n+1}), & (x, y) \in \mathbf{G}, \\ \tilde{u}^{n+1/2}(0, y) = (\mathbf{I} + \Delta t \mathbf{L}_2^{n+1}) \mathbf{s}(0, y, t_{n+1}) - \Delta t g_2(0, y, t_{n+1}), \\ \tilde{u}^{n+1/2}(1, y) = (\mathbf{I} + \Delta t \mathbf{L}_2^{n+1}) \mathbf{s}(1, y, t_{n+1}) - \Delta t g_2(1, y, t_{n+1}). \end{cases} \quad (3.35)$$

Using the argument of Kellogg and Tsan technique [61], one can obtain that

$$\left| \frac{\partial \tilde{u}^{n+1/2}(x, y)}{\partial x} \right| \leq C \left[1 + \varepsilon^{-1} \exp(-\mathbf{m}_1(1-x)/\varepsilon) \right], \quad (x, y) \in \bar{\mathbf{G}}. \quad (3.36)$$

Let $\zeta_1(x, y) = \mathbf{L}_{1,\varepsilon}^{n+1} \zeta(x, y)$, which satisfies that

$$\begin{cases} (\mathbf{I} + \Delta t \mathbf{L}_{1,\varepsilon}^{n+1}) \zeta_1(x, y) = -(\mathbf{L}_{1,\varepsilon}^{n+1})^2 u(x, y, t_n) + \mathbf{L}_{1,\varepsilon}^{n+1} g_1(x, y, t_{n+1}) \equiv \mathcal{H}_2(x, y), \\ \zeta_1(0, y) = -\frac{\zeta(0, y)}{\Delta t} + \frac{1}{\Delta t} \left[g_1(0, y, t_{n+1}) - \mathbf{L}_{1,\varepsilon}^{n+1} u(0, y, t_n) \right], \\ \zeta_1(1, y) = -\frac{\zeta(1, y)}{\Delta t} + \frac{1}{\Delta t} \left[g_1(1, y, t_{n+1}) - \mathbf{L}_{1,\varepsilon}^{n+1} u(1, y, t_n) \right]. \end{cases} \quad (3.37)$$

Let $|\mathbf{L}_{1,\varepsilon}^{n+1})^2 u(x, y, t_n)| \leq C$, then $|\mathcal{H}_2(x, y)| \leq C$. Now, from the compatibility conditions (3.3), one can obtain that

$$\begin{aligned} \frac{ds(0, y, t_n)}{dt} &= -\mathbf{L}_\varepsilon^n \mathbf{s}(0, y, t_n) + g(0, y, t_n), \\ \frac{ds(1, y, t_n)}{dt} &= -\mathbf{L}_\varepsilon^n \mathbf{s}(1, y, t_n) + g(1, y, t_n). \end{aligned} \quad (3.38)$$

By using the equations (3.37) and (3.38), we get

$$\begin{cases} (\mathbf{I} + \Delta t \mathbf{L}_{1,\varepsilon}^{n+1}) \zeta_1(x, y) = \mathcal{H}_2(x, y), \\ \zeta_1(0, y) = \frac{\partial g(0, y, t_n)}{\partial t} - \mathbf{L}_{2,\varepsilon}^{n+1} \frac{\partial \mathbf{s}(0, y, t_n)}{\partial t} + C_1, \\ \zeta_1(1, y) = \frac{\partial g(1, y, t_n)}{\partial t} - \mathbf{L}_{2,\varepsilon}^{n+1} \frac{\partial \mathbf{s}(1, y, t_n)}{\partial t} + C_2, \end{cases} \quad (3.39)$$

where C_1 and C_2 are independent of ε and Δt . We see that $\mathcal{H}_2(x, y) = -(\mathbf{L}_{1,\varepsilon}^{n+1})^2 u(x, y, t_n) + \mathbf{L}_{1,\varepsilon}^{n+1} g_1(x, y, t_{n+1})$ is bounded (ε -uniformly) and boundary conditions are $(\varepsilon, \Delta t)$ -uniformly bounded. Hence, applying Lemma

3.3 , we obtain that $|\zeta_1(x, y)| \leq C$. Afterwards, one can deduce that

$$\left| \frac{\partial \zeta(x, y)}{\partial x} \right| \leq C \left[1 + \varepsilon^{-1} \exp(-\mathfrak{m}_1(1-x)/\varepsilon) \right], \quad (x, y) \in \bar{\mathbf{G}}, \quad (3.40)$$

by invoking Kellogg and Tsan technique [61] to the following BVP:

$$\begin{cases} \mathbf{L}_{1,\varepsilon}^{n+1} \zeta(x, y) = \zeta_1(x, y), \\ \zeta(0, y) = \mathbf{L}_{2,\varepsilon}^{n+1} \mathbf{s}(0, y, t_{n+1}) - \mathfrak{g}_2(0, y, t_{n+1}) + \frac{d\mathbf{s}(0, y, t_n)}{dt} + O(\Delta t), \\ \zeta(1, y) = \mathbf{L}_{2,\varepsilon}^{n+1} \mathbf{s}(1, y, t_{n+1}) - \mathfrak{g}_2(1, y, t_{n+1}) + \frac{d\mathbf{s}(1, y, t_n)}{dt} + O(\Delta t). \end{cases} \quad (3.41)$$

Now, differentiate (3.35) with respect to x , we consider that $\bar{\zeta}(x, y) = \frac{\partial \tilde{u}^{n+1/2}}{\partial x}$ satisfies the following problem

$$\begin{cases} \mathbf{L}_{1,\varepsilon}^{n+1} \bar{\zeta}(x, y) = \mathcal{H}_3(x, y), \\ \bar{\zeta}(0, y) = C_1, \quad \bar{\zeta}(1, y) = C_2 \varepsilon^{-1}, \end{cases} \quad (3.42)$$

where $\mathcal{H}_3(x, y) = -\frac{\partial \zeta(x, y)}{\partial x} + \frac{\partial \mathfrak{g}_1(x, y, t_{n+1})}{\partial x} - \frac{\partial v_1(x, y, t_{n+1})}{\partial x} \frac{\partial \tilde{u}^{n+1/2}}{\partial x} - \frac{\partial b_1(x, y, t_{n+1})}{\partial x} \tilde{u}^{n+1/2}(x, y)$ and we obtain that

$$|\mathcal{H}_3(x, y)| \leq C \left[1 + \varepsilon^{-1} \exp(-\mathfrak{m}_1(1-x)/\varepsilon) \right], \quad (x, y) \in \bar{\mathbf{G}}.$$

Again, using the argument of Kellogg and Tsan technique [61] for (3.42), we get

$$\left| \frac{\partial \bar{\zeta}(x, y)}{\partial x} \right| = \left| \frac{\partial^2 \tilde{u}^{n+1/2}(x, y)}{\partial x^2} \right| \leq C \left[1 + \varepsilon^{-2} \exp(-\mathfrak{m}_1(1-x)/\varepsilon) \right], \quad (x, y) \in \bar{\mathbf{G}}.$$

To establish result for $j = 3$, we follow the similar procedure. Firstly, we consider the function $\zeta_2(x, y) = (\mathbf{L}_{1,\varepsilon}^{n+1})^2 \zeta(x, y)$ as the solution of the following BVP:

$$\begin{cases} (\mathbf{I} + \Delta t \mathbf{L}_{1,\varepsilon}^{n+1}) \zeta_2(x, y) = -(\mathbf{L}_{1,\varepsilon}^{n+1})^3 u(x, y, t_n) + (\mathbf{L}_{1,\varepsilon}^{n+1})^2 \mathfrak{g}_1(x, y, t_{n+1}) \equiv \mathcal{H}_4(x, y), \\ \zeta_2(0, y) = \frac{1}{\Delta t} \left[-\mathbf{L}_{1,\varepsilon}^{n+1} \zeta(0, y) + \left(\mathbf{L}_{1,\varepsilon}^{n+1} \mathfrak{g}_1(0, y, t_{n+1}) - \mathbf{L}_{1,\varepsilon}^{n+1} \mathbf{L}_{1,\varepsilon}^{n+1} u(0, y, t_n) \right) \right], \\ \zeta_2(1, y) = \frac{1}{\Delta t} \left[-\mathbf{L}_{1,\varepsilon}^{n+1} \zeta(1, y) + \left(\mathbf{L}_{1,\varepsilon}^{n+1} \mathfrak{g}_1(1, y, t_{n+1}) - \mathbf{L}_{1,\varepsilon}^{n+1} \mathbf{L}_{1,\varepsilon}^{n+1} u(1, y, t_n) \right) \right]. \end{cases} \quad (3.43)$$

We simplify the boundary conditions of the problem (3.43) by using the compatibility conditions (3.38), to get

$$\begin{cases} (\mathbf{I} + \Delta t \mathbf{L}_{1,\varepsilon}^{n+1}) \zeta_2(x, y) = \mathcal{H}_4(x, y), \\ \zeta_2(0, y) = \left(\frac{1}{2} \mathbf{L}_{1,\varepsilon}^{n+1} \frac{\partial^2 \mathbf{s}}{\partial t^2} \right)(0, y, t_{n+1}) + \left(\mathbf{L}_{1,\varepsilon}^{n+1} \mathbf{L}_{1,\varepsilon}^{n+1} \frac{\partial \mathbf{s}}{\partial t} \right)(0, y, t_{n+1}) + O(\Delta t), \\ \zeta_2(1, y) = \left(\frac{1}{2} \mathbf{L}_{1,\varepsilon}^{n+1} \frac{\partial^2 \mathbf{s}}{\partial t^2} \right)(1, y, t_{n+1}) + \left(\mathbf{L}_{1,\varepsilon}^{n+1} \mathbf{L}_{1,\varepsilon}^{n+1} \frac{\partial \mathbf{s}}{\partial t} \right)(1, y, t_{n+1}) + O(\Delta t). \end{cases} \quad (3.44)$$

We see that $\mathcal{H}_4(x, y) = -(\mathbf{L}_{1,\varepsilon}^{n+1})^3 u(x, y, t_n) + (\mathbf{L}_{1,\varepsilon}^{n+1})^2 \mathfrak{g}_1(x, y, t_{n+1})$ is bounded (ε -uniformly) and boundary conditions are $(\varepsilon, \Delta t)$ -uniformly bounded. Hence, applying Lemma 3.3 , we obtain that $|\zeta_2(x, y)| \leq C$. Now,

similar arguments can be applied for the following BVP:

$$\begin{cases} \mathbf{L}_{1,\varepsilon}^{n+1} \zeta_1(x, y) = \zeta_2(x, y), \\ \zeta_1(0, y) = \frac{\partial g(0, y, t_n)}{\partial t} - \mathbf{L}_{2,\varepsilon}^{n+1} \frac{\partial \mathbf{s}(0, y, t_n)}{\partial t} + C_1, \\ \zeta_1(1, y) = \frac{\partial g(1, y, t_n)}{\partial t} - \mathbf{L}_{2,\varepsilon}^{n+1} \frac{\partial \mathbf{s}(1, y, t_n)}{\partial t} + C_2, \end{cases} \quad (3.45)$$

to prove that

$$\left| \frac{\partial^2 \zeta(x, y)}{\partial^2 x} \right| \leq C \left[1 + \varepsilon^{-2} \exp(-\mathbf{m}_1(1-x)/\varepsilon) \right], \quad (x, y) \in \bar{\mathbf{G}}. \quad (3.46)$$

Now, we differentiate (3.42) with respect to x , we consider that $\bar{\zeta}_1(x, y) = \frac{\partial^2 \tilde{u}^{n+1/2}(x, y)}{\partial x^2}$ satisfies the following problem:

$$\begin{cases} \mathbf{L}_{1,\varepsilon}^{n+1} \bar{\zeta}_1(x, y) = \mathcal{H}_5(x, y), \\ \bar{\zeta}_1(0, y) = C_1, \quad \bar{\zeta}_1(1, y) = C_2 \varepsilon^{-2}, \end{cases} \quad (3.47)$$

where $|\mathcal{H}_5(x, y)| \leq C \left[1 + \varepsilon^{-2} \exp(-\mathbf{m}_1(1-x)/\varepsilon) \right]$, $(x, y) \in \bar{\mathbf{G}}$. From the argument of Kellogg and Tsan technique [61] for (3.47), we get

$$\left| \frac{\partial \bar{\zeta}_1(x, y)}{\partial x} \right| = \left| \frac{\partial^3 \tilde{u}^{n+1/2}(x, y)}{\partial x^3} \right| \leq C \left[1 + \varepsilon^{-3} \exp(-\mathbf{m}_1(1-x)/\varepsilon) \right], \quad (x, y) \in \bar{\mathbf{G}}.$$

Similar way one can obtain the bound for $j = 4$.

We now derive the bound of $\tilde{u}^{n+1/2}(x, y)$ by differentiating the auxiliary BVP (3.14) at the first half with respect to y , and we get

$$\begin{cases} (\mathbf{I} + \Delta t \mathbf{L}_{1,\varepsilon}^{n+1}) \frac{\partial \tilde{u}^{n+1/2}(x, y)}{\partial y} = \frac{\partial u(x, y, t_n)}{\partial y} + \Delta t \frac{\partial g_1(x, y, t_{n+1})}{\partial y} - \frac{\partial v_1(x, y, t_{n+1})}{\partial y} \frac{\partial \tilde{u}^{n+1/2}(x, y)}{\partial x} \\ \quad - \frac{\partial b_1(x, y, t_{n+1})}{\partial y} \tilde{u}^{n+1/2}(x, y), \\ \frac{\partial \tilde{u}^{n+1/2}(0, y)}{\partial y} = (\mathbf{I} + \Delta t \mathbf{L}_2^{n+1}) \frac{\partial \mathbf{s}(0, y, t_{n+1})}{\partial y} + \Delta t \frac{\partial v_2(0, y, t_{n+1})}{\partial y} \frac{\partial \mathbf{s}(0, y, t_{n+1})}{\partial y} + \\ \quad \Delta t \frac{\partial b_2(0, y, t_{n+1})}{\partial y} \mathbf{s}(0, y, t_{n+1}) - \Delta t \frac{\partial g_2(0, y, t_{n+1})}{\partial y}, \quad y \in [0, 1], \\ \frac{\partial \tilde{u}^{n+1/2}(1, y)}{\partial y} = (\mathbf{I} + \Delta t \mathbf{L}_2^{n+1}) \frac{\partial \mathbf{s}(1, y, t_{n+1})}{\partial y} + \Delta t \frac{\partial v_2(1, y, t_{n+1})}{\partial y} \frac{\partial \mathbf{s}(1, y, t_{n+1})}{\partial y} + \\ \quad \Delta t \frac{\partial b_2(1, y, t_{n+1})}{\partial y} \mathbf{s}(1, y, t_{n+1}) - \Delta t \frac{\partial g_2(1, y, t_{n+1})}{\partial y}, \quad y \in [0, 1]. \end{cases} \quad (3.48)$$

The following bounds are proven by using the bounds of $\frac{\partial^j \tilde{u}^{n+1/2}(x, y)}{\partial x^j}$ for $j = 0, 1, 2, 3, 4$,

$$\left| \frac{\partial^j \tilde{u}^{n+1/2}(x, y)}{\partial y^j} \right| \leq C \left[1 + \varepsilon^{-j} \exp(-\mathbf{m}_2(1-y)/\varepsilon) \right], \quad (x, y) \in \bar{\mathbf{G}}, \text{ for } j = 0, 1, 2, 3, 4. \quad (3.49)$$

Part-II: Here, we prove the result (3.30) for $\tilde{u}^{n+1}(x, y)$. We suppose that, based on prior technical criterion,

$$\|\mathbf{L}_{2,\varepsilon}^{n+1} \tilde{u}^{n+1/2}(x, y)\|_{\bar{\mathbf{G}}} \leq C, \quad \|(\mathbf{L}_{2,\varepsilon}^{n+1})^2 \tilde{u}^{n+1/2}(x, y)\|_{\bar{\mathbf{G}}} \leq C, \quad \|(\mathbf{L}_{2,\varepsilon}^{n+1})^3 \tilde{u}^{n+1/2}(x, y)\|_{\bar{\mathbf{G}}} \leq C.$$

Define the following auxiliary boundary value problems:

$$\begin{cases} (\mathbf{I} + \Delta t \mathbf{L}_{2,\varepsilon}^{n+1}) \Lambda(x, y) = -\mathbf{L}_{2,\varepsilon}^{n+1} \tilde{u}^{n+1/2}(x, y) + \mathcal{G}_2(x, y, t_{n+1}) \equiv \mathcal{F}_1(x, y), \\ \Lambda(x, 0) = -\mathbf{L}_{2,\varepsilon}^{n+1} \mathbf{s}(x, 0, t_{n+1}) + \mathcal{G}_2(x, 0, t_{n+1}), \\ \Lambda(x, 1) = -\mathbf{L}_{2,\varepsilon}^{n+1} \mathbf{s}(x, 1, t_{n+1}) + \mathcal{G}_2(x, 1, t_{n+1}), \end{cases} \quad (3.50)$$

where $\Lambda(x, y) = \frac{\tilde{u}^{n+1}(x, y) - \tilde{u}^{n+1/2}(x, y)}{\Delta t}$. We see that boundary conditions are $(\varepsilon, \Delta t)$ -uniformly bounded and $|\mathcal{F}_1(x, y)| \leq C$. Hence, applying Lemma 3.3, we obtain that $|\Lambda(x, y)| \leq C$. We have

$$\begin{cases} \mathbf{L}_{2,\varepsilon}^{n+1} \tilde{u}^{n+1}(x, y) = -\Lambda(x, y) + \mathcal{G}_2(x, y, t_{n+1}), \\ \tilde{u}^{n+1}(x, 0) = \mathbf{s}(x, 0, t_{n+1}), \quad \tilde{u}^{n+1}(x, 1) = \mathbf{s}(x, 1, t_{n+1}). \end{cases} \quad (3.51)$$

Using the argument of Kellogg and Tsan technique [61], one can obtain that

$$\left| \frac{\partial \tilde{u}^{n+1}(x, y)}{\partial y} \right| \leq C \left[1 + \varepsilon^{-1} \exp(-\mathfrak{m}_2(1-y)/\varepsilon) \right] \quad (x, y) \in \bar{\mathbb{G}}. \quad (3.52)$$

We introduce the function $\Lambda_1(x, y) = \mathbf{L}_{2,\varepsilon}^{n+1} \Lambda(x, y)$, which is a solution of the following BVP:

$$\begin{cases} (\mathbf{I} + \Delta t \mathbf{L}_{2,\varepsilon}^{n+1}) \Lambda_1(x, y) = -(\mathbf{L}_{2,\varepsilon}^{n+1})^2 \tilde{u}^{n+1/2}(x, y) + \mathbf{L}_{2,\varepsilon}^{n+1} \mathcal{G}_2(x, y, t_{n+1}) \equiv \mathcal{F}_2(x, y), \\ \Lambda_1(x, 0) = -\mathbf{L}_{2,\varepsilon}^{n+1} \mathbf{L}_{2,\varepsilon}^{n+1} \mathbf{s}(x, 0, t_{n+1}) + \mathbf{L}_{2,\varepsilon}^{n+1} \mathcal{G}_2(x, 0, t_{n+1}), \\ \Lambda_1(x, 1) = -\mathbf{L}_{2,\varepsilon}^{n+1} \mathbf{L}_{2,\varepsilon}^{n+1} \mathbf{s}(x, 1, t_{n+1}) + \mathbf{L}_{2,\varepsilon}^{n+1} \mathcal{G}_2(x, 1, t_{n+1}). \end{cases} \quad (3.53)$$

We see that $\mathcal{F}_2(x, y) = -(\mathbf{L}_{2,\varepsilon}^{n+1})^2 \tilde{u}^{n+1/2}(x, y) + \mathbf{L}_{2,\varepsilon}^{n+1} \mathcal{G}_2(x, y, t_{n+1})$ is bounded (ε -uniformly) and boundary conditions are $(\varepsilon, \Delta t)$ -uniformly bounded. Hence, applying Lemma 3.3, we obtain that $|\Lambda_1(x, y)| \leq C$. Afterwards, one can deduce that

$$\left| \frac{\partial \Lambda(x, y)}{\partial y} \right| \leq C \left[1 + \varepsilon^{-1} \exp(-\mathfrak{m}_2(1-y)/\varepsilon) \right], \quad (x, y) \in \bar{\mathbb{G}}, \quad (3.54)$$

by invoking Kellogg and Tsan technique [61] to the following BVP:

$$\begin{cases} \mathbf{L}_{2,\varepsilon}^{n+1} \Lambda(x, y) = \Lambda_1(x, y), \\ \Lambda(x, 0) = -\mathbf{L}_{2,\varepsilon}^{n+1} \mathbf{s}(x, 0, t_{n+1}) + \mathcal{G}_2(x, 0, t_{n+1}), \\ \Lambda(x, 1) = -\mathbf{L}_{2,\varepsilon}^{n+1} \mathbf{s}(x, 1, t_{n+1}) + \mathcal{G}_2(x, 1, t_{n+1}). \end{cases} \quad (3.55)$$

For second order derivative bound of $\tilde{u}^{n+1}(x, y)$, we differentiate (3.51) with respect y , to get

$$\begin{cases} \mathbf{L}_{2,\varepsilon}^{n+1} \bar{\Lambda}(x, y) = \mathcal{F}_3(x, y), \\ \bar{\Lambda}(x, 0) = C_1, \quad \bar{\Lambda}(x, 1) = C_2 \varepsilon^{-1}, \end{cases} \quad (3.56)$$

where

$$\mathcal{F}_3(x, y) = -\frac{\partial \Lambda(x, y)}{\partial y} + \frac{\partial \mathcal{G}_2(x, y, t_{n+1})}{\partial y} - \frac{\partial v_2(x, y, t_{n+1})}{\partial y} \frac{\partial \tilde{u}^{n+1}(x, y)}{\partial y} - \frac{\partial b_2(x, y, t_{n+1})}{\partial y} \tilde{u}^{n+1}(x, y),$$

and $\bar{\Lambda}(x, y) = \frac{\partial \tilde{u}^{n+1}(x, y)}{\partial y}$. We obtain that $|\mathcal{F}_3(x, y)| \leq C[1 + \varepsilon^{-1} \exp(-\mathfrak{m}_2(1 - y)/\varepsilon)]$, $(x, y) \in \bar{\mathcal{G}}$. Applying the methodology of Kellogg and Tsan to (3.56), we deduce that

$$\left| \frac{\partial \bar{\Lambda}(x, y)}{\partial y} \right| = \left| \frac{\partial^2 \tilde{u}^{n+1}(x, y)}{\partial y^2} \right| \leq C[1 + \varepsilon^{-2} \exp(-\mathfrak{m}_2(1 - y)/\varepsilon)], \quad (x, y) \in \bar{\mathcal{G}}. \quad (3.57)$$

We introduce the function $\Lambda_2(x, y) = (\mathbf{L}_{2,\varepsilon}^{n+1})^2 \Lambda(x, y)$ which is solution of the following BVP:

$$\begin{cases} (\mathbf{I} + \Delta t \mathbf{L}_{2,\varepsilon}^{n+1}) \Lambda_2(x, y) = -(\mathbf{L}_{2,\varepsilon}^{n+1})^3 \tilde{u}^{n+1/2}(x, y) + (\mathbf{L}_{2,\varepsilon}^{n+1})^2 \mathcal{G}_2(x, y, t_{n+1}) \equiv \mathcal{F}_4(x, y), \\ \Lambda_2(x, 0) = -(\mathbf{L}_{2,\varepsilon}^{n+1})^3 \mathbf{s}(x, 0, t_{n+1}) + (\mathbf{L}_{2,\varepsilon}^{n+1})^2 \mathcal{G}_2(x, 0, t_{n+1}), \\ \Lambda_2(x, 1) = -(\mathbf{L}_{2,\varepsilon}^{n+1})^3 \mathbf{s}(x, 1, t_{n+1}) + (\mathbf{L}_{2,\varepsilon}^{n+1})^2 \mathcal{G}_2(x, 1, t_{n+1}). \end{cases} \quad (3.58)$$

We observe that $\mathcal{F}_4(x, y) = -(\mathbf{L}_{2,\varepsilon}^{n+1})^3 \tilde{u}^{n+1/2}(x, y) + (\mathbf{L}_{2,\varepsilon}^{n+1})^2 \mathcal{G}_2(x, y, t_{n+1})$ is bounded (ε -uniformly) and boundary conditions are $(\varepsilon, \Delta t)$ -uniformly bounded. Hence, applying Lemma 3.3, we obtain that $|\Lambda_2(x, y)| \leq C$. Now, similar arguments can be applied for the following BVP:

$$\begin{cases} \mathbf{L}_{2,\varepsilon}^{n+1} \Lambda_1(x, y) = \Lambda_2(x, y), \\ \Lambda_1(x, 0) = -\mathbf{L}_{2,\varepsilon}^{n+1} \mathbf{L}_{2,\varepsilon}^{n+1} \mathbf{s}(x, 0, t_{n+1}) + \mathbf{L}_{2,\varepsilon}^{n+1} \mathcal{G}_2(x, 0, t_{n+1}), \\ \Lambda_1(x, 1) = -\mathbf{L}_{2,\varepsilon}^{n+1} \mathbf{L}_{2,\varepsilon}^{n+1} \mathbf{s}(x, 1, t_{n+1}) + \mathbf{L}_{2,\varepsilon}^{n+1} \mathcal{G}_2(x, 1, t_{n+1}), \end{cases} \quad (3.59)$$

to prove that

$$\left| \frac{\partial^2 \Lambda(x, y)}{\partial y^2} \right| \leq C[1 + \varepsilon^{-2} \exp(-\mathfrak{m}_2(1 - y)/\varepsilon)], \quad (x, y) \in \bar{\mathcal{G}}. \quad (3.60)$$

To establish result for $j = 3$, we follow the similar procedure. Firstly, we differentiate (3.56) with respect to y and rewrite in the form

$$\begin{cases} \mathbf{L}_{2,\varepsilon}^{n+1} \bar{\Lambda}_1(x, y) = \mathcal{F}_5(x, y), \\ \bar{\Lambda}_1(x, 0) = C_1, \quad \bar{\Lambda}_1(x, 1) = C_2 \varepsilon^{-2}, \end{cases} \quad (3.61)$$

where $\bar{\Lambda}_1(x, y) = \frac{\partial^2 \tilde{u}^{n+1}(x, y)}{\partial y^2}$ and $|\mathcal{F}_5(x, y)| \leq C[1 + \varepsilon^{-2} \exp(-\mathfrak{m}_2(1 - x)/\varepsilon)]$, $(x, y) \in \bar{\mathcal{G}}$. Applying the same methodology of Kellogg and Tsan to (3.61) we deduce that

$$\left| \frac{\partial \bar{\Lambda}_1(x, y)}{\partial y} \right| = \left| \frac{\partial^3 \tilde{u}^{n+1}(x, y)}{\partial y^3} \right| \leq [1 + \varepsilon^{-3} \exp(-\mathfrak{m}_2(1 - y)/\varepsilon)]. \quad (3.62)$$

Similarly, way one can prove the bound for $j = 4$. ■

Lemma 3.7. *The exact solutions $\tilde{u}^{n+1/2}(x, y)$ and $\tilde{u}^{n+1}(x, y)$ of the time semidiscrete scheme (3.14) can be*

decomposed as

$$\begin{cases} \tilde{u}^{n+1/2}(x, y) = \tilde{p}^{n+1/2}(x, y) + \gamma_1 \tilde{q}^{n+1/2}(x, y), \\ \tilde{u}^{n+1}(x, y) = \tilde{p}^{n+1}(x, y) + \gamma_2 \tilde{q}^{n+1}(x, y), \end{cases}$$

where $y \in (0, 1)$ the components of $\tilde{u}^{n+1/2}(x, y)$ satisfy

$$\begin{cases} \left| \frac{\partial^j \tilde{p}^{n+1/2}}{\partial x^j} \right| \leq C \left(1 + \varepsilon^{-j+1} \exp\left(-\frac{\mathfrak{m}_1(1-x)}{\varepsilon}\right) \right), \quad j = 0, 1, 2, 3, 4, \\ \tilde{q}^{n+1}(x, y) = \exp(-v_1(1, y, t_{n+1})(1-x)/\varepsilon), \quad \gamma_1 = \frac{\varepsilon}{v_1(1, y, t_{n+1})} \frac{d\tilde{u}^{n+1}}{dx}(1, y), \end{cases}$$

and for $x \in (0, 1)$ the components of $\tilde{u}^{n+1}(x, y)$ satisfy

$$\begin{cases} \left| \frac{\partial^j \tilde{p}^{n+1}}{\partial y^j} \right| \leq C \left(1 + \varepsilon^{-j+1} \exp\left(-\frac{\mathfrak{m}_2(1-y)}{\varepsilon}\right) \right), \quad j = 0, 1, 2, 3, 4, \\ \tilde{q}^{n+1}(x, y) = \exp(-v_2(x, 1, t_{n+1})(1-y)/\varepsilon), \quad \gamma_2 = \frac{\varepsilon}{v_2(x, 1, t_{n+1})} \frac{d\tilde{u}^{n+1}}{dy}(x, 1), \end{cases}$$

Proof. The proof was carried out by using Lemma 3.6 and the approach described in ([24], Appendix A). ■

Next, we state several important lemmas which will be used in the next section.

Lemma 3.8. Consider the following mesh functions $\Theta_{l,k}(\lambda_l)$ with $l = 1, 2$

$$\begin{cases} \Theta_{1,k}(\lambda_1) = \prod_{j=k+1}^N \left(1 + \frac{\lambda_1 h_{x_k}}{\varepsilon} \right)^{-1}, \quad \text{for } 0 \leq k \leq N-1, \quad \Theta_{1,N}(\lambda_1) = 1, \\ \Theta_{2,k}(\lambda_2) = \prod_{j=k+1}^N \left(1 + \frac{\lambda_2 h_{y_k}}{\varepsilon} \right)^{-1}, \quad \text{for } 0 \leq k \leq N-1, \quad \Theta_{2,N}(\lambda_2) = 1, \end{cases}$$

where λ_l is a positive constant. Then, we have the following inequalities:

(i) If $\lambda_l < \mathfrak{m}_l/2$, then

$$\begin{cases} \exp(-\mathfrak{m}_1(1-x_k)/\varepsilon) \leq \Theta_{1,k}(\lambda_1), \quad \text{for } 0 \leq k \leq N-1, \\ \exp(-\mathfrak{m}_2(1-y_k)/\varepsilon) \leq \Theta_{2,k}(\lambda_2), \quad \text{for } 0 \leq k \leq N-1, \end{cases} \quad (3.63)$$

$$(ii) \quad \Theta_{l,N/2}(\lambda_l) \leq CN^{-\lambda_l \eta_{l,0}}, \quad (3.64)$$

for some constant C .

Proof. Use the arguments given in [84, Lemma 5] for the proof of (i) and (ii). ■

Lemma 3.9. *If $\lambda_l < m_l/2$, $l = 1, 2$, then under the hypothesis (3.27) of Lemma 3.5, it follows that*

$$\mathbf{L}_{l,\varepsilon}^{N,\Delta t} \Theta_{l,k}(\lambda_l) \geq \begin{cases} \frac{C\Delta t}{\varepsilon} \Theta_{2,k}(\lambda_l), & \text{for } 1 \leq k \leq N/2, \text{ and when } \varepsilon > \|v_l\|N^{-1}, \\ \frac{C\Delta t}{H_l} \Theta_{l,k}(\lambda_l), & \text{for } 1 \leq k \leq N/2, \text{ and when } \varepsilon \leq \|v_l\|N^{-1}, \\ \frac{C\Delta t}{\varepsilon} \Theta_{l,k}(\lambda_l), & \text{for } N/2 < k \leq N-1. \end{cases}$$

Proof. The argument given in [Chapter 2, Lemma 12] can be used to prove this lemma. ■

3.4.2.1 Error due to spatial discretization

In order to estimate the spatial error related to the fully discrete scheme (3.22), we consider the spatial discretization of the auxiliary problem (3.14) using the new finite difference scheme as described in Section 3.4.1. Hence, we obtain the following discrete problem:

$$\left\{ \begin{array}{l} \tilde{U}_{i,j}^0 = q_0(x_i, y_j), \quad 0 \leq i, j \leq N, \\ \left\{ \begin{array}{l} \mathbf{L}_{1,\varepsilon}^{N,\Delta t} \tilde{U}_{i,j}^{n+1/2} \equiv \mu_{x_i}^- \tilde{U}_{i-1,j}^{n+1/2} + \mu_{x_i}^c \tilde{U}_{i,j}^{n+1/2} + \mu_{x_i}^+ \tilde{U}_{i+1,j}^{n+1/2} = \tilde{\mathbf{F}}_1^{\Delta t}(x_i, y_j), \\ \qquad \qquad \qquad \text{for } 1 \leq i, j \leq N-1, \\ \tilde{U}^{n+1/2}(x, y) = \mathbf{s}^{n+1/2}(x, y), \quad (x, y) \in \{0, 1\} \times \bar{\mathbf{G}}_y^N, \\ \mathbf{L}_{2,\varepsilon}^{N,\Delta t} \tilde{U}_{i,j}^{n+1} \equiv \mu_{y_j}^- \tilde{U}_{i,j-1}^{n+1} + \mu_{y_j}^c \tilde{U}_{i,j}^{n+1} + \mu_{y_j}^+ \tilde{U}_{i,j+1}^{n+1} = \tilde{\mathbf{F}}_2^{n+1}(x_i, y_j), \\ \qquad \qquad \qquad \text{for } 1 \leq i, j \leq N-1, \\ \tilde{U}^{n+1}(x, y) = \mathbf{s}^{n+1}(x, y), \quad (x, y) \in \bar{\mathbf{G}}_x^N \times \{0, 1\}, \\ \text{for } n = 0, \dots, M-1, \end{array} \right. \end{array} \right. \quad (3.65)$$

where the coefficients $\mu_{x_i}^-, \mu_{x_i}^c, \mu_{x_i}^+, \mu_{y_j}^-, \mu_{y_j}^c, \mu_{y_j}^+$ are described in (3.26); and the terms $\tilde{\mathbf{F}}_1^{\Delta t}(x_i, y_j), \tilde{\mathbf{F}}_2^{\Delta t}(x_i, y_j)$ are respectively given by

$$\tilde{\mathbf{F}}_1^{\Delta t}(x_i, y_j) = \begin{cases} \frac{1}{2}(u(x_{i-1}, y_j, t_n) + \Delta t g_{1,i-1,j}^{n+1}) + \frac{1}{2}(u(x_i, y_j, t_n) + \Delta t g_{1,i,j}^{n+1}), \\ \qquad \qquad \qquad \text{for } 1 \leq i \leq N/2, \text{ and when } \varepsilon \leq \|v_1\|N^{-1}, \quad y_j \in \mathbf{G}_y^N, \\ u(x_i, y_j, t_n) + \Delta t g_{1,i,j}^{n+1}, \quad \text{for } 1 \leq i \leq N/2, \text{ and when } \varepsilon > \|v_1\|N^{-1}, \quad y_j \in \mathbf{G}_y^N, \\ u(x_i, y_j, t_n) + \Delta t g_{1,i,j}^{n+1}, \quad \text{for } N/2 < i \leq N-1, \quad y_j \in \mathbf{G}_y^N, \end{cases} \quad (3.66)$$

and

$$\tilde{F}_2^{\Delta t}(x_i, y_j) = \begin{cases} \frac{1}{2}(\tilde{U}_{i,j-1}^{n+1/2} + \Delta t g_{2,i,j-1}^{n+1}) + \frac{1}{2}(\tilde{U}_{i,j}^{n+1/2} + \Delta t g_{2,i,j}^{n+1}), \\ \quad \text{for } 1 \leq j \leq N/2, \text{ and when } \varepsilon \leq \|v_2\|N^{-1}, \quad x_i \in \mathbf{G}_x^N, \\ \tilde{U}_{i,j}^{n+1/2} + \Delta t g_{2,i,j}^{n+1}, \quad \text{for } 1 \leq j \leq N/2, \text{ and when } \varepsilon > \|v_2\|N^{-1}, \quad x_i \in \mathbf{G}_x^N, \\ \tilde{U}_{i,j}^{n+1/2} + \Delta t g_{2,i,j}^{n+1}, \quad \text{for } N/2 < j \leq N-1, \quad x_i \in \mathbf{G}_x^N. \end{cases} \quad (3.67)$$

At first, we derive the estimate for the local error $|\tilde{U}_{i,j}^{n+1/2} - \tilde{u}^{n+1/2}(x_i, y_j)|$. Here, for the discrete problem (3.65), the local truncation error at the first half is defined as

$$\begin{aligned} \mathcal{T}_{x_i, \tilde{u}^{n+1/2}}^{N, \Delta t} &= \mathbf{L}_{1, \varepsilon}^{N, \Delta t} [\tilde{U}_{i,j}^{n+1/2} - \tilde{u}^{n+1/2}(x_i, y_j)], \\ &= \begin{cases} \mu_{x_i}^- \tilde{U}_{i-1,j}^{n+1/2} + \mu_{x_i}^c \tilde{U}_{i,j}^{n+1/2} + \mu_{x_i}^+ \tilde{U}_{i+1,j}^{n+1/2} - \left(\tilde{u}^{n+1/2}(x_i, y_j) + \Delta t \mathbf{L}_{1, \varepsilon}^{n+1} \tilde{u}^{n+1/2}(x_i, y_j) \right), \\ \quad \text{for } 1 \leq i \leq N/2, \text{ and when } \varepsilon > \|v_1\|N^{-1}, \\ \mu_{x_i}^- \tilde{U}_{i-1,j}^{n+1/2} + \mu_{x_i}^c \tilde{U}_{i,j}^{n+1/2} + \mu_{x_i}^+ \tilde{U}_{i+1,j}^{n+1/2} - \frac{1}{2} \left(\tilde{u}^{n+1/2}(x_i, y_j) + \Delta t \mathbf{L}_{1, \varepsilon}^{n+1} \tilde{u}^{n+1/2}(x_i, y_j) \right) \\ \quad - \frac{1}{2} \left(\tilde{u}^{n+1/2}(x_{i-1}, y_j) + \Delta t \mathbf{L}_{1, \varepsilon}^{n+1} \tilde{u}^{n+1/2}(x_{i-1}, y_j) \right), \\ \quad \text{for } 1 \leq i \leq N/2, \text{ when } \varepsilon \leq \|v_1\|N^{-1}, \\ \mu_{x_i}^- \tilde{U}_{i-1,j}^{n+1/2} + \mu_{x_i}^c \tilde{U}_{i,j}^{n+1/2} + \mu_{x_i}^+ \tilde{U}_{i+1,j}^{n+1/2} - \left(\tilde{u}^{n+1/2}(x_i, y_j) + \Delta t \mathbf{L}_{1, \varepsilon}^{n+1} \tilde{u}^{n+1/2}(x_i, y_j) \right), \\ \quad \text{for } N/2 < i \leq N-1, \end{cases} \\ &= \begin{cases} \Delta t \left[\mathbf{L}_{1, N, mcd}^{n+1} \tilde{u}^{n+1/2}(x_i, y_j) - (\mathbf{L}_{1, \varepsilon}^{n+1} \tilde{u}^{n+1/2})(x_i, y_j) \right], \\ \quad \text{for } 1 \leq i \leq N/2, \text{ and when } \varepsilon > \|v_1\|N^{-1}, \\ \Delta t \left[\mathbf{L}_{1, N, mup}^{n+1} \tilde{u}^{n+1/2}(x_i, y_j) - (\mathbf{L}_{1, \varepsilon}^{n+1} \tilde{u}^{n+1/2})_{i-1/2, j} \right], \\ \quad \text{for } 1 \leq i \leq N/2, \text{ and when } \varepsilon \leq \|v_1\|N^{-1}, \\ \Delta t \left[\mathbf{L}_{1, N, mcd}^{n+1} \tilde{u}^{n+1/2}(x_i, y_j) - (\mathbf{L}_{1, \varepsilon}^{n+1} \tilde{u}^{n+1/2})(x_i, y_j) \right], \quad \text{for } N/2 < i \leq N-1. \end{cases} \quad (3.68) \end{aligned}$$

By using Lemma 3.7 and the arguments given in [Chapter 2, Lemma 2.10], we can deduce from (3.68) that

$$|\mathcal{T}_{x_i, \tilde{u}^{n+1/2}}^{N, \Delta t}| \leq \begin{cases} C\Delta t \left[H_1^2 + \varepsilon^{-1} \exp(-\mathfrak{m}_1(1 - x_i)/\varepsilon) \right], & \text{for } 1 \leq i < N/2, \text{ and when } \varepsilon > \|v_1\|N^{-1}, \\ C\Delta t \left[(\varepsilon + H_1)H_1 + H_1^{-1} \exp(-\mathfrak{m}_1(1 - x_{i+1})/\varepsilon) \right], & \text{for } 1 \leq i < N/2, \text{ and when } \varepsilon \leq \|v_1\|N^{-1}, \\ C\Delta t \left[(\varepsilon + H_1)H_1 + \varepsilon^{-1} \exp(-\mathfrak{m}_1(1 - x_i)/\varepsilon) \right], & \text{for } i = N/2, \text{ and when } \varepsilon > \|v_1\|N^{-1}, \\ C\Delta t \left[(\varepsilon + H_1)H_1 + \varepsilon^{-1} \exp(-\mathfrak{m}_1(1 - x_{i+1})/\varepsilon) \right], & \text{for } i = N/2, \text{ and when } \varepsilon \leq \|v_1\|N^{-1}, \\ C\Delta t \left[h_1^2 + h_1^2 \varepsilon^{-3} \exp(-\mathfrak{m}_1(1 - x_i)/\varepsilon) \right], & \text{for } N/2 < i \leq N - 1. \end{cases}$$

We now pursue the error analysis at the first half by considering two parts. We assume that $\lambda_1 < \mathfrak{m}_1/2$ and let $y_j \in \bar{\mathbf{G}}_y^N$.

Part-I: When $\varepsilon > \|v_1\|N^{-1}$, for sufficiently large C , we consider the following discrete function:

$$\Phi_{1,i}(\lambda_1) = C \left[H_1^2(1 + x_i) + H_1^2 \varphi_{1,i} + \Theta_{1,i}(\lambda_1) \right], \quad \text{for } 0 \leq i \leq N,$$

where

$$\varphi_{1,i} = \begin{cases} \frac{x_i}{1 - \eta_1}, & \text{for } 0 \leq i \leq N/2, \\ 1, & \text{for } N/2 \leq i \leq N. \end{cases}$$

Then, using the inequality (3.63) and Lemma 3.9, we get

$$\mathbf{L}_{1,\varepsilon}^{N, \Delta t} \Phi_{1,i}(\lambda_1) \geq |\mathcal{T}_{x_i, \tilde{u}^{n+1/2}}^{N, \Delta t}|, \quad \text{for } 1 \leq i \leq N - 1.$$

Thus, by applying Lemma 3.5 to $\Phi_{1,i}(\lambda_1) \pm (\tilde{U}_{i,j}^{n+1/2} - \tilde{u}^{n+1/2}(x_i, y_j))$, for $x_i \in \bar{\mathbf{G}}_x^N$, and using the inequality (3.63), we get

$$\begin{aligned} |\tilde{U}_{i,j}^{n+1/2} - \tilde{u}^{n+1/2}(x_i, y_j)| &\leq C \left[H_1^2 + \Theta_{1,N/2}(\lambda_1) \right], \\ &\leq C \left[N^{-2} + N^{-\lambda_1, \eta_1, 0} \right], \quad \text{for } 0 \leq i \leq N/2. \end{aligned} \tag{3.69}$$

When $\varepsilon \leq \|v_1\|N^{-1}$, for sufficiently large C , we consider the following discrete function:

$$\Psi_{1,i}(\lambda_1) = \begin{cases} C \left[(\varepsilon + H_1)H_1(1 + x_i) + \Theta_{1,i+1}(\lambda_1) \right], & \text{for } 0 \leq i \leq N/2, \\ C \left[(\varepsilon + H_1)H_1(1 + x_i) + \left(1 + \frac{\lambda_1 h_1}{\varepsilon}\right) \Theta_{1,i}(\lambda_1) \right], & \text{for } N/2 < i \leq N. \end{cases}$$

Since the assumption (3.27) yields $\mathfrak{m}_1 h_1 / \varepsilon < 2$, using the inequality (3.63) and Lemma 3.9, we have

$$\mathbf{L}_{1,\varepsilon}^{N,\Delta t} \Psi_{1,i}(\lambda_1) \geq |\mathcal{T}_{x_i, \tilde{u}^{n+1/2}}^{N,\Delta t}|, \quad \text{for } 1 \leq i \leq N-1.$$

Thus, by applying Lemma 3.5 to $\Psi_{1,i}(\lambda_1) \pm (\tilde{U}_{i,j}^{n+1/2} - \tilde{u}^{n+1/2}(x_i, y_j))$, for $x_i \in \bar{\mathbf{G}}_x^N$, and utilizing (3.64), $\mathfrak{m}_1 h_1 / \varepsilon < 2$, we have

$$\begin{aligned} |\tilde{U}_{i,j}^{n+1/2} - \tilde{u}^{n+1/2}(x_i, y_j)| &\leq C \left[(\varepsilon + H_1) H_1 + \left(1 + \frac{\lambda_1 h_1}{\varepsilon} \right) \Theta_{1,N/2}(\lambda_1) \right], \\ &\leq C \left[(\varepsilon + N^{-1}) N^{-1} + N^{-\lambda_1, \eta_{1,0}} \right], \quad \text{for } 0 \leq i \leq N/2. \end{aligned} \quad (3.70)$$

Part-II: For sufficiently large C , we consider the following discrete function:

$$\Upsilon_{1,i}(\lambda_1) = C \left[(N^{-2} + N^{-\lambda_1 \eta_{1,0}}) (1 + x_i) + h_1^2 \varepsilon^{-2} \Theta_{1,i}(\lambda_1) \right], \quad \text{for } N/2 \leq i \leq N.$$

Then, it implies that

$$\begin{cases} \Upsilon_{1,N/2}(\lambda_1) \geq |\tilde{U}_{N/2,j}^{n+1/2} - \tilde{u}^{n+1/2}(x_{N/2}, y_j)|, & \Upsilon_{1,N}(\lambda_1) \geq |\tilde{U}_{N,j}^{n+1/2} - \tilde{u}^{n+1/2}(x_N, y_j)|, \\ \mathbf{L}_{1,\varepsilon}^{N,\Delta t} \Upsilon_{1,i}(\lambda_1) \geq |\mathcal{T}_{x_i, \tilde{u}^{n+1/2}}^{N,\Delta t}|, & \text{for } N/2 + 1 \leq i \leq N-1, \end{cases}$$

and applying Lemma 3.5 to $\Upsilon_{1,i}(\lambda_1) \pm (\tilde{U}_{i,j}^{n+1/2} - \tilde{u}^{n+1/2}(x_i, y_j))$, for $x_i \in [1 - \eta_1, 1] \times \bar{\mathbf{G}}_x^N$, we obtain that

$$|\tilde{U}_{i,j}^{n+1/2} - \tilde{u}^{n+1/2}(x_i, y_j)| \leq C \left(\eta_{1,0}^2 N^{-2} \ln^2 N + N^{-\lambda_1 \eta_{1,0}} \right), \quad \text{for } N/2 + 1 \leq i \leq N. \quad (3.71)$$

Therefore, by combining (3.69), (3.70) and (3.71), we obtain the following estimate at $(n + \frac{1}{2})^{th}$ time level.

Lemma 3.10. *Let $y_j \in \bar{\mathbf{G}}_y^N$. If $\lambda_1 < \mathfrak{m}_1/2$, the local error associated with the discrete problem (3.65) at $(n + 1/2)^{th}$ time level satisfies the following estimate:*

$$|\tilde{U}_{i,j}^{n+1/2} - \tilde{u}^{n+1/2}(x_i, y_j)| \leq \begin{cases} C \left((N^{-1} + \chi_{1,\varepsilon}) N^{-1} + N^{-\lambda_1 \eta_{1,0}} \right), & \text{for } x_i \in [0, 1 - \eta_1] \cap \bar{\mathbf{G}}_x^N, \\ C \left(\eta_{1,0}^2 N^{-2} \ln^2 N + N^{-\lambda_1 \eta_{1,0}} \right), & \text{for } x_i \in (1 - \eta_1, 1] \cap \bar{\mathbf{G}}_x^N, \end{cases} \quad (3.72)$$

where

$$\chi_{1,\varepsilon} = \begin{cases} \varepsilon, & \text{when } \varepsilon \leq \|v_1\| N^{-1}, \\ 0, & \text{when } \varepsilon > \|v_1\| N^{-1}. \end{cases}$$

Next, we proceed to estimate the local error $|\tilde{U}_{i,j}^{n+1} - \tilde{u}^{n+1}(x_i, y_j)|$. Here, for the discrete problem (3.65), the

local truncation error at the second half is defined as

$$\begin{aligned}
\mathcal{T}_{y_j, \tilde{u}^{n+1}}^{N, \Delta t} &= \mathbf{L}_{2, \varepsilon}^{N, \Delta t} [\tilde{U}_{i, j}^{n+1} - \tilde{u}^{n+1}(x_i, y_j)] \\
&= \begin{cases} \tilde{U}_{i, j}^{n+1/2} - \tilde{u}^{n+1/2}(x_i, y_j) + \Delta t \left(\mathbf{L}_{2, \varepsilon}^{n+1} \tilde{u}^{n+1}(x_i, y_j) - \mathbf{L}_{2, N, mcd}^{n+1} \tilde{u}^{n+1}(x_i, y_j) \right), \\ \quad \text{for } 1 \leq j \leq N/2, \text{ when } \varepsilon > \|v_2\| N^{-1}, \\ \frac{1}{2} \left(\tilde{U}_{i, j}^{n+1/2} - \tilde{u}^{n+1/2}(x_i, y_j) \right) + \frac{1}{2} \left(\tilde{U}_{i, j-1}^{n+1/2} - \tilde{u}^{n+1/2}(x_i, y_{j-1}) \right) + \\ \quad \Delta t \left(\mathbf{L}_{2, \varepsilon}^{n+1} \tilde{u}^{n+1}(x_i, y_{j-1/2}) - \mathbf{L}_{2, N, mup}^{n+1} \tilde{u}^{n+1}(x_i, y_j) \right), \text{ for } 1 \leq j \leq N/2, \text{ when } \varepsilon \leq \|v_2\| N^{-1}, \\ \tilde{U}_{i, j}^{n+1/2} - \tilde{u}^{n+1/2}(x_i, y_j) + \Delta t \left(\mathbf{L}_{2, \varepsilon}^{n+1} \tilde{u}^{n+1}(x_i, y_j) - \mathbf{L}_{2, N, mcd}^{n+1} \tilde{u}^{n+1}(x_i, y_j) \right), \text{ for } N/2 < j < N. \end{cases}
\end{aligned} \tag{3.73}$$

From (3.72) and (3.73), we get the following bounds of the local truncation error for the $(n+1)^{th}$ time level.

For $1 \leq j < N/2$ and when $\varepsilon > \|v_2\| N^{-1}$,

$$\left| \mathcal{T}_{y_j, \tilde{u}^{n+1}}^{N, \Delta t} \right| \leq \begin{cases} C((N^{-1} + \chi_{1, \varepsilon})N^{-1} + N^{-\lambda_1 \eta_{1,0}}) + C\Delta t \left[H_2^2 + \varepsilon^{-1} \exp(-\mathfrak{m}_2(1 - y_j)/\varepsilon) \right], \\ \quad \text{for } 1 \leq i \leq N/2, \\ C(\eta_{1,0}^2 N^{-2} \ln^2 N + N^{-\lambda_1 \eta_{1,0}}) + C\Delta t \left[H_2^2 + \varepsilon^{-1} \exp(-\mathfrak{m}_2(1 - y_j)/\varepsilon) \right], \\ \quad \text{for } N/2 < i < N, \end{cases}$$

for $j = N/2$ and when $\varepsilon > \|v_2\| N^{-1}$,

$$\left| \mathcal{T}_{y_j, \tilde{u}^{n+1}}^{N, \Delta t} \right| \leq \begin{cases} C((N^{-1} + \chi_{1, \varepsilon})N^{-1} + N^{-\lambda_1 \eta_{1,0}}) + C\Delta t \left[(\varepsilon + H_2)H_2 + \varepsilon^{-1} \exp(-\mathfrak{m}_2(1 - y_{j+1})/\varepsilon) \right], \\ \quad \text{for } 1 \leq i \leq N/2, \\ C(\eta_{1,0}^2 N^{-2} \ln^2 N + N^{-\lambda_1 \eta_{1,0}}) + C\Delta t \left[(\varepsilon + H_2)H_2 + \varepsilon^{-1} \exp(-\mathfrak{m}_2(1 - y_{j+1})/\varepsilon) \right], \\ \quad \text{for } N/2 < i < N, \end{cases}$$

for $1 \leq j < N/2$ and when $\varepsilon \leq \|v_2\| N^{-1}$,

$$\left| \mathcal{T}_{y_j, \tilde{u}^{n+1}}^{N, \Delta t} \right| \leq \begin{cases} C((N^{-1} + \chi_{1, \varepsilon})N^{-1} + N^{-\lambda_1 \eta_{1,0}}) + C\Delta t \left[(\varepsilon + H_2)H_2 + H_2^{-1} \exp(-\mathfrak{m}_2(1 - y_{j+1})/\varepsilon) \right], \\ \quad \text{for } 1 \leq i \leq N/2, \\ C(\eta_{1,0}^2 N^{-2} \ln^2 N + N^{-\lambda_1 \eta_{1,0}}) + C\Delta t \left[(\varepsilon + H_2)H_2 + H_2^{-1} \exp(-\mathfrak{m}_2(1 - y_{j+1})/\varepsilon) \right], \\ \quad \text{for } N/2 < i < N, \end{cases}$$

for $j = N/2$ and when $\varepsilon \leq \|v_2\|N^{-1}$,

$$|\mathcal{T}_{y_j, \tilde{u}^{n+1}}^{N, \Delta t}| \leq \begin{cases} C((N^{-1} + \chi_{1, \varepsilon})N^{-1} + N^{-\lambda_1 \eta_{1,0}}) + C\Delta t \left[(\varepsilon + H_2)H_2 + \varepsilon^{-1} \exp(-\mathfrak{m}_2(1 - y_{j+1})/\varepsilon) \right], \\ \text{for } 1 \leq i \leq N/2, \\ C(\eta_{1,0}^2 N^{-2} \ln^2 N + N^{-\lambda_1 \eta_{1,0}}) + C\Delta t \left[(\varepsilon + H_2)H_2 + \varepsilon^{-1} \exp(-\mathfrak{m}_2(1 - y_{j+1})/\varepsilon) \right], \\ \text{for } N/2 < i < N, \end{cases}$$

and finally, for $N/2 < j < N$,

$$|\mathcal{T}_{y_j, \tilde{u}^{n+1}}^{N, \Delta t}| \leq \begin{cases} C((N^{-1} + \chi_{1, \varepsilon})N^{-1} + N^{-\lambda_1 \eta_{1,0}}) + C\Delta t \left[h_2^2 + h_2^2 \varepsilon^{-3} \exp(-\mathfrak{m}_2(1 - y_j)/\varepsilon) \right], \\ \text{for } 1 \leq i \leq N/2, \\ C(\eta_{1,0}^2 N^{-2} \ln^2 N + N^{-\lambda_1 \eta_{1,0}}) + C\Delta t \left[h_2^2 + h_2^2 \varepsilon^{-3} \exp(-\mathfrak{m}_2(1 - y_j)/\varepsilon) \right], \\ \text{for } N/2 < i < N. \end{cases}$$

In the following, we consider two parts: $x_i \in [0, 1 - \eta_1] \cap \bar{\mathbf{G}}_x^N$ and $x_i \in (1 - \eta_1, 1] \cap \bar{\mathbf{G}}_x^N$.

Part-I: Here, we consider two subparts.

(a) When $\varepsilon > \|v_2\|N^{-1}$, for sufficiently large C , we consider the following discrete function

$$\Phi_{2,j}(\lambda_2) = C \left[((N^{-1} + \chi_{1, \varepsilon})N^{-1} + N^{-\lambda_1 \eta_{1,0}}) (1 + y_j) + H_2^2 \varphi_{2,j} + \Theta_{2,j}(\lambda_2) \right], \quad \text{for } 0 \leq j \leq N,$$

where

$$\varphi_{2,j} = \begin{cases} \frac{y_j}{1 - \eta_2}, & \text{for } 0 \leq j \leq N/2, \\ 1, & \text{for } N/2 \leq j \leq N. \end{cases}$$

Then, from Lemma 3.9, and the inequality (3.63), we get

$$\mathbf{L}_{2, \varepsilon}^{N, \Delta t} \Phi_{2,j}(\lambda_2) \geq |\mathcal{T}_{y_j, \tilde{u}^{n+1}}^{N, \Delta t}|, \quad \text{for } 1 \leq j \leq N - 1.$$

Thus, by applying Lemma 3.5 to $\Phi_{2,j}(\lambda_2) \pm (\tilde{U}_{i,j}^{n+1} - \tilde{u}^{n+1}(x_i, y_j))$, for $y_j \in \bar{\mathbf{G}}_y^N$, and using the inequality (3.63), we get

$$|\tilde{U}_{i,j}^{n+1} - \tilde{u}^{n+1}(x_i, y_j)| \leq C \left[(N^{-1} + \chi_{1, \varepsilon})N^{-1} + N^{-2} + N^{-\lambda_1 \eta_{1,0}} + N^{-\lambda_2 \eta_{2,0}} \right], \quad \text{for } 0 \leq j \leq N/2.$$

When $\varepsilon \leq \|v_2\|N^{-1}$, for sufficiently large C , we consider the following discrete function

$$\Psi_{2,j}(\lambda_2) = \begin{cases} C \left[((N^{-1} + \chi_{1,\varepsilon})N^{-1} + N^{-\lambda_1\eta_{1,0}})(1 + y_j) + (\varepsilon + H_2)H_2(1 + y_j) + \Theta_{2,j+1}(\lambda_2) \right], & \text{for } 0 \leq j \leq N/2, \\ C \left[((N^{-1} + \chi_{1,\varepsilon})N^{-1} + N^{-\lambda_1\eta_{1,0}})(1 + y_j) + (\varepsilon + H_2)H_2(1 + y_j) + \left(1 + \frac{\lambda_2 h_2}{\varepsilon}\right) \Theta_{2,j}(\lambda_2) \right], & \text{for } N/2 \leq j \leq N. \end{cases}$$

Then, from Lemma 3.5, and the inequality (3.63), we get

$$\mathbf{L}_{2,\varepsilon}^{N,\Delta t} \Psi_{2,j}(\lambda_2) \geq |\mathcal{T}_{y_j, \tilde{u}^{n+1}}^{N,\Delta t}|, \quad \text{for } 1 \leq j \leq N-1.$$

Thus, by applying Lemma 3.5 to $\Psi_{2,j}(\gamma) \pm (\tilde{U}_{i,j}^{n+1} - \tilde{u}^{n+1}(x_i, y_j))$, for $y_j \in \bar{\mathbf{G}}_y^N$, and using (3.64), $\mathfrak{m}_2 h_2 / \varepsilon < 2$, we get

$$\begin{aligned} |\tilde{U}_{i,j}^{n+1} - \tilde{u}^{n+1}(x_i, y_j)| &\leq C \left[(N^{-1} + \chi_{1,\varepsilon})N^{-1} + \varepsilon H_2 + H_2^2 + N^{-\lambda_1\eta_{1,0}} + \Theta_{2,N/2}(\lambda_2) \right], \\ &\leq C \left((N^{-1} + \chi_{1,\varepsilon})N^{-1} + (\varepsilon + N^{-1})N^{-1} + N^{-\lambda_1\eta_{1,0}} + N^{-\lambda_2\eta_{2,0}} \right), \quad \text{for } 0 \leq j \leq N/2. \end{aligned}$$

(b) For sufficiently large C , we consider the following discrete function

$$\Upsilon_{2,j}(\lambda_2) = C \left[((N^{-1} + \chi_{1,\varepsilon})N^{-1} + N^{-\lambda_1\eta_{1,0}} + N^{-\lambda_1\eta_{2,0}})(1 + y_j) + h_2^2 \varepsilon^{-2} \Theta_{2,j}(\lambda_2) \right], \quad N/2 \leq j \leq N,$$

and by applying Lemma 3.5 to $\Upsilon_{2,j}(\gamma) \pm (\tilde{U}_{i,j}^{n+1} - \tilde{u}^{n+1}(x_i, y_j))$, over $[1 - \eta_2, 1] \cap \bar{\mathbf{G}}_y^N$, we have

$$\begin{aligned} |\tilde{U}_{i,j}^{n+1} - \tilde{u}^{n+1}(x_i, y_j)| &\leq \Upsilon_{2,j}(\lambda_2), \\ &\leq C \left[((N^{-1} + \chi_{1,\varepsilon})N^{-1} + \eta_{2,0}^2 N^{-2} \ln^2 N + N^{-\lambda_1\eta_{1,0}} + N^{-\lambda_2\eta_{2,0}}) \right], \quad N/2 + 1 \leq j \leq N. \end{aligned}$$

Part-II: As like the previous part, one can suitably choose $\Phi_{2,j}(\lambda_2)$, for $0 \leq j \leq N$, and when $\varepsilon > \|v_2\|N^{-1}$, $\Psi_{2,j}(\lambda_2)$, for $0 \leq j \leq N$, and when $\varepsilon \leq \|v_2\|N^{-1}$, $\Upsilon_{2,j}(\lambda_2)$, for $N/2 \leq j \leq N$, and arguing similar way as in the previous case, one can obtain the desired result. Therefore, from the above derivations, we deduce the following estimate at $(n+1)^{th}$ time level.

Lemma 3.11. *If $\lambda_l < \mathfrak{m}_l/2$, $l = 1, 2$, the local error associated with the discrete problem (3.65) at $(n+1)^{th}$*

time level satisfies the following estimate:

$$|\tilde{U}_{i,j}^{n+1} - \tilde{u}^{n+1}(x_i, y_j)| \leq \begin{cases} C\left((N^{-1} + \chi_{1,\varepsilon})N^{-1} + (N^{-1} + \chi_{2,\varepsilon})N^{-1} + N^{-\lambda_1\eta_{1,0}} + N^{-\lambda_2\eta_{2,0}}\right), \\ \quad \text{for } (x_i, y_j) \in ([0, 1 - \eta_1] \cap \bar{\mathbf{G}}_x^N) \times ([0, 1 - \eta_2] \cap \bar{\mathbf{G}}_y^N), \\ C\left((N^{-1} + \chi_{1,\varepsilon})N^{-1} + \eta_{2,0}^2 N^{-2} \ln^2 N + N^{-\lambda_1\eta_{1,0}} + N^{-\lambda_2\eta_{2,0}}\right), \\ \quad \text{for } (x_i, y_j) \in ([0, 1 - \eta_1] \cap \bar{\mathbf{G}}_x^N) \times ((1 - \eta_2, 1] \cap \bar{\mathbf{G}}_y^N), \\ C\left((N^{-1} + \chi_{2,\varepsilon})N^{-1} + \eta_{1,0}^2 N^{-2} \ln^2 N + N^{-\lambda_1\eta_{1,0}} + N^{-\lambda_2\eta_{2,0}}\right), \\ \quad \text{for } (x_i, y_j) \in ((1 - \eta_1, 1] \cap \bar{\mathbf{G}}_x^N) \times ([0, 1 - \eta_2] \cap \bar{\mathbf{G}}_y^N), \\ C\left((\eta_{1,0}^2 + \eta_{2,0}^2)N^{-2} \ln^2 N + N^{-\lambda_1\eta_{1,0}} + N^{-\lambda_2\eta_{2,0}}\right), \\ \quad \text{for } (x_i, y_j) \in ((1 - \eta_1, 1] \cap \bar{\mathbf{G}}_x^N) \times ((1 - \eta_2, 1] \cap \bar{\mathbf{G}}_y^N), \end{cases}$$

where

$$\chi_{1,\varepsilon} = \begin{cases} \varepsilon, & \text{when } \varepsilon \leq \|v_1\|N^{-1} \\ 0, & \text{when } \varepsilon > \|v_1\|N^{-1}, \end{cases} \quad \text{and} \quad \chi_{2,\varepsilon} = \begin{cases} \varepsilon, & \text{when } \varepsilon \leq \|v_2\|N^{-1} \\ 0, & \text{when } \varepsilon > \|v_2\|N^{-1}. \end{cases}$$

Corollary 3.1. Lemma 3.11 implies that for fixed $\eta_{l,0} \geq 2/\lambda_l$, $l = 1, 2$, and for some constant C

$$|\tilde{U}_{i,j}^{n+1} - \tilde{u}^{n+1}(x_i, y_j)| \leq \begin{cases} C(N^{-1} + \chi_{1,\varepsilon})N^{-1} + C(N^{-1} + \chi_{2,\varepsilon})N^{-1}, \\ \quad \text{for } (x_i, y_j) \in ([0, 1 - \eta_1] \times [0, 1 - \eta_2]) \cap \bar{\mathbf{G}}^N, \\ CN^{-2} \ln^2 N, \quad \text{otherwise.} \end{cases} \quad (3.74)$$

3.4.2.2 Uniform convergence of the fully discrete scheme

We define $E^{n+1}(x_i, y_j) = [U_{i,j}^{n+1} - u(x_i, y_j, t_{n+1})]$, for $(x_i, y_j) \in \bar{\mathbf{G}}^N$, as the global error related to the fully discrete scheme (3.22) at the time level t_{n+1} . Now, to show the ε -uniform convergence of the fully discrete scheme (3.22), we rewrite the global error in the following form:

$$E^{n+1}(x_i, y_j) = \tilde{e}^{n+1}(x_i, y_j) + \tilde{E}^{n+1}(x_i, y_j) + [U_{i,j}^{n+1} - \tilde{U}_{i,j}^{n+1}]. \quad (3.75)$$

Here, $\tilde{e}^{n+1}(x_i, y_j) = [\tilde{u}^{n+1}(x_i, y_j) - u(x_i, y_j, t_{n+1})]$ and $\tilde{E}^{n+1}(x_i, y_j) = [\tilde{U}_{i,j}^{n+1} - \tilde{u}^{n+1}(x_i, y_j)]$, respectively, denote the local error related to the time semidiscrete scheme and the spatial discretization of the auxiliary problem (3.14) at the time level t_{n+1} . The term $[U_{i,j}^{n+1} - \tilde{U}_{i,j}^{n+1}]$ can be written as the solution of the following systems:

$$\begin{cases} \mathbf{L}_{1,\varepsilon}^{N,\Delta t} \mathbf{L}_{2,\varepsilon}^{N,\Delta t} R^{n+1}(x_i, y_j) = U_{i,j}^n - u(x_i, y_j, t_n) + O(\Delta t)^2, & (x_i, y_j) \in \mathbf{G}^N, \\ R^{n+1}(x_i, y_j) = 0, & (x_i, y_j) \in \partial \mathbf{G}^N, \end{cases}$$

where $R^{n+1}(x_i, y_j) = [U_{i,j}^{n+1} - \tilde{U}_{i,j}^{n+1}]$, and by employing the discrete maximum principle in Lemma 3.5, we obtain that

$$\left\| \left\{ R^{n+1}(x_i, y_j) \right\}_{i,j} \right\| \leq \left\| \left\{ E^n(x_i, y_j) \right\}_{i,j} \right\| + C(\Delta t)^2. \quad (3.76)$$

Afterwards, from (3.75) and (3.76), we obtain that

$$\begin{aligned} \left\| \left\{ E^{n+1}(x_i, y_j) \right\}_{i,j} \right\| &\leq \left\| \left\{ \tilde{e}^{n+1}(x_i, y_j) \right\}_{i,j} \right\| + \left\| \left\{ \tilde{E}^{n+1}(x_i, y_j) \right\}_{i,j} \right\| + \left\| \left\{ E^n(x_i, y_j) \right\}_{i,j} \right\| + C(\Delta t)^2, \\ &\text{for } (x_i, y_j) \in \bar{\mathbf{G}}^N. \end{aligned} \quad (3.77)$$

Now, by invoking the estimate obtained in Lemma 3.4 and the estimate (3.74) in (3.77), with the assumption that $N^{-\delta} \leq C\Delta t$, $0 < \delta < 1$, we obtain the following estimate of the global error.

Theorem 3.2 (Global error). *Assume that the conditions given in (3.27) hold for $N \geq N_0$. Then, if $\lambda_l < \mathfrak{m}_l/2$, $\eta_{l,0} \geq 2/\lambda_l$, $l = 1, 2$, the global error associated with the fully discrete scheme (3.22) at time level t_{n+1} , satisfies the following estimate:*

$$\left\| \left\{ U_{i,j}^{n+1} \right\}_{i,j} - \left\{ u(x_i, y_j, t_{n+1}) \right\}_{i,j} \right\| \leq \begin{cases} C(N^{-2+\delta} + \chi_{1,\varepsilon} N^{-1+\delta} + \chi_{2,\varepsilon} N^{-1+\delta} + \Delta t), \\ \text{for } (x_i, y_j) \in ([0, 1 - \eta_1] \times [0, 1 - \eta_2]) \cap \bar{\mathbf{G}}^N, \\ C(N^{-2+\delta} \ln^2 N + \Delta t), \quad \text{for otherwise,} \end{cases} \quad (3.78)$$

where N and Δt are such that $N^{-\delta} \leq C\Delta t$ with $0 < \delta < 1$.

Remark 3.2. The error estimate (3.78) implies that the global error takes the form

$$U_{i,j}^{n+1} - u(x_i, y_j, t_{n+1}) = \begin{cases} O(N^{-2+\delta}) + O(\Delta t), & \text{for } (x_i, y_j) \in ([0, 1 - \eta_1] \times [0, 1 - \eta_2]) \cap \bar{\mathbf{G}}^N, \\ O(N^{-2+\delta} \ln^2 N) + O(\Delta t), & \text{for otherwise,} \end{cases} \quad (3.79)$$

not only for $\varepsilon \leq \|v_l\|N^{-1}$ but also for $\varepsilon > \|v_l\|N^{-1}$, $l = 1, 2$. Note that the temporal accuracy in (3.79) holds under the alternative boundary data given in (3.13).

3.5 Error analysis for temporal Richardson extrapolation

In this section, we analyze the Richardson extrapolation in the time variable in order to improve the order of uniform convergence in the temporal direction established in Theorem 3.1 so that we can produce higher-order accurate numerical solution at low computational cost. On the domain $[0, T]$, we construct a fine mesh, denoted by $\Lambda^{\Delta t/2} = \{\tilde{t}_n\}_{n=0}^{2M}$, by bisecting each mesh interval of $\Lambda^{\Delta t}$. So, $\tilde{t}_{n+1} - \tilde{t}_n = T/2M = \Delta t/2$ is the step-size. Let $U^{N,\Delta t}(x_i, y_j, t_{n+1})$ and $U^{N,\Delta t/2}(x_i, y_j, \tilde{t}_{n+1})$ be the respective solutions of the fully discrete problem

(3.22) on the mesh $\bar{\mathbf{G}}^N \times \Lambda^{\Delta t}$ and $\bar{\mathbf{G}}^N \times \Lambda^{\Delta t/2}$. Then, from (3.79), on $\bar{\mathbf{G}}^N \times \Lambda^{\Delta t}$ we have

$$\left\{ \begin{array}{l} \left(2U^{N,\Delta t/2}(x_i, y_j, t_{n+1}) - U^{N,\Delta t}(x_i, y_j, t_{n+1}) \right) - u(x_i, y_j, t_{n+1}) = o(\Delta t) + O(N^{-2+\delta}), \\ \quad \text{for } (x_i, y_j) \in ([0, 1 - \eta_1] \times [0, 1 - \eta_2]) \cap \bar{\mathbf{G}}^N, \\ \left(2U^{N,\Delta t/2}(x_i, y_j, t_{n+1}) - U^{N,\Delta t}(x_i, y_j, t_{n+1}) \right) - u(x_i, y_j, t_{n+1}) = o(\Delta t) + O(N^{-2+\delta} \ln^2 N), \\ \quad \text{for otherwise.} \end{array} \right. \quad (3.80)$$

Remark 3.3. We set $U_{extp}^{N,\Delta t}(x_i, y_j, t_{n+1}) = \left(2U^{N,\Delta t/2}(x_i, y_j, t_{n+1}) - U^{N,\Delta t}(x_i, y_j, t_{n+1}) \right)$ as the extrapolation formula so that the time accuracy can be improved from $O(\Delta t)$ to $O(\Delta t^k)$, $k > 1$. To determine the exact value of k , we analyze the global error related to temporal extrapolation of the solution to the time semidiscrete problem 3.11. However, it is clear from (3.80) that the spatial accuracy remains unchanged due to the Richardson extrapolation only in time variable.

Now, let $u^{\Delta t}(x, y, t_{n+1})$ and $u^{\Delta t/2}(x, y, \tilde{t}_{n+1})$ be the respective solutions of the time-semidiscrete problem (3.11) on the mesh $\bar{\mathbf{G}} \times \Lambda^{\Delta t}$ and $\bar{\mathbf{G}} \times \Lambda^{\Delta t/2}$, such that $u^{\Delta t}(x_i, y_j, t_{n+1}) \approx U^{N,\Delta t}(x_i, y_j, t_{n+1})$ and $u^{\Delta t/2}(x_i, y_j, \tilde{t}_{n+1}) \approx U^{N,\Delta t/2}(x_i, y_j, \tilde{t}_{n+1})$, $(x_i, y_j) \in \bar{\mathbf{G}}^N$. Utilizing the global error in Theorem 3.1, one can show that when $\Delta t \rightarrow 0$, the following relation holds for the global error of the time semidiscrete scheme (3.11):

$$u^{\Delta t}(x, y, t_{n+1}) = u(x, y, t_{n+1}) + \Delta t \Psi(x, y, t_{n+1}) + \mathbf{R}(x, y, t_{n+1}), \quad (3.81)$$

where Ψ is a certain smooth function defined on $\bar{\mathbf{G}} \times \Lambda^{\Delta t}$ and independent of Δt ; \mathbf{R} is the remainder term defined on $\bar{\mathbf{G}} \times \Lambda^{\Delta t}$. We begin by assuming that the expansion (3.81) is valid. We substitute $u^{\Delta t}(x, y, t_{n+1})$ in (3.11) and obtain that

$$\left\{ \begin{array}{l} u(x, y, 0) + \Delta t \Psi(x, y, 0) + \mathbf{R}(x, y, 0) = \mathbf{q}_0(x, y), \quad (x, y) \in \bar{\mathbf{G}}, \\ (\mathbf{I} + \Delta t \mathbf{L}_{1,\varepsilon}^{n+1}) \left[(\mathbf{I} + \Delta t \mathbf{L}_{2,\varepsilon}^{n+1}) (u(x, y, t_{n+1}) + \Delta t \Psi(x, y, t_{n+1}) + \mathbf{R}(x, y, t_{n+1})) - \Delta t \mathbf{g}_2(x, y, t_{n+1}) \right] = \\ u(x, y, t_n) + \Delta t \Psi(x, y, t_n) + \mathbf{R}(x, y, t_n) + \Delta t \mathbf{g}_1(x, y, t_{n+1}), \quad (x, y) \in \mathbf{G}, \\ u(x, y, t_{n+1}) + \Delta t \Psi(x, y, t_{n+1}) + \mathbf{R}(x, y, t_{n+1}) = \mathbf{s}(x, y, t_{n+1}), \quad (x, y) \in \partial \mathbf{G} \times \Lambda^{\Delta t}, \\ n = 0, 1, \dots, M-1. \end{array} \right. \quad (3.82)$$

By following the approach in [104, 60] to the problem (3.82), we get the function $\Psi(x, y, t)$ is the solution of the following IBVP:

$$\left\{ \begin{array}{l} \left(\frac{\partial}{\partial t} + \mathbf{L}_\varepsilon \right) \Psi(x, y, t) = \frac{1}{2} \frac{\partial^2 u(x, y, t)}{\partial t^2} + \mathbf{L}_{1,\varepsilon} \mathbf{g}_2(x, y, t) - \mathbf{L}_{1,\varepsilon} \mathbf{L}_{2,\varepsilon} u(x, y, t), \quad (x, y, t) \in \mathbf{D}, \\ \Psi(x, y, 0) = 0, \quad (x, y) \in \bar{\mathbf{G}}, \\ \Psi(x, y, t) = 0, \quad \text{in } \partial \mathbf{G} \times (0, T]. \end{array} \right. \quad (3.83)$$

Since $\frac{1}{2} \frac{\partial^2 u(x, y, t)}{\partial t^2} + \mathbf{L}_{1,\varepsilon} \mathbf{g}_2(x, y, t) - \mathbf{L}_{1,\varepsilon} \mathbf{L}_{2,\varepsilon} u(x, y, t)$ is ε -uniformly bounded, one can derive that $\|\Psi(x, y, t)\|_{\bar{\mathbf{D}}} \leq$

C . To establish the bounds of the derivatives up to second order in time in Lemma 3.12, we require $\Psi(x, y, t) \in \mathcal{C}^{4+\gamma}(\bar{\mathcal{D}})$.

Lemma 3.12. *The function $\Psi(x, y, t)$ solution of (3.83) satisfies the bounds*

$$\left| \frac{\partial^k \Psi(x, y, t)}{\partial t^k} \right| \leq C, \quad k = 0, 1, 2.$$

Proof. The proof of this lemma is obtained by using the argument given in [20]. ■

Lemma 3.13. *The remainder term $\mathcal{R}(x, y, t)$ given in (3.81), satisfies the bound*

$$|\mathcal{R}(x, y, t_n)| \leq C(\Delta t)^2, \quad 0 \leq n \leq M. \quad (3.84)$$

Proof. From the equation (3.82), we get

$$\begin{aligned} & (\mathcal{I} + \Delta t \mathcal{L}_{1,\varepsilon}^{n+1})(\mathcal{I} + \Delta t \mathcal{L}_{2,\varepsilon}^{n+1})u(x, y, t_{n+1}) + \Delta t(\mathcal{I} + \Delta t \mathcal{L}_{1,\varepsilon}^{n+1})(\mathcal{I} + \Delta t \mathcal{L}_{2,\varepsilon}^{n+1})\Psi(x, y, t_{n+1}) + \\ & (\mathcal{I} + \Delta t \mathcal{L}_{1,\varepsilon}^{n+1})(\mathcal{I} + \Delta t \mathcal{L}_{2,\varepsilon}^{n+1})\mathcal{R}(x, y, t_{n+1}) = \\ & u(x, y, t_n) + \Delta t \Psi(x, y, t_n) + \mathcal{R}(x, y, t_n) + \Delta t g_1(x, y, t_{n+1}). \end{aligned}$$

Further simplification yields that

$$\begin{aligned} & u(x, y, t_{n+1}) + \Delta t \Psi(x, y, t_{n+1}) + \Delta t \mathcal{L}_{\varepsilon}^{n+1}u(x, y, t_{n+1}) + (\Delta t)^2 \mathcal{L}_{\varepsilon}^{n+1}\Psi(x, y, t_{n+1}) + \\ & (\mathcal{I} + \Delta t \mathcal{L}_{1,\varepsilon}^{n+1})(\mathcal{I} + \Delta t \mathcal{L}_{2,\varepsilon}^{n+1})\mathcal{R}(x, y, t_{n+1}) = u(x, y, t_n) + \Delta t \Psi(x, y, t_n) + \mathcal{R}(x, y, t_n) + \\ & \Delta t g(x, y, t_{n+1}) + (\Delta t)^2 \mathcal{L}_{1,\varepsilon}^{n+1}g_2(x, y, t_{n+1}) - (\Delta t)^2 \mathcal{L}_{1,\varepsilon}^{n+1}\mathcal{L}_{2,\varepsilon}^{n+1}u(x, y, t_{n+1}) - \\ & (\Delta t)^3 \mathcal{L}_{1,\varepsilon}^{n+1}\mathcal{L}_{2,\varepsilon}^{n+1}\Psi(x, y, t_{n+1}). \end{aligned} \quad (3.85)$$

Using the equation (3.83) and the Taylor-series expansion of the functions u and Ψ with respect to time variable t in (3.85), the remainder term in (3.81) is the solution of the following IBVP:

$$\begin{cases} \mathcal{R}(x, y, 0) = 0, & (x, y) \in \bar{\mathcal{G}}, \\ (\mathcal{I} + \Delta t \mathcal{L}_{2,\varepsilon}^{n+1})(\mathcal{I} + \Delta t \mathcal{L}_{1,\varepsilon}^{n+1})\mathcal{R}(x, y, t_{n+1}) = \mathcal{R}(x, y, t_n) + O(\Delta t)^3, & (x, y) \in \mathcal{G}, \\ \mathcal{R}(x, y, t_{n+1}) = 0, & (x, y, t_{n+1}) \in \partial \mathcal{G} \times \Lambda^{\Delta t}. \end{cases} \quad (3.86)$$

Finally, using the above relation recursively and by invoking the stability in Lemma 3.3, we obtain the desired bound of the remainder term. ■

Theorem 3.3. *Let $u^{\Delta t}(x, y, t_{n+1})$ and $u^{\Delta t/2}(x, y, \tilde{t}_{n+1})$ be the respective solutions of the time-semidiscrete problem (3.11) on the mesh $\bar{\mathcal{G}} \times \Lambda^{\Delta t}$ and $\bar{\mathcal{G}} \times \Lambda^{\Delta t/2}$; and let $u(x, y, t_{n+1})$ be the exact solution of the IBVP (3.1)-(3.2) on the mesh $\bar{\mathcal{G}} \times \Lambda^{\Delta t}$. Then the error due to the temporal extrapolation defined by*

$$u_{extp}^{\Delta t}(x, y, t_{n+1}) = \left(2u^{\Delta t/2}(x, y, t_{n+1}) - u^{\Delta t}(x, y, t_{n+1}) \right), \quad (x, y, t_{n+1}) \in \bar{\mathcal{G}} \times \Lambda^{\Delta t},$$

satisfies that

$$|u_{exp}^{\Delta t}(x, y, t_{n+1}) - u(x, y, t_{n+1})| \leq C(\Delta t)^2, \quad (x, y, t_{n+1}) \in \bar{\mathbf{G}} \times \Lambda^{\Delta t}.$$

Proof. From (3.81) and (3.84), we have

$$u(x, y, t_{n+1}) = u^{\Delta t}(x, y, t_{n+1}) - \Delta t \Psi(x, y, t_{n+1}) + O(\Delta t)^2, \quad (x, y, t_{n+1}) \in \bar{\mathbf{G}}^N \times \Lambda^{\Delta t}.$$

Similarly, we have

$$u(x, y, \tilde{t}_{n+1}) = u^{\Delta t/2}(x, y, \tilde{t}_{n+1}) - (\Delta t/2) \Psi(x, y, \tilde{t}_{n+1}) + O(\Delta t)^2, \quad (x, y, \tilde{t}_{n+1}) \in \bar{\mathbf{G}}^N \times \Lambda^{\Delta t/2}.$$

Now, using the above two expressions, we obtain the desired result. ■

3.6 Numerical experiments

We provide numerical results obtained with the algorithm given here to solve effectively several problems of type (3.1)-(3.2) in this section. We used the same decomposition for the reaction term in all of the test examples: $b_1(x, y, t) = b_2(x, y, t) = b(x, y, t)/2$. In this case, the right-hand side is decomposed in the form $g(x, y, t) = g_1(x, y, t) + g_2(x, y, t)$, where $g_2(x, y, t) = g(x, 0, t) + y(g(x, 1, t) - g(x, 0, t))$, $g_1(x, y, t) = g(x, y, t) - g_2(x, y, t)$. For all the test examples, we choose $\eta_0 = 4.2$ to define the transition parameters of meshes $\bar{\mathbf{G}}_x^N$ and $\bar{\mathbf{G}}_y^N$ respectively, and implement the Thomas algorithm to solve the tridiagonal linear systems involved in our methods. The numerical results are also compared with the implicit upwind method [22].

3.6.1 Test examples

Example 3.1. Consider the following parabolic IBVP:

$$\begin{cases} \frac{\partial u}{\partial t} - \varepsilon \Delta u + (1 + x(1 - x)) \frac{\partial u}{\partial x} + (1 + y(1 - y)) \frac{\partial u}{\partial y} = g(x, y, t), & \text{in } \mathbf{G} \times (0, 1], \\ u(x, y, 0) = q_0(x, y), & \text{in } \bar{\mathbf{G}}, \\ u(x, y, t) = s(x, y, t), & \text{in } \partial \mathbf{G} \times (0, T], \end{cases} \quad (3.87)$$

where g, q_0, s are obtained from the exact solution which is given by

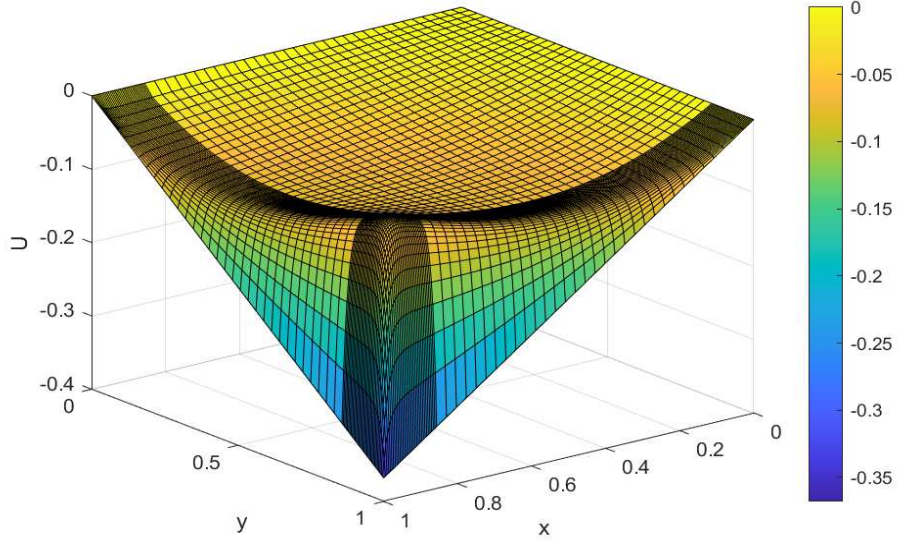
$$u(x, y, t) = \exp(-t) \left[\left(\frac{1 - \exp(-(1 - x)/\varepsilon)}{1 - \exp(-1/\varepsilon)} - \cos\left(\frac{\pi x}{2}\right) \right) \left(\frac{1 - \exp(-(1 - y)/\varepsilon)}{1 - \exp(-1/\varepsilon)} - \cos\left(\frac{\pi y}{2}\right) \right) - xy \right].$$

In Fig 3.2, we draw surface plot of numerical solution for Example 3.1 and it shows that the solution generates boundary layers closer to the outflow boundaries $x = 1$ and $y = 1$. Global errors are displayed to demonstrate the uniform convergence of the method. For each ε , we calculate the maximum point-wise errors $e_\varepsilon^{N, \Delta t}$ corresponding to the proposed numerical method before and after extrapolation, respectively by

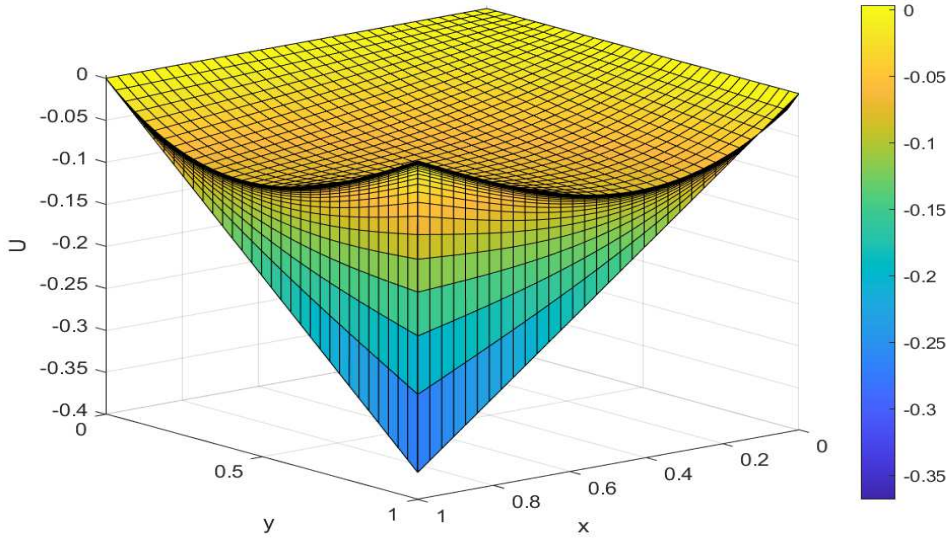
$$\max_{0 \leq i \leq N} \max_{0 \leq j \leq N} \max_{0 \leq n \leq M} |U^{N, \Delta t}(x_i, y_j, t_n) - u(x_i, y_j, t_n)|,$$

and

$$\max_{0 \leq i \leq N} \max_{0 \leq j \leq N} \max_{0 \leq n \leq M} |U_{exp}^{N, \Delta t}(x_i, y_j, t_n) - u(x_i, y_j, t_n)|,$$



(a) for $\varepsilon = 2^{-6}$



(b) for $\varepsilon = 2^{-14}$

Figure 3.2: Graphs of numerical solution for Example 3.1 $N = 64$, $M = 32$ at $t = 1$.

and the corresponding orders of convergence are calculated by $r_\varepsilon^{N,\Delta t} = \log_2 \left(\frac{e_\varepsilon^{N,\Delta t}}{e_\varepsilon^{2N,\Delta t/2}} \right)$. Here, $U^{N,\Delta t}(x_i, y_j, t_n)$ and $U_{extp}^{N,\Delta t}(x_i, y_j, t_n)$, respectively denote the numerical solutions of the proposed method (3.22) obtained at $(x_i, y_j, t_n) \in \bar{D}^{N,\Delta t}$. Further, for each N and Δt , we calculate the ε -uniform maximum point-wise error and the corresponding ε -uniform order of convergence, respectively by

$$e^{N,\Delta t} = \max_\varepsilon e_\varepsilon^{N,\Delta t} \quad \text{and} \quad r^{N,\Delta t} = \log_2 \left(\frac{e^{N,\Delta t}}{e^{2N,\Delta t/2}} \right).$$

We also compute the local errors in time to illustrate the numerical behavior of the method. The local errors at the mesh points are computed by

$$e_{loc}^{N,\Delta t} = \max_{0 \leq i \leq M} \max_{0 \leq j \leq M} \max_{0 \leq n \leq M} |\tilde{U}^{N,\Delta t}(x_i, y_j, t_n) - u(x_i, y_j, t_n)|,$$

where $\tilde{U}^{N,\Delta t}(x_i, y_j, t_n)$ is solution of the discrete problem (3.65)-(3.67) and the corresponding local order of convergence computed by

$$r_{loc}^{N,\Delta t} = \frac{\log(e_{loc}^{N,\Delta t}/e_{loc}^{N,\Delta t/2})}{\ln 2}.$$

Note that the corresponding orders of consistency are given by $r_{loc}^{N,\Delta t} - 1$.

Example 3.2. Consider the following parabolic IBVP:

$$\begin{cases} \frac{\partial u}{\partial t} - \varepsilon \Delta u + \frac{\partial u}{\partial x} + \frac{\partial u}{\partial y} + (1 + t^2 xy)u = g(x, y, t), & \text{in } \mathbf{G} \times (0, 1], \\ u(x, y, 0) = 0, & \text{in } \bar{\mathbf{G}}, \\ u(x, y, t) = (e^{-t} - 1)(1 + x)y, & (x, y, t) \in \partial \mathbf{G} \times (0, 1], \end{cases} \quad (3.88)$$

where $g(x, y, t) = [1 + rt^2 xy][\Phi(x)\Phi(y) - (1 + x)y] + rm_2[\Phi(x) + \Phi(y)] - r(1 + x + y)$ and $\Phi(z) = m_1 + m_2 z + \exp(-(1 - z)/\varepsilon)$, $m_1 = -\exp(-1/\varepsilon)$, $m_2 = -1 - m_1$ and $r = 1 - e^{-t}$.

In Fig 3.3, we draw surface plot of numerical solution for Example 3.2 and it shows that the solution generates boundary layers closer to the outflow boundaries $x = 1$ and $y = 1$. As we are not acquainted with the exact solution of Example 3.2, we calculate the maximum point-wise errors $\hat{e}_\varepsilon^{N,\Delta t}$ corresponding to the proposed numerical method before and after extrapolation, respectively by

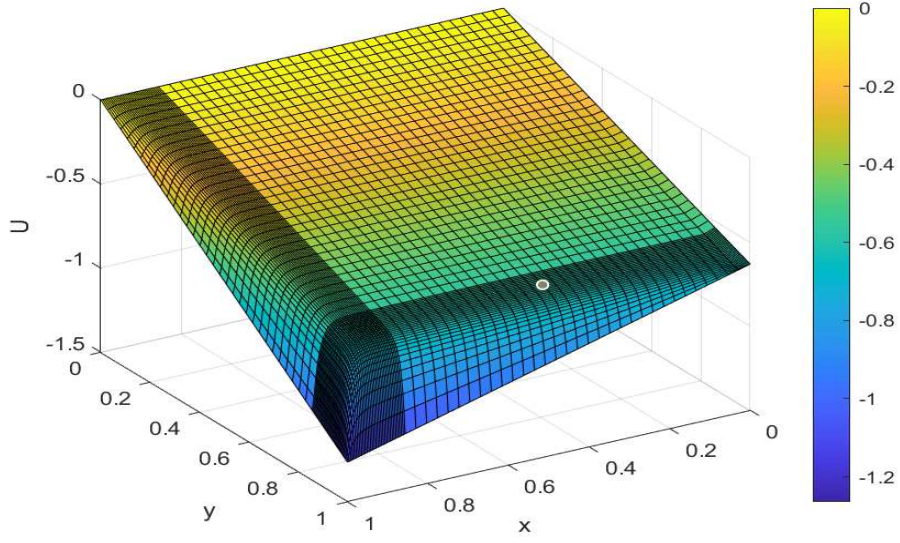
$$\max_{0 \leq i \leq N} \max_{0 \leq j \leq N} \max_{0 \leq n \leq M} |U^{N,\Delta t}(x_i, y_j, t_n) - \hat{U}^{2N,\Delta t/2}(x_i, y_j, t_n)|,$$

and

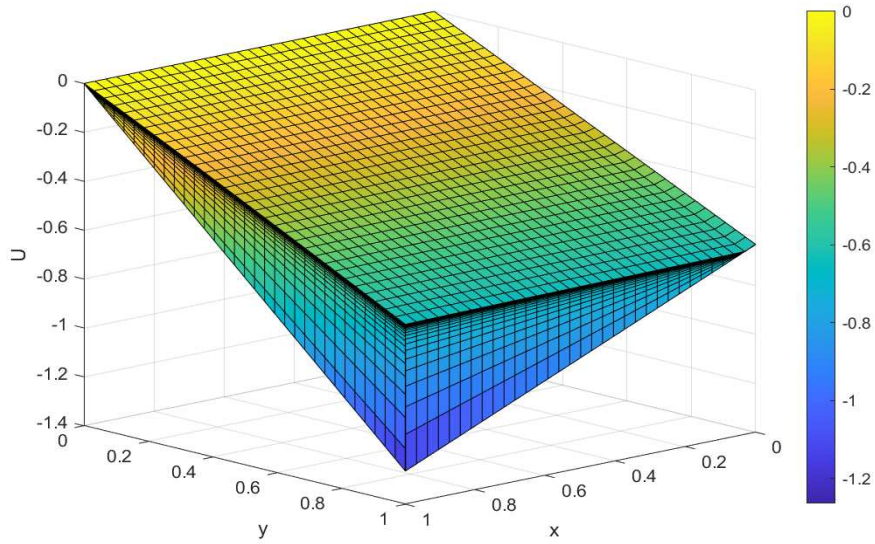
$$\max_{0 \leq i \leq N} \max_{0 \leq j \leq N} \max_{0 \leq n \leq M} |U_{extp}^{N,\Delta t}(x_i, y_j, t_n) - \hat{U}_{extp}^{2N,\Delta t/2}(x_i, y_j, t_n)|,$$

and the corresponding orders of convergence are calculated by $\hat{r}_\varepsilon^{N,\Delta t} = \log_2 \left(\frac{\hat{e}_\varepsilon^{N,\Delta t}}{\hat{e}_\varepsilon^{2N,\Delta t/2}} \right)$. Here,

$\hat{U}^{2N,\Delta t/2}(x_i, y_j, t_n)$ and $\hat{U}_{extp}^{2N,\Delta t/2}(x_i, y_j, t_n)$, respectively denote the numerical solution and the extrapolated



(a) for $\varepsilon = 2^{-6}$



(b) for $\varepsilon = 2^{-14}$

Figure 3.3: Graphs of numerical solution for Example 3.2 $N = 64$, $M = 32$ at $t = 1$.

numerical solution obtained at $(x_i, y_j, t_n) \in \widehat{\mathcal{D}}^{2N, \Delta t/2} = \widehat{\mathcal{G}}^{2N} \times \Lambda^{\Delta t/2}$, where $\Delta t/2 = T/2M$, and $\widehat{\mathcal{G}}^{2N}$ is a piecewise-uniform Shishkin mesh with $2N$ mesh-intervals in both the x - and y -directions and having the same transition parameter η_l , $l = 1, 2$, as that of $\bar{\mathcal{G}}^N$ such that the $(i^{\text{th}}, j^{\text{th}})$ point of $\bar{\mathcal{G}}^N$ becomes $(2i^{\text{th}}, 2j^{\text{th}})$ point of $\widehat{\mathcal{G}}^{2N}$, for $i, j = 0, 1, \dots, N$. Finally, for each N and Δt , we compute the quantities $\widehat{e}^{N, \Delta t}$ and $\widehat{r}^{N, \Delta t}$ analogously to $e^{N, \Delta t}$ and $r^{N, \Delta t}$.

Furthermore, we compute the local errors for the second example in the same way that we did for the first example. Because we do not know the exact solution, to approximate $\widetilde{U}^{N, \Delta t}(x_i, y_j, t_n)$ we use one step of the fully discrete scheme given in (3.22) and we replace the numerical solution $U^{N, \Delta t}(x_i, y_j, t_{n-1})$ by the numerical solution obtained on the finest mesh, which is a sufficiently good approximation to $u(x_i, y_j, t_{n-1})$. Finally, the local errors are computed by

$$\widehat{e}_{loc}^{N, \Delta t} = \max_{0 \leq i \leq M} \max_{0 \leq j \leq M} \max_{0 \leq n \leq M} |\widetilde{U}^{N, \Delta t}(x_i, y_j, t_n) - u_{2048, 1024}(x_i, y_j, t_n)|,$$

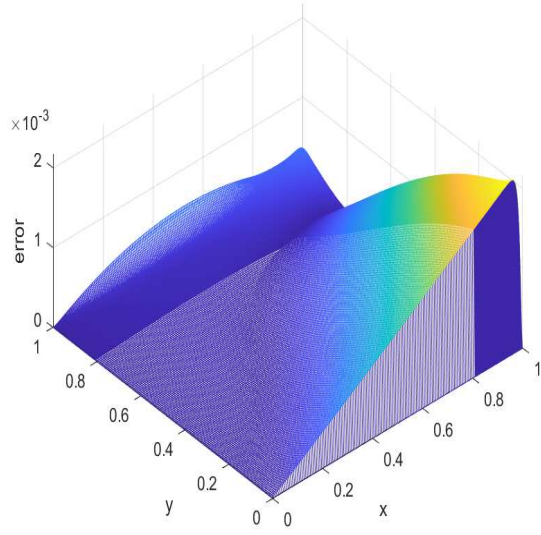
where $\widetilde{U}^{N, \Delta t}(x_i, y_j, t_n)$ is solution of the discrete problem (3.65)-(3.67) and the corresponding local order of convergence computed by

$$\widehat{r}_{loc}^{N, \Delta t} = \frac{\log(\widehat{e}_{loc}^{N, \Delta t} / \widehat{e}_{loc}^{N, \Delta t/2})}{\log 2}.$$

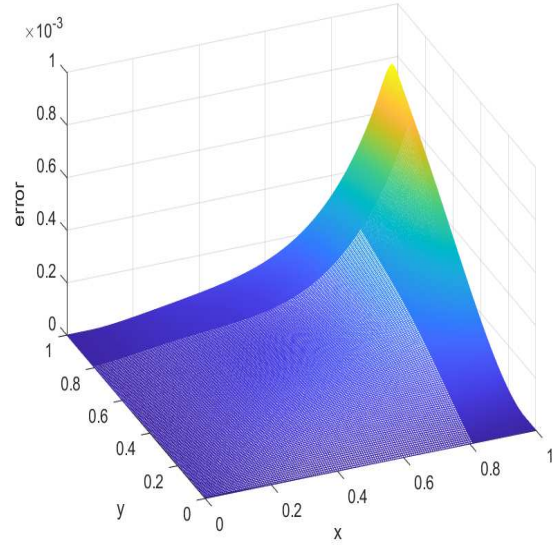
Note that the corresponding orders of consistency are given by $\widehat{r}_{loc}^{N, \Delta t} - 1$.

3.6.2 Numerical results and observations

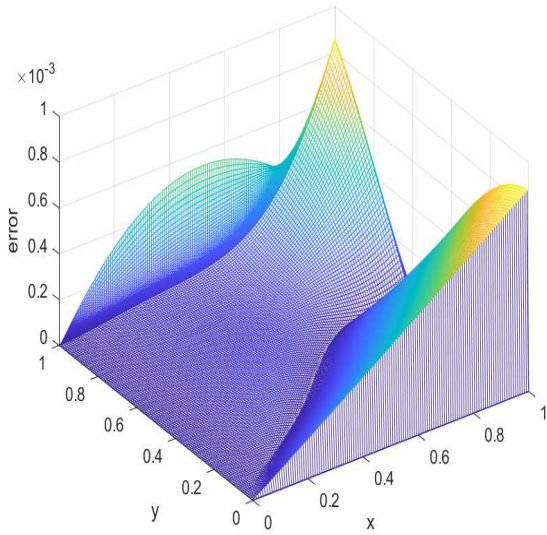
We choose all the values of ε from $\mathbb{S}_\varepsilon = \{2^0, 2^{-2}, \dots, 2^{-20}\}$, for computation of ε -uniform errors. For different values of ε , N and Δt , the computed ε -uniform errors and order of convergence are displayed in Tables 3.1 and 3.2 for both the choices of boundary conditions (3.12) and (3.13), without using the temporal Richardson extrapolation, respectively for Examples 3.1 and 3.2. This shows the monotonically decreasing behavior of the ε -uniform errors with increasing N , and it represents the ε -uniform convergence of the proposed method (3.22) for both the choice of boundary conditions. For the sake of clarity, the computed ε -uniform errors in Tables 3.1 and 3.2 are depicted in Figs 3.6 and 3.7, respectively for Examples 3.1 and 3.2. Further, Tables 3.1 and 3.2 show that the ε -uniform maximum point-wise errors of the proposed method (3.22) with alternative boundary conditions (3.13) are smaller than the ε -uniform maximum point-wise errors of proposed method (3.22) with natural boundary conditions (3.12) and moreover, we notice that proposed method (3.22) gives better result in comparison with classical upwind scheme [22]. To complement this observation, surface plots of the error corresponding to the Examples 3.1 and 3.2 computed at $t = 1$ are also depicted in Figs 3.4 and 3.5 for $N = 256$ and $\Delta t = \frac{1}{160}$ with natural and alternative boundary conditions, respectively. In the Tables 3.3 and 3.4, we present the numerical local errors and local order of convergence corresponding to the two choices of the boundary data. To reduce the influence of the local spatial error, we take sufficiently large the discretization parameter $N = 2048$. It is observed that when the alternative boundary data is chosen, the local errors are significantly reduced; and the numerical order of consistency (*i.e.*, $(\widehat{r}_{loc}^{N, \Delta t} - 1)$ for Example 3.1 and $(\widehat{r}_{loc}^{N, \Delta t} - 1)$ for Example 3.2) is one, whereas for the classical evaluation the numerical order of consistency is near to zero. This observation reveals that the option (3.13) for evaluation of the boundary data is evidently better than the conventional one as claimed in Remark 3.1. For clear illustration of the influence of the alternative the boundary data (3.13) over the classical the boundary data (3.12), the computed maximum point-wise local errors in Tables



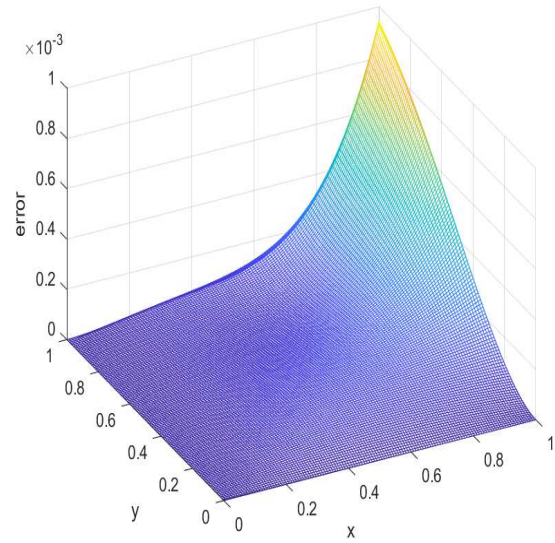
(a)



(b)

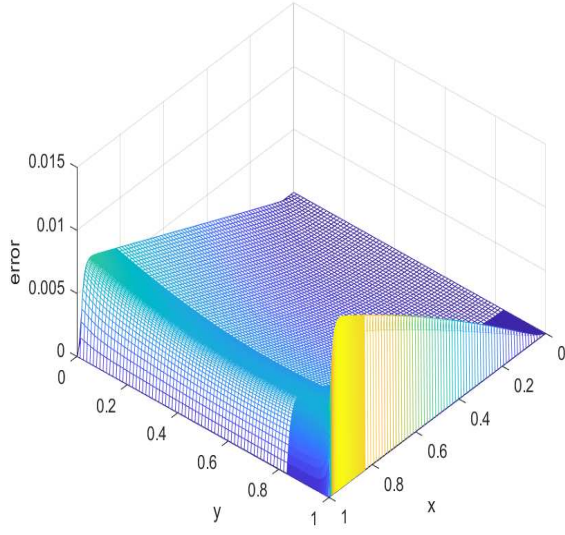


(c)

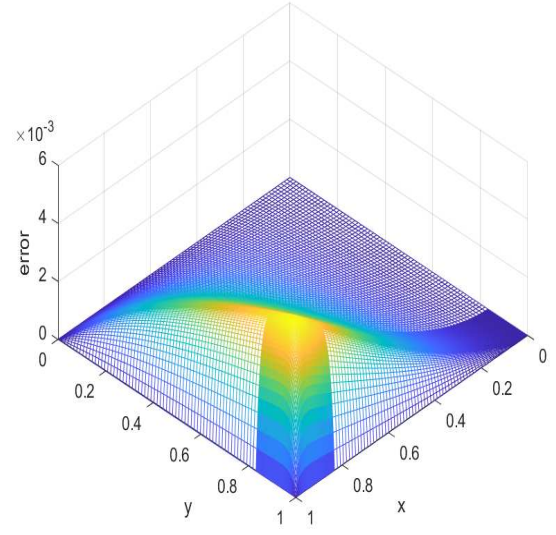


(d)

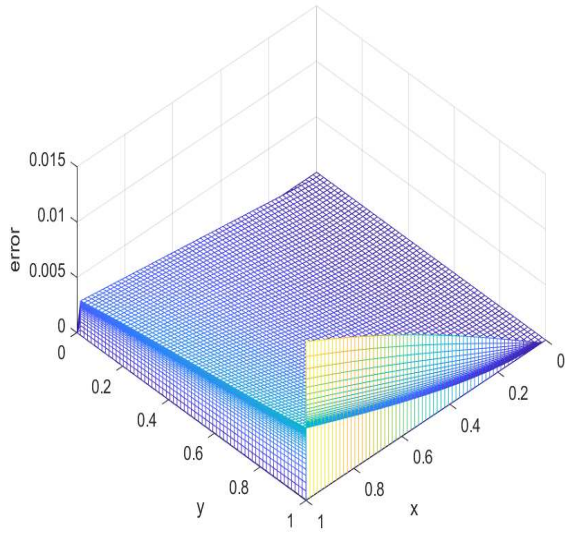
Figure 3.4: Graphs of error $|U^{N,\Delta t} - u|$ corresponding to Example 3.1 for $\varepsilon = 2^{-6}$ using (a) natural b.c (b) alternative b.c and for $\varepsilon = 2^{-14}$ using (c) natural b.c (d) alternative b.c at $t = 1$



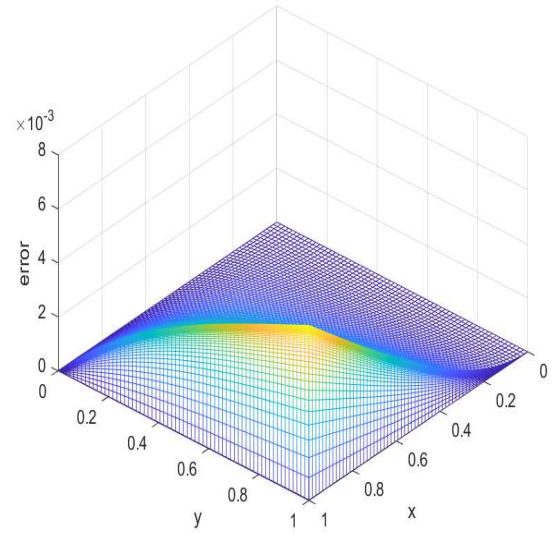
(a)



(b)



(c)



(d)

Figure 3.5: Graphs of error $|U^{N,\Delta t} - U^{2N,\Delta t/2}|$ corresponding to Example 3.2 for $\varepsilon = 2^{-6}$ using (a) natural b.c (b) alternative b.c and for $\varepsilon = 2^{-14}$ using (c) natural b.c (d) alternative b.c at $t = 1$

3.3 and 3.4 are depicted in Figs 3.8 and 3.9, respectively for Examples 3.1 and 3.2.

Next, in order to visualize the effect of the temporal Richardson extrapolation, we choose a suitably large N to reduce the influence of the spatial error. In Tables 3.7 and 3.8, we display the numerical results for Example 3.1, after the temporal extrapolation of the proposed method (3.22). This shows that the improvement in the temporal order of convergence after employing the Richardson extrapolation in the time variable, as claimed in Theorem 3.3. Tables 3.7 and 3.8 show that the temporal errors of proposed method (3.22) after temporal extrapolation with alternative boundary conditions (3.13) are smaller than the temporal errors of proposed scheme (3.22) with natural boundary conditions (3.12). The above numerical experiment indicates that by using the temporal Richardson extrapolation, one can check the spatial accuracy by choosing $\Delta t = 1/N$. Following this, in Tables 3.9 and 3.10, we compare the region-wise spatial accuracy of the proposed method given in (3.22) with the classical implicit upwind scheme, for Examples 3.1 and 3.2, respectively. These computational results match very well with the spatial error established in Theorem 3.2; and also clearly reflects the robustness of the proposed method (3.22) in comparison with the implicit upwind method in terms of order of accuracy, irrespective of the smaller and the larger values of ε .

3.7 Conclusion

In this chapter, we provide parameter-uniform convergence analysis for higher-order numerical approximation of a class of two-dimensional singularly perturbed parabolic convection-diffusion problems of the form (3.1)-(3.2) with non-homogeneous boundary data by proposing a new FSFMM followed the temporal Richardson extrapolation. The ε -uniform error estimate of the newly proposed method is carried out by invoking a two-stage discretization technique, which discretizes first in time and later in space.

(i) At first, we prove that the order reduction in time associated with the classical evaluation of the time-dependent boundary conditions can be eliminated by choosing appropriate evaluation of the boundary data.

(ii) Next, we prove that the corresponding fully discrete scheme is ε -uniformly convergent in the discrete supremum norm; and show that the spatial accuracy is at least two in the outer region and is almost two in the boundary layer region, regardless of the larger and smaller values of ε .

(iii) Further, we derive the ε -uniform error estimate associated with temporal Richardson extrapolation for improving the temporal order of convergence.

As a result, the resulting numerical solution is proved to be second-order uniformly convergent in both the spatial and temporal variables. Finally, we perform several numerical experiments to confirm that those theoretical outcomes. Further, we demonstrate that the newly developed FSFMM is robust in comparison with the implicit upwind method [22].

This is the first attempt in the literature to achieve cost-effective high-order parameter-uniform numerical solution for two-dimensional singularly perturbed linear parabolic convection-diffusion problems with non-homogeneous boundary data. This approach plays vital role to pursue convergence analysis for higher-order numerical approximation of two-dimensional singularly perturbed nonlinear problem as discussed in Chapter 5.

Table 3.1: Comparison of ε -uniform errors and order of convergence for Example 3.1 computed using $\Delta t = 1.6/N$ without temporal extrapolation

$\varepsilon \in \mathbb{S}_\varepsilon$	Number of mesh intervals N / time step size Δt				
	$64 / \frac{1}{40}$	$128 / \frac{1}{80}$	$256 / \frac{1}{160}$	$512 / \frac{1}{320}$	$1024 / \frac{1}{640}$
upwind scheme with alternative boundary conditions [22]					
$e^{N,\Delta t}$	1.1142e-01	7.1687e-02	4.3516e-02	2.5390e-02	1.4404e-02
$r^{N,\Delta t}$	0.63617	0.72018	0.77729	0.81779	
proposed method (3.22) with natural boundary conditions (3.12)					
$e^{N,\Delta t}$	3.7271e-02	1.8094e-02	1.0503e-02	5.5237e-03	2.9347e-03
$r^{N,\Delta t}$	1.0425	0.78475	0.92704	0.91240	
proposed method (3.22) with alternative boundary conditions (3.13)					
$e^{N,\Delta t}$	3.7016e-02	1.4197e-02	5.3925e-03	2.1507e-03	9.0979e-04
$r^{N,\Delta t}$	1.3825	1.3966	1.3261	1.2412	

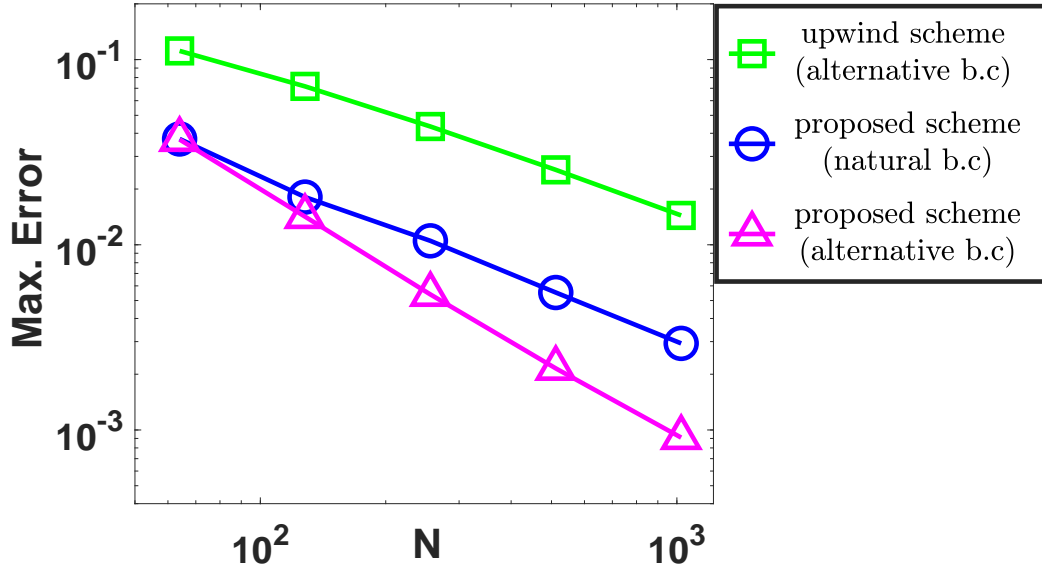


Figure 3.6: Loglog plot for comparison of the ε -uniform errors $e^{N,\Delta t}$ for Example 3.1

Table 3.2: Comparison of ε -uniform errors and order of convergence for Example 3.2 computed using $\Delta t = 1.6/N$ without temporal extrapolation

$\varepsilon \in \mathbb{S}_\varepsilon$	Number of mesh intervals N / time step size Δt				
	$64 / \frac{1}{40}$	$128 / \frac{1}{80}$	$256 / \frac{1}{160}$	$512 / \frac{1}{320}$	$1024 / \frac{1}{640}$
upwind scheme with alternative boundary conditions [22]					
$\hat{e}^{N,\Delta t}$	5.8496e-02	3.9579e-02	2.5215e-02	1.5255e-02	8.8471e-03
$\hat{r}^{N,\Delta t}$	0.56363	0.65042	0.72501	0.78601	
proposed method (3.22) with natural boundary conditions (3.12)					
$\hat{e}^{N,\Delta t}$	3.3637e-02	2.2012e-02	1.2872e-02	7.0903e-03	3.8038e-03
$\hat{r}^{N,\Delta t}$	0.61179	0.77404	0.86031	0.89842	
proposed method (3.22) with alternative boundary conditions (3.13)					
$\hat{e}^{N,\Delta t}$	2.4898e-02	1.2804e-02	6.4916e-03	3.2684e-03	1.6399e-03
$\hat{r}^{N,\Delta t}$	0.95946	0.97990	0.98999	0.99500	

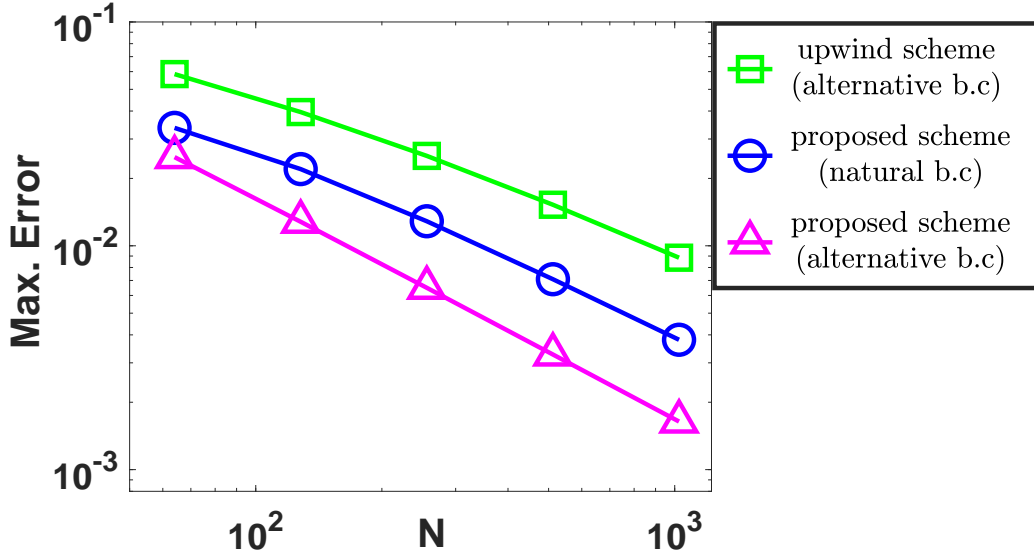


Figure 3.7: Loglog plot for comparison of the ε -uniform errors $\hat{e}^{N,\Delta t}$ for Example 3.2.

Table 3.3: Maximum point-wise local errors $e_{loc}^{N,\Delta t}$ and order of convergence $r_{loc}^{N,\Delta t}$ for Example 3.1 with natural boundary conditions (3.12)

ε	Number of mesh intervals $N = 2048$			
	M=16	M=32	M=64	M=128
2^{-3}	4.1048e-02	2.3271e-02	1.2582e-02	6.6195e-03
	0.81880	0.88714	0.92659	
2^{-6}	5.0417e-02	2.7105e-02	1.4029e-02	7.1115e-03
	0.89534	0.95016	0.98019	
2^{-14}	5.3945e-02	2.8395e-02	1.4217e-02	6.7896e-03
	0.92585	0.99802	0.10662	
2^{-20}	5.3981e-02	2.8411e-02	1.4221e-02	6.7863e-03
	0.92602	0.99839	1.0674	

Table 3.4: Maximum point-wise local errors $e_{loc}^{N,\Delta t}$ and order of convergence $r_{loc}^{N,\Delta t}$ for Example 3.1 with alternative boundary conditions (3.13)

ε	Number of mesh intervals $N = 2048$			
	M=16	M=32	M=64	M=128
2^{-3}	2.7823e-03	9.3463e-04	2.8070e-04	7.8404e-05
	1.5738	1.7354	1.8400	
2^{-6}	4.8208e-03	1.5150e-03	4.4089e-04	1.2514e-04
	1.6699	1.7809	1.8168	
2^{-14}	5.7823e-03	1.6911e-03	4.5544e-04	1.2987e-04
	1.7737	1.8926	1.8102	
2^{-20}	5.7966e-03	1.6947e-03	4.5600e-04	1.2990e-04
	1.7742	1.8939	1.8117	

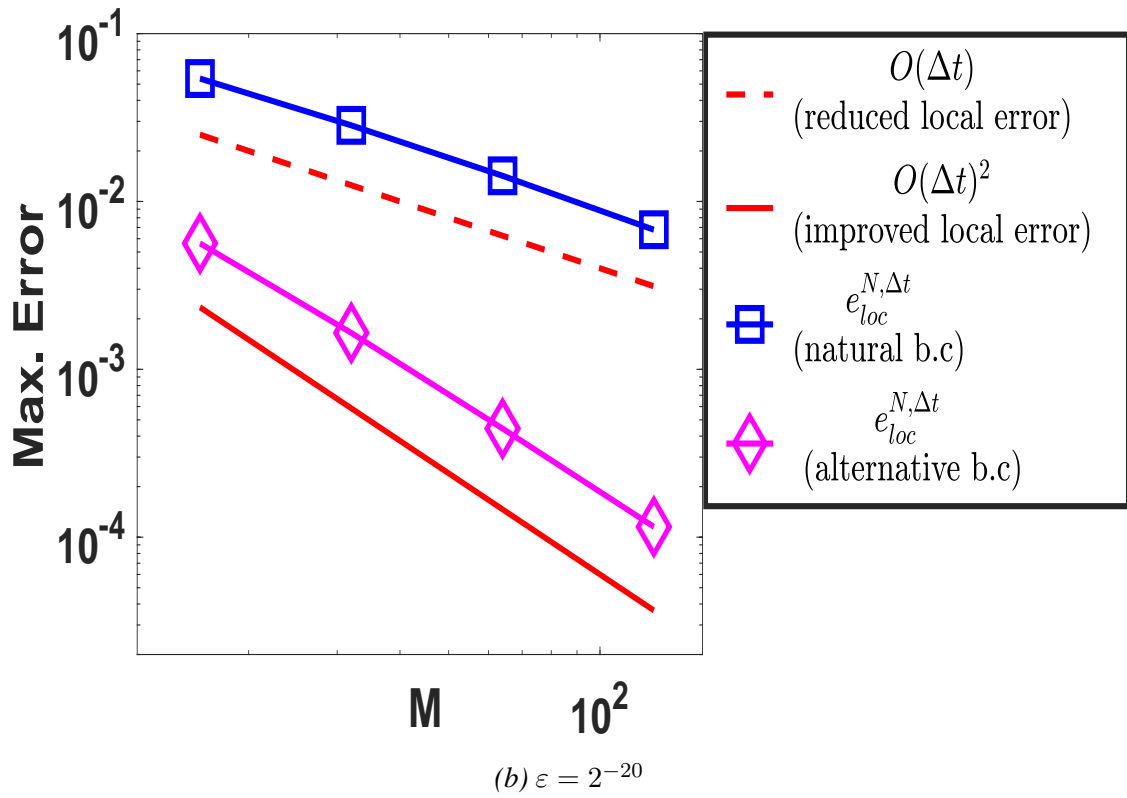
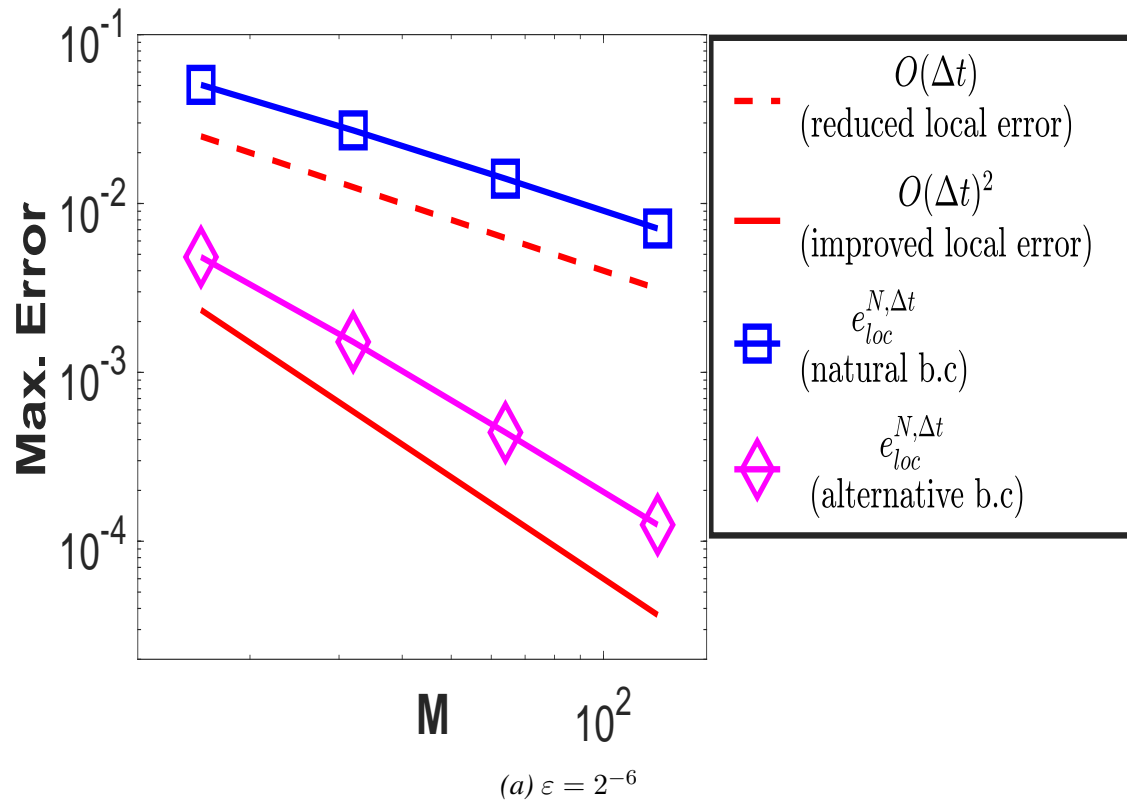


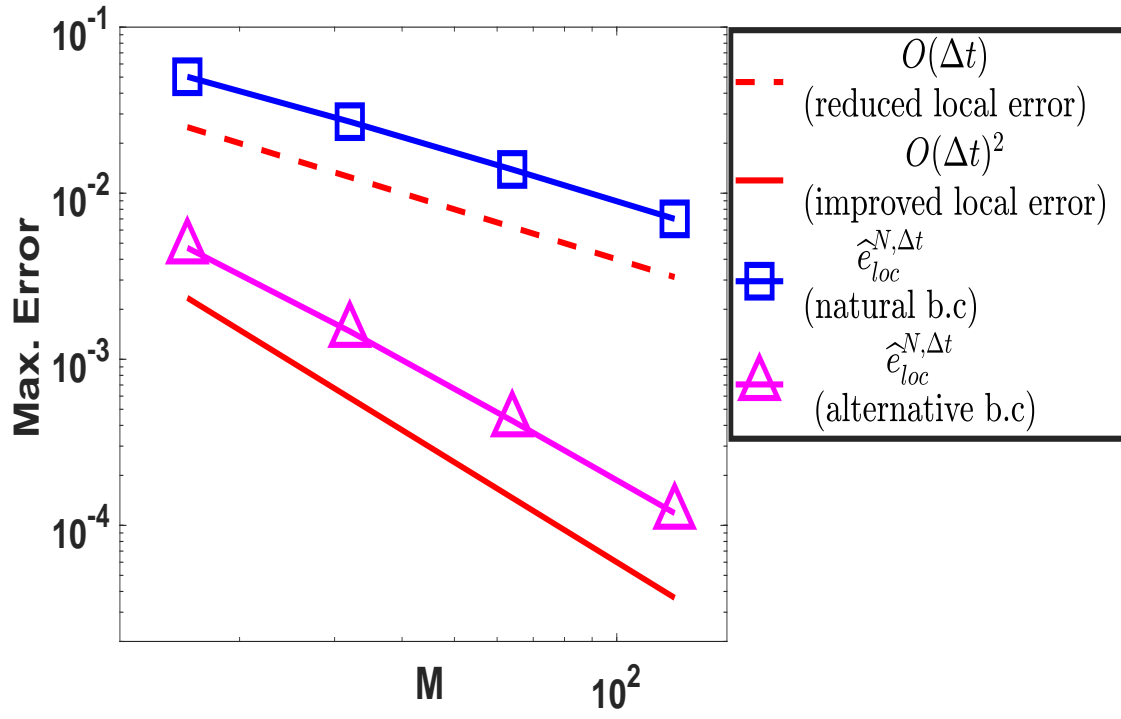
Figure 3.8: Loglog plot for comparison of the local temporal errors without extrapolation using the proposed scheme (3.22) for Example 3.1

Table 3.5: Maximum point-wise local errors $\hat{e}_{loc}^{N,\Delta t}$ and order of convergence $\hat{r}_{loc}^{N,\Delta t}$ for Example 3.2 with natural boundary conditions(3.12)

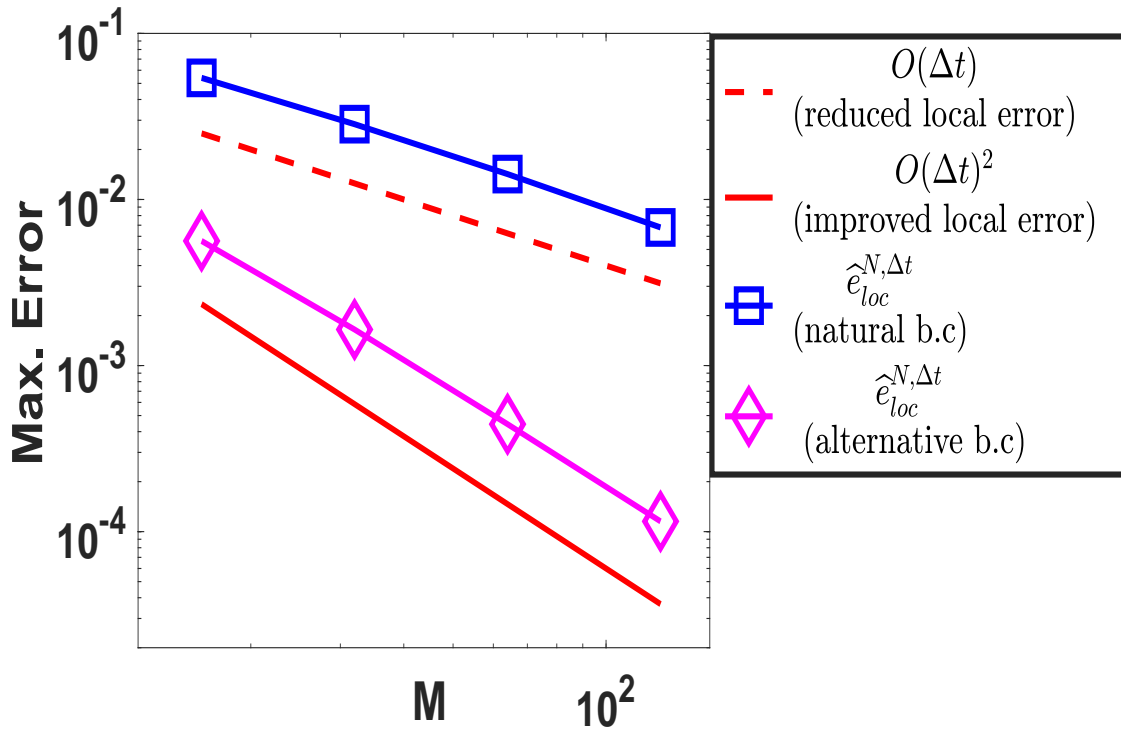
ε	Number of mesh intervals $N = 512$			
	M=16	M=32	M=64	M=128
2^{-3}	4.1048e-02	2.3271e-02	1.2582e-02	6.6195e-03
	0.89873	0.95555	0.98838	
2^{-6}	5.0262e-02	2.6959e-02	1.3901e-02	7.0068e-03
	0.92587	0.99806	1.0663	
2^{-14}	5.3944e-02	2.8394e-02	1.4216e-02	6.7888e-03
	0.92601	0.99839	1.0674	
2^{-20}	5.3981e-02	2.8411e-02	1.4221e-02	6.7863e-03
	0.81880	0.88714	0.92659	

Table 3.6: Maximum point-wise local errors $\hat{e}_{loc}^{N,\Delta t}$ and order of convergence $\hat{r}_{loc}^{N,\Delta t}$ for Example 3.2 with alternative boundary conditions (3.13)

ε	Number of mesh intervals $N = 512$			
	M=16	M=32	M=64	M=128
2^{-3}	2.7796e-03	9.3539e-04	2.8154e-04	7.8802e-05
	1.5713	1.7322	1.8370	
2^{-6}	4.6890e-03	1.4747e-03	4.2654e-04	1.1848e-04
	1.6689	1.7897	1.8481	
2^{-14}	5.6131e-03	1.6448e-03	4.4289e-04	1.1524e-04
	1.7709	1.8929	1.9423	
2^{-20}	5.6273e-03	1.6485e-03	4.4375e-04	1.1532e-04
	1.7713	1.8933	1.9441	



(a) $\varepsilon = 2^{-6}$



(b) $\varepsilon = 2^{-20}$

Figure 3.9: Loglog plot for comparison of the local temporal errors without extrapolation using the proposed scheme (3.22) for Example 3.2

Table 3.7: Comparison of temporal accuracy with natural and alternative boundary conditions after temporal Richardson extrapolation for Example 3.1

ε	Number of mesh intervals $N = 4096$			
	M=8	M=16	M=32	M=64
	with natural boundary conditions (3.12)			
2^{-6}	3.7679e-03 1.3295	1.4993e-03 0.89988	8.0354e-04 0.80125	4.6111e-04
2^{-20}	4.0595e-03 1.6006	1.3386e-03 1.2478	5.6366e-04 1.3116	2.2708e-04
	with alternative boundary conditions (3.13)			
2^{-6}	1.4013e-03 1.7465	4.1762e-04 1.8086	1.1922e-04 1.8533	3.2995e-05
2^{-20}	1.8114e-03 1.6838	5.6383e-04 1.7440	1.6833e-04 1.8115	4.7957e-05

Table 3.8: Comparison of temporal accuracy with natural and alternative boundary conditions after temporal Richardson extrapolation for Example 3.2

ε	Number of mesh intervals $N = 2048$			
	M=8	M=16	M=32	M=64
	with natural boundary conditions (3.12)			
2^{-6}	1.9871e-02 1.5629	6.7257e-03 0.11664	2.9966e-03 0.88323	1.6246e-03
2^{-20}	1.9935e-02 1.5960	6.5946e-03 1.0688	3.1439e-03 1.0397	1.5293e-03
	with alternative boundary conditions (3.13)			
2^{-6}	3.8994e-03 1.9352	1.0196e-03 1.9378	2.6615e-04 1.9581	6.8500e-05
2^{-20}	4.4127e-03 1.9403	1.1497e-03 1.9182	3.0420e-04 1.9445	7.9030e-05

Table 3.9: Comparison (region wise) of maximum point-wise errors and order of convergence for Example 3.1, with alternative boundary data and using temporal Richardson extrapolation with $\Delta t = \frac{1}{N}$.

	Outer region $[0, 1 - \eta_1] \times [0, 1 - \eta_2]$	Right boundary layer region $(1 - \eta_1, 1] \times [0, 1 - \eta_2]$	Top boundary layer region $[0, 1 - \eta_1] \times (1 - \eta_2, 1]$	Corner layer region $(1 - \eta_1, 1] \times (1 - \eta_2, 1]$
N	proposed scheme			
	$\varepsilon = 2^{-4}$			
128	2.2443e-06 1.9875	4.5694e-05 1.9997	4.8835e-05 2.0000	1.9999e-04 1.9997
256	5.6596e-07 1.9936	1.1426e-05 2.0004	1.2209e-05 1.9990	5.0010e-05 2.0004
	$\varepsilon = 2^{-6}$			
128	7.2420e-06 2.4714	5.8724e-04 1.8242	5.9304e-04 1.8265	1.5524e-03 1.6194
256	1.3058e-06 2.4543	1.6583e-04 1.8715	1.6721e-04 1.8726	5.0528e-04 1.6644
	$\varepsilon = 2^{-14}$			
128	2.0939e-05 1.8757	1.1412e-03 1.6272	1.1414e-03 1.6272	1.6144e-03 1.6140
256	5.7058e-06 1.8650	3.6943e-04 1.6571	3.6948e-04 1.6570	5.2741e-04 1.6622
N	implicit upwind scheme [22]			
	$\varepsilon = 2^{-4}$			
128	3.8131e-04 1.0078	1.3172e-03 0.95803	1.3151e-03 0.95706	7.3201e-03 0.95556
256	1.8963e-04 1.0041	6.7802e-04 0.97850	6.7741e-04 0.97788	3.7746e-03 0.97729
	$\varepsilon = 2^{-6}$			
128	1.0196e-03 1.3462	8.4117e-03 0.91080	8.4084e-03 0.91057	2.3877e-02 0.71482
256	4.0103e-04 1.3703	4.4741e-03 0.98075	4.4731e-03 0.98059	1.4548e-02 0.77735
	$\varepsilon = 2^{-14}$			
128	2.9420e-03 1.0425	1.7299e-02 0.71644	1.7300e-02 0.71650	2.5364e-02 0.71766
256	1.4283e-03 1.0236	1.0528e-02 0.76587	1.0528e-02 0.76588	1.5423e-02 0.77642

Table 3.10: Comparison (region wise) of maximum point-wise errors and order of convergence for Example 3.2, with alternative boundary data and using temporal Richardson extrapolation with $\Delta t = \frac{1}{N}$.

	Outer region $[0, 1 - \eta_1] \times$ $[0, 1 - \eta_2]$	Right boundary layer region $(1 - \eta_1, 1] \times$ $[0, 1 - \eta_2]$	Top boundary layer region $[0, 1 - \eta_1] \times$ $(1 - \eta_2, 1]$	Corner layer region $(1 - \eta_1, 1] \times$ $(1 - \eta_2, 1]$
N	proposed scheme			
	$\varepsilon = 2^{-4}$			
128	7.6843e-06 1.9832	7.7947e-05 2.0024	7.4252e-05 2.0033	1.9508e-04 2.0018
256	3.1.9436e-06 1.9915	1.9455e-05 2.0007	1.8520e-05 2.0004	4.8711e-05 2.0012
	$\varepsilon = 2^{-6}$			
128	1.3183e-05 2.0691	9.3152e-04 1.7295	9.2664e-04 1.7289	1.8468e-03 1.6178
256	3.1417e-06 2.0859	2.8091e-04 1.7714	2.7955e-04 1.7710	6.0177e-04 1.6617
	$\varepsilon = 2^{-14}$			
128	2.2066e-05 1.9745	1.4778e-03 1.6302	1.4778e-03 1.6302	2.0878e-03 1.6170
256	5.6146e-06 1.9821	4.7740e-04 1.6578	4.7739e-04 1.6578	6.8067e-04 1.6632
N	implicit upwind scheme [22]			
	$\varepsilon = 2^{-4}$			
128	3.0207e-05 1.2841	2.4924e-03 0.94564	2.4964e-03 0.94690	6.1400e-03 0.94401
256	1.2404e-05 1.1670	1.2940e-03 0.97309	1.2950e-03 0.97366	3.1915e-03 0.97067
	$\varepsilon = 2^{-6}$			
128	1.2733e-05 2.0469	9.6326e-03 0.79539	9.6372e-03 0.79570	1.9279e-02 0.70014
256	3.0816e-06 2.0727	5.5502e-03 0.87188	5.5516e-03 0.87207	1.1866e-02 0.76242
	$\varepsilon = 2^{-14}$			
128	1.9245e-05 1.9542	1.5331e-02 0.69155	1.5332e-02 0.69161	2.1915e-02 0.70649
256	4.9665e-06 1.9705	9.4926e-03 0.76550	9.4928e-03 0.76552	1.3430e-02 0.76347

Chapter 4

Convergence Analysis of Higher-Order Parameter Uniform Numerical Methods for Singularly Perturbed 1D Semilinear Parabolic PDEs with Smooth Data

This chapter deals with a class of singularly perturbed semilinear parabolic convection-diffusion initial-boundary-value problems exhibiting a boundary layer. This type of model problem often appears in modeling various physical phenomena, particularly in mathematical biology, and thus requires effective numerical techniques for analyzing computationally. For this purpose, we approximate the model problem by developing two new efficient numerical methods followed by the extrapolation technique. The first one is the fully-implicit fitted mesh method which utilizes the implicit-Euler method for the temporal discretization, and the other one is the implicit-explicit (IMEX) fitted mesh method which utilizes the IMEX-Euler method for the temporal discretization. The spatial discretization for both numerical methods is based on a new finite difference scheme. To accomplish this, the spatial domain is discretized by an appropriate layer-adapted mesh and the time domain by an equidistant mesh. At first, we analyze stability and study the asymptotic behavior of the analytical solution of the nonlinear governing problem. Then, we perform stability analysis and establish the parameter-uniform convergence of both the newly proposed methods in the discrete supremum norm. Thereafter, we analyze the Richardson extrapolation solely for the time variable to improve the order of uniform convergence in the temporal direction; and, consequently, achieve globally (with respect to both space and time) second-order accurate numerical solutions. Hereby, we indeed provide a complete convergence analysis towards higher-order numerical approximations for the considered nonlinear problem on a nonuniform grid. The theoretical outcomes are finally supported by the extensive numerical experiments, which also include a comparison of the proposed numerical methods along with the fully-implicit upwind method in terms of the order of accuracy and the computational cost.

4.1 Introduction

We consider the following class of semilinear singularly perturbed parabolic initial-boundary-value problems (IBVPs) on the domain $\mathfrak{D} = \Omega \times (0, T] = (0, 1) \times (0, T]$:

$$\begin{cases} \mathbb{T}_\varepsilon y(x, t) \equiv \frac{\partial y(x, t)}{\partial t} + \mathbb{L}_{x, \varepsilon} y(x, t) + b(x, t, y(x, t)) = g(x, t), & (x, t) \in \mathfrak{D}, \\ y(x, 0) = q_0(x), & x \in \overline{\Omega} = [0, 1], \\ y(0, t) = s_l(t), \quad y(1, t) = s_r(t), & t \in (0, T], \end{cases} \quad (4.1)$$

where

$$\mathbb{L}_{x, \varepsilon} y(x, t) = -\varepsilon \frac{\partial^2 y(x, t)}{\partial x^2} + a(x) \frac{\partial y(x, t)}{\partial x},$$

ε is a small parameter such that $0 < \varepsilon \leq 1$. We assume that the convection coefficient $a(x)$ is sufficiently smooth on $\overline{\Omega}$, and satisfies the condition

$$a(x) \geq m > 0, \quad \text{on } \overline{\Omega}. \quad (4.2)$$

Further, it is assumed that the nonlinear term $b(x, t, y)$ is sufficiently smooth on $\overline{\mathfrak{D}} \times \mathbb{R}$, and satisfies the condition

$$\frac{\partial b(x, t, y)}{\partial y} \geq \beta > 0, \quad (x, t, y) \in \overline{\mathfrak{D}} \times \mathbb{R}. \quad (4.3)$$

Moreover, the data s_l, s_r, q_0 , and the source term $g(x, t)$ are supposed to be sufficiently smooth and satisfy the following compatibility conditions at the corner points $(0, 0)$ and $(1, 0)$:

$$q_0(0) = s_l(0), \quad q_0(1) = s_r(0), \quad (4.4)$$

$$\begin{cases} \frac{ds_l(0)}{dt} = g(0, 0) + \varepsilon \frac{d^2 q_0(0)}{dx^2} - a(0) \frac{dq_0(0)}{dx} - b(0, 0, q_0(0)), \\ \frac{ds_r(0)}{dt} = g(1, 0) + \varepsilon \frac{d^2 q_0(1)}{dx^2} - a(1) \frac{dq_0(1)}{dx} - b(1, 0, q_0(1)), \end{cases} \quad (4.5)$$

and

$$\begin{cases} \frac{d^2 s_l(0)}{dt^2} = \frac{\partial g(0, 0)}{\partial t} - \frac{\partial b(0, 0, q_0(0))}{\partial t} - \left(\mathbb{L}_{x, \varepsilon} + \frac{\partial b(x, t, q_0)}{\partial y} \right) (g - \mathbb{L}_{x, \varepsilon} q_0 - b(x, t, q_0))(0, 0), \\ \frac{d^2 s_r(0)}{dt^2} = \frac{\partial g(1, 0)}{\partial t} - \frac{\partial b(1, 0, q_0(1))}{\partial t} - \left(\mathbb{L}_{x, \varepsilon} + \frac{\partial b(x, t, q_0)}{\partial y} \right) (g - \mathbb{L}_{x, \varepsilon} q_0 - b(x, t, q_0))(1, 0). \end{cases} \quad (4.6)$$

The above assumptions guarantee that the nonlinear IBVP (4.1)-(4.3) has a unique solution $y(x, t) \in \mathcal{C}^{4+\gamma}(\overline{\mathfrak{D}})$, which follows from [Chapter 7, §4] of the book [41] by Friedman. Here, the solution $y(x, t)$ generally possesses a boundary layer of width $O(\varepsilon)$ at $x = 1$ (see [12]). The layout of the rest of this chapter is given as follows. In Section 4.2, a comparison principle as well as some a-priori bounds of the analytical solution and its derivatives are stated and proven. Apart from this, the bounds of the decomposition of the solution (into

the smooth and the layer components) and their derivatives are also derived. In Section 4.3, we construct an appropriate piecewise-uniform Shishkin mesh adapted to the boundary layer. Then, the fully-implicit FMM and the IMEX-FMM are formulated respectively, in (4.29) and (4.30). We establish ε -uniform convergence of the proposed IMEX-FMM in Section 4.4; and that of the proposed fully-implicit FMM in Section 4.5. Further, we discuss convergence analysis related to the temporal Richardson extrapolation to the nonlinear discrete problem (4.71), in Section 4.6. Finally, numerical experiments are carried out in Section 4.7, to demonstrate the accuracy and the efficiency of the proposed FMMs. The conclusions of this chapter is provided in Section 4.8.

4.2 Properties of the analytical solution

Lemma 4.1 (Comparison Principle). *Let the functions $v, w \in \mathcal{C}^0(\overline{\mathcal{D}}) \cap \mathcal{C}^2(\mathcal{D})$ be such that $v \leq w$ on $\partial\mathcal{D}$ and $\mathbb{T}_\varepsilon v \leq \mathbb{T}_\varepsilon w$ in \mathcal{D} , then it implies that $v \leq w$ on $\overline{\mathcal{D}}$.*

Proof: Here, we use method of contradiction. Firstly, we suppose that there exists $(x^*, t^*) \in \overline{\mathcal{D}}$ such that $v(x^*, t^*) > w(x^*, t^*)$. Since, $v - w \in \mathcal{C}^0(\overline{\mathcal{D}})$, without loss of generality, we assume that $v - w$ takes positive maximum at (x^*, t^*) . Now, in conformity with the hypothesis of the comparison principle, $v - w \leq 0$ on $\partial\mathcal{D} \implies (x^*, t^*) \notin \partial\mathcal{D}$. Therefore, under the above assumption, we have

$$\begin{aligned} & (\mathbb{T}_\varepsilon v - \mathbb{T}_\varepsilon w)(x^*, t^*) \\ &= \frac{\partial(v - w)(x^*, t^*)}{\partial t} + \mathbb{L}_{x,\varepsilon}(v - w)(x^*, t^*) + b(x^*, t^*, v(x^*, t^*)) - b(x^*, t^*, w(x^*, t^*)), \\ &\geq \left[\int_0^1 \frac{b(x^*, t^*, w + \xi(v - w))}{\partial y} d\xi \right] (v - w)(x^*, t^*). \end{aligned} \quad (4.7)$$

Thus, from (4.7) and the assumption (4.3), we have $\mathbb{T}_\varepsilon v(x^*, t^*) > \mathbb{T}_\varepsilon w(x^*, t^*)$ and this contradicts that $\mathbb{T}_\varepsilon v(x, t) \leq \mathbb{T}_\varepsilon w(x, t)$ for all $(x, t) \in \mathcal{D}$. Hence, the proof is over. \blacksquare

The following result follows from Lemma 4.1.

Corollary 4.1. *Let the function $\Phi \in \mathcal{C}^0(\overline{\mathcal{D}}) \cap \mathcal{C}^2(\mathcal{D})$. For any given functions $v, w \in \mathcal{C}^0(\overline{\mathcal{D}})$, the differential operator $\tilde{\mathbb{T}}_{\varepsilon,(v,w)}$ given by*

$$\tilde{\mathbb{T}}_{\varepsilon,(v,w)}\Phi = \frac{\partial\Phi}{\partial t} + \mathbb{L}_{x,\varepsilon}\Phi + \left[\int_0^1 \frac{\partial b(x, t, w + \xi(v - w))}{\partial y} d\xi \right] \Phi,$$

satisfies the maximum principle, i.e., if $\Phi \leq 0$ on $\partial\mathcal{D}$ and $\tilde{\mathbb{T}}_{\varepsilon,(v,w)}\Phi \leq 0$ in \mathcal{D} , then it implies that $\Phi \leq 0$ on $\overline{\mathcal{D}}$.

The following lemma provides ε -uniform stability and uniqueness of the analytical solution of the nonlinear IBVP (4.1)-(4.3).

Lemma 4.2 (Stability). *Let the functions $v, w \in \mathcal{C}^0(\overline{\mathcal{D}}) \cap \mathcal{C}^2(\mathcal{D})$. Then, we have*

$$\|v - w\|_{\overline{\mathcal{D}}} \leq \|v - w\|_{\partial\mathcal{D}} + \frac{1}{\beta} \|\mathbb{T}_\varepsilon v - \mathbb{T}_\varepsilon w\|_{\overline{\mathcal{D}}}. \quad (4.8)$$

Proof. Consider the functions

$$\Phi^\pm(x, t) = -\|v - w\|_{\partial\mathfrak{D}} - \frac{1}{\beta} \|\mathbb{T}_\varepsilon v - \mathbb{T}_\varepsilon w\|_{\overline{\mathfrak{D}}} \pm (v - w)(x, t), \quad (x, t) \in \overline{\mathfrak{D}}.$$

Note that $\Phi^\pm(x, t) \leq 0$, $(x, t) \in \partial\mathfrak{D}$, and

$$\|\tilde{\mathbb{T}}_{\varepsilon, (v, w)}(v - w)\| \leq \left[\int_0^1 \frac{\partial b(x, t, w + \xi(v - w))}{\partial y} d\xi \right] \left(\frac{1}{\beta} \|\mathbb{T}_\varepsilon v - \mathbb{T}_\varepsilon w\| \right) \Rightarrow \tilde{\mathbb{T}}_{\varepsilon, (v, w)} \Phi^\pm(x, t) \leq 0.$$

Then, Corollary 4.1 implies that $\Phi^\pm(x, t) \leq 0$ for all $(x, t) \in \overline{\mathfrak{D}}$, from which the desired result follows immediately. \blacksquare

Next, for the purpose of deriving the bounds on the derivatives of $y(x, t)$, we extend the approach given in [23] to the considered model problem.

Theorem 4.1. *The solution $y(x, t)$ of the nonlinear IBVP (4.1)-(4.3) and its derivatives satisfy that*

$$\left| \frac{\partial^{j+k} y(x, t)}{\partial x^j \partial t^k} \right| \leq C \left(1 + \varepsilon^{-j} \exp(-\mathfrak{m}(1-x)/\varepsilon) \right), \quad (x, t) \in \overline{\mathfrak{D}}, \quad (4.9)$$

$\forall j, k \in \mathbb{N} \cup \{0\}$, satisfying $0 \leq j + 2k \leq 4$.

Proof: The above bounds are obtained by considering following cases.

Case 1: Let $j = 0$ and $k = 0$. Choose $v = y$ and $w = 0$. Then, Lemma 4.2 implies that

$$|y(x, t)| \leq C, \quad (x, t) \in \overline{\mathfrak{D}}. \quad (4.10)$$

Remark 4.1. The a-priori bound (independent of ε) obtained in (4.10) and the sufficient smoothness assumption on the nonlinear term ‘ b ’ yields the following ε -uniform boundedness property:

$$\left| \frac{\partial^{j+k+m} b(x, t, y)}{\partial x^j \partial t^k \partial y^m} \right|_{y=y(x, t)} \leq C, \quad (x, t) \in \overline{\mathfrak{D}}, \quad (4.11)$$

$\forall j, k, m \in \mathbb{N} \cup \{0\}$, satisfying $0 \leq j + 2k + 2m \leq \ell$; and this property is being frequently used as pointed out below.

Case 2: Let $j = 0$ and $k = 1, 2$. Differentiating (4.1) with respect to t , we consider that $\omega(x, t) = \frac{\partial y(x, t)}{\partial t}$ satisfies the following problem:

$$\begin{cases} \frac{\partial \omega}{\partial t} + \mathbb{L}_{x, \varepsilon} \omega + \frac{\partial b(x, t, y)}{\partial y} \omega = \mathcal{F}_1(x, t), & (x, t) \in \mathfrak{D}, \\ \omega(x, 0) = g(x, 0) - \mathbb{L}_{x, \varepsilon} q_0(x) - b(x, 0, q_0(x)), & x \in \overline{\Omega}, \\ \omega(0, t) = \frac{ds_l(t)}{dt}, \quad \omega(1, t) = \frac{ds_r(t)}{dt}, & t \in (0, T], \end{cases} \quad (4.12)$$

where $\mathcal{F}_1(x, t) = \frac{\partial g(x, t)}{\partial t} - \frac{\partial b(x, t, y)}{\partial t}$ is bounded (ε -uniformly) on $\overline{\mathfrak{D}}$ because of the smoothness assumption on g ; and the term $\frac{\partial b(x, t, y)}{\partial t}$ being bounded (ε -uniformly) follows from the property (4.11). Here, the compati-

bility conditions in (4.5) ensure that $\omega \in \mathcal{C}^0(\overline{\mathfrak{D}})$. Afterwards, introducing the differential operator $\widetilde{\mathbb{T}}_{\varepsilon,(y,y)}$ given by $\widetilde{\mathbb{T}}_{\varepsilon,(y,y)}\omega = \frac{\partial\omega}{\partial t} + \mathbb{L}_{x,\varepsilon}\omega + \frac{\partial b(x,t,y)}{\partial y}\omega$, one can obtain from Corollary 4.1 that

$$|\omega(x,t)| = \left| \frac{\partial y(x,t)}{\partial t} \right| \leq C, \quad (x,t) \in \overline{\mathfrak{D}}.$$

Next, we obtain the bound on $\frac{\partial^2 y}{\partial t^2}$. Differentiating (4.12) with respect to t , we consider that $\omega_1(x,t) = \frac{\partial\omega(x,t)}{\partial t}$ satisfies the following problem:

$$\begin{cases} \frac{\partial\omega_1}{\partial t} + \mathbb{L}_{x,\varepsilon}\omega_1 + \frac{\partial b(x,t,y)}{\partial y}\omega_1 = \mathcal{F}_2(x,t), & (x,t) \in \mathfrak{D}, \\ \omega_1(x,0) = \frac{\partial g(x,0)}{\partial t} - \mathbb{L}_{x,\varepsilon}\omega(x,0) - \frac{\partial b(x,0,\mathbf{q}_0(x))}{\partial y}\omega(x,0) - \frac{\partial b(x,t,\mathbf{q}_0(x))}{\partial t}, & x \in \overline{\Omega}, \\ \omega_1(0,t) = \frac{d^2 \mathbf{s}_l(t)}{dt^2}, \quad \omega_1(1,t) = \frac{d^2 \mathbf{s}_r(t)}{dt^2}, & t \in (0,T], \end{cases} \quad (4.13)$$

where $\mathcal{F}_2(x,t) = \frac{\partial^2 g}{\partial t^2} - \frac{\partial^2 b(x,t,y)}{\partial t^2} - 2 \frac{\partial^2 b(x,t,y)}{\partial t \partial y} \frac{\partial y}{\partial t} - \frac{\partial^2 b(x,t,y)}{\partial y^2} \left(\frac{\partial y}{\partial t} \right)^2$. The property (4.11) guarantees that the terms $\frac{\partial^2 b(x,t,y)}{\partial t^2}$, $\frac{\partial^2 b(x,t,y)}{\partial t \partial y}$, $\frac{\partial^2 b(x,t,y)}{\partial y^2}$ are bounded (ε -uniformly). Then, the smoothness assumption on g and the bound on $\frac{\partial y}{\partial t}$ implies that $\mathcal{F}_2(x,t)$ is bounded (ε -uniformly) on $\overline{\mathfrak{D}}$. Here, the compatibility condition in (4.6) ensure that $\omega_1 \in \mathcal{C}^0(\overline{\mathfrak{D}})$. Thereafter, similarly one can get

$$|\omega_1(x,t)| = \left| \frac{\partial^2 y(x,t)}{\partial t^2} \right| \leq C, \quad (x,t) \in \overline{\mathfrak{D}}.$$

Case 3. Let $j = 1$ and $k = 0, 1$. We rearrange the terms in (4.1) to consider the following form:

$$\begin{cases} \mathbb{L}_{x,\varepsilon}y + \left(\int_0^1 \frac{\partial b(x,t,\xi y)}{\partial y} d\xi \right) y = \mathcal{F}_3(x,t), & (x,t) \in \mathfrak{D}, \\ y(0,1) = \mathbf{s}_l(t), \quad y(1,t) = \mathbf{s}_r(t), & t \in (0,T], \end{cases} \quad (4.14)$$

where $\mathcal{F}_3(x,t) = g(x,t) - \frac{\partial y}{\partial t} - b(x,t,0)$. It is obvious that $b(x,t,0)$ is bounded (ε -uniformly). Then, the smoothness assumption on g together with the bound on $\frac{\partial y}{\partial t}$ implies that $\mathcal{F}_3(x,t)$ is bounded (ε -uniformly) on $\overline{\mathfrak{D}}$. Now, fixing $t \in [0,T]$ and using the argument of Kellogg and Tsan [61] on the line segment $\{(x,t), x \in [0,1]\}$ for (4.14), we have

$$\left| \frac{\partial y(x,t)}{\partial x} \right| \leq C \left(1 + \varepsilon^{-1} \exp(-m(1-x)/\varepsilon) \right), \quad (x,t) \in \overline{\mathfrak{D}}.$$

Again, rearranging the terms in (4.12), we consider the following form:

$$\begin{cases} \mathbb{L}_{x,\varepsilon}\omega + \frac{\partial b(x,t,y)}{\partial y}\omega = \mathcal{F}_4(x,t), & (x,t) \in \mathfrak{D}, \\ \omega(0,t) = \frac{ds_l(t)}{dt}, \quad \omega(1,t) = \frac{ds_r(t)}{dt}, & t \in (0,T], \end{cases} \quad (4.15)$$

where $\mathcal{F}_4(x,t) = \frac{\partial g}{\partial t} - \frac{\partial \omega}{\partial t} - \frac{\partial b(x,t,y)}{\partial t}$. From the previous argument we know that $\frac{\partial b(x,t,y)}{\partial t}$ is bounded (ε -uniformly) on $\overline{\mathfrak{D}}$. Then, the smoothness assumption on g together with the bound on $\frac{\partial \omega}{\partial t}$ implies that $\mathcal{F}_4(x,t)$ is bounded (ε -uniformly) on $\overline{\mathfrak{D}}$. Afterwards, applying the methodology of Kellogg and Tsan [61] for (4.15), we have

$$\left| \frac{\partial \omega(x,t)}{\partial x} \right| = \left| \frac{\partial^2 y(x,t)}{\partial t \partial x} \right| \leq C \left(1 + \varepsilon^{-1} \exp(-\mathfrak{m}(1-x)/\varepsilon) \right), \quad (x,t) \in \overline{\mathfrak{D}}.$$

Case 4. Let $j = 2$ and $k = 0$. Differentiating (4.1) with respect to x and rearranging the terms, we consider that $\overline{\omega}_1(x,t) = \frac{\partial y(x,t)}{\partial x}$ satisfies the following problem:

$$\begin{cases} \mathbb{L}_{x,\varepsilon}\overline{\omega}_1 + \frac{\partial b(x,t,y)}{\partial y}\overline{\omega}_1 = \mathcal{F}_5(x,t), & (x,t) \in \mathfrak{D}, \\ \overline{\omega}_1(0,t) = C_1, \quad \overline{\omega}_1(1,t) = C_2\varepsilon^{-1}, & t \in (0,T], \end{cases} \quad (4.16)$$

where $\mathcal{F}_5(x,t) = \frac{\partial g(x,t)}{\partial x} - \frac{\partial \overline{\omega}_1}{\partial t} - \frac{da}{dx} \frac{\partial y}{\partial x} - \frac{\partial b(x,t,y)}{\partial x}$. Using similar arguments for g and $b(x,t,y)$ as mentioned previously; and applying the bounds on $\frac{\partial y}{\partial x}$ and $\frac{\partial \overline{\omega}_1}{\partial t} = \frac{\partial \omega}{\partial x}$, we have

$$|\mathcal{F}_5(x,t)| \leq C \left(1 + \varepsilon^{-1} \exp(-\mathfrak{m}(1-x)/\varepsilon) \right), \quad (x,t) \in \overline{\mathfrak{D}}.$$

Thereafter, applying the similar technique in [61] for (4.16), we have

$$\left| \frac{\partial \overline{\omega}_1(x,t)}{\partial x} \right| = \left| \frac{\partial^2 y(x,t)}{\partial x^2} \right| \leq C \left(1 + \varepsilon^{-2} \exp(-\mathfrak{m}(1-x)/\varepsilon) \right), \quad (x,t) \in \overline{\mathfrak{D}}.$$

Finally, by adopting the approach mentioned above, one can obtain the required bounds on the spatial derivatives of $y(x,t)$ for $j = 3, 4$. ■

4.2.1 Decomposition of the analytical solution

Consider the decomposition of the solution $y = p + q$ into the smooth component p and the layer component q . Here, the smooth component p is decomposed in the following form

$$p = p_0 + \varepsilon p_1 + \varepsilon^2 p_2 + \varepsilon^3 p_3, \text{ in } \mathfrak{D}, \quad (4.17)$$

where the functions p_0, p_1, p_2 and p_3 , receptively, satisfy the following problems:

$$\begin{cases} \frac{\partial p_0}{\partial t} + a(x) \frac{\partial p_0}{\partial x} + b(x,t,p_0) = g, & \text{in } \mathfrak{D}, \\ p_0(x,0) = q_0(x), \quad x \in \overline{\Omega}, \quad p_0(0,t) = p(0,t), & t \in (0,T], \end{cases} \quad (4.18)$$

$$\begin{cases} \frac{\partial p_1}{\partial t} + a(x) \frac{\partial p_1}{\partial x} + \frac{1}{\varepsilon} [b(x, t, p_0 + \varepsilon p_1) - b(x, t, p_0)] = \frac{\partial^2 p_0}{\partial x^2}, & \text{in } \mathfrak{D}, \\ p_1(x, 0) = 0, \quad x \in \overline{\Omega}, \quad p_1(0, t) = 0, \quad t \in (0, T], \end{cases} \quad (4.19)$$

$$\begin{cases} \frac{\partial p_2}{\partial t} + a(x) \frac{\partial p_2}{\partial x} + \frac{1}{\varepsilon^2} [b(x, t, p_0 + \varepsilon p_1 + \varepsilon^2 p_2) - b(x, t, p_0 + \varepsilon p_1)] = \frac{\partial^2 p_1}{\partial x^2}, & \text{in } \mathfrak{D}, \\ p_2(x, 0) = 0, \quad x \in \overline{\Omega}, \quad p_2(0, t) = 0, \quad t \in (0, T], \end{cases} \quad (4.20)$$

and

$$\begin{cases} \frac{\partial p_3}{\partial t} + \mathbb{L}_{x, \varepsilon} p_3 + \frac{1}{\varepsilon^3} [b(x, t, p) - b(x, t, p_0 + \varepsilon p_1 + \varepsilon^2 p_2)] = \frac{\partial^2 p_2}{\partial x^2}, & \text{in } \mathfrak{D}, \\ p_3(x, 0) = 0, \quad x \in \overline{\Omega}, \quad p_3(0, t) = 0, \quad p_3(1, t) = 0, \quad t \in (0, T]. \end{cases} \quad (4.21)$$

Thus, the smooth component p satisfies that

$$\begin{cases} \mathbb{T}_\varepsilon p = g, & \text{in } \mathfrak{D}, \\ p(x, 0) = q_0(x), \quad x \in \overline{\Omega}, \\ p(0, t) = s_l(t), \quad p(1, t) = p_0(1, t) + \varepsilon p_1(1, t) + \varepsilon^2 p_2(1, t), \quad t \in (0, T]. \end{cases} \quad (4.22)$$

Theorem 4.2. *The smooth component p and its derivatives satisfy that*

$$\left| \frac{\partial^{j+k} p(x, t)}{\partial x^j \partial t^k} \right| \leq C (1 + \varepsilon^{3-j}), \quad (x, t) \in \overline{\mathfrak{D}}, \quad (4.23)$$

$\forall j, k \in \mathbb{N} \cup \{0\}$, satisfying $0 \leq j + 2k \leq 4$.

Proof: We obtain the strong bounds on the smooth component p and its derivatives, by deriving the corresponding bounds separately for the functions p_i , $i = 0, 1, 2, 3$.

The function p_0 is the solution of the IVP (4.18), which is independent of ε . Henceforth, assuming sufficient smoothness on the data associated with the IVP (4.18) and imposing necessary compatibility conditions at $(0, 0)$, which can be obtained by extending the result of Bobisud [4] for the existence of higher order derivatives of p_0 , one can obtain that

$$\left| \frac{\partial^{j+k} p_0(x, t)}{\partial x^j \partial t^k} \right| \leq C, \quad (x, t) \in \overline{\mathfrak{D}}, \quad \text{for } 0 \leq j + 2k \leq 4. \quad (4.24)$$

Again, the IVPs (4.19) and (4.20), respectively, can be rewritten in the following forms:

$$\begin{cases} \frac{\partial p_1}{\partial t} + a(x) \frac{\partial p_1}{\partial x} + \int_0^1 \frac{\partial b(x, t, p_0 + \xi \varepsilon p_1)}{\partial y} d\xi p_1 = \frac{\partial^2 p_0}{\partial x^2}, & \text{in } \mathfrak{D}, \\ p_1(x, 0) = 0, \quad x \in \overline{\Omega}, \quad p_1(0, t) = 0, \quad t \in (0, T], \end{cases}$$

and

$$\begin{cases} \frac{\partial p_2}{\partial t} + a(x) \frac{\partial p_2}{\partial x} + \int_0^1 \frac{\partial b(x, t, p_0 + \varepsilon p_1 + \xi \varepsilon^2 p_2)}{\partial y} d\xi p_2 = \frac{\partial^2 p_1}{\partial x^2}, & \text{in } \mathfrak{D}, \\ p_2(x, 0) = 0, \quad x \in \overline{\Omega}, \quad p_2(0, t) = 0, \quad t \in (0, T]. \end{cases}$$

Henceforth, applying the above arguments for the functions p_i , $i = 1, 2$, one can get

$$\left| \frac{\partial^{j+k} p_i(x, t)}{\partial x^j \partial t^k} \right| \leq C, \quad (x, t) \in \overline{\mathfrak{D}}, \text{ for } 0 \leq j + 2k \leq 4. \quad (4.25)$$

Furthermore, the IBVP (4.21) can be rewritten in the following form:

$$\begin{cases} \frac{\partial p_3}{\partial t} + \mathbb{L}_{x,\varepsilon} p_3 + \int_0^1 \frac{\partial b(x, t, p_0 + \varepsilon p_1 + \varepsilon^2 p_2 + \xi \varepsilon^3 p_3)}{\partial y} d\xi p_3 = \frac{\partial^2 p_2}{\partial x^2}, & \text{in } \mathfrak{D}, \\ p_3(x, 0) = 0, \quad x \in \overline{\Omega}, \quad p_3(0, t) = 0, \quad p_3(1, t) = 0, & t \in (0, T], \end{cases}$$

which is similar to the IBVP (4.1), and henceforth, applying the result (4.9) analogously to the function p_3 , one can have

$$\left| \frac{\partial^{j+k} p_3(x, t)}{\partial x^j \partial t^k} \right| \leq C \left(1 + \varepsilon^{-j} \exp(-\mathfrak{m}(1-x)/\varepsilon) \right), \quad (x, t) \in \overline{\mathfrak{D}}, \text{ for } 0 \leq j + 2k \leq 4. \quad (4.26)$$

Finally, the desired result (4.23) is obtained by invoking the bounds (4.24)-(4.26) to the decomposition (4.17). ■

We now define the layer component q as the solution of the following nonlinear IBVP:

$$\begin{cases} \frac{\partial q}{\partial t} + \mathbb{L}_{x,\varepsilon} q + b(x, t, p + q) - b(x, t, p) = 0, & \text{in } \mathfrak{D}, \\ q(x, 0) = 0, \quad x \in \overline{\Omega}, \\ q(0, t) = 0, \quad q(1, t) = y(1, t) - p(1, t), & t \in (0, T]. \end{cases} \quad (4.27)$$

Theorem 4.3. *The layer component q and its derivatives satisfy that*

$$\left| \frac{\partial^{j+k} q(x, t)}{\partial x^j \partial t^k} \right| \leq C \left(\varepsilon^{-j} \exp(-\mathfrak{m}(1-x)/\varepsilon) \right), \quad (x, t) \in \overline{\mathfrak{D}}, \quad (4.28)$$

$\forall j, k \in \mathbb{N} \cup \{0\}$, satisfying $0 \leq j + 2k \leq 4$.

Proof: The IBVP (4.27) can be rewritten in the following form:

$$\begin{cases} \frac{\partial q}{\partial t} + \mathbb{L}_{x,\varepsilon} q + \left[\int_0^1 \frac{\partial b(x, t, p + \xi(y - p))}{\partial y} d\xi \right] q = 0, & \text{in } \mathfrak{D}, \\ q(x, 0) = 0, \quad x \in \overline{\Omega}, \\ q(0, t) = 0, \quad q(1, t) = y(1, t) - p(1, t), & t \in (0, T]. \end{cases}$$

Here, we introduce a differential operator $\widetilde{\mathbb{T}}_{\varepsilon, (y, p)}$ such that

$$\widetilde{\mathbb{T}}_{\varepsilon, (y, p)} q = \frac{\partial q}{\partial t} + \mathbb{L}_{x,\varepsilon} q + \left[\int_0^1 \frac{\partial b(x, t, p + \xi(y - p))}{\partial y} d\xi \right] q.$$

Now, we choose the functions

$$\Phi^\pm(x, t) = -C \exp(-\mathfrak{m}(1-x)/\varepsilon) \pm q(x, t), \quad (x, t) \in \overline{\mathfrak{D}},$$

for sufficiently large C . Note that $\Phi^\pm(x, t) \leq 0$, $(x, t) \in \partial\mathfrak{D}$, and

$$\begin{aligned} \tilde{\mathbb{T}}_{\varepsilon, (y, p)} \Phi^\pm(x, t) &\leq -C \exp(-\mathfrak{m}(1-x)/\varepsilon) \left[\frac{-\mathfrak{m}^2}{\varepsilon} + \frac{a(x)\mathfrak{m}}{\varepsilon} + \int_0^1 \frac{\partial b(x, t, q + \xi(y-p))}{\partial y} d\xi \right], \\ &\leq 0, \quad (x, t) \in \mathfrak{D}. \end{aligned}$$

Since the Corollary 4.1 shows that $\tilde{\mathbb{T}}_{\varepsilon, (y, p)}$ satisfies the maximum principle, we have

$$\Phi^\pm(x, t) \leq 0 \implies |q(x, t)| \leq C \exp(-\mathfrak{m}(1-x)/\varepsilon), \quad (x, t) \in \overline{\mathfrak{D}}.$$

The bounds on the derivatives of q are derived from the argument presented in [99], and thus the proof is complete. ■

4.3 Formulation of the discrete problems

On the domain $\overline{\mathfrak{D}}$, we construct a mesh $\overline{\mathfrak{D}}^{N, \Delta t} = \overline{\Omega}^N \times \Lambda^{\Delta t}$, where $\overline{\Omega}^N$ is the piecewise-uniform Shishkin mesh on the spatial domain $\overline{\Omega}$ and $\Lambda^{\Delta t}$ is the equidistant mesh on the temporal domain $[0, T]$. The detailed description is given in [Chapter 2, Section 2.3.1].

Now, for a given mesh function $\Psi_j^n = \Psi(x_j, t_n)$ defined on $\overline{\mathfrak{D}}^{N, \Delta t}$, we denote $\Psi_{j-\frac{1}{2}}^n = \frac{\Psi_j^n + \Psi_{j-1}^n}{2}$, $a_{j-\frac{1}{2}} = \frac{a_j + a_{j-1}}{2}$, $g_{j-\frac{1}{2}}^n = \frac{g_j^n + g_{j-1}^n}{2}$.

4.3.1 The fully-implicit FMM

Here, we discretize the nonlinear IBVP (4.1)-(4.3) by utilizing the implicit-Euler method with respect to the temporal variable. The implicit-Euler method treats both the linear and the nonlinear parts of the governing differential equation implicitly. Further, we propose a new hybrid finite difference scheme for the spatial discretization. The new hybrid scheme combines the midpoint upwind scheme in the outer region $(0, 1 - \eta]$ and a modified central difference scheme in the boundary layer region $(1 - \eta, 1)$, whenever $\varepsilon \leq \|a\|N^{-1}$; and selects the modified central difference scheme whenever $\varepsilon > \|a\|N^{-1}$. Then, the fully discrete scheme takes

the following form on $\overline{\mathcal{D}}^{N,\Delta t}$:

$$\left\{ \begin{array}{l} Y_j^0 = q_0(x_j), \quad 0 \leq j \leq N, \\ \left\{ \begin{array}{l} D_t^- Y_j^{n+1} + \mathbb{L}_{mcd}^N Y_j^{n+1} + b(x_j, t_{n+1}, Y_j^{n+1}) = g_j^{n+1}, \\ \text{for } 1 \leq j \leq N/2, \text{ and when } \varepsilon > \|a\|N^{-1}, \\ D_t^- Y_{j-\frac{1}{2}}^{n+1} + \mathbb{L}_{mup}^N Y_j^{n+1} + b(x_{j-\frac{1}{2}}, t_{n+1}, Y_{j-\frac{1}{2}}^{n+1}) = g_{j-\frac{1}{2}}^{n+1}, \\ \text{for } 1 \leq j \leq N/2, \text{ and when } \varepsilon \leq \|a\|N^{-1}, \\ D_t^- Y_j^{n+1} + \mathbb{L}_{mcd}^N Y_j^{n+1} + b(x_j, t_{n+1}, Y_j^{n+1}) = g_j^{n+1}, \\ \text{for } N/2 < j \leq N-1, \end{array} \right. \\ Y_0^{n+1} = s_l(t_{n+1}), \quad Y_N^{n+1} = s_r(t_{n+1}), \quad \text{for } n = 0, \dots, M-1. \end{array} \right. \quad (4.29)$$

Here, $\mathbb{L}_{mup}^N Y_j^{n+1} = -\varepsilon \delta_x^2 Y_j^{n+1} + a_{j-\frac{1}{2}} D_x^- Y_j^{n+1}$, and $\mathbb{L}_{mcd}^N Y_j^{n+1} = -\varepsilon \delta_x^2 Y_j^{n+1} + a_j D_x^* Y_j^{n+1}$.

4.3.2 The implicit-explicit FMM

Here, we discretize the nonlinear IBVP (4.1)-(4.3) by utilizing the IMEX-Euler method with respect to the temporal variable. The IMEX method treats the linear part of the governing differential equation implicitly and the nonlinear part explicitly. Further, we consider the framework of the new hybrid scheme for the spatial discretization. Then, the fully discrete scheme takes the following form on $\overline{\mathcal{D}}^{N,\Delta t}$:

$$\left\{ \begin{array}{l} y_j^0 = q_0(x_j), \quad 0 \leq j \leq N, \\ \left\{ \begin{array}{l} Y_j^{n+1} + \Delta t \mathbb{L}_{mcd}^N Y_j^{n+1} + \Delta t b(x_j, t_n, Y_j^n) = Y_j^n + \Delta t g_j^{n+1}, \\ \text{for } 1 \leq j \leq N/2, \text{ and when } \varepsilon > \|a\|N^{-1}, \\ Y_{j-\frac{1}{2}}^{n+1} + \Delta t \mathbb{L}_{mup}^N Y_j^{n+1} + \Delta t b(x_{j-\frac{1}{2}}, t_n, Y_{j-\frac{1}{2}}^n) = Y_{j-\frac{1}{2}}^n + \Delta t g_{j-\frac{1}{2}}^{n+1}, \\ \text{for } 1 \leq j \leq N/2, \text{ and when } \varepsilon \leq \|a\|N^{-1}, \\ Y_j^{n+1} + \Delta t \mathbb{L}_{mcd}^N Y_j^{n+1} + \Delta t b(x_j, t_n, Y_j^n) = Y_j^n + \Delta t g_j^{n+1}, \\ \text{for } N/2 < j \leq N-1, \end{array} \right. \\ Y_0^{n+1} = s_l(t_{n+1}), \quad Y_N^{n+1} = s_r(t_{n+1}), \quad \text{for } n = 0, \dots, M-1. \end{array} \right. \quad (4.30)$$

Remark 4.2. One can see that the fully-implicit FMM (4.29) results in a nonlinear-system (4.71), which requires to solve at each time step by employing an iterative method. To avoid this computational cost, we introduce the IMEX-FMM (4.30), which results in a linearized system (4.31); and thus produces cost effective numerical solution (see comparison of computational time in Table 4.11). Further, one can observe that the linearization in case of the IMEX scheme does not cause reduction in the order of uniform convergence (with respect to both space and time) achieved in case of the nonlinear scheme. To illustrate this, a detailed convergence analysis is presented for both the FMMs in the subsequent sections (Section 4.4 and Section 4.5).

4.4 Convergence analysis for the IMEX-FMM

For the convergence analysis, the fully discrete scheme (4.30) is written in the following form:

$$\left\{ \begin{array}{l} Y_j^0 = \mathbf{q}_0(x_j), \quad 0 \leq j \leq N, \\ \left\{ \begin{array}{l} \mathbb{L}_\varepsilon^{N,\Delta t} Y_j^{n+1} \equiv \nu_j^- Y_{j-1}^{n+1} + \nu_j^c Y_j^{n+1} + \nu_j^+ Y_{j+1}^{n+1} = \mathbb{F}_j^{n+1}, \\ \text{for } 1 \leq j \leq N-1, \end{array} \right. \\ Y_0^{n+1} = \mathbf{s}_l(t_{n+1}), \quad Y_N^{n+1} = \mathbf{s}_r(t_{n+1}), \quad \text{for } n = 0, \dots, M-1, \end{array} \right. \quad (4.31)$$

where the right hand side vector \mathbb{F}_j^{n+1} is given by

$$\mathbb{F}_j^{n+1} = \left\{ \begin{array}{l} \frac{1}{2}(Y_{j-1}^n + \Delta t g_{j-1}^{n+1}) + \frac{1}{2}(Y_j^n + \Delta t g_j^{n+1}) - \Delta t b(x_{j-\frac{1}{2}}, t_n, Y_{j-\frac{1}{2}}^n), \\ \text{for } 1 \leq j \leq N/2, \text{ and when } \varepsilon \leq \|a\|N^{-1}, \\ Y_j^n + \Delta t g_j^{n+1} - \Delta t b(x_j, t_n, Y_j^n), \text{ for } 1 \leq j \leq N/2, \text{ and when } \varepsilon > \|a\|N^{-1}, \\ Y_j^n + \Delta t g_j^{n+1} - \Delta t b(x_j, t_n, Y_j^n), \text{ for } N/2 < j \leq N-1. \end{array} \right. \quad (4.32)$$

Here, the coefficients $\nu_j^-, \nu_j^c, \nu_j^+$ are given by

$$\left\{ \begin{array}{l} \nu_j^- = \Delta t \nu_{mcd,j}^-, \quad \nu_j^c = \Delta t \nu_{mcd,j}^c + 1, \quad \nu_j^+ = \Delta t \nu_{mcd,j}^+, \\ \text{for } 1 \leq j \leq N/2, \text{ and when } \varepsilon > \|a\|N^{-1}, \\ \nu_j^- = \Delta t \nu_{mup,j}^- + \frac{1}{2}, \quad \nu_j^c = \Delta t \nu_{mup,j}^c + \frac{1}{2}, \quad \nu_j^+ = \Delta t \nu_{mup,j}^+, \\ \text{for } 1 \leq j \leq N/2, \text{ and when } \varepsilon \leq \|a\|N^{-1}, \\ \nu_j^- = \Delta t \nu_{mcd,j}^-, \quad \nu_j^c = \Delta t \nu_{mcd,j}^c + 1, \quad \nu_j^+ = \Delta t \nu_{mcd,j}^+, \\ \text{for } N/2 < j \leq N-1, \end{array} \right. \quad (4.33)$$

where

$$\left\{ \begin{array}{l} \nu_{mup,j}^- = -\frac{2\varepsilon}{\widehat{h}_j h_j} - \frac{a_{j-\frac{1}{2}}}{h_j}, \quad \nu_{mup,j}^c = \frac{2\varepsilon}{h_j h_{j+1}} + \frac{a_{j-\frac{1}{2}}}{h_j}, \quad \nu_{mup,j}^+ = -\frac{2\varepsilon}{\widehat{h}_j h_{j+1}}, \text{ and} \\ \nu_{mcd,j}^- = -\frac{2\left(\varepsilon - \frac{a_j h_j}{2}\right)}{\widehat{h}_j h_j} - \frac{a_j}{h_j}, \quad \nu_{mcd,j}^c = \frac{2\left(\varepsilon - \frac{a_j h_j}{2}\right)}{h_j h_{j+1}} + \frac{a_j}{h_j}, \quad \nu_{mcd,j}^+ = -\frac{2\left(\varepsilon - \frac{a_j h_j}{2}\right)}{\widehat{h}_j h_{j+1}}. \end{array} \right. \quad (4.34)$$

Next, we follow the two-stage discretization method in (4.30)-(4.32). The error analysis *via* two-stage discretization method involves error estimate due to the time semidiscretization and afterwards, that due to the spatial discretization.

4.4.1 Error estimate for the time semidiscretization

Let $y^n(x)$ denotes the semidiscrete approximation to the exact solution $y(x, t)$ of (4.1) at the time level $t_n = n \Delta t$. Then, the semidiscrete scheme, generated by temporal discretization of the nonlinear IBVP (4.1) using the IMEX-Euler method, takes the following form:

$$\begin{cases} y^0(x) = q_0(x), & x \in \overline{\Omega}, \\ (I + \Delta t \mathbb{L}_{x,\varepsilon}) y^{n+1}(x) + \Delta t b(x, t_n, y^n(x)) = y^n(x) + \Delta t g(x, t_{n+1}), & x \in \Omega, \\ y^{n+1}(0) = s_l(t_{n+1}), & y^{n+1}(1) = s_r(t_{n+1}). \end{cases} \quad (4.35)$$

One can prove in the classical way that the operator $(I + \Delta t \mathbb{L}_{x,\varepsilon})$ satisfies the maximum principle as stated in the following lemma.

Lemma 4.3 (Maximum principle). *Let the function $\psi \in \mathcal{C}^0(\overline{\Omega}) \cap \mathcal{C}^2(\Omega)$. If ψ satisfies $\psi(0) \leq 0$, $\psi(1) \leq 0$ and $(I + \Delta t \mathbb{L}_{x,\varepsilon})\psi(x) \leq 0$ for all $x \in \Omega$, then it implies that $\psi(x) \leq 0$ for all $x \in \overline{\Omega}$.*

Lemma 4.4. *Let the function $\mathcal{V} \in \mathcal{C}^0(\overline{\Omega}) \cap \mathcal{C}^2(\Omega)$. Then we have*

$$\|\mathcal{V}\| \leq \|\mathcal{V}\|_{\partial\Omega} + \|(I + \Delta t \mathbb{L}_{x,\varepsilon})\mathcal{V}\|_{\overline{\Omega}}.$$

Proof: Consider the following functions

$$\psi^\pm(x) = -\|\mathcal{V}\|_{\partial\Omega} - \|(I + \Delta t \mathbb{L}_{x,\varepsilon})\mathcal{V}\|_{\overline{\Omega}} \pm \mathcal{V}(x), \quad x \in \overline{\Omega}.$$

Note that $\psi^\pm(0) \leq 0$, $\psi^\pm(1) \leq 0$, and

$$(I + \Delta t \mathbb{L}_{x,\varepsilon})\psi^\pm(x) \leq -(I + \Delta t \mathbb{L}_{x,\varepsilon})\|(I + \Delta t \mathbb{L}_{x,\varepsilon})\mathcal{V}\| \pm (I + \Delta t \mathbb{L}_{x,\varepsilon})\mathcal{V}(x) \leq 0, \quad x \in \Omega.$$

Then, the desired result is obtained by applying Lemma 4.3. ■

Lemma 4.3 guarantees that the scheme (4.35) has a unique solution $y^n(x)$ at each time step t_n . Further, using Lemma 4.3 below it is shown that the solution $y^n(x)$ becomes ε -uniformly bounded.

Lemma 4.5. *The solution $y^n(x)$ of the semidiscrete problem (4.35) at the time level t_n satisfies that*

$$|y^n(x)| \leq C, \quad x \in \overline{\Omega}. \quad (4.36)$$

Proof: Due to the continuity of $q_0(x)$ on $\overline{\Omega}$. It is clear that

$$|y^0(x)| \leq C, \quad x \in \overline{\Omega},$$

and hence, $|b(x, t, y^0(x))| \leq C$, $x \in \overline{\Omega}$. Then, applying Lemma 4.4, we obtain from (4.35) that

$$|y^1(x)| \leq C, \quad x \in \overline{\Omega},$$

and hence, $|b(x, t, y^1(x))| \leq C$, $x \in \bar{\Omega}$. Thereafter, arguing previously, we obtain that

$$|y^2(x)| \leq C, \quad x \in \bar{\Omega}. \quad (4.37)$$

Thus, one can proceed in the same way to obtain the desired result. ■

Now, let us define $\tilde{e}^{n+1}(x) = y(x, t_{n+1}) - \tilde{y}^{n+1}(x)$, as the local error associated with the time semidiscrete scheme (4.35) at the time level t_{n+1} , where $\tilde{y}^{n+1}(x)$ is defined as the solution of the following auxiliary BVP:

$$\begin{cases} (I + \Delta t \mathbb{L}_{x,\varepsilon}) \tilde{y}^{n+1}(x) + \Delta t b(x, t_n, y(x, t_n)) = y(x, t_n) + \Delta t g(x, t_{n+1}), & x \in \Omega, \\ \tilde{y}^{n+1}(0) = \mathbf{s}_l(t_{n+1}), \quad \tilde{y}^{n+1}(1) = \mathbf{s}_r(t_{n+1}). \end{cases} \quad (4.38)$$

Lemma 4.6 (Local error). *The local error $\tilde{e}^{n+1}(x)$ satisfies the following estimate at the time level t_{n+1} :*

$$\|\tilde{e}^{n+1}\| \leq C(\Delta t)^2. \quad (4.39)$$

Proof: Using Taylor's theorem on $y(x, t)$ with respect to the temporal variable, we get

$$y(x, t_n) = (I + \Delta t \mathbb{L}_{x,\varepsilon}) y(x, t_{n+1}) + \Delta t b(x, t_{n+1}, y(x, t_{n+1})) - \Delta t g(x, t_{n+1}) + \frac{(\Delta t)^2}{2} \frac{\partial^2 y(x, s)}{\partial t^2},$$

where $t_n < s < t_{n+1}$. Again, from (4.38), we have

$$y(x, t_n) = (I + \Delta t \mathbb{L}_{x,\varepsilon}) \tilde{y}^{n+1}(x) + \Delta t b(x, t_n, y(x, t_n)) - \Delta t g(x, t_{n+1}).$$

Therefore,

$$(I + \Delta t \mathbb{L}_{x,\varepsilon}) \tilde{e}^{n+1}(x) + \Delta t \left[b(x, t_{n+1}, y(x, t_{n+1})) - b(x, t_n, y(x, t_n)) \right] = O(\Delta t)^2, \quad (4.40)$$

where we apply the bound on $\frac{\partial^2 y}{\partial t^2}$ from Theorem 4.1. Further, one can deduce that

$$\begin{aligned} & b(x, t_{n+1}, y(x, t_{n+1})) - b(x, t_n, y(x, t_n)) \\ &= \Delta t \left[\frac{\partial b(x, s, y(x, s))}{\partial t} + \frac{\partial b(x, s, y(x, s))}{\partial y} \frac{\partial y(x, s)}{\partial t} \right], \quad t_n < s < t_{n+1}, \\ &= O(\Delta t), \end{aligned} \quad (4.41)$$

where the bound on $\frac{\partial y}{\partial t}$ from Theorem 4.1 and the property (4.11) are utilized. Now, combining (4.40) and (4.41), we obtain that

$$\begin{cases} (I + \Delta t \mathbb{L}_{x,\varepsilon}) \tilde{e}^{n+1}(x) = O(\Delta t)^2, & x \in \Omega, \\ \tilde{e}^{n+1}(0) = 0 = \tilde{e}^{n+1}(1). \end{cases}$$

Henceforth, applying Lemma 4.4 on \tilde{e}^{n+1} , we get the desire result estimate. ■

Next, we define $e^{n+1}(x) = y(x, t_{n+1}) - y^{n+1}(x)$, as the global error associated with the time semidiscrete

scheme (4.35) at the time level t_{n+1} .

Theorem 4.4 (Global error). *The global error $e^{n+1}(x)$ satisfies the following estimate the time level t_{n+1} :*

$$\sup_{(n+1)\Delta t \leq T} \|e^{n+1}\| \leq C\Delta t. \quad (4.42)$$

Proof: The global error can be written as

$$e^{n+1}(x) = \tilde{e}^{n+1}(x) + d^{n+1}(x), \quad (4.43)$$

where the term $d^{n+1}(x)$ satisfies that

$$\begin{cases} (I + \Delta t \mathbb{L}_{x,\varepsilon}) d^{n+1}(x) + \Delta t [b(x, t_n, y(x, t_n)) - b(x, t_n, y^n(x))] = e^n(x), & x \in \Omega, \\ d^{n+1}(0) = 0 = d^{n+1}(1). \end{cases} \quad (4.44)$$

Further, one can deduce that

$$b(x, t_n, y(x, t_n)) - b(x, t_n, y^n(x)) = \left[\int_0^1 \frac{\partial b(x, t_n, y^n + \xi(y(t_n) - y^n))}{\partial y} d\xi \right] e^n(x). \quad (4.45)$$

Now, since the solutions y^n and $y(t_n)$ are bounded ε -uniformly, the smoothness assumption of $b(x, t, y)$ implies that there exists a constant $\mathfrak{M}_0(> 0)$ (independent of ε) such that

$$\mathfrak{M}_0 = \sup \left\{ \left| \frac{\partial b(x, t, y)}{\partial y} \right|, \quad (x, t) \in \overline{\mathfrak{D}}, \quad |y| \leq C_0 \right\},$$

where $C_0 = \max \left\{ \|y^n\|, \|y(t_n)\|, \quad \text{for } n = 0, 1, \dots, M \right\}$. Then, combining (4.43), (4.44), (4.45); and applying Lemma 4.4 on $d^{n+1}(x)$, we have

$$\|e^{n+1}\| \leq \|\tilde{e}^{n+1}\| + (1 + \mathfrak{M}_0 \Delta t) \|e^n\|.$$

Finally, the desired estimate follows from the above recurrence relation and by utilizing Lemma 4.6 and the inequality $(1 + \mathfrak{M}_0 \Delta t)^n \leq \exp(n \Delta t \mathfrak{M}_0) \leq \exp(T \mathfrak{M}_0)$. ■

4.4.1.1 Properties of the semidiscrete solution

The following lemma shows that although the problem (4.38) seems to be a double parameter $(\varepsilon, \Delta t)$ singularly perturbed problem at first sight, nevertheless the spatial derivatives of the solution $\tilde{y}^{n+1}(x)$ indeed maintain the same asymptotic behavior as that of the solution $y(x, t)$ of the model problem with respect to the parameter ε only. To establish the following result we adopt the approach of [23]. For the proof, apart from the requirement of ε -uniform boundedness of the reaction term ‘ b ’ and smoothness criterion on the given data, we also need certain compatibility conditions at $(0, t_n)$ and $(1, t_n)$ as mentioned in (4.50) and (4.53).

Lemma 4.7. *The solution $\tilde{y}^{n+1}(x)$ of the auxiliary BVP (4.38) and its derivatives satisfy that*

$$\left| \frac{d^j \tilde{y}^{n+1}(x)}{dx^j} \right| \leq C \left(1 + \varepsilon^{-j} \exp(-m(1-x)/\varepsilon) \right), \quad x \in \overline{\Omega}, \quad \text{for } 0 \leq j \leq 4. \quad (4.46)$$

Proof: The above bounds are obtained by considering following cases.

Case 1. Let $j = 0$. From the property (4.11), we have $|b(x, t_n, y(x, t_n))| \leq C$, $x \in \overline{\Omega}$. Then, using the continuity of g on $\overline{\Omega}$ and Lemma 4.4 in the scheme(4.38), we have

$$|\widetilde{y}^{n+1}(x)| \leq C, \quad x \in \overline{\Omega}.$$

Case 2. Let $j = 1$. We consider the function $\zeta(x) = \frac{\widetilde{y}^{n+1}(x) - y(x, t_n)}{\Delta t}$ as the solution of the following BVP:

$$\begin{cases} (I + \Delta t \mathbb{L}_{x,\varepsilon})\zeta(x) = \mathcal{H}_1(x), & x \in \Omega, \\ \zeta(0) = \frac{d\mathbf{s}_l(t_n)}{dt} + C_1\Delta t, \quad \zeta(1) = \frac{d\mathbf{s}_r(t_n)}{dt} + C_2\Delta t, \end{cases} \quad (4.47)$$

where $\mathcal{H}_1(x) = -\mathbb{L}_{x,\varepsilon}y(x, t_n) + g(x, t_{n+1}) - b(x, t_n, y(x, t_n))$ is bounded (ε -uniformly) on $\overline{\Omega}$; and hence, using Lemma 4.4 for (4.47), we obtain that $|\zeta(x)| \leq C$. We now rewrite (4.47) to get the following BVP:

$$\begin{cases} \mathbb{L}_{x,\varepsilon}\widetilde{y}^{n+1}(x) = \mathcal{H}_2(x), & x \in \Omega, \\ \widetilde{y}^{n+1}(0) = \mathbf{s}_l(t), \quad \widetilde{y}^{n+1}(1) = \mathbf{s}_r(t), \end{cases} \quad (4.48)$$

where $\mathcal{H}_2(x) = -\zeta(x) + g(x, t_{n+1}) - b(x, t_n, y(x, t_n))$ is bounded (ε -uniformly) on $\overline{\Omega}$; and hence, using the argument of Kellogg and Tsan [61] for (4.48), we have the required bound (4.46) for $j = 1$.

Case 3. Let $j = 2$. We consider the function $\zeta_1(x) = \mathbb{L}_{x,\varepsilon}\zeta(x)$ as the solution of the following BVP:

$$\begin{cases} (I + \Delta t \mathbb{L}_{x,\varepsilon})\zeta_1(x) = \mathcal{H}_3(x), & x \in \Omega, \\ \zeta_1(0) = \frac{1}{\Delta t} \left[-\frac{d\mathbf{s}_l(t_n)}{dt} + C_1\Delta t + g(0, t_{n+1}) - \mathbb{L}_{x,\varepsilon}y(0, t_n) - b(0, t_n, y(0, t_n)) \right], \\ \zeta_1(1) = \frac{1}{\Delta t} \left[-\frac{d\mathbf{s}_r(t_n)}{dt} + C_2\Delta t + g(1, t_{n+1}) - \mathbb{L}_{x,\varepsilon}y(1, t_n) - b(1, t_n, y(1, t_n)) \right], \end{cases} \quad (4.49)$$

where $\mathcal{H}_3(x) = -\mathbb{L}_{x,\varepsilon}^2 y(x, t_n) + \mathbb{L}_{x,\varepsilon}g(x, t_{n+1}) - \mathbb{L}_{x,\varepsilon}b(x, t_n, y(x, t_n))$ is bounded (ε -uniformly) on $\overline{\Omega}$ due to the smoothness assumption on g , the property (4.11) and Theorem 4.1. Further, from $\frac{\partial y}{\partial t} \in \mathcal{C}^0(\overline{\Omega})$, we obtain the following compatibility conditions:

$$\begin{cases} \frac{d\mathbf{s}_l(t_n)}{dt} = g(0, t_n) - \mathbb{L}_{x,\varepsilon}y(0, t_n) - b(0, t_n, y(0, t_n)), \\ \frac{d\mathbf{s}_r(t_n)}{dt} = g(1, t_n) - \mathbb{L}_{x,\varepsilon}y(1, t_n) - b(1, t_n, y(1, t_n)), \end{cases} \quad (4.50)$$

which yields that

$$\zeta_1(0) = \frac{dg(0, t_n)}{dt} + C_1, \quad \text{and} \quad \zeta_1(1) = \frac{dg(1, t_n)}{dt} + C_2.$$

Therefore, the boundary conditions are $(\varepsilon, \Delta t)$ - uniformly bounded. Thus, applying Lemma 4.4 for (4.49), we obtain that $|\zeta_1(x)| \leq C$, $x \in \overline{\Omega}$. Afterwards, one can deduce that

$$\left| \frac{d\zeta(x)}{dx} \right| \leq C \left(1 + \varepsilon^{-1} \exp(-\mathbf{m}(1-x)/\varepsilon) \right), \quad x \in \overline{\Omega},$$

by invoking Lemma 4.4 to the following BVP:

$$\begin{cases} \mathbb{L}_{x,\varepsilon}\zeta(x) = \zeta_1(x), & x \in \Omega, \\ \zeta(0) = \frac{d\mathbf{s}_l(t_n)}{dt} + C_1\Delta t, & \zeta(1) = \frac{d\mathbf{s}_r(t_n)}{dt} + C_2\Delta t. \end{cases}$$

Now, differentiating (4.48) with respect to x , we consider that $\bar{\zeta}(x) = \frac{d\tilde{y}^{n+1}}{dx}$ satisfies the following problem:

$$\begin{cases} \mathbb{L}_{x,\varepsilon}\bar{\zeta}(x) = \mathcal{H}_4(x), & x \in \Omega, \\ \bar{\zeta}(0) = C_1, & \bar{\zeta}(1) = C_2\varepsilon^{-1}, \end{cases} \quad (4.51)$$

where $\mathcal{H}_4(x) = -\frac{d\zeta(x)}{dx} + \frac{dg(x, t_{n+1})}{dx} - \frac{da(x)}{dx} \frac{d\tilde{y}^{n+1}(x)}{dx} - \left(\frac{\partial b(x, t_n, y(x, t_n))}{\partial x} + \frac{\partial b(x, t_n, y(x, t_n))}{\partial y} \frac{\partial y(x, t_n)}{\partial x} \right)$.

Then, the bound on $\frac{d\zeta}{dx}$, the smoothness assumption on g , the property (4.11) and Theorem 4.1 imply that

$$|\mathcal{H}_4(x)| \leq C \left(1 + \varepsilon^{-1} \exp(-\mathfrak{m}(1-x)/\varepsilon) \right), \quad x \in \bar{\Omega}.$$

Hence, using the argument of Kellogg and Tsan [61] for (4.51), we have the required bound (4.46) for $j = 2$.

Case 4. Let $j = 3, 4$. Here, we derive the result (4.46) for $j = 3$, likewise Case 3 and the similar procedure can be followed for $j = 4$. Firstly, we consider the function $\zeta_2(x) = \mathbb{L}_{x,\varepsilon}^2 \zeta(x)$ as the solution of the following BVP:

$$\begin{cases} (I + \Delta t \mathbb{L}_{x,\varepsilon})\zeta_2(x) = \mathcal{H}_5(x), & x \in \Omega, \\ \zeta_2(x) = \frac{1}{\Delta t} \mathbb{L}_{x,\varepsilon} [g(x, t_{n+1}) - g(x, t_n)] + \\ \frac{1}{\Delta t^2} \left[\zeta(x) + \mathbb{L}_{x,\varepsilon} y(x, t_n) - g(x, t_{n+1}) + b(x, t_n, y(x, t_n)) + \Delta t \mathbb{L}_{x,\varepsilon} \frac{\partial y(x, t_n)}{\partial t} \right], & \text{for } x = 0, 1, \end{cases} \quad (4.52)$$

where following the similar arguments as in Case 3, one can show that $\mathcal{H}_5(x) = -\mathbb{L}_{x,\varepsilon}^3 y(x, t_n) + \mathbb{L}_{x,\varepsilon}^2 g(x, t_{n+1}) - \mathbb{L}_{x,\varepsilon}^2 b(x, t_n, y(x, t_n))$ is bounded (ε -uniformly) on $\bar{\Omega}$. Further, the boundary conditions are $(\varepsilon, \Delta t)$ - uniformly bounded, since $\zeta_2(0)$ and $\zeta_2(1)$ can be rewritten in the following form:

$$\zeta_2(0) = (\mathbb{L}_{x,\varepsilon} g_t)(0, s) - \frac{1}{2} (\mathbb{L}_{x,\varepsilon} y_{tt})(0, s), \quad \text{and} \quad \zeta_2(1) = (\mathbb{L}_{x,\varepsilon} g_t)(1, s) - \frac{1}{2} (\mathbb{L}_{x,\varepsilon} y_{tt})(1, s),$$

where $t_n < s < t_{n+1}$, which follows from the compatibility conditions

$$\begin{cases} \zeta(0) + \Delta t (\mathbb{L}_{x,\varepsilon} y_t)(0, t_n) + \mathbb{L}_{x,\varepsilon} y(0, t_n) - g(0, t_{n+1}) + b(0, t_n, y(0, t_n)) = \frac{-\Delta t^2}{2} (\mathbb{L}_{x,\varepsilon} y_{tt})(0, s), \\ \zeta(1) + \Delta t (\mathbb{L}_{x,\varepsilon} y_t)(1, t_n) + \mathbb{L}_{x,\varepsilon} y(1, t_n) - g(1, t_{n+1}) + b(1, t_n, y(1, t_n)) = \frac{-\Delta t^2}{2} (\mathbb{L}_{x,\varepsilon} y_{tt})(1, s), \end{cases} \quad (4.53)$$

obtained from (4.49). Therefore, applying Lemma 4.4 for (4.52), we obtain that $|\zeta_2(x)| \leq C$, $x \in \bar{\Omega}$. Now,

similar arguments can be applied for the following BVP:

$$\begin{cases} \mathbb{L}_{x,\varepsilon}\zeta_1(x) = \zeta_2(x), & x \in \Omega, \\ \zeta_1(0) = \frac{d\mathbf{s}_l(t_n)}{dt} + C_1\Delta t, & \zeta_1(1) = \frac{d\mathbf{s}_r(t_n)}{dt} + C_2\Delta t, \end{cases}$$

to prove that

$$\left| \frac{d^2\zeta(x)}{dx^2} \right| \leq C \left(1 + \varepsilon^{-2} \exp(-\mathfrak{m}(1-x)/\varepsilon) \right), \quad x \in \overline{\Omega}.$$

Now, differentiating (4.51) with respect to x , we consider that $\bar{\zeta}_1(x) = \frac{d^2\tilde{y}^{n+1}}{dx^2}$ satisfies the following problem:

$$\begin{cases} \mathbb{L}_{x,\varepsilon}\bar{\zeta}_1(x) = \mathcal{H}_6(x), & x \in \Omega, \\ \bar{\zeta}_1(0) = C_1, & \bar{\zeta}_1(1) = C_2\varepsilon^{-2}, \end{cases} \quad (4.54)$$

where

$$\begin{aligned} \mathcal{H}_6(x) = & -\frac{d^2\zeta(x)}{dx^2} + \frac{d^2g(x, t_{n+1})}{dx^2} - 2\frac{da(x)}{dx} \frac{d^2\tilde{y}^{n+1}(x)}{dx^2} - \frac{d^2a(x)}{dx^2} \frac{d\tilde{y}^{n+1}}{dx} - \\ & \left[\frac{\partial^2 b}{\partial x^2} + \frac{\partial^2 b}{\partial x \partial y} \frac{\partial y}{\partial x} + \left(\frac{\partial^2 b}{\partial y \partial x} + \frac{\partial^2 b}{\partial y^2} \frac{\partial y}{\partial x} \right) \frac{\partial y}{\partial x} + \frac{\partial b}{\partial y} \frac{\partial^2 y}{\partial x^2} \right]. \end{aligned}$$

Since, $|\mathcal{H}_6(x)| \leq C \left(1 + \varepsilon^{-2} \exp(-\mathfrak{m}(1-x)/\varepsilon) \right)$, $x \in \overline{\Omega}$, using the same argument as in Case 3, one can derive the required bound (4.46) for $j = 3$. ■

Further, we need decomposition of the exact solution $\tilde{y}^{n+1}(x)$ of the BVP (4.38) in order to establish bound of the truncation error in the subsequent section.

Lemma 4.8. *The solution $\tilde{y}^{n+1}(x)$ can be decomposed in the form*

$$\tilde{y}^{n+1}(x) = \tilde{p}^{n+1}(x) + \gamma \tilde{q}^{n+1}(x),$$

where

$$\begin{cases} \tilde{q}^{n+1}(x) = \exp\left(-\frac{a(1)(1-x)}{\varepsilon}\right), & \gamma = \frac{\varepsilon}{a(1)} \frac{d\tilde{y}^{n+1}(1)}{dx}, \\ \text{and } \left| \frac{d^j \tilde{p}^{n+1}(x)}{dx^j} \right| \leq C \left(1 + \varepsilon^{-j+1} \exp(-\mathfrak{m}(1-x)/\varepsilon) \right), & x \in \overline{\Omega}, \text{ for } 0 \leq j \leq 4. \end{cases}$$

Proof. Let $\tilde{p}^{n+1}(x) = \tilde{y}^{n+1}(x) - \gamma \tilde{q}^{n+1}(x)$. Then, we have

$$\mathbb{L}_{x,\varepsilon}\tilde{p}^{n+1}(x) = \mathcal{R}_1(x), \quad x \in \Omega, \quad (4.55)$$

where $\mathcal{R}_1(x) = \mathcal{H}_2(x) + \gamma(a(1) - a(x)) \frac{d\tilde{q}^{n+1}(x)}{dx}$; and differentiating (4.55) with respect to x , it yields that

$$\mathbb{L}_{x,\varepsilon} \frac{d\tilde{p}^{n+1}(x)}{dx} = \mathcal{R}_2(x), \quad x \in \Omega, \quad (4.56)$$

where $\mathcal{R}_2(x) = \mathcal{H}_4(x) - \frac{da(x)}{dx} \frac{d\tilde{q}^{n+1}(x)}{dx} - \gamma \frac{da(x)}{dx} \frac{d\tilde{q}^{n+1}(x)}{dx} + \gamma(a(1) - a(x)) \frac{d^2\tilde{q}^{n+1}(x)}{dx^2}$. Now, one can show that

$\mathcal{R}_1(x)$ bounded (ε -uniformly) on $\overline{\Omega}$ and

$$|\mathcal{R}_2(x)| \leq C \left(1 + \varepsilon^{-1} \exp \left(-\mathfrak{m}(1-x)/\varepsilon \right) \right), \quad x \in \overline{\Omega}.$$

Also, it holds that

$$|\tilde{p}^{n+1}(0)| \leq C, \quad |\tilde{p}^{n+1}(1)| \leq C, \quad \left| \frac{d\tilde{p}^{n+1}(0)}{dx} \right| \leq C, \quad \frac{d\tilde{p}^{n+1}(1)}{dx} = 0.$$

Therefore, using the argument of [61] for (4.55) and (4.56), it follows that

$$\left| \frac{d^j \tilde{p}^{n+1}(x)}{dx^j} \right| \leq C \left(1 + \varepsilon^{-j+1} \exp \left(-\mathfrak{m}(1-x)/\varepsilon \right) \right), \quad x \in \overline{\Omega}, \quad j = 1, 2. \quad (4.57)$$

Finally, by adopting the approach as mentioned above, one can obtain the required bounds on the spatial derivatives of $\tilde{p}^{n+1}(x)$ for $j = 3, 4$. ■

4.4.2 Error estimate for the spatial discretization

Here, we analyze the following discrete problem, which is obtained by discretizing (4.38) with respect to the spatial variable using the proposed hybrid scheme:

$$\begin{cases} \mathbb{L}_\varepsilon^{N,\Delta t} \tilde{Y}_j^{n+1} \equiv \nu_j^- \tilde{Y}_{j-1}^{n+1} + \nu_j^c \tilde{Y}_j^{n+1} + \nu_j^+ \tilde{Y}_{j+1}^{n+1} = \tilde{\mathbb{F}}_j^{n+1}, \\ \quad \text{for } 1 \leq j \leq N-1, \\ \tilde{Y}_0^{n+1} = \mathbf{s}_l(t_{n+1}), \quad \tilde{Y}_N^{n+1} = \mathbf{s}_r(t_{n+1}), \end{cases} \quad (4.58)$$

where the coefficients ν_j^- , ν_j^+ , ν_j^c are described in (4.31)-(4.33) and $\tilde{\mathbb{F}}_j^{n+1}$ is given by

$$\tilde{\mathbb{F}}_j^{n+1} = \begin{cases} \frac{1}{2}(y(x_{j-1}, t_n) + \Delta t g_{j-1}^{n+1}) + \frac{1}{2}(y(x_j, t_n) + \Delta t g_j^{n+1}) - \Delta t b(x_{j-\frac{1}{2}}, t_n, y(x_{j-\frac{1}{2}}, t_n)), \\ \quad \text{for } 1 \leq j \leq N/2, \text{ and when } \varepsilon \leq \|a\| N^{-1}, \\ y(x_j, t_n) + \Delta t g_j^{n+1} - \Delta t b(x_j, t_n, y(x_j, t_n)), \\ \quad \text{for } 1 \leq j \leq N/2, \text{ and when } \varepsilon > \|a\| N^{-1}, \\ y(x_j, t_n) + \Delta t g_j^{n+1} - \Delta t b(x_j, t_n, y(x_j, t_n)), \text{ for } N/2 < j \leq N-1. \end{cases} \quad (4.59)$$

The following lemma shows that the difference operator $\mathbb{L}_\varepsilon^{N,\Delta t}$ satisfies the discrete maximum principle.

Lemma 4.9 (Discrete Maximum Principle). *Assume that the following conditions hold for $N \geq N_0$:*

$$N/\ln N > \eta_0 \|a\|, \quad (4.60)$$

$$\text{and } \mathfrak{m}N \geq \frac{1}{\Delta t}. \quad (4.61)$$

For fixed n , suppose that the mesh function $\psi_j^{n+1} = \psi^{n+1}(x_j)$ defined on $\overline{\Omega}^N$ satisfies that $\psi_0^{n+1} \leq 0$, $\psi_N^{n+1} \leq$

0, and $\mathbb{L}_\varepsilon^{N,\Delta t} \psi_j^{n+1} \leq 0$, for $1 \leq j \leq N-1$. Then, we have $\psi_j^{n+1} \leq 0$, for all j .

Proof. See [Chapter 2, Lemma 7.2.7] for the proof. ■

Next, we derive the local truncation error $\mathcal{T}_{j,\tilde{y}^{n+1}}^{N,\Delta t} = \mathbb{L}_\varepsilon^{N,\Delta t} [\tilde{y}_j^{n+1} - \tilde{Y}_j^{n+1}]$ for the scheme (4.58)-(4.59). Let $1 \leq j \leq N/2$. Then, we have for $\varepsilon > \|a\|N^{-1}$,

$$\mathcal{T}_{j,\tilde{y}^{n+1}}^{N,\Delta t} = \nu_j^- \tilde{y}_{j-1}^{n+1} + \nu_j^c \tilde{y}_j^{n+1} + \nu_j^+ \tilde{y}_{j+1}^{n+1} - \Delta t \left[g(x_j, t_{n+1}) - b(x_j, t_n, y(x_j, t_n)) \right] - y(x_j, t_n), \quad (4.62)$$

and for $\varepsilon \leq \|a\|N^{-1}$,

$$\begin{aligned} \mathcal{T}_{j,\tilde{y}^{n+1}}^{N,\Delta t} &= \nu_j^- \tilde{y}_{j-1}^{n+1} + \nu_j^c \tilde{y}_j^{n+1} + \nu_j^+ \tilde{y}_{j+1}^{n+1} - \Delta t \left[\frac{g(x_j, t_{n+1}) + g(x_{j-1}, t_{n+1})}{2} \right] \\ &\quad - \Delta t \left[\frac{b(x_j, t_n, y(x_j, t_n)) + b(x_{j-1}, t_n, y(x_{j-1}, t_n))}{2} \right] - \frac{y(x_j, t_n) + y(x_{j-1}, t_n)}{2} + O(\Delta t h_j^2). \end{aligned} \quad (4.63)$$

Next, for $N/2 < j \leq N-1$,

$$\mathcal{T}_{j,\tilde{y}^{n+1}}^{N,\Delta t} = \nu_j^- \tilde{y}_{j-1}^{n+1} + \nu_j^c \tilde{y}_j^{n+1} + \nu_j^+ \tilde{y}_{j+1}^{n+1} - \Delta t \left[g(x_j, t_{n+1}) - b(x_j, t_n, y(x_j, t_n)) \right] - y(x_j, t_n). \quad (4.64)$$

Then, the truncation error can be written in the following form

$$\mathcal{T}_{j,\tilde{y}^{n+1}}^{N,\Delta t} = \begin{cases} \Delta t \mathcal{T}_{j,\tilde{y}^{n+1}}^N, & \text{for } 1 \leq j \leq N/2, \text{ and when } \varepsilon > \|a\|N^{-1}, \\ \Delta t \mathcal{T}_{j,\tilde{y}^{n+1}}^N + O(\Delta t h_j^2), & \text{for } 1 \leq j \leq N/2, \text{ and when } \varepsilon \leq \|a\|N^{-1}, \\ \Delta t \mathcal{T}_{j,\tilde{y}^{n+1}}^N, & \text{for } N/2 < j \leq N-1, \end{cases}$$

where

$$\mathcal{T}_{j,\tilde{y}^{n+1}}^N = \begin{cases} \mathbb{L}_{mcd}^N \tilde{y}_j^{n+1} - (\mathbb{L}_{x,\varepsilon} \tilde{y}^{n+1})(x_j), & \text{for } 1 \leq j \leq N/2, \text{ and when } \varepsilon > \|a\|N^{-1}, \\ \mathbb{L}_{mup}^N \tilde{y}_j^{n+1} - (\mathbb{L}_{x,\varepsilon} \tilde{y}^{n+1})_{j-\frac{1}{2}}, & \text{for } 1 \leq j \leq N/2, \text{ and when } \varepsilon \leq \|a\|N^{-1}, \\ \mathbb{L}_{mcd}^N \tilde{y}_j^{n+1} - (\mathbb{L}_{x,\varepsilon} \tilde{y}^{n+1})(x_j), & \text{for } N/2 < j \leq N-1. \end{cases}$$

We now provide a brief outline of the proof for the error estimate stated in Theorem 4.5. At first, using the decomposition of \tilde{y}^{n+1} in Lemma 4.8, we decompose $\mathcal{T}_{j,\tilde{y}^{n+1}}^N$, as

$$\mathcal{T}_{j,\tilde{y}^{n+1}}^N = \mathcal{T}_{j,\tilde{p}^{n+1}}^N + \mathcal{T}_{j,\tilde{q}^{n+1}}^N, \quad (4.65)$$

where $\mathcal{T}_{j,\tilde{p}^{n+1}}^N$ and $\mathcal{T}_{j,\tilde{q}^{n+1}}^N$ denote the truncation errors corresponding to $\tilde{p}^{n+1}(x)$ and $\tilde{q}^{n+1}(x)$, respectively. Then, utilizing (4.65), (4.65) and Lemma 4.8, we obtain the bounds of $\mathcal{T}_{j,\tilde{y}^{n+1}}^{N,\Delta t}$ (see [Chapter 2, Lemma 2.10]). Further, we require the following important result for the error analysis.

Lemma 4.10. Consider the mesh function

$$\mathcal{S}_j(\theta) = \begin{cases} \prod_{k=j+1}^N \left(1 + \frac{\theta h_k}{\varepsilon}\right)^{-1}, & \text{for } 0 \leq j \leq N-1, \\ 1, & \text{for } j = N, \end{cases}$$

where θ is a positive constant such that $\theta < \mathfrak{m}/2$. Then, under the hypothesis (4.60)-(4.60) of Lemma 4.9, we have

$$\mathbb{L}_\varepsilon^{N,\Delta t} \mathcal{S}_j(\theta) \geq \begin{cases} \frac{C\Delta t}{\varepsilon} \mathcal{S}_j(\theta), & \text{for } 1 \leq j \leq N/2, \text{ and when } \varepsilon > \|a\|N^{-1}, \\ \frac{C\Delta t}{H} \mathcal{S}_j(\theta), & \text{for } 1 \leq j \leq N/2, \text{ and when } \varepsilon \leq \|a\|N^{-1}, \\ \frac{C\Delta t}{\varepsilon} \mathcal{S}_j(\theta), & \text{for } N/2 < j \leq N-1. \end{cases}$$

Proof: From (4.31)-(4.34), we obtain that

$$\mathbb{L}_\varepsilon^{N,\Delta t} \mathcal{S}_j(\theta) = \begin{cases} \Delta t \mathbb{L}_{mcd}^N \mathcal{S}_j(\theta) + \mathcal{S}_j(\theta), & \text{for } 1 \leq j \leq N/2, \text{ and when } \varepsilon > \|a\|N^{-1} \\ \Delta t \mathbb{L}_{mup}^N \mathcal{S}_j(\theta) + \frac{1}{2} \left(1 + \frac{\varepsilon}{\varepsilon + \theta h_j}\right) \mathcal{S}_j(\theta), & \text{for } 1 \leq j \leq N/2, \text{ and when } \varepsilon \leq \|a\|N^{-1}, \\ \Delta t \mathbb{L}_{mcd}^N \mathcal{S}_j(\theta) + \mathcal{S}_j(\theta), & \text{for } N/2 < j \leq N-1. \end{cases} \quad (4.66)$$

The rest of the proof follows from [Chapter 2, Lemma 2.12]. ■

Afterwards, by making use of Lemma 4.9 together with the bounds of $\mathcal{T}_{j,\tilde{y}^{n+1}}^{N,\Delta t}$ and Lemma 4.10, one can derive the following result.

Theorem 4.5 (Spatial error). *Let $\theta < \mathfrak{m}/2$ and $\eta_0 \geq 2/\theta$. Then, under the conditions (4.60) and (4.61), the following error estimate holds related to the discrete problem (4.58):*

$$\left| \tilde{y}^{n+1}(x_j) - \tilde{Y}_j^{n+1} \right| \leq \begin{cases} CN^{-2}, & \text{for } 1 \leq j \leq N/2, \\ CN^{-2} \ln^2 N, & \text{for } N/2 < j \leq N-1. \end{cases} \quad (4.67)$$

4.4.3 Convergence result for the IMEX-FMM

Theorem 4.6 (Global error). *Let $y(x, t)$ be the exact solution of the problem (4.1)-(4.3), and Y_j^{n+1} be the discrete solution of the fully discrete scheme (4.30), at time level t_{n+1} . If $\theta < \frac{\mathfrak{m}}{2}$ and $\eta_0 \geq \frac{2}{\theta}$, under the assumptions (4.60) and (4.61), the following error estimate holds:*

$$\left\| \{y(x_j, t_{n+1})\}_j - \{Y_j^{n+1}\}_j \right\| \leq \begin{cases} C(N^{-2+\delta} + \Delta t), & \text{for } 1 \leq j \leq N/2, \\ C(N^{-2+\delta} \ln^2 N + \Delta t), & \text{for } N/2 < j \leq N-1, \end{cases} \quad (4.68)$$

where N and Δt are such that $N^{-\delta} \leq C\Delta t$ with $0 < \delta < 1$.

Proof. The global error can be written as

$$E^{n+1}(x_j) = \tilde{e}^{n+1}(x_j) + \tilde{E}^{n+1}(x_j) + R_j^{n+1}, \quad (4.69)$$

where $\tilde{e}^{n+1}(x_j) = [y(x_j, t_{n+1}) - \tilde{y}^{n+1}(x_j)]$, $\tilde{E}^{n+1}(x_j) = [\tilde{y}^{n+1}(x_j) - \tilde{Y}_j^{n+1}]$, and the term R_j^{n+1} satisfies that

$$\begin{cases} \mathbb{L}_\varepsilon^{N, \Delta t} R_j^{n+1} = -\Delta t [b(x_j, t_n, y(x_j, t_n)) - b(x_j, t_n, Y_j^n)] + y(x_j, t_n) - Y_j^n, & 1 \leq j \leq N-1. \\ R_0^{n+1} = R_N^{n+1} = 0. \end{cases}$$

Next, applying discrete maximum principle for the operator $\mathbb{L}_\varepsilon^{N, \Delta t}$, one can deduce that

$$\|\{R_j^{n+1}\}_j\| \leq (1 + \mathfrak{M}_1 \Delta t) \|\{y(x_j, t_n)\}_j - \{Y_j^n\}_j\|, \quad \text{for } 0 \leq j \leq N, \quad (4.70)$$

where \mathfrak{M}_1 is a constant (>0) (independent of ε) such that

$$\mathfrak{M}_1 = \sup \left\{ \left| \frac{\partial b(x, t, y)}{\partial y} \right|, \quad (x, t) \in \overline{\mathfrak{D}}, \quad |y| \leq C_1 \right\},$$

and $C_1 = \max \left\{ \|Y^n\|, \|y(t_n)\|, \quad \text{for } n = 0, 1, \dots, M \right\}$. Thereafter, using (4.69) and (4.70) together with Lemma 4.6, Theorem 4.5, and the assumption $N^{-\delta} \leq C \Delta t$ with $0 < \delta < 1$, we obtain that

$$\|\{E^{n+1}(x_j)\}_j\| \leq \begin{cases} C \Delta t (\Delta t + N^{-2+\delta}) + (1 + \mathfrak{M}_1 \Delta t) \|\{E^n(x_j)\}_j\|, & \text{for } 1 \leq j \leq N/2, \\ C \Delta t (\Delta t + N^{-2+\delta} \ln^2 N) + (1 + \mathfrak{M}_1 \Delta t) \|\{E^n(x_j)\}_j\|, & \text{for } N/2 < j \leq N. \end{cases}$$

Hence, we establish the estimate in (4.68) by using $(1 + \mathfrak{M}_1 \Delta t)^n \leq \exp(\mathfrak{M}_1 T)$. ■

Remark 4.3. In this section, we carry out the error analysis by invoking the two-stage discretization technique keeping in mind the extension of the proposed method for solving multi-dimensional nonlinear parabolic PDEs. One can further note that the theoretical restriction $N^{-\delta} \leq C \Delta t$ with $0 < \delta < 1$ in Theorem 4.6 is no longer appear in the numerical results of the proposed IMEX method; and can be eliminated by estimating the error separately for the smooth component and the layer component as like the error analysis in the next section.

4.5 Convergence analysis for the fully-implicit FMM

For the convergence analysis, we rewrite the fully discrete scheme (4.31) in the following form:

$$\begin{cases} y_j^0 = q_0(x_j), \quad 0 \leq j \leq N, \\ \begin{cases} \mathbb{T}_\varepsilon^{N, \Delta t} Y_j^{n+1} = \mathbb{G}_j^{n+1}, & \text{for } 1 \leq j \leq N-1, \\ Y_0^{n+1} = \mathbf{s}_l(t_{n+1}), \quad Y_N^{n+1} = \mathbf{s}_r(t_{n+1}), & \text{for } n = 0, 1, \dots, M-1, \end{cases} \end{cases} \quad (4.71)$$

where the nonlinear discrete operator $\mathbb{T}_\varepsilon^{N,\Delta t}$ is given by

$$\mathbb{T}_\varepsilon^{N,\Delta t} Y_j^{n+1} = \begin{cases} D_t^- Y_j^{n+1} + \mathbb{L}_{mcd}^N Y_j^{n+1} + b(x_j, t_{n+1}, Y_j^{n+1}), & \text{for } 1 \leq j \leq N/2, \text{ and when } \varepsilon > \|a\|N^{-1}, \\ D_t^- Y_{j-\frac{1}{2}}^{n+1} + \mathbb{L}_{mup}^N Y_j^{n+1} + b(x_{j-\frac{1}{2}}, t_{n+1}, Y_{j-\frac{1}{2}}^{n+1}), & \text{for } 1 \leq j \leq N/2, \text{ and when } \varepsilon \leq \|a\|N^{-1}, \\ D_t^- Y_j^{n+1} + \mathbb{L}_{mcd}^N Y_j^{n+1} + b(x_j, t_{n+1}, Y_j^{n+1}), & \text{for } N/2 < j \leq N-1, \end{cases}$$

and the right-hand side vector \mathbb{G}^{n+1} is given by

$$\mathbb{G}_j^{n+1} = \begin{cases} g_{j-\frac{1}{2}}^{n+1}, & \text{for } 1 \leq j \leq N/2, \text{ and when } \varepsilon \leq \|a\|N^{-1}, \\ g_j^{n+1}, & \text{for } 1 \leq j \leq N/2, \text{ and when } \varepsilon > \|a\|N^{-1}, \\ g_j^{n+1}, & \text{for } N/2 < j \leq N-1. \end{cases}$$

For the sake of convenience, we set $g_{j-1/2}^{n+1} = g(x_{j-1/2}, t_{n+1})$ and $a_{j-1/2} = a(x_{j-1/2})$, in the rest of the chapter.

Lemma 4.11 (Discrete Comparison Principle). *Assume that the following conditions hold for $N \geq N_0$:*

$$N/\ln N > \eta_0 \|a\|, \quad (4.72)$$

$$\text{and } \mathfrak{m}N \geq \left(\left\| \frac{\partial b}{\partial y} \right\| + \frac{1}{\Delta t} \right). \quad (4.73)$$

Suppose that two mesh functions V and W defined on $\overline{\mathfrak{D}}^{N,\Delta t}$ satisfies that $V \leq W$ on $\partial \mathfrak{D}^{N,\Delta t}$ and $\mathbb{T}_\varepsilon^{N,\Delta t} V \leq \mathbb{T}_\varepsilon^{N,\Delta t} W$ in $\mathfrak{D}^{N,\Delta t}$. Then, we have $V \leq W$ on $\overline{\mathfrak{D}}^{N,\Delta t}$.

Proof: Let $\omega_j^n \leq 0$, for all j and n . Then, inconformity with the hypothesis of the discrete comparison principle, we assume that $V_j^0 - W_j^0 = \omega_j^0$ for $0 \leq j \leq N$ and consider the following system:

$$\begin{cases} \mathbb{T}_\varepsilon^{N,\Delta t} V_j^{n+1} - \mathbb{T}_\varepsilon^{N,\Delta t} W_j^{n+1} = \omega_j^{n+1}, & \text{for } 1 \leq j \leq N-1, \\ V_0^{n+1} - W_0^{n+1} = \omega_0^{n+1}, \quad V_N^{n+1} - W_N^{n+1} = \omega_N^{n+1}, & \text{for } n = 0, 1, \dots, M-1. \end{cases} \quad (4.74)$$

Now, let $U_j^n = V_j^n - W_j^n$ for all n . Then, we have

$$\begin{aligned} \mathbb{T}_\varepsilon^{N,\Delta t} V_j^{n+1} - \mathbb{T}_\varepsilon^{N,\Delta t} W_j^{n+1} = & \\ \left\{ \begin{array}{l} D_t^- U_j^{n+1} + \mathbb{L}_{mcd}^N U_j^{n+1} + \left[\int_0^1 \frac{\partial b(x_j, t_{n+1}, W_j^{n+1} + \xi(V_j^{n+1} - W_j^{n+1})) d\xi}{\partial y} \right] U_j^{n+1}, \\ \quad \text{for } 1 \leq j \leq N/2 \text{ and when } \varepsilon > \|a\|N^{-1}, \\ D_t^- U_{j-\frac{1}{2}}^{n+1} + \mathbb{L}_{mup}^N U_{j-\frac{1}{2}}^{n+1} + \left[\int_0^1 \frac{\partial b(x_{j-\frac{1}{2}}, t_{n+1}, W_{j-\frac{1}{2}}^{n+1} + \xi(V_{j-\frac{1}{2}}^{n+1} - W_{j-\frac{1}{2}}^{n+1})) d\xi}{\partial y} \right] U_{j-\frac{1}{2}}^{n+1}, \\ \quad \text{for } 1 \leq j \leq N/2 \text{ and when } \varepsilon \leq \|a\|N^{-1}, \\ D_t^- U_j^{n+1} + \mathbb{L}_{mcd}^N U_j^{n+1} + \left[\int_0^1 \frac{\partial b(x_j, t_{n+1}, W_j^{n+1} + \xi(V_j^{n+1} - W_j^{n+1})) d\xi}{\partial y} \right] U_j^{n+1}, \\ \quad \text{for } N/2 < j \leq N. \end{array} \right. \quad (4.75) \end{aligned}$$

For simplifying the proof, we set $U^n = (U_0^n, U_1^n, \dots, U_N^n)$ and $\omega^n = (\omega_0^n, \omega_1^n, \dots, \omega_N^n)$, for $n = 0, 1, \dots, M$. Here, by employing equation (4.75), we can rewrite equation (4.74) in the following form:

$$\mathbf{A}U^{n+1} - \mathbf{B}U^n = \omega^{n+1}, \text{ for } n = 0, 1, \dots, M-1.$$

Here, the matrix \mathbf{A} is given by $\mathbf{A}_{j,j} = 1$, for $j = 0, N$, and

$$\left\{ \begin{array}{l} \mathbf{A}_{j,j-1} = \tilde{\nu}_{mcd,j}^-, \mathbf{A}_{j,j} = \tilde{\nu}_{mcd,j}^c + \frac{1}{\Delta t}, \mathbf{A}_{j,j+1} = \tilde{\nu}_{mcd,j}^+ \\ \quad \text{for } 1 \leq j \leq N/2 \text{ and when } \varepsilon > \|a\|N^{-1}, \\ \mathbf{A}_{j,j-1} = \tilde{\nu}_{mup,j}^- + \frac{1}{2\Delta t}, \mathbf{A}_{j,j} = \tilde{\nu}_{mup,j}^c + \frac{1}{2\Delta t}, \mathbf{A}_{j,j+1} = \tilde{\nu}_{mup,j}^+ \\ \quad \text{for } 1 \leq j \leq N/2 \text{ and when } \varepsilon \leq \|a\|N^{-1}, \\ \mathbf{A}_{j,j-1} = \tilde{\nu}_{mcd,j}^-, \mathbf{A}_{j,j} = \tilde{\nu}_{mcd,j}^c + \frac{1}{\Delta t}, \mathbf{A}_{j,j+1} = \tilde{\nu}_{mcd,j}^+ \text{ for } N/2 < j < N, \end{array} \right.$$

where

$$\left\{ \begin{array}{l} \tilde{\nu}_{mup,j}^- = \nu_{mup,j}^- + \frac{1}{2} \left[\int_0^1 \frac{\partial b(x_{j-\frac{1}{2}}, t_{n+1}, W_{j-\frac{1}{2}}^{n+1} + \xi(V_{j-\frac{1}{2}}^{n+1} - W_{j-\frac{1}{2}}^{n+1})) d\xi}{\partial y} \right], \\ \tilde{\nu}_{mup,j}^c = \nu_{mup,j}^c + \frac{1}{2} \left[\int_0^1 \frac{\partial b(x_{j-\frac{1}{2}}, t_{n+1}, W_{j-\frac{1}{2}}^{n+1} + \xi(V_{j-\frac{1}{2}}^{n+1} - W_{j-\frac{1}{2}}^{n+1})) d\xi}{\partial y} \right], \\ \tilde{\nu}_{mup,j}^+ = \nu_{mup,j}^+, \end{array} \right.$$

and

$$\left\{ \begin{array}{l} \tilde{\nu}_{mcd,j}^- = \nu_{mcd,j}^-, \\ \tilde{\nu}_{mcd,j}^c = \nu_{mcd,j}^c + \left[\int_0^1 \frac{\partial b(x_j, t_{n+1}, W_j^{n+1} + \xi(V_j^{n+1} - W_j^{n+1})) d\xi}{\partial y} \right], \\ \tilde{\nu}_{mcd,j}^+ = \nu_{mcd,j}^+. \end{array} \right.$$

One can show that, under the conditions (4.72) and (4.73), the matrix \mathbf{A} is an M-matrix (see the proof in Lemma 2.7 of Chapter 2) and it is straightforward that the matrix $\mathbf{B} \geq 0$. Therefore, the proof follows from [99, Lemma 3.12]. \blacksquare

Remark 4.4. From the discrete comparison principle, one can obtain the existence and uniqueness of the solution to the discrete problem (4.71)(see the Hadamard's Theorem 5.3.10 in [91]).

Corollary 4.2. *Let Ψ be any mesh function defined on $\overline{\mathfrak{D}}^{N,\Delta t}$. Then, for any given mesh functions V and W defined on $\overline{\mathfrak{D}}^{N,\Delta t}$, the difference operator $\tilde{\mathbb{T}}_{\varepsilon,(V,W)}^{N,\Delta t}$ given by*

$$\tilde{\mathbb{T}}_{\varepsilon,(V,W)}^{N,\Delta t} \Psi_j^{n+1} = \begin{cases} D_t^- \Psi_j^{n+1} + \mathbb{L}_{mcd}^N \Psi_j^{n+1} + \left[\int_0^1 \frac{\partial b(x_j, t_{n+1}, W_j^{n+1} + \xi(V_j^{n+1} - W_j^{n+1}))}{\partial y} d\xi \right] \Psi_j^{n+1}, \\ \quad \text{for } 1 \leq j \leq N/2 \text{ and when } \varepsilon > \|a\|N^{-1}, \\ \\ D_t^- \Psi_{j-\frac{1}{2}}^{n+1} + \mathbb{L}_{mup}^N \Psi_j^{n+1} + \left[\int_0^1 \frac{\partial b(x_{j-\frac{1}{2}}, t_{n+1}, W_{j-\frac{1}{2}}^{n+1} + \xi(V_{j-\frac{1}{2}}^{n+1} - W_{j-\frac{1}{2}}^{n+1}))}{\partial y} d\xi \right] \Psi_{j-\frac{1}{2}}^{n+1}, \\ \quad \text{for } 1 \leq j \leq N/2 \text{ and when } \varepsilon \leq \|a\|N^{-1}, \\ \\ D_t^- \Psi_j^{n+1} + \mathbb{L}_{mcd}^N \Psi_j^{n+1} + \left[\int_0^1 \frac{\partial b(x_j, t_{n+1}, W_j^{n+1} + \xi(V_j^{n+1} - W_j^{n+1}))}{\partial y} d\xi \right] \Psi_j^{n+1}, \\ \quad \text{for } N/2 < j \leq N, \end{cases}$$

satisfies the discrete maximum principle, i.e., if $\Psi \leq 0$, on $\partial \mathfrak{D}^{N,\Delta t}$ and $\tilde{\mathbb{T}}_{\varepsilon,(V,W)}^{N,\Delta t} \Psi \leq 0$, in $\mathfrak{D}^{N,\Delta t}$, then it implies that $\Psi \leq 0$, on $\overline{\mathfrak{D}}^{N,\Delta t}$.

Lemma 4.12 (Stability). *Let V and W be two mesh function defined on $\overline{\mathfrak{D}}^{N,\Delta t}$. Then, under the conditions (4.72) and (4.73), we have*

$$\|V - W\|_{\overline{\mathfrak{D}}^{N,\Delta t}} \leq \|V - W\|_{\partial \mathfrak{D}^{N,\Delta t}} + \frac{1}{\beta} \|\mathbb{T}_{\varepsilon}^{N,\Delta t} V - \mathbb{T}_{\varepsilon}^{N,\Delta t} W\|_{\overline{\mathfrak{D}}^{N,\Delta t}}. \quad (4.76)$$

Proof. Consider the mesh functions

$$\Psi^{\pm}(x_j, t_n) = -\|V - W\|_{\partial \mathfrak{D}^{N,\Delta t}} - \frac{1}{\beta} \|\mathbb{T}_{\varepsilon}^{N,\Delta t} V - \mathbb{T}_{\varepsilon}^{N,\Delta t} W\| \pm (V - W)(x_j, t_n), \quad (x_j, t_n) \in \overline{\mathfrak{D}}^{N,\Delta t}.$$

Note that $\Psi^{\pm}(x_j, t_n) \leq 0$, on $\partial \mathfrak{D}^{N,\Delta t}$, and $\tilde{\mathbb{T}}_{\varepsilon,(V,W)}^{N,\Delta t} \Psi^{\pm}(x_j, t_{n+1}) \leq 0$, in $\mathfrak{D}^{N,\Delta t}$. Then, Corollary 4.2 implies that $\Psi^{\pm}(x_j, t_n) \leq 0$, for all $(x_j, t_n) \in \overline{\mathfrak{D}}^{N,\Delta t}$. Hence, the proof is over. \blacksquare

Before we proceed for the error analysis, we provide the following important result which is used in the subsequent section.

Lemma 4.13. *Consider the mesh function*

$$\mathcal{S}_j(\theta) = \begin{cases} \prod_{k=j+1}^N \left(1 + \frac{\theta h_k}{\varepsilon}\right)^{-1}, & \text{for } 0 \leq j \leq N-1, \\ 1, & \text{for } j = N, \end{cases}$$

where θ is a positive constant such that $\theta < \mathfrak{m}/2$. Then, under the hypothesis (4.72)-(4.73) of Lemma 4.11, we have

$$\tilde{\mathbb{T}}_{\varepsilon, (V, W)}^{N, \Delta t} \mathcal{S}_j(\theta) \geq \begin{cases} \frac{C}{\varepsilon} \mathcal{S}_j(\theta), & \text{for } 1 \leq j \leq N/2, \text{ and when } \varepsilon > \|a\|N^{-1}, \\ \frac{C}{H} \mathcal{S}_j(\theta), & \text{for } 1 \leq j \leq N/2, \text{ and when } \varepsilon \leq \|a\|N^{-1}, \\ \frac{C}{\varepsilon} \mathcal{S}_j(\theta), & \text{for } N/2 < j \leq N-1. \end{cases} \quad (4.77)$$

4.5.1 Decomposition of the discrete solution and error estimates

We decompose the numerical solution Y_j^{n+1} into the smooth component P_j^{n+1} and the layer component Q_j^{n+1} such that $Y_j^{n+1} = P_j^{n+1} + Q_j^{n+1}$. Here, P_j^{n+1} satisfies the following discrete problem:

$$\begin{cases} P_j^0 = p(x_j, 0), & 0 \leq j \leq N, \\ \mathbb{T}_{\varepsilon}^{N, \Delta t} P_j^{n+1} = \mathbb{G}_j^{n+1}, & 1 \leq j \leq N-1, \\ P_0^{n+1} = p(0, t_{n+1}), & P_N^{n+1} = p(1, t_{n+1}). \end{cases} \quad (4.78)$$

Lemma 4.14. *Let the assumptions (4.72) and (4.73) of Lemma 4.11 hold. Then, the error related to the smooth component satisfies the following estimate:*

$$\left| P_j^{n+1} - p(x_j, t_{n+1}) \right| \leq C(N^{-2} + \Delta t), \quad \text{for } 1 \leq j \leq N-1. \quad (4.79)$$

Proof. For $1 \leq j \leq N/2$ and when $\varepsilon \leq \|a\|N^{-1}$, we have

$$\begin{aligned} & D_t^- P_{j-\frac{1}{2}}^{n+1} + \mathbb{L}_{mup}^N P_j^{n+1} + b(x_{j-\frac{1}{2}}, t_{n+1}, P_{j-\frac{1}{2}}^{n+1}) - b(x_{j-\frac{1}{2}}, t_{n+1}, p(x_{j-\frac{1}{2}}, t_{n+1})) \\ &= \frac{\partial p(x_{j-\frac{1}{2}}, t_{n+1})}{\partial t} + \mathbb{L}_{x, \varepsilon} p(x_{j-\frac{1}{2}}, t_{n+1}). \end{aligned}$$

Utilizing the derivative bound of p from Theorem 4.2 and the following relation

$$b(x_{j-1/2}, t_{n+1}, p(x_{j-1/2}, t_{n+1})) = b\left(x_{j-1/2}, t_{n+1}, \frac{p(x_j, t_{n+1}) + p(x_{j-1}, t_{n+1})}{2}\right) + O(h_j^2),$$

the above equation can be rewritten in the following form:

$$\begin{aligned} & D_t^- \left(P_{j-\frac{1}{2}}^{n+1} - \frac{p(x_j, t_{n+1}) + p(x_{j-1}, t_{n+1})}{2} \right) + \mathbb{L}_{mup}^N (P_j^{n+1} - p(x_j, t_{n+1})) \\ &+ \left[\int_0^1 \frac{\partial b(x_{j-\frac{1}{2}}, t_{n+1}, P_{j-\frac{1}{2}}^{*, n+1}(\xi))}{\partial y} d\xi \right] \left(P_{j-\frac{1}{2}}^{n+1} - \frac{p(x_j, t_{n+1}) + p(x_{j-1}, t_{n+1})}{2} \right) \\ &= \left(\frac{\partial}{\partial t} - D_t^- \right) p(x_{j-\frac{1}{2}}, t_{n+1}) - \varepsilon \left(\frac{\partial^2 p(x_{j-\frac{1}{2}}, t_{n+1})}{\partial x^2} - \delta_x^2 p(x_j, t_{n+1}) \right) \\ &+ a(x_{j-\frac{1}{2}}) \left(\frac{\partial p(x_{j-\frac{1}{2}}, t_{n+1})}{\partial x} - D_x^- p(x_j, t_{n+1}) \right) + O(h_j^2), \end{aligned} \quad (4.80)$$

where $P_{j-\frac{1}{2}}^{*,n+1}(\xi) = p_{j-1/2}^{n+1} + \xi(P_{j-\frac{1}{2}}^{n+1} - p_{j-1/2}^{n+1})$. On the other hand, for $1 \leq j \leq N/2$ and when $\varepsilon > \|a\|N^{-1}$, and for $N/2 < j \leq N-1$, we have

$$\begin{aligned} & \left[D_t^- + \mathbb{L}_{mcd}^N + \int_0^1 \frac{\partial b(x_j, t_{n+1}, P_j^{*,n+1}(\xi))}{\partial y} d\xi \right] (P_j^{n+1} - p(x_j, t_{n+1})) \\ &= \left(\frac{\partial}{\partial t} - D_t^- \right) p(x_j, t_{n+1}) - \varepsilon \left(\frac{\partial^2}{\partial x^2} - \delta_x^2 \right) p(x_j, t_{n+1}) + a_j \left(\frac{\partial}{\partial x} - D_x^* \right) p(x_j, t_{n+1}), \end{aligned} \quad (4.81)$$

where $P_j^{*,n+1}(\xi) = p(x_j, t_{n+1}) + \xi(P_j^{n+1} - p(x_j, t_{n+1}))$. Now, for any mesh function Ψ we introduce a discrete operator $\mathbb{L}_{\varepsilon, P^*}^{N, \Delta t}$ given by

$$\mathbb{L}_{\varepsilon, P^*}^{N, \Delta t} \Psi = \tilde{\mathbb{T}}_{\varepsilon, (P, p)}^{N, \Delta t} \Psi.$$

Afterwards, we derive bounds of the truncation errors from (4.80) and (4.81) by using the derivative bounds of $p(x, t)$ given in Theorem 4.2. For $1 \leq j < N/2$, to the case $\varepsilon > \|a\|N^{-1}$, we obtain that

$$\begin{aligned} |\mathbb{L}_{\varepsilon, P^*}^{N, \Delta t}(P_j^{n+1} - p(x_j, t_{n+1}))| &\leq C\varepsilon h_j \int_{x_{j-1}}^{x_{j+1}} \left| \frac{\partial^4 p}{\partial s^4} \right| ds + Ch_j \int_{x_{j-1}}^{x_{j+1}} \left| \frac{\partial^3 p}{\partial s^3} \right| ds + \Delta t \left\| \frac{\partial^2 p}{\partial t^2} \right\|, \\ &\leq C[N^{-2} + \Delta t], \end{aligned} \quad (4.82)$$

and for $j = N/2$, to the case $\varepsilon > \|a\|N^{-1}$,

$$\begin{aligned} |\mathbb{L}_{\varepsilon, P^*}^{N, \Delta t}(P_j^{n+1} - p(x_j, t_{n+1}))| &\leq C\varepsilon \int_{x_{j-1}}^{x_{j+1}} \left| \frac{\partial^3 p}{\partial s^3} \right| ds + Ch_j \int_{x_{j-1}}^{x_{j+1}} \left| \frac{\partial^3 p}{\partial s^3} \right| ds + \Delta t \left\| \frac{\partial^2 p}{\partial t^2} \right\|, \\ &\leq C[(\varepsilon + N^{-1})N^{-1} + \Delta t]. \end{aligned} \quad (4.83)$$

Next, for $1 \leq j \leq N/2$, to the case $\varepsilon \leq \|a\|N^{-1}$, we deduce that

$$\begin{aligned} |\mathbb{L}_{\varepsilon, P^*}^{N, \Delta t}(P_j^{n+1} - p(x_j, t_{n+1}))| &\leq C\varepsilon \int_{x_{j-1}}^{x_{j+1}} \left| \frac{\partial^3 p}{\partial s^3} \right| ds + Ch_j \int_{x_{j-1}}^{x_{j+1}} \left| \frac{\partial^3 p}{\partial s^3} \right| ds + \Delta t \left\| \frac{\partial^2 p}{\partial t^2} \right\| + Ch_j^2, \\ &\leq C[N^{-2} + \Delta t]. \end{aligned} \quad (4.84)$$

Finally, for $N/2 < j < N$,

$$\begin{aligned} |\mathbb{L}_{\varepsilon, P^*}^{N, \Delta t}(P_j^{n+1} - p(x_j, t_{n+1}))| &\leq C\varepsilon h_j \int_{x_{j-1}}^{x_{j+1}} \left| \frac{\partial^4 p}{\partial s^4} \right| ds + Ch_j \int_{x_{j-1}}^{x_{j+1}} \left| \frac{\partial^3 p}{\partial s^3} \right| ds + \Delta t \left\| \frac{\partial^2 p}{\partial t^2} \right\|, \\ &\leq C[N^{-2} + \Delta t]. \end{aligned} \quad (4.85)$$

Consider the discrete functions in the domain $0 \leq j \leq N$, for the case $\varepsilon > \|a\|N^{-1}$,

$$\Psi^\pm(x_j, t_{n+1}) = -C(N^{-2} + \Delta t)x_j - CN^{-2}\varphi_j \pm (P_j^{n+1} - p(x_j, t_{n+1})),$$

where

$$\varphi_j = \begin{cases} \frac{x_j}{1-\eta}, & \text{for } 0 \leq j \leq N/2, \\ 1, & \text{for } N/2 \leq j \leq N, \end{cases}$$

and apply Corollary 4.2 for the operator $\mathbb{L}_{\varepsilon, P^*}^{N, \Delta t}$ together with the truncation error bounds in (4.82), (4.83) and (4.85) to obtain that

$$|P_j^{n+1} - p(x_j, t_{n+1})| \leq C(N^{-2} + \Delta t), \quad \text{for } 1 \leq j \leq N-1.$$

In the same way, we choose the discrete functions in the domain $0 \leq j \leq N$, for the case $\varepsilon \leq \|a\|N^{-1}$,

$$\Psi^\pm(x_j, t_{n+1}) = -C(N^{-2} + \Delta t)x_j \pm (P_j^{n+1} - p(x_j, t_{n+1})),$$

and apply Corollary 4.2 for the operator $\mathbb{L}_{\varepsilon, P^*}^{N, \Delta t}$ together with the truncation error bounds in (4.84) and (4.85), to obtain that

$$|P_j^{n+1} - p(x_j, t_{n+1})| \leq C(N^{-2} + \Delta t), \quad \text{for } 1 \leq j \leq N-1.$$

Hence, the proof is over. ■

In the next lemma, we deduce the error estimate corresponding to the layer component Q_j^{n+1} which is the solution of the following discrete problem:

$$\left\{ \begin{array}{l} Q_j^0 = 0, \quad 0 \leq j \leq N, \\ D_t^- Q_j^{n+1} + \mathbb{L}_{mcd}^N Q_j^{n+1} + b(x_j, t_{n+1}, Y_j^{n+1}) - b(x_j, t_{n+1}, P_j^{n+1}) = 0, \\ \quad \text{for } 1 \leq j \leq N/2, \text{ and when } \varepsilon > \|a\|N^{-1}, \\ D_t^- Q_{j-\frac{1}{2}}^{n+1} + \mathbb{L}_{mup}^N Q_j^{n+1} + b(x_{j-\frac{1}{2}}, t_{n+1}, Y_{j-\frac{1}{2}}^{n+1}) - b(x_{j-\frac{1}{2}}, t_{n+1}, P_{j-\frac{1}{2}}^{n+1}) = 0, \\ \quad \text{for } 1 \leq j \leq N/2, \text{ and when } \varepsilon \leq \|a\|N^{-1}, \\ D_t^- Q_j^{n+1} + \mathbb{L}_{mcd}^N Q_j^{n+1} + b(x_j, t_{n+1}, Y_j^{n+1}) - b(x_j, t_{n+1}, P_j^{n+1}) = 0, \\ \quad \text{for } N/2 < j \leq N-1, \\ Q_0^{n+1} = q(0, t_{n+1}), \quad Q_N^{n+1} = q(1, t_{n+1}). \end{array} \right. \quad (4.86)$$

Lemma 4.15. *Let the assumptions (4.72) and (4.73) of Lemma 4.11 hold. Then, if $\theta < \mathfrak{m}/2$ and $\eta_0 \geq 2/\theta$, the error related to the layer component satisfies the following estimate:*

$$|Q_j^{n+1} - q(x_j, t_{n+1})| \leq \begin{cases} CN^{-2}, & \text{for } 1 \leq j \leq N/2, \\ C(N^{-2} \ln^2 N + \Delta t), & \text{for } N/2 < j \leq N-1. \end{cases} \quad (4.87)$$

Proof. Here, for any mesh function Ψ , we introduce a discrete operator $\mathbb{L}_{\varepsilon, Q^*}^{N, \Delta t}$ defined by

$$\mathbb{L}_{\varepsilon, Q^*}^{N, \Delta t} \Psi = \widetilde{\mathbb{T}}_{\varepsilon, (Y, P)}^{N, \Delta t} \Psi,$$

where $Q_j^{*,n+1}(\xi) = P_j^{n+1} + \xi(Y_j^{n+1} - P_j^{n+1})$. Then, we rewrite the discrete problem (4.86) in the following form:

$$\begin{cases} Q_j^0 = 0, & 0 \leq j \leq N, \\ \mathbb{L}_{\varepsilon, Q^*}^{N, \Delta t} Q_j^{n+1} = 0, & \text{for } 1 \leq j \leq N-1, \\ Q_0^{n+1} = q(0, t_{n+1}), & Q_N^{n+1} = q(1, t_{n+1}). \end{cases}$$

By (4.27) and Theorem 4.3, we have $Q_0^{n+1} = 0$ and $|Q_N^{n+1}| = |q(1, t_{n+1})| \leq C$. We choose the discrete functions for $0 \leq j \leq N$,

$$\Psi^\pm(x_j, t_{n+1}) = -CS_j(\theta) \pm Q_j^{n+1},$$

for sufficiently large C . By Corollary 4.2 for the operator $\mathbb{L}_{\varepsilon, Q^*}^{N, \Delta t}$ and invoking Lemma 4.13, we obtain that

$$|Q_j^{n+1}| \leq CS_j(\theta). \quad (4.88)$$

Now, for $\theta < \mathfrak{m}/2$, combining (4.88) and Theorem 4.3, we get

$$|Q_j^{n+1} - q(x_j, t_{n+1})| \leq |Q_j^{n+1}| + |q(x_j, t_{n+1})| \leq CS_j(\theta). \quad (4.89)$$

Again, for $\eta_0 \geq \frac{2}{\theta}$, it follows from [109, Lemma 3.1] that

$$S_j(\theta) \leq CN^{-4(1-j/N)}, \quad \text{for } N/2 \leq j < N, \quad (4.90)$$

and hence, in particular for $1 \leq j \leq N/2$, (4.89) and (4.90) together imply that

$$|Q_j^{n+1} - q(x_j, t_{n+1})| \leq CN^{-2}. \quad (4.91)$$

Next, we estimate $|Q_j^{n+1} - q(x_j, t_{n+1})|$ on the fine part of the mesh by using consistency and barrier function argument on the interval $[1-\eta, 1]$, since we have $|Q_{N/2}^{n+1} - q(x_{N/2}, t_{n+1})| \leq CN^{-2}$ and $|Q_N^{n+1} - q(x_N, t_{n+1})| = 0$. From (4.27) and (4.86), we derive that for $N/2 < j < N$,

$$\begin{aligned} & D_t^- Q_j^{n+1} + \mathbb{L}_{mcd}^N Q_j^{n+1} + b(x_j, t_{n+1}, Y_j^{n+1}) - b(x_j, t_{n+1}, y(x_j, t_{n+1})) \\ &= \frac{\partial q(x_j, t_{n+1})}{\partial t} + \mathbb{L}_{x, \varepsilon} q(x_j, t_{n+1}) + b(x_j, t_{n+1}, P_j^{n+1}) - b(x_j, t_{n+1}, p(x_j, t_{n+1})). \end{aligned}$$

From the above equation, we have

$$\begin{aligned} & \left[D_t^- + \mathbb{L}_{mcd}^N + \int_0^1 \frac{\partial b(x_j, t_{n+1}, Y_j^{*,n+1}(\xi))}{\partial y} d\xi \right] (Q_j^{n+1} - q(x_j, t_{n+1})) \\ &= \left(\frac{\partial}{\partial t} - D_t^- \right) q(x_j, t_{n+1}) + \left(\mathbb{L}_{x, \varepsilon} - \mathbb{L}_{mcd}^N \right) q(x_j, t_{n+1}) + \left[\int_0^1 \frac{\partial b(x_j, t_{n+1}, P_j^{*,n+1}(\xi))}{\partial y} d\xi \right. \\ & \quad \left. - \int_0^1 \frac{\partial b(x_j, t_{n+1}, Y_j^{*,n+1}(\xi))}{\partial y} d\xi \right] (P_j^{n+1} - p(x_j, t_{n+1})), \end{aligned} \quad (4.92)$$

where $Y_j^{*,n+1}(\xi) = y(x_j, t_{n+1}) + \xi(Y_j^{n+1} - y(x_j, t_{n+1}))$. Now, for any mesh function Ψ , we introduce a discrete operator $\mathbb{L}_{\varepsilon, Y^*}^{N, \Delta t}$ given by

$$\mathbb{L}_{\varepsilon, Y^*}^{N, \Delta t} \Psi = \widetilde{\mathbb{T}}_{\varepsilon, (Y, y)}^{N, \Delta t} \Psi,$$

where $Y_j^{*,n+1}(\xi) = y(x_j, t_{n+1}) + \xi(Y_j^{n+1} - y(x_j, t_{n+1}))$. Now, using derivative bound of $q(x, t)$ from Theorem 4.3, and Lemma 4.14, we obtain from (4.92) that for $N/2 < j < N$,

$$\begin{aligned} |\mathbb{L}_{\varepsilon, Y^*}^{N, \Delta t}(Q_j^{n+1} - q(x_j, t_{n+1}))| &\leq C\varepsilon h_j \int_{x_{j-1}}^{x_{j+1}} \left| \frac{\partial^4 q}{\partial s^4} \right| ds + Ch_j \int_{x_{j-1}}^{x_{j+1}} \left| \frac{\partial^3 q}{\partial s^3} \right| ds \\ &\quad + \Delta t \left\| \frac{\partial^2 q}{\partial t^2} \right\| + C(N^{-2} + \Delta t) \\ &\leq CN^{-2} \ln^2 N \varepsilon^{-1} \exp(-\mathfrak{m}(1 - x_j)/\varepsilon) + C(N^{-2} + \Delta t). \end{aligned} \quad (4.93)$$

We choose the discrete functions for $N/2 \leq j \leq N$,

$$\Psi^\pm(x_j, t_{n+1}) = -C(N^{-2} + \Delta t)x_j - C(N^{-2} \ln^2 N)S_j(\theta) \pm (Q_j^{n+1} - q(x_j, t_{n+1})).$$

Lemma 4.13 implies that $\mathbb{L}_{\varepsilon, Y^*}^{N, \Delta t} S_j(\theta) \geq \frac{C}{\varepsilon} S_j(\theta)$, for $N/2 < j < N$, and hence, use of (4.93) for $\theta < \mathfrak{m}/2$ yields that

$$\mathbb{L}_{\varepsilon, Y^*}^{N, \Delta t} \Psi^\pm(x_j, t_{n+1}) \leq 0.$$

Now, apply Corollary 4.2 for the operator $\mathbb{L}_{\varepsilon, Y^*}^{N, \Delta t}$ to get $\Psi^\pm(x_j, t_{n+1}) \leq 0$, for all $N/2 \leq j \leq N$. Hence, the proof is over. ■

4.5.2 Convergence result for the fully-implicit FMM

We decompose the error in the numerical solution can also be decomposed as

$$Y_j^{n+1} - y(x_j, t_{n+1}) = P_j^{n+1} - p(x_j, t_{n+1}) + Q_j^{n+1} - q(x_j, t_{n+1}), \quad (x_j, t_{n+1}) \in \overline{\mathfrak{D}}^{N, \Delta t}. \quad (4.94)$$

Hence, the required ε -uniform error estimate given in the following Theorem.

Theorem 4.7 (Global error). *Let y be the solution of the nonlinear problem (4.1)-(4.3) and Y_j^{n+1} be the solution of the discrete problem (4.71). Then, the following ε -uniform error estimate holds:*

$$\left\| \{Y_j^{n+1}\}_j - \{y(x_j, t_{n+1})\}_j \right\| \leq \begin{cases} C(N^{-2} + \Delta t), & \text{for } 0 \leq j \leq N/2, \\ C(N^{-2} \ln^2 N + \Delta t), & \text{for } N/2 < j \leq N, \end{cases}$$

Proof. This immediately follows from Lemmas 4.14 and 4.15. ■

4.6 The temporal Richardson extrapolation

In this section, we analyze the Richardson extrapolation in the time variable in order to improve the order of uniform convergence in the temporal direction established in Theorem 4.7 so that we can produce higher-order accurate numerical solution at low computational cost.

On the domain $[0, T]$, we construct a fine mesh, denoted by $\Lambda^{\Delta t/2} = \{\tilde{t}_n\}_{n=0}^{2M}$, by bisecting each mesh

interval of $\Lambda^{\Delta t}$. So, $\tilde{t}_{n+1} - \tilde{t}_n = T/2M = \Delta t/2$ is the step-size. Let $Y^{N,\Delta t}(x_j, t_{n+1})$ and $Y^{N,\Delta t/2}(x_j, \tilde{t}_{n+1})$ be the respective solutions of the fully discrete problem (4.29) on the mesh $\bar{\Omega}^N \times \Lambda^{\Delta t}$ and $\bar{\Omega}^N \times \Lambda^{\Delta t/2}$. Then, from Theorem 4.7, we have

$$\left\{ \begin{array}{l} \left(2Y^{N,\Delta t/2}(x_j, t_{n+1}) - Y^{N,\Delta t}(x_j, t_{n+1}) \right) - y(x_j, t_{n+1}) = o(\Delta t) + O(N^{-2}), \\ \quad \text{for } 0 \leq j \leq N/2, t_{n+1} \in \Lambda^{\Delta t}, \\ \left(2Y^{N,\Delta t/2}(x_j, t_{n+1}) - Y^{N,\Delta t}(x_j, t_{n+1}) \right) - y(x_j, t_{n+1}) = o(\Delta t) + O(N^{-2} \ln^2 N), \\ \quad \text{for } N/2 < j \leq N, t_{n+1} \in \Lambda^{\Delta t}. \end{array} \right. \quad (4.95)$$

Remark 4.5. We set $Y_{exp}^{N,\Delta t}(x_j, t_{n+1}) = \left(2Y^{N,\Delta t/2}(x_j, t_{n+1}) - Y^{N,\Delta t}(x_j, t_{n+1}) \right)$ as the temporal Richardson extrapolation formula so that the time accuracy can be improved from $O(\Delta t)$ to $O(\Delta t^2)$.

Likewise (4.94), we now consider the decomposition of $(2Y^{N,\Delta t/2} - Y^{N,\Delta t})$ so that

$$Y_{exp}^{N,\Delta t}(x_j, t_{n+1}) - y(x_j, t_{n+1}) = \underbrace{P_{exp}^{N,\Delta t}(x_j, t_{n+1}) - p(x_j, t_{n+1})}_{\text{smooth part}} + \underbrace{Q_{exp}^{N,\Delta t}(x_j, t_{n+1}) - q(x_j, t_{n+1})}_{\text{remainder}}. \quad (4.96)$$

4.6.1 Error for the smooth part after extrapolation

We show that when $\Delta t \rightarrow 0$ and $N \rightarrow \infty$, the following error relation holds:

$$P^{N,\Delta t}(x_j, t_{n+1}) - p(x_j, t_{n+1}) = \Delta t \phi_p(x_j, t_{n+1}) + \mathcal{R}_p(x_j, t_{n+1}), \quad (x_j, t_{n+1}) \in \bar{\Omega}^N \times \Lambda^{\Delta t}, \quad (4.97)$$

where ϕ_p is a certain smooth function defined on $\bar{\Omega}^N \times \Lambda^{\Delta t}$, and is independent of $\Delta t, N$; $\mathcal{R}_p(x_j, t_{n+1})$ is the remainder term defined on $\bar{\Omega}^N \times \Lambda^{\Delta t}$. We begin by assuming that the expansion in (4.97) is valid. By following the approach in [60], we define ϕ_p is the smooth component of the function ϕ , which is the solution of the following IBVP:

$$\left\{ \begin{array}{l} \frac{\partial \phi(x, t)}{\partial t} + \mathbb{L}_{x,\varepsilon} \phi(x, t) + \frac{\partial}{\partial y} b(x, t, p(x, t)) \phi = \frac{1}{2} \frac{\partial^2 p(x, t)}{\partial t^2}, \quad \text{in } \mathfrak{D}, \\ \phi(x, 0) = 0, \quad \text{on } \bar{\Omega}, \\ \phi(0, t) = \phi(1, t) = 0, \quad t \in (0, T]. \end{array} \right. \quad (4.98)$$

Since, Theorem 4.2 implies that $\left\| \frac{\partial^2 p}{\partial t^2} \right\|_{\bar{\mathfrak{D}}} \leq C$, one can derive that $\|\phi\|_{\bar{\mathfrak{D}}} \leq C$. To establish the bounds of the derivatives up to fourth-order in space and second order in time in Lemma 4.16, we require $\phi \in \mathcal{C}^{4+\gamma}(\bar{\mathfrak{D}})$. This is guaranteed by the assumption that $g = \frac{1}{2} \frac{\partial^2 p}{\partial t^2}$ must satisfies the compatibility conditions mentioned in (4.5), (4.6), at the corner points $(0, 0)$ and $(1, 0)$.

Lemma 4.16. *The derivatives of the solution $\phi(x, t)$ of the IBVP (4.98) satisfy the bounds*

$$\left| \frac{\partial^{j+k} \phi(x, t)}{\partial x^j \partial t^k} \right|_{\bar{\mathfrak{D}}} \leq C \varepsilon^{-j}, \quad \forall j, k \in \mathbb{N} \cup \{0\}, \text{ and for } 0 \leq j + 2k \leq 4.$$

Proof: By changing the independent variable x to the new variable $\tilde{x} = \frac{1-x}{\varepsilon}$ and letting $\tilde{\phi}(\tilde{x}, t) = \phi(x, t)$ with similar definitions of \tilde{a} , $\frac{\partial \tilde{b}}{\partial y}$ and \tilde{p} ; the IBVP (4.98) is transformed to the following form:

$$\begin{cases} -\frac{\partial^2 \tilde{\phi}}{\partial \tilde{x}^2} - \tilde{a} \frac{\partial \tilde{\phi}}{\partial \tilde{x}} + \varepsilon \frac{\partial}{\partial y} \tilde{b}(\tilde{x}, t, \tilde{p}(\tilde{x}, t)) \tilde{\phi} - \varepsilon \frac{\partial \tilde{\phi}}{\partial t} = \frac{\varepsilon}{2} \frac{\partial^2 \tilde{p}}{\partial t^2}, & \text{in } \tilde{\mathfrak{D}}, \\ \tilde{\phi}(\tilde{x}, t) = 0, & \text{on } \partial \tilde{\mathfrak{D}}, \end{cases}$$

where $\tilde{\mathfrak{D}} = (0, \frac{1}{\varepsilon}) \times (0, T]$ and $\partial \tilde{\mathfrak{D}} = \tilde{\mathfrak{D}} \setminus \tilde{\mathfrak{D}}$. The rest of the proof follows from [Chapter 2, Lemma 2.17]. ■

Lemma 4.17. *The functions ϕ_p and its derivatives, satisfy that*

$$\left| \frac{\partial^{j+k} \phi_p(x, t)}{\partial x^j \partial t^k} \right|_{\tilde{\mathfrak{D}}} \leq C(1 + \varepsilon^{3-j}), \quad \forall j, k \in \mathbb{N} \cup \{0\}, \text{ and for } 0 \leq j + 2k \leq 4.$$

Proof. The proof was obtained by using Lemma 4.16 and the approach described in [75, Theorem 4]. ■

Now, we substitute $P^{N, \Delta t}(x_j, t_{n+1})$ in (4.78) and applying the Taylor-series expansion of the functions p and ϕ_p , invoking Theorem 4.2, Lemma 4.17, and finally, after utilizing the Taylor-expansion for the function b , it provides for $\varepsilon > \|a\|N^{-1}$ that

$$\left\{ \begin{array}{l} p(x_j, 0) + \Delta t \phi_p(x_j, 0) + \mathcal{R}_p(x_j, 0) = p(x_j, 0), \quad 0 \leq j \leq N, \\ p_t(x_j, t_{n+1}) - \varepsilon p_{xx}(x_j, t_{n+1}) + a(x_j) p_x(x_j, t_{n+1}) + b(x_j, t_{n+1}, p(x_j, t_{n+1})) + \\ \Delta t \left[\phi_{p,t}(x_j, t_{n+1}) - \varepsilon \phi_{p,xx}(x_j, t_{n+1}) + a(x_j) \phi_{p,x}(x_j, t_{n+1}) + \right. \\ \left. \frac{\partial b(x_j, t_{n+1}, p(x_j, t_{n+1}))}{\partial y} \phi_p(x_j, t_{n+1}) - \frac{1}{2} p_{tt}(x_j, t_{n+1}) \right] + D_t^- \mathcal{R}_p(x_j, t_{n+1}) + \mathbb{L}_{mcd}^N \mathcal{R}_p(x_j, t_{n+1}) + \\ \left. + \frac{\partial b(x_j, t_{n+1}, \alpha_{p,j}^{n+1})}{\partial y} \mathcal{R}_p(x_j, t_{n+1}) + O(N^{-2}) + O(\Delta t)^2 = g(x_j, t_{n+1}), \quad \text{for } 1 \leq j < N/2, \text{ and } N/2 < j < N, \right. \\ p_t(x_j, t_{n+1}) - \varepsilon p_{xx}(x_j, t_{n+1}) + a(x_j) p_x(x_j, t_{n+1}) + b(x_j, t_{n+1}, p(x_j, t_{n+1})) + \\ \Delta t \left[\phi_{p,t}(x_j, t_{n+1}) - \varepsilon \phi_{p,xx}(x_j, t_{n+1}) + a(x_j) \phi_{p,x}(x_j, t_{n+1}) + \right. \\ \left. \frac{\partial b(x_j, t_{n+1}, p(x_j, t_{n+1}))}{\partial y} \phi_p(x_j, t_{n+1}) - \frac{1}{2} p_{tt}(x_j, t_{n+1}) \right] + D_t^- \mathcal{R}_p(x_j, t_{n+1}) + \mathbb{L}_{mcd}^N \mathcal{R}_p(x_j, t_{n+1}) + \\ \left. \frac{\partial b(x_j, t_{n+1}, \alpha_{p,j}^{n+1})}{\partial y} \mathcal{R}_p(x_j, t_{n+1}) + O((\varepsilon + N^{-1})N^{-1}) + O(\Delta t)^2 = g(x_j, t_{n+1}), \quad \text{for } j = N/2, \right. \\ p(0, t_{n+1}) + \Delta t \phi_p(0, t_{n+1}) + \mathcal{R}_p(0, t_{n+1}) = p(0, t_{n+1}), \quad t_{n+1} \in \Lambda^{\Delta t}, \\ p(1, t_{n+1}) + \Delta t \phi_p(1, t_{n+1}) + \mathcal{R}_p(1, t_{n+1}) = p(1, t_{n+1}), \quad t_{n+1} \in \Lambda^{\Delta t}. \end{array} \right.$$

Next, we consider the case $\varepsilon \leq \|a\|N^{-1}$, and obtain that

$$\left\{ \begin{array}{l} p(x_j, 0) + \Delta t \Phi_p(x_j, 0) + \mathcal{R}_p(x_j, 0) = p(x_j, 0), \quad 0 \leq j \leq N, \\ p_t(x_{j-1/2}, t_{n+1}) - \varepsilon p_{xx}(x_{j-1/2}, t_{n+1}) + a(x_{j-\frac{1}{2}})p_x(x_{j-1/2}, t_{n+1}) + b(x_{j-1/2}, t_{n+1}, p(x_{j-1/2}, t_{n+1})) \\ + \Delta t \left[\Phi_{p,t}(x_{j-1/2}, t_{n+1}) - \varepsilon \Phi_{p,xx}(x_{j-1/2}, t_{n+1}) + a(x_{j-\frac{1}{2}})\Phi_{p,x}(x_{j-1/2}, t_{n+1}) + \right. \\ \left. \frac{\partial b(x_{j-1/2}, t_{n+1}, p(x_{j-1/2}, t_{n+1}))}{\partial y} \Phi_p(x_{j-1/2}, t_{n+1}) - \frac{1}{2} p_{tt}(x_{j-1/2}, t_{n+1}) \right] \\ + D_t^- \frac{\mathcal{R}_p(x_j, t_{n+1}) + \mathcal{R}_p(x_{j-1}, t_{n+1})}{2} + \mathbb{L}_{mup}^N \mathcal{R}_p(x_j, t_{n+1}) + \frac{\partial b(x_{j-1/2}, t_{n+1}, \alpha_{p,j-\frac{1}{2}}^{n+1})}{\partial y} \frac{\mathcal{R}_p(x_j, t_{n+1}) + \mathcal{R}_p(x_{j-1}, t_{n+1})}{2} \\ + O(\Delta t)^2 + O(N^{-2}) = g(x_{j-\frac{1}{2}}, t_{n+1}), \quad \text{for } 1 \leq j \leq N/2, \\ p_t(x_j, t_{n+1}) - \varepsilon p_{xx}(x_j, t_{n+1}) + a(x_j)p_x(x_j, t_{n+1}) + b(x_j, t_{n+1}, p(x_j, t_{n+1})) \\ + \Delta t \left[\Phi_{p,t}(x_j, t_{n+1}) - \varepsilon \Phi_{p,xx}(x_j, t_{n+1}) + a(x_j)\Phi_{p,x}(x_j, t_{n+1}) + \right. \\ \left. \frac{\partial b(x_j, t_{n+1}, p(x_j, t_{n+1}))}{\partial y} \Phi_p(x_j, t_{n+1}) - \frac{1}{2} p_{tt}(x_j, t_{n+1}) \right] + D_t^- \mathcal{R}_p(x_j, t_{n+1}) + \mathbb{L}_{mcd}^N \mathcal{R}_p(x_j, t_{n+1}) \\ + \frac{\partial b(x_j, t_{n+1}, \alpha_{p,j}^{n+1})}{\partial y} \mathcal{R}_p(x_j, t_{n+1}) + O(\Delta t)^2 + O(N^{-2}) = g(x_j, t_{n+1}), \quad \text{for } N/2 < j < N, \\ p(0, t_{n+1}) + \Delta t \Phi_p(0, t_{n+1}) + \mathcal{R}_p(0, t_{n+1}) = p(0, t_{n+1}), \quad t_{n+1} \in \Lambda^{\Delta t}, \\ p(1, t_{n+1}) + \Delta t \Phi_p(1, t_{n+1}) + \mathcal{R}_p(1, t_{n+1}) = p(1, t_{n+1}), \quad t_{n+1} \in \Lambda^{\Delta t}. \end{array} \right.$$

From the above expressions, we obtain the remainder term $\mathcal{R}_p(x_j, t_{n+1})$ is the solution of the following discrete problem:

$$\left\{ \begin{array}{l} D_t^- \mathcal{R}_p(x_j, t_{n+1}) + \mathbb{L}_{mcd}^{N, \Delta t} \mathcal{R}_p(x_j, t_{n+1}) + \frac{\partial b(x_j, t_{n+1}, \alpha_{p,j}^{n+1})}{\partial y} \mathcal{R}_p(x_j, t_{n+1}) = \\ O((\Delta t)^2) + O(N^{-2}), \quad \text{for } 1 \leq j < N/2, \text{ and when } \varepsilon > \|a\|N^{-1}, \\ D_t^- \mathcal{R}_p(x_j, t_{n+1}) + \mathbb{L}_{mcd}^{N, \Delta t} \mathcal{R}_p(x_j, t_{n+1}) + \frac{\partial b(x_j, t_{n+1}, \alpha_{p,j}^{n+1})}{\partial y} \mathcal{R}_p(x_j, t_{n+1}) = \\ O((\Delta t)^2) + O((\varepsilon + N^{-1})N^{-1}), \quad \text{for } j = N/2, \text{ and when } \varepsilon > \|a\|N^{-1}, \\ D_t^- \frac{\mathcal{R}_p(x_j, t_{n+1}) + \mathcal{R}_p(x_{j-1}, t_{n+1})}{2} + \mathbb{L}_{mup}^{N, \Delta t} \mathcal{R}_p(x_j, t_{n+1}) + \frac{\partial b(x_{j-\frac{1}{2}}, t_{n+1}, \alpha_{p,j-\frac{1}{2}}^{n+1})}{\partial y} \\ \frac{\mathcal{R}_p(x_j, t_{n+1}) + \mathcal{R}_p(x_{j-1}, t_{n+1})}{2} = O(\Delta t)^2 + O(N^{-2}), \quad \text{for } 1 \leq j \leq N/2, \text{ and when } \varepsilon \leq \|a\|N^{-1}, \\ D_t^- \mathcal{R}_p(x_j, t_{n+1}) + \mathbb{L}_{mcd}^{N, \Delta t} \mathcal{R}_p(x_j, t_{n+1}) + \frac{\partial b(x_j, t_{n+1}, \alpha_{p,j}^{n+1})}{\partial y} \mathcal{R}_p(x_j, t_{n+1}) = \\ O((\Delta t)^2) + O(N^{-2}), \quad \text{for } N/2 < j \leq N-1, \\ \mathcal{R}_p(x_j, 0) = 0, \quad \text{for } 0 \leq j \leq N, \\ \mathcal{R}_p(0, t_{n+1}) = 0, \quad \mathcal{R}_p(1, t_{n+1}) = -\Delta t \Phi_p(1, t), \quad \text{for } t_{n+1} \in \Lambda^{\Delta t}, \end{array} \right. \quad (4.99)$$

where $\alpha_{p,j}^{n+1}$ belong to some finite interval $[-C, C]$ due to stability bound of the functions $P^{N,\Delta t}$, p and ϕ_p . To prove the uniform convergence of the temporal Richardson extrapolation method, we need to derive bound of the remainder term $\mathcal{R}_p(x, t)$ on $\bar{\Omega}^N \times \Lambda^{\Delta t}$.

Lemma 4.18. *The remainder term \mathcal{R}_p , given in (4.99), satisfies that*

$$|\mathcal{R}_p(x_j, t_{n+1})| \leq C(N^{-2} + (\Delta t)^2), \quad \text{for } 0 \leq j \leq N.$$

Proof Now, for any mesh function Ψ , we introduce a discrete operator $\mathbb{L}_{\varepsilon, \alpha_p}^{N, \Delta t}$ defined by

$$\mathbb{L}_{\varepsilon, \alpha_p}^{N, \Delta t} \Psi = \tilde{\mathbb{T}}_{\varepsilon, (\alpha_p, \alpha_p)}^{N, \Delta t} \Psi.$$

Now, the equation (4.99) implies that

$$|\mathbb{L}_{\varepsilon, \alpha_p}^{N, \Delta t} \mathcal{R}_p(x_j, t_{n+1})| \leq \begin{cases} C(N^{-2} + \Delta t^2), & \text{for } 0 \leq j < N/2, \text{ and when } \varepsilon \geq \|a\|N^{-1}, \\ C((\varepsilon + N^{-1})N^{-1} + \Delta t^2), & \text{for } j = N/2, \text{ when } \varepsilon \geq \|a\|N^{-1}, \\ C(N^{-2} + \Delta t^2), & \text{for } 0 \leq j \leq N/2, \text{ and when } \varepsilon \leq \|a\|N^{-1}, \\ C(N^{-2} + \Delta t^2), & \text{for } N/2 < j \leq N. \end{cases}$$

Then, by using the discrete maximum principle (Corollary 4.2) for the operator $\mathbb{L}_{\varepsilon, \alpha_p}^{N, \Delta t}$ to the suitable barrier functions, we get the desired result. ■

Therefore, from (4.97) and Lemma 4.18, we obtain that

$$\begin{aligned} P^{N, \Delta t}(x_j, t_{n+1}) - p(x_j, t_{n+1}) &= \Delta t \phi_p(x_j, t_{n+1}) + O(\Delta t^2) + O(N^{-2}), \\ &\text{for } 0 \leq j \leq N, \quad t_{n+1} \in \Lambda^{\Delta t}. \end{aligned}$$

Similarly, we have

$$\begin{aligned} P^{N, \Delta t/2}(x_j, \tilde{t}_{n+1}) - p(x_j, \tilde{t}_{n+1}) &= \Delta t/2 \phi_p(x_j, \tilde{t}_{n+1}) + O(\Delta t^2) + O(N^{-2}), \\ &\text{for } 0 \leq j \leq N, \quad \tilde{t}_{n+1} \in \Lambda^{\Delta t/2}. \end{aligned}$$

Finally, we obtain that

$$|P_{extp}^{N, \Delta t}(x_j, t_{n+1}) - p(x_j, t_{n+1})| \leq C(N^{-2} + (\Delta t)^2), \quad \text{for } 0 \leq j \leq N. \quad (4.100)$$

4.6.2 Error for the layer part after extrapolation

From the Lemma 4.15, for the region $0 \leq j \leq N/2$, $t_{n+1} \in \Lambda^{\Delta t}$, we have $|(Q_j^{N, \Delta t} - q(x_j, t_{n+1}))| \leq CN^{-2}$. Similarly $|(Q_j^{N, \Delta t/2} - q(x_j, t_{n+1}))| \leq CN^{-2}$. Hence, we obtain that

$$|Q_{extp}^{N, \Delta t}(x_j, t_{n+1}) - q(x_j, t_{n+1})| \leq CN^{-2}, \quad 0 \leq j \leq N/2. \quad (4.101)$$

To analyze the effect of extrapolation in time variable on $(1 - \eta, 1) \times \Lambda^{\Delta t}$, we show that when $\Delta t \rightarrow 0$ and $N \rightarrow \infty$ the following error relation hold:

$$\begin{aligned} Q^{N, \Delta t}(x_j, t_{n+1}) - q(x_j, t_{n+1}) &= \Delta t \phi_q(x_j, t_{n+1}) + \mathcal{R}_q(x_j, t_{n+1}), \\ \text{for } N/2 < j \leq N, \quad t_{n+1} &\in \Lambda^{\Delta t}, \end{aligned} \quad (4.102)$$

where ϕ_q is a certain smooth function defined on $\overline{\Omega}^N \times \Lambda^{\Delta t}$, and is independent of $\Delta t, N$ and $\mathcal{R}_q(x_j, t_{n+1})$ is remainder term defined on $\overline{\Omega}^N \times \Lambda^{\Delta t}$. We begin by assuming that the expansion (4.102) is valid. We define ϕ_q is the solution of the following IBVP:

$$\begin{cases} \frac{\partial \phi_q}{\partial t} - \varepsilon \frac{\partial^2 \phi_q}{\partial x^2} + a(x) \frac{\partial \phi_q}{\partial x} + \frac{\partial b(x, t, y)}{\partial y} \phi_q = \frac{1}{2} \frac{\partial^2 q}{\partial t^2} - \frac{\partial b(x, t, y)}{\partial y} \phi_p + \frac{\partial b(x, t, p)}{\partial y} \phi_p, \\ \hspace{15em} \text{in } (1 - \eta, 1) \times (0, T], \\ \phi_q(x, 0) = 0, \quad \text{in } [1 - \eta, 1], \\ \phi_q(1 - \eta, t) = 0, \quad \phi_q(1, t) = 0, \quad t \in (0, T]. \end{cases} \quad (4.103)$$

Since, Theorem 4.3 implies that $\left\| \frac{\partial^2 q}{\partial t^2} \right\|_{\overline{\mathfrak{D}}} \leq C$, Lemma 4.17 gives $\|\phi_p\| \leq C$ and the equation (4.11) implies that $\left\| \frac{\partial b}{\partial y} \right\| \leq C$, one can derive that $\|\phi_q\| \leq C$.

Lemma 4.19. *The functions ϕ_q and its derivatives, satisfy that*

$$\left| \frac{\partial^{j+k} \phi_q(x, t)}{\partial x^j \partial t^k} \right| \leq C \left(\varepsilon^{-j} \exp(-m(1-x)/\varepsilon) \right), \quad \text{in } [1 - \eta, 1] \times (0, T],$$

$\forall j, k \in \mathbb{N} \cup \{0\}$, and for $0 \leq j + 2k \leq 4$.

Proof. The proof is obtained by the approach described in [86, Theorem 4.8]. ■

Now, we substitute $Q^{N, \Delta t}(x_j, t_{n+1})$ into (4.86) and we applying the Taylor-series expansion of the functions q and ϕ_q , invoking Theorem 4.3, Lemma 4.19, and finally, after utilizing the Taylor-expansion for the function b , it gives

$$\begin{cases} q(x_j, 0) + \Delta t \phi_q(x_j, 0) + \mathcal{R}_q(x_j, 0) = q(x_j, 0), \quad N/2 \leq j \leq N, \\ q_t(x_j, t_{n+1}) + \mathbb{L}_{x, \varepsilon} q(x_j, t_{n+1}) + b(x_j, t_{n+1}, y(x_j, t_{n+1})) - b(x_j, t_{n+1}, p(x_j, t_{n+1})) + \\ O(\Delta t)^2 + O(N^{-2}) + O(N^{-2} \ln^2 N \varepsilon^{-1} \exp(-m(1-x)/\varepsilon)) + \Delta t \left[\phi_{q,t}(x_j, t_{n+1}) + \right. \\ \mathbb{L}_{x, \varepsilon} \phi_q(x_j, t_{n+1}) + \frac{\partial b(x_j, t_{n+1}, y(x_j, t_{n+1}))}{\partial y} \phi_q(x_j, t_{n+1}) - \frac{1}{2} \frac{\partial^2 q(x_j, t_{n+1})}{\partial t^2} + \\ \left. \frac{\partial b(x_j, t_{n+1}, y(x_j, t_{n+1}))}{\partial y} \phi_p(x_j, t_{n+1}) - \frac{\partial b(x_j, t_{n+1}, p(x_j, t_{n+1}))}{\partial y} \phi_p(x_j, t_{n+1}) \right] + \\ D_t^- \mathcal{R}_q(x_j, t_{n+1}) + \mathbb{L}_{mcd}^N \mathcal{R}_q(x_j, t_{n+1}) + \frac{\partial b(x_j, t_{n+1}, \alpha_{q,j}^{n+1})}{\partial y} \mathcal{R}_q(x_j, t_{n+1}) = 0, \quad N/2 < j < N, \\ q(1 - \eta, t_{n+1}) + \Delta t \phi_q(1 - \eta, t_{n+1}) + \mathcal{R}_q(1 - \eta, t_{n+1}) = q(1 - \eta, t_{n+1}), \quad t_{n+1} \in \Lambda^{\Delta t}, \\ q(1, t_{n+1}) + \Delta t \phi_q(1, t_{n+1}) + \mathcal{R}_q(1, t_{n+1}) = q(1, t_{n+1}), \quad t_{n+1} \in \Lambda^{\Delta t}. \end{cases} \quad (4.104)$$

The equations (4.27) and (4.103) together implies that the remainder term $\mathcal{R}_q(x_j, t_{n+1})$ is the solution of the following discrete problem:

$$\begin{cases} D_t^- \mathcal{R}_q(x_j, t_{n+1}) + \mathbb{L}_{mcd}^N \mathcal{R}_q(x_j, t_{n+1}) + \frac{\partial b(x_j, t_{n+1}, \alpha_{q,j}^{n+1})}{\partial y} \mathcal{R}_q(x_j, t_{n+1}) = \\ O(N^{-2} + \Delta t^2) + O(N^{-2} \ln^2 N \varepsilon^{-1} \exp(-\mathfrak{m}(1 - x_j)/\varepsilon)), \quad \text{in } [1 - \eta, 1] \times (0, T], \\ \mathcal{R}_q(x_j, 0) = 0, \quad \text{in } [1 - \eta, 1], \\ \mathcal{R}_q(1 - \eta, t_{n+1}) = 0, \quad \mathcal{R}_q(1, t_{n+1}) = 0, \quad t_{n+1} \in [0, T], \end{cases} \quad (4.105)$$

where $\alpha_{q,j}^{n+1} \in [-C, C]$, for some constant C .

Lemma 4.20. *The remainder term \mathcal{R}_q , given in (4.105), satisfies that*

$$|\mathcal{R}_q(x_j, t_{n+1})| \leq C(N^{-2} \ln^2 N + (\Delta t)^2), \text{ for } N/2 < j \leq N.$$

Proof. Now, for any mesh function Ψ , we introduce a discrete operator $\mathbb{L}_{\varepsilon, \alpha_q}^{N, \Delta t}$ defined by

$$\mathbb{L}_{\varepsilon, \alpha_q}^{N, \Delta t} \Psi = \tilde{\mathbb{T}}_{\varepsilon, (\alpha_q, \alpha_q)}^{N, \Delta t} \Psi.$$

From the equation (4.105), we get

$$|\mathbb{L}_{\varepsilon, \alpha_q}^{N, \Delta t} \mathcal{R}_q(x_j, t_{n+1})| \leq O(N^{-2} + \Delta t^2) + O(N^{-2} \ln^2 N \varepsilon^{-1} \exp(-\mathfrak{m}(1 - x_j)/\varepsilon)),$$

for $N/2 < j < N$.

Then, by using the discrete maximum principle (Corollary 4.2) for the operator $\mathbb{L}_{\varepsilon, \alpha_q}^{N, \Delta t}$ to the suitable barrier functions, we get the desired result for $N/2 < j \leq N$. ■

From the equation (4.102) and Lemma 4.20, we obtain that

$$Q^{N, \Delta t}(x_j, t_{n+1}) = q(x_j, t_{n+1}) + \Delta t \phi_q(x_j, t_{n+1}) + O(N^{-2} \ln^2 N) + O(\Delta t^2),$$

for $N/2 < j \leq N, t_{n+1} \in \Lambda^{\Delta t}$.

Similarly, we have

$$Q^{N, \Delta t/2}(x_j, \tilde{t}_{n+1}) = q(x_j, \tilde{t}_{n+1}) + \Delta t/2 \phi_q(x_j, \tilde{t}_{n+1}) + O(N^{-2} \ln^2 N) + O(\Delta t^2),$$

for $N/2 < j \leq N, \tilde{t}_{n+1} \in \Lambda^{\Delta t/2}$.

Finally, we obtain that

$$|Q_{extp}^{N, \Delta t}(x_j, t_{n+1}) - q(x_j, t_{n+1})| \leq C(N^{-2} \ln^2 N + \Delta t^2),$$

for $N/2 < j \leq N, t_{n+1} \in \Lambda^{\Delta t}$. (4.106)

4.6.3 Convergence result after extrapolation

Now, the equations (4.96), (4.100), (4.101) and (4.106) yields the following ε -uniform error bounds after using the temporal Richardson extrapolation .

Theorem 4.8 (Global error). *Let y be the solution of the nonlinear problem (4.1)-(4.3) and $Y_{exp}^{N,\Delta t}$ be the solution of the discretized problem (4.71) after using the temporal Richardson extrapolation. Then, the following ε -uniform error estimate holds:*

$$|Y_{exp}^{N,\Delta t}(x_j, t_{n+1}) - y(x_j, t_{n+1})| \leq \begin{cases} C(N^{-2} + (\Delta t)^2), & \text{for } 0 \leq j \leq N/2, t_{n+1} \in \Lambda^{\Delta t}, \\ C(N^{-2} \ln^2 N + (\Delta t)^2), & \text{for } N/2 < j \leq N, t_{n+1} \in \Lambda^{\Delta t}. \end{cases}$$

4.7 Numerical experiments

In this section, we present the numerical results before and after applying the extrapolation technique for two test problems of the form (4.1)-(4.3), utilizing the proposed FMMs in (4.29) and (4.30). For all the test examples, we choose $\eta_0 = 2.2$ and implement the Thomas algorithm to solve the tridiagonal linear systems involved in our methods. The numerical results are also compared with the fully-implicit upwind FMM, which is mentioned below as well.

4.7.1 The fully-implicit upwind FMM

In this section, we approximate the problem (4.1)-(4.3) by a fully implicit numerical method that combines an implicit Euler method to discretize in the temporal direction and a classical upwind scheme to discretize in the spatial direction. Then, the fully-implicit method takes the following form on $\overline{\mathfrak{D}}^{N,\Delta t}$:

$$\begin{cases} Y_j^0 = q_0(x_j), & 0 \leq j \leq N, \\ D_t^- Y_j^{n+1} + \mathbb{L}_{up}^N Y_j^{n+1} + b(x_j, t_{n+1}, Y_j^{n+1}) = g_j^{n+1}, & \text{for } 1 \leq j \leq N-1, \\ Y_0^{n+1} = s_l(t_{n+1}), \quad Y_N^{n+1} = s_r(t_{n+1}), & \text{for } n = 0, \dots, M-1, \end{cases} \quad (4.107)$$

where

$$\mathbb{L}_{up}^N Y_j^{n+1} = -\varepsilon \delta_x^2 Y_j^{n+1} + a_j D_x^- Y_j^{n+1}.$$

The existence and stability of the solution Y_j^{n+1} of the nonlinear discrete problem (4.107) can be obtained in the same way as in Section 4.5. Furthermore, following the error analysis given in Section 4.5, one can prove ε -uniform error estimate for the FMM (4.107).

Theorem 4.9 (Global Error). *Let y be the solution of the problem (4.1)-(4.3) and Y_j^{n+1} be the solution of the discretized problem (4.107). Then, the following ε -uniform error estimate holds:*

$$\left\| \{Y_j^{n+1}\}_j - \{y(x_j, t_{n+1})\}_j \right\| \leq \begin{cases} C(N^{-1} + \Delta t), & \text{for } 0 \leq j \leq N/2, \\ C(N^{-1} \ln N + \Delta t), & \text{for } N/2 < j \leq N. \end{cases}$$

4.7.2 Test Examples

Example 4.1. Consider the following parabolic nonlinear IBVP:

$$\begin{cases} \frac{\partial y}{\partial t} - \varepsilon \frac{\partial^2 y}{\partial x^2} + (1 + x - x^2) \frac{\partial y}{\partial x} + (1 + xt)y \exp(y^2) = g(x, t), & (x, t) \in (0, 1) \times (0, 1], \\ y(x, 0) = q_0(x), & x \in [0, 1], \\ y(0, t) = 0, \quad y(1, t) = 0, & t \in (0, 1], \end{cases}$$

where the exact solution $y(x, t)$ is given by

$$y(x, t) = \exp(-t)((1 - \exp(-(1 - x)/\varepsilon))/(1 - \exp(-1/\varepsilon)) - \cos(\pi/2x)).$$

and accordingly, we choose the initial data $q_0(x)$ and source function $g(x, t)$. In Fig 4.1, we draw surface plot and contour plot of numerical solution for Example 4.1 and it shows that the solution generates boundary layer closer to $x = 1$. Here, for each ε , we calculate the maximum point-wise errors $e_\varepsilon^{N, \Delta t}$ corresponding to the proposed numerical methods before and after extrapolation, respectively by

$$\max_{0 \leq j \leq N} \max_{0 \leq n \leq M} |Y^{N, \Delta t}(x_j, t_n) - y(x_j, t_n)|,$$

and

$$\max_{0 \leq j \leq N} \max_{0 \leq n \leq M} |Y_{extp}^{N, \Delta t}(x_j, t_n) - y(x_j, t_n)|,$$

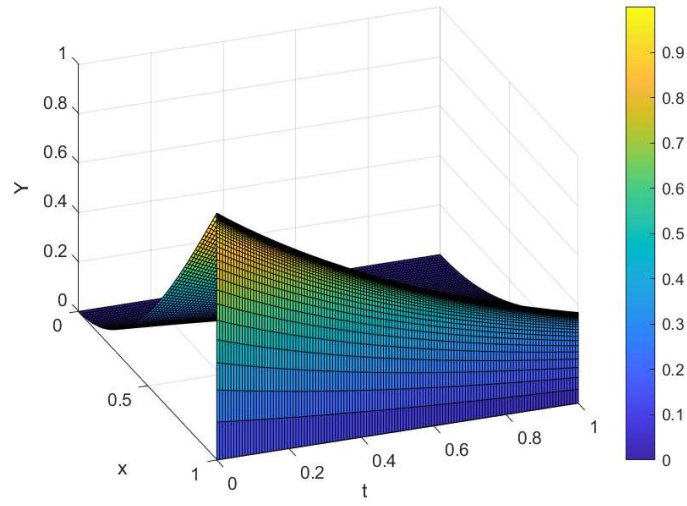
and the corresponding orders of convergence are calculated by $r_\varepsilon^{N, \Delta t} = \log_2 \left(\frac{e_\varepsilon^{N, \Delta t}}{e_\varepsilon^{2N, \Delta t/2}} \right)$. Here, $Y^{N, \Delta t}(x_j, t_n)$ and $Y_{extp}^{N, \Delta t}(x_j, t_n)$, respectively denote the numerical solution obtained at $(x_j, t_{n+1}) \in \overline{\mathcal{D}}^{N, \Delta t}$. Further, for each N and Δt , we calculate the ε -uniform maximum point-wise error and the corresponding ε -uniform order of convergence, respectively by

$$e^{N, \Delta t} = \max_\varepsilon e_\varepsilon^{N, \Delta t} \quad \text{and} \quad r^{N, \Delta t} = \log_2 \left(\frac{e^{N, \Delta t}}{e^{2N, \Delta t/2}} \right).$$

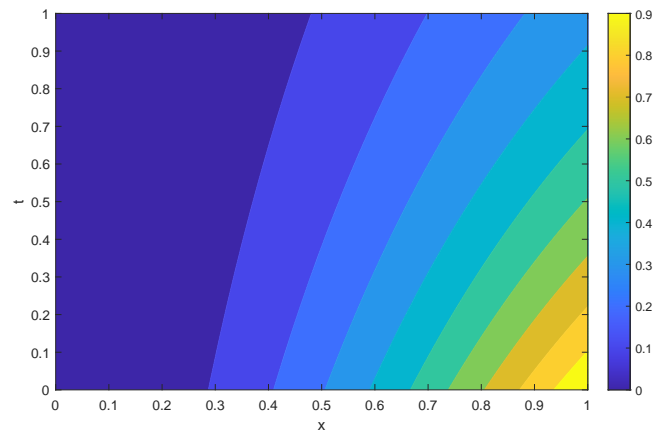
Example 4.2. Consider the following parabolic nonlinear IBVP:

$$\begin{cases} \frac{\partial y}{\partial t} - \varepsilon \frac{\partial^2 y}{\partial x^2} + (2 - x^2 t^2) \frac{\partial y}{\partial x} + \exp(-t) \exp(2y) - y \sin(y) = 2 + 10t^2 \exp(-t)x(1 - x), & (x, t) \in (0, 1) \times (0, 1], \\ y(x, 0) = 0, & x \in [0, 1], \\ y(0, t) = 1 - \exp(-t), \quad y(1, t) = t, & t \in (0, 1], \end{cases}$$

In Fig 4.2, we draw surface plot and contour plot of numerical solution for Example 4.2 and it shows that the numerical solution generates boundary layer closer to $x = 1$. As we are not acquainted with the exact solution of Example 4.2, we calculate the maximum point-wise errors $\widehat{e}_\varepsilon^{N, \Delta t}$ corresponding to the proposed numerical

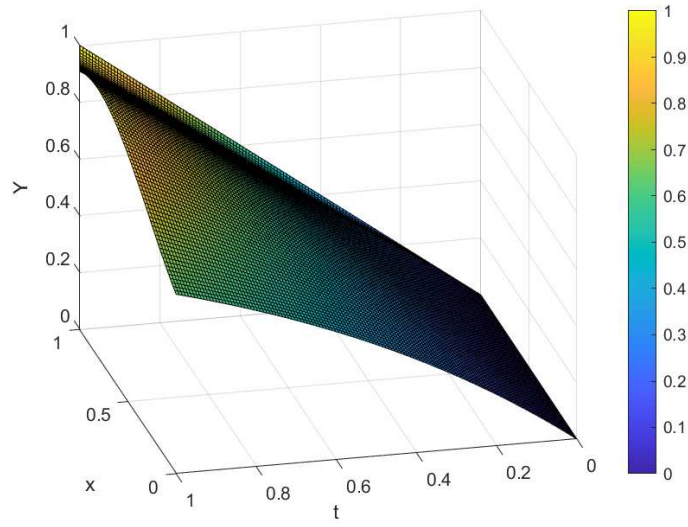


(a) Surface plot

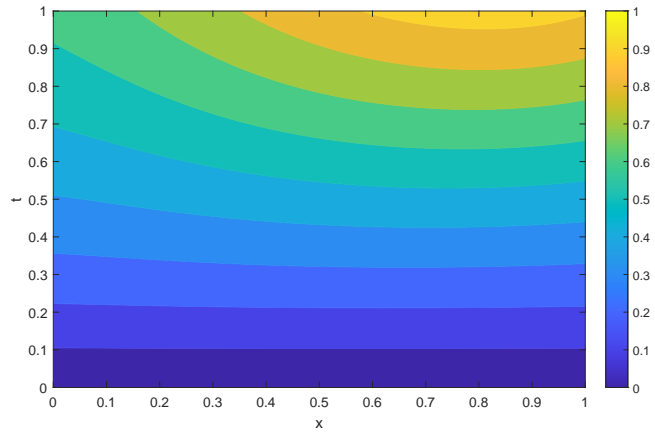


(b) Contour plot

Figure 4.1: Plots of Example 4.1 for $\varepsilon = 2^{-20}$, $N = 128$.



(a) Surface plot



(b) Contour plot

Figure 4.2: Plots of Example 4.2 for $\varepsilon = 2^{-20}$, $N = 128$.

method before and after extrapolation, respectively by

$$\max_{0 \leq j \leq N} \max_{0 \leq n \leq M} |Y^{N,\Delta t}(x_j, t_n) - \hat{Y}^{2N,\Delta t/2}(x_j, t_n)|,$$

and

$$\max_{0 \leq j \leq N} \max_{0 \leq n \leq M} |Y_{extp}^{N,\Delta t}(x_j, t_n) - \hat{Y}_{extp}^{2N,\Delta t/2}(x_j, t_n)|,$$

and the corresponding orders of convergence are calculated by $\hat{r}_\varepsilon^{N,\Delta t} = \log_2 \left(\frac{\hat{e}_\varepsilon^{N,\Delta t}}{\hat{e}_\varepsilon^{2N,\Delta t/2}} \right)$. Here, $\hat{Y}^{2N,\Delta t/2}(x_j, t_n)$

and $\hat{Y}_{extp}^{2N,\Delta t/2}(x_j, t_n)$, respectively denote the numerical solution and the extrapolated numerical solution obtained at $(x_j, t_n) \in \hat{\mathcal{D}}^{2N,\Delta t/2} = \hat{\Omega}^{2N} \times \Lambda^{\Delta t/2}$, where $\Delta t/2 = T/2M$ and $\hat{\Omega}^{2N}$ is a piecewise-uniform Shishkin mesh with $2N$ mesh-intervals and having the same transition parameter η as that of $\bar{\Omega}^N$ such that the j^{th} point of $\bar{\Omega}^N$ becomes $2j^{\text{th}}$ point of $\hat{\Omega}^{2N}$, for $j = 0, 1, \dots, N$. Finally, for each N and Δt , we compute the quantities $\hat{e}^{N,\Delta t}$ and $\hat{r}^{N,\Delta t}$ analogously to $e^{N,\Delta t}$ and $r^{N,\Delta t}$. To compute the numerical solution of the FMMs in (4.29) and (4.107) for Examples 4.1 and 4.2, a nonlinear system needs to be solved at each time step. For that, we use the Newton's method with the following stopping criterion

$$\max_{0 \leq j \leq N} \max_{0 \leq n \leq M} |Y_{k+1}^{N,\Delta t}(x_j, t_{n+1}) - Y_k^{N,\Delta t}(x_j, t_{n+1})| < 10^{-5}, \quad (4.108)$$

where $Y_k^{N,\Delta t}(x_j, t_n)$ is the approximation of $Y^{N,\Delta t}(x_j, t_n)$ given by the k^{th} iteration of the Newton's method. Here, we have chosen $Y_0^{N,\Delta t}(x_j, t_n) = 0$ as an initial guess for all the values of ε .

4.7.3 Numerical results and observations

We choose all the values of ε from $\mathcal{S} = \{2^0, 2^{-2}, \dots, 2^{-20}\}$, for computation of ε -uniform errors. For different values of ε , N and Δt , the computed ε -uniform errors and order of convergence are displayed in Tables 4.1 and 4.2, without using the temporal Richardson extrapolation, respectively for Examples 4.1 and 4.2. This shows the monotonically decreasing behavior of the ε -uniform errors with increasing N , and it definitely represents the ε -uniform convergence of the FMMs given in (4.29), (4.30) and (4.107). For the sake of clarity, the computed ε -uniform errors in Tables 4.1 and 4.2 are depicted in Figs 4.3 and 4.4, respectively for Examples 4.1 and 4.2. At the same time, these computational results clearly illustrate the influence of the temporal error over the global error. The computed order of convergence shown in Tables 4.1 and 4.2, does not truly reflect the spatial order of convergence of the proposed FMMs in (4.29) and (4.30), because of the dominance of the temporal error over the spatial error according to Theorems 4.4 and 4.7.

Next, in order to visualize the effect of the temporal Richardson extrapolation, we choose a suitably large N to reduce the influence of the spatial error. In Tables 4.3 and 4.4, we display the numerical results for Example 4.1, before and after the temporal extrapolation of the proposed FMMs in (4.29) and (4.30), respectively. Similar computational results are also displayed in Tables 4.5 and 4.6 for Example 4.2. For the sake of clarity, the computed maximum point-wise errors in Tables 4.3-4.6 are depicted in Figs 4.5 and 4.6, respectively for Examples 4.1 and 4.2. This shows that the improvement in the temporal order of convergence after employing the Richardson extrapolation in the time variable, as claimed in Theorem 4.8.

The above numerical experiment indicates that by using the temporal Richardson extrapolation, one can

check the spatial accuracy by choosing $\Delta t = 1/N$. Following this, in Tables 4.7 and 4.8, we compare the region-wise spatial accuracy of the FMMs given in (4.29), (4.30) and (4.107), for Example 4.1. Similar computational results are also displayed in Tables 4.9 and 4.10 for Example 4.2. For the sake of clarity, the computed maximum point-wise errors for $\varepsilon = 2^{-6}, 2^{-20}$ in Tables 4.7- 4.10 are graphically presented in Figs 4.7 and 4.8, respectively for Examples 4.1 and 4.2. These computational results match very well with the spatial error established in Theorems 4.5 , 4.7 and 4.9; and also clearly reflects the robustness of the fully-implicit FMM (4.29) and the IMEX FMM (4.30) in comparison with the upwind FMM (4.107) in terms of order of accuracy, irrespective of the smaller and the larger values of ε .

Finally, to demonstrate computational efficiency, we compare the computational time of the proposed FMMs in (4.29) and (4.30) using the Thomas algorithm in Table 4.11 for Examples 4.1 and 4.2. From these results, we see that the IMEX-FMM (4.30) takes comparatively less computation time than the fully-implicit FMM (4.29), irrespective of the parameter ε .

4.8 Conclusion

In this chapter, we provide a complete convergence analysis for higher-order numerical approximation of a class of singularly perturbed nonlinear parabolic IBVPs of the form (4.1)-(4.3), by proposing two new FMMs followed the temporal Richardson extrapolation. Apart from studying the asymptotic properties of the analytical solution of the governing nonlinear problem, the entire convergence analysis is splitted into three major parts.

(i) In the first part, ε -uniform error estimate of the newly proposed IMEX-FMM (4.30) is carried out by invoking two-stage discretization technique, which discretizes first in time and later in space. This technique is useful for extending the proposed IMEX method for multi-dimensional nonlinear parabolic problems. We prove that the corresponding fully discrete scheme is ε -uniformly convergent in the discrete supremum norm; and show that the spatial accuracy is at least two in the outer region and is almost two in the boundary layer region, regardless of the larger and smaller values of ε .

(ii) In the second part, we carry out ε -uniform error estimate of the newly proposed fully-implicit FMM (4.29) by analyzing the error separately for the smooth component and the layer component, which finally contribute to the global error associated with the fully discrete scheme. We prove that the associated fully discrete scheme is ε -uniformly convergent in the discrete supremum norm; and also achieves the similar order of accuracy as that of the present IMEX-FMM.

(iii) In the third part, we focus on the ε -uniform error estimate related to the temporal Richardson extrapolation for enhancing the temporal order of convergence.

The error estimates in (i) and (ii), justify that although the IMEX method leads to a linearized system at each time step, but it does not cause reduction in the order of convergence with respect to both space and time, corresponding to the present fully-implicit method that indeed leads to a nonlinear-system at each time step. Finally, the error estimate in (iii) shows that the resulting numerical solution is second-order uniformly convergent with respect to both the spatial and the temporal variables. Finally, we perform the several numerical experiments to confirm that those theoretical outcomes match very well with the numerical results. Further, we demonstrate that the newly developed FMMs are robust in comparison with the upwind FMM (4.107) with regard to the order of accuracy; and the proposed IMEX-FMM is a cost-effective numerical scheme than the proposed fully-implicit FMM.

In a nutshell, the work of this chapter can be considered as a stepping stone to develop and analyze the robust numerical methods for one-dimensional singularly perturbed nonlinear parabolic convection-diffusion problems; and moreover for two-dimensional problems as well. The further investigation of the proposed algorithms for two-dimensional nonlinear parabolic problem is carried out in Chapter 5 as a continuation of the present work.

Table 4.1: Comparison of ε -uniform maximum point-wise errors for Example 4.1 .

$\varepsilon \in \mathcal{S}_\varepsilon$	Number of mesh intervals N / time step size Δt ($\Delta t = 0.8/N$)				
	$64 / \frac{1}{80}$	$128 / \frac{1}{160}$	$256 / \frac{1}{320}$	$512 / \frac{1}{640}$	$1024 / \frac{1}{1280}$
IMEX-FMM (4.30)					
$e^{N,\Delta t}$	9.9649e-04	4.7367e-04	2.3146e-04	1.1453e-04	5.6993e-05
$r^{N,\Delta t}$	1.0730	1.0331	1.0150	1.0069	
fully-implicit FMM (4.29)					
$e^{N,\Delta t}$	1.2458e-03	5.0386e-04	1.9860e-04	8.4765e-05	3.7479e-05
$r^{N,\Delta t}$	1.3060	1.3431	1.2283	1.1774	
upwind FMM (4.107)					
$e^{N,\Delta t}$	1.3954e-02	8.7427e-03	5.2698e-03	3.0723e-03	1.7505e-03
$r^{N,\Delta t}$	0.67450	0.73032	0.77843	0.81158	

Table 4.2: Comparison of ε -uniform maximum point-wise errors for Example 4.2 .

$\varepsilon \in \mathcal{S}_\varepsilon$	Number of mesh intervals N / time step size Δt ($\Delta t = 0.8/N$)				
	$64 / \frac{1}{80}$	$128 / \frac{1}{160}$	$256 / \frac{1}{320}$	$512 / \frac{1}{640}$	$1024 / \frac{1}{1280}$
IMEX-FMM (4.30)					
$\widehat{e}^{N,\Delta t}$	7.3370e-04	3.9862e-04	1.6843e-04	8.6622e-05	4.0807e-05
$\widehat{r}^{N,\Delta t}$	0.88017	1.2429	0.95935	1.0859	
fully-implicit FMM (4.29)					
$\widehat{e}^{N,\Delta t}$	3.9859e-04	2.0286e-04	7.3029e-05	3.6852e-05	1.6888e-05
$\widehat{r}^{N,\Delta t}$	0.97440	1.4740	0.98673	1.1257	
upwind FMM (4.107)					
$\widehat{e}^{N,\Delta t}$	3.4854e-03	1.7738e-03	8.9403e-04	4.4872e-04	2.2477e-04
$\widehat{r}^{N,\Delta t}$	0.97453	0.98842	0.99452	0.99735	

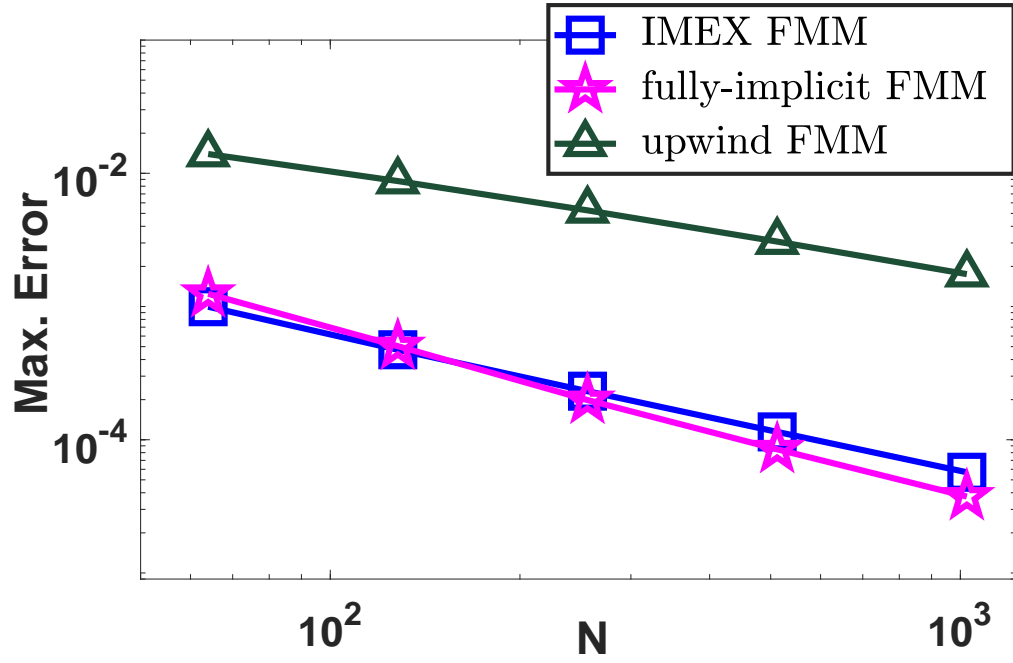


Figure 4.3: Loglog plot for comparison of the ε -uniform errors for Example 4.1.

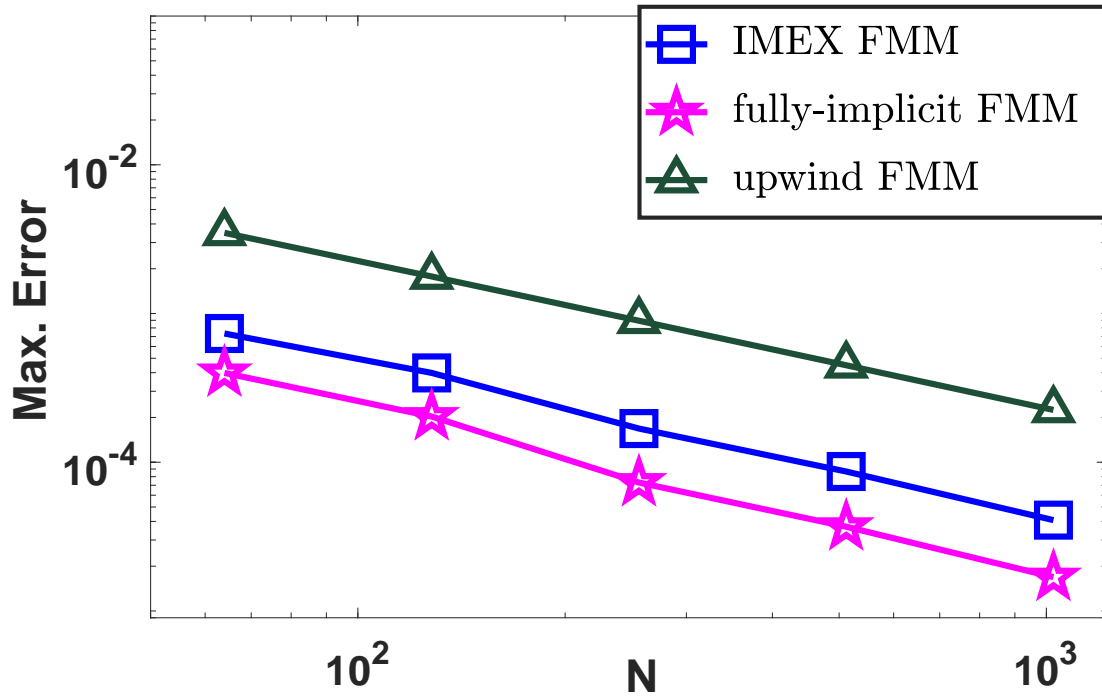


Figure 4.4: Loglog plot for comparison of the ε -uniform errors for Example 4.1.

Table 4.3: Comparison of the temporal accuracy for Example 4.1 computed using the IMEX-FMM (4.30)

ε	Number of space intervals $N = 8192$				
	$\Delta t = \frac{1}{8}$	$\Delta t = \frac{1}{16}$	$\Delta t = \frac{1}{32}$	$\Delta t = \frac{1}{64}$	$\Delta t = \frac{1}{128}$
2^{-8}	without temporal extrapolation				
	8.8104e-03	4.3045e-03	2.1270e-03	1.0571e-03	5.2694e-04
	1.0334	1.0170	1.0087	1.0044	
	with temporal extrapolation				
	2.0146e-04	5.0561e-05	1.2731e-05	3.2515e-06	9.1795e-07
	1.9944	1.9897	1.9692	1.8246	
2^{-20}	without temporal extrapolation				
	9.5233e-03	4.6517e-03	2.2982e-03	1.1421e-03	5.6930e-04
	1.0337	1.0173	1.0088	1.0044	
	with temporal extrapolation				
	2.1986e-04	5.5347e-05	1.3936e-05	3.5177e-06	9.5905e-07
	1.9900	1.9897	1.9861	1.8750	

Table 4.4: Comparison of the temporal accuracy for Example 4.1 computed using the fully-implicit FMM (4.29)

ε	Number of space intervals $N = 8192$				
	$\Delta t = \frac{1}{8}$	$\Delta t = \frac{1}{16}$	$\Delta t = \frac{1}{32}$	$\Delta t = \frac{1}{64}$	$\Delta t = \frac{1}{128}$
2^{-8}	without temporal extrapolation				
	5.5218e-03	2.7254e-03	1.3500e-03	6.7128e-04	3.3465e-04
	1.0187	1.0135	1.0080	1.0043	
	with temporal extrapolation				
	7.6162e-05	2.5687e-05	7.5004e-06	2.0003e-06	5.0636e-07
	1.5680	1.7760	1.9067	1.9820	
2^{-20}	without temporal extrapolation				
	5.7745e-03	2.8511e-03	1.4124e-03	7.0223e-04	3.5004e-04
	1.0182	1.0134	1.0081	1.0044	
	with temporal extrapolation				
	7.8881e-05	2.6711e-05	7.9001e-06	2.1374e-06	5.5066e-07
	1.5622	1.7575	1.8860	1.9566	

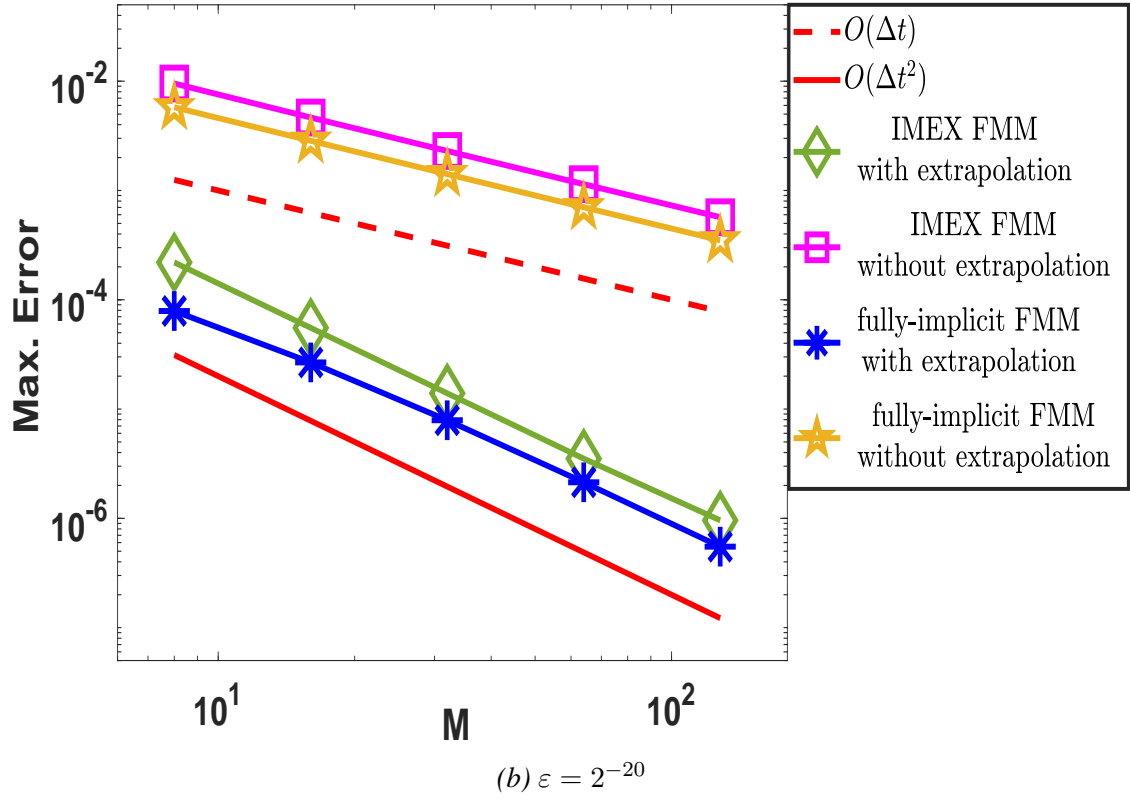
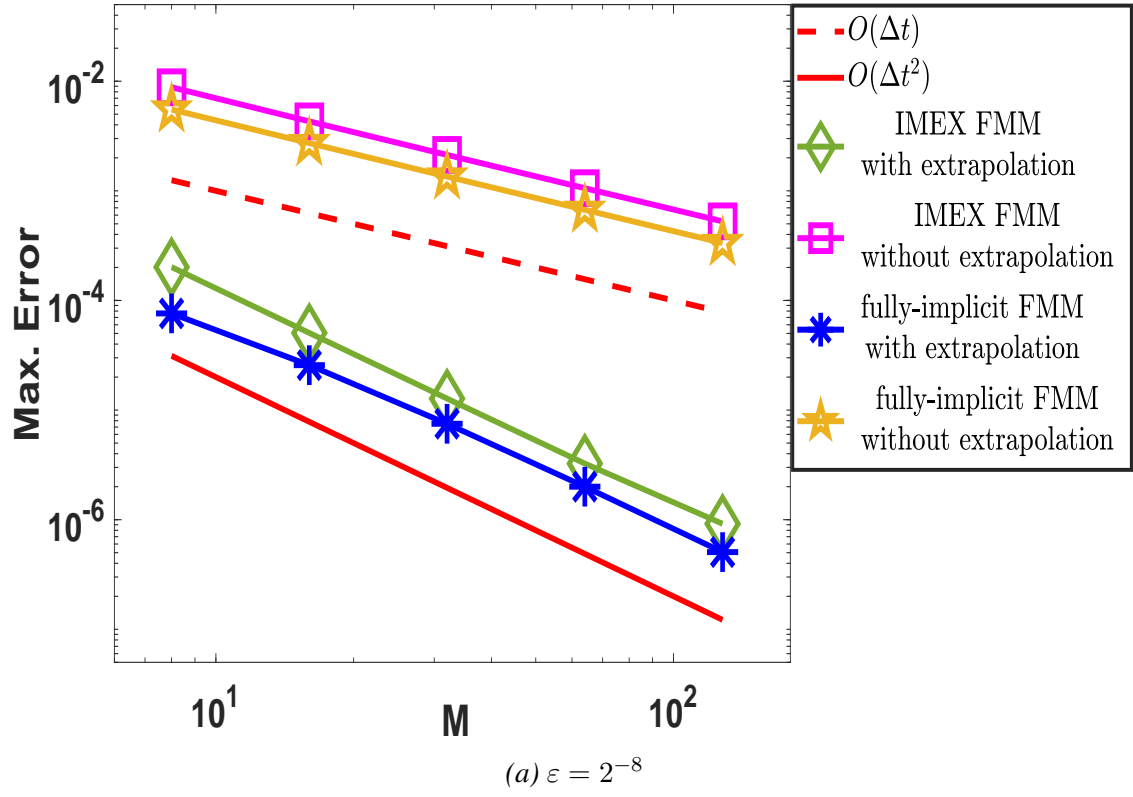


Figure 4.5: Loglog plot for comparison of the temporal order of convergence for Example 4.1

Table 4.5: Comparison of the temporal accuracy for Example 4.2 computed using the IMEX-FMM (4.30)

ε	Number of space intervals $N = 8192$				
	$\Delta t = \frac{1}{8}$	$\Delta t = \frac{1}{16}$	$\Delta t = \frac{1}{32}$	$\Delta t = \frac{1}{64}$	$\Delta t = \frac{1}{128}$
2^{-8}	without temporal extrapolation				
	5.7624e-03	3.0397e-03	1.5591e-03	7.8930e-04	3.9708e-04
	0.92275	0.96321	0.98205	0.99114	
	with temporal extrapolation				
	3.1742e-04	7.8648e-05	1.9562e-05	4.8727e-06	1.2108e-06
	2.0129	2.0074	2.0053	2.0088	
2^{-20}	without temporal extrapolation				
	5.8165e-03	3.0682e-03	1.5737e-03	7.9670e-04	4.0081e-04
	0.92279	0.96322	0.98204	0.99112	
	with temporal extrapolation				
	3.2026e-04	7.9374e-05	1.9754e-05	4.9303e-06	1.2347e-06
	2.0125	2.0065	2.0024	1.9976	

Table 4.6: Comparison of the temporal accuracy for Example 4.2 using the fully-implicit FMM (4.29)

ε	Number of space intervals $N = 8192$				
	$\Delta t = \frac{1}{8}$	$\Delta t = \frac{1}{16}$	$\Delta t = \frac{1}{32}$	$\Delta t = \frac{1}{64}$	$\Delta t = \frac{1}{128}$
2^{-8}	without temporal extrapolation				
	2.3672e-03	1.2260e-03	6.3430e-04	3.2141e-04	1.6169e-04
	0.94915	0.95078	0.98076	0.99118	
	with temporal extrapolation				
	2.1813e-04	4.3563e-05	8.6666e-06	2.0023e-06	4.8800e-07
	2.3240	2.3296	2.1138	2.0367	
2^{-20}	without temporal extrapolation				
	2.3801e-03	1.2541e-03	6.5187e-04	3.3090e-04	1.6660e-04
	0.92440	0.94398	0.97820	0.98995	
	with temporal extrapolation				
	2.4413e-04	4.9651e-05	9.9248e-06	2.3130e-06	5.6376e-07
	2.2978	2.3227	2.1013	2.0366	

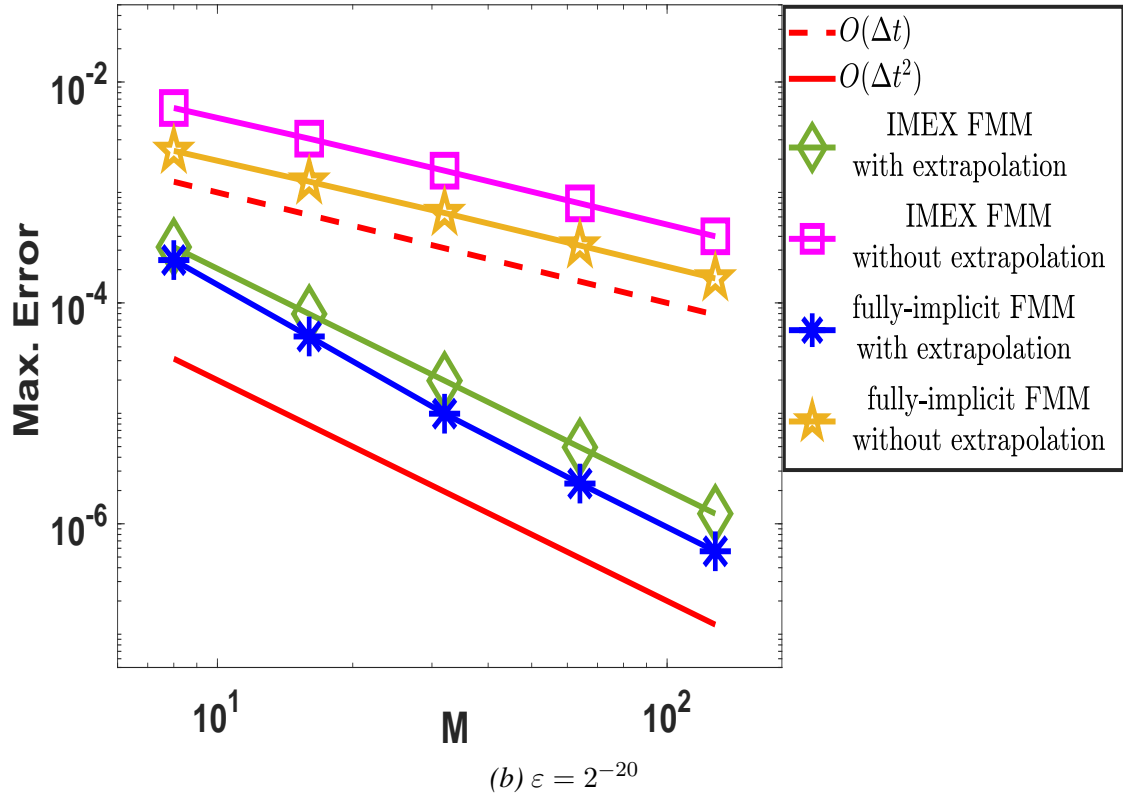
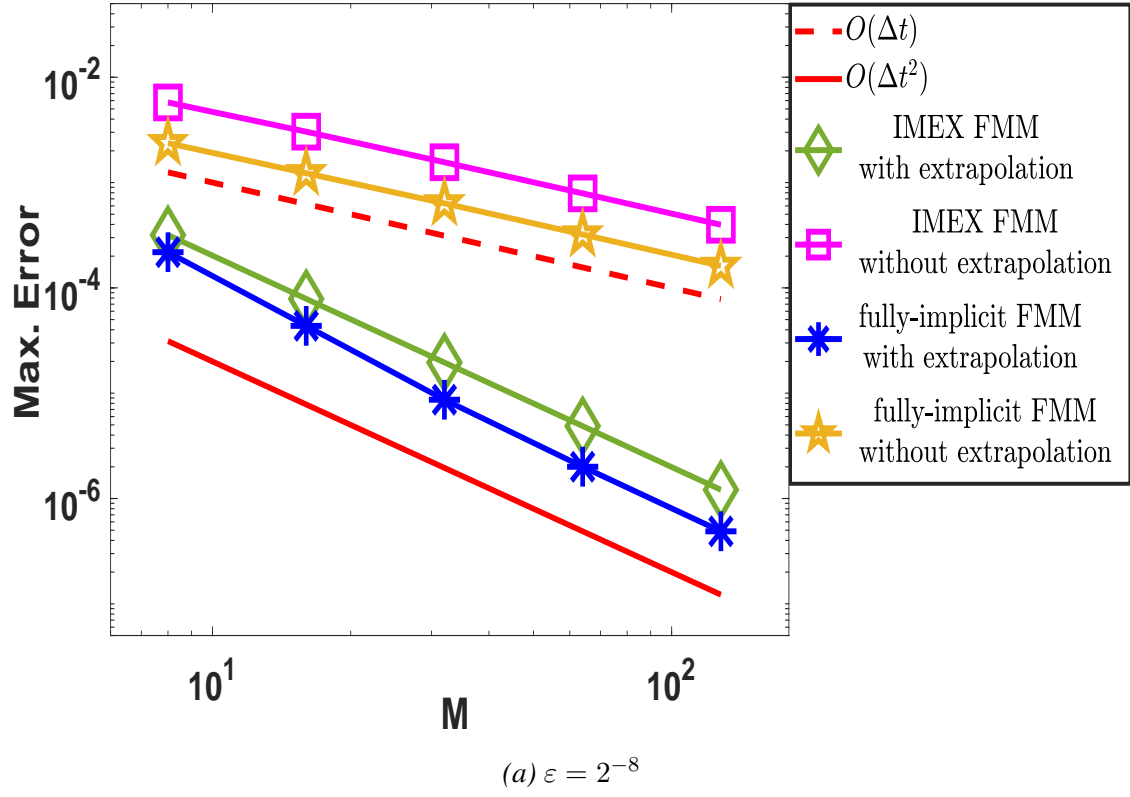


Figure 4.6: Loglog plot for comparison of the temporal order of convergence for Example 4.2

Table 4.7: Comparison of the spatial accuracy in the outer region, i.e., $[0, 1 - \eta]$ for Example 4.1

	maximum errors in $[0, 1 - \eta]$		
N	IMEX-FMM (4.30)	fully-implicit FMM (4.29)	upwind FMM (4.107)
	$\varepsilon = 2^{-4}$		
128	3.5572e-06 1.9993	3.3779e-06 1.9996	1.4327e-03 0.99511
256	8.8973e-07 1.9998	8.4474e-07 1.9999	7.1876e-04 0.99767
512	2.2246e-07 2.0000	2.1119e-07 2.0000	3.5996e-04 0.99886
1024	5.5616e-08	5.2798e-08	1.8012e-04
	$\varepsilon = 2^{-6}$		
128	1.7688e-05 2.2251	1.6955e-05 2.2286	3.0035e-03 1.0326
256	3.7833e-06 2.1625	3.6175e-06 2.1630	1.4682e-03 1.0389
512	8.4509e-07 2.1527	8.0776e-07 2.1527	7.1454e-04 1.0444
1024	1.9005e-07	1.8166e-07	3.4645e-04
	$\varepsilon = 2^{-14}$		
128	1.7633e-05 2.1323	1.9047e-05 2.1207	3.6522e-03 0.99515
256	4.0220e-06 2.0829	4.3794e-06 2.0758	1.8323e-03 0.99791
512	9.4936e-07 2.0112	1.0388e-06 2.0103	9.1746e-04 0.99902
1024	2.3550e-07	2.5785e-07	4.5904e-04
	$\varepsilon = 2^{-20}$		
128	1.7490e-05 2.1528	1.8907e-05 2.1394	3.6547e-03 0.99502
256	3.9331e-06 2.1286	4.2915e-06 2.1173	1.8337e-03 0.99778
512	8.9940e-07 2.1076	9.8911e-07 2.0976	9.1825e-04 0.99890
1024	2.0869e-07	2.3111e-07	4.5948e-04

Table 4.8: Comparison of the spatial accuracy in the layer region, i.e., $(\eta, 1]$ for Example 4.1

	maximum errors in $(\eta, 1]$		
N	IMEX-FMM (4.30)	fully-implicit FMM (4.29)	upwind FMM (4.107)
	$\varepsilon = 2^{-4}$		
128	1.7779e-04 2.0020	1.7733e-04 2.0020	6.3143e-03 0.96077
256	4.4388e-05 2.0002	4.4270e-05 2.0002	3.2442e-03 0.97982
512	1.1095e-05 2.0001	1.1066e-05 2.0001	1.6449e-03 0.98976
1024	2.7737e-06	2.7664e-06	8.2833e-04
	$\varepsilon = 2^{-6}$		
128	3.2023e-04 1.6345	3.1947e-04 1.6337	8.6126e-03 0.72370
256	1.0314e-04 1.6686	1.0296e-04 1.6682	5.2153e-03 0.77548
512	3.2443e-05 1.7015	3.2394e-05 1.7010	3.0467e-03 0.81049
1024	9.9753e-06	9.9635e-06	1.7372e-03
	$\varepsilon = 2^{-14}$		
128	3.0337e-04 1.6019	3.0248e-04 1.6008	8.7022e-03 0.72936
256	9.9943e-05 1.6515	9.9723e-05 1.6508	5.2489e-03 0.77765
512	3.1814e-05 1.6906	3.1758e-05 1.6901	3.0618e-03 0.81107
1024	9.8559e-06	9.8418e-06	1.7451e-03
	$\varepsilon = 2^{-20}$		
128	3.0348e-04 1.6016	3.0258e-04 1.6005	8.7033e-03 0.72939
256	1.0000e-04 1.6508	9.9782e-05 1.6502	5.2494e-03 0.77766
512	3.1846e-05 1.6895	3.1791e-05 1.6891	3.0621e-03 0.81107
1024	9.8731e-06	9.8591e-06	1.7453e-03

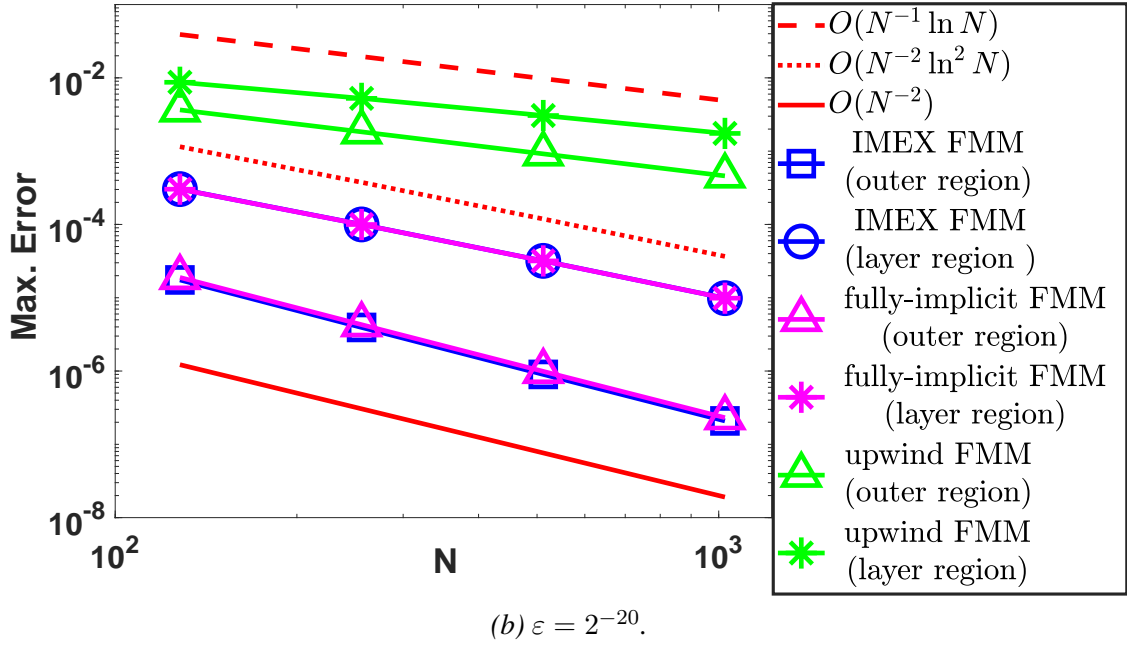
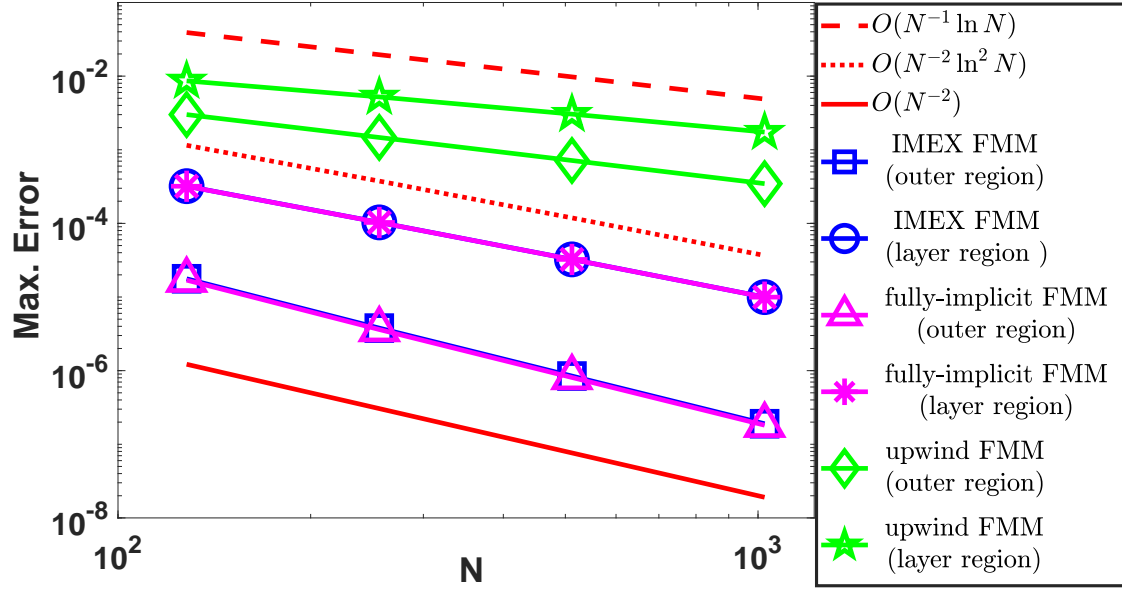


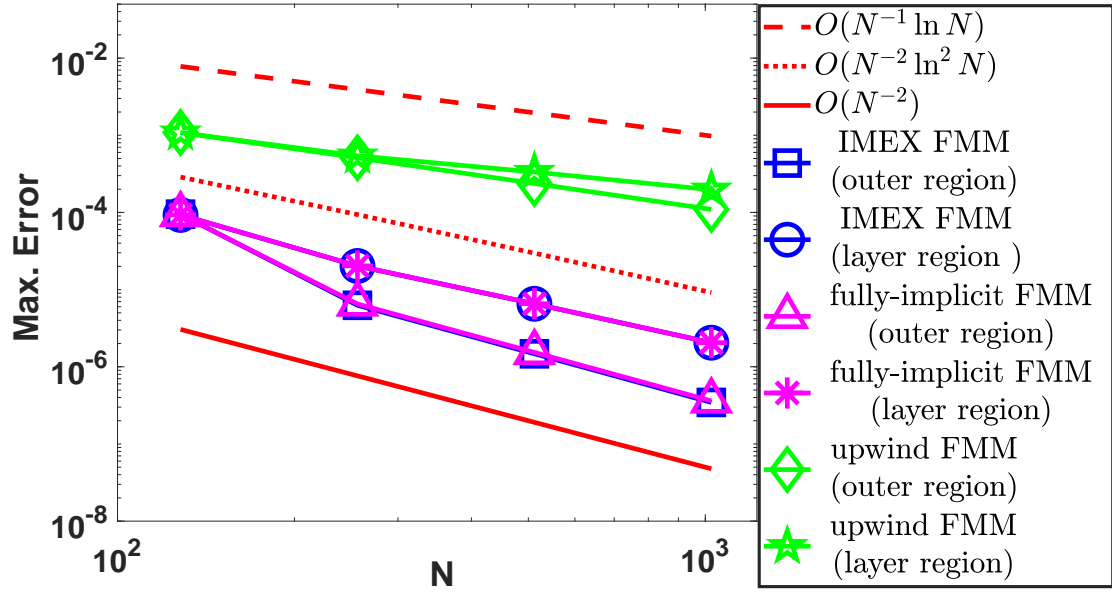
Figure 4.7: Loglog plot for comparison of the spatial order of convergence for Example 4.1

Table 4.9: Comparison of the spatial accuracy in the outer region, i.e., $[0, 1 - \eta]$ for Example 4.2

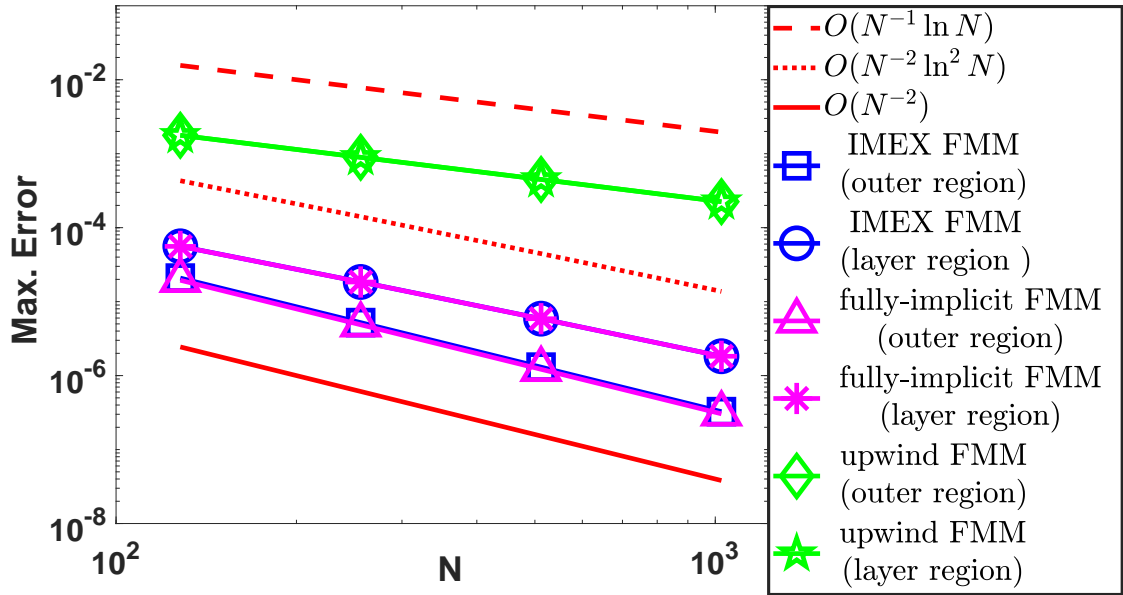
	maximum errors in $[0, 1 - \eta]$		
N	IMEX-FMM (4.30)	fully-implicit FMM (4.29)	upwind FMM (4.107)
$\varepsilon = 2^{-4}$			
128	7.9584e-06 1.9997	8.8874e-06 1.9999	2.6618e-04 0.99695
256	1.9900e-067 1.9999	2.2220e-06 1.9999	1.3337e-04 0.99850
512	4.9755e-07 1.9999	5.5553e-07 2.0000	6.6756e-05 0.99926
1024	1.2439e-07	1.3889e-07	3.3395e-05
$\varepsilon = 2^{-6}$			
128	9.4962e-05 3.9220	9.3866e-05 3.8477	1.0854e-03 1.0876
256	6.2648e-06 2.0889	6.5198e-06 2.0856	5.1072e-04 1.1049
512	1.4726e-06 2.0919	1.5361e-06 2.0882	2.3745e-04 1.1166
1024	3.4544e-07	3.6124e-07	1.0950e-04
$\varepsilon = 2^{-14}$			
128	2.0950e-05 1.9894	1.9587e-05 1.9881	1.7701e-03 0.98880
256	5.2761e-06 1.9784	4.9373e-06 1.9767	8.9195e-04 0.99488
512	1.3389e-06 1.9573	1.2544e-06 1.9542	4.4756e-04 0.99768
1024	3.4479e-07	3.2372e-07	2.2414e-04
$\varepsilon = 2^{-20}$			
128	2.0821e-05 2.0001	1.9458e-05 1.9997	1.7738e-03 0.98842
256	5.2050e-06 1.9997	4.8656e-06 1.9997	8.9403e-04 0.99452
512	1.3015e-06 1.9993	1.2167e-06 1.9992	4.4872e-04 0.99735
1024	3.2552e-07	3.0433e-07	2.2477e-04

Table 4.10: Comparison of the spatial accuracy in the layer region, i.e., $(\eta, 1]$ for Example 4.2

	maximum errors in $(\eta, 1]$		
N	IMEX-FMM (4.30)	fully-implicit FMM (4.29)	upwind FMM (4.107)
$\varepsilon = 2^{-4}$			
128	4.5383e-05 2.0037	4.5749e-05 2.0040	6.3875e-04 0.91539
256	1.1317e-05 2.0009	1.1405e-05 2.0010	3.3867e-04 0.95708
512	2.8276e-06 2.0002	2.8493e-06 2.0003	1.7445e-04 0.97782
1024	7.0680e-07	7.1219e-07	8.8575e-05
$\varepsilon = 2^{-6}$			
128	9.2843e-05 2.1975	9.3066e-05 2.1973	1.0792e-03 0.99260
256	2.0241e-05 1.6277	2.0293e-05 1.6286	5.4235e-04 0.70089
512	6.5500e-06 1.6738	6.5629e-06 1.6744	3.3365e-04 0.76230
1024	2.0529e-06	2.0561e-06	1.9671e-04
$\varepsilon = 2^{-14}$			
128	5.6115e-05 1.5996	5.6004e-05 1.5990	1.7698e-03 0.98861
256	1.8517e-05 1.6469	1.8487e-05 1.6465	8.9191e-04 0.99484
512	5.9128e-06 1.6838	5.9051e-06 1.6835	4.4755e-04 0.99767
1024	1.8404e-06	1.8384e-06	2.2414e-04
$\varepsilon = 2^{-20}$			
128	5.5953e-05 1.6005	5.5838e-05 1.6000	1.7735e-03 0.98824
256	1.8451e-05 1.6488	1.8420e-05 1.6484	8.9401e-04 0.99450
512	5.8841e-06 1.6871	5.8761e-06 1.6868	4.4871e-04 0.99734
1024	1.8273e-06	1.8253e-06	2.2477e-04



(a) $\varepsilon = 2^{-6}$.



(b) $\varepsilon = 2^{-20}$.

Figure 4.8: Loglog plot for comparison of the spatial order of convergence for Example 4.2

Table 4.11: Comparison of computational time (in seconds), taking $\Delta t = \frac{1}{N}$.

N	64	128	256	512	1024
for Example 4.1					
$\varepsilon = 2^{-14}$					
IMEX-FMM (4.30)	0.031944	0.134318	0.561493	1.668808	5.190696
fully-implicit FMM (4.29)	0.130007	0.636498	2.492893	9.787806	33.590889
$\varepsilon = 2^{-20}$					
IMEX-FMM (4.30)	0.033153	0.136713	2.718047	1.636886	5.151719
fully-implicit FMM (4.29)	0.142311	0.647636	3.165477	14.589820	41.411865
for Example 4.2					
$\varepsilon = 2^{-14}$					
IMEX-FMM (4.30)	0.159617	0.672547	2.138652	8.102781	23.756256
fully-implicit FMM (4.29)	1.061960	4.167360	13.470426	41.194917	174.114664
$\varepsilon = 2^{-20}$					
IMEX-FMM (4.30)	0.158384	0.668101	2.063758	8.793906	24.746797
fully-implicit FMM (4.29)	1.221180	5.930538	18.249831	54.942602	186.518022

Chapter 5

Higher-order Efficient Numerical Methods for Singularly Perturbed 2D Semilinear Parabolic PDEs with Non-homogeneous Boundary Data: ε -Uniform Convergence and Order Reduction Analysis

This chapter aims to provide a complete convergence analysis toward cost-effective higher-order numerical approximations for a class of two-dimensional singularly perturbed semilinear parabolic convection-diffusion problems with non-homogeneous boundary data. For this purpose, we developed two novel computational methods followed by the extrapolation technique to approximate the model problem. The first one is the implicit-explicit (IMEX) fractional-step method, which utilizes the fractional IMEX-Euler method for temporal discretization. The other is the fully-implicit fractional-step method, which uses the fractional-step implicit-Euler method for temporal discretization. The spatial discretization for both numerical methods is based on a new finite difference scheme. An appropriate non-uniform rectangular mesh is used to discretize the spatial domain, and an equidistant mesh is used to discretize the time domain. We begin our analysis by investigating the stability and asymptotic behavior of the analytical solution to the nonlinear governing problem. The error analysis is performed in two steps, first in time and then in space, for both the newly proposed methods. In addition to this, we proposed an appropriate choice of the boundary data to avoid the order reduction phenomena caused by the classical evaluation of the time-dependent boundary conditions. After that, we apply the Richardson extrapolation solely to the time variable to increase the order of uniform convergence in the temporal direction. As a result, we obtain second-order accurate numerical solutions globally (in both space and time). Finally, we carry out extensive numerical experiments to validate the theoretical findings. Moreover, the numerical results of the proposed methods are compared with the fractional-step implicit upwind finite difference scheme to examine the robustness of the newly developed methods.

5.1 Introduction

Here, we consider the following class of singularly perturbed 2D semilinear parabolic convection-diffusion IBVPs posed on the domain $\mathcal{D} = \mathcal{G} \times (0, T] = (0, 1)^2 \times (0, T]$; $\bar{\mathcal{G}} = [0, 1]^2$:

$$\begin{cases} \mathbb{T}_\varepsilon u(x, y, t) = \frac{\partial u(x, y, t)}{\partial t} + \mathbb{L}_\varepsilon u(x, y, t) + b(x, y, t, u(x, y, t)) = g(x, y, t), & \text{in } \mathcal{D}, \\ u(x, y, 0) = q_0(x, y), & \text{in } \bar{\mathcal{G}}, \\ u(x, y, t) = s(x, y, t), & \text{in } \partial\mathcal{G} \times (0, T], \end{cases} \quad (5.1)$$

where

$$\begin{cases} \mathbb{L}_\varepsilon u = -\varepsilon \Delta u + \vec{v}(x, y, t) \cdot \vec{\nabla} u, \\ \vec{v}(x, y, t) = (v_1(x, y, t), v_2(x, y, t)), \end{cases}$$

and ε is a small parameter such that $\varepsilon \in (0, 1]$. The convection coefficient $\vec{v}(x, y, t)$ is considered to be sufficiently smooth on $\bar{\mathcal{D}}$ with

$$v_1(x, y, t) \geq m_1 > 0, \quad v_2(x, y, t) \geq m_2 > 0, \quad \text{on } \bar{\mathcal{D}}. \quad (5.2)$$

In addition, it is assumed that the nonlinear term $b(x, y, t, u)$ is sufficiently smooth on $\bar{\mathcal{D}} \times \mathbb{R}$ and satisfies the condition

$$\frac{\partial b(x, y, t, u)}{\partial u} \geq \beta > 0, \quad (x, y, t, u) \in \bar{\mathcal{D}} \times \mathbb{R}. \quad (5.3)$$

The solution of the IBVP (5.1)-(5.3) has exponential layers when $\varepsilon \ll 1$ at the outflow boundaries $x = 1$ and $y = 1$ (see [5]). We set $\mathbb{L}_\varepsilon = \mathbb{L}_{1,\varepsilon} + \mathbb{L}_{2,\varepsilon}$, where the differential operators $\mathbb{L}_{1,\varepsilon}$, $\mathbb{L}_{2,\varepsilon}$ are defined by

$$\begin{cases} \mathbb{L}_{1,\varepsilon} u = -\varepsilon \frac{\partial^2 u}{\partial x^2} + v_1(x, y, t) \frac{\partial u}{\partial x}, \\ \mathbb{L}_{2,\varepsilon} u = -\varepsilon \frac{\partial^2 u}{\partial y^2} + v_2(x, y, t) \frac{\partial u}{\partial y}, \end{cases}$$

with $g = g_1 + g_2$. We further assume that the initial and boundary data of the problem are sufficiently smooth functions and also assume that necessary compatibility conditions hold among them in order to $u(x, y, t) \in \mathcal{C}^{4+\gamma}(\bar{\mathcal{D}})$, which has continuous derivatives up to fourth-order in space and second-order in time. The existence of the solution $u(x, y, t)$ of the nonlinear IBVP (5.1)-(5.3) follows from [Chapter 7, §4] of the book [41] by Friedman.

The compatibility conditions are given below:

$$\left\{ \begin{array}{l} \mathbf{s}(x, y, 0) = \mathbf{q}_0(x, y), \quad \text{on } \partial\mathbf{G}, \\ \frac{\partial \mathbf{s}(x, y, 0)}{\partial t} = -\mathbb{L}_\varepsilon(0)\mathbf{q}_0(x, y) - b(x, y, 0, \mathbf{q}_0(x, y)) + g(x, y, 0), \quad \text{on } \partial\mathbf{G} \\ \frac{\partial^2 \mathbf{s}(x, y, 0)}{\partial t^2} = -\mathbb{L}_\varepsilon g(x, y, 0) + \mathbb{L}_\varepsilon^2(0)\mathbf{q}_0(x, y) + \frac{\partial g(x, y, 0)}{\partial t} - \frac{\partial b(x, y, 0, \mathbf{q}_0(x, y))}{\partial t} - \\ \frac{\partial b(x, y, 0, \mathbf{q}_0(x, y))}{\partial u} g(x, y, 0) + \frac{\partial b(x, y, 0, \mathbf{q}_0(x, y))}{\partial u} b(x, y, 0, \mathbf{q}_0(x, y)) + \\ \frac{\partial b(x, y, 0, \mathbf{q}_0(x, y))}{\partial u} \mathbb{L}_\varepsilon(0)\mathbf{q}_0(x, y), \quad \text{on } \partial\mathbf{G}, \\ \frac{\partial \mathbf{s}(x, y, t)}{\partial t} = -\mathbb{L}_\varepsilon \mathbf{s}(x, y, t) - b(x, y, t, \mathbf{s}(x, y, t)) + g(x, y, t), \\ (x, y) \in \{0, 1\} \times \{0, 1\} \times (0, T]. \end{array} \right. \quad (5.4)$$

The rest of this chapter is organized as follows. Section 5.2 presents comparison principle as well as some a-priori bounds of the analytical solution and its derivatives. The implicit-explicit fractional-step FMM is formulated and analyzed in Section 5.3. The fully implicit fractional-step FMM is formulated and analyzed in Section 5.4. In Section 5.5, we discuss convergence analysis for the temporal Richardson extrapolation to the nonlinear discrete problem (5.102). Finally, numerical experiments are performed in Section 5.6 to demonstrate the accuracy and efficiency of the proposed FMMs. The conclusion of this chapter is provided in 5.7.

5.2 Properties of the analytical solution

Lemma 5.1 (Comparison Principle). *Let the functions $v, w \in \mathcal{C}^0(\bar{\mathbf{D}}) \cap \mathcal{C}^2(\mathbf{D})$ be such that $v \leq w$, on $\partial\mathbf{D}$ and $\mathbb{T}_\varepsilon v \leq \mathbb{T}_\varepsilon w$, in \mathbf{D} , then it implies that $v \leq w$, on $\bar{\mathbf{D}}$.*

Proof. Here, we use method of contradiction. Firstly, we suppose that there exists $(x^*, y^*, t^*) \in \bar{\mathbf{D}}$ such that $v(x^*, y^*, t^*) > w(x^*, y^*, t^*)$. Since, $v - w \in \mathcal{C}^0(\bar{\mathbf{D}})$, without loss of generality, we assume that $v - w$ takes positive maximum at (x^*, y^*, t^*) . Now, in conformity with the hypothesis of the comparison principle, $v - w \leq 0$ on $\partial\mathbf{D} \implies (x^*, y^*, t^*) \notin \partial\mathbf{D}$. Therefore, under the above assumption and applying mean value theorem, we have

$$\begin{aligned} & (\mathbb{T}_\varepsilon v - \mathbb{T}_\varepsilon w)(x^*, y^*, t^*) \\ &= \frac{\partial(v - w)(x^*, y^*, t^*)}{\partial t} + \mathbb{L}_{x, \varepsilon}(v - w)(x^*, y^*, t^*) + b(x^*, y^*, t^*, v(x^*, y^*, t^*)) \\ & \quad - b(x^*, y^*, t^*, w(x^*, y^*, t^*)), \\ & \geq \left[\int_0^1 \frac{b(x^*, y^*, t^*, w(x^*, y^*, t^*)) + \xi(v - w)(x^*, y^*, t^*)}{\partial y} d\xi \right] (v - w)(x^*, y^*, t^*). \end{aligned} \quad (5.5)$$

Thus, from (5.5) and the assumption (5.3), we have $\mathbb{T}_\varepsilon v(x^*, y^*, t^*) > \mathbb{T}_\varepsilon w(x^*, y^*, t^*)$ and this contradicts that $\mathbb{T}_\varepsilon v(x, y, t) \leq \mathbb{T}_\varepsilon w(x, y, t)$ for all $(x, y, t) \in \mathbf{D}$. Hence, the proof is over. ■

The following result follows from Lemma 5.1.

Corollary 5.1. *Let the function $\Phi \in \mathcal{C}^0(\bar{\mathcal{D}}) \cap \mathcal{C}^2(\mathcal{D})$. For any given functions $v, w \in \mathcal{C}^0(\bar{\mathcal{D}})$, the linear differential operator $\tilde{\mathbb{T}}_{\varepsilon, (v, w)}$ defined by*

$$\tilde{\mathbb{T}}_{\varepsilon, (v, w)}\Phi = \frac{\partial \Phi}{\partial t} + \mathbb{L}_{x, \varepsilon}\Phi + \left(\int_0^1 \frac{\partial b(x, y, t, w(x, y, t) + \xi(v - w)(x, y, t))}{\partial u} d\xi \right) \Phi,$$

satisfies the maximum principle, i.e., if $\Phi \leq 0$, on $\partial\mathcal{D}$ and $\tilde{\mathbb{T}}_{\varepsilon, (v, w)}\Phi \leq 0$, in \mathcal{D} , then it implies that $\Phi \leq 0$, on $\bar{\mathcal{D}}$.

Corollary 5.1 is used to deduce the following ε -uniform stability result.

Lemma 5.2 (Stability). *Let the functions $v, w \in \mathcal{C}^0(\bar{\mathcal{D}}) \cap \mathcal{C}^2(\mathcal{D})$, then it satisfies*

$$\|v - w\|_{\bar{\mathcal{D}}} \leq \|v - w\|_{\partial\mathcal{D}} + \frac{1}{\beta} \|\mathbb{T}_{\varepsilon}v - \mathbb{T}_{\varepsilon}w\|_{\mathcal{D}}. \quad (5.6)$$

Proof. Consider the functions

$$\Phi^{\pm}(x, y, t) = -\|v - w\|_{\partial\mathcal{D}} - \frac{1}{\beta} \|\mathbb{T}_{\varepsilon}v - \mathbb{T}_{\varepsilon}w\|_{\bar{\mathcal{D}}} \pm (v - w)(x, y, t), \quad (x, y, t) \in \bar{\mathcal{D}}.$$

Note that $\Phi^{\pm}(x, y, t) \leq 0$, $(x, y, t) \in \partial\mathcal{D}$, and

$$\|\tilde{\mathbb{T}}_{\varepsilon, (v, w)}(v - w)\| \leq \left[\int_0^1 \frac{\partial b(x, y, t, w + \xi(v - w))}{\partial u} d\xi \right] \left(\frac{1}{\beta} \|\mathbb{T}_{\varepsilon}v - \mathbb{T}_{\varepsilon}w\| \right) \Rightarrow \tilde{\mathbb{T}}_{\varepsilon, (v, w)}\Phi^{\pm} \leq 0.$$

Then, Corollary 5.1 implies that $\Phi^{\pm}(x, y, t) \leq 0$, for all $(x, y, t) \in \bar{\mathcal{D}}$, from which the desired result follows immediately. ■

By selecting $v = u$ and $w = 0$, Lemma 5.2 implies that

$$|u(x, y, t)| \leq C_0, \quad (x, y, t) \in \bar{\mathcal{D}}. \quad (5.7)$$

Remark 5.1. Note that using the a-priori bound (5.7) (independent of ε) and the smoothness assumption on the nonlinear term ‘ b ’ one can obtain the following ε -uniform boundedness property:

$$\left| \frac{\partial^{j+k+m} b(x, y, t, u)}{\partial x^{j_1} \partial y^{j_2} \partial t^k \partial u^m} \right|_{u=u(x, y, t)} \leq C, \quad (x, y, t) \in \bar{\mathcal{D}}, \quad (5.8)$$

$\forall j, k, m \in \mathbb{N} \cup \{0\}$, satisfying $j = j_1 + j_2$, $0 \leq j + 2k + 2m \leq N$; and we use this property later in this chapter.

Next, we derive the bounds on the derivatives of $u(x, y, t)$ with respect to space variables x, y and time variable t by extending the approach given in [24]. The solution $u(x, y, t)$ of the nonlinear IBVP (5.1)-(5.3) can be decomposed as

$$u(x, y, t) = s(x, y, t) + z(x, y, t), \quad (x, y, t) \in \bar{\mathcal{D}},$$

where $s(x, y, t)$ is the smooth component and z is the singular component. Again, the component $z(x, y, t)$

which can be decomposed in the form

$$z(x, y, t) = z_1(x, y, t) + z_2(x, y, t) + z_{11}(x, y, t), \quad (x, t, t) \in \bar{D},$$

where z_1 , z_2 are the exponential layers near the sides $x = 1$ and $y = 1$ of G , respectively and z_{11} is the corner layer near the point $(1, 1)$. The smooth component $s(x, y, t)$ is the restriction of $s^*(x, y, t)$ to D , where $s^*(x, y, t)$ is the solution of the following nonlinear problem:

$$\begin{cases} \frac{\partial s^*}{\partial t} + \mathbb{L}_\varepsilon^* s^* + b^*(x, y, t, s^*) = g^*(x, y, t), & \text{in } D^* = G^* \times (0, T], \\ s^*(x, y, 0) = q_0^*(x, y), & \text{in } \bar{G}^*, \\ s^*(x, y, t) = s^*(x, y, t), & \text{in } \partial G^* \times (0, T], \end{cases} \quad (5.9)$$

where $\mathbb{L}_\varepsilon^* = -\varepsilon \Delta + \vec{v}^*(x, y, t) \cdot \vec{\nabla}$, G^* is a smooth extension of G , and \vec{v}^* , b^* , g^* , q_0^* , s^* are smooth extension of \vec{v} , b , g , q_0 , s to their respective domains. Hence, the singular component z satisfies that

$$\begin{cases} \frac{\partial z}{\partial t} + \mathbb{L}_\varepsilon z + b(x, y, t, u) - b(x, y, t, s) = 0, & \text{in } D, \\ z(x, y, 0) = 0, & \text{in } \bar{G}, \\ z(x, y, t) = u(x, y, t) - s(x, y, t), & \text{in } \partial G \times (0, T]. \end{cases} \quad (5.10)$$

By applying mean value theorem, the nonlinear IBVPs (5.9) and (5.10) can be reduced to the following respective linear problems:

$$\begin{cases} \frac{\partial s^*}{\partial t} + \mathbb{L}_\varepsilon^* s^* + \left(\int_0^1 \frac{\partial b^*(x, y, t, \xi s^*)}{\partial u} d\xi \right) s^* = g^*(x, y, t) - b^*(x, y, t, 0), & \text{in } D^*, \\ s^*(x, y, 0) = q_0^*(x, y), & \text{in } \bar{G}^*, \\ s^*(x, y, t) = s^*(x, y, t), & \text{in } \partial G^* \times (0, T], \end{cases} \quad (5.11)$$

and

$$\begin{cases} \frac{\partial z}{\partial t} + \mathbb{L}_\varepsilon z + \left(\int_0^1 \frac{\partial b(x, y, t, s + \xi(u - s))}{\partial u} d\xi \right) z = 0, & \text{in } D, \\ z(x, y, 0) = 0, & \text{in } \bar{G}, \\ z(x, y, t) = u(x, y, t) - s(x, y, t), & \text{in } \partial G \times (0, T]. \end{cases} \quad (5.12)$$

Now, following the approach given in [24], one can show that the components of $u(x, y, t)$ satisfies the following bounds:

$$\left| \frac{\partial^{j+k} s(x, y, t)}{\partial x^{j_1} \partial y^{j_2} \partial t^k} \right| \leq C, \quad (5.13)$$

$$\left| \frac{\partial^{j+k} z_1(x, y, t)}{\partial x^{j_1} \partial y^{j_2} \partial t^k} \right| \leq C \varepsilon^{-j_1} \exp \left(-\frac{m_1(1-x)}{\varepsilon} \right), \quad (5.14)$$

$$\left| \frac{\partial^{j+k} z_2(x, y, t)}{\partial x^{j_1} \partial y^{j_2} \partial t^k} \right| \leq C \varepsilon^{-j_2} \exp \left(-\frac{\mathfrak{m}_2(1-y)}{\varepsilon} \right), \quad (5.15)$$

$$\left| \frac{\partial^{j+k} z_{11}(x, y, t)}{\partial x^{j_1} \partial y^{j_2} \partial t^k} \right| \leq C \varepsilon^{-j} \min \left\{ \exp \left(-\frac{\mathfrak{m}_1(1-x)}{\varepsilon} \right), \exp \left(-\frac{\mathfrak{m}_2(1-y)}{\varepsilon} \right) \right\}, \quad (5.16)$$

where $\forall j_1, j_2, k \in \mathbb{N} \cup \{0\}$, $j = j_1 + j_2$, $0 \leq j + 2k \leq 4$ and $(x, y, t) \in \bar{D}$.

Lemma 5.3. *The derivatives of the solution $u(x, y, t)$ of the nonlinear IBVP (5.1)-(5.3) satisfy the following bounds:*

$$\left| \frac{\partial^k u(x, y, t)}{\partial t^k} \right| \leq C, \quad (5.17)$$

$$\left| \frac{\partial^{j_1} u(x, y, t)}{\partial x^{j_1}} \right| \leq C \varepsilon^{-j_1} \exp \left(-\frac{\mathfrak{m}_1(1-x)}{\varepsilon} \right), \quad (5.18)$$

$$\left| \frac{\partial^{j_2} u(x, y, t)}{\partial y^{j_2}} \right| \leq C \varepsilon^{-j_2} \exp \left(-\frac{\mathfrak{m}_2(1-y)}{\varepsilon} \right), \quad (5.19)$$

where $j = j_1 + j_2$, $0 \leq j + 2k \leq 4$ and $(x, y, t) \in \bar{D}$.

5.3 The discrete problem-I

The purpose of this section is to introduce and analyze the implicit-explicit fractional-step FMM for discretization of the nonlinear IBVP (5.1)-(5.3). At first, we estimate the error for the time semidiscretization and later, for the fully discrete problem. We write $b(x, y, t, u) = b_1(x, y, t, u) + b_2(x, y, t, u)$, where b_1 and b_2 also satisfy similar smoothness assumption as like the reaction term b .

5.3.1 Time semidiscretization: fractional-steps implicit-explicit scheme

Here, we consider the fractional-step IMEX-Euler method to discretize the nonlinear IBVP (5.1)-(5.3) with respect to the temporal variable. The fractional-step IMEX-method can be written as two half scheme and in each half, the method treats the linear part of the governing differential equation implicitly and the nonlinear

part explicitly. Let $u^n(x, y) \approx u(x, y, t_n)$. Then, the semidiscrete problem takes the following form:

(i) (initial condition)

$$u^0(x, y) = q_0(x, y), \quad (x, y) \in \bar{\mathbf{G}},$$

(ii) (first half)

$$\begin{cases} (\mathbf{I} + \Delta t \mathbb{L}_{1,\varepsilon}^{n+1}) u^{n+1/2}(x, y) + \Delta t b_1(x, y, t_n, u^n(x, y)) = u^n(x, y) + \Delta t g_1(x, y, t_{n+1}), \\ (x, y) \in \mathbf{G}, \\ u^{n+1/2}(x, y) = \mathbf{s}^{n+1/2}(x, y), \quad (x, y) \in \{0, 1\} \times [0, 1], \end{cases} \quad (5.20)$$

(iii) (second half)

$$\begin{cases} (\mathbf{I} + \Delta t \mathbb{L}_{2,\varepsilon}^{n+1}) u^{n+1}(x, y) + \Delta t b_2(x, y, t_n, u^n(x, y)) = u^{n+1/2}(x, y) + \Delta t g_2(x, y, t_{n+1}), \\ (x, y) \in \mathbf{G}, \\ u^{n+1}(x, y) = \mathbf{s}^{n+1}(x, y), \quad (x, y) \in [0, 1] \times \{0, 1\}, \end{cases}$$

for $n = 0, \dots, M - 1$, where the operators $\mathbb{L}_{1,\varepsilon}^{n+1}$ and $\mathbb{L}_{2,\varepsilon}^{n+1}$ are defined by

$$\begin{cases} \mathbb{L}_{1,\varepsilon}^{n+1} \equiv -\varepsilon \frac{\partial^2}{\partial x^2} + v_1(x, y, t_{n+1}) \frac{\partial}{\partial x}, \\ \mathbb{L}_{2,\varepsilon}^{n+1} \equiv -\varepsilon \frac{\partial^2}{\partial y^2} + v_2(x, y, t_{n+1}) \frac{\partial}{\partial y}. \end{cases}$$

The classical choice of boundary conditions is given by

$$\begin{cases} \mathbf{s}^{n+1/2}(x, y) = \mathbf{s}(x, y, t_{n+1}), \quad (x, y) \in \{0, 1\} \times [0, 1], \\ \mathbf{s}^{n+1}(x, y) = \mathbf{s}(x, y, t_{n+1}), \quad (x, y) \in [0, 1] \times \{0, 1\}. \end{cases} \quad (5.21)$$

In most cases, this option causes a sharp increase in the global error which finally become $O(1)$. To avoid this order reduction, we propose an alternative choice of boundary data which is given by

$$\begin{cases} \mathbf{s}^{n+1/2}(x, y) = (\mathbf{I} + \Delta t \mathbb{L}_{2,\varepsilon}^{n+1}) \mathbf{s}(x, y, t_{n+1}) + \Delta t b_2(x, y, t_n, u^n(x, y)) - \Delta t g_2(x, y, t_{n+1}), \\ (x, y) \in \{0, 1\} \times [0, 1], \\ \mathbf{s}^{n+1}(x, y) = \mathbf{s}(x, y, t_{n+1}), \quad (x, y) \in [0, 1] \times \{0, 1\}. \end{cases} \quad (5.22)$$

One can show that the operators $(\mathbf{I} + \Delta t \mathbb{L}_{1,\varepsilon}^{n+1})$ and $(\mathbf{I} + \Delta t \mathbb{L}_{2,\varepsilon}^{n+1})$ satisfy the following maximum principle.

Lemma 5.4 (Maximum principle). *Let the function $\psi \in \mathcal{C}^0(\bar{\mathbf{G}}) \cap \mathcal{C}^2(\mathbf{G})$ be such that $\psi(x, y) \leq 0$, on $\partial \mathbf{G}$ and $(\mathbf{I} + \Delta t \mathbb{L}_{k,\varepsilon}^{n+1}) \psi(x, y) \leq 0$, $k = 1, 2$, for all $(x, y) \in \mathbf{G}$. Then, it implies that $\psi(x, y) \leq 0$, for all $(x, y) \in \bar{\mathbf{G}}$.*

Proof. See [Chapter 3, Lemma 3.2] for the proof. ■

Lemma 5.5 (Stability). *Let the function $\mathcal{V} \in \mathcal{C}^0(\bar{\mathbf{G}}) \cap \mathcal{C}^2(\mathbf{G})$. Then, we have*

$$\|\mathcal{V}\|_{\bar{\mathbf{G}}} \leq \|\mathcal{V}\|_{\partial\mathbf{G}} + \|(\mathbf{I} + \Delta t \mathbb{L}_{k,\varepsilon}^{n+1})\mathcal{V}\|_{\bar{\mathbf{G}}},$$

where $k = 1, 2$.

Proof. Consider the following functions

$$\Psi^\pm(x, y) = -\|\mathcal{V}\|_{\partial\mathbf{G}} - \|(\mathbf{I} + \Delta t \mathbb{L}_{k,\varepsilon}^{n+1})\mathcal{V}\|_{\bar{\mathbf{G}}} \pm \mathcal{V}(x, y), \quad (x, y) \in \bar{\mathbf{G}},$$

where $k = 1, 2$. It is obvious that $\Psi^\pm(x, y) \leq 0$ on $\partial\mathbf{G}$ and

$$(\mathbf{I} + \Delta t \mathbb{L}_{k,\varepsilon}^{n+1})\Psi^\pm(x, y) \leq -\|(\mathbf{I} + \Delta t \mathbb{L}_{k,\varepsilon}^{n+1})\mathcal{V}\|_{\bar{\mathbf{G}}} \pm (\mathbf{I} + \Delta t \mathbb{L}_{k,\varepsilon}^{n+1})\mathcal{V} \leq 0,$$

by applying Lemma 5.4, we obtain the desired result. ■

Lemma 5.5 guarantees that the scheme (5.20) has a unique solution $u^n(x, y)$ at each time level t_n . Further, using Lemma 5.5 below it is shown that the solution $u^n(x, y)$ becomes ε -uniformly bounded.

Lemma 5.6. *The solution $u^n(x, y)$ of the semidiscrete problem (5.20) at the time level t_n satisfies that*

$$|u^n(x, y)| \leq C_0, \quad \text{in } \bar{\mathbf{G}}. \quad (5.23)$$

Proof. It is clear that

$$|u^0(x, y)| \leq C_0, \quad \text{in } \bar{\mathbf{G}},$$

due to the continuity of $q_0(x)$ on $\bar{\mathbf{G}}$, and hence, implies that $|b(x, y, t, u^0(x, y))| \leq C_0$, in $\bar{\mathbf{G}}$. Then, applying Lemma 5.5, we obtain from (5.20) that

$$|u^1(x, y)| \leq C_0, \quad \text{in } \bar{\mathbf{G}},$$

and hence, implies that $|b(x, y, t, u^1(x, y))| \leq C_0$, in $\bar{\mathbf{G}}$. Thereafter, arguing previously, we obtain that

$$|u^2(x, y)| \leq C_0, \quad \text{in } \bar{\mathbf{G}}. \quad (5.24)$$

Thus, one can proceed in the same way to obtain the desired result. ■

5.3.1.1 Error analysis

Let us denote \tilde{e}^{n+1} as the local truncation error of scheme (5.20) at the time level t_{n+1} i.e., $\tilde{e}^{n+1}(x, y) = \tilde{u}^{n+1}(x, y) - u(x, y, t_{n+1})$, where \tilde{u}^{n+1} is the solution of the following auxiliary problem:

$$\begin{aligned}
 (i) \quad & u^0(x, y) = q_0(x, y), \quad (x, y) \in \bar{G}, \\
 (ii) \quad & \begin{cases} (\mathbf{I} + \Delta t \mathbb{L}_{1,\varepsilon}^{n+1}) \tilde{u}^{n+1/2}(x, y) + \Delta t b_1(x, y, t_n, u(x, y, t_n)) = u(x, y, t_n) + \Delta t g_1(x, y, t_{n+1}), \\ (x, y) \in G, \\ \tilde{u}^{n+1/2}(x, y) = \mathbf{s}^{n+1/2}(x, y), \quad (x, y) \in \{0, 1\} \times [0, 1], \end{cases} \\
 (iii) \quad & \begin{cases} (\mathbf{I} + \Delta t \mathbb{L}_{2,\varepsilon}^{n+1}) \tilde{u}^{n+1}(x, y) + \Delta t b_2(x, y, t_n, u(x, y, t_n)) = \tilde{u}^{n+1/2}(x, y) + \Delta t g_2(x, y, t_{n+1}), \\ (x, y) \in G, \\ \tilde{u}^{n+1}(x, y) = \mathbf{s}^{n+1}(x, y), \quad (x, y) \in [0, 1] \times \{0, 1\}, \end{cases}
 \end{aligned} \tag{5.25}$$

for $n = 0, \dots, M - 1$.

Lemma 5.7 (Local error). *Under the alternative boundary data $\mathbf{s}^{n+1/2}$ and \mathbf{s}^{n+1} are given in (5.22), the local error at the time level t_{n+1} satisfies that*

$$\|\tilde{e}^{n+1}\|_{\bar{G}} \leq C(\Delta t)^2.$$

Proof. From (5.25), we easily deduce that

$$\begin{aligned}
 & (\mathbf{I} + \Delta t \mathbb{L}_{1,\varepsilon}^{n+1}) \left((\mathbf{I} + \Delta t \mathbb{L}_{2,\varepsilon}^{n+1}) \tilde{u}^{n+1}(x, y) + \Delta t b_2(x, y, t_n, u(x, y, t_n)) \right. \\
 & \left. - \Delta t g_2(x, y, t_{n+1}) \right) + \Delta t b_1(x, y, t_n, u(x, y, t_n)) = u(x, y, t_n) + \Delta t g_1(x, y, t_{n+1}).
 \end{aligned}$$

Further, we obtain that

$$\begin{aligned}
 & (\mathbf{I} + \Delta t \mathbb{L}_{1,\varepsilon}^{n+1}) (\mathbf{I} + \Delta t \mathbb{L}_{2,\varepsilon}^{n+1}) \tilde{u}^{n+1}(x, y) + \Delta t b(x, y, t_n, u(x, y, t_n)) \\
 & = u(x, y, t_n) + \Delta t g(x, y, t_{n+1}) + O(\Delta t)^2.
 \end{aligned} \tag{5.26}$$

We expand Taylor's series expansion of the function $u(x, y, t_n)$ with respect to time to have

$$u(x, y, t_n) = u(x, y, t_{n+1}) - \Delta t \frac{\partial u(x, y, t_{n+1})}{\partial t} + O(\Delta t)^2, \tag{5.27}$$

and by using equation (5.1), we can write

$$\begin{aligned}
 & (\mathbf{I} + \Delta t \mathbb{L}_{1,\varepsilon}^{n+1}) (\mathbf{I} + \Delta t \mathbb{L}_{2,\varepsilon}^{n+1}) u(x, y, t_{n+1}) + \Delta t b(x, y, t_{n+1}, u(x, y, t_{n+1})) \\
 & = u(x, y, t_n) + \Delta t g(x, y, t_{n+1}) + O(\Delta t)^2.
 \end{aligned} \tag{5.28}$$

Subtracting equation (5.26) and (5.28), we get

$$\begin{aligned} & (\mathbf{I} + \Delta t \mathbb{L}_{1,\varepsilon}^{n+1})(\mathbf{I} + \Delta t \mathbb{L}_{2,\varepsilon}^{n+1})\tilde{e}^{n+1}(x, y) + \Delta t [b(x, y, t_{n+1}, u(x, y, t_{n+1})) - b(x, y, t_n, u(x, y, t_n))] \\ & = O(\Delta t)^2, \end{aligned}$$

where we apply the bound $\frac{\partial^2 u}{\partial t^2}$ from Lemma 5.3. Further, one can deduce that

$$b(x, y, t_{n+1}, u(x, y, t_{n+1})) - b(x, y, t_n, u(x, y, t_n)) \quad (5.29)$$

$$\begin{aligned} & = \Delta t \left[\frac{\partial b(x, y, s, u(x, y, s))}{\partial t} + \frac{\partial b(x, y, s, u(x, y, s))}{\partial u} \frac{\partial u(x, y, s)}{\partial t} \right], \quad t_n < s < t_{n+1}, \\ & = O(\Delta t), \end{aligned} \quad (5.30)$$

where the bound on $\frac{\partial u}{\partial t}$ from Lemma 5.3 and the property (5.8) are utilized. Now, by using alternative boundary data given in (5.22), the local error can be written as the solution of a following problem

$$\begin{cases} (\mathbf{I} + \Delta t \mathbb{L}_{1,\varepsilon}^{n+1})\tilde{e}^{n+1/2}(x, y) = O(\Delta t)^2, & (x, y) \in \mathbb{G}, \\ \tilde{e}^{n+1/2}(0, y) = 0, \quad \tilde{e}^{n+1/2}(1, y) = 0, & y \in [0, 1], \end{cases} \quad (5.31)$$

$$\begin{cases} (\mathbf{I} + \Delta t \mathbb{L}_{2,\varepsilon}^{n+1})\tilde{e}^{n+1}(x, y) = \tilde{e}^{n+1/2}(x, y), & (x, y) \in \mathbb{G}, \\ \tilde{e}^{n+1}(x, 0) = 0, \quad \tilde{e}^{n+1}(x, 1) = 0, & x \in [0, 1]. \end{cases} \quad (5.32)$$

From (5.31) and (5.32), and using the stability property of Lemma 5.5, we get desired bound of the local error. ■

Let us introduce the global error of the time semidiscrete scheme (5.20) at the time level t_{n+1} i.e., $e^{n+1}(x, y) = u(x, y, t_{n+1}) - u^{n+1}(x, y)$. The following result shows that the fractional-step implicit-explicit Euler method converges uniformly with first-order accurate in time.

Theorem 5.1 (Global error). *Under the alternative boundary data of $\mathbf{s}^{n+1/2}$ and \mathbf{s}^{n+1} are given in (5.22), the global error $e^{n+1}(x, y)$ satisfies that*

$$\sup_{(n+1)\Delta t \leq T} \|e^{n+1}\|_{\mathbb{G}} \leq C\Delta t.$$

Proof. We rewrite the global error as

$$e^{n+1}(x, y) = \tilde{e}^{n+1}(x, y) + d^{n+1}(x, y), \quad (5.33)$$

where the term $d^{n+1}(x, y) = \tilde{u}^{n+1}(x, y) - u^{n+1}(x, y)$ can be deduced from the following problems:

$$\begin{cases} (\mathbf{I} + \Delta t \mathbb{L}_{1,\varepsilon}^{n+1})d^{n+1/2}(x, y) + \Delta t [b_1(x, y, t_n, u(x, y, t_n)) - b_1(x, y, t_n, u^n(x, y))] \\ = e^n(x, y), & \text{in } \mathbb{G}, \\ d^{n+1/2}(0, y) = 0, \quad d^{n+1/2}(1, y) = 0, & \text{in } [0, 1], \end{cases} \quad (5.34)$$

and

$$\begin{cases} (\mathbb{I} + \Delta t \mathbb{L}_{2,\varepsilon}^{n+1})d^{n+1}(x, y) + \Delta t \left[b_2(x, y, t_n, u(x, y, t_n)) - b_2(x, y, t_n, u^n(x, y)) \right] \\ = d^{n+1/2}(x, y), \quad \text{in } \mathbb{G}, \\ d^{n+1}(x, 0) = 0, \quad d^{n+1}(x, 1) = 0, \quad \text{in } [0, 1]. \end{cases} \quad (5.35)$$

Since, the solution $u^n(x, y)$ and $u(x, y, t_n)$ are bounded ε -uniformly, the smoothness assumption of $b_k(x, y, t, u)$ implies that there exist a constant $\mathfrak{K}_0(> 0)$ (independent of ε) such that

$$\mathfrak{K}_0 = \sup \left\{ \left| \frac{\partial b_k(x, y, t, u)}{\partial u} \right|, \quad (x, y, t) \in \bar{\mathbb{D}}, \quad |u| \leq C_0, \quad k = 1, 2 \right\},$$

where $C_0 = \max \left\{ \|u^n\|, \|u(t_n)\|, \quad \text{for } n = 0, 1, \dots, M \right\}$. Therefore, one can deduce that for $k = 1, 2$,

$$|b_k(x, y, t_n, u(x, y, t_n)) - b_k(x, y, t_n, u^n(x, y))| \leq \mathfrak{K}_0 |e^n(x, y)|, \quad (x, y) \in \bar{\mathbb{G}}. \quad (5.36)$$

Now, we apply Lemma 5.5 to the equations (5.34) and (5.35), and utilizing (5.33) and (5.36), we get

$$\|e^{n+1}\| \leq \|\tilde{e}^{n+1}\| + (1 + 2\mathfrak{K}_0\Delta t)\|e^n\|.$$

Finally, the desired result follows from the above recurrence relation and by utilizing Lemma 5.7 and the inequality $(1 + 2\mathfrak{K}_0\Delta t)^n \leq \exp(2n\Delta t\mathfrak{K}_0) \leq \exp(2T\mathfrak{K}_0)$. ■

5.3.2 The fully discrete scheme

On the domain $\bar{\mathbb{D}}$, we construct a mesh $\bar{\mathbb{D}}^{N,\Delta t} = \bar{\mathbb{G}}^N \times \Lambda^{\Delta t}$, where $\bar{\mathbb{G}}^N$ is the rectangular piecewise-uniform Shishkin mesh on the spatial domain $\bar{\mathbb{G}}$ and $\Lambda^{\Delta t}$ is the equidistant mesh on the temporal domain $[0, T]$. The detailed description is given in [Chapter 3, Section 3.4]. For a given function $\Psi_{i,j}^n = \Psi(x_i, y_j, t_n)$, defined on the mesh $\bar{\mathbb{D}}^{N,\Delta t} = \bar{\mathbb{G}}^N \times \Lambda^{\Delta t}$, we define $\Psi_{i-\frac{1}{2},j}^n = \frac{\Psi_{i,j}^n + \Psi_{i-1,j}^n}{2}$, $\Psi_{i,j-\frac{1}{2}}^n = \frac{\Psi_{i,j}^n + \Psi_{i,j-1}^n}{2}$. Let us denote $\mathbb{G}_x^N = \bar{\mathbb{G}}_x^N \cap (0, 1)$ and $\mathbb{G}_y^N = \bar{\mathbb{G}}_y^N \cap (0, 1)$. In order to constitute the fully discrete scheme for the nonlinear problem (5.1)-(5.3), we consider the framework of the new hybrid finite difference scheme given in Chapter 3

for the spatial discretization of (5.20) on the mesh $\bar{\mathbf{D}}^{N,\Delta t}$, the fully discrete scheme takes the following form:

$$\begin{aligned}
(i) \quad & U_{i,j}^0 = \mathbf{q}_0(x_i, y_j), \quad \text{for } (x_i, y_j) \in \bar{\mathbf{G}}^N, \\
(ii) \quad & \left\{ \begin{aligned} & U_{i,j}^{n+1/2} + \Delta t \mathbb{L}_{1,\varepsilon,mcd}^{n+1} U_{i,j}^{n+1/2} + \Delta t b_1(x_i, y_j, t_n, U_{i,j}^n) = U_{i,j}^n + \Delta t g_1(x_i, y_j, t_{n+1}), \\ & \quad \text{for } 1 \leq i \leq N/2, \ y_j \in \mathbf{G}_y^N \text{ and when } \varepsilon > \|v_1\| N^{-1}, \\ & U_{i-\frac{1}{2},j}^{n+1/2} + \Delta t \mathbb{L}_{1,\varepsilon,mup}^{n+1} U_{i,j}^{n+1/2} + \Delta t b_1(x_{i-\frac{1}{2}}, y_j, t_n, U_{i-\frac{1}{2},j}^n) = U_{i-\frac{1}{2},j}^n + \Delta t g_{1,i-\frac{1}{2},j}^{n+1}, \\ & \quad \text{for } 1 \leq i \leq N/2, \ y_j \in \mathbf{G}_y^N \text{ and when } \varepsilon \leq \|v_1\| N^{-1}, \\ & U_{i,j}^{n+1/2} + \Delta t \mathbb{L}_{1,\varepsilon,mcd}^{n+1} U_{i,j}^{n+1/2} + \Delta t b_1(x_i, y_j, t_n, U_{i,j}^n) = U_{i,j}^n + \Delta t g_1(x_i, y_j, t_{n+1}), \\ & \quad \text{for } N/2 < i \leq N-1, \ y_j \in \mathbf{G}_y^N \\ & U_{i,j}^{n+1/2} = \mathbf{s}^{n+1/2}(x_i, y_j), \quad i = 0, N, \quad y_j \in \bar{\mathbf{G}}_y^N, \end{aligned} \right. \quad (5.37) \\
(iii) \quad & \left\{ \begin{aligned} & U_{i,j}^{n+1} + \Delta t \mathbb{L}_{2,\varepsilon,mcd}^{n+1} U_{i,j}^{n+1} + \Delta t b_2(x_i, y_j, t_n, U_{i,j}^n) = U_{i,j}^{n+1/2} + \Delta t g_2(x_i, y_j, t_{n+1}), \\ & \quad \text{for } 1 \leq j \leq N/2, \ x_i \in \mathbf{G}_x^N \text{ and when } \varepsilon > \|v_2\| N^{-1}, \\ & U_{i,j-\frac{1}{2}}^{n+1} + \Delta t \mathbb{L}_{2,\varepsilon,mup}^{n+1} U_{i,j}^{n+1} + \Delta t b_2(x_i, y_{j-\frac{1}{2}}, t_n, U_{i,j-\frac{1}{2}}^n) = U_{i,j-\frac{1}{2}}^{n+1/2} + \Delta t g_{2,i,j-\frac{1}{2}}^{n+1}, \\ & \quad \text{for } 1 \leq j \leq N/2, \ x_i \in \mathbf{G}_x^N \text{ and when } \varepsilon \leq \|v_2\| N^{-1}, \\ & U_{i,j}^{n+1} + \Delta t \mathbb{L}_{2,\varepsilon,mcd}^{n+1} U_{i,j}^{n+1} + \Delta t b_2(x_i, y_j, t_n, U_{i,j}^n) = U_{i,j}^{n+1/2} + \Delta t g_2(x_i, y_j, t_{n+1}), \\ & \quad \text{for } N/2 < j \leq N-1, \ x_i \in \mathbf{G}_x^N \\ & U_{i,j}^{n+1} = \mathbf{s}^{n+1}(x_i, y_j), \quad j = 0, N, \quad x_i \in \bar{\mathbf{G}}_x^N, \end{aligned} \right.
\end{aligned}$$

where $\mathbf{s}^{n+1/2}, \mathbf{s}^{n+1}$ are defined in (5.22) and $\mathbb{L}_{1,N,mcd}^{n+1}, \mathbb{L}_{1,N,mup}^{n+1}, \mathbb{L}_{2,N,mcd}^{n+1}, \mathbb{L}_{2,N,mup}^{n+1}$ are given by

$$\left\{ \begin{aligned} & \mathbb{L}_{1,N,mcd}^{n+1} U_{i,j}^{n+1/2} = -\varepsilon \delta_x^2 U_{i,j}^{n+1/2} + v_1^{n+1}(x_i, y_j, t_{n+1}) D_x^* U_{i,j}^{n+1/2}, \\ & \mathbb{L}_{1,N,mup}^{n+1} U_{i,j}^{n+1/2} = -\varepsilon \delta_x^2 U_{i,j}^{n+1/2} + v_{1,i-\frac{1}{2},j}^{n+1} D_x^- U_{i,j}^{n+1/2}, \\ & \mathbb{L}_{2,N,mcd}^{n+1} U_{i,j}^{n+1} = -\varepsilon \delta_y^2 U_{i,j}^{n+1} + v_2^{n+1}(x_i, y_j, t_{n+1}) D_y^* U_{i,j}^{n+1}, \\ & \mathbb{L}_{2,N,mup}^{n+1} U_{i,j}^{n+1} = -\varepsilon \delta_y^2 U_{i,j}^{n+1} + v_{2,i,j-\frac{1}{2}}^{n+1} D_y^- U_{i,j}^{n+1}. \end{aligned} \right. \quad (5.38)$$

Let $\rho_{x_i} = \left(\varepsilon - \frac{v_1 h_{x_i}}{2}\right)$ and $\rho_{y_j} = \left(\varepsilon - \frac{v_2 h_{y_j}}{2}\right)$. After rearranging the term in (5.37), the fully discrete scheme is written as follows:

$$\left\{ \begin{array}{l} U_{i,j}^0 = \mathbf{q}_0(x_i, y_j), \quad \text{for } (x_i, y_j) \in \bar{\mathbf{G}}^N, \\ \left\{ \begin{array}{l} \mathbb{L}_{1,\varepsilon}^{N,\Delta t} U_{i,j}^{n+1/2} \equiv \mu_{x_i}^- U_{i-1,j}^{n+1/2} + \mu_{x_i}^c U_{i,j}^{n+1/2} + \mu_{x_i}^+ U_{i+1,j}^{n+1/2} = \mathbb{F}_1^{\Delta t}(x_i, y_j), \\ \text{for } 1 \leq i \leq N-1, \quad y_j \in \mathbf{G}_y^N, \\ U_{i,j}^{n+1/2} = \mathbf{s}^{n+1/2}(x_i, y_j), \quad i = 0, N, \quad y_j \in \bar{\mathbf{G}}_y^N, \\ \mathbb{L}_{2,\varepsilon}^{N,\Delta t} U_{i,j}^{n+1} \equiv \mu_{y_j}^- U_{i,j-1}^{n+1} + \mu_{y_j}^c U_{i,j}^{n+1} + \mu_{y_j}^+ U_{i,j+1}^{n+1} = \mathbb{F}_2^{\Delta t}(x_i, y_j), \\ \text{for } 1 \leq j \leq N-1, \quad x_i \in \mathbf{G}_x^N \\ U_{i,j}^{n+1} = \mathbf{s}^{n+1}(x_i, y_j), \quad j = 0, N, \quad x_i \in \bar{\mathbf{G}}_x^N, \\ \text{for } n = 0, \dots, M-1, \end{array} \right. \end{array} \right. \quad (5.39)$$

where the right hand side vector $\mathbb{F}_1^{\Delta t}(x_i, y_j), \mathbb{F}_2^{\Delta t}(x_i, y_j)$ in (5.39) are given by

$$\mathbb{F}_1^{\Delta t}(x_i, y_j) = \left\{ \begin{array}{l} \frac{1}{2}(U_{i-1,j}^n + \Delta t g_1(x_{i-1}, y_j, t_{n+1})) + \frac{1}{2}(U_{i,j}^n + \Delta t g_1(x_i, y_j, t_{n+1})) - \\ \Delta t b_1(x_{i-\frac{1}{2}}, y_j, t_n, U_{i-\frac{1}{2},j}^n), \quad \text{for } 1 \leq i \leq N/2, \text{ and when } \varepsilon \leq \|v_1\|N^{-1}, \quad y_j \in \mathbf{G}_y^N, \\ U_{i,j}^n + \Delta t g_1(x_i, y_j, t_{n+1}) - \Delta t b_1(x_i, y_j, t_n, U_{i,j}^n), \\ \text{for } 1 \leq i \leq N/2, \text{ and when } \varepsilon > \|v_1\|N^{-1}, \quad y_j \in \mathbf{G}_y^N, \\ U_{i,j}^n + \Delta t g_1(x_i, y_j, t_{n+1}) - \Delta t b_1(x_i, y_j, t_n, U_{i,j}^n), \quad \text{for } N/2 < i \leq N-1, \quad y_j \in \mathbf{G}_y^N, \end{array} \right. \quad (5.40)$$

and

$$\mathbb{F}_2^{\Delta t}(x_i, y_j) = \left\{ \begin{array}{l} \frac{1}{2}(U_{i,j-1}^{n+1/2} + \Delta t g_2(x_i, y_{j-1}, t_{n+1})) + \frac{1}{2}(U_{i,j}^{n+1/2} + \Delta t g_2(x_i, y_j, t_{n+1})) - \\ \Delta t b_2(x_i, y_{j-\frac{1}{2}}, t_n, U_{i,j-\frac{1}{2}}^n), \quad \text{for } 1 \leq j \leq N/2, \text{ and when } \varepsilon \leq \|v_2\|N^{-1}, \quad x_i \in \mathbf{G}_x^N, \\ U_{i,j}^{n+1/2} + \Delta t g_2(x_i, y_j, t_{n+1}) - \Delta t b_2(x_i, y_j, t_n, U_{i,j}^n), \\ \text{for } 1 \leq j \leq N/2, \text{ and when } \varepsilon > \|v_2\|N^{-1}, \quad x_i \in \mathbf{G}_x^N, \\ U_{i,j}^{n+1/2} + \Delta t g_2(x_i, y_j, t_{n+1}) - \Delta t b_2(x_i, y_j, t_n, U_{i,j}^n), \quad \text{for } N/2 < j \leq N-1, \quad x_i \in \mathbf{G}_x^N. \end{array} \right. \quad (5.41)$$

Here, the coefficients $\mu_{z_k}^-, \mu_{z_k}^c, \mu_{z_k}^+$ for $z_k = x_k/y_k$, $k = i$ or j and $l = 1, 2$ are given by

$$\left\{ \begin{array}{l} \mu_{z_k}^- = \Delta t \mu_{mcd, z_k}^-, \quad \mu_{z_k}^c = \Delta t \mu_{mcd, z_k}^c + 1, \quad \mu_{z_k}^+ = \Delta t \mu_{mcd, z_k}^+, \\ \text{for } 1 \leq k \leq N/2, \text{ and when } \varepsilon > \|v_l\| N^{-1}, \\ \mu_{z_k}^- = \Delta t \mu_{mup, z_k}^- + \frac{1}{2}, \quad \mu_{z_k}^c = \Delta t \mu_{mup, z_k}^c + \frac{1}{2}, \quad \mu_{z_k}^+ = \Delta t \mu_{mup, z_k}^+, \\ \text{for } 1 \leq k \leq N/2, \text{ and when } \varepsilon \leq \|v_l\| N^{-1}, \\ \mu_{z_k}^- = \Delta t \mu_{mcd, z_k}^-, \quad \mu_{z_k}^c = \Delta t \mu_{mcd, z_k}^c + 1, \quad \mu_{z_k}^+ = \Delta t \mu_{mcd, z_k}^+, \\ \text{for } N/2 < k \leq N-1, \end{array} \right. \quad (5.42)$$

where

$$\left\{ \begin{array}{l} \mu_{mup, z_k}^- = -\frac{2\varepsilon}{\tilde{h}_{z_k} h_{z_k}} - \frac{v_{1, i-\frac{1}{2}, j}^{n+1}}{h_{z_k}}, \\ \mu_{mup, z_k}^c = \frac{2\varepsilon}{h_{z_k} h_{z_{k+1}}} + \frac{v_{1, i-\frac{1}{2}, j}^{n+1}}{h_{z_k}}, \\ \mu_{mup, z_k}^+ = -\frac{2\varepsilon}{\tilde{h}_{z_k} h_{z_{k+1}}}, \end{array} \right. \text{ and } \left\{ \begin{array}{l} \mu_{mcd, z_k}^- = -\frac{2\rho_{z_k}}{\tilde{h}_{z_k} h_{z_k}} - \frac{v_{1, i, j}^{n+1}}{h_{z_k}}, \\ \mu_{mcd, z_k}^c = \frac{2\rho_{z_k}}{h_{z_k} h_{z_{k+1}}} + \frac{v_{1, i, j}^{n+1}}{h_{z_k}}, \\ \mu_{mcd, z_k}^+ = -\frac{2\rho_{z_k}}{\tilde{h}_{z_k} h_{z_{k+1}}}, \end{array} \right.$$

It is shown that the difference operators $\mathbb{L}_{1, \varepsilon}^{N, \Delta t}, \mathbb{L}_{2, \varepsilon}^{N, \Delta t}$ defined in (5.39) satisfies the following discrete maximum principle.

Lemma 5.8 (Discrete maximum principle). *Suppose that the following conditions hold for $N \geq N_0$:*

$$\frac{N}{\ln N} > \eta_{k,0} \|v_k\| \text{ and } \mathfrak{m}_k N \geq \frac{1}{\Delta t}, \quad k = 1, 2, \quad (5.43)$$

where N_0 is a positive integer. If any mesh function $Z_{i,j} = Z(x_i, y_j)$ defined on $\bar{\mathbb{G}}^N$ satisfies that $Z_{i,j} \leq 0$, on $\partial \mathbb{G}^N$ and $\mathbb{L}_{k, \varepsilon}^{N, \Delta t} Z_{i,j} \leq 0$, $k = 1, 2$, for $(x_i, y_j) \in \mathbb{G}^N$, then it implies that $Z_{i,j} \leq 0$, for all i, j .

Proof. See [Chapter 3, Lemma 3.5] for the proof. ■

5.3.2.1 Error analysis

In the beginning, we study the asymptotic behavior of the analytical solution of the semidiscrete problem (5.25) and its derivatives. This will be used later to derive the bounds of the truncation errors $\mathcal{T}_{x_i, \tilde{u}^{n+1/2}}^{N, \Delta t}$ and $\mathcal{T}_{y_j, \tilde{u}^{n+1}}^{N, \Delta t}$. From Lemma 5.5, it is clear that $\|\tilde{u}^{n+1/2}\| \leq C$ and $\|\tilde{u}^{n+1}\| \leq C$, since $u(x, y, t_n)$, b_1 , b_2 , g_1, g_2 , $\mathfrak{s}^{n+1/2}$ and \mathfrak{s}^{n+1} are ε -uniformly bounded. At first, we deduce a priori bounds for $\tilde{u}^{n+1/2}(x, y)$ and its derivatives in the x -direction and also for $\tilde{u}^{n+1}(x, y)$ and its derivatives in the y -direction. For the proof of Lemma 5.9, apart from the requirement of ε -uniform boundedness and smoothness criterion on the given data, we also need certain compatibility conditions at $(0, t_n)$ and $(1, t_n)$ as mentioned in (5.53). Note that the corresponding derivation take care of the presence of the non-homogeneous boundary data $\mathfrak{s}^{n+1/2}, \mathfrak{s}^{n+1}$.

Lemma 5.9. *The solutions $\tilde{u}^{n+1/2}(x, y)$ and $\tilde{u}^{n+1}(x, y)$ of the time semidiscrete scheme (5.25) and their deriva-*

tives satisfy that

$$\left| \frac{\partial^j \tilde{u}^{n+1/2}(x, y)}{\partial x^j} \right| \leq C(1 + \varepsilon^{-j} \exp(-\mathfrak{m}_1(1-x)/\varepsilon)), \quad j = 0, 1, 2, 3, 4, \quad (5.44)$$

and

$$\left| \frac{\partial^j \tilde{u}^{n+1}(x, y)}{\partial y^j} \right| \leq C(1 + \varepsilon^{-j} \exp(-\mathfrak{m}_2(1-y)/\varepsilon)), \quad j = 0, 1, 2, 3, 4, \quad (5.45)$$

for all $(x, y) \in \bar{\mathcal{G}}$.

Proof. We split up the proof into two parts. In the first part, we derive the result (5.44) for $\tilde{u}^{n+1/2}(x, y)$ and the second part, the result (5.45) is established for $\tilde{u}^{n+1}(x, y)$.

Part-I: Consider the auxiliary BVP:

$$(\mathbf{I} + \Delta t \mathbb{L}_{1,\varepsilon}^{n+1}) \zeta(x, y) = -\mathbb{L}_{1,\varepsilon}^{n+1} u(x, y, t_n) - b_1(x, y, t_n, u(x, y, t_n)) + g_1(x, y, t_{n+1}) \equiv \mathcal{H}_1(x, y), \quad (5.46)$$

where

$$\zeta(x, y) = \frac{\tilde{u}^{n+1/2}(x, y) - u(x, y, t_n)}{\Delta t},$$

with boundary conditions:

$$\begin{aligned} \zeta(0, y) &= \frac{\tilde{u}^{n+1/2}(0, y) - u(0, y, t_n)}{\Delta t}, \\ &= \frac{(\mathbf{I} + \Delta t \mathbb{L}_{2,\varepsilon}^{n+1}) \mathbf{s}(0, y, t_{n+1}) + \Delta t b_2(x, y, t_n, \mathbf{s}(0, y, t_n)) - \Delta t g_2(0, y, t_{n+1}) - \mathbf{s}(0, y, t_n)}{\Delta t}, \\ &= \mathbb{L}_{2,\varepsilon}^{n+1} \mathbf{s}(0, y, t_{n+1}) + b_2(0, y, t_n, \mathbf{s}(0, y, t_n)) - g_2(0, y, t_{n+1}) + \frac{\partial \mathbf{s}(0, y, t_n)}{\partial t} + O(\Delta t), \end{aligned} \quad (5.47)$$

$$\zeta(1, y) = \mathbb{L}_{2,\varepsilon}^{n+1} \mathbf{s}(1, y, t_{n+1}) + b_2(1, y, t_n, \mathbf{s}(1, y, t_n)) - g_2(1, y, t_{n+1}) + \frac{\partial \mathbf{s}(1, y, t_n)}{\partial t} + O(\Delta t). \quad (5.48)$$

Therefore, the boundary value problem (5.46)-(5.48) reduces to the following form:

$$\begin{cases} (\mathbf{I} + \Delta t \mathbb{L}_{1,\varepsilon}^{n+1}) \zeta(x, y) = \mathcal{H}_1(x, y), \\ \zeta(0, y) = \mathbb{L}_{2,\varepsilon}^{n+1} \mathbf{s}(0, y, t_{n+1}) + b_2(0, y, t_n, \mathbf{s}(0, y, t_n)) - g_2(0, y, t_{n+1}) + \frac{\partial \mathbf{s}(0, y, t_n)}{\partial t} + O(\Delta t), \\ \zeta(1, y) = \mathbb{L}_{2,\varepsilon}^{n+1} \mathbf{s}(1, y, t_{n+1}) + b_2(1, y, t_n, \mathbf{s}(0, y, t_n)) - g_2(1, y, t_{n+1}) + \frac{\partial \mathbf{s}(1, y, t_n)}{\partial t} + O(\Delta t). \end{cases} \quad (5.49)$$

We see boundary conditions of problem (5.49) are $(\varepsilon, \Delta t)$ -uniformly bounded. Let $|\mathbb{L}_{1,\varepsilon}^{n+1} u(x, y, t_n)| \leq C$, then $|\mathcal{H}_1(x, y)| \leq C$. Hence, applying Lemma 5.5, we obtain that $|\zeta(x, y)| \leq C$. Next, we have the BVP:

$$\begin{cases} \mathbb{L}_{1,\varepsilon}^{n+1} \tilde{u}^{n+1/2}(x, y) = -\zeta(x, y) - b_1(x, y, t_n, u(x, y, t_n)) + g_1(x, y, t_{n+1}), \\ \tilde{u}^{n+1/2}(0, y) = (\mathbf{I} + \Delta t \mathbb{L}_{2,\varepsilon}^{n+1}) \mathbf{s}(0, y, t_{n+1}) + b_2(0, y, t_n, \mathbf{s}(0, y, t_n)) - \Delta t g_2(0, y, t_{n+1}), \\ \tilde{u}^{n+1/2}(1, y) = (\mathbf{I} + \Delta t \mathbb{L}_{2,\varepsilon}^{n+1}) \mathbf{s}(1, y, t_{n+1}) + b_2(1, y, t_n, \mathbf{s}(0, y, t_n)) - \Delta t g_2(1, y, t_{n+1}). \end{cases} \quad (5.50)$$

Using the argument of Kellogg and Tsan technique [61], one can obtain that

$$\left| \frac{\partial \tilde{u}^{n+1/2}(x, y)}{\partial x} \right| \leq C \left[1 + \varepsilon^{-1} \exp(-\mathfrak{m}_1(1-x)/\varepsilon) \right], \quad (x, y) \in \bar{\mathbf{G}}. \quad (5.51)$$

Let $\zeta_1(x, y) = \mathbb{L}_{1,\varepsilon}^{n+1} \zeta(x, y)$, which satisfies that

$$\begin{cases} (\mathbf{I} + \Delta t \mathbb{L}_{1,\varepsilon}^{n+1}) \zeta_1(x, y) = \\ -(\mathbb{L}_{1,\varepsilon}^{n+1})^2 u(x, y, t_n) - \mathbb{L}_{1,\varepsilon}^{n+1} b_1(x, y, t_n, u(x, y, t_n)) + \mathbb{L}_{1,\varepsilon}^{n+1} g_1(x, y, t_{n+1}) \equiv \mathcal{H}_2(x, y), \\ \zeta_1(0, y) = \frac{1}{\Delta t} \left[-\zeta(0, y) + g_1(0, y, t_{n+1}) - b_1(0, y, t_n, \mathbf{s}(0, y, t_n)) - \mathbb{L}_{1,\varepsilon}^{n+1} \mathbf{s}(0, y, t_n) \right], \\ \zeta_1(1, y) = \frac{1}{\Delta t} \left[-\zeta(1, y) + g_1(1, y, t_{n+1}) - b_1(1, y, t_n, \mathbf{s}(1, y, t_n)) - \mathbb{L}_{1,\varepsilon}^{n+1} \mathbf{s}(1, y, t_n) \right]. \end{cases} \quad (5.52)$$

Let $|(\mathbb{L}_{1,\varepsilon}^{n+1})^2 u(x, y, t_n)| \leq C$, then $|\mathcal{H}_2(x, y)| \leq C$, by invoking smoothness property (5.8). Now, from the compatibility conditions (5.4), one can obtain that

$$\begin{aligned} \frac{\partial \mathbf{s}(0, y, t_n)}{\partial t} &= -\mathbb{L}_{\varepsilon}^n \mathbf{s}(0, y, t_n) - b(x, y, t_n, u(0, y, t_n)) + g(0, y, t_n), \\ \frac{\partial \mathbf{s}(1, y, t_n)}{\partial t} &= -\mathbb{L}_{\varepsilon}^n \mathbf{s}(1, y, t_n) - b(x, y, t_n, u(0, y, t_n)) + g(1, y, t_n). \end{aligned} \quad (5.53)$$

Now, by using the boundary conditions of the problem (5.49), the equation (5.52) and (5.53), we get

$$\begin{cases} (\mathbf{I} + \Delta t \mathbb{L}_{1,\varepsilon}^{n+1}) \zeta_1(x, y) = \mathcal{H}_2(x, y), \\ \zeta_1(0, y) = \frac{\partial g(0, y, t_n)}{\partial t} - \mathbb{L}_{2,\varepsilon}^{n+1} \frac{\partial \mathbf{s}(0, y, t_n)}{\partial t} + C_1, \\ \zeta_1(1, y) = \frac{\partial g(1, y, t_n)}{\partial t} - \mathbb{L}_{2,\varepsilon}^{n+1} \frac{\partial \mathbf{s}(1, y, t_n)}{\partial t} + C_2. \end{cases} \quad (5.54)$$

We see that $\mathcal{H}_2(x, y) = -(\mathbb{L}_{1,\varepsilon}^{n+1})^2 u(x, y, t_n) - \mathbb{L}_{1,\varepsilon}^{n+1} b_1(x, y, t_n, u(x, y, t_n)) + \mathbb{L}_{1,\varepsilon}^{n+1} g_1(x, y, t_{n+1})$ is bounded (ε -uniformly) by invoking smoothness property (5.8) and boundary conditions are $(\varepsilon, \Delta t)$ -uniformly bounded. Hence, applying Lemma 5.5, we obtain that $|\zeta_1(x, y)| \leq C$. Afterwards, one can deduce that

$$\left| \frac{\partial \zeta(x, y)}{\partial x} \right| \leq C \left[1 + \varepsilon^{-1} \exp(-\mathfrak{m}_1(1-x)/\varepsilon) \right], \quad (x, y) \in \bar{\mathbf{G}}, \quad (5.55)$$

by invoking Kellogg and Tsan technique [61] to the following BVP:

$$\begin{cases} \mathbb{L}_{1,\varepsilon}^{n+1} \zeta(x, y) = \zeta_1(x, y), \\ \zeta(0, y) = \mathbb{L}_{2,\varepsilon}^{n+1} \mathbf{s}(0, y, t_{n+1}) - g_2(0, y, t_{n+1}) + \frac{d\mathbf{s}(0, y, t_n)}{dt} + O(\Delta t), \\ \zeta(1, y) = \mathbb{L}_{2,\varepsilon}^{n+1} \mathbf{s}(1, y, t_{n+1}) - g_2(1, y, t_{n+1}) + \frac{d\mathbf{s}(1, y, t_n)}{dt} + O(\Delta t). \end{cases} \quad (5.56)$$

Now, differentiate (5.50) with respect to x , we consider that $\bar{\zeta}(x, y) = \frac{\partial \tilde{u}^{n+1/2}}{\partial x}$ satisfies the following problem

$$\begin{cases} \mathbb{L}_{1,\varepsilon}^{n+1} \bar{\zeta}(x, y) = \mathcal{H}_3(x, y), & (x, y) \in \mathbb{G}, \\ \bar{\zeta}(0, y) = C_1, \quad \bar{\zeta}(1, y) = C_2 \varepsilon^{-1}, \end{cases} \quad (5.57)$$

where $\mathcal{H}_3(x, y) = -\frac{\partial \zeta(x, y)}{\partial x} + \frac{\partial g_1(x, y, t_{n+1})}{\partial x} - \frac{\partial v_1(x, y, t_{n+1})}{\partial x} \frac{\partial \tilde{u}^{n+1/2}}{\partial x} - \left(\frac{\partial b_1(x, y, t_n, u(x, y, t_n))}{\partial x} + \frac{\partial b_1(x, y, t_n, u(x, y, t_n))}{\partial u} \frac{\partial u}{\partial x} \right)$ and we obtain that

$$|\mathcal{H}_3(x, y)| \leq C \left[1 + \varepsilon^{-1} \exp(-\mathfrak{m}_1(1-x)/\varepsilon) \right], \quad (x, y) \in \bar{\mathbb{G}}.$$

Again, using the argument of Kellogg and Tsan technique [61] for (5.57), we get

$$\left| \frac{\partial \bar{\zeta}(x, y)}{\partial x} \right| = \left| \frac{\partial^2 \tilde{u}^{n+1/2}(x, y)}{\partial x^2} \right| \leq C \left[1 + \varepsilon^{-2} \exp(-\mathfrak{m}_1(1-x)/\varepsilon) \right], \quad (x, y) \in \bar{\mathbb{G}}.$$

Similar way, we obtained the bound (5.44) for $j = 3, 4$. We now derive the bound of $\tilde{u}^{n+1/2}(x, y)$ with respect to y by differentiating the auxiliary BVP (5.25) at the first half with respect to y , and we get

$$\begin{cases} (\mathbb{I} + \Delta t \mathbb{L}_{1,\varepsilon}^{n+1}) \frac{\partial \tilde{u}^{n+1/2}(x, y)}{\partial y} = \frac{\partial u(x, y, t_n)}{\partial y} + \Delta t \frac{\partial g_1(x, y, t_{n+1})}{\partial y} - \frac{\partial v_1(x, y, t_{n+1})}{\partial y} \frac{\partial \tilde{u}^{n+1/2}(x, y)}{\partial x} - \\ \left(\frac{\partial b_1(x, y, t_n, u(x, y, t_n))}{\partial y} + \frac{\partial b_1(x, y, t_n, u(x, y, t_n))}{\partial u} \frac{\partial u}{\partial y} \right), \\ \frac{\partial \tilde{u}^{n+1/2}(0, y)}{\partial y} = (\mathbb{I} + \Delta t \mathbb{L}_2^{n+1}) \frac{\partial \mathfrak{s}(0, y, t_{n+1})}{\partial y} + \Delta t \frac{\partial v_2(0, y, t_{n+1})}{\partial y} \frac{\partial \mathfrak{s}(0, y, t_{n+1})}{\partial y} + \\ \Delta t \left(\frac{b_2(0, y, t_n, \mathfrak{s}(0, y, t_n))}{\partial y} + \frac{b_2(0, y, t_n, \mathfrak{s}(0, y, t_n))}{\partial u} \frac{\partial \mathfrak{s}(0, y, t_n)}{\partial y} \right) - \Delta t \frac{\partial g_2(0, y, t_{n+1})}{\partial y}, \\ \frac{\partial \tilde{u}^{n+1/2}(1, y)}{\partial y} = (\mathbb{I} + \Delta t \mathbb{L}_2^{n+1}) \frac{\partial \mathfrak{s}(1, y, t_{n+1})}{\partial y} + \Delta t \frac{\partial v_2(1, y, t_{n+1})}{\partial y} \frac{\partial \mathfrak{s}(1, y, t_{n+1})}{\partial y} + \\ \Delta t \left(\frac{b_2(1, y, t_n, \mathfrak{s}(1, y, t_n))}{\partial y} + \frac{b_2(1, y, t_n, \mathfrak{s}(1, y, t_n))}{\partial u} \frac{\partial \mathfrak{s}(1, y, t_n)}{\partial y} \right) - \Delta t \frac{\partial g_2(1, y, t_{n+1})}{\partial y}. \end{cases} \quad (5.58)$$

The following bounds are proven by using the bounds of $\frac{\partial^j \tilde{u}^{n+1/2}(x, y)}{\partial x^j}$ for $j = 0, 1, 2, 3, 4$:

$$\left| \frac{\partial^j \tilde{u}^{n+1/2}}{\partial y^j}(x, y) \right| \leq C \left[1 + \varepsilon^{-j} \exp(-\mathfrak{m}_2(1-y)/\varepsilon) \right], \quad (x, y) \in \bar{\mathbb{G}}, \text{ for } j = 0, 1, 2, 3, 4. \quad (5.59)$$

Part-II: Here, we prove bounds (5.45) for $\tilde{u}^{n+1}(x, y)$. We suppose that, based on prior technical criterion,

$$\|\mathbb{L}_{2,\varepsilon}^{n+1} \tilde{u}^{n+1/2}(x, y)\|_{\bar{\mathbb{G}}} \leq C, \quad \|(\mathbb{L}_{2,\varepsilon}^{n+1})^2 \tilde{u}^{n+1/2}(x, y)\|_{\bar{\mathbb{G}}} \leq C, \quad \|(\mathbb{L}_{2,\varepsilon}^{n+1})^3 \tilde{u}^{n+1/2}(x, y)\|_{\bar{\mathbb{G}}} \leq C.$$

Define the following auxiliary BVP:

$$\begin{cases} (\mathbb{I} + \Delta t \mathbb{L}_{2,\varepsilon}^{n+1})\Lambda(x, y) + b_2(x, y, t_n, u(x, y, t_n)) = -\mathbb{L}_{2,\varepsilon}^{n+1}\tilde{u}^{n+1/2}(x, y) + \mathcal{G}_2(x, y, t_{n+1}) \equiv \mathcal{F}_1(x, y), \\ \Lambda(x, 0) = -\mathbb{L}_{2,\varepsilon}^{n+1}\mathbf{s}(x, 0, t_{n+1}) - b_2(x, 0, t_n, \mathbf{s}(x, 0, t_n)) + \mathcal{G}_2(x, 0, t_{n+1}), \\ \Lambda(x, 1) = -\mathbb{L}_{2,\varepsilon}^{n+1}\mathbf{s}(x, 1, t_{n+1}) - b_2(x, 1, t_n, \mathbf{s}(x, 1, t_n)) + \mathcal{G}_2(x, 1, t_{n+1}). \end{cases} \quad (5.60)$$

where $\Lambda(x, y) = \frac{\tilde{u}^{n+1}(x, y) - \tilde{u}^{n+1/2}(x, y)}{\Delta t}$. We see that boundary conditions are $(\varepsilon, \Delta t)$ -uniformly bounded and $|\mathcal{F}_1(x, y)| \leq C$. Hence, applying Lemma 5.5, we obtain that $|\Lambda(x, y)| \leq C$. we have

$$\begin{cases} \mathbb{L}_{2,\varepsilon}^{n+1}\tilde{u}^{n+1}(x, y) = -\Lambda(x, y) - b_2(x, y, t_n, u(x, y, t_n)) + \mathcal{G}_2(x, y, t_{n+1}), \\ \tilde{u}^{n+1}(x, 0) = \mathbf{s}(x, 0, t_{n+1}), \quad \tilde{u}^{n+1}(x, 1) = \mathbf{s}(x, 1, t_{n+1}). \end{cases} \quad (5.61)$$

Using the argument of Kellogg and Tsan technique [61], one can obtain that

$$\left| \frac{\partial \tilde{u}^{n+1}(x, y)}{\partial y} \right| \leq C \left[1 + \varepsilon^{-1} \exp(-\mathfrak{m}_2(1-y)/\varepsilon) \right] \quad (x, y) \in \bar{\mathbf{G}}. \quad (5.62)$$

We introduce the function $\Lambda_1(x, y) = \mathbb{L}_{2,\varepsilon}^{n+1}\Lambda(x, y)$, which is a solution of

$$\begin{cases} (\mathbb{I} + \Delta t \mathbb{L}_{2,\varepsilon}^{n+1})\Lambda_1(x, y) = -(\mathbb{L}_{2,\varepsilon}^{n+1})^2\tilde{u}^{n+1/2}(x, y) - \\ \quad \mathbb{L}_{2,\varepsilon}^{n+1}b_2(x, y, t_n, u(x, y, t_n)) + \mathbb{L}_{2,\varepsilon}^{n+1}\mathcal{G}_2(x, y, t_{n+1}) \equiv \mathcal{F}_2(x, y), \\ \Lambda_1(x, 0) = -\mathbb{L}_{2,\varepsilon}^{n+1}\mathbb{L}_{2,\varepsilon}^{n+1}\mathbf{s}(x, 0, t_{n+1}) - \mathbb{L}_{2,\varepsilon}^{n+1}b_2(x, 0, t_n, \mathbf{s}(x, 0, t_n)) + \mathbb{L}_{2,\varepsilon}^{n+1}\mathcal{G}_2(x, 0, t_{n+1}), \\ \Lambda_1(x, 1) = -\mathbb{L}_{2,\varepsilon}^{n+1}\mathbb{L}_{2,\varepsilon}^{n+1}\mathbf{s}(x, 1, t_{n+1}) - \mathbb{L}_{2,\varepsilon}^{n+1}b_2(x, 1, t_n, \mathbf{s}(x, 1, t_n)) + \mathbb{L}_{2,\varepsilon}^{n+1}\mathcal{G}_2(x, 1, t_{n+1}). \end{cases} \quad (5.63)$$

We see that $\mathcal{F}_2(x, y) = -(\mathbb{L}_{2,\varepsilon}^{n+1})^2\tilde{u}^{n+1/2}(x, y) - \mathbb{L}_{2,\varepsilon}^{n+1}b_2(x, y, t_n, u(x, y, t_n)) + \mathbb{L}_{2,\varepsilon}^{n+1}\mathcal{G}_2(x, y, t_{n+1})$ is bounded (ε -uniformly) and boundary conditions are $(\varepsilon, \Delta t)$ -uniformly bounded. Hence, applying Lemma 5.5, we obtain that $|\Lambda_1(x, y)| \leq C$. Afterwards, one can deduce that

$$\left| \frac{\partial \Lambda(x, y)}{\partial y} \right| \leq C \left[1 + \varepsilon^{-1} \exp(-\mathfrak{m}_2(1-y)/\varepsilon) \right], \quad (x, y) \in \bar{\mathbf{G}}, \quad (5.64)$$

by invoking Kellogg and Tsan technique [61] to the following BVPs:

$$\begin{cases} \mathbb{L}_{2,\varepsilon}^{n+1}\Lambda(x, y) = \Lambda_1(x, y), \\ \Lambda(x, 0) = -\mathbb{L}_{2,\varepsilon}^{n+1}\mathbf{s}(x, 0, t_{n+1}) - b_2(x, 0, t_n, \mathbf{s}(x, 0, t_n)) + \mathcal{G}_2(x, 0, t_{n+1}), \\ \Lambda(x, 1) = -\mathbb{L}_{2,\varepsilon}^{n+1}\mathbf{s}(x, 1, t_{n+1}) - b_2(x, 1, t_n, \mathbf{s}(x, 1, t_n)) + \mathcal{G}_2(x, 1, t_{n+1}). \end{cases} \quad (5.65)$$

For second order derivative bound of $\tilde{u}^{n+1}(x, y)$, we differentiate (5.61) with respect y , to get

$$\begin{cases} \mathbb{L}_{2,\varepsilon}^{n+1}\bar{\Lambda}(x, y) = \mathcal{F}_3(x, y), \\ \bar{\Lambda}(x, 0) = C_1, \quad \bar{\Lambda}(x, 1) = C_2\varepsilon^{-1}, \end{cases} \quad (5.66)$$

where

$$\mathcal{F}_3(x, y) = -\frac{\partial \Lambda(x, y)}{\partial y} + \frac{\partial g_2(x, y, t_{n+1})}{\partial y} - \frac{\partial v_2(x, y, t_{n+1})}{\partial y} \frac{\partial \tilde{u}^{n+1}(x, y)}{\partial y} - \left(\frac{\partial b_2(x, y, t_n, u(x, y, t_n))}{\partial y} + \frac{\partial b_2(x, y, t_n, u(x, y, t_n))}{\partial u} \frac{\partial u}{\partial y} \right),$$

and $\bar{\Lambda}(x, y) = \frac{\partial \tilde{u}^{n+1}(x, y)}{\partial y}$. We obtain that $|\mathcal{F}_3(x, y)| \leq C[1 + \varepsilon^{-1} \exp(-\mathfrak{m}_2(1 - y)/\varepsilon)]$, $(x, y) \in \bar{\mathbb{G}}$. Applying the methodology of Kellogg and Tsan to (5.66), we deduce that

$$\left| \frac{\partial \bar{\Lambda}(x, y)}{\partial y} \right| = \left| \frac{\partial^2 \tilde{u}^{n+1}(x, y)}{\partial y^2} \right| \leq C \left[1 + \varepsilon^{-2} \exp(-\mathfrak{m}_2(1 - y)/\varepsilon) \right], \quad (x, y) \in \bar{\mathbb{G}}. \quad (5.67)$$

Similar way, we obtained the bound (5.45) for $j = 3, 4$. ■

Lemma 5.10. *The exact solutions $\tilde{u}^{n+1/2}(x, y)$ and $\tilde{u}^{n+1}(x, y)$ of time semidiscrete scheme (5.25) can be decomposed as*

$$\begin{cases} \tilde{u}^{n+1/2}(x, y) = \tilde{p}^{n+1/2}(x, y) + \gamma_1 \tilde{q}^{n+1/2}(x, y), \\ \tilde{u}^{n+1}(x, y) = \tilde{p}^{n+1}(x, y) + \gamma_2 \tilde{q}^{n+1}(x, y), \end{cases}$$

where $y \in (0, 1)$ the components of $\tilde{u}^{n+1/2}(x, y)$ satisfy

$$\begin{cases} \tilde{q}^{n+1}(x, y) = \exp(-v_1(1, y, t_{n+1})(1 - x)/\varepsilon), \quad \gamma_1 = \frac{\varepsilon}{v_1(1, y, t_{n+1})} \frac{\partial \tilde{u}^{n+1}}{\partial x}(1, y), \\ \left| \frac{\partial^j \tilde{p}^{n+1/2}}{\partial x^j} \right| \leq C \left(1 + \varepsilon^{-j+1} \exp \left(-\frac{\mathfrak{m}_1(1 - x)}{\varepsilon} \right) \right), \quad j = 0, 1, 2, 3, 4, \end{cases}$$

and for $x \in (0, 1)$ the components of $\tilde{u}^{n+1}(x, y)$ satisfy

$$\begin{cases} \tilde{q}^{n+1}(x, y) = \exp(-v_2(x, 1, t_{n+1})(1 - y)/\varepsilon), \quad \gamma_2 = \frac{\varepsilon}{v_2(x, 1, t_{n+1})} \frac{\partial \tilde{u}^{n+1}}{\partial y}(x, 1), \\ \left| \frac{\partial^j \tilde{p}^{n+1}}{\partial y^j} \right| \leq C \left(1 + \varepsilon^{-j+1} \exp \left(-\frac{\mathfrak{m}_2(1 - y)}{\varepsilon} \right) \right), \quad j = 0, 1, 2, 3, 4. \end{cases}$$

Proof. Let $\tilde{p}^{n+1/2}(x, y) = \tilde{u}^{n+1/2}(x, y) - \gamma_1 \tilde{q}^{n+1/2}(x, y)$. Then, we have

$$\mathbb{L}_{1,\varepsilon}^{n+1} \tilde{p}^{n+1/2}(x, y) = \mathcal{R}_1(x, y), \quad \text{in } \mathbb{G}, \quad (5.68)$$

where $\mathcal{R}_1(x, y) = -\zeta(x, y) - b_1(x, y, t_n, u(x, y, t_n)) + g_1(x, y, t_{n+1}) + \gamma_1(v_1(1, y, t_{n+1}) - v_1(x, y, t_{n+1})) \frac{\partial \tilde{q}^{n+1/2}(x, y)}{\partial x}$; and differentiating (5.68) with respect to x , it yields that

$$\mathbb{L}_{1,\varepsilon}^{n+1} \frac{\partial \tilde{p}^{n+1/2}(x, y)}{\partial x} = \mathcal{R}_2(x, y), \quad \text{in } \mathbb{G}, \quad (5.69)$$

where $\mathcal{R}_2(x, y) = \mathcal{H}_3(x, y) - \frac{\partial v_1(x, y, t_{n+1})}{\partial x} \frac{\partial \tilde{q}^{n+1/2}(x, y)}{\partial x} - \gamma_1 \frac{\partial v_1(x, y, t_{n+1})}{\partial x} \frac{\partial \tilde{q}^{n+1/2}(x, y)}{\partial x} + \gamma_1(v_1(1, y, t_{n+1}) - v_1(x, y, t_{n+1})) \frac{\partial^2 \tilde{q}^{n+1/2}(x, y)}{\partial x^2}$. Now one can show that $\mathcal{R}_1(x, y)$ bounded ε -uniformly on

$\bar{\mathbf{G}}$ and

$$|\mathcal{R}_2(x, y)| \leq C \left(1 + \varepsilon^{-1} \exp(-\mathbf{m}_1(1-x)/\varepsilon) \right), \quad \text{in } \bar{\mathbf{G}}.$$

Also, it holds that for $y \in [0, 1]$

$$|\tilde{p}^{n+1/2}(0, y)| \leq C, \quad |\tilde{p}^{n+1/2}(1, y)| \leq C, \quad \left| \frac{\partial \tilde{p}^{n+1/2}(0, y)}{\partial x} \right| \leq C, \quad \frac{\partial \tilde{p}^{n+1/2}(1, y)}{\partial x} = 0.$$

Therefore, using the argument of [61] for (5.68) and (5.69), it follows that

$$\left| \frac{\partial^j \tilde{p}^{n+1/2}}{\partial x^j} \right| \leq C \left(1 + \varepsilon^{-j+1} \exp \left(-\frac{\mathbf{m}_1(1-x)}{\varepsilon} \right) \right), \quad j = 1, 2. \quad (5.70)$$

Finally, by adopting the approach as mentioned above, one can obtain the required bound on the spatial derivative of $\tilde{p}^{n+1/2}(x, y)$ for $j = 3, 4$. We have derived derivative bound of component $\tilde{u}^{n+1}(x, y)$ by using the above approach described at $(n+1/2)^{th}$ level. ■

In order to estimate the spatial error related to the fully discrete scheme (5.37), we consider the spatial discretization of the auxiliary problem (5.25) using the new finite difference scheme as described in Section 5.3.2. Hence, we obtain the following discrete problem:

$$\left\{ \begin{array}{l} \tilde{U}_{i,j}^0 = q_0(x_i, y_j), \quad \text{for } (x_i, y_j) \in \bar{\mathbf{G}}^N, \\ \mathbb{L}_{1,\varepsilon}^{N,\Delta t} \tilde{U}_{i,j}^{n+1/2} \equiv \mu_{x_i}^- \tilde{U}_{i-1,j}^{n+1/2} + \mu_{x_i}^c \tilde{U}_{i,j}^{n+1/2} + \mu_{x_i}^+ \tilde{U}_{i+1,j}^{n+1/2} = \tilde{\mathbb{F}}_1^{\Delta t}(x_i, y_j), \\ \hspace{15em} \text{for } 1 \leq i \leq N-1, \quad y_j \in \mathbf{G}_y^N, \\ \tilde{U}_{i,j}^{n+1/2} = \mathbf{s}^{n+1/2}(x_i, y_j), \quad i = 0, N, \quad y_j \in \bar{\mathbf{G}}_y^N, \\ \mathbb{L}_{2,\varepsilon}^{N,\Delta t} \tilde{U}_{i,j}^{n+1} \equiv \mu_{y_j}^- \tilde{U}_{i,j-1}^{n+1} + \mu_{y_j}^c \tilde{U}_{i,j}^{n+1} + \mu_{y_j}^+ \tilde{U}_{i,j+1}^{n+1} = \tilde{\mathbb{F}}_2^{\Delta t}(x_i, y_j), \\ \hspace{15em} \text{for } 1 \leq i, j \leq N-1, \\ \tilde{U}_{i,j}^{n+1} = \mathbf{s}^{n+1}(x_i, y_j), \quad j = 0, N, \quad x_i \in \bar{\mathbf{G}}_x^N, \\ \text{for } n = 0, \dots, M-1, \end{array} \right. \quad (5.71)$$

where the coefficients $\mu_{x_i}^-, \mu_{x_i}^c, \mu_{x_i}^+, \mu_{y_j}^-, \mu_{y_j}^c, \mu_{y_j}^+$ are described in (5.42) and $\tilde{\mathbb{F}}_1^{\Delta t}(x_i, y_j), \tilde{\mathbb{F}}_2^{\Delta t}(x_i, y_j)$ are respectively given by

$$\tilde{\mathbb{F}}_1^{\Delta t}(x_i, y_j) = \left\{ \begin{array}{l} \frac{1}{2}(u(x_{i-1}, y_j, t_n) + \Delta t g_1(x_{i-1}, y_j, t_{n+1})) + \frac{1}{2}(u(x_i, y_j, t_n) + \Delta t g_1(x_i, y_j, t_{n+1})) - \\ \Delta t b_1(x_{i-\frac{1}{2}}, y_j, t_n, u(x_{i-\frac{1}{2}}, y_j, t_n)), \quad \text{for } 1 \leq i \leq N/2, \text{ and when } \varepsilon \leq \|v_1\|N^{-1}, \\ u(x_i, y_j, t_n) + \Delta t g_1(x_i, y_j, t_{n+1}) - \Delta t b_1(x_i, y_j, t_n, u(x_i, y_j, t_n)), \\ \hspace{15em} \text{for } 1 \leq i \leq N/2, \text{ and when } \varepsilon > \|v_1\|N^{-1}, \\ u(x_i, y_j, t_n) + \Delta t g_1(x_i, y_j, t_{n+1}) - \Delta t b_1(x_i, y_j, t_n, u(x_i, y_j, t_n)), \\ \hspace{15em} \text{for } N/2 < i \leq N-1, \end{array} \right. \quad (5.72)$$

and

$$\tilde{\mathbb{F}}_2^{\Delta t}(x_i, y_j) = \begin{cases} \frac{1}{2}(\tilde{U}_{i,j-1}^{n+1/2} + \Delta t g_2(x_i, y_{j-1}, t_{n+1})) + \frac{1}{2}(\tilde{U}_{i,j}^{n+1/2} + \Delta t g_2(x_i, y_j, t_{n+1})) - \\ \Delta t b_2(x_i, y_{j-\frac{1}{2}}, t_n, u(x_i, y_{j-\frac{1}{2}})), \text{ for } 1 \leq j \leq N/2, \text{ and when } \varepsilon \leq \|v_2\|N^{-1}, \\ \tilde{U}_{i,j}^{n+1/2} + \Delta t g_2(x_i, y_j, t_{n+1}) - \Delta t b_2(x_i, y_j, t_n, u(x_i, y_j, t_n)), \\ \text{for } 1 \leq j \leq N/2, \text{ and when } \varepsilon > \|v_2\|N^{-1}, \\ \tilde{U}_{i,j}^{n+1/2} + \Delta t g_2(x_i, y_j, t_{n+1}) - \Delta t b_2(x_i, y_j, t_n, u(x_i, y_j, t_n)), \\ \text{for } N/2 < j \leq N-1. \end{cases} \quad (5.73)$$

The local truncation error at the first half for the numerical scheme (5.71)-(5.73) is defined as

$$\begin{aligned} \mathfrak{T}_{x_i, \tilde{u}^{n+1/2}}^{N, \Delta t} &= \mathbb{L}_{1, \varepsilon}^{N, \Delta t} [\tilde{U}_{i,j}^{n+1/2} - \tilde{u}^{n+1/2}(x_i, y_j)], \\ &= \begin{cases} \mu_{x_i}^- \tilde{U}_{i-1,j}^{n+1/2} + \mu_{x_i}^c \tilde{U}_{i,j}^{n+1/2} + \mu_{x_i}^+ \tilde{U}_{i+1,j}^{n+1/2} - \Delta t [g_1(x_i, y_j, t_{n+1}) - b_1(x_i, y_j, t_n, u(x_i, y_j, t_n))] \\ - u(x_i, y_j, t_n), \quad \text{for } 1 \leq i \leq N/2, \text{ and when } \varepsilon > \|v_1\|N^{-1}, \\ \mu_{x_i}^- \tilde{U}_{i-1,j}^{n+1/2} + \mu_{x_i}^c \tilde{U}_{i,j}^{n+1/2} + \mu_{x_i}^+ \tilde{U}_{i+1,j}^{n+1/2} - \Delta t \left[\frac{g_1(x_i, y_j, t_{n+1}) + g_1(x_{i-1}, y_j, t_{n+1})}{2} \right] + \\ \Delta t \left[\frac{b_1(x_i, y_j, t_n, u(x_i, y_j, t_n)) + b_1(x_{i-1}, y_j, t_n, u(x_{i-1}, y_j, t_n))}{2} \right] - \frac{u(x_i, y_j, t_n) + u(x_{i-1}, y_j, t_n)}{2} \\ + O(\Delta t h_{x_i}^2), \quad \text{for } 1 \leq i \leq N/2, \text{ when } \varepsilon \leq \|v_1\|N^{-1}, \\ \mu_{x_i}^- \tilde{U}_{i-1,j}^{n+1/2} + \mu_{x_i}^c \tilde{U}_{i,j}^{n+1/2} + \mu_{x_i}^+ \tilde{U}_{i+1,j}^{n+1/2} - \Delta t [g_1(x_i, y_j, t_{n+1}) - b_1(x_i, y_j, t_n, u(x_i, y_j, t_n))] \\ - u(x_i, y_j, t_n), \quad \text{for } N/2 < i \leq N-1, \end{cases} \\ &= \begin{cases} \Delta t \left[\mathbb{L}_{1, N, mcd}^{n+1} \tilde{u}^{n+1/2}(x_i, y_j) - (\mathbb{L}_{1, \varepsilon}^{n+1} \tilde{u}^{n+1/2})(x_i, y_j) \right], \\ \text{for } 1 \leq i \leq N/2, \text{ and when } \varepsilon > \|v_1\|N^{-1}, \quad y_j \in \mathbf{G}_y^N, \\ \Delta t \left[\mathbb{L}_{1, N, mup}^{n+1} \tilde{u}^{n+1/2}(x_i, y_j) - (\mathbb{L}_{1, \varepsilon}^{n+1} \tilde{u}^{n+1/2})_{i-\frac{1}{2}, j} \right] + O(\Delta t h_{x_i}^2), \\ \text{for } 1 \leq i \leq N/2, \text{ and when } \varepsilon \leq \|v_1\|N^{-1}, \quad y_j \in \mathbf{G}_y^N, \\ \Delta t \left[\mathbb{L}_{1, N, mcd}^{n+1} \tilde{u}^{n+1/2}(x_i, y_j) - (\mathbb{L}_{1, \varepsilon}^{n+1} \tilde{u}^{n+1/2})(x_i, y_j) \right], \quad \text{for } N/2 < i \leq N-1, \quad y_j \in \mathbf{G}_y^N. \end{cases} \quad (5.74) \end{aligned}$$

Further, we state the following important results for the error analysis.

Lemma 5.11. Consider the following mesh functions $\Theta_{l,k}(\lambda_l)$ with $l = 1, 2$

$$\begin{cases} \Theta_{1,k}(\lambda_1) = \prod_{j=k+1}^N \left(1 + \frac{\lambda_1 h_{x_k}}{\varepsilon}\right)^{-1}, \quad \text{for } 0 \leq k \leq N-1, \quad \Theta_{1,N}(\lambda_1) = 1, \\ \Theta_{2,k}(\lambda_2) = \prod_{j=k+1}^N \left(1 + \frac{\lambda_2 h_{y_k}}{\varepsilon}\right)^{-1}, \quad \text{for } 0 \leq k \leq N-1, \quad \Theta_{2,N}(\lambda_2) = 1, \end{cases}$$

where λ_l is a positive constant, such that $\lambda_l < \mathfrak{m}_l/2$, $l = 1, 2$. Then, under the hypothesis (5.43) of Lemma 5.8, it follows that for $l = 1, 2$,

$$\mathbb{I}_{l,\varepsilon}^{N,\Delta t} \Theta_{l,k}(\lambda_l) \geq \begin{cases} \frac{C\Delta t}{\varepsilon} \Theta_{2,k}(\lambda_l), & \text{for } 1 \leq k \leq N/2, \text{ and when } \varepsilon > \|v_l\|N^{-1}, \\ \frac{C\Delta t}{H_l} \Theta_{l,k}(\lambda_l), & \text{for } 1 \leq k \leq N/2, \text{ and when } \varepsilon \leq \|v_l\|N^{-1}, \\ \frac{C\Delta t}{\varepsilon} \Theta_{l,k}(\lambda_l), & \text{for } N/2 < k \leq N-1. \end{cases}$$

Proof. The arguments given in [Chapter 2, Lemma 2.12] can be used to prove this lemma. ■

At first, we derive the bounds of $\mathcal{T}_{x_i, \tilde{u}^{n+1/2}}^{N,\Delta t}$ (see Chapter 3) by using Lemma 5.10 in (5.74). Then, following the approach given in [Chapter 3, Lemma 3.10] and invoking Lemma 5.11 and the discrete maximum principle in Lemma 5.8, we deduce the following result.

Lemma 5.12. *Let $y_j \in \bar{\mathbf{G}}_y^N$. If $\lambda_1 < \mathfrak{m}_1/2$, the local error associated with the discrete problem (5.71)-(5.73) at $(n+1/2)^{th}$ time level satisfies the following estimate:*

$$|\tilde{U}_{i,j}^{n+1/2} - \tilde{u}^{n+1/2}(x_i, y_j)| \leq \begin{cases} C((N^{-1} + \chi_{1,\varepsilon})N^{-1} + N^{-\lambda_1\eta_{1,0}}), & \text{for } x_i \in [0, 1 - \eta_1] \cap \bar{\mathbf{G}}_x^N, \\ C(\eta_{1,0}^2 N^{-2} \ln^2 N + N^{-\lambda_1\eta_{1,0}}), & \text{for } x_i \in (1 - \eta_1, 1] \cap \bar{\mathbf{G}}_x^N, \end{cases} \quad (5.75)$$

where

$$\chi_{1,\varepsilon} = \begin{cases} \varepsilon, & \text{when } \varepsilon \leq \|v_1\|N^{-1}, \\ 0, & \text{when } \varepsilon > \|v_1\|N^{-1}. \end{cases}$$

Now, we proceed to estimate the local truncation error $|\tilde{U}_{i,j}^{n+1} - \tilde{u}^{n+1}(x_i, y_j)|$ obtained in the y -direction. Here, for the numerical scheme (5.71)-(5.73), the bound of the local truncation error $\mathcal{T}_{y_j, \tilde{u}^{n+1}}^{N,\Delta t} = \mathbb{I}_{2,\varepsilon}^{N,\Delta t} [\tilde{U}_{i,j}^{n+1} - \tilde{u}^{n+1}(x_i, y_j)]$ can be obtain by invoking Lemmas 5.10, 5.11 and 5.12. Further, following that arguments given in [Chapter 3, Lemma 3.11] and finally we get the following result by invoking Lemma 5.11 and the discrete maximum principle in Lemma 5.8.

Theorem 5.2. *Let $\eta_{l,0} \geq 2/\lambda_l, l = 1, 2$. If $\lambda_l < \mathfrak{m}_l/2$, the local error associated with the discrete problem (5.71)-(5.73) at $(n+1)^{th}$ time level satisfies the following estimate:*

$$|\tilde{U}_{i,j}^{n+1} - \tilde{u}^{n+1}(x_i, y_j)| \leq \begin{cases} C(N^{-1} + \chi_{1,\varepsilon})N^{-1} + C(N^{-1} + \chi_{2,\varepsilon})N^{-1}, \\ \quad \text{for } (x_i, y_j) \in ([0, 1 - \eta_1] \times [0, 1 - \eta_2]) \cap \bar{\mathbf{G}}^N, \\ CN^{-2} \ln^2 N, & \text{otherwise,} \end{cases} \quad (5.76)$$

where

$$\chi_{1,\varepsilon} = \begin{cases} \varepsilon, & \text{when } \varepsilon \leq \|v_1\|N^{-1} \\ 0, & \text{when } \varepsilon > \|v_1\|N^{-1}, \end{cases} \quad \text{and} \quad \chi_{2,\varepsilon} = \begin{cases} \varepsilon, & \text{when } \varepsilon \leq \|v_2\|N^{-1}, \\ 0, & \text{when } \varepsilon > \|v_2\|N^{-1}. \end{cases}$$

5.3.2.2 Uniform convergence of the proposed IMEX fractional step-method

We define $E^{n+1}(x_i, y_j) = [U_{i,j}^{n+1} - u(x_i, y_j, t_{n+1})]$, for $(x_i, y_j) \in \bar{\mathbf{G}}^N$, as the global error related to the fully discrete scheme (5.37) at the time level t_{n+1} . Now, to show the ε -uniform convergence of the fully discrete scheme (5.37), we rewrite the global error in the following form:

$$E^{n+1}(x_i, y_j) = \tilde{e}^{n+1}(x_i, y_j) + \tilde{E}^{n+1}(x_i, y_j) + [U_{i,j}^{n+1} - \tilde{U}_{i,j}^{n+1}]. \quad (5.77)$$

Here, $\tilde{e}^{n+1}(x_i, y_j) = [\tilde{u}^{n+1}(x_i, y_j) - u(x_i, y_j, t_{n+1})]$ and $\tilde{E}^{n+1}(x_i, y_j) = [\tilde{U}_{i,j}^{n+1} - \tilde{u}^{n+1}(x_i, y_j)]$, respectively, denote the local error related to the time semidiscrete scheme and the spatial discretization of the auxiliary problem (5.25) at the time level t_{n+1} . The term $[U_{i,j}^{n+1} - \tilde{U}_{i,j}^{n+1}]$ can be written as the solution of the following systems:

$$\begin{cases} \mathbb{L}_{1,\varepsilon}^{N,\Delta t} \mathbb{L}_{2,\varepsilon}^{N,\Delta t} R^{n+1}(x_i, y_j) = -\Delta t \left[b(x_i, y_j, t_n, U_{i,j}^n) - b(x_i, y_j, t_n, u(x_i, y_j, t_n)) \right] + \\ \quad U_{i,j}^n - u(x_i, y_j, t_n) + O(\Delta t)^2, \quad (x_i, y_j) \in \mathbf{G}^N, \\ R^{n+1}(x_i, y_j) = 0, \quad \partial \mathbf{G}^N, \end{cases}$$

where $R^{n+1}(x_i, y_j) = [U_{i,j}^{n+1} - \tilde{U}_{i,j}^{n+1}]$, and by employing the discrete maximum principle in Lemma 5.8, we obtain that

$$\left\| \left\{ R^{n+1}(x_i, y_j) \right\}_{i,j} \right\| \leq (1 + \mathfrak{K}_1 \Delta t) \left\| \left\{ E^n(x_i, y_j) \right\}_{i,j} \right\| + C(\Delta t)^2. \quad (5.78)$$

where \mathfrak{K}_1 is a constant(>0)(independent of ε) such that

$$\mathfrak{K}_1 = \sup \left\{ \left| \frac{\partial b(x, y, t, u)}{\partial u} \right|, \quad (x, y, t) \in \bar{\mathbf{D}}, \quad |u| \leq C_1 \right\},$$

and $C_1 = \max \left\{ \|U^n\|, \|u(t_n)\|, \quad \text{for } n = 0, 1, \dots, M \right\}$. Afterwards, from (5.77) and (5.78), we get

$$\begin{aligned} \left\| \left\{ E^{n+1}(x_i, y_j) \right\}_{i,j} \right\| &\leq \left\| \left\{ \tilde{e}^{n+1}(x_i, y_j) \right\}_{i,j} \right\| + \left\| \left\{ \tilde{E}^{n+1}(x_i, y_j) \right\}_{i,j} \right\| + \\ &\quad (1 + \mathfrak{K}_1 \Delta t) \left\| \left\{ E^n(x_i, y_j) \right\}_{i,j} \right\| + C(\Delta t)^2, \quad (x_i, y_j) \in \bar{\mathbf{G}}^N. \end{aligned} \quad (5.79)$$

Now, using the estimates derived in Lemma 5.7 and Theorem 5.2 in (5.79), with the assumption that $N^{-\delta} \leq C\Delta t$, $0 < \delta < 1$, and by using $(1 + \mathfrak{K}_1 \Delta t)^n \leq \exp(\mathfrak{K}_1 T)$, we obtain the following estimate of the global error.

Theorem 5.3 (Global error). *Assume that the conditions given in (5.43) hold for $N \geq N_0$. Then, if $\lambda_l < \mathfrak{m}_l/2$, $\eta_{l,0} \geq 2/\lambda_l$, $l = 1, 2$, the global error associated with the fully discrete scheme (5.37) at time level t_{n+1} , satisfies the following estimate:*

$$\left\| \left\{ U_{i,j}^{n+1} \right\}_{i,j} - \left\{ u(x_i, y_j, t_{n+1}) \right\}_{i,j} \right\| \leq \begin{cases} C \left(N^{-2+\delta} + \chi_{1,\varepsilon} N^{-1+\delta} + \chi_{2,\varepsilon} N^{-1+\delta} + \Delta t \right), \\ \text{for } (x_i, y_j) \in ([0, 1 - \eta_1] \times [0, 1 - \eta_2]) \cap \bar{\mathbf{G}}^N, \\ C \left(N^{-2+\delta} \ln^2 N + \Delta t \right), \quad \text{for otherwise,} \end{cases} \quad (5.80)$$

where N and Δt are such that $N^{-\delta} \leq C\Delta t$ with $0 < \delta < 1$.

Remark 5.2. Note that the temporal accuracy in the result (5.80) holds under the alternative boundary data given in 5.22. In order to confirm that both the proposed IMEX-FSFM (a linearized scheme) and the proposed fully-implicit FSFM (a nonlinear scheme) achieve the same order of accuracy as obtained in Theorem 5.3, we provide a detailed convergence analysis for the fractional fully-implicit method in the next section.

5.4 The discrete problem-II

This section introduces and analyses the fully-implicit fractional-step FMM for discretizing the nonlinear IBVP (5.1)-(5.3). First, we estimate the error for the time semidiscretization problem, and then we estimate the error for the fully discrete problem.

5.4.1 Time semidiscretization: fractional fully-implicit scheme

The fractional-step implicit-Euler method is used here to discretize the nonlinear IBVP (5.1)-(5.3) with respect to the temporal variable. The fractional-step implicit-Euler method can be written as two-half scheme, and in the first half, the method treats the linear part of the governing differential equation implicitly, and in the second half, the method treats both the linear and the nonlinear parts of the governing differential equation implicitly. Let $u^n(x, y) \approx u(x, y, t_n)$. Then, the semidiscrete problem takes the following form:

(i) (initial condition)

$$u^0(x, y) = q_0(x, y), \quad (x, y) \in \bar{G},$$

(ii) (first half)

$$\begin{cases} \mathbb{T}_{1,\varepsilon}^{\Delta t} u^{n+1}(x, y) = u^n(x, y) + \Delta t g_1(x, y, t_{n+1}), & (x, y) \in G, \\ u^{n+1/2}(x, y) = s^{n+1/2}(x, y), & (x, y) \in \{0, 1\} \times [0, 1], \end{cases} \quad (5.81)$$

(iii) (second half)

$$\begin{cases} \mathbb{T}_{2,\varepsilon}^{\Delta t} u^{n+1}(x, y) = u^{n+1/2}(x, y) + \Delta t g_2(x, y, t_{n+1}), & (x, y) \in G, \\ u^{n+1}(x, y) = s^{n+1}(x, y), & (x, y) \in \{0, 1\} \times [0, 1], \end{cases}$$

where

$$\begin{cases} \mathbb{T}_{1,\varepsilon}^{\Delta t} u^{n+1}(x, y) &= (\mathbb{I} + \Delta t \mathbb{L}_{1,\varepsilon}^{n+1}) u^{n+1/2}(x, y), \\ \mathbb{T}_{2,\varepsilon}^{\Delta t} u^{n+1}(x, y) &= (\mathbb{I} + \Delta t \mathbb{L}_{2,\varepsilon}^{n+1}) u^{n+1/2}(x, y) + \Delta t b(x, y, t_{n+1}, u^{n+1/2}(x, y)). \end{cases}$$

The natural choice of the boundary data is given by

$$\begin{cases} s^{n+1/2}(x, y) = s(x, y, t_{n+1}), & (x, y) \in \{0, 1\} \times [0, 1], \\ s^{n+1}(x, y) = s(x, y, t_{n+1}), & (x, y) \in [0, 1] \times \{0, 1\}. \end{cases} \quad (5.82)$$

To avoid the order reduction in time due to (5.82), we propose an alternative choice of boundary conditions which is given by

$$\begin{cases} \mathbf{s}^{n+1/2}(x, y) = (\mathbf{I} + \Delta t \mathbb{L}_{2,\varepsilon}^{n+1})\mathbf{s}(x, y, t_{n+1}) + \Delta t b(x, y, t_{n+1}, \mathbf{s}(x, y, t_{n+1})) - \\ \quad \Delta t g_2(x, y, t_{n+1}), \quad (x, y) \in \{0, 1\} \times [0, 1], \\ \mathbf{s}^{n+1}(x, y) = \mathbf{s}(x, y, t_{n+1}), \quad (x, y) \in [0, 1] \times \{0, 1\}. \end{cases} \quad (5.83)$$

One can show that the operator $\mathbb{T}_{1,\varepsilon}^{\Delta t}$ satisfy the following maximum principle.

Lemma 5.13 (Maximum principle). *Let the function $\Phi \in \mathcal{C}^0(\bar{\mathcal{G}}) \cap \mathcal{C}^2(\mathcal{G})$ be such that $\Phi(x, y) \leq 0$ on $\partial\mathcal{G}$ and $\mathbb{T}_{1,\varepsilon}^{\Delta t}\Phi(x, y) \leq 0$, in \mathcal{G} . Then, it implies that $\Phi(x, y) \leq 0$ for all $(x, y) \in \bar{\mathcal{G}}$.*

Lemma 5.14 (Stability). *Let the functions $v^{n+1/2}, w^{n+1/2} \in \mathcal{C}^0(\bar{\mathcal{G}}) \cap \mathcal{C}^2(\mathcal{G})$. Then, we have*

$$\|v^{n+1/2} - w^{n+1/2}\|_{\bar{\mathcal{G}}} \leq \|v^{n+1/2} - w^{n+1/2}\|_{\partial\mathcal{G}} + \|\mathbb{T}_{1,\varepsilon}^{\Delta t}v^{n+1/2} - \mathbb{T}_{1,\varepsilon}^{\Delta t}w^{n+1/2}\|_{\bar{\mathcal{G}}}. \quad (5.84)$$

Proof. Consider the functions

$$\Phi^{\pm, n+1/2}(x, y) = -\|v^{n+1/2} - w^{n+1/2}\|_{\partial\mathcal{G}} - \|\mathbb{T}_{1,\varepsilon}^{\Delta t}v^{n+1/2} - \mathbb{T}_{1,\varepsilon}^{\Delta t}w^{n+1/2}\|_{\bar{\mathcal{G}}} \pm (v^{n+1} - w^{n+1})(x, y), \quad (x, y) \in \bar{\mathcal{G}}.$$

Since, $\mathbb{T}_{1,\varepsilon}^{\Delta t}v^{n+1/2} - \mathbb{T}_{1,\varepsilon}^{\Delta t}w^{n+1/2} = \mathbb{T}_{1,\varepsilon}^{\Delta t}(v^{n+1/2} - w^{n+1/2})$, by applying Lemma 5.13, we obtain the desired result. \blacksquare

Lemma 5.14 ensure that the scheme (5.81) produces a unique solution at the first half.

Lemma 5.15 (Comparison principle). *Let the functions $v^{n+1}, w^{n+1} \in \mathcal{C}^0(\bar{\mathcal{G}}) \cap \mathcal{C}^2(\mathcal{G})$ be such that $v^{n+1}(x, y) \leq w^{n+1}(x, y)$ on $\partial\mathcal{G}$ and $\mathbb{T}_{2,\varepsilon}^{\Delta t}v^{n+1}(x, y) \leq \mathbb{T}_{2,\varepsilon}^{\Delta t}w^{n+1}(x, y)$ in \mathcal{G} , then it implies that $v^{n+1}(x, y) \leq w^{n+1}(x, y)$ in $\bar{\mathcal{G}}$.*

Proof: Here, we use method of contradiction. Let us fix $x \in [0, 1]$. Firstly, we suppose that there exists $(x, y^*) \in \bar{\mathcal{G}}$ such that $v^{n+1}(x, y^*) > w^{n+1}(x, y^*)$. Since, $v^{n+1} - w^{n+1} \in \mathcal{C}^0(\bar{\mathcal{G}})$, without loss of generality, we assume that $v^{n+1} - w^{n+1}$ takes positive maximum at (x, y^*) . Now, in conformity with the hypothesis of the comparison principle, $v^{n+1} - w^{n+1} \leq 0$ on $\partial\mathcal{G} \implies (x, y^*) \notin \partial\mathcal{G}$. Therefore, under the above assumption and applying mean value theorem, we have

$$\begin{aligned} & (\mathbb{T}_{2,\varepsilon}^{\Delta t}v^{n+1} - \mathbb{T}_{2,\varepsilon}^{\Delta t}w^{n+1})(x, y^*) \\ &= (\mathbf{I} + \Delta t \mathbb{L}_{2,\varepsilon}^{n+1})(v^{n+1} - w^{n+1})(x, y^*) + \Delta t b(x, y^*, t_{n+1}, v^{n+1}(x, y^*)) \\ & \quad - \Delta t b(x, y^*, t_{n+1}, w^{n+1}(x, y^*)), \\ & \geq \left[\int_0^1 \frac{b(x, y^*, t_{n+1}, (w^{n+1} + \xi(v^{n+1} - w^{n+1}))(x, y^*))}{\partial u} d\xi \right] (v^{n+1} - w^{n+1})(x, y^*). \end{aligned} \quad (5.85)$$

Thus, from (5.85) and the assumption (5.3), we have $\mathbb{T}_{2,\varepsilon}^{\Delta t}v^{n+1}(x, y^*) > \mathbb{T}_{2,\varepsilon}^{\Delta t}w^{n+1}(x, y^*)$ and this contradicts that $\mathbb{T}_{2,\varepsilon}^{\Delta t}v^{n+1}(x, y) \leq \mathbb{T}_{2,\varepsilon}^{\Delta t}w^{n+1}(x, y)$ for all $(x, y) \in \mathcal{G}$. Hence, the proof is over. \blacksquare

Corollary 5.2. *Let the function $\Phi^{n+1} \in \mathcal{C}^0(\bar{\mathcal{G}}) \cap \mathcal{C}^2(\mathcal{G})$. For any given functions $v^{n+1}, w^{n+1} \in \mathcal{C}^0(\bar{\mathcal{G}})$, the linear differential operator $\tilde{\mathbb{T}}_{2,\varepsilon,(v,w)}^{\Delta t}$ defined by*

$$\begin{aligned} \tilde{\mathbb{T}}_{2,\varepsilon,(v,w)}^{\Delta t} \Phi^{n+1} = \\ (\mathbb{I} + \Delta t \mathbb{L}_{2,\varepsilon}^{n+1}) \Phi^{n+1} + \Delta t \left(\int_0^1 \frac{\partial b(x, y, t_{n+1}, w^{n+1} + \xi(v^{n+1} - w^{n+1}))}{\partial u} d\xi \right) \Phi^{n+1}, \end{aligned} \quad (5.86)$$

satisfies the maximum principle, i.e., if $\Phi^{n+1}(x, y) \leq 0$ on $\partial\mathcal{G}$ and $\tilde{\mathbb{T}}_{2,\varepsilon,(v,w)}^{\Delta t} \Phi^{n+1}(x, y) \leq 0$ in \mathcal{G} , then it implies that $\Phi^{n+1} \leq 0$, for all $(x, y) \in \bar{\mathcal{G}}$.

Corollary 5.2 is used to deduce the following ε -uniform stability result.

Lemma 5.16 (Stability). *Let the functions $v^{n+1}, w^{n+1} \in \mathcal{C}^0(\bar{\mathcal{G}}) \cap \mathcal{C}^2(\mathcal{G})$. Then, we have*

$$\|v^{n+1} - w^{n+1}\|_{\bar{\mathcal{G}}} \leq \|v^{n+1} - w^{n+1}\|_{\partial\mathcal{G}} + \frac{1}{1 + \Delta t \beta} \|\mathbb{T}_{2,\varepsilon}^{\Delta t} v^{n+1} - \mathbb{T}_{2,\varepsilon}^{\Delta t} w^{n+1}\|_{\bar{\mathcal{G}}}. \quad (5.87)$$

Proof. Consider the functions

$$\Phi^{\pm, n+1}(x, y) = -\|v^{n+1} - w^{n+1}\|_{\partial\mathcal{G}} - \frac{1}{1 + \Delta t \beta} \|\mathbb{T}_{2,\varepsilon}^{\Delta t} v - \mathbb{T}_{2,\varepsilon}^{\Delta t} w\|_{\bar{\mathcal{G}}} \pm (v^{n+1} - w^{n+1})(x, y), \quad (x, y) \in \bar{\mathcal{G}}.$$

Note that $\Phi^{\pm, n+1}(x, y) \leq 0$, $(x, y) \in \partial\mathcal{G}$, and

$$\begin{aligned} \|\tilde{\mathbb{T}}_{2,\varepsilon,(v,w)}^{\Delta t} (v^{n+1} - w^{n+1})\| &\leq \\ \left[\mathbb{I} + \Delta t \int_0^1 \frac{\partial b(x, y, t_{n+1}, w^{n+1} + \xi(v^{n+1} - w^{n+1}))}{\partial u} d\xi \right] \left(\frac{1}{1 + \Delta t \beta} \|\mathbb{T}_{2,\varepsilon}^{\Delta t} v^{n+1} - \mathbb{T}_{2,\varepsilon}^{\Delta t} w^{n+1}\| \right) \\ \Rightarrow \tilde{\mathbb{T}}_{2,\varepsilon,(v,w)}^{\Delta t} \Phi^{\pm, n+1}(x, t) &\leq 0. \end{aligned} \quad (5.88)$$

Then, Corollary 5.2 implies that $\Phi^{\pm, n+1}(x, y) \leq 0$ for all $(x, y) \in \bar{\mathcal{G}}$, from which the desired result follows immediately. ■

Lemma 5.16 ensure that the scheme (5.81) produces a unique solution at the second half.

Lemma 5.17. *The solution $u^n(x, y)$ of the semidiscrete problem (5.81) at the time level t_n satisfies that*

$$|u^n(x, y)| \leq C_0, \quad \text{in } \bar{\mathcal{G}}. \quad (5.89)$$

5.4.1.1 Error analysis

Let us denote \tilde{e}^{n+1} the local truncation error of scheme (5.81) at the time t_{n+1} , i.e., $\tilde{e}^{n+1}(x, y) = \tilde{u}^{n+1}(x, y) - u(x, y, t_{n+1})$, where $\tilde{u}^{n+1}(x, y)$ is the solution of the following auxiliary problem:

$$\begin{aligned}
(i) \quad & \tilde{u}^0(x, y) = \mathbf{q}_0(x, y), \quad \text{in } \mathbf{G}, \\
(ii) \quad & \begin{cases} \mathbb{T}_{1,\varepsilon}^{\Delta t} \tilde{u}^{n+1/2}(x, y) = u(x, y, t_n) + \Delta t g_1(x, y, t_{n+1}), & \text{in } \mathbf{G}, \\ \tilde{u}^{n+1/2}(x, y) = \mathbf{s}^{n+1/2}(x, y), & \text{in } \{0, 1\} \times [0, 1], \end{cases} \\
(iii) \quad & \begin{cases} \mathbb{T}_{2,\varepsilon}^{\Delta t} \tilde{u}^{n+1}(x, y) = \tilde{u}^{n+1/2}(x, y) + \Delta t g_2(x, y, t_{n+1}), & \text{in } \mathbf{G}, \\ \tilde{u}^{n+1}(x, y) = \mathbf{s}^{n+1}(x, y), & \text{in } \{0, 1\} \times [0, 1]. \end{cases}
\end{aligned} \tag{5.90}$$

Lemma 5.18 (Local error). *Under the alternative boundary data $\mathbf{s}^{n+1/2}$ and \mathbf{s}^{n+1} given in (5.83), the local error \tilde{e}^{n+1} at the time level t_{n+1} satisfies that*

$$\|\tilde{e}^{n+1}\|_{\bar{\mathbf{G}}} \leq C(\Delta t)^2.$$

Proof. From (5.90), we easily deduce that

$$\mathbb{T}_{1,\varepsilon}^{\Delta t} \left(\mathbb{T}_{2,\varepsilon}^{\Delta t} \tilde{u}^{n+1}(x, y) - \Delta t g_2(x, y, t_{n+1}) \right) = u(x, y, t_n) + \Delta t g_1(x, y, t_{n+1}), \quad \text{in } \mathbf{G}.$$

Further, we obtain that

$$\mathbb{T}_{1,\varepsilon}^{\Delta t} \mathbb{T}_{2,\varepsilon}^{\Delta t} \tilde{u}^{n+1}(x, y) = u(x, y, t_n) + \Delta t g(x, y, t_{n+1}) + O(\Delta t)^2, \quad \text{in } \mathbf{G}. \tag{5.91}$$

We expand Taylor's series expansion of the function $u(x, y, t_n)$ in the time variable to get

$$u(x, y, t_n) = u(x, y, t_{n+1}) - \Delta t \frac{\partial u(x, y, t_{n+1})}{\partial t} + O(\Delta t)^2,$$

and by using equation (5.1), one can write

$$\begin{aligned}
& (\mathbf{I} + \Delta t \mathbb{L}_{1,\varepsilon}^{n+1})(\mathbf{I} + \Delta t \mathbb{L}_{2,\varepsilon}^{n+1})u(x, y, t_{n+1}) + \Delta t b(x, y, t_{n+1}, u(x, y, t_{n+1})) = \\
& (\Delta t)^2 \mathbb{L}_{1,\varepsilon}^{n+1} \mathbb{L}_{2,\varepsilon}^{n+1} u(x, y, t_{n+1}) + u(x, y, t_n) + \Delta t g(x, y, t_{n+1}) + O(\Delta t)^2.
\end{aligned} \tag{5.92}$$

Subtracting equation (5.91) and (5.92), we obtain that

$$\begin{aligned}
& (\mathbf{I} + \Delta t \mathbb{L}_{1,\varepsilon}^{n+1})(\mathbf{I} + \Delta t \mathbb{L}_{2,\varepsilon}^{n+1})\tilde{e}^{n+1}(x, y) + \Delta t [b(x, y, t_{n+1}, \tilde{u}^{n+1}(x, y)) - b(x, y, t_{n+1}, u(x, y, t_{n+1}))] \\
& + (\Delta t)^2 \mathbb{L}_{1,\varepsilon}^{n+1} [b(x, y, t_{n+1}, \tilde{u}^{n+1}(x, y)) + g_2(x, y, t_{n+1}) + \mathbb{L}_{2,\varepsilon}^{n+1} \tilde{u}^{n+1}(x, y)] = O(\Delta t)^2.
\end{aligned}$$

Further, we have

$$\begin{aligned} & (\mathbf{I} + \Delta t \mathbb{L}_{1,\varepsilon}^{n+1})(\mathbf{I} + \Delta t \mathbb{L}_{2,\varepsilon}^{n+1})\tilde{e}^{n+1}(x, y) + \Delta t [b(x, y, t_{n+1}, \tilde{u}^{n+1}(x, y)) - b(x, y, t_{n+1}, u(x, y, t_{n+1}))] \\ & + (\Delta t)^2 \mathbb{L}_{1,\varepsilon}^{n+1} [b(x, y, t_{n+1}, \tilde{u}^{n+1}(x, y)) - b(x, y, t_{n+1}, u(x, y, t_{n+1}))] = O(\Delta t)^2. \end{aligned} \quad (5.93)$$

Again, one can deduce that

$$\begin{aligned} & b(x, y, t_{n+1}, \tilde{u}^{n+1}) - b(x, y, t_{n+1}, u(t_{n+1})) \\ & = \left[\int_0^1 \frac{\partial b(x, y, t_{n+1}, u(t_{n+1}) + \xi(\tilde{u}^{n+1} - u(t_{n+1})))}{\partial u} d\xi \right] \tilde{e}^{n+1}(x, y). \end{aligned} \quad (5.94)$$

The equations (5.93) and (5.94) together imply that

$$\begin{aligned} & (\mathbf{I} + \Delta t \mathbb{L}_{1,\varepsilon}^{n+1})(\mathbf{I} + \Delta t \mathbb{L}_{2,\varepsilon}^{n+1})\tilde{e}^{n+1}(x, y) + \Delta t (\mathbf{I} + \Delta t \mathbb{L}_{1,\varepsilon}^{n+1}) \\ & \left[\int_0^1 \frac{\partial b(x, y, t_{n+1}, u(x, y, t_{n+1}) + \xi(\tilde{u}^{n+1}(x, y) - u(x, y, t_{n+1})))}{\partial u} d\xi \right] \tilde{e}^{n+1}(x, y) \\ & = O(\Delta t)^2. \end{aligned} \quad (5.95)$$

Now, by using the alternative boundary conditions (5.83), and the equation (5.95), the local error \tilde{e}^{n+1} can be written as the solution of the following problems:

$$\begin{cases} \mathbb{T}_{1,\varepsilon}^{\Delta t} \tilde{e}^{n+1/2}(x, y) = O(\Delta t)^2, & \text{in } \mathbf{G}, \\ \tilde{e}^{n+1/2}(0, y) = 0, \quad \tilde{e}^{n+1/2}(1, y) = 0, & \text{in } [0, 1], \end{cases} \quad (5.96)$$

and

$$\begin{cases} \tilde{\mathbb{T}}_{2,\varepsilon,(\tilde{u}^{n+1}, u(t_{n+1}))}^{\Delta t} \tilde{e}^{n+1}(x, y) = \tilde{e}^{n+1/2}(x, y), & \text{in } \mathbf{G}, \\ \tilde{e}^{n+1}(x, 0) = 0, \quad \tilde{e}^{n+1}(x, 1) = 0, & \text{in } [0, 1]. \end{cases} \quad (5.97)$$

We use Lemma 5.14 to the equation (5.96) to obtain $\|\tilde{e}^{n+1/2}(x, y)\|_{\bar{\mathbf{G}}} = O(\Delta t)^2$. Further, by applying Lemma 5.16 to the equation (5.97), we get desired bound of the local error. \blacksquare

Let us introduce the global error of the scheme (5.81) at time t_{n+1} as usual, i.e., $e^{n+1}(x, y) = u^{n+1}(x, y) - u(x, y, t_{n+1})$. The following result shows that the fractional-step implicit-Euler method converges uniformly with first-order accurate in time.

Theorem 5.4 (Global error). *Under the alternative boundary data of $\mathbf{s}^{n+1/2}$ and \mathbf{s}^{n+1} given in (5.83), the global error $e^{n+1}(x, y)$ satisfies that*

$$\sup_{(n+1)\Delta t \leq T} \|e^{n+1}\|_{\bar{\mathbf{G}}} \leq C\Delta t.$$

Proof. We rewrite the global error as

$$e^{n+1}(x, y) = \tilde{e}^{n+1}(x, y) + d^{n+1}(x, y), \quad (5.98)$$

where the term $d^{n+1}(x, y) = u^{n+1}(x, y) - \tilde{u}^{n+1}(x, y)$ can be deduced from the following problems:

$$\begin{cases} \mathbb{T}_{1,\varepsilon}^{\Delta t} d^{n+1/2}(x, y) = e^n(x, y), & \text{in } \mathbf{G} \\ d^{n+1/2}(0, y) = 0, \quad d^{n+1/2}(1, y) = 0, & \text{in } [0, 1], \end{cases} \quad (5.99)$$

and

$$\begin{cases} \tilde{\mathbb{T}}_{2,\varepsilon,(u^{n+1}, \tilde{u}^{n+1})}^{\Delta t} d^{n+1}(x, y) = d^{n+1/2}(x, y), & \text{in } \mathbf{G}, \\ d^{n+1}(x, 0) = 0, \quad d^{n+1}(x, 1) = 0, & \text{in } [0, 1], \end{cases} \quad (5.100)$$

which utilizes the the following expression:

$$\begin{aligned} & b(x, y, t_{n+1}, u^{n+1}(x, y)) - b(x, y, t_{n+1}, \tilde{u}^{n+1}(x, y)) = \\ & \left[\int_0^1 \frac{\partial b(x, y, t_{n+1}, \tilde{u}^{n+1}(x, y) + \xi(u^{n+1}(x, y) - \tilde{u}^{n+1}(x, y)))}{\partial u} d\xi \right] d^{n+1}(x, y). \end{aligned} \quad (5.101)$$

Firstly, we apply Lemma 5.14 to the equation 5.99 and Lemma 5.16 to the equation 5.100; and utilizing (5.98), we get

$$\|e^{n+1}\|_{\bar{\mathbf{G}}} \leq \|\tilde{e}^{n+1}\|_{\bar{\mathbf{G}}} + \|e^n\|_{\bar{\mathbf{G}}}.$$

Finally, the desired estimate follows from the above recurrence relation and utilizing Lemma 5.18. ■

5.4.2 The fully discrete scheme

We consider the framework of the new hybrid FMM for the spatial discretization of the time semidiscrete problem (5.90). Then, the fully discrete scheme takes the following form on $\bar{\mathbf{D}}^{N,\Delta t}$:

$$\begin{aligned} (i) \quad & U_{i,j}^0 = \mathbf{q}_0(x_i, y_j), \quad \text{for } i, j = 0, 1, \dots, N, \\ (ii) \quad & \begin{cases} \mathbb{T}_{1,\varepsilon}^{N,\Delta t} U_{i,j}^{n+1/2} = \mathbb{G}_1^{\Delta t}(x_i, y_j), & 1 \leq i \leq N-1, \quad y_j \in \mathbf{G}_y^N, \\ U_{i,j}^{n+1/2} = \mathbf{s}^{n+1/2}(x_i, y_j), & i = 0, N, \quad y_j \in \bar{\mathbf{G}}_y^N, \end{cases} \\ (iii) \quad & \begin{cases} \mathbb{T}_{2,\varepsilon}^{N,\Delta t} U_{i,j}^{n+1} = \mathbb{G}_2^{\Delta t}(x_i, y_j), & 1 \leq j \leq N-1, \quad x_i \in \mathbf{G}_x^N, \\ U_{i,j}^{n+1} = \mathbf{s}^{n+1}(x_i, y_j), & j = 0, N, \quad x_i \in \bar{\mathbf{G}}_x^N, \end{cases} \end{aligned} \quad (5.102)$$

where the discrete operators $\mathbb{T}_{1,\varepsilon}^{N,\Delta t}$ and $\mathbb{T}_{2,\varepsilon}^{N,\Delta t}$ are given by

$$\mathbb{T}_{1,\varepsilon}^{N,\Delta t} U_{i,j}^{n+1/2} = \begin{cases} (\mathbb{I} + \Delta t \mathbb{L}_{1,N,mcd}^{n+1}) U_{i,j}^{n+1/2}, \\ \quad \text{for } 1 \leq i \leq N/2, y_j \in \mathbb{G}_y^N \text{ and when } \varepsilon > \|v_1\| N^{-1}, \\ U_{i-1/2,j}^{n+1/2} + \Delta t \mathbb{L}_{1,N,mup}^{n+1} U_{i,j}^{n+1/2}, \\ \quad \text{for } 1 \leq i \leq N/2, y_j \in \mathbb{G}_y^N \text{ and when } \varepsilon \leq \|v_1\| N^{-1}, \\ (\mathbb{I} + \Delta t \mathbb{L}_{1,N,mcd}^{n+1}) U_{i,j}^{n+1/2}, \quad \text{for } N/2 < i \leq N-1, y_j \in \mathbb{G}_y^N, \end{cases}$$

and

$$\mathbb{T}_{2,\varepsilon}^{N,\Delta t} U_{i,j}^{n+1} = \begin{cases} (\mathbb{I} + \Delta t \mathbb{L}_{2,N,mcd}^{n+1}) U_{i,j}^{n+1} + \Delta t b(x_i, y_j, t_{n+1}, U_{i,j}^{n+1}), \\ \quad \text{for } 1 \leq j \leq N/2, x_i \in \mathbb{G}_x^N \text{ and when } \varepsilon > \|v_2\| N^{-1}, \\ U_{i,j-1/2}^{n+1} + \Delta t \mathbb{L}_{2,N,mup}^{n+1} U_{i,j}^{n+1} + \Delta t b(x_i, y_{j-1/2}, t_{n+1}, U_{i,j-1/2}^{n+1}), \\ \quad \text{for } 1 \leq j \leq N/2, x_i \in \mathbb{G}_x^N \text{ and when } \varepsilon \leq \|v_2\| N^{-1}, \\ (\mathbb{I} + \Delta t \mathbb{L}_{2,N,mcd}^{n+1}) U_{i,j}^{n+1} + \Delta t b(x_i, y_j, t_{n+1}, U_{i,j}^{n+1}), \\ \quad \text{for } N/2 < j \leq N-1, x_i \in \mathbb{G}_x^N, \end{cases}$$

and the right-side vectors $\mathbb{G}_1^{\Delta t}(x_i, y_j)$ and $\mathbb{G}_2^{\Delta t}(x_i, y_j)$ are given by

$$\mathbb{G}_1^{\Delta t}(x_i, y_j) = \begin{cases} U_{i,j}^n + \Delta t g_1(x_i, y_j, t_{n+1}), \\ \quad \text{for } 1 \leq i \leq N/2, y_j \in \mathbb{G}_y^N \text{ and when } \varepsilon > \|v_1\| N^{-1}, \\ U_{i-1/2,j}^n + \Delta t g_{1,i-\frac{1}{2},j}^{n+1}, \\ \quad \text{for } 1 \leq i \leq N/2, y_j \in \mathbb{G}_y^N \text{ and when } \varepsilon \leq \|v_1\| N^{-1}, \\ U_{i,j}^n + \Delta t g_1(x_i, y_j, t_{n+1}), \quad \text{for } N/2 < i \leq N-1, y_j \in \mathbb{G}_y^N, \end{cases}$$

and

$$\mathbb{G}_2^{\Delta t}(x_i, y_j) = \begin{cases} U_{i,j}^{n+1/2} + \Delta t g_2(x_i, y_j, t_{n+1}), \\ \quad \text{for } 1 \leq j \leq N/2, x_i \in \mathbb{G}_x^N \text{ and when } \varepsilon > \|v_2\| N^{-1}, \\ U_{i,j-1/2}^{n+1/2} + \Delta t g_{2,i,j-\frac{1}{2}}^{n+1}, \\ \quad \text{for } 1 \leq j \leq N/2, x_i \in \mathbb{G}_x^N \text{ and when } \varepsilon \leq \|v_2\| N^{-1}, \\ U_{i,j}^{n+1/2} + \Delta t g_2(x_i, y_j, t_{n+1}), \quad \text{for } N/2 < j \leq N-1, x_i \in \mathbb{G}_x^N, \end{cases}$$

and $\mathbf{s}^{n+1/2}(x, y)$, $\mathbf{s}^{n+1}(x, y)$ are defined in (5.83), the operators $\mathbb{L}_{1,N,mcd}^{n+1}$, $\mathbb{L}_{1,N,mup}^{n+1}$, $\mathbb{L}_{2,N,mcd}^{n+1}$, $\mathbb{L}_{2,N,mup}^{n+1}$ are given in (5.38).

Lemma 5.19 (Discrete comparison principle). *Suppose that there exists a positive integer N_0 such that the*

following conditions hold for $N \geq N_0$:

$$\frac{N}{\ln N} > \eta_{1,0} \|v_1\|, \quad \mathfrak{m}_1 N \geq \frac{1}{\Delta t}, \quad (5.103)$$

and

$$\frac{N}{\ln N} > \eta_{2,0} \|v_2\|, \quad \mathfrak{m}_2 N \geq \left(\left\| \frac{\partial b}{\partial u} \right\| + \frac{1}{\Delta t} \right). \quad (5.104)$$

If two arbitrary mesh function V and W defined on $\bar{\mathcal{D}}^{N,\Delta t}$ satisfies that $V \leq W$ on $\partial \mathcal{D}^{N,\Delta t}$ and $\mathbb{T}_{k,\varepsilon}^{N,\Delta t} V \leq \mathbb{T}_{k,\varepsilon}^{N,\Delta t} W$ in $\mathcal{D}^{N,\Delta t}$, where $k = 1, 2$, then it implies that $V \leq W$ on $\bar{\mathcal{D}}^{N,\Delta t}$.

Proof. The linear discrete operator $\mathbb{T}_{1,\varepsilon}^{N,\Delta t}$ satisfies the discrete comparison principle, and the proof is obtained by [Chapter 3, Lemma 3.5].

Now, we prove the discrete comparison principle for the nonlinear discrete operator $\mathbb{T}_{2,\varepsilon}^{N,\Delta t}$. In conformity with the hypothesis of the discrete comparison principle, without loss of generality we consider $V_{i,j} = V_j$ for any fixed i ; and consider the following system

$$\begin{cases} \mathbb{T}_{2,\varepsilon}^{N,\Delta t} V_j - \mathbb{T}_{2,\varepsilon}^{N,\Delta t} W_j = \omega_j, & 1 \leq j \leq N-1, \\ V_0 - W_0 = \omega_0, & V_N - W_N = \omega_N, \end{cases} \quad (5.105)$$

where $\omega_j \leq 0$, for $0 \leq j \leq N$. Now, let $Z_j = V_j - W_j$ and we have

$$\mathbb{T}_{2,\varepsilon}^{N,\Delta t} V_j - \mathbb{T}_{2,\varepsilon}^{N,\Delta t} W_j = \begin{cases} Z_j + \Delta t \mathbb{L}_{2,N,mcd}^{n+1} Z_j + \Delta t \left[\int_0^1 \frac{\partial b(x_i, y_j, t_{n+1}, W_j + \xi(V_j - W_j))}{\partial u} d\xi \right] Z_j, \\ \quad 1 \leq j \leq N/2 \text{ and when } \varepsilon > \|v_2\| N^{-1}, \\ Z_{j-\frac{1}{2}} + \Delta t \mathbb{L}_{2,N,mup}^{n+1} Z_j + \Delta t \left[\int_0^1 \frac{\partial b(x_i, y_{j-\frac{1}{2}}, t_{n+1}, W_{j-\frac{1}{2}} + \xi(V_{j-\frac{1}{2}} - W_{j-\frac{1}{2}}))}{\partial u} d\xi \right] Z_{j-\frac{1}{2}}, \\ \quad 1 \leq j \leq N/2 \text{ and when } \varepsilon \leq \|v_2\| N^{-1}, \\ Z_j + \Delta t \mathbb{L}_{2,N,mcd}^{n+1} Z_j + \Delta t \left[\int_0^1 \frac{\partial b(x_i, y_j, t_{n+1}, W_j + \xi(V_j - W_j))}{\partial u} d\xi \right] Z_j, & N/2 < j < N. \end{cases} \quad (5.106)$$

By using the equation (5.106), we can rewrite the equation (5.105) in the following form:

$$\mathbf{A}Z = \omega. \quad (5.107)$$

Here, the matrix \mathbf{A} is given by $\mathbf{A}_{j,j} = 1$, for $j = 0, N$, and

$$\begin{cases} \mathbf{A}_{j,j-1} = \Delta t \tilde{\mu}_{mcd,y_j}^-, & \mathbf{A}_{j,j} = \Delta t \tilde{\mu}_{mcd,y_j}^c + 1, & \mathbf{A}_{j,j+1} = \Delta t \tilde{\mu}_{mcd,y_j}^+, \\ \quad 1 \leq j \leq N/2 \text{ and when } \varepsilon > \|v_2\| N^{-1}, \\ \mathbf{A}_{j,j-1} = \Delta t \tilde{\mu}_{mup,y_j}^- + \frac{1}{2}, & \mathbf{A}_{j,j} = \Delta t \tilde{\mu}_{mup,y_j}^c + \frac{1}{2}, & \mathbf{A}_{j,j+1} = \Delta t \tilde{\mu}_{mup,y_j}^+, \\ \quad 1 \leq j \leq N/2 \text{ and when } \varepsilon \leq \|v_2\| N^{-1}, \\ \mathbf{A}_{j,j-1} = \Delta t \tilde{\mu}_{mcd,y_j}^-, & \mathbf{A}_{j,j} = \Delta t \tilde{\mu}_{mcd,y_j}^c + 1, & \mathbf{A}_{j,j+1} = \Delta t \tilde{\mu}_{mcd,y_j}^+, & N/2 < j < N, \end{cases}$$

where

$$\begin{cases} \tilde{\mu}_{mcd,y_j}^- = \mu_{mcd,y_j}^-, \\ \tilde{\mu}_{mcd,y_j}^c = \mu_{mcd,y_j}^c + \left[\int_0^1 \frac{\partial b(x_i, y_j, t_{n+1}, W_j + \xi(V_j - W_j))}{\partial u} d\xi \right], \\ \tilde{\mu}_{mcd,y_j}^+ = \mu_{mcd,y_j}^+, \end{cases}$$

and

$$\begin{cases} \tilde{\mu}_{mup,y_j}^- = \mu_{mup,y_j}^- + \frac{1}{2} \left[\int_0^1 \frac{\partial b(x_i, y_{j-\frac{1}{2}}, t_{n+1}, W_{j-\frac{1}{2}} + \xi(V_{j-\frac{1}{2}} - W_{j-\frac{1}{2}}))}{\partial u} d\xi \right], \\ \tilde{\mu}_{mup,y_j}^c = \mu_{mup,y_j}^c + \frac{1}{2} \left[\int_0^1 \frac{\partial b(x_i, y_{j-\frac{1}{2}}, t_{n+1}, W_{j-\frac{1}{2}} + \xi(V_{j-\frac{1}{2}} - W_{j-\frac{1}{2}}))}{\partial u} d\xi \right], \\ \tilde{\mu}_{mcd,y_j}^+ = \mu_{mup,y_j}^+. \end{cases}$$

One can show that, under the conditions (5.103) and (5.104), the matrix \mathbf{A} is an M-matrix (see the proof in [Chapter 3, Lemma 3.5]). ■

Remark 5.3. From the discrete comparison principle, one can obtain the existence and uniqueness of the solution to the discrete problem (5.102)(see the Hadamard's Theorem 5.3.10 in [91]).

Corollary 5.3. *Let Ψ be any mesh function defined on $\bar{\mathcal{D}}^{N,\Delta t}$. Then, for any given mesh functions V and W defined on $\bar{\mathcal{D}}^{N,\Delta t}$, the difference operators $\tilde{\mathbb{T}}_{1,\varepsilon,(V,W)}^{N,\Delta t}$ defined by*

$$\tilde{\mathbb{T}}_{1,\varepsilon,(V,W)}^{N,\Delta t} \Psi_{i,j} = \mathbb{T}_{1,\varepsilon}^{N,\Delta t} \Psi_{i,j}, \quad \text{for } 1 \leq i, j \leq N-1, \quad (5.108)$$

and

$$\tilde{\mathbb{T}}_{2,\varepsilon,(V,W)}^{N,\Delta t} \Psi_{i,j} = \begin{cases} \left(\mathbb{I} + \Delta t \mathbb{L}_{2,N,mcd}^{n+1} \right) \Psi_{i,j} + \Delta t \left[\int_0^1 \frac{\partial b(x_i, y_j, t_{n+1}, W_{i,j} + \xi(V_{i,j} - W_{i,j}))}{\partial u} d\xi \right] \Psi_{i,j}, \\ \quad \text{for } 1 \leq j \leq N/2, \ 1 \leq i \leq N, \text{ and when } \varepsilon > \|v_2\|N^{-1}, \\ \left(\mathbb{I} + \Delta t \mathbb{L}_{2,N,mcd}^{n+1} \right) \Psi_{i,j-1/2} + \Delta t \left[\int_0^1 \frac{\partial b(x_i, y_{j-1/2}, t_{n+1}, W_{i,j-1/2} + \xi(V_{i,j-1/2} - W_{i,j-1/2}))}{\partial u} d\xi \right] \Psi_{i,j-1/2}^{n+1}, \\ \quad \text{for } 1 \leq j \leq N/2, \ 1 \leq i \leq N, \text{ and when } \varepsilon \leq \|v_2\|N^{-1}, \\ \left(\mathbb{I} + \Delta t \mathbb{L}_{2,N,mcd}^{n+1} \right) \Psi_{i,j} + \Delta t \left[\int_0^1 \frac{\partial b(x_i, y_j, t_{n+1}, W_{i,j} + \xi(V_{i,j} - W_{i,j}))}{\partial u} d\xi \right] \Psi_{i,j}, \\ \quad \text{for } N/2 < j \leq N-1, \ 1 \leq i \leq N, \end{cases} \quad (5.109)$$

satisfies the discrete maximum principle, i.e., if $\Psi \leq 0$ on $\partial \bar{\mathcal{D}}^{N,\Delta t}$ and $\tilde{\mathbb{T}}_{k,\varepsilon,(V,W)}^{N,\Delta t} \Psi_{i,j} \leq 0$, for $k = 1, 2$, in $\mathcal{D}^{N,\Delta t}$, then it implies that $\Psi_{i,j} \leq 0$ on $\bar{\mathcal{D}}^{N,\Delta t}$.

Lemma 5.20 (Stability). *If two arbitrary mesh functions V and W defined on $\bar{\mathcal{G}}^N$. Then, under the assumptions*

(5.103) and (5.104), we have

$$\begin{aligned} \|V - W\|_{\bar{\mathcal{D}}^{N,\Delta t}} &\leq \|V - W\|_{\partial\bar{\mathcal{D}}^{N,\Delta t}} + \|\mathbb{T}_{1,\varepsilon}^{N,\Delta t}V - \mathbb{T}_{1,\varepsilon}^{N,\Delta t}W\|_{\bar{\mathcal{D}}^{N,\Delta t}}, \\ \text{and } \|V - W\|_{\bar{\mathcal{D}}^{N,\Delta t}} &\leq \|V - W\|_{\partial\bar{\mathcal{D}}^{N,\Delta t}} + \frac{1}{1 + \Delta t\beta} \|\mathbb{T}_{2,\varepsilon}^{N,\Delta t}V - \mathbb{T}_{2,\varepsilon}^{N,\Delta t}W\|_{\bar{\mathcal{D}}^{N,\Delta t}}. \end{aligned} \quad (5.110)$$

Proof. First, we consider the mesh functions for $k = 1$,

$$\Psi_1^\pm(x_i, y_j) = -\|V - W\|_{\partial\mathcal{D}^{N,\Delta t}} - \|\mathbb{T}_{1,\varepsilon}^{N,\Delta t}V - \mathbb{T}_{1,\varepsilon}^{N,\Delta t}W\|_{\bar{\mathcal{D}}^{N,\Delta t}} \pm (V - W)(x_i, y_j), \quad \text{in } \bar{\mathcal{D}}^{N,\Delta t}.$$

Note that $\Psi_1^\pm(x_i, y_j) \leq 0$ on $\partial\mathcal{D}^{N,\Delta t}$, and $\tilde{\mathbb{T}}_{1,\varepsilon,(V,W)}^{N,\Delta t}\Psi_1^\pm(x_i, y_j) \leq 0$, in $\mathcal{D}^{N,\Delta t}$. Then, Corollary 5.3 implies that $\Psi_1^\pm(x_i, y_j) \leq 0$ on $\bar{\mathcal{D}}^{N,\Delta t}$. Now, we consider the mesh function for $k = 2$,

$$\Psi_2^\pm(x_i, y_j) = -\|V - W\|_{\partial\mathcal{D}^{N,\Delta t}} - \frac{1}{1 + \Delta t\beta} \|\mathbb{T}_{2,\varepsilon}^{N,\Delta t}V - \mathbb{T}_{2,\varepsilon}^{N,\Delta t}W\|_{\bar{\mathcal{D}}^{N,\Delta t}} \pm (V - W)(x_i, y_j), \quad \text{in } \bar{\mathcal{D}}^{N,\Delta t}.$$

Here also, $\Psi_2^\pm(x_i, y_j) \leq 0$ on $\partial\mathcal{D}^{N,\Delta t}$, and $\tilde{\mathbb{T}}_{2,\varepsilon,(V,W)}^{N,\Delta t}\Psi_2^\pm(x_i, y_j) \leq 0$, in $\mathcal{D}^{N,\Delta t}$. Then, Corollary 5.3 implies that $\Psi_2^\pm(x_i, y_j) \leq 0$ on $\bar{\mathcal{D}}^{N,\Delta t}$. Hence, the proof is over. \blacksquare

5.4.2.1 Error analysis

At first, we investigate the asymptotic behavior of the analytical solution of the semidiscrete problem (5.90) and its derivatives. This will be used later to derive the truncation error bounds. It is clear from Lemma 5.14 and 5.16 that $\|\tilde{u}^{n+1/2}\| \leq C$ and $\|\tilde{u}^{n+1}\| \leq C$, because $u(x, y, t_n), g_1, g_2, \mathbf{s}^{n+1/2}$ and \mathbf{s}^{n+1} are ε -uniformly bounded. We begin by deducing a-priori bounds for $\tilde{u}^{n+1/2}(x, y)$ and its derivatives in the x -direction, as well as $\tilde{u}^{n+1}(x, y)$ and its derivatives in the y -direction. For the proof of Lemma 5.21, apart from the requirement of ε -uniform boundedness and smoothness criterion on the given data, we also need certain compatibility conditions at $(0, t_n)$ and $(1, t_n)$ as mentioned in (5.120). It should be noted that the corresponding derivation consider the take care of non-homogeneous boundary data $\mathbf{s}^{n+1/2}, \mathbf{s}^{n+1}$.

Lemma 5.21. *The solutions $\tilde{u}^{n+1/2}(x, y)$ and $\tilde{u}^{n+1}(x, y)$ of the time semidiscrete scheme (5.90) and their derivatives satisfy that*

$$\left| \frac{\partial^j \tilde{u}^{n+1/2}(x, y)}{\partial x^j} \right| \leq C(1 + \varepsilon^{-j} \exp(-m_1(1 - x)/\varepsilon)), \quad j = 0, 1, 2, 3, 4, \quad (5.111)$$

and

$$\left| \frac{\partial^j \tilde{u}^{n+1}(x, y)}{\partial y^j} \right| \leq C(1 + \varepsilon^{-j} \exp(-m_2(1 - y)/\varepsilon)), \quad j = 0, 1, 2, 3, 4, \quad (5.112)$$

for all $(x, y) \in \bar{\mathcal{G}}$.

Proof. We split up the proof into two parts. In the first part, we derive the result (5.111) for $\tilde{u}^{n+1/2}(x, y)$ and in the second part, the result (5.112) is established for $\tilde{u}^{n+1}(x, y)$.

Part-I: Consider the auxiliary BVP:

$$(\mathbb{I} + \Delta t \mathbb{L}_{1,\varepsilon}^{n+1})\zeta(x, y) = -\mathbb{L}_{1,\varepsilon}^{n+1}u(x, y, t_n) + g_1(x, y, t_{n+1}) \equiv \mathcal{H}_1(x, y), \quad (5.113)$$

where

$$\zeta(x, y) = \frac{\tilde{u}^{n+1/2}(x, y) - u(x, y, t_n)}{\Delta t},$$

with boundary conditions:

$$\begin{aligned} \zeta(0, y) &= \frac{\tilde{u}^{n+1/2}(0, y) - u(0, y, t_n)}{\Delta t}, \\ &= \frac{(\mathbf{I} + \Delta t \mathbb{L}_{2, \varepsilon}^{n+1})u(0, y, t_{n+1}) - \Delta t b(0, y, t_{n+1}, u(0, y, t_{n+1})) - \Delta t g_2(0, y, t_{n+1}) - u(0, y, t_n)}{\Delta t}, \\ &= \frac{(\mathbf{I} + \Delta t \mathbb{L}_{2, \varepsilon}^{n+1})\mathbf{s}(0, y, t_{n+1}) - \Delta t b(0, y, t_{n+1}, \mathbf{s}(0, y, t_{n+1})) - \Delta t g_2(0, y, t_{n+1}) - \mathbf{s}(0, y, t_n)}{\Delta t}, \\ &= \mathbb{L}_{2, \varepsilon}^{n+1} \mathbf{s}(0, y, t_{n+1}) + b(0, y, t_{n+1}, \mathbf{s}(0, y, t_{n+1})) - g_2(0, y, t_{n+1}) + \frac{\partial \mathbf{s}(0, y, t_{n+1})}{\partial t} + O(\Delta t), \end{aligned} \quad (5.114)$$

$$\zeta(1, y) = \mathbb{L}_{2, \varepsilon}^{n+1} \mathbf{s}(1, y, t_{n+1}) + b(1, y, t_{n+1}, \mathbf{s}(1, y, t_{n+1})) - g_2(1, y, t_{n+1}) + \frac{\partial \mathbf{s}(1, y, t_{n+1})}{\partial t} + O(\Delta t). \quad (5.115)$$

Therefore, the BVP (5.113)-(5.115) reduces to the following form:

$$\left\{ \begin{array}{l} (\mathbf{I} + \Delta t \mathbb{L}_{1, \varepsilon}^{n+1})\zeta(x, y) = \mathcal{H}_1(x, y), \\ \zeta(0, y) = \mathbb{L}_{2, \varepsilon}^{n+1} \mathbf{s}(0, y, t_{n+1}) + b(0, y, t_{n+1}, \mathbf{s}(0, y, t_{n+1})) - g_2(0, y, t_{n+1}) + \\ \quad \frac{\partial \mathbf{s}(0, y, t_{n+1})}{\partial t} + O(\Delta t), \\ \zeta(1, y) = \mathbb{L}_{2, \varepsilon}^{n+1} \mathbf{s}(1, y, t_{n+1}) + b(1, y, t_{n+1}, \mathbf{s}(1, y, t_{n+1})) - g_2(1, y, t_{n+1}) + \\ \quad \frac{\partial \mathbf{s}(1, y, t_{n+1})}{\partial t} + O(\Delta t). \end{array} \right. \quad (5.116)$$

We see that boundary conditions of the problem (5.116) are $(\varepsilon, \Delta t)$ -uniformly bounded. Let $|\mathbb{L}_{1, \varepsilon}^{n+1} u(x, y, t_n)| \leq C$, then $|\mathcal{H}_1(x, y)| \leq C$. Hence, applying Lemma 5.14, we obtain that $|\zeta(x, y)| \leq C$. Next, we write the BVP:

$$\left\{ \begin{array}{l} \mathbb{L}_{1, \varepsilon}^{n+1} \tilde{u}^{n+1/2}(x, y) = -\zeta(x, y) + g_1(x, y, t_{n+1}), \\ \tilde{u}^{n+1/2}(0, y) = (\mathbf{I} + \Delta t \mathbb{L}_2^{n+1})\mathbf{s}(0, y, t_{n+1}) + b(0, y, t_{n+1}, \mathbf{s}(0, y, t_{n+1})) - \Delta t g_2(0, y, t_{n+1}), \\ \tilde{u}^{n+1/2}(1, y) = (\mathbf{I} + \Delta t \mathbb{L}_2^{n+1})\mathbf{s}(1, y, t_{n+1}) + b(1, y, t_{n+1}, \mathbf{s}(0, y, t_{n+1})) - \Delta t g_2(1, y, t_{n+1}). \end{array} \right. \quad (5.117)$$

Using the argument of Kellogg and Tsan technique [61], one can obtain that

$$\left| \frac{\partial \tilde{u}^{n+1/2}(x, y)}{\partial x} \right| \leq C \left[1 + \varepsilon^{-1} \exp(-\mathfrak{m}_1(1-x)/\varepsilon) \right], \quad (x, y) \in \bar{\mathbf{G}}. \quad (5.118)$$

Let $\zeta_1(x, y) = \mathbb{L}_{1,\varepsilon}^{n+1} \zeta(x, y)$, which satisfies that

$$\begin{cases} (\mathbb{I} + \Delta t \mathbb{L}_{1,\varepsilon}^{n+1}) \zeta_1(x, y) = -(\mathbb{L}_{1,\varepsilon}^{n+1})^2 u(x, y, t_n) + \mathbb{L}_{1,\varepsilon}^{n+1} g_1(x, y, t_{n+1}) \equiv \mathcal{H}_2(x, y), & \text{in } \mathbb{G}, \\ \zeta_1(0, y) = \frac{1}{\Delta t} \left[-\zeta(0, y) + g_1(0, y, t_{n+1}) - \mathbb{L}_{1,\varepsilon}^{n+1} u(0, y, t_n) \right], \\ \zeta_1(1, y) = \frac{1}{\Delta t} \left[-\zeta(1, y) + g_1(1, y, t_{n+1}) - \mathbb{L}_{1,\varepsilon}^{n+1} u(1, y, t_n) \right]. \end{cases} \quad (5.119)$$

Let $|(\mathbb{L}_{1,\varepsilon}^{n+1})^2 u(x, y, t_n)| \leq C$, then $|\mathcal{H}_2(x, y)| \leq C$. Now, from the compatibility conditions (5.4), one can obtain that

$$\begin{aligned} \frac{\partial \mathbf{s}(0, y, t_n)}{\partial t} &= -\mathbb{L}_\varepsilon^n \mathbf{s}(0, y, t_n) - b(x, y, t_n, u(x, y, t_n)) + g(0, y, t_n), \\ \frac{\partial \mathbf{s}(1, y, t_n)}{\partial t} &= -\mathbb{L}_\varepsilon^n \mathbf{s}(1, y, t_n) - b(x, y, t_n, u(x, y, t_n)) + g(1, y, t_n). \end{aligned} \quad (5.120)$$

Now, by using the boundary conditions of the problem (5.116), from the equations (5.119) and (5.120), we get

$$\begin{cases} (\mathbb{I} + \Delta t \mathbb{L}_{1,\varepsilon}^{n+1}) \zeta_1(x, y) = \mathcal{H}_2(x, y), \\ \zeta_1(0, y) = \mathbb{L}_{2,\varepsilon}^{n+1} \frac{\partial \mathbf{s}(0, y, t_{n+1})}{\partial t} + C_1, \\ \zeta_1(1, y) = \mathbb{L}_{2,\varepsilon}^{n+1} \frac{\partial \mathbf{s}(1, y, t_{n+1})}{\partial t} + C_2. \end{cases} \quad (5.121)$$

We see that $\mathcal{H}_2(x, y) = -(\mathbb{L}_{1,\varepsilon}^{n+1})^2 u(x, y, t_n) + \mathbb{L}_{1,\varepsilon}^{n+1} g_1(x, y, t_{n+1})$ is bounded (ε -uniformly) and boundary conditions are $(\varepsilon, \Delta t)$ -uniformly bounded. Hence, applying Lemma 5.14, we obtain that $|\zeta_1(x, y)| \leq C$. Afterwards, one can deduce that

$$\left| \frac{\partial \zeta(x, y)}{\partial x} \right| \leq C \left[1 + \varepsilon^{-1} \exp(-\mathfrak{m}_1(1-x)/\varepsilon) \right], \quad (x, y) \in \bar{\mathbb{G}}, \quad (5.122)$$

by invoking Kellogg and Tsan technique [61] to the following BVP:

$$\begin{cases} \mathbb{L}_{1,\varepsilon}^{n+1} \zeta(x, y) = \zeta_1(x, y), \\ \zeta(0, y) = \mathbb{L}_{2,\varepsilon}^{n+1} \mathbf{s}(0, y, t_{n+1}) + b(0, y, t_{n+1}, \mathbf{s}(0, y, t_{n+1})) - g_2(0, y, t_{n+1}) + \\ \quad \frac{\partial \mathbf{s}(0, y, t_{n+1})}{\partial t} + O(\Delta t), \\ \zeta(1, y) = \mathbb{L}_{2,\varepsilon}^{n+1} \mathbf{s}(1, y, t_{n+1}) + b(1, y, t_{n+1}, \mathbf{s}(1, y, t_{n+1})) - g_2(1, y, t_{n+1}) + \\ \quad \frac{\partial \mathbf{s}(1, y, t_{n+1})}{\partial t} + O(\Delta t). \end{cases} \quad (5.123)$$

Now, differentiate (5.117) with respect to x , we consider that $\bar{\zeta}(x, y) = \frac{\partial \tilde{u}^{n+1/2}}{\partial x}$ satisfies the following problem

$$\begin{cases} \mathbb{L}_{1,\varepsilon}^{n+1} \bar{\zeta}(x, y) = \mathcal{H}_3(x, y), \\ \bar{\zeta}(0, y) = C_1, \quad \bar{\zeta}(1, y) = C_2 \varepsilon^{-1}, \end{cases} \quad (5.124)$$

where $\mathcal{H}_3(x, y) = -\frac{\partial \zeta(x, y)}{\partial x} + \frac{\partial g_1(x, y, t_{n+1})}{\partial x} - \frac{\partial v_1(x, y, t_{n+1})}{\partial x} \frac{\partial \tilde{u}^{n+1/2}}{\partial x}$ and we obtain that

$$|\mathcal{H}_3(x, y)| \leq C \left[1 + \varepsilon^{-1} \exp(-\mathfrak{m}_1(1-x)/\varepsilon) \right], \quad (x, y) \in \bar{\mathbf{G}}.$$

Again, using the argument of Kellogg and Tsan technique [61] for (5.124), we get

$$\left| \frac{\partial \bar{\zeta}(x, y)}{\partial x} \right| = \left| \frac{\partial^2 \tilde{u}^{n+1/2}(x, y)}{\partial x^2} \right| \leq C \left[1 + \varepsilon^{-2} \exp(-\mathfrak{m}_1(1-x)/\varepsilon) \right], \quad (x, y) \in \bar{\mathbf{G}}.$$

Similar way, we obtained the bound (5.111) for $j = 3, 4$.

We now derive the bound of $\tilde{u}^{n+1/2}(x, y)$ with respect to y by differentiating the auxiliary BVP (5.90) at the first half with respect to y , and we get

$$\left\{ \begin{aligned} & (\mathbf{I} + \Delta t \mathbb{L}_{1,\varepsilon}^{n+1}) \frac{\partial \tilde{u}^{n+1/2}(x, y)}{\partial y} = \\ & \frac{\partial u(x, y, t_n)}{\partial y} + \Delta t \frac{\partial g_1(x, y, t_{n+1})}{\partial y} - \frac{\partial v_1(x, y, t_{n+1})}{\partial y} \frac{\partial \tilde{u}^{n+1/2}(x, y)}{\partial x}, \\ & \frac{\partial \tilde{u}^{n+1/2}(0, y)}{\partial y} = (\mathbf{I} + \Delta t \mathbb{L}_2^{n+1}) \frac{\partial \mathbf{s}(0, y, t_{n+1})}{\partial y} + \Delta t \frac{\partial v_2(0, y, t_{n+1})}{\partial y} \frac{\partial \mathbf{s}(0, y, t_{n+1})}{\partial y} + \\ & \Delta t \left(\frac{b(0, y, t_{n+1}, \mathbf{s}(0, y, t_{n+1}))}{\partial y} + \frac{b(0, y, t_{n+1}, \mathbf{s}(0, y, t_{n+1}))}{\partial u} \frac{\partial \mathbf{s}(0, y, t_{n+1})}{\partial y} \right) - \Delta t \frac{\partial g_2(0, y, t_{n+1})}{\partial y}, \\ & \frac{\partial \tilde{u}^{n+1/2}(1, y)}{\partial y} = (\mathbf{I} + \Delta t \mathbb{L}_2^{n+1}) \frac{\partial \mathbf{s}(1, y, t_{n+1})}{\partial y} + \Delta t \frac{\partial v_2(1, y, t_{n+1})}{\partial y} \frac{\partial \mathbf{s}(1, y, t_{n+1})}{\partial y} + \\ & \Delta t \left(\frac{b(1, y, t_{n+1}, \mathbf{s}(1, y, t_{n+1}))}{\partial y} + \frac{b(1, y, t_{n+1}, \mathbf{s}(1, y, t_{n+1}))}{\partial u} \frac{\partial \mathbf{s}(1, y, t_{n+1})}{\partial y} \right) - \Delta t \frac{\partial g_2(1, y, t_{n+1})}{\partial y}. \end{aligned} \right. \quad (5.125)$$

The following bounds are proven by using the bounds of $\frac{\partial^j \tilde{u}^{n+1/2}(x, y)}{\partial x^j}$ for $j = 0, 1, 2, 3, 4$,

$$\left| \frac{\partial^j \tilde{u}^{n+1/2}}{\partial y^j}(x, y) \right| \leq C \left[1 + \varepsilon^{-j} \exp(-\mathfrak{m}_2(1-y)/\varepsilon) \right], \quad (x, y) \in \bar{\mathbf{G}}, \text{ for } j = 0, 1, 2, 3, 4. \quad (5.126)$$

Part-II: Here, we prove bounds (5.112) for $\tilde{u}^{n+1}(x, y)$. We suppose that, based on prior technical criterion,

$$\|\mathbb{L}_{2,\varepsilon}^{n+1} \tilde{u}^{n+1/2}(x, y)\|_{\bar{\mathbf{G}}} \leq C, \quad \|(\mathbb{L}_{2,\varepsilon}^{n+1})^2 \tilde{u}^{n+1/2}(x, y)\|_{\bar{\mathbf{G}}} \leq C, \quad \|(\mathbb{L}_{2,\varepsilon}^{n+1})^3 \tilde{u}^{n+1/2}(x, y)\|_{\bar{\mathbf{G}}} \leq C.$$

We have

$$\left\{ \begin{aligned} & (\mathbf{I} + \Delta t \mathbb{L}_{2,\varepsilon}^{n+1}) \tilde{u}^{n+1}(x, y) + \Delta t \left[\int_0^1 \frac{\partial b(x, y, t_{n+1}, \xi \tilde{u}^{n+1}(x, y))}{\partial u} d\xi \right] \tilde{u}^{n+1}(x, y) = \\ & \tilde{u}^{n+1/2}(x, y) + \Delta t [g_2(x, y, t_{n+1}) - b(x, y, t_{n+1}, 0)], \\ & \tilde{u}^{n+1}(x, 0) = \mathbf{s}(x, 0, t_{n+1}), \quad \tilde{u}^{n+1}(x, 1) = \mathbf{s}(x, 1, t_{n+1}). \end{aligned} \right. \quad (5.127)$$

Further, we define the operator

$$\tilde{\mathbb{L}}_{2,\varepsilon}^{n+1} = \mathbb{L}_{2,\varepsilon}^{n+1} + \left[\int_0^1 \frac{\partial b(x, y, t_{n+1}, \xi \tilde{u}^{n+1}(x, y))}{\partial u} d\xi \right],$$

and define the following auxiliary BVP:

$$\begin{cases} (\mathbb{I} + \Delta t \tilde{\mathbb{L}}_{2,\varepsilon}^{n+1}) \Lambda(x, y) = -\tilde{\mathbb{L}}_{2,\varepsilon}^{n+1} \tilde{u}^{n+1/2}(x, y) + g_2(x, y, t_{n+1}) - b(x, y, t_{n+1}, 0) \equiv \mathcal{F}_1(x, y), \\ \Lambda(x, 0) = -\mathbb{L}_{2,\varepsilon}^{n+1} \mathbf{s}(x, 0, t_{n+1}) - b(x, 0, t_{n+1}, \mathbf{s}(x, 0, t_{n+1})) + g_2(x, 0, t_{n+1}), \\ \Lambda(x, 1) = -\mathbb{L}_{2,\varepsilon}^{n+1} \mathbf{s}(x, 1, t_{n+1}) - b(x, 1, t_{n+1}, \mathbf{s}(x, 1, t_{n+1})) + g_2(x, 1, t_{n+1}), \end{cases} \quad (5.128)$$

where $\Lambda(x, y) = \frac{\tilde{u}^{n+1}(x, y) - \tilde{u}^{n+1/2}(x, y)}{\Delta t}$. We see that boundary conditions are $(\varepsilon, \Delta t)$ -uniformly bounded and $|\mathcal{F}_1(x, y)| \leq C$. Hence, applying Lemma 5.16, we obtain that $|\Lambda(x, y)| \leq C$. Next, we have

$$\begin{cases} \tilde{\mathbb{L}}_{2,\varepsilon}^{n+1} \tilde{u}^{n+1}(x, y) = -\Lambda(x, y) - b(x, y, t_n, 0) + g_2(x, y, t_{n+1}), \\ \tilde{u}^{n+1}(x, 0) = \mathbf{s}(x, 0, t_{n+1}), \quad \tilde{u}^{n+1}(x, 1) = \mathbf{s}(x, 1, t_{n+1}). \end{cases} \quad (5.129)$$

Using the argument of Kellogg and Tsan technique [61], one can obtain that

$$\left| \frac{\partial \tilde{u}^{n+1}(x, y)}{\partial y} \right| \leq C \left[1 + \varepsilon^{-1} \exp(-\mathfrak{m}_2(1-y)/\varepsilon) \right] \quad \text{in } \bar{\mathbb{G}}. \quad (5.130)$$

We introduce the function $\Lambda_1(x, y) = \tilde{\mathbb{L}}_{2,\varepsilon}^{n+1} \Lambda(x, y)$, which is a solution of

$$\begin{cases} (\mathbb{I} + \Delta t \tilde{\mathbb{L}}_{2,\varepsilon}^{n+1}) \Lambda_1(x, y) = \\ -(\tilde{\mathbb{L}}_{2,\varepsilon}^{n+1})^2 \tilde{u}^{n+1/2}(x, y) - \tilde{\mathbb{L}}_{2,\varepsilon}^{n+1} b(x, y, t_{n+1}, 0) + \tilde{\mathbb{L}}_{2,\varepsilon}^{n+1} g_2(x, y, t_{n+1}) \equiv \mathcal{F}_2(x, y), \\ \Lambda_1(x, 0) = -\tilde{\mathbb{L}}_{2,\varepsilon}^{n+1} \mathbb{L}_{2,\varepsilon}^{n+1} \mathbf{s}(x, 0, t_{n+1}) - \tilde{\mathbb{L}}_{2,\varepsilon}^{n+1} b(x, 0, t_{n+1}, 0) + \tilde{\mathbb{L}}_{2,\varepsilon}^{n+1} g_2(x, 0, t_{n+1}), \\ \Lambda_1(x, 1) = -\tilde{\mathbb{L}}_{2,\varepsilon}^{n+1} \mathbb{L}_{2,\varepsilon}^{n+1} \mathbf{s}(x, 1, t_{n+1}) - \tilde{\mathbb{L}}_{2,\varepsilon}^{n+1} b(x, 1, t_{n+1}, 0) + \tilde{\mathbb{L}}_{2,\varepsilon}^{n+1} g_2(x, 1, t_{n+1}). \end{cases} \quad (5.131)$$

We see that $\mathcal{F}_2(x, y) = -(\tilde{\mathbb{L}}_{2,\varepsilon}^{n+1})^2 \tilde{u}^{n+1/2}(x, y) - \tilde{\mathbb{L}}_{2,\varepsilon}^{n+1} b(x, y, t_{n+1}, 0) + \tilde{\mathbb{L}}_{2,\varepsilon}^{n+1} g_2(x, y, t_{n+1})$ is bounded (ε) -uniformly and boundary conditions are $(\varepsilon, \Delta t)$ -uniformly bounded. Hence, applying Lemma 5.16, we obtain that $|\Lambda_1(x, y)| \leq C$. Afterwards, one can deduce that

$$\left| \frac{\partial \Lambda_1(x, y)}{\partial y} \right| \leq C \left[1 + \varepsilon^{-1} \exp(-\mathfrak{m}_2(1-y)/\varepsilon) \right], \quad (x, y) \in \bar{\mathbb{G}}, \quad (5.132)$$

by invoking Kellogg and Tsan technique [61] to the following BVP:

$$\begin{cases} \tilde{\mathbb{L}}_{2,\varepsilon}^{n+1} \Lambda(x, y) = \Lambda_1(x, y), \\ \Lambda(x, 0) = -\mathbb{L}_{2,\varepsilon}^{n+1} \mathbf{s}(x, 0, t_{n+1}) - b(x, 0, t_{n+1}, \mathbf{s}(x, 0, t_{n+1})) + g_2(x, 0, t_{n+1}), \\ \Lambda(x, 1) = -\mathbb{L}_{2,\varepsilon}^{n+1} \mathbf{s}(x, 1, t_{n+1}) - b(x, 1, t_{n+1}, \mathbf{s}(x, 1, t_{n+1})) + g_2(x, 1, t_{n+1}). \end{cases} \quad (5.133)$$

For second order derivative bound of $\tilde{u}^{n+1}(x, y)$, we differentiate (5.90) with respect y ,

$$\begin{cases} \mathbb{L}_{2,\varepsilon}^{n+1}\bar{\Lambda}(x, y) = \mathcal{F}_3(x, y), \\ \bar{\Lambda}(x, 0) = C_1, \quad \bar{\Lambda}(x, 1) = C_2\varepsilon^{-1}, \end{cases} \quad (5.134)$$

where

$$\begin{aligned} \mathcal{F}_3(x, y) = & -\frac{\partial \Lambda(x, y)}{\partial y} + \frac{\partial g_2(x, y, t_{n+1})}{\partial y} - \frac{\partial v_2(x, y, t_{n+1})}{\partial y} \frac{\partial \tilde{u}^{n+1}(x, y)}{\partial y} - \\ & \left(\frac{\partial b(x, y, t_{n+1}, \tilde{u}^{n+1}(x, y))}{\partial y} + \frac{\partial b(x, y, t_{n+1}, \tilde{u}^{n+1}(x, y))}{\partial u} \frac{\partial \tilde{u}^{n+1}(x, y)}{\partial y} \right), \end{aligned}$$

and $\bar{\Lambda}(x, y) = \frac{\partial \tilde{u}^{n+1}(x, y)}{\partial y}$. We obtain that $|\mathcal{F}_3(x, y)| \leq C[1 + \varepsilon^{-1} \exp(-\mathfrak{m}_2(1 - y)/\varepsilon)]$, $(x, y) \in \bar{\mathbf{G}}$. Applying the same methodology of Kellogg and Tsan to (5.134) we deduce that

$$\left| \frac{\partial \bar{\Lambda}(x, y)}{\partial y} \right| = \left| \frac{\partial^2 \tilde{u}^{n+1}(x, y)}{\partial y^2} \right| \leq C \left[1 + \varepsilon^{-2} \exp(-\mathfrak{m}_2(1 - y)/\varepsilon) \right], \quad (x, y) \in \bar{\mathbf{G}}. \quad (5.135)$$

Similar way, we obtained the bound (5.112) for $j = 3, 4$. ■

We need stronger bound on the derivatives of $\tilde{u}^{n+1/2}(x, y)$ and $\tilde{u}^{n+1}(x, y)$ for the semidiscrete problem (5.90) to establish the ε -uniform error estimate at $(n + 1/2)^{th}$ and $(n + 1)^{th}$ time levels. These are obtained by decomposing the solution $\tilde{u}^{n+1/2}(x, y)$ into smooth and layer components, as given below:

$$\tilde{u}^{n+1/2}(x, y) = \tilde{s}^{n+1/2}(x, y) + \tilde{z}^{n+1/2}(x, y), \quad \text{in } \bar{\mathbf{G}}, \quad (5.136)$$

where $\tilde{s}^{n+1/2}(x, y)$ can be decomposed in the form:

$$\tilde{s}^{n+1/2}(x, y) = \tilde{s}_0^{n+1/2}(x, y) + \varepsilon \tilde{s}_1^{n+1/2}(x, y) + \varepsilon^2 \tilde{s}_2^{n+1/2}(x, y) + \varepsilon^3 \tilde{s}_3^{n+1/2}(x, y), \quad \text{in } \bar{\mathbf{G}}.$$

Here, $\tilde{s}_0^{n+1/2}$, $\tilde{s}_1^{n+1/2}$, $\tilde{s}_2^{n+1/2}$ and $\tilde{s}_3^{n+1/2}$ are defined to be solutions of suitable partial differential equations so that the smooth component $\tilde{s}^{n+1/2}$ and the layer component $\tilde{z}^{n+1/2}$ respectively satisfy the following linear IBVPs:

$$\begin{cases} \tilde{s}^0(x, y) = \mathbf{q}_0(x, y), & \text{in } \bar{\mathbf{G}}, \\ \mathbb{T}_{1,\varepsilon}^{\Delta t} \tilde{s}^{n+1/2}(x, y) = s(x, y, t_n) + \Delta t g_1(x, y, t_{n+1}), & \text{in } \mathbf{G}, \\ \tilde{s}^{n+1/2}(0, y) = \tilde{u}^{n+1/2}(0, y), & \text{in } [0, 1], \\ \tilde{s}^{n+1/2}(1, y) = \tilde{s}_0^{n+1/2}(1, y) + \varepsilon \tilde{s}_1^{n+1/2}(1, y) + \varepsilon^2 \tilde{s}_2^{n+1/2}(1, y), & \text{in } [0, 1], \end{cases} \quad (5.137)$$

and

$$\begin{cases} \tilde{z}^0(x, y) = 0, & \text{in } \bar{\mathbf{G}}, \\ \mathbb{T}_{1,\varepsilon}^{\Delta t} \tilde{z}^{n+1/2}(x, y) = z(x, y, t_n), & \text{in } \mathbf{G}, \\ \tilde{z}^{n+1/2}(0, y) = 0, \quad \tilde{z}^{n+1/2}(1, y) = \tilde{u}^{n+1/2}(1, y) - \tilde{s}^{n+1/2}(1, y), & \text{in } [0, 1]. \end{cases} \quad (5.138)$$

The following Lemma can be proved by using Lemma 5.21

Lemma 5.22. *The solution $\tilde{s}^{n+1/2}$ and $\tilde{z}^{n+1/2}$ of the respective problems (5.137) and (5.138), and their deriva-*

tives satisfy the bounds

$$\begin{aligned} \left| \frac{\partial^j \tilde{s}^{n+1/2}(x, y)}{\partial x^j} \right| &\leq C(1 + \varepsilon^{3-j}), \\ \left| \frac{\partial^j \tilde{z}^{n+1/2}(x, y)}{\partial x^j} \right| &\leq C\left(\varepsilon^{-j} \exp\left(-\frac{\mathfrak{m}_1(1-x)}{\varepsilon}\right)\right), \end{aligned} \quad (5.139)$$

for $j = 0, 1, 2, 3, 4$.

Note that the similar bounds for $\frac{\partial^j \tilde{s}^{n+1/2}}{\partial y^j}$ and $\frac{\partial^j \tilde{z}^{n+1/2}}{\partial y^j}$ can be obtained as given in (5.139), which will be used to prove Lemma 5.23.

In the same way, we decompose the solution $\tilde{u}^{n+1}(x, y)$ into smooth and layer components, as given below:

$$\tilde{u}^{n+1}(x, y) = \tilde{s}^{n+1}(x, y) + \tilde{z}^{n+1}(x, y), \quad (x, y) \in \bar{\mathbf{G}}, \quad (5.140)$$

where $\tilde{s}^{n+1}(x, y)$ can be written in the form:

$$\tilde{s}^{n+1}(x, y) = \tilde{s}_0^{n+1}(x, y) + \varepsilon \tilde{s}_1^{n+1}(x, y) + \varepsilon^2 \tilde{s}_2^{n+1}(x, y) + \varepsilon^3 \tilde{s}_3^{n+1}(x, y), \quad \text{in } \bar{\mathbf{G}}.$$

Here, \tilde{s}_0^{n+1} , \tilde{s}_1^{n+1} , \tilde{s}_2^{n+1} and \tilde{s}_3^{n+1} are solutions of some partial differential equations so that the smooth component $\tilde{s}^{n+1}(x, y)$ and the layer component $\tilde{z}^{n+1}(x, y)$ satisfy the following nonlinear IBVPs:

$$\begin{cases} \mathbb{T}_{2,\varepsilon}^{\Delta t} \tilde{s}^{n+1}(x, y) = \tilde{s}^{n+1/2}(x, y) + \Delta t g_2(x, y, t_{n+1}), & \text{in } \mathbf{G}, \\ \tilde{s}^{n+1}(x, 0) = \tilde{u}^{n+1}(x, 0), & \text{in } [0, 1], \\ \tilde{s}^{n+1}(x, 1) = \tilde{s}_0^{n+1}(x, 1) + \varepsilon \tilde{s}_1^{n+1}(x, 1) + \varepsilon^2 \tilde{s}_2^{n+1}(x, 1), & \text{in } [0, 1], \end{cases} \quad (5.141)$$

and

$$\begin{cases} (\mathbb{I} + \Delta t \mathbb{L}_{2,\varepsilon}^{n+1}) \tilde{z}^{n+1}(x, y) + \Delta t [b(x, y, t_{n+1}, \tilde{u}^{n+1}) - b(x, y, t_{n+1}, \tilde{s}^{n+1})] = \tilde{z}^{n+1/2}(x, y), & \text{in } \mathbf{G}, \\ \tilde{z}^{n+1}(x, 0) = 0, \quad \tilde{z}^{n+1}(x, 1) = \tilde{u}^{n+1}(x, 1) - \tilde{s}^{n+1}(x, 1), & \text{in } [0, 1]. \end{cases} \quad (5.142)$$

Lemma 5.23. *The solution \tilde{s}^{n+1} and \tilde{z}^{n+1} of problems (5.141) and (5.142), and their derivatives satisfy the bounds*

$$\begin{aligned} \left| \frac{\partial^j \tilde{s}^{n+1}(x, y)}{\partial y^j} \right| &\leq C(1 + \varepsilon^{3-j}), \quad \text{in } \bar{\mathbf{G}}, \\ \left| \frac{\partial^j \tilde{z}^{n+1}(x, y)}{\partial y^j} \right| &\leq C\left(\varepsilon^{-j} \exp\left(-\frac{\mathfrak{m}_2(1-y)}{\varepsilon}\right)\right), \quad \text{in } \bar{\mathbf{G}}, \end{aligned} \quad (5.143)$$

for $j = 0, 1, 2, 3, 4$.

Proof. The proof can be obtained by using Lemma 5.21, and the approach described in [Chapter 4, Section 4.2.1]. ■

Here, we analyze the following discrete problem, which is obtained by discretizing the semidiscrete problem

(5.90) with respect to the spatial variable using the new finite difference scheme:

$$\begin{cases} \mathbb{T}_{1,\varepsilon}^{N,\Delta t} \tilde{U}_{i,j}^{n+1/2} = \mathbb{G}_{1,u}^{\Delta t}(x_i, y_j), & 1 \leq i, j \leq N-1, \\ \tilde{U}_{i,j}^{n+1/2} = \mathbf{s}^{n+1/2}(x_i, y_j), & i = 0, N, \quad y_j \in \bar{\mathbf{G}}_y^N, \\ \mathbb{T}_{2,\varepsilon}^{N,\Delta t} \tilde{U}_{i,j}^{n+1} = \mathbb{G}_{2,\tilde{U}}^{\Delta t}(x_i, y_j), & 1 \leq i, j \leq N-1, \\ \tilde{U}_{i,j}^{n+1} = \mathbf{s}^{n+1}(x_i, y_j), & j = 0, N, \quad x_i \in \bar{\mathbf{G}}_x^N, \quad 0 \leq n \leq M-1, \end{cases} \quad (5.144)$$

where the discrete operators $\mathbb{T}_{1,\varepsilon}^{N,\Delta t}$ and $\mathbb{T}_{2,\varepsilon}^{N,\Delta t}$ are given by

$$\mathbb{T}_{1,\varepsilon}^{N,\Delta t} \tilde{U}_{i,j}^{n+1/2} = \begin{cases} (\mathbb{I} + \Delta t \mathbb{L}_{1,N,mcd}^{n+1}) \tilde{U}_{i,j}^{n+1/2}, \\ \text{for } 1 \leq i \leq N/2, \quad y_j \in \mathbf{G}_y^N, \text{ and when } \varepsilon > \|v_1\| N^{-1}, \\ \tilde{U}_{i-1/2,j}^{n+1/2} + \Delta t \mathbb{L}_{1,N,mup}^{n+1} \tilde{U}_{i,j}^{n+1/2}, \\ \text{for } 1 \leq i \leq N/2, \quad y_j \in \mathbf{G}_y^N, \text{ and when } \varepsilon \leq \|v_1\| N^{-1}, \\ (\mathbb{I} + \Delta t \mathbb{L}_{1,N,mcd}^{n+1}) \tilde{U}_{i,j}^{n+1/2}, \text{ for } N/2 < i \leq N-1, \quad y_j \in \mathbf{G}_y^N, \end{cases}$$

and

$$\mathbb{T}_{2,\varepsilon}^{N,\Delta t} \tilde{U}_{i,j}^{n+1} = \begin{cases} (\mathbb{I} + \Delta t \mathbb{L}_{2,N,mcd}^{n+1}) \tilde{U}_{i,j}^{n+1} + \Delta t b(x_i, y_j, t_{n+1}, \tilde{U}_{i,j}^{n+1}), \\ \text{for } 1 \leq j \leq N/2, \quad x_i \in \mathbf{G}_x^N, \text{ and when } \varepsilon > \|v_2\| N^{-1}, \\ \tilde{U}_{i,j-1/2}^{n+1} + \Delta t \mathbb{L}_{2,N,mup}^{n+1} \tilde{U}_{i,j}^{n+1} + \Delta t b(x_i, y_{j-1/2}, t_{n+1}, \tilde{U}_{i,j-1/2}^{n+1}), \\ \text{for } 1 \leq j \leq N/2, \quad x_i \in \mathbf{G}_x^N, \text{ and when } \varepsilon \leq \|v_2\| N^{-1}, \\ (\mathbb{I} + \Delta t \mathbb{L}_{2,N,mcd}^{n+1}) \tilde{U}_{i,j}^{n+1} + \Delta t b(x_i, y_j, t_{n+1}, \tilde{U}_{i,j}^{n+1}), \\ \text{for } N/2 < j \leq N-1, \quad x_i \in \mathbf{G}_x^N, \end{cases}$$

and right-side vectors $\mathbb{G}_{1,u}^{\Delta t}(x_i, y_j)$ and $\mathbb{G}_{2,\tilde{U}}^{\Delta t}(x_i, y_j)$ are given by

$$\mathbb{G}_{1,u}^{\Delta t}(x_i, y_j) = \begin{cases} u(x_i, y_j, t_n) + \Delta t g_1(x_i, y_j, t_{n+1}), \\ \text{for } 1 \leq i \leq N/2, \quad y_j \in \mathbf{G}_y^N, \text{ and when } \varepsilon > \|v_1\| N^{-1}, \\ \frac{u(x_i, y_j, t_n) + u(x_{i-1}, y_j, t_n)}{2} + \Delta t g_{1,i-\frac{1}{2},j}^{n+1}, \\ \text{for } 1 \leq i \leq N/2, \quad y_j \in \mathbf{G}_y^N, \text{ and when } \varepsilon \leq \|v_1\| N^{-1}, \\ u(x_i, y_j, t_n) + \Delta t g_1(x_i, y_j, t_{n+1}), \text{ for } N/2 < i \leq N-1, \quad y_j \in \mathbf{G}_y^N, \end{cases}$$

and

$$\mathbb{G}_{2,\tilde{U}}^{\Delta t}(x_i, y_j) = \begin{cases} \tilde{U}_{i,j}^{n+1/2} + \Delta t g_2(x_i, y_j, t_{n+1}), \\ \text{for } 1 \leq j \leq N/2, \quad x_i \in \bar{\mathbb{G}}_x^N, \text{ and when } \varepsilon > \|v_2\|N^{-1}, \\ \tilde{U}_{i,j-1/2}^{n+1/2} + \Delta t g_{2,i,j-1/2}^{n+1}, \\ \text{for } 1 \leq j \leq N/2, \quad x_i \in \bar{\mathbb{G}}_x^N, \text{ and when } \varepsilon \leq \|v_2\|N^{-1}, \\ \tilde{U}_{i,j}^{n+1/2} + \Delta t g_2(x_i, y_j, t_{n+1}), \quad \text{for } 1 \leq j \leq N/2, \quad x_i \in \bar{\mathbb{G}}_x^N. \end{cases}$$

Here, we set

$$g_{1,i-\frac{1}{2},j}^{n+1} = g_1(x_{i-\frac{1}{2}}, y_j, t_{n+1}), \quad v_{1,i-\frac{1}{2},j}^{n+1} = v_1(x_{i-\frac{1}{2}}, y_j, t_{n+1}),$$

and

$$g_{2,i,j-\frac{1}{2}}^{n+1} = g_2(x_i, y_{j-\frac{1}{2}}, t_{n+1}), \quad v_{2,i,j-\frac{1}{2}}^{n+1} = v_2(x_i, y_{j-\frac{1}{2}}, t_{n+1}),$$

As like the continuous solution, we consider decomposition of the numerical solution into the smooth component and layer component, i.e., we decompose $\tilde{U}_{i,j}^{n+1/2}$ and $\tilde{U}_{i,j}^{n+1}$ as

$$\tilde{U}_{i,j}^{n+1/2} = \tilde{S}_{i,j}^{n+1/2} + \tilde{Z}_{i,j}^{n+1/2}, \quad \tilde{U}_{i,j}^{n+1} = \tilde{S}_{i,j}^{n+1} + \tilde{Z}_{i,j}^{n+1}, \quad \text{in } \bar{\mathbb{G}}^N,$$

where the discrete functions $\tilde{S}^{n+1/2}$, $\tilde{Z}^{n+1/2}$, \tilde{S}^{n+1} and \tilde{Z}^{n+1} are respectively the solutions of the following problems:

$$\begin{cases} \mathbb{T}_{1,\varepsilon}^{N,\Delta t} \tilde{S}_{i,j}^{n+1/2} = \mathbb{G}_{1,s}^{\Delta t}(x_i, y_j), \quad 1 \leq i, j \leq N-1, \\ \tilde{S}_{0,j}^{n+1/2} = \tilde{s}^{n+1/2}(0, y_j, t_{n+1}), \quad \tilde{S}_{N,j}^{n+1/2} = \tilde{s}^{n+1/2}(1, y_j, t_{n+1}), \quad y_j \in \bar{\mathbb{G}}_y^N, \\ \mathbb{T}_{1,\varepsilon}^{N,\Delta t} \tilde{Z}_{i,j}^{n+1/2} = z(x_i, y_j, t_n), \quad 1 \leq i, j \leq N-1, \\ \tilde{Z}_{0,j}^{n+1/2} = \tilde{z}^{n+1/2}(0, y_j, t_{n+1}), \quad \tilde{Z}_{N,j}^{n+1/2} = \tilde{z}^{n+1/2}(1, y_j, t_{n+1}), \quad y_j \in \bar{\mathbb{G}}_y^N, \end{cases} \quad (5.145)$$

and

$$\begin{cases} \mathbb{T}_{2,\varepsilon}^{N,\Delta t} \tilde{S}_{i,j}^{n+1} = \mathbb{G}_{2,\tilde{S}}^{\Delta t}(x_i, y_j), \quad 1 \leq i, j \leq N-1, \\ \tilde{S}_{i,0}^{n+1} = \tilde{s}^{n+1}(x_i, 0, t_{n+1}), \quad \tilde{S}_{i,N}^{n+1} = \tilde{s}^{n+1}(x_i, 1, t_{n+1}), \quad x_i \in \bar{\mathbb{G}}_x^N, \\ \mathbb{T}_{2,\varepsilon}^{N,\Delta t} \tilde{U}_{i,j}^{n+1} - \mathbb{T}_{2,\varepsilon}^{N,\Delta t} \tilde{S}_{i,j}^{n+1} = \tilde{Z}_{i,j}^{n+1/2}, \quad 1 \leq i, j \leq N-1, \\ \tilde{Z}_{i,0}^{n+1} = \tilde{z}^{n+1}(x_i, 0, t_{n+1}), \quad \tilde{Z}_{i,N}^{n+1} = \tilde{z}^{n+1}(x_i, 1, t_{n+1}), \quad x_i \in \bar{\mathbb{G}}_x^N. \end{cases} \quad (5.146)$$

At first, we proceed to estimate the local error $|\tilde{U}_{i,j}^{n+1/2} - \tilde{u}^{n+1/2}(x_i, y_j)|$.

Lemma 5.24. *Let $y_j \in \bar{\mathbb{G}}_y^N$. Then, the local error associated to the smooth component at $(n+1/2)^{th}$ time level satisfies the following estimate:*

$$|\tilde{S}_{i,j}^{n+1/2} - \tilde{s}^{n+1/2}(x_i, y_j)| \leq CN^{-2}, \quad \text{for } x_i \in \bar{\mathbb{G}}_x^N. \quad (5.147)$$

Proof. From problems (5.137) and (5.145), we derive bound of the local truncation error $\tau_{1,\tilde{s}^{n+1/2}}^{N,\Delta t}(x_i, y_j) = \mathbb{T}_{1,\varepsilon}^{N,\Delta t} [\tilde{S}_{i,j}^{n+1/2} - \tilde{s}^{n+1/2}(x_i, y_j)]$ by using the derivative bound of $\tilde{s}^{n+1/2}$ and Lemma 5.22. For $1 \leq i < N/2$

and when $\varepsilon > \|v_1\|N^{-1}$, the local truncation error is given by

$$\begin{aligned}\tau_{1,\tilde{s}^{n+1/2}}^{N,\Delta t}(x_i, y_j) &= \Delta t [\mathbb{L}_{1,\varepsilon}^{n+1} - \mathbb{L}_{1,N,mcd}^{n+1}] \tilde{s}^{n+1/2}(x_i, y_j). \\ \therefore \quad \left| \tau_{1,\tilde{s}^{n+1/2}}^{N,\Delta t}(x_i, y_j) \right| &\leq \Delta t \left[C\varepsilon h_{x_i} \int_{x_{i-1}}^{x_{i+1}} \left| \frac{\partial^4 \tilde{s}^{n+1/2}}{\partial \xi^4} \right| d\xi + Ch_{x_i} \int_{x_{i-1}}^{x_{i+1}} \left| \frac{\partial^3 \tilde{s}^{n+1/2}}{\partial \xi^3} \right| d\xi \right], \\ &\leq C\Delta t N^{-2}.\end{aligned}\tag{5.148}$$

Next, for $i = N/2$ and when $\varepsilon > \|v_1\|N^{-1}$, we deduce that

$$\begin{aligned}\left| \tau_{1,\tilde{s}^{n+1/2}}^{N,\Delta t}(x_i, y_j) \right| &\leq \Delta t [\mathbb{L}_{1,\varepsilon}^{n+1} - \mathbb{L}_{1,N,mcd}^{n+1}] \tilde{s}^{n+1/2}(x_i, y_j), \\ &\leq C\Delta t (\varepsilon + N^{-1}) N^{-1}.\end{aligned}\tag{5.149}$$

Now, for $1 \leq i \leq N/2$ and when $\varepsilon \leq \|v_1\|N^{-1}$, the truncation error is given by

$$\begin{aligned}\tau_{1,\tilde{s}^{n+1/2}}^{N,\Delta t}(x_i, y_j) &= \Delta t \left[(\mathbb{L}_{1,\varepsilon}^{n+1} \tilde{s}^{n+1/2})_{i-\frac{1}{2},j} - \mathbb{L}_{1,N,mup}^{n+1} \tilde{s}^{n+1/2}(x_i, y_j) \right]. \\ \therefore \quad \left| \tau_{1,\tilde{s}^{n+1/2}}^{N,\Delta t}(x_i, y_j) \right| &\leq \Delta t \left[C\varepsilon \int_{x_{i-1}}^{x_{i+1}} \left| \frac{\partial^3 \tilde{s}^{n+1/2}}{\partial \xi^3} \right| d\xi + Ch_{x_i} \int_{x_{i-1}}^{x_{i+1}} \left| \frac{\partial^3 \tilde{s}^{n+1/2}}{\partial \xi^3} \right| d\xi \right], \\ &\leq C\Delta t N^{-2}.\end{aligned}\tag{5.150}$$

Finally, for $N/2 < i < N$,

$$\begin{aligned}\left| \tau_{1,\tilde{s}^{n+1/2}}^{N,\Delta t}(x_i, y_j) \right| &\leq \Delta t \left[C\varepsilon h_{x_i} \int_{x_{i-1}}^{x_{i+1}} \left| \frac{\partial^4 \tilde{s}^{n+1/2}}{\partial \xi^4} \right| d\xi + Ch_{x_i} \int_{x_{i-1}}^{x_{i+1}} \left| \frac{\partial^3 \tilde{s}^{n+1/2}}{\partial \xi^3} \right| d\xi \right], \\ &\leq C\Delta t N^{-2}.\end{aligned}\tag{5.151}$$

Consider the following discrete functions in the domain $0 \leq i \leq N$, for the case $\varepsilon > \|v_1\|N^{-1}$:

$$\Psi^\pm(x_i, y_j) = -CN^{-2}x_i - CN^{-2}\varphi_{1,i} \pm (\tilde{S}_{i,j}^{n+1/2} - \tilde{s}^{n+1/2}(x_i, y_j)),$$

where

$$\varphi_{1,i} = \begin{cases} \frac{x_i}{1 - \eta_1}, & \text{for } 0 \leq i \leq N/2, \\ 1, & \text{for } N/2 \leq i \leq N, \end{cases}$$

and apply Corollary 5.3 for the operator $\tilde{\mathbb{T}}_{1,\varepsilon,(V,W)}^{N,\Delta t}$ together with the local truncation bounds in (5.148), (5.149) and (5.151), we obtain that

$$\left| \tilde{S}_{i,j}^{n+1/2} - \tilde{s}^{n+1/2}(x_i, y_j) \right| \leq CN^{-2}, \quad \text{for } 0 \leq i \leq N.\tag{5.152}$$

In the same way, we choose the following discrete functions in the domain $0 \leq i \leq N$, for the case $\varepsilon \leq$

$\|v_1\|N^{-1}$:

$$\Psi^\pm(x_i, y_j) = -CN^{-2}x_i \pm (\tilde{S}_{i,j}^{n+1/2} - \tilde{s}^{n+1/2}(x_i, y_j)),$$

and apply Corollary 5.3 for the operator $\tilde{\mathbb{T}}_{1,\varepsilon,(V,W)}^{N,\Delta t}$ together with the local truncation bounds in (5.150) and (5.151), to obtain that

$$|\tilde{S}_{i,j}^{n+1/2} - \tilde{s}^{n+1/2}(x_i, y_j)| \leq CN^{-2}, \quad \text{for } 0 \leq i \leq N. \quad (5.153)$$

Hence, the proof is over. ■

Lemma 5.25. *Let λ_l is a positive constant such that $\lambda_l < \mathfrak{m}_l/2$, $l = 1, 2$. Then, under the hypothesis (5.103) and (5.104) of Lemma 5.19, it follows that for $l = 1, 2$,*

$$\tilde{\mathbb{T}}_{l,\varepsilon,(V,W)}^{N,\Delta t} \Theta_{l,k}(\lambda_l) \geq \begin{cases} \frac{C\Delta t}{\varepsilon} \Theta_{2,k}(\lambda_l), & \text{for } 1 \leq k \leq N/2, \text{ and when } \varepsilon > \|v_l\|N^{-1}, \\ \frac{C\Delta t}{H_l} \Theta_{l,k}(\lambda_l), & \text{for } 1 \leq k \leq N/2, \text{ and when } \varepsilon \leq \|v_l\|N^{-1}, \\ \frac{C\Delta t}{\varepsilon} \Theta_{l,k}(\lambda_l), & \text{for } N/2 < k \leq N-1. \end{cases}$$

Proof. The approach described in [Chapter 2, Lemma 2.12] was used to prove this lemma. ■

In the next lemma, we deduce the error estimate corresponding to the layer component $\tilde{Z}_{i,j}^{n+1/2}$.

Lemma 5.26. *Let $y_j \in \bar{\mathfrak{G}}_y^N$. If $\lambda_1 < \mathfrak{m}_1/2$ and $\eta_{1,0} \geq 2/\lambda_1$, the local error associated to the layer component at $(n+1/2)^{th}$ time level satisfies the following estimate:*

$$|\tilde{Z}_{i,j}^{n+1/2} - \tilde{z}^{n+1/2}(x_i, y_j)| \leq \begin{cases} CN^{-2}, & \text{for } x_i \in [0, 1 - \eta_1] \cap \bar{\mathfrak{G}}_x^N, \\ CN^{-2} \ln^2 N, & \text{for } x_i \in (1 - \eta_1, 1] \cap \bar{\mathfrak{G}}_x^N. \end{cases} \quad (5.154)$$

Proof. From the equation (5.138) and Lemma 5.22, we have $\tilde{Z}_{0,j}^{n+1/2} = 0$ and $|\tilde{Z}_{N,j}^{n+1/2}| = |\tilde{z}^{n+1/2}(1, y_j)| \leq C$. We choose the discrete functions for $0 \leq i \leq N$,

$$\Psi^\pm(x_i, y_j) = -C\Theta_{1,i}(\lambda_1) \pm \tilde{Z}_{i,j}^{n+1/2}, \quad (5.155)$$

for sufficiently large C . By Corollary 5.3 for the operator $\tilde{\mathbb{T}}_{1,\varepsilon,(V,W)}^{N,\Delta t}$ and invoking Lemma 5.25, we obtain that

$$|\tilde{Z}_{i,j}^{n+1/2}| \leq C\Theta_{1,i}(\lambda_1). \quad (5.156)$$

Now, for $\lambda_1 < \mathfrak{m}_1/2$, combining (5.156) and Lemma 5.22, we get

$$|\tilde{Z}_{i,j}^{n+1/2} - \tilde{z}^{n+1/2}(x_i, y_j)| \leq |\tilde{Z}_{i,j}^{n+1/2}| + |\tilde{z}^{n+1/2}(x_i, y_j)| \leq C\Theta_{1,i}(\lambda_1). \quad (5.157)$$

Again, for $\eta_{1,0} \geq \frac{2}{\lambda_1}$, it follows from [Chapter 3, Lemma 3.8] that

$$\Theta_{1,N/2}(\lambda_1) \leq CN^{-2}, \quad (5.158)$$

and hence, in particular for $1 \leq i \leq N/2$, the equations (5.157) and (5.158) together imply that

$$|\tilde{Z}_{i,j}^{n+1/2} - \tilde{z}^{n+1/2}(x_i, y_j)| \leq CN^{-2}. \quad (5.159)$$

Next, we estimate $|\tilde{Z}_{i,j}^{n+1/2} - \tilde{z}^{n+1/2}(x_i, y_j)|$ on the fine part of the mesh by using consistency and barrier function argument on the interval $[1 - \eta_1, 1] \times [0, 1]$. Here, we have $|\tilde{Z}_{N/2,j}^{n+1/2} - \tilde{z}^{n+1/2}(x_{N/2}, y_j)| \leq CN^{-2}$ and $|\tilde{Z}_{N,j}^{n+1/2} - \tilde{z}^{n+1/2}(x_N, y_j)| = 0$. From (5.138) and (5.145), we obtain the local truncation error by using the derivative bound of $\tilde{z}^{n+1/2}$ and the Lemma 5.22. For $N/2 < i < N$, we have

$$\begin{aligned} \tau_{1,\tilde{z}^{n+1/2}}^{N,\Delta t}(x_i, y_j) &= \Delta t [\mathbb{L}_{1,\varepsilon}^{n+1} - \mathbb{L}_{1,N,med}^{n+1}] \tilde{z}^{n+1/2}(x_i, y_j), \\ \therefore |\tau_{1,\tilde{z}^{n+1/2}}^{N,\Delta t}(x_i, y_j)| &\leq \Delta t \left[C\varepsilon h_{x_i} \int_{x_{i-1}}^{x_{i+1}} \left| \frac{\partial^4 \tilde{z}^{n+1/2}}{\partial \xi^4} \right| d\xi + Ch_{x_i} \int_{x_{i-1}}^{x_{i+1}} \left| \frac{\partial^3 \tilde{z}^{n+1/2}}{\partial \xi^3} \right| d\xi \right], \\ &\leq C\Delta t N^{-2} \ln^2 N \varepsilon^{-1} \exp(-\mathfrak{m}_1(1 - x_i)/\varepsilon). \end{aligned} \quad (5.160)$$

We choose the discrete functions for $N/2 \leq i \leq N$,

$$\Psi^\pm(x_i, y_j) = -C(N^{-2} \ln^2 N) \Theta_{1,i}(\lambda_1) \pm (\tilde{Z}_{i,j}^{n+1/2} - \tilde{z}^{n+1/2}(x_i, y_j)),$$

Lemma 5.25 implies that $\tilde{\mathbb{T}}_{1,\varepsilon,(V,W)}^{N,\Delta t} \Theta_{1,i}(\lambda_1) \geq \frac{C\Delta t}{\varepsilon} \Theta_{1,i}(\lambda_1)$, for $N/2 < i \leq N-1$, and hence, use of (5.160) for $\lambda_1 < \mathfrak{m}_1/2$ yields that

$$\tilde{\mathbb{T}}_{1,\varepsilon,(V,W)}^{N,\Delta t} \Psi^\pm(x_i, y_j) \leq 0.$$

Now, apply Corollary 5.3 for the operator $\tilde{\mathbb{T}}_{1,\varepsilon,(V,W)}^{N,\Delta t}$ to get $\Psi^\pm(x_i, y_j) \leq 0$, for all $N/2 \leq i \leq N$. Hence, the proof is over. ■

We decompose the error at $(n + 1/2)^{th}$ level in the following form:

$$\tilde{U}_{i,j}^{n+1/2} - \tilde{u}^{n+1/2}(x_i, y_j) = \tilde{S}_{i,j}^{n+1/2} - \tilde{s}^{n+1/2}(x_i, y_j) + \tilde{Z}_{i,j}^{n+1/2} - \tilde{z}^{n+1/2}(x_i, y_j), \quad 0 \leq i, j \leq N.$$

Hence, the required ε -uniform error estimate at $(n + 1/2)^{th}$ level are given in the following Lemma.

Lemma 5.27. *Let $y_j \in \bar{\mathbb{G}}_y^N$. If $\lambda_1 < \mathfrak{m}_1/2$, the local error associated with the discrete problem (5.144) at $(n + 1/2)^{th}$ time level satisfies the following estimate:*

$$|\tilde{U}_{i,j}^{n+1/2} - \tilde{u}^{n+1/2}(x_i, y_j)| \leq \begin{cases} CN^{-2}, & \text{for } x_i \in [0, 1 - \eta_1] \cap \bar{\mathbb{G}}_x^N, \\ CN^{-2} \ln^2 N, & \text{for } x_i \in (1 - \eta_1, 1] \cap \bar{\mathbb{G}}_x^N. \end{cases} \quad (5.161)$$

Next, we proceed to estimate the local error $|\tilde{U}_{i,j}^{n+1} - \tilde{u}^{n+1}(x_i, y_j)|$.

Lemma 5.28. *Let $x_i \in \bar{\mathbb{G}}_x^N$. Then, the local error associated to the smooth component at $(n + 1)^{th}$ time level satisfies the following estimate:*

$$|\tilde{S}_{i,j}^{n+1} - \tilde{s}^{n+1}(x_i, y_j)| \leq CN^{-2}, \quad \text{for } y_j \in \bar{\mathbb{G}}_y^N. \quad (5.162)$$

Proof. For $1 \leq j < N$ and when $\varepsilon > \|v_2\|N^{-1}$, from the problems (5.141) and (5.146), we obtain that

$$\begin{aligned} & \left(\mathbf{I} + \Delta t \mathbb{L}_{2, mcd, N}^{n+1} \right) \tilde{S}_{i,j}^{n+1} + \Delta t \left[b(x_i, y_j, t_{n+1}, \tilde{S}_{i,j}^{n+1}) - b(x_i, y_j, t_{n+1}, \tilde{s}^{n+1}(x_i, y_j)) \right] \\ &= \tilde{S}_{i,j}^{n+1/2} - \tilde{s}^{n+1/2}(x_i, y_j) + \left(\mathbf{I} + \Delta t \mathbb{L}_{2, \varepsilon}^{n+1} \right) \tilde{s}^{n+1}(x_i, y_j). \end{aligned}$$

The above equation can be rewritten in the following form:

$$\begin{aligned} & \left(\mathbf{I} + \Delta t \mathbb{L}_{2, mcd, N}^{n+1} \right) (\tilde{S}_{i,j}^{n+1} - \tilde{s}^{n+1}(x_i, y_j)) + \Delta t \left[\int_0^1 \frac{\partial b(x_i, y_j, t_{n+1}, \tilde{S}_{i,j}^{*,n+1}(\xi))}{\partial u} d\xi \right] (\tilde{S}_{i,j}^{n+1} - \tilde{s}^{n+1}(x_i, y_j)) \\ &= \tilde{S}_{i,j}^{n+1/2} - \tilde{s}^{n+1/2}(x_i, y_j) + \Delta t \left[-\varepsilon \left(\frac{\partial^2}{\partial y^2} - \delta_y^2 \right) \tilde{s}^{n+1}(x_i, y_j) + v_2(x_i, y_j, t_{n+1}) \left(\frac{\partial}{\partial y} - D_y^* \right) \tilde{s}^{n+1}(x_i, y_j) \right], \end{aligned} \quad (5.163)$$

where $\tilde{S}_{i,j}^{*,n+1}(\xi) = \tilde{s}^{n+1}(x_i, y_j) + \xi(\tilde{S}_{i,j}^{n+1} - \tilde{s}^{n+1}(x_i, y_j))$. Now, for any mesh function Ψ we introduce a discrete operator $\mathbb{L}_{\varepsilon, \tilde{S}^*}^{N, \Delta t}$ given by

$$\mathbb{L}_{2, \varepsilon, \tilde{S}^*}^{N, \Delta t} \Psi = \tilde{\mathbb{T}}_{2, \varepsilon, (\tilde{S}, \tilde{s})}^{N, \Delta t} \Psi.$$

Afterwards, we derive bounds of the local truncation error $\tau_{2, \tilde{s}^{n+1}}^{N, \Delta t}(x_i, y_j) = \mathbb{L}_{2, \varepsilon, \tilde{S}^*}^{N, \Delta t} [\tilde{S}_{i,j}^{n+1} - \tilde{s}^{n+1}(x_i, y_j)]$ from (5.163) by using the derivative bounds of \tilde{s}^{n+1} given in Lemma 5.23. For $1 \leq j < N/2$, to the case $\varepsilon > \|v_2\|N^{-1}$, we obtain that

$$\begin{aligned} |\tau_{2, \tilde{s}^{n+1}}^{N, \Delta t}(x_i, y_j)| &\leq |(\tilde{S}_{i,j}^{n+1/2} - \tilde{s}^{n+1/2}(x_i, y_j))| + \\ &\quad \Delta t \left[C\varepsilon h_{y_j} \int_{y_{j-1}}^{y_{j+1}} \left| \frac{\partial^4 \tilde{s}^{n+1}}{\partial \xi^4} \right| d\xi + Ch_{y_j} \int_{y_{j-1}}^{y_{j+1}} \left| \frac{\partial^3 \tilde{s}^{n+1}}{\partial \xi^3} \right| d\xi \right], \\ &\leq CN^{-2} + C\Delta t N^{-2}, \end{aligned} \quad (5.164)$$

and for $j = N/2$, to the case $\varepsilon > \|v_2\|N^{-1}$,

$$\begin{aligned} |\tau_{2, \tilde{s}^{n+1}}^{N, \Delta t}(x_i, y_j)| &\leq |(\tilde{S}_{i,j}^{n+1/2} - \tilde{s}^{n+1/2}(x_i, y_j))| + \\ &\quad \Delta t \left[C\varepsilon \int_{y_{j-1}}^{y_{j+1}} \left| \frac{\partial^3 \tilde{s}^{n+1}}{\partial \xi^3} \right| d\xi + Ch_{y_j} \int_{y_{j-1}}^{y_{j+1}} \left| \frac{\partial^3 \tilde{s}^{n+1}}{\partial \xi^3} \right| d\xi \right], \\ &\leq CN^{-2} + C\Delta t(\varepsilon + N^{-1})N^{-1}. \end{aligned} \quad (5.165)$$

Now, for the region $1 \leq j \leq N/2$, when $\varepsilon \leq \|v_2\|N^{-1}$, we deduce that

$$\begin{aligned} & \tilde{S}_{i, j-\frac{1}{2}}^{n+1} + \Delta t \mathbb{L}_{2, mup, N}^{n+1} \tilde{S}_{i,j}^{n+1} + \Delta t \left[b(x_i, y_{j-\frac{1}{2}}, t_{n+1}, \tilde{S}_{i, j-\frac{1}{2}}^{n+1}) - b(x_i, y_{j-\frac{1}{2}}, t_{n+1}, \tilde{s}^{n+1}(x_i, y_{j-\frac{1}{2}})) \right] \\ &= \tilde{S}_{i, j-\frac{1}{2}}^{n+1/2} - \tilde{s}^{n+1/2}(x_i, y_{j-\frac{1}{2}}) + \tilde{s}^{n+1}(x_i, y_{j-\frac{1}{2}}) + \Delta t \mathbb{L}_{2, \varepsilon}^{n+1} \tilde{s}^{n+1}(x_i, y_{j-\frac{1}{2}}). \end{aligned} \quad (5.166)$$

We rewrite the above equation as follows:

$$\begin{aligned}
& \left(\tilde{S}_{i,j-\frac{1}{2}}^{n+1} - \frac{\tilde{s}^{n+1}(x_i, y_{j-1}) + \tilde{s}^{n+1}(x_i, y_j)}{2} \right) + \Delta t \mathbb{L}_{2,mup,N}^{n+1}(\tilde{S}_{i,j}^{n+1} - \tilde{s}^{n+1}(x_i, y_j)) + \\
& \Delta t \left[\int_0^1 \frac{\partial b(x_i, y_{j-\frac{1}{2}}, t_{n+1}, \tilde{S}_{i,j-\frac{1}{2}}^{*,n+1}(\xi))}{\partial u} d\xi \right] \left(\tilde{S}_{i,j-\frac{1}{2}}^{n+1} - \frac{\tilde{s}^{n+1}(x_i, y_{j-1}) + \tilde{s}^{n+1}(x_i, y_j)}{2} \right) \\
& = \tilde{S}_{i,j-\frac{1}{2}}^{n+1/2} - \tilde{s}^{n+1/2}(x_i, y_{j-\frac{1}{2}}) + \Delta t \left[\left(\mathbb{L}_{2,\varepsilon}^{n+1} \tilde{s}^{n+1} \right)_{i,j-\frac{1}{2}} - \mathbb{L}_{2,mup,N}^{n+1} \tilde{s}^{n+1}(x_i, y_j) \right] + O(h_{y_j})^2,
\end{aligned} \tag{5.167}$$

where $\tilde{S}_{i,j-\frac{1}{2}}^{*,n+1}(\xi) = \frac{\tilde{s}^{n+1}(x_i, y_{j-1}) + \tilde{s}^{n+1}(x_i, y_j)}{2} + \xi \left(\tilde{S}_{i,j-\frac{1}{2}}^{n+1} - \frac{\tilde{s}^{n+1}(x_i, y_{j-1}) + \tilde{s}^{n+1}(x_i, y_j)}{2} \right)$. Afterwards, from (5.167) and by using the derivative bounds of \tilde{s}^{n+1} given in Lemma 5.23, we obtain that

$$\begin{aligned}
& |\tau_{2,\tilde{s}^{n+1}}^{N,\Delta t}(x_i, y_j)| \leq |(\tilde{S}_{i,j-1/2}^{n+1/2} - \tilde{s}^{n+1/2}(x_i, y_{j-1/2}))| + \\
& \Delta t \left[C\varepsilon \int_{y_{j-1}}^{y_{j+1}} \left| \frac{\partial^3 \tilde{s}^{n+1}}{\partial \xi^3} \right| d\xi + Ch_{y_j} \int_{y_{j-1}}^{y_{j+1}} \left| \frac{\partial^3 \tilde{s}^{n+1}}{\partial \xi^3} \right| d\xi \right], \\
& \leq CN^{-2} + C\Delta t N^{-2}.
\end{aligned} \tag{5.168}$$

Finally, for $N/2 < j < N$,

$$\begin{aligned}
& |\tau_{2,\tilde{s}^{n+1}}^{N,\Delta t}(x_i, y_j)| \leq |(\tilde{S}_{i,j}^{n+1/2} - \tilde{s}^{n+1/2}(x_i, y_j))| + \\
& \Delta t \left[C\varepsilon h_{y_j} \int_{y_{j-1}}^{y_{j+1}} \left| \frac{\partial^4 \tilde{s}^{n+1}}{\partial \xi^4} \right| d\xi + Ch_{y_j} \int_{y_{j-1}}^{y_{j+1}} \left| \frac{\partial^3 \tilde{s}^{n+1}}{\partial \xi^3} \right| d\xi \right], \\
& \leq CN^{-2} + C\Delta t N^{-2}.
\end{aligned} \tag{5.169}$$

Consider the following discrete functions in the domain $0 \leq j \leq N$, for the case $\varepsilon > \|v_2\|N^{-1}$:

$$\Psi^\pm(x_i, y_j) = -CN^{-2}y_j - CN^{-2}\varphi_{2,j} \pm (\tilde{S}_{i,j}^{n+1} - \tilde{s}^{n+1}(x_i, y_j)),$$

where

$$\varphi_{2,j} = \begin{cases} \frac{y_j}{1-\eta_2}, & \text{for } 0 \leq j \leq N/2, \\ 1, & \text{for } N/2 \leq j \leq N, \end{cases}$$

and apply Corollary 5.3 for the operator $\mathbb{L}_{2,\varepsilon,\tilde{S}^*}^{N,\Delta t}$ together with the local truncation bound in (5.164), (5.165) and (5.169), to obtain that

$$|\tilde{S}_{i,j}^{n+1} - \tilde{s}^{n+1}(x_i, y_j)| \leq CN^{-2}, \quad \text{for } 0 \leq j \leq N. \tag{5.170}$$

In the same way, we choose the following discrete functions in the domain $0 \leq j \leq N$, for the case $\varepsilon \leq \|v_2\|N^{-1}$:

$$\Psi^\pm(x_i, y_j) = -CN^{-2}y_j \pm (\tilde{S}_{i,j}^{n+1} - \tilde{s}^{n+1}(x_i, y_j)),$$

and apply Corollary 5.3 for the operator $\mathbb{L}_{2,\varepsilon,\tilde{S}^*}^{N,\Delta t}$ together with the local truncation bound in (5.168) and (5.169), to obtain that

$$|\tilde{S}_{i,j}^{n+1} - \tilde{s}^{n+1}(x_i, y_j)| \leq CN^{-2}, \quad \text{for } 0 \leq j \leq N. \quad (5.171)$$

Hence, the proof is over. ■

Lemma 5.29. *Let $x_i \in \bar{\mathbf{G}}_x^N$. If $\lambda_l < \mathfrak{m}_l/2$ and $\eta_{l,0} \geq 2/\lambda_l$, $l = 1, 2$, the local error associated to the layer component at $(n+1)^{\text{th}}$ time level satisfies the following estimate:*

$$|\tilde{Z}_{i,j}^{n+1} - \tilde{z}^{n+1}(x_i, y_j)| \leq \begin{cases} CN^{-2}, & \text{for } y_j \in [0, 1 - \eta_2] \cap \bar{\mathbf{G}}_y^N, \\ CN^{-2} \ln^2 N, & \text{for } y_j \in (1 - \eta_2, 1] \cap \bar{\mathbf{G}}_y^N. \end{cases} \quad (5.172)$$

Proof. Here, for any mesh function Ψ , we introduce a linear discrete operator $\mathbb{L}_{2,\varepsilon,\tilde{Z}^*}^{N,\Delta t}$ defined by

$$\mathbb{L}_{2,\varepsilon,\tilde{Z}^*}^{N,\Delta t} \Psi = \tilde{\mathbb{T}}_{2,\varepsilon,(\tilde{U},\tilde{S})}^{N,\Delta t} \Psi,$$

where $\tilde{Z}_j^{*,n+1}(\xi) = \tilde{S}_{i,j}^{n+1} + \xi(\tilde{U}_{i,j}^{n+1} - \tilde{S}_{i,j}^{n+1})$. Then, we rewrite the discrete problem (5.146) in the following form:

$$\begin{cases} \mathbb{L}_{2,\varepsilon,\tilde{Z}^*}^{N,\Delta t} \tilde{Z}_{i,j}^{n+1} = \tilde{Z}_{i,j}^{n+1/2}, & \text{for } 1 \leq i, j \leq N-1, \\ \tilde{Z}_{i,0}^{n+1} = \tilde{z}^{n+1}(x_i, y_0), & \tilde{Z}_{i,N}^{n+1} = \tilde{z}^{n+1}(x_i, y_N). \end{cases}$$

From the equation (5.142) and Lemma 5.23, we have $\tilde{Z}_{0,j}^{n+1} = 0$ and $|\tilde{Z}_{N,j}^{n+1}| = |\tilde{z}^{n+1}(1, y_j)| \leq C$. We choose the discrete functions for $0 \leq j \leq N$,

$$\Psi^\pm(x_i, y_j) = -C\Theta_{2,j}(\lambda_2) \pm \tilde{Z}_{i,j}^{n+1}, \quad (5.173)$$

for sufficiently large C . By Corollary 5.3 for the operator $\mathbb{L}_{2,\varepsilon,\tilde{Z}^*}^{N,\Delta t}$ and invoking Lemma 5.25, we obtain that

$$|\tilde{Z}_{i,j}^{n+1}| \leq C\Theta_{2,j}(\lambda_2). \quad (5.174)$$

Now, for $\lambda_2 < \mathfrak{m}_2/2$, combining (5.174) and Lemma 5.23, we get

$$|\tilde{Z}_{i,j}^{n+1} - \tilde{z}^{n+1}(x_i, y_j)| \leq |\tilde{Z}_{i,j}^{n+1}| + |\tilde{z}^{n+1}(x_i, y_j)| \leq C\Theta_{2,j}(\lambda_2). \quad (5.175)$$

Again, for $\eta_{2,0} \geq \frac{2}{\lambda_2}$, it follows from [Chapter 3, Lemma 3.8] and the equation (5.175) for $1 \leq j \leq N/2$,

$$|\tilde{Z}_{i,j}^{n+1} - \tilde{z}^{n+1}(x_i, y_j)| \leq CN^{-2}. \quad (5.176)$$

Next, we estimate $|\tilde{Z}_{i,j}^{n+1} - \tilde{z}^{n+1}(x_i, y_j)|$ on the fine part of the mesh by using consistency and barrier function argument on the interval $[0, 1] \times [1 - \eta_2, 1]$. Here, we have $|\tilde{Z}_{i,N/2}^{n+1} - \tilde{z}^{n+1}(x_i, y_{N/2})| \leq CN^{-2}$ and $|\tilde{Z}_{i,N}^{n+1/2} - \tilde{z}^{n+1/2}(x_i, y_N)| = 0$. From (5.142) and (5.146), we obtain local truncation error by using the derivative bound

of \tilde{z}^{n+1} , from the Lemma 5.23. For $N/2 < j < N$, we have

$$\begin{aligned} & \left(\mathbf{I} + \Delta t \mathbb{L}_{2, mcd, N}^{n+1} \right) \tilde{Z}_{i,j}^{n+1} + \Delta t \left[b(x_i, y_j, t_{n+1}, \tilde{U}_{i,j}^{n+1}) - b(x_i, y_j, t_{n+1}, \tilde{u}^{n+1}(x_i, y_j)) \right] \\ &= \tilde{Z}_{i,j}^{n+1/2} - \tilde{z}^{n+1/2}(x_i, y_j) + \left(\mathbf{I} + \Delta t \mathbb{L}_{2, \varepsilon}^{n+1} \right) \tilde{z}^{n+1}(x_i, y_j) + \\ & \Delta t \left[b(x_i, y_j, t_{n+1}, \tilde{S}_{i,j}^{n+1}) - b(x_i, y_j, t_{n+1}, \tilde{s}^{n+1}(x_i, y_j)) \right]. \end{aligned} \quad (5.177)$$

From the above equation, we have

$$\begin{aligned} & \left(\mathbf{I} + \Delta t \mathbb{L}_{2, mcd, N}^{n+1} \right) (\tilde{Z}_{i,j}^{n+1} - \tilde{z}^{n+1}(x_i, y_j)) + \Delta t \left[\int_0^1 \frac{\partial b(x_i, y_j, t_{n+1}, \tilde{U}_{i,j}^{*,n+1}(\xi))}{\partial u} d\xi \right] (\tilde{Z}_{i,j}^{n+1} - \tilde{z}^{n+1}(x_i, y_j)) \\ &= \tilde{Z}_{i,j}^{n+1/2} - \tilde{z}^{n+1/2}(x_i, y_j) + \Delta t \left[-\varepsilon \left(\frac{\partial^2}{\partial y^2} - \delta_y^2 \right) \tilde{z}^{n+1}(x_i, y_j) + v_2(x_i, y_j, t_{n+1}) \left(\frac{\partial}{\partial y} - D_y^* \right) \tilde{z}^{n+1}(x_i, y_j) \right] + \\ & \Delta t \left[\int_0^1 \frac{\partial b(x_i, y_j, t_{n+1}, \tilde{S}_{i,j}^{*,n+1}(\xi))}{\partial u} d\xi - \int_0^1 \frac{\partial b(x_i, y_j, t_{n+1}, \tilde{U}_{i,j}^{*,n+1}(\xi))}{\partial u} d\xi \right] (\tilde{S}_{i,j}^{n+1} - \tilde{s}^{n+1}(x_i, y_j)), \end{aligned} \quad (5.178)$$

where $\tilde{S}_{i,j}^{*,n+1}(\xi) = \tilde{s}^{n+1}(x_i, y_j) + \xi(\tilde{S}_{i,j}^{n+1} - \tilde{s}^{n+1}(x_i, y_j))$ and $\tilde{U}_{i,j}^{*,n+1}(\xi) = \tilde{u}^{n+1}(x_i, y_j) + \xi(\tilde{U}_{i,j}^{n+1} - \tilde{u}^{n+1}(x_i, y_j))$. Now, for any mesh function Ψ , we introduce a discrete operator $\mathbb{L}_{2, \varepsilon, \tilde{U}^*}^{N, \Delta t}$ given by

$$\mathbb{L}_{2, \varepsilon, \tilde{U}^*}^{N, \Delta t} \Psi = \tilde{\mathbb{T}}_{2, \varepsilon, (\tilde{U}, \tilde{u})}^{N, \Delta t} \Psi.$$

Now, using derivative bound of $\tilde{z}^{n+1}(x, y)$ from Lemma 5.23, and Lemma 5.28, we obtain from (5.178) that for $N/2 < j < N$,

$$\begin{aligned} & \left| \mathbb{L}_{2, \varepsilon, \tilde{U}^*}^{N, \Delta t} (\tilde{Z}_{i,j}^{n+1} - \tilde{z}^{n+1}(x_i, y_j)) \right| \leq \left| (\tilde{Z}_{i,j}^{n+1/2} - \tilde{z}^{n+1/2}(x_i, y_j)) \right| + \\ & \Delta t \left[C\varepsilon h_{y_j} \int_{y_{j-1}}^{y_{j+1}} \left| \frac{\partial^4 \tilde{z}^{n+1}}{\partial \xi^4} \right| d\xi + Ch_{y_j} \int_{y_{j-1}}^{y_{j+1}} \left| \frac{\partial^3 \tilde{z}^{n+1}}{\partial \xi^3} \right| d\xi \right] + C\Delta t |\tilde{S}_{i,j}^{n+1} - \tilde{s}^{n+1}(x_i, y_j)|, \quad (5.179) \\ & \leq CN^{-2} \ln^2 N + C\Delta t N^{-2} \ln^2 N \varepsilon^{-1} \exp(-\mathfrak{m}_2(1 - y_j)/\varepsilon) + C\Delta t N^{-2}. \end{aligned}$$

We choose the discrete functions for $N/2 \leq j \leq N$,

$$\Psi^\pm(x_i, y_j) = -C(N^{-2} \ln^2 N) y_j - C(N^{-2} \ln^2 N) \Theta_{2,j}(\lambda_2) \pm (\tilde{Z}_{i,j}^{n+1} - \tilde{z}^{n+1}(x_i, y_j)).$$

Lemma 5.25 implies that $\mathbb{L}_{2, \varepsilon, \tilde{U}^*}^{N, \Delta t} \Theta_{2,j}(\lambda_2) \geq \frac{C\Delta t}{\varepsilon} \Theta_{2,j}(\lambda_2)$, for $N/2 < j \leq N-1$, and hence, use of (5.179) for $\lambda_2 < \mathfrak{m}_2/2$ yields that

$$\mathbb{L}_{2, \varepsilon, \tilde{U}^*}^{N, \Delta t} \Psi^\pm(x_i, y_j) \leq 0.$$

Now, apply Corollary 5.3 for the operator $\mathbb{L}_{2, \varepsilon, \tilde{U}^*}^{N, \Delta t}$ to get $\Psi^\pm(x_i, y_j) \leq 0$, for all $N/2 \leq j \leq N$. Hence, the proof is over. ■

We decompose the error at $(n+1)^{th}$ level in the following form:

$$\tilde{U}_{i,j}^{n+1} - \tilde{u}^{n+1}(x_i, y_j) = \tilde{S}_{i,j}^{n+1} - \tilde{s}^{n+1}(x_i, y_j) + \tilde{Z}_{i,j}^{n+1} - \tilde{z}^{n+1}(x_i, y_j), \quad 0 \leq i, j \leq N.$$

Hence, the required ε -uniform error estimate at $(n+1)^{th}$ level are given in the following Lemma.

Lemma 5.30. *If $\lambda_l < \mathfrak{m}_l/2$ and $\eta_{l,0} \geq 2/\lambda_l$, $l = 1, 2$, the error associated with the discrete problem (5.144) at $(n+1)^{th}$ time level satisfies the following estimate:*

$$|\tilde{U}_{i,j}^{n+1} - \tilde{u}^{n+1}(x_i, y_j)| \leq \begin{cases} CN^{-2}, & \text{for } (x_i, y_j) \in ([0, 1 - \eta_1] \times [0, 1 - \eta_2]) \cap \bar{\mathbf{G}}^N, \\ CN^{-2} \ln^2 N, & \text{otherwise.} \end{cases} \quad (5.180)$$

5.4.2.2 Uniform convergence of the proposed fractional-step method

We define $E^{n+1}(x_i, y_j) = [U_{i,j}^{n+1} - u(x_i, y_j, t_{n+1})]$, for $(x_i, y_j) \in \bar{\mathbf{G}}^N$, as the global error related to the fully discrete scheme (5.102) at the time level t_{n+1} . Now, to show the ε -uniform convergence of the fully discrete scheme (5.102), we rewrite the global error in the following form:

$$E^{n+1}(x_i, y_j) = \tilde{e}^{n+1}(x_i, y_j) + \tilde{E}^{n+1}(x_i, y_j) + [U_{i,j}^{n+1} - \tilde{U}_{i,j}^{n+1}]. \quad (5.181)$$

Here, $\tilde{e}^{n+1}(x_i, y_j) = [\tilde{u}^{n+1}(x_i, y_j) - u(x_i, y_j, t_{n+1})]$ and $\tilde{E}^{n+1}(x_i, y_j) = [\tilde{U}_{i,j}^{n+1} - \tilde{u}^{n+1}(x_i, y_j)]$, respectively, denote the local error related to the time semidiscretization of the IBVP (5.1)-(5.3) and the spatial discretization of the auxiliary BVP (5.90) at time level t_{n+1} . We see that, the term $[U_{i,j}^{n+1} - \tilde{U}_{i,j}^{n+1}]$ can be written as the solution of the following systems:

$$\begin{cases} \mathbb{L}_{1,\varepsilon}^{N,\Delta t} \mathbb{L}_{2,\varepsilon}^{N,\Delta t} R^{n+1}(x_i, y_j) + \Delta t \left[\int_0^1 \frac{\partial b(x_i, y_j, t_{n+1}, \tilde{U}_{i,j}^{n+1} + \xi(U_{i,j}^{n+1} - \tilde{U}_{i,j}^{n+1}))}{\partial u} d\xi \right] R^{n+1}(x_i, y_j) = \\ U_{i,j}^n - u(x_i, y_j, t_n) + O(\Delta t)^2, & \text{in } \mathbf{G}^N, \\ R^{n+1}(x_i, y_j) = 0, & \partial \mathbf{G}^N, \end{cases}$$

where $R^{n+1}(x_i, y_j) = [U_{i,j}^{n+1} - \tilde{U}_{i,j}^{n+1}]$, and by employing the discrete maximum principle in Lemma 5.20, we obtain that

$$\left\| \left\{ R^{n+1}(x_i, y_j) \right\}_{i,j} \right\| \leq \left\| \left\{ E^n(x_i, y_j) \right\}_{i,j} \right\| + C(\Delta t)^2. \quad (5.182)$$

Afterwards, from (5.181) and (5.182), we obtain that

$$\left\| \left\{ E^{n+1}(x_i, y_j) \right\}_{i,j} \right\| \leq \left\| \left\{ \tilde{e}^{n+1}(x_i, y_j) \right\}_{i,j} \right\| + \left\| \left\{ \tilde{E}^{n+1}(x_i, y_j) \right\}_{i,j} \right\| + \left\| \left\{ E^n(x_i, y_j) \right\}_{i,j} \right\| + C(\Delta t)^2, \\ \text{for } (x_i, y_j) \in \bar{\mathbf{G}}^N. \quad (5.183)$$

Now, by invoking the estimate obtained in Lemma 5.18 and the estimate 5.180 in (5.183), with the assumption that $N^{-\delta} \leq C\Delta t$, $0 < \delta < 1$, we obtain the following estimate of the global error.

Theorem 5.5 (Global error). *Assume that the conditions given in (5.103) and (5.104) hold for $N \geq N_0$. Then, if $\lambda_l < \mathfrak{m}_l/2$, $\eta_{l,0} \geq 2/\lambda_l$, $l = 1, 2$, the global error associated with the fully discrete scheme (5.102) at time*

level t_{n+1} , satisfies the following estimate:

$$\left\| \left\{ U_{i,j}^{n+1} \right\}_{i,j} - \left\{ u(x_i, y_j, t_{n+1}) \right\}_{i,j} \right\| \leq \begin{cases} C(N^{-2+\delta} + \Delta t), \\ \text{for } (x_i, y_j) \in ([0, 1 - \eta_1] \times [0, 1 - \eta_2]) \cap \bar{\mathcal{G}}^N, \\ C(N^{-2+\delta} \ln^2 N + \Delta t), \quad \text{for otherwise,} \end{cases} \quad (5.184)$$

where N and Δt are such that $N^{-\delta} \leq C\Delta t$ with $0 < \delta < 1$.

Remark 5.4. Note the temporal accuracy in Theorem 5.4 holds under the alternative boundary data given in (5.83).

5.5 The temporal Richardson extrapolation

In this section, we analyze the Richardson extrapolation in the time variable in order to improve the order of uniform convergence in the temporal direction established in Theorem 5.5 so that we can produce higher-order accurate numerical solution at low computational cost. On the domain $[0, T]$, we construct a fine mesh, denoted by $\Lambda^{\Delta t/2} = \{\tilde{t}_n\}_{n=0}^{2M}$, by bisecting each mesh interval of $\Lambda^{\Delta t}$. So, $\tilde{t}_{n+1} - \tilde{t}_n = T/2M = \Delta t/2$ is the step-size $\Lambda^{\Delta t/2}$. To serve this purpose, we follow the approach given in [Chapter 3, Section 3.5].

Let $u^{\Delta t}(x, y, t_{n+1})$ and $u^{\Delta t/2}(x, y, \tilde{t}_{n+1})$ be the respective solutions of the time-semidiscrete problem (5.81) on the mesh $\bar{\mathcal{G}} \times \Lambda^{\Delta t}$ and $\bar{\mathcal{G}} \times \Lambda^{\Delta t/2}$ such that $u^{\Delta t}(x_i, y_j, t_{n+1}) \approx U^{N, \Delta t}(x_i, y_j, t_{n+1})$ and $u^{\Delta t/2}(x_i, y_j, \tilde{t}_{n+1}) \approx U^{N, \Delta t/2}(x_i, y_j, \tilde{t}_{n+1})$, $(x_i, y_j) \in \bar{\mathcal{G}}^N$. Utilizing global error Theorem 5.4, one can show that when $\Delta t \rightarrow 0$, the global error of time semidiscrete scheme (5.81) hold the relation

$$u^{\Delta t}(x, y, t_{n+1}) = u(x, y, t_{n+1}) + \Delta t \Psi(x, y, t_{n+1}) + \mathcal{R}(x, y, t_{n+1}), \quad (5.185)$$

where Ψ is a certain smooth function defined on $\bar{\mathcal{G}} \times \Lambda^{\Delta t}$ and independent of Δt ; \mathcal{R} is the remainder term defined on $\bar{\mathcal{G}} \times \Lambda^{\Delta t}$. We begin by assuming that the expansion (5.185) is valid. We substitute $u^{\Delta t}(x, y, t_{n+1})$ in (5.81) and obtain that

$$\left\{ \begin{array}{l} u(x, y, 0) + \Delta t \Psi(x, y, 0) + \mathcal{R}(x, y, 0) = \mathbf{q}_0(x, y), \quad (x, y) \in \bar{\mathcal{G}}, \\ (\mathbf{I} + \Delta t \mathbb{L}_{1, \varepsilon}^{n+1}) \left[(\mathbf{I} + \Delta t \mathbb{L}_{2, \varepsilon}^{n+1}) (u(x, y, t_{n+1}) + \Delta t \Psi(x, y, t_{n+1}) + \mathcal{R}(x, y, t_{n+1})) + \right. \\ \left. \Delta t b(x, y, t_{n+1}, u(x, y, t_{n+1}) + \Delta t \Psi(x, y, t_{n+1}) + \mathcal{R}(x, y, t_{n+1})) - \Delta t g_2(x, y, t_{n+1}) \right] = \\ u(x, y, t_n) + \Delta t \Psi(x, y, t_n) + \mathcal{R}(x, y, t_n) + \Delta t g_1(x, y, t_{n+1}), \quad (x, y, t_{n+1}) \in \mathcal{G} \times \Lambda^{\Delta t}, \\ u(x, y, t_{n+1}) + \Delta t \Psi(x, y, t_{n+1}) + \mathcal{R}(x, y, t_{n+1}) = \mathbf{s}(x, y, t_{n+1}), \quad (x, y) \in \partial \mathcal{G} \times \Lambda^{\Delta t}, \\ n = 0, 1, \dots, M-1. \end{array} \right. \quad (5.186)$$

By following the approach in [60] to the problem (5.186), we get the function $\Psi(x, y, t)$ is the solution of the

following IBVP:

$$\left\{ \begin{array}{l} \left(\frac{\partial}{\partial t} + \mathbb{L}_\varepsilon + \frac{\partial b(x, y, t, u(x, y, t))}{\partial u} \right) \Psi(x, y, t) = \frac{1}{2} \frac{\partial^2 u(x, y, t)}{\partial t^2} + \\ \mathbb{L}_{1,\varepsilon} \left(g_2(x, y, t) - b(x, y, t, u(x, y, t)) \right) - \mathbb{L}_{1,\varepsilon} \mathbb{L}_{2,\varepsilon} u(x, y, t), \\ \Psi(x, y, 0) = 0, \quad (x, y) \in \bar{\mathbf{G}} \\ \Psi(x, y, t) = 0, \quad \text{in } \partial \mathbf{G} \times (0, T]. \end{array} \right. \quad (5.187)$$

Since $\frac{1}{2} \frac{\partial^2 u(x, y, t)}{\partial t^2} + \mathbb{L}_{1,\varepsilon} \left(g_2(x, y, t) - b(x, y, t, u(x, y, t)) \right) - \mathbb{L}_{1,\varepsilon} \mathbb{L}_{2,\varepsilon} u(x, y, t)$ is ε -uniformly bounded, one can derive that $\|\Psi(x, y, t)\|_{\bar{\mathbf{D}}} \leq C$. To establish the bounds of the derivatives up to second order in time in Lemma 5.31, we require $\Psi(x, y, t) \in \mathcal{C}^{4+\gamma}(\bar{\mathbf{D}})$.

Lemma 5.31. *The function $\Psi(x, y, t)$ solution of (5.187) satisfies the bounds*

$$\left| \frac{\partial^k \Psi(x, y, t)}{\partial t^k} \right| \leq C, \quad k = 0, 1, 2.$$

Proof. The proof of this lemma is obtained by using the argument given in [20]. ■

Lemma 5.32. *The remainder term $\mathbf{R}(x, y, t)$ given in (5.185), satisfies the bound*

$$|\mathbf{R}(x, y, t_n)| \leq C(\Delta t)^2, \quad 0 \leq n \leq M. \quad (5.188)$$

Proof. Using the equation (5.187) and the Taylor-series expansion of the functions u and Ψ with respect to time variable t in (5.186), the remainder term in (5.185) is the solution of the following IBVP:

$$\left\{ \begin{array}{l} \mathbf{R}(x, y, 0) = 0, \quad (x, y) \in \bar{\mathbf{G}}, \\ (\mathbf{I} + \Delta t \mathbb{L}_{2,\varepsilon}^{n+1}) \left[(\mathbf{I} + \Delta t \mathbb{L}_{1,\varepsilon}^{n+1}) \mathbf{R}(x, y, t_{n+1}) + \Delta t \frac{\partial b(x, y, t_{n+1}, \eta^{\Delta t}(x, y))}{\partial u} \mathbf{R}(x, y, t_{n+1}) \right] = \\ \mathbf{R}(x, y, t_n) + O(\Delta t)^3, \quad (x, y) \in \mathbf{G}, \\ \mathbf{R}(x, y, t_{n+1}) = 0, \quad (x, y) \in \partial \mathbf{G}, \quad n = 0, \dots, M-1, \end{array} \right. \quad (5.189)$$

where $\eta^{\Delta t}$ belong to some finite interval $[-C, C]$. Finally, using the above relation recursively and by invoking the stability in Lemmas 5.14 and 5.16, we obtain the desired bound of the remainder term. ■

Theorem 5.6. *Let $u^{\Delta t}(x, y, t_{n+1})$ and $u^{\Delta t/2}(x, y, \tilde{t}_{n+1})$ be the respective solutions of the time-semidiscrete problem (5.81) on the mesh $\bar{\mathbf{G}} \times \wedge^{\Delta t}$ and $\bar{\mathbf{G}} \times \wedge^{\Delta t/2}$; and let $u(x, y, t_{n+1})$ be the exact solution of the IBVP (5.1)-(5.3) on the mesh $\bar{\mathbf{G}} \times [0, T]$. Then the error due to the temporal extrapolation defined by*

$$u_{extp}^{\Delta t}(x, y, t_{n+1}) = \left(2u^{\Delta t/2}(x, y, t_{n+1}) - u^{\Delta t}(x, y, t_{n+1}) \right), \quad (x, y, t_{n+1}) \in \bar{\mathbf{G}} \times \wedge^{\Delta t},$$

satisfies that

$$|u_{extp}^{\Delta t}(x, y, t_{n+1}) - u(x, y, t_{n+1})| \leq C(\Delta t)^2, \quad (x, y, t_{n+1}) \in \bar{\mathbf{G}} \times \wedge^{\Delta t}.$$

Proof. From the equation (5.185) and Lemma 5.32, we obtain that

$$u(x, y, t_{n+1}) = u^{\Delta t}(x, y, t_{n+1}) - \Delta t \Psi(x, y, t_{n+1}) + O(\Delta t)^2, \quad (x, y, t_{n+1}) \in \bar{\mathbf{G}}^N \times \Lambda^{\Delta t}.$$

Similarly, we have

$$u(x, y, \tilde{t}_{n+1}) = u^{\Delta t/2}(x, y, \tilde{t}_{n+1}) - (\Delta t/2) \Psi(x, y, \tilde{t}_{n+1}) + O(\Delta t)^2, \quad (x, y, \tilde{t}_{n+1}) \in \bar{\mathbf{G}}^N \times \Lambda^{\Delta t/2}.$$

Now, using the above two expressions, we obtain the desired result.

5.6 Numerical experiments

In this section, we present the numerical results before and after applying the extrapolation technique for the test problem of the form (5.1)-(5.3), utilizing the proposed FMMs in (5.37) and (5.102). For all the test examples, we choose $\eta_0 = 2.2$ and implement the Thomas algorithm to solve the tridiagonal linear systems involved in our methods. The numerical results are also compared with the fully-implicit upwind FMM, which is mentioned below as well. In this case, we decompose the right-hand side in the form $g(x, y, t) = g_1(x, y, t) + g_2(x, y, t)$, where $g_2(x, y, t) = g(x, 0, t) + y(g(x, 1, t) - g(x, 0, t))$, $g_1(x, y, t) = g(x, y, t) - g_2(x, y, t)$.

5.6.1 The fully-implicit upwind FSFMM

Then, the fully discrete scheme takes the following form on $\bar{\mathbf{D}}^{N, \Delta t}$:

$$\begin{aligned} (i) \quad & U_{i,j}^0 = q_0(x_i, y_j), \quad \text{for } i, j = 0, 1, \dots, N, \\ (ii) \quad & \begin{cases} U_{i,j}^{n+1/2} + \Delta t \mathbb{L}_{1,\varepsilon,up}^{n+1} U_{i,j}^{n+1/2} = U_{i,j}^n + \Delta t g_1(x_i, y_j, t_{n+1}), & \text{for } 1 \leq i \leq N, \quad y_j \in \mathbf{G}_y^N, \\ U_{i,j}^{n+1/2} = \mathbf{s}^{n+1/2}(x_i, y_j), & i = 0, N, \quad y_j \in \bar{\mathbf{G}}_y^N, \end{cases} \\ (iii) \quad & \begin{cases} U_{i,j}^{n+1} + \Delta t \mathbb{L}_{2,\varepsilon,up}^{n+1} U_{i,j}^{n+1} + \Delta t b(x_i, y_j, t_{n+1}, U_{i,j}^{n+1}) = U_{i,j}^{n+1/2} + \Delta t g_2(x_i, y_j, t_{n+1}), \\ & \text{for } 1 \leq j \leq N-1, \quad x_i \in \mathbf{G}_x^N \\ U_{i,j}^{n+1} = \mathbf{s}^{n+1}(x_i, y_j), & j = 0, N, \quad x_i \in \bar{\mathbf{G}}_x^N, \end{cases} \end{aligned} \quad (5.190)$$

where $\mathbf{s}^{n+1/2}(x_i, y_j)$, $\mathbf{s}^{n+1}(x, y)$ are defined in (5.83) and $\mathbb{L}_{1,N,up}^{n+1}$, $\mathbb{L}_{2,N,up}^{n+1}$ are given by

$$\begin{cases} \mathbb{L}_{1,N,up}^{n+1} U_{i,j}^{n+1/2} = -\varepsilon \delta_x^2 U_{i,j}^{n+1/2} + v_1(x_i, y_j, t_{n+1}) D_x^- U_{i,j}^{n+1/2}, \\ \mathbb{L}_{2,N,up}^{n+1} U_{i,j}^{n+1} = -\varepsilon \delta_y^2 U_{i,j}^{n+1} + v_2(x_i, y_j, t_{n+1}) D_y^- U_{i,j}^{n+1}. \end{cases}$$

The existence and stability of the solution $U_{i,j}^{n+1}$ of the nonlinear discrete problem (5.190) can be obtained in the same way as in Section 5.3.2. Furthermore, following the error analysis given in Section 5.3.2, one can prove ε -uniform error estimate for the FMM (5.190).

Theorem 5.7 (Global error). *Let $u(x, y, t)$ be the exact solution of the IVBP (5.1)-(5.3) and $U_{i,j}^{n+1}$ be the discrete solution of the fully discrete scheme (5.190), at time level t_{n+1} . Then, if $\lambda_l < \frac{m_l}{2}$, $\eta_{l,0} \geq \frac{2}{\lambda_l}$, $l = 1, 2$, the error*

associated with the fully discrete scheme (5.190) at time level t_{n+1} satisfies the following estimate:

$$\left\| \left\{ U_{i,j}^{n+1} \right\}_{i,j} - \left\{ u(x_i, y_j, t_{n+1}) \right\}_{i,j} \right\| \leq \begin{cases} C(N^{-1+\delta} + \Delta t), & \text{for } 0 \leq i, j \leq N/2, \\ C(N^{-1+\delta} \ln N + \Delta t), & \text{for otherwise,} \end{cases}$$

where N and Δt are such that $N^{-\delta} \leq C\Delta t$ with $0 < \delta < 1$.

5.6.2 Test example

Example 5.1. Consider the following parabolic IBVP:

$$\begin{cases} \frac{\partial u}{\partial t} - \varepsilon \Delta u + (1+x(1-x)) \frac{\partial u}{\partial x} + (1+y(1-y)) \frac{\partial u}{\partial y} + \frac{u-4}{5-u} = g(x, y, t), & \text{in } D, \\ u(x, y, t) = q_0(x, y), & \text{in } \bar{G}, \\ u(x, y, t) = s(x, y, t), & \text{in } \partial G \times (0, T], \end{cases} \quad (5.191)$$

where g, q_0, s are obtained from the exact solution which is given by

$$u(x, y, t) = \exp(-t) \left[\left(\frac{1 - \exp(-(1-x)/\varepsilon)}{1 - \exp(-1/\varepsilon)} \right) \left(\frac{1 - \exp(-(1-y)/\varepsilon)}{1 - \exp(-1/\varepsilon)} \right) - xy \right].$$

In the same way as we computed the results in Chapter 3, we determine the maximum nodal error and the related order of convergence for each ε .

To compute the numerical solution of the FMMs in (5.102) and (5.190) for Example 5.1, a nonlinear system needs to be solved at each time step. For that, we use the Newton's iterative method as we define in Chapter 4.

5.6.3 Numerical results and observations

We choose all the values of ε from $\mathbb{S}_\varepsilon = \{2^0, 2^{-2}, \dots, 2^{-20}\}$, for computation of ε -uniform errors. For different values of ε, N and Δt , the computed ε -uniform errors and order of convergence are displayed in Tables 5.1 and 5.2 for both choices of boundary conditions (5.21), (5.22), (5.82) and (5.83) without using the temporal Richardson extrapolation for Examples 5.1. This shows the monotonically decreasing behavior of the ε -uniform errors with increasing N , and it represents the ε -uniform convergence of the FSFMMs given in (5.37) and (5.102). For the sake of clarity, the computed ε -uniform errors in Tables 5.1 and 5.2 are depicted in Figs 5.1 and 5.2, for Examples 5.1. At the same time, these computational results clearly illustrate the influence of the temporal error over the global error. The computed order of convergence shown in Tables 5.1 and 5.2, does not truly reflect the spatial order of convergence of the proposed FMMs in (5.37) and (5.102), because of the dominance of the temporal error over the spatial error according to Theorems 5.3 and 5.5. Tables 5.1 and 5.2 show that the ε -uniform maximum point-wise errors of proposed schemes (5.37) and (5.102) with alternative boundary conditions (5.22) and (5.83) are smaller than the ε -uniform maximum point-wise errors of proposed schemes (5.37) and (5.102) with natural boundary conditions (5.21) and (5.82). To the best of our knowledge, no such technique has been used in the any context of uniform convergence analysis of singularly perturbed of this type.

In the Tables 5.3, 5.4, 5.5 and 5.6, we show these numerical local errors $e_{loc}^{N, \Delta t}$ and corresponding order of convergence $r_{loc}^{N, \Delta t}$ for the two choices of the boundary data. To reduce the influence of the local spatial

error, we take sufficiently large the discretization parameter $N = 2048$. It is worth noting that when the non-natural alternative boundary conditions are chosen, the local errors are significantly reduced; also, the order of consistency is one, whereas for classical evaluation it's zero. The option (5.22) for IMEX-FSFMM (5.37) and (5.83) for fully-implicit FSFMM (5.102) is evidently better than the conventional one.

Next, in order to visualize the effect of the temporal Richardson extrapolation, we choose a suitably large N to reduce the influence of the spatial error. In Tables 5.8 and 5.9, we display the numerical results for Example 5.1, after the temporal extrapolation of the proposed schemes (5.37) and (5.102). This shows that the improvement in the temporal order of convergence after employing the Richardson extrapolation in the time variable, as claimed in Theorem 5.6. Tables 5.8 and 5.9 show that the temporal errors of proposed schemes (5.37) and (5.102) after temporal extrapolation with alternative boundary conditions (5.22) and (5.83) are smaller than the temporal errors of proposed schemes (5.37) and (5.102) with natural boundary conditions (5.21) and (5.82).

The above numerical experiment indicates that by using the temporal Richardson extrapolation, one can check the spatial accuracy by choosing $\Delta t = 1/N$. Following this, in Tables 5.7, we compare the region-wise spatial accuracy of the FSFMMs given in (5.37), (5.102) and (5.190), for Example 5.1. These computational results match very well with the spatial error established in Theorems 5.3, 5.5 and 5.7; and also clearly reflects the robustness of the fully-implicit FSFMM (5.102) and the IMEX-FSFMM (5.37) in comparison with the upwind FSFMM (5.190) in terms of order of accuracy, irrespective of the smaller and the larger values of ε . This is the first comprehensive analysis of this type for two-dimensional semilinear parabolic convection-diffusion-reaction problems discretized using high-order fitted mesh methods.

5.7 Conclusion

In this chapter, we provide a complete convergence analysis for the higher-order numerical approximation of a class of two-dimensional singularly perturbed nonlinear parabolic convection-diffusion problems (5.1)-(5.3) with non-homogeneous boundary data by proposing two new FMMs followed the temporal Richardson extrapolation. Apart from studying the asymptotic properties of the analytical solution of the nonlinear governing problem, the entire convergence analysis is split into three major parts.

(i) In the first part, ε -uniform error estimate of the newly proposed fractional step IMEX-FMM (5.37) is carried out by invoking two-stage discretization technique, which discretizes first in time and later in space. We also proved that the order reduction in time associated with the classical evaluation of time-dependent boundary conditions could be eliminated by choosing appropriate boundary data. Further, we prove that the corresponding fully discrete scheme is ε -uniformly convergent in the discrete supremum norm; and show that the spatial accuracy is at least two in the outer region and is almost two in the boundary layer region, regardless of the larger and smaller values of ε .

(ii) In the second part, we carry out ε -uniform error estimate of the newly proposed fractional-step fully-implicit FMM (5.102) by invoking the two-stage discretization technique. Here also, We proved that the order reduction in time associated with the classical evaluation of time-dependent boundary conditions could be eliminated by choosing appropriate boundary data. Finally, we prove that the associated fully discrete scheme is ε -uniformly convergent in the discrete supremum norm; and also achieves a similar order of accuracy as that of the present fractional IMEX-FMM.

(iii) The third part focuses on the ε -uniform error estimate associated with temporal Richardson extrapolation.

tion for improving the temporal order of convergence.

The error estimates in (i) and (ii) demonstrate that, while the proposed fractional IMEX method produces a linearized system at each time step, it does not cause a reduction in the order of convergence in both space and time, corresponding to the present proposed fractional fully-implicit method, which produces a nonlinear system at each time step. Finally, the error estimate in (iii) demonstrates that the resulting numerical solution is second-order uniformly convergent in both the spatial and temporal variables. Finally, we perform several numerical experiments to confirm that those theoretical outcomes. Further, we demonstrate that the newly developed fractional FMMs are robust in comparison with the upwind fractional-step FMM (5.190).

This is the first detailed convergence analysis for two-dimensional singularly perturbed nonlinear parabolic convection-diffusion problems with non-homogeneous boundary data. Our unique technical approach opens the door for more difficult nonlinear model problems to be solved numerically.

Table 5.1: Comparison of ε -uniform errors and order of convergence for Example 5.1 using the IMEX-FSFMM (5.37) computed with $\Delta t = 1.6/N$ without using Richardson extrapolation in time

$\varepsilon \in \mathbb{S}_\varepsilon$	Number of mesh intervals N / time step size Δt				
	$64 / \frac{1}{40}$	$128 / \frac{1}{80}$	$256 / \frac{1}{160}$	$512 / \frac{1}{320}$	$1024 / \frac{1}{640}$
with natural boundary conditions (5.21)					
$e^{N,\Delta t}$	1.8074e-02	1.0394e-02	5.4734e-03	2.9316e-03	1.4884e-03
$r^{N,\Delta t}$	0.79821	0.92521	0.90077	0.97791	
with alternative boundary conditions (5.22)					
$e^{N,\Delta t}$	6.4681e-03	3.0900e-03	1.5096e-03	7.5303e-04	3.7816e-04
$r^{N,\Delta t}$	1.0657	1.0334	1.0034	0.99369	

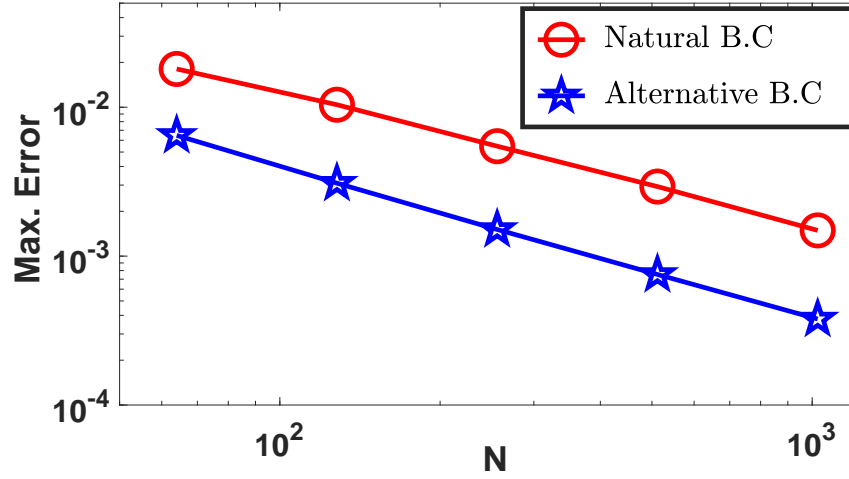


Figure 5.1: Loglog plot for comparison of the ε -uniform errors for Example 5.1.

Table 5.2: Comparison of ε -uniform errors and order of convergence for Example 5.1 using the fully-implicit FSFMM (5.102) computed with $\Delta t = 1.6/N$ without using Richardson extrapolation in time

$\varepsilon \in \mathbb{S}_\varepsilon$	Number of mesh intervals N / time step size Δt				
	$64 / \frac{1}{40}$	$128 / \frac{1}{80}$	$256 / \frac{1}{160}$	$512 / \frac{1}{320}$	$1024 / \frac{1}{640}$
with natural boundary conditions (5.82)					
$e^{N,\Delta t}$	3.1016e-02	1.8073e-02	1.0394e-02	5.4733e-03	2.9315e-03
$r^{N,\Delta t}$	0.77919	0.79814	0.92519	0.90076	
with alternative boundary conditions (5.83)					
$e^{N,\Delta t}$	1.3511e-02	6.4469e-03	3.0773e-03	1.5026e-03	7.4932e-04
$r^{N,\Delta t}$	1.0675	1.0670	1.0341	1.0038	

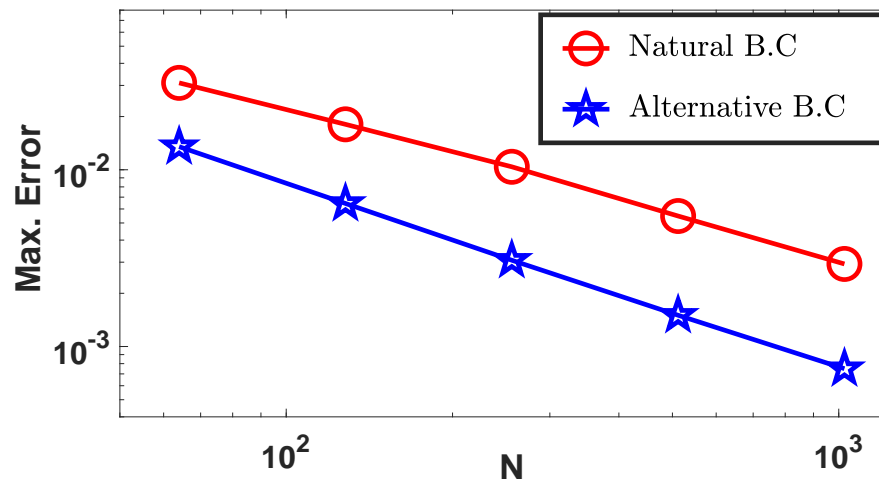


Figure 5.2: Loglog plot for comparison of the ε -uniform errors for Example 5.1.

Table 5.3: Maximum point-wise local errors $e_{loc}^{N,\Delta t}$ and order of convergence $r_{loc}^{N,\Delta t}$ for Example 5.1 using the IMEX-FSMM (5.37) for natural boundary conditions (5.21) and without using Richardson extrapolation in time

ε	Number of mesh intervals $N = 2048$			
	M=16	M=32	M=64	M=128
2^{-3}	4.1048e-02	2.3271e-02	1.2582e-02	6.6195e-03
	0.89873	0.95555	0.98838	
2^{-6}	5.0262e-02	2.6959e-02	1.3901e-02	7.0068e-03
	0.92587	0.99806	1.0663	
2^{-14}	5.3944e-02	2.8394e-02	1.4216e-02	6.7888e-03
	0.92601	0.99839	1.0674	
2^{-20}	5.3981e-02	2.8411e-02	1.4221e-02	6.7863e-03
	0.81880	0.88714	0.92659	

Table 5.4: Maximum point-wise local errors $e_{loc}^{N,\Delta t}$ and order of convergence $r_{loc}^{N,\Delta t}$ for Example 5.1 using the IMEX-FSMM (5.37) for alternative boundary conditions (5.22) and without using Richardson extrapolation in time

ε	Number of mesh intervals $N = 2048$			
	M=16	M=32	M=64	M=128
2^{-3}	2.7796e-03	9.3539e-04	2.8154e-04	7.8802e-05
	1.5713	1.7322	1.8370	
2^{-6}	4.6890e-03	1.4747e-03	4.2654e-04	1.1848e-04
	1.6689	1.7897	1.8481	
2^{-14}	5.6131e-03	1.6448e-03	4.4289e-04	1.1524e-04
	1.7709	1.8929	1.9423	
2^{-20}	5.6273e-03	1.6485e-03	4.4375e-04	1.1532e-04
	1.7713	1.8933	1.9441	

Table 5.5: Maximum point-wise local errors $e_{loc}^{N,\Delta t}$ and order of convergence $r_{loc}^{N,\Delta t}$ for Example 5.1 using the fully-implicit FSFMM (5.102) for natural boundary conditions (5.82) and without using Richardson extrapolation in time

ε	Number of mesh intervals $N = 2048$			
	M=16	M=32	M=64	M=128
2^{-3}	4.0964e-02	2.3245e-02	1.2575e-02	6.6175e-03
	0.81743	0.88637	0.92618	
2^{-6}	5.0149e-02	2.6927e-02	1.3893e-02	7.0046e-03
	0.89719	0.95471	0.98795	
2^{-14}	5.3821e-02	2.8360e-02	1.4207e-02	6.7867e-03
	0.92430	0.99722	1.0659	
2^{-20}	5.3858e-02	2.8377e-02	1.4213e-02	6.7842e-03
	0.92445	0.99754	1.0669	

Table 5.6: Maximum point-wise local errors $e_{loc}^{N,\Delta t}$ and order of convergence $r_{loc}^{N,\Delta t}$ for Example 5.1 using the fully-implicit FSFMM (5.102) for alternative boundary conditions (5.83) and without using Richardson extrapolation in time

ε	Number of mesh intervals $N = 2048$			
	M=16	M=32	M=64	M=128
2^{-3}	2.7307e-03	9.2104e-04	2.7747e-04	7.7675e-05
	1.5679	1.7309	1.8368	
2^{-6}	4.6636e-03	1.4684e-03	4.2484e-04	1.1799e-04
	1.6672	1.7893	1.8483	
2^{-14}	5.5968e-03	1.6423e-03	4.4254e-04	1.1518e-04
	1.7689	1.8918	1.9419	
2^{-20}	5.6110e-03	1.6460e-03	4.4340e-04	1.1526e-04
	1.7693	1.8923	1.9437	

Table 5.7: Comparison (region-wise) of maximum point-wise errors and order of convergence for Example 5.1, with alternative boundary conditions (5.22) and (5.83)

	with using temporal Richardson extrapolation	outer region $[0, 1 - \eta_1] \times$ $[0, 1 - \eta_2]$	right boundary layer region $(1 - \eta_1, 1] \times$ $[0, 1 - \eta_2]$	top boundary layer region $[0, 1 - \eta_1] \times$ $(1 - \eta_2, 1]$	corner layer region $(1 - \eta_1, 1] \times$ $(1 - \eta_2, 1]$
N	$\varepsilon = 2^{-4}$				
128	IMEX-FSFMM (5.37)	2.1639e-06	4.5559e-05	4.8590e-05	1.9927e-04
		1.9877	1.9996	2.0000	1.9996
	fully-implicit FSFMM (5.102)	2.1768e-06	4.5555e-05	4.8617e-05	1.9925e-04
		1.9878	1.9996	2.0000	1.9996
	upwind-FSFMM (5.190)	3.7900e-04	1.3175e-03	1.3155e-03	7.3076e-03
		1.0077	0.95807	0.95713	0.95560
256	IMEX-FSFMM (5.37)	5.4560e-07	1.1393e-05	1.2147e-05	4.9830e-05
		1.9937	2.0004	1.9989	2.0004
	fully-implicit FSFMM (5.102)	5.4882e-07	1.1392e-05	1.2154e-05	4.9827e-05
		1.9938	2.0004	1.9989	2.0004
	upwind-FSFMM (5.190)	1.8850e-04	6.7818e-04	6.7758e-04	3.7680e-03
		1.0040	0.97852	0.97792	0.97731
N	$\varepsilon = 2^{-6}$				
128	IMEX-FSFMM (5.37)	2.2276e-05	2.4411e-04	2.4846e-04	4.3807e-04
		2.3258	1.7252	1.7257	1.6338
	fully-implicit FSFMM (5.102)	2.2259e-05	2.4410e-04	2.4845e-04	4.3804e-04
		2.3259	1.7252	1.7257	1.6338
	upwind-FSFMM (5.190)	1.8732e-03	6.2279e-03	6.2256e-03	1.2558e-02
		1.1349	0.79954	0.79939	0.73913
256	IMEX-FSFMM (5.37)	4.4432e-06	7.3834e-05	7.5120e-05	1.4116e-04
		2.2517	1.7557	1.7579	1.6719
	fully-implicit FSFMM (5.102)	4.4396e-06	7.3831e-05	7.5117e-05	1.4116e-04
		2.2517	1.7556	1.7578	1.671
	upwind-FSFMM (5.190)	8.5296e-04	3.5781e-03	3.5772e-03	7.5236e-03
		1.1364	0.85619	0.85602	0.78626
N	$\varepsilon = 2^{-14}$				
128	IMEX-FSFMM (5.37)	3.9181e-05	2.8937e-04	2.8944e-04	4.2160e-04
		2.1338	1.5798	1.5774	1.5914
	fully-implicit FSFMM (5.102)	3.9258e-05	2.8934e-04	2.8939e-04	4.2156e-04
		2.1332	1.5798	1.5773	1.5914
	upwind-FSFMM (5.190)	2.8500e-03	8.8276e-03	8.8282e-03	1.3352e-02
		1.0254	0.72372	0.72378	0.74025
256	IMEX-FSFMM (5.37)	8.9276e-06	9.6800e-05	9.6989e-05	1.3990e-04
		2.0921	1.6384	1.6385	1.6476
	fully-implicit FSFMM (5.102)	8.9489e-06	9.6791e-05	9.6976e-05	1.3989e-04
		2.0916	1.6384	1.6385	1.6476
	upwind-FSFMM (5.190)	1.4002e-03	5.3454e-03	5.3455e-03	7.9931e-03
		1.0167	0.77768	0.77769	0.78829

Table 5.8: Comparison of temporal accuracy for IMEX-FSFMM (5.37) with natural and alternative boundary conditions after Richardson extrapolation for the time variable for Example 5.1

ε	Number of mesh intervals $N = 2048$			
	M=8	M=16	M=32	M=64
	with natural boundary conditions (5.21)			
2^{-6}	1.5480e-02 1.2167	6.6605e-03 1.1498	3.0018e-03 1.0403	1.4596e-03
2^{-20}	1.8973e-02 1.1094	8.7934e-03 1.1258	4.0294e-03 1.2126	1.7386e-03
	with alternative boundary conditions (5.22)			
2^{-6}	2.5541e-03 1.7421	7.6350e-04 1.8501	2.1178e-04 1.8535	5.8604e-05
2^{-20}	3.4663e-03 1.7558	1.0264e-03 1.8453	2.8563e-04 1.8312	8.0274e-05

Table 5.9: Comparison of temporal accuracy for fully-implicit FSFMM (5.102) with natural and alternative boundary conditions after Richardson extrapolation for the time variable for Example 5.1

ε	Number of mesh intervals $N = 2048$			
	M=8	M=16	M=32	M=64
	with natural boundary conditions (5.82)			
2^{-6}	1.5621e-02 1.2195	6.7079e-03 1.1536	3.0153e-03 1.0432	1.4632e-03
2^{-20}	1.9101e-02 1.1124	8.8347e-03 1.1284	4.0413e-03 1.2145	1.7414e-03
	with alternative boundary conditions (5.83)			
2^{-6}	2.5608e-03 1.7399	7.6667e-04 1.8499	2.1268e-04 1.8538	5.8840e-05
2^{-20}	3.4790e-03 1.7560	1.0300e-03 1.8438	2.8696e-04 1.8351	8.0428e-05

Chapter 6

Convergence Analysis of New Efficient Numerical Methods for Singularly Perturbed Linear Parabolic PDEs with Nonsmooth Data

This chapter addresses efficient numerical methods for solving two different classes of singularly perturbed parabolic PDEs with nonsmooth data. At first, we deal with a class of singularly perturbed parabolic convection-diffusion IBVPs possessing strong interior layers. Aiming to get a better numerical approximation to the solutions to this class of problems, we devise a new hybrid finite difference scheme on a layer-resolving piecewise-uniform Shishkin mesh in the spatial direction, and the time derivative is discretized by the backward-Euler method in the temporal direction. We discuss the stability of the proposed method and establish the parameter-uniform error estimate in the discrete supremum norm. Numerical results are also displayed to support the theoretical findings and compared with the existing hybrid scheme to show the improvement in terms of spatial order of convergence. Furthermore, we carry out numerical experiments for the semi-linear parabolic IBVPs.

Next, we consider a class of singularly perturbed parabolic convection-diffusion IBVPs exhibiting both boundary and weak interior layers. To solve this class of problems with better accuracy, we discretize the time derivative by the backward-Euler method; and a new finite difference scheme is proposed for the spatial discretization. To accomplish this purpose, we construct a modified layer-adapted mesh, a modification of the standard Shishkin mesh adapted to both boundary and weak interior layers. Utilizing the modified layer-adapted mesh, we overcome the difficulty in proving the inverse monotonicity of the finite difference operator on the standard Shishkin mesh; and we establish the parameter-uniform error estimate in the discrete supremum norm. Numerical results are presented to validate the theoretical findings and are compared with the implicit upwind finite difference scheme. Furthermore, we extend numerical experiments to the semi-linear parabolic IBVPs.

6.1 Introduction

In the beginning, for describing the model problem, we introduce the following notations:

$$\begin{cases} \mathfrak{D}^- = \Omega^- \times (0, T] = (0, \mathfrak{d}) \times (0, T], & \mathfrak{D}^+ = \Omega^+ \times (0, T] = (\mathfrak{d}, 1) \times (0, T], & 0 < \mathfrak{d} < 1, \\ \mathfrak{D} = \Omega \times (0, T] = (0, 1) \times (0, T], & \overline{\mathfrak{D}} = \overline{\Omega} \times [0, T] = [0, 1] \times (0, T]. \end{cases}$$

Here, we consider the following class of singularly perturbed parabolic IBVPs:

$$\begin{cases} \left(\mathcal{L}_{x,\varepsilon} - \frac{\partial}{\partial t} \right) y(x, t) = g(x, t), & (x, t) \in \mathfrak{D}^- \cup \mathfrak{D}^+, \\ y(x, 0) = q_0(x), & x \in \bar{\Omega}, \\ y(0, t) = s_l(t), \quad y(1, t) = s_r(t), & t \in (0, T], \end{cases} \quad (6.1)$$

where

$$\mathcal{L}_{x,\varepsilon} y = \varepsilon \frac{\partial^2 y}{\partial x^2} + a(x) \frac{\partial y}{\partial x} - b(x, t) y,$$

together with the following interface conditions:

$$[y](d, t) = 0, \quad \left[\frac{\partial y}{\partial x} \right](d, t) = 0, \quad t \in (0, T]. \quad (6.2)$$

Here, ε is a small parameter such that $\varepsilon \in (0, 1]$; and we assume that the convection coefficient $a(x)$, the reaction term $b(x, t)$, and the source term $g(x, t)$ are sufficiently smooth on $\Omega^- \cup \Omega^+$, $\bar{\mathfrak{D}}$ and $\mathfrak{D}^- \cup \mathfrak{D}^+$, respectively; such that

$$\begin{cases} |[a](d)| \leq C, \quad |[g](d, t)| \leq C, \\ b(x, t) \geq \beta \geq 0, \quad \text{on } \bar{\mathfrak{D}}. \end{cases} \quad (6.3)$$

We consider two cases for the convection coefficient:

$$\textbf{Case I} : -m_1^* < a(x) < -m_1 < 0, \quad x < d, \quad m_2^* > a(x) > m_2 > 0, \quad x > d, \quad (6.4)$$

$$\textbf{Case II} : a(x) \geq m_0 > 0, \quad \bar{\Omega}^- \cup \bar{\Omega}^+. \quad (6.5)$$

The boundary and the initial data, *i.e.*, *i.e.*, s_l, s_r and q_0 are also assumed to be sufficiently smooth. Here, $[g](d, t) = g(d^+, t) - g(d^-, t)$, where $g(d^\pm, t) = \lim_{x \rightarrow d^\pm} g(x, t)$. In **Case I**, the solution of the IBVP (6.1)-(6.3) generally possess strong interior layers of width $O(\varepsilon)$ in the vicinity of the point $x = d$ (see [89]); and in **Case II**, the solution of the IBVP (6.1)-(6.3) with (6.5) generally possess a boundary layer at the left boundary $x = 0$ and a weak interior layer in the right side of the point $x = d$ of width $O(\varepsilon)$ (see [33]). Firstly, we analyze the model problem (6.1)-(6.3) along with (6.4) in Section 6.2-6.7; and afterwards, we consider the model problem (6.1)-(6.3) along with (6.5) in Section 6.8-6.11. The conclusion of this chapter is given in Section 6.12.

Efficient Numerical Method for Model problem-I

This type of model problem with the alternative sign pattern of the convection-coefficient can viewed as the linearized version of the time-dependent viscous Burgers' equation exhibiting shock layer (see [88]).

The content of this part is given here: In Section 6.2, we discuss properties of the analytical solution which includes the stability of the analytical solution as well as the asymptotic behavior of the smooth and the layer components. Section 6.3 introduces the suitable mesh for discretizing the domain $\bar{\mathfrak{D}}$ and provides description of the newly proposed numerical method. Further, the stability of the proposed method is also discussed here.

In Section 6.4, we present several technical lemmas to be used in the convergence analysis. Afterwards, we decompose the discrete solution in Section 6.5 and establish the main convergence result in connection with the ε -uniform error estimate of the proposed method. Further, Section 6.6 introduces the Newton's linearization technique for solving the semi-linear singularly perturbed parabolic IBVPs having discontinuous convection coefficient. Finally in Section 6.7, we display the numerical results for couple of test examples to confirm the theoretical findings; and we also compare the computational time and the accuracy of the present method with the existing hybrid scheme [83].

6.2 The analytical solution of model problem-I

In this section, we present the results associated with the stability bound of the analytical solution of the IBVP (6.1)-(6.3) with (6.4) as well as the bounds of the derivatives of the smooth and the layer components. It will be required for analyzing the numerical approximation of the IBVP (6.1)-(6.3) with (6.4). In addition to the smoothness assumption imposed on a, b and g , we assume that the data associated with the boundary and the initial conditions, *i.e.*, q_0, s_l and s_r are sufficiently smooth functions and satisfy the compatibility conditions at the corner points $(0, 0)$ and $(1, 0)$, as listed below:

$$q_0(0) = s_l(0), \quad q_0(1) = s_r(0),$$

$$\begin{cases} -\frac{ds_l(0)}{dt} = g(0, 0) - \varepsilon \frac{d^2 q_0(0)}{dx^2} - a(0) \frac{dq_0(0)}{dx} + b(0, 0)q_0(0), \\ -\frac{ds_r(0)}{dt} = g(1, 0) - \varepsilon \frac{d^2 q_0(1)}{dx^2} - a(1) \frac{dq_0(1)}{dx} + b(1, 0)q_0(1), \end{cases}$$

and

$$\begin{cases} \frac{d^2 s_l(0)}{dt^2} = \mathcal{L}_{x,\varepsilon}(\mathcal{L}_{x,\varepsilon} q_0 - g)(0, 0) - q_0(0) \frac{\partial b(0, 0)}{\partial t} - \frac{\partial g(0, 0)}{\partial t}, \\ \frac{d^2 s_r(1)}{dt^2} = \mathcal{L}_{x,\varepsilon}(\mathcal{L}_{x,\varepsilon} q_0 - g)(1, 0) - q_0(1) \frac{\partial b(1, 0)}{\partial t} - \frac{\partial g(1, 0)}{\partial t}. \end{cases}$$

We also assume the necessary compatibility conditions at the point $(d, 0)$. Then, under these hypothesis the IBVP (6.1)-(6.3) with (6.4) possesses a unique solution $y \in \mathcal{C}^{1+\gamma}(\mathcal{D}) \cap \mathcal{C}^{4+\gamma}(\mathcal{D}^- \cup \mathcal{D}^+)$ (see [65, Chapter 3]).

6.2.1 Stability

At first, we show that the maximum principle holds for the differential operator $\mathcal{L}_\varepsilon \equiv \left(\mathcal{L}_{x,\varepsilon} - \frac{\partial}{\partial t} \right)$ in the following Lemma. For clarity of the presentation, the outline of the proof of Lemma 6.1 is given below. Let $\partial\mathcal{D} = \overline{\mathcal{D}} \setminus \mathcal{D}$.

Lemma 6.1. *If a function $\phi \in \mathcal{C}^0(\overline{\mathcal{D}}) \cap \mathcal{C}^2(\mathcal{D}^- \cup \mathcal{D}^+)$ satisfies that $\phi \leq 0$, on $\partial\mathcal{D}$, $\left[\frac{\partial \phi}{\partial x} \right](d, t) \geq 0$, for $t > 0$; and $\mathcal{L}_\varepsilon \phi \geq 0$, in $\mathcal{D}^- \cup \mathcal{D}^+$, then $\phi \leq 0$, on $\overline{\mathcal{D}}$.*

Proof: Let the function f defined on $\overline{\mathcal{D}}$ be such that

$$\phi(x, t) = \exp(-m|x - d|/2\varepsilon)f(x, t),$$

where $m = \min\{m_1, m_2\}$. We assume that f attains its maximum value at (s, τ) in $\overline{\mathcal{D}}$ and $f(s, \tau) > 0$. From the

hypothesis of the maximum principle, either $(s, \tau) \in \mathfrak{D}^- \cup \mathfrak{D}^+$ or $(s, \tau) = (d, \tau)$. Therefore, if $(s, \tau) \in \mathfrak{D}^-$, then we have

$$\begin{aligned} \mathcal{L}_\varepsilon \phi(s, \tau) &= \exp(-m_1(d-s)/2\varepsilon) \left(\varepsilon \frac{\partial^2 f}{\partial x^2} + (a(s) + m_1) \frac{\partial f}{\partial x} + \left(\frac{m_1}{2\varepsilon} \left(\frac{m_1}{2} + a(s) \right) - b(s, \tau) \right) f - \frac{\partial f}{\partial t} \right) (s, \tau) \\ &< 0, \end{aligned}$$

and if $(s, \tau) \in \mathfrak{D}^+$, we have

$$\begin{aligned} \mathcal{L}_\varepsilon \phi(s, \tau) &= \exp(-m_2(s-d)/2\varepsilon) \left(\varepsilon \frac{\partial^2 f}{\partial x^2} + (a(s) - m_2) \frac{\partial f}{\partial x} + \left(\frac{m_2}{2\varepsilon} \left(\frac{m_2}{2} - a(s) \right) - b(s, \tau) \right) f - \frac{\partial f}{\partial t} \right) (s, \tau) \\ &< 0, \end{aligned}$$

which contradicts the hypothesis that $\mathcal{L}_\varepsilon \phi(x, t) \geq 0$, $(x, t) \in \mathfrak{D}^- \cup \mathfrak{D}^+$. Next, if $(s, \tau) = (d, \tau)$, $\left[\frac{\partial \phi}{\partial x} \right](d, \tau) = \left[\frac{\partial f}{\partial x} \right](d, \tau) - ((m_1 + m_2)/2\varepsilon)f(d, \tau)$, and since, we assume that f has a maximum at (d, τ) , it implies that $\left[\frac{\partial \phi}{\partial x} \right](d, \tau) \leq 0$, which also leads to a contradiction. Hence, the proof is complete. ■

Now, consequently using Lemma 6.1, one can deduce the following stability result.

Lemma 6.2. *The following bound holds for the solution $y(x, t)$ of the IBVP (6.1)–(6.3) with (6.4):*

$$\|y(x, t)\|_{\overline{\mathfrak{D}}} \leq \|y\|_{\partial \mathfrak{D}} + \frac{1}{\gamma} \|g\|_{\overline{\mathfrak{D}}},$$

where $\gamma = \min\{m_1/d, m_2/(1-d)\}$.

Proof: See [89] for the proof. ■

6.2.2 Decomposition of the analytical solution

The solution y is now decomposed into the smooth component v and the layer component z such that $y = v + z$. Here, the smooth component y satisfies that

$$\left\{ \begin{array}{l} \mathcal{L}_\varepsilon v = g, \quad \text{in } \mathfrak{D}^- \cup \mathfrak{D}^+, \\ v(x, 0) = q_0(x), \quad x \in \overline{\Omega}, \\ v(0, t) = s_l(t), \quad v(1, t) = s_r(t), \\ v(d^-, t) = \psi_1(t), \quad v(d^+, t) = \psi_2(t), \quad t \in (0, T], \end{array} \right. \quad (6.6)$$

where for the suitable choices of the functions $\psi_1(t)$, $\psi_2(t)$, one can refer to the proof of [83, Theorem 3.4]. Now, the interior layer component z is defined as follows :

$$\begin{cases} \mathcal{L}_\varepsilon z = 0, & \text{in } \mathfrak{D}^+ \cup \mathfrak{D}^-, \\ z(x, 0) = 0, & x \in \bar{\Omega}, \\ z(0, t) = 0, \quad z(1, t) = 0, \\ [z](\mathfrak{d}, t) = -[v](\mathfrak{d}, t), \quad \left[\frac{\partial z}{\partial x} \right](\mathfrak{d}, t) = - \left[\frac{\partial v}{\partial x} \right](\mathfrak{d}, t), \quad t \in (0, T]. \end{cases} \quad (6.7)$$

Without loss of generality, suppose that $y \equiv 0$ on $\partial\mathfrak{D}$ and afterwards, we follow the approach given in [83, Theorem 3.4] to derive the bounds of the derivative of v and z in Theorem 6.1.

Theorem 6.1. $\forall j, k \in \mathbb{N} \cup \{0\}$ satisfying $0 \leq j \leq 3$ and $0 \leq j + 2k \leq 4$, the smooth component v given in (6.6) satisfies the bounds

$$\left\| \frac{\partial^{j+k} v}{\partial x^j \partial t^k} \right\|_{\mathfrak{D} \cup \mathfrak{D}^+} \leq C, \quad \left\| \frac{\partial^4 v}{\partial x^4} \right\|_{\mathfrak{D} \cup \mathfrak{D}^+} \leq C\varepsilon^{-1},$$

and the layer component z given in (6.7) satisfies the bounds

$$\left| \frac{\partial^{j+k} z(x, t)}{\partial x^j \partial t^k} \right| \leq \begin{cases} C \left(\varepsilon^{-j} \exp(-\mathfrak{m}_1(\mathfrak{d} - x)/\varepsilon) \right), & (x, t) \in \mathfrak{D}^-, \\ C \left(\varepsilon^{-j} \exp(-\mathfrak{m}_2(x - \mathfrak{d})/\varepsilon) \right), & (x, t) \in \mathfrak{D}^+, \end{cases}$$

and

$$\left| \frac{\partial^4 z(x, t)}{\partial x^4} \right| \leq \begin{cases} C \left(\varepsilon^{-4} \exp(-\mathfrak{m}_1(\mathfrak{d} - x)/\varepsilon) \right), & (x, t) \in \mathfrak{D}^-, \\ C \left(\varepsilon^{-4} \exp(-\mathfrak{m}_2(x - \mathfrak{d})/\varepsilon) \right), & (x, t) \in \mathfrak{D}^+. \end{cases}$$

6.3 The discrete solution of model problem-I

In this section, we introduce the suitable mesh to discretize the domain $\bar{\mathfrak{D}}$ and provide the description of the proposed numerical method for discretizing the IBVP (6.1)-(6.3) with (6.4). Further, the stability of the proposed method is discussed.

6.3.1 Discretization of the domain

Let us choose $N (\geq 8)$ as an even positive integer. Now, on the domain $\bar{\mathfrak{D}}$, we construct a mesh $\bar{\mathfrak{D}}^{N, \Delta t} = \bar{\Omega}^N \times \wedge^{\Delta t}$. Here, $\wedge^{\Delta t} := \{t_n\}_{n=0}^M$, denotes the equidistant mesh with uniform step-size $\Delta t = T/M$ and with M mesh-intervals in the temporal direction; whereas $\bar{\Omega}^N$ denotes the piecewise-uniform Shishkin mesh defined on the spatial domain $\bar{\Omega}$ as depicted in Fig 6.1. $\bar{\Omega}^N$ is constructed by partitioning $\bar{\Omega}$ into four sub-intervals as $\bar{\Omega} = [0, \mathfrak{d} - \eta_1] \cup [\mathfrak{d} - \eta_1, \mathfrak{d}] \cup [\mathfrak{d}, \mathfrak{d} + \eta_2] \cup [\mathfrak{d} + \eta_2, 1]$, where the transition parameters η_1 and η_2 are given by

$$\eta_1 = \min \left\{ \frac{\mathfrak{d}}{2}, \eta_0 \varepsilon \ln N \right\}, \quad \eta_2 = \min \left\{ \frac{1 - \mathfrak{d}}{2}, \eta_0 \varepsilon \ln N \right\},$$

where $\eta_0 = 2/\theta$ and θ is a positive constant to be chosen suitably later on.

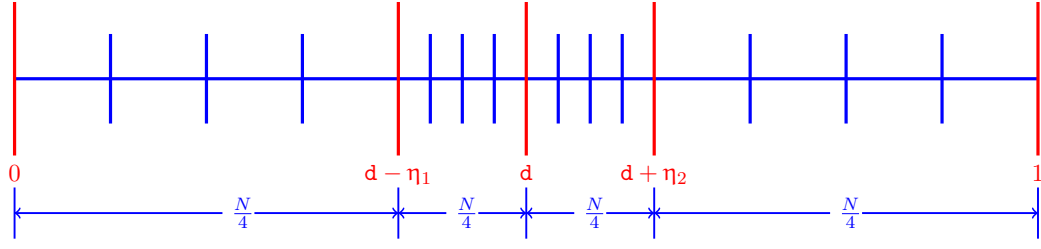


Figure 6.1: Shishkin mesh in spatial direction

Now, we place the equidistant mesh with $N/4$ mesh-intervals in each sub-interval such that $\bar{\Omega}^N = \{x_j\}_{j=0}^N$, where

$$x_j = \begin{cases} \frac{4(d - \eta_1)j}{N}, & \text{for } 0 \leq j \leq N/4, \\ (d - \eta_1) + \left(j - \frac{N}{4}\right) \frac{4\eta_1}{N}, & \text{for } N/4 < j \leq N/2, \\ d + \left(j - \frac{N}{2}\right) \frac{4\eta_2}{N}, & \text{for } N/2 < j \leq 3N/4, \\ (d + \eta_2) + \left(j - \frac{3N}{4}\right) \frac{4(1 - d - \eta_2)}{N}, & \text{for } 3N/4 < j \leq N. \end{cases}$$

Further, the mesh widths in the spatial direction are denoted by $h_j = x_j - x_{j-1}$, $1 \leq j \leq N$, with $\hat{h}_j = h_j + h_{j+1}$, $1 \leq j \leq N - 1$, and from the definition of x_j 's, it follows that

$$h_j = \begin{cases} H_l = \frac{4(d - \eta_1)}{N}, & \text{for } 1 \leq j \leq \frac{N}{4}, \\ h_l = \frac{4\eta_1}{N}, & \text{for } \frac{N}{4} < j \leq \frac{N}{2}, \\ h_r = \frac{4\eta_2}{N}, & \text{for } \frac{N}{2} < j \leq \frac{3N}{4}, \\ H_r = \frac{4(1 - d - \eta_2)}{N}, & \text{for } \frac{3N}{4} < j \leq N. \end{cases}$$

6.3.2 Proposed numerical method

Let $\Psi_j^n = \Psi(x_j, t_n)$ be the mesh function defined on $\bar{\mathcal{D}}^{N, \Delta t}$. We define

$$\Psi_{j \pm \frac{1}{2}}^n = \frac{\Psi(x_j, t_n) + \Psi(x_{j \pm 1}, t_n)}{2}, \quad a_{j \pm \frac{1}{2}} = \frac{a_j + a_{j \pm 1}}{2}, \quad b_{j \pm \frac{1}{2}}^n = \frac{b_j^n + b_{j \pm 1}^n}{2}, \quad g_{j \pm \frac{1}{2}}^n = \frac{g_j^n + g_{j \pm 1}^n}{2}.$$

In the following, we describe the proposed numerical method for discretizing the IBVP (6.1)–(6.3) with (6.4). We use the backward-Euler method to approximate the time derivative; and for the spatial discretization, we propose a new hybrid finite difference scheme which is comprised of a modified central difference scheme whenever $\varepsilon > 2\|a\|N^{-1}$; and a combination of the midpoint upwind scheme in the outer regions $(0, d - \eta]$, $[d + \eta_2, 1)$ and the modified central difference scheme in the interior layer regions $(d - \eta_1, d)$, $(d, d + \eta_2)$, whenever $\varepsilon \leq 2\|a\|N^{-1}$. Further, we use the second order one-sided difference approximation at the point of discontinuity. Thus, we solve the IBVP (6.1)-(6.3) with (6.4) numerically using the fully discrete finite

difference scheme, which takes the following form on $\overline{\mathfrak{D}}^{N,\Delta t}$:

$$\left\{ \begin{array}{l} Y_j^0 = \mathbf{q}_0(x_j), \quad \text{for } 0 \leq j \leq N, \\ \left\{ \begin{array}{ll} \mathcal{L}_{mcd}^{N,\Delta t} Y_j^{n+1} = g_j^{n+1}, & \text{for } 1 \leq j \leq N/4 \text{ and } 3N/4 \leq j \leq N-1, \\ & \text{and when } \varepsilon > 2\|a\|N^{-1}, \\ \mathcal{L}_{mup}^{N,\Delta t,(-)} Y_j^{n+1} = g_{j-1/2}^{n+1}, & \text{for } 1 \leq j \leq N/4, \\ & \text{and when } \varepsilon \leq 2\|a\|N^{-1}, \\ \mathcal{L}_{mup}^{N,\Delta t,(+)} Y_j^{n+1} = g_{j+1/2}^{n+1}, & \text{for } 3N/4 \leq j \leq N-1, \\ & \text{and when } \varepsilon \leq 2\|a\|N^{-1}, \\ \mathcal{L}_{mcd}^{N,\Delta t} Y_j^{n+1} = g_j^{n+1}, & \text{for } N/4 < j < N/2, \\ & \text{and } N/2 < j \leq 3N/4 - 1, \\ D_x^F Y_j^{n+1} - D_x^B Y_j^{n+1} = 0, & \text{for } j = N/2, \\ Y_0^{n+1} = \mathbf{s}_l(t_{n+1}), \quad Y_N^{n+1} = \mathbf{s}_r(t_{n+1}), & n = 0, 1, \dots, M-1, \end{array} \right. \end{array} \right. \quad (6.8)$$

where

$$\left\{ \begin{array}{l} \mathcal{L}_{mup}^{N,\Delta t,(-)} Y_j^{n+1} = \varepsilon \delta_x^2 Y_j^{n+1} + a_{j-1/2} D_x^- Y_j^{n+1} - b_{j-1/2}^{n+1} Y_{j-1/2}^{n+1} - D_t^- Y_{j-1/2}^{n+1}, \\ \mathcal{L}_{mcd}^{N,\Delta t} Y_j^{n+1} = \varepsilon \delta_x^2 Y_j^{n+1} + a_j D_x^* Y_j^{n+1} - b_j^{n+1} Y_j^{n+1} - D_t^- Y_j^{n+1}, \\ \mathcal{L}_{mup}^{N,\Delta t,(+)} Y_j^{n+1} = \varepsilon \delta_x^2 Y_j^{n+1} + a_{j+1/2} D_x^+ Y_j^{n+1} - b_{j+1/2}^{n+1} Y_{j+1/2}^{n+1} - D_t^- Y_{j+1/2}^{n+1}, \end{array} \right. \quad (6.9)$$

and

$$\left\{ \begin{array}{l} D_x^F Y_j^{n+1} = [-Y_{N/2+2}^{n+1} + 4Y_{N/2+1}^{n+1} - 3Y_{N/2}^{n+1}]/2h_r, \\ D_x^B Y_j^{n+1} = [Y_{N/2-2}^{n+1} - 4Y_{N/2-1}^{n+1} + 3Y_{N/2}^{n+1}]/2h_l. \end{array} \right. \quad (6.10)$$

Next, the difference scheme in (6.8) is rewritten into the following form:

$$\left\{ \begin{array}{l} Y_j^0 = \mathbf{q}_0(x_j), \quad \text{for } 0 \leq j \leq N, \\ \left\{ \begin{array}{l} \mathcal{L}_\varepsilon^{N,\Delta t} Y_j^{n+1} = g_j^{n+1}, \quad \text{for } 1 \leq j \leq N-1, \\ Y_0^{n+1} = \mathbf{s}_l(t_{n+1}), \quad Y_N^{n+1} = \mathbf{s}_r(t_{n+1}), \quad n = 0, 1, \dots, M-1, \end{array} \right. \end{array} \right. \quad (6.11)$$

where the difference operator $\mathcal{L}_\varepsilon^{N,\Delta t}$ is given by

$$\mathcal{L}_\varepsilon^{N,\Delta t} Y_j^{n+1} = \begin{cases} \left[\mu_j^- Y_{j-1}^{n+1} + \mu_j^c Y_j^{n+1} + \mu_j^+ Y_{j+1}^{n+1} \right] + \left[\lambda_j^- Y_{j-1}^n + \lambda_j^c Y_j^n + \lambda_j^+ Y_{j+1}^n \right], \\ \text{for } 1 \leq j < N/2 \text{ and } N/2 < j \leq N-1, \\ \left[\nu_j^{-,2} Y_{j-2}^{n+1} + \nu_j^{-,1} Y_{j-1}^{n+1} + \nu_j^c Y_j^{n+1} + \nu_j^{+,1} Y_{j+1}^{n+1} + \nu_j^{+,2} Y_{j+2}^{n+1} \right], \\ \text{for } j = N/2, \end{cases} \quad (6.12)$$

and the term \mathcal{G}_j^{n+1} is given by

$$\mathcal{G}_j^{n+1} = \begin{cases} g_j^{n+1}, & \text{for } 1 \leq j \leq N/4 \text{ and } 3N/4 \leq j \leq N-1, \text{ and when } \varepsilon > 2\|a\|N^{-1}, \\ g_{j-1/2}^{n+1}, & \text{for } 1 \leq j \leq N/4, \text{ and when } \varepsilon \leq 2\|a\|N^{-1}, \\ g_{j+1/2}^{n+1}, & \text{for } 3N/4 \leq j \leq N-1, \text{ and when } \varepsilon \leq 2\|a\|N^{-1}, \\ g_j^{n+1}, & \text{for } N/4 < j < N/2 \text{ and } N/2 < j < 3N/4, \\ 0, & \text{for } j = N/2. \end{cases} \quad (6.13)$$

We denote that

$$\mathbf{p}_j = \varepsilon + a_j h_j / 2, \quad \text{for } 1 \leq j < N/2, \quad \text{and} \quad \mathbf{q}_j = \varepsilon - a_j h_{j+1} / 2, \quad \text{for } N/2 < j \leq N-1.$$

When $\varepsilon > 2\|a\|N^{-1}$, the coefficients in (6.12), respectively, for $1 \leq j < N/2$ and $N/2 < j \leq N-1$ are given by

$$\left\{ \begin{array}{l} \mu_j^- = \frac{2\mathbf{p}_j}{h_j \widehat{h_j}} - \frac{a_j}{h_j}, \\ \mu_j^c = \frac{-2\mathbf{p}_j}{h_j h_{j+1}} + \frac{a_j}{h_j} - b_j^{n+1} - \frac{1}{\Delta t}, \\ \mu_j^+ = \frac{2\mathbf{p}_j}{h_{j+1} \widehat{h_j}}, \\ \lambda_j^- = 0, \quad \lambda_j^c = \frac{1}{\Delta t}, \quad \lambda_j^+ = 0, \end{array} \right. \quad \text{and} \quad \left\{ \begin{array}{l} \mu_j^- = \frac{2\mathbf{q}_j}{h_j \widehat{h_j}}, \\ \mu_j^c = \frac{-2\mathbf{q}_j}{h_j h_{j+1}} - \frac{a_j}{h_{j+1}} - b_j^{n+1} - \frac{1}{\Delta t}, \\ \mu_j^+ = \frac{2\mathbf{q}_j}{h_{j+1} \widehat{h_j}} + \frac{a_j}{h_{j+1}}, \\ \lambda_j^- = 0, \quad \lambda_j^c = \frac{1}{\Delta t}, \quad \lambda_j^+ = 0. \end{array} \right.$$

Next, when $\varepsilon \leq 2||a||N^{-1}$, the coefficients in (6.12), respectively for $1 \leq j \leq N/4$ and $N/4 < j < N/2$ are given by

$$\left\{ \begin{array}{l} \mu_j^- = \frac{2\varepsilon}{h_j \hat{h}_j} - \frac{a_{j-1/2}}{h_j} - \frac{b_{j-1/2}^{n+1}}{2} - \frac{1}{2\Delta t}, \\ \mu_j^c = \frac{-2\varepsilon}{h_j h_{j+1}} + \frac{a_{j-1/2}}{h_j} - \frac{b_{j-1/2}^{n+1}}{2} - \frac{1}{2\Delta t}, \\ \mu_j^+ = \frac{2\varepsilon}{h_{j+1} \hat{h}_j}, \\ \lambda_j^- = \frac{1}{2\Delta t}, \quad \lambda_j^c = \frac{1}{2\Delta t}, \quad \lambda_j^+ = 0, \end{array} \right. \text{ and } \left\{ \begin{array}{l} \mu_j^- = \frac{2\mathbf{p}_j}{h_j \hat{h}_j} - \frac{a_j}{h_j}, \\ \mu_j^c = \frac{-2\mathbf{p}_j}{h_j h_{j+1}} + \frac{a_j}{h_j} - b_j^{n+1} - \frac{1}{\Delta t}, \\ \mu_j^+ = \frac{2\mathbf{p}_j}{h_{j+1} \hat{h}_j}, \\ \lambda_j^- = 0, \quad \lambda_j^c = \frac{1}{\Delta t}, \quad \lambda_j^+ = 0, \end{array} \right.$$

and for $N/2 < j < 3N/4$ and $3N/4 \leq j \leq N-1$ are respectively given by

$$\left\{ \begin{array}{l} \mu_j^- = \frac{2\mathbf{q}_j}{h_j \hat{h}_j}, \\ \mu_j^c = \frac{-2\mathbf{q}_j}{h_j h_{j+1}} - \frac{a_j}{h_{j+1}} - b_j^{n+1} - \frac{1}{\Delta t}, \\ \mu_j^+ = \frac{2\mathbf{q}_j}{h_{j+1} \hat{h}_j} + \frac{a_j}{h_{j+1}}, \\ \lambda_j^- = 0, \quad \lambda_j^c = \frac{1}{\Delta t}, \quad \lambda_j^+ = 0, \end{array} \right. \text{ and } \left\{ \begin{array}{l} \mu_j^- = \frac{2\varepsilon}{h_j \hat{h}_j}, \\ \mu_j^c = \frac{-2\varepsilon}{h_j h_{j+1}} - \frac{a_{j+1/2}}{h_{j+1}} - \frac{b_{j+1/2}^{n+1}}{2} - \frac{1}{2\Delta t}, \\ \mu_j^+ = \frac{2\varepsilon}{h_{j+1} \hat{h}_j} + \frac{a_{j+1/2}}{h_{j+1}} - \frac{b_{j+1/2}^{n+1}}{2} - \frac{1}{2\Delta t}, \\ \lambda_j^- = 0, \quad \lambda_j^c = \frac{1}{2\Delta t}, \quad \lambda_j^+ = \frac{1}{2\Delta t}. \end{array} \right.$$

Finally, for $j = N/2$, the coefficient in (6.12) are given by

$$\nu_{N/2}^{-,2} = \frac{-1}{2h_l}, \quad \nu_{N/2}^{-,1} = \frac{2}{h_l}, \quad \nu_{N/2}^c = \frac{-3}{2} \left(\frac{1}{h_l} + \frac{1}{h_r} \right), \quad \nu_{N/2}^{+,1} = \frac{2}{h_r}, \quad \nu_{N/2}^{+,2} = \frac{-1}{2h_r}.$$

6.3.3 Stability

Here, the stability of the fully discrete scheme (6.11)-(6.13) is discussed. We consider non-uniform mesh in the analysis and assume that $\eta_1 = \eta_2 = \eta = \eta_0 \varepsilon \ln N$. Then, $h_l = h_r = h$, say. It is obvious that the discrete maximum principle does not hold for the difference operator defined in (6.12). We overcome this difficulty by replacing $Y_{N/2-2}^{n+1}$ and $Y_{N/2+2}^{n+1}$ in the equation corresponding to the point $x_{N/2} = d$ given by (6.11), with the following expressions

$$\left\{ \begin{array}{l} Y_{N/2-2}^{n+1} = \frac{1}{\mu_{N/2-1}^-} \left[g_{N/2-1}^{n+1} - \mu_{N/2-1}^c Y_{N/2-1}^{n+1} - \mu_{N/2-1}^+ Y_{N/2}^{n+1} - \frac{1}{\Delta t} U_{N/2-1}^n \right], \\ Y_{N/2+2}^{n+1} = \frac{1}{\mu_{N/2+1}^+} \left[g_{N/2+1}^{n+1} - \mu_{N/2+1}^c Y_{N/2+1}^{n+1} - \mu_{N/2+1}^- Y_{N/2}^{n+1} - \frac{1}{\Delta t} U_{N/2+1}^n \right]. \end{array} \right. \quad (6.14)$$

Thus, we modify the system of equations in (6.11) to the following tri-diagonal form:

$$\begin{cases} Y_j^0 = \mathbf{q}_0(x_j), & \text{for } 0 \leq j \leq N, \\ \begin{cases} \mathbf{L}_{hyb}^{N,\Delta t} Y_j^{n+1} = \tilde{\mathcal{G}}_j^{n+1}, & \text{for } 1 \leq j \leq N, \\ Y_0^{n+1} = \mathbf{s}_l(t_{n+1}), \quad Y_N^{n+1} = \mathbf{s}_r(t_{n+1}), & n = 0, 1, \dots, M-1. \end{cases} \end{cases} \quad (6.15)$$

Here, the difference operator $\mathbf{L}_{hyb}^{N,\Delta t}$ and the term $\tilde{\mathcal{G}}_j^{n+1}$ are respectively given by

$$\mathbf{L}_{hyb}^{N,\Delta t} Y_j^{n+1} = \begin{cases} \left[\mu_j^- Y_{j-1}^{n+1} + \mu_j^c Y_j^{n+1} + \mu_j^+ Y_{j+1}^{n+1} \right] + \left[\lambda_j^- Y_{j-1}^n + \lambda_j^c Y_j^n + \lambda_j^+ Y_{j+1}^n \right], & \text{for } j = N/2, \\ \mathcal{L}_\varepsilon^{N,\Delta t} Y_j^{n+1}, & \text{for } j \neq N/2, \end{cases} \quad (6.16)$$

and

$$\tilde{\mathcal{G}}_j^{n+1} = \begin{cases} \frac{h/2}{\mathbf{p}_{j-1} - a_{j-1}h} g_{j-1}^{n+1} + \frac{h/2}{\mathbf{q}_{j+1} + a_{j+1}h} g_{j+1}^{n+1}, & \text{for } j = N/2, \\ g_j^{n+1}, & \text{for } j \neq N/2, \end{cases} \quad (6.17)$$

where

$$\begin{cases} \mu_{N/2}^- = \frac{1}{2h} \left[4 - \frac{2\mathbf{p}_{N/2-1} - a_{N/2-1}h + b_{N/2-1}^{n+1}h^2 + \frac{h^2}{\Delta t}}{\mathbf{p}_{N/2-1} - a_{N/2-1}h} \right], \\ \mu_{N/2}^c = \frac{1}{2h} \left[-6 + \frac{\mathbf{p}_{N/2-1}}{\mathbf{p}_{N/2-1} - a_{N/2-1}h} + \frac{\mathbf{q}_{N/2+1}}{\mathbf{q}_{N/2+1} + a_{N/2+1}h} \right], \\ \mu_{N/2}^+ = \frac{1}{2h} \left[4 - \frac{2\mathbf{q}_{N/2+1} + a_{N/2+1}h + b_{N/2+1}^{n+1}h^2 + \frac{h^2}{\Delta t}}{\mathbf{q}_{N/2+1} + a_{N/2+1}h} \right], \\ \lambda_{N/2}^- = \frac{h/2}{(\mathbf{p}_{N/2-1} - a_{N/2-1}h)\Delta t}, \quad \lambda_{N/2}^c = 0, \quad \lambda_{N/2}^+ = \frac{h/2}{(\mathbf{q}_{N/2+1} + a_{N/2+1}h)\Delta t}. \end{cases} \quad (6.18)$$

Next, we prove that the difference operator $\mathbf{L}_{hyb}^{N,\Delta t}$ given in (6.16) satisfies the discrete maximum principle in the following lemma.

Let $\mathfrak{D}^{N,\Delta t} = \mathfrak{D} \cap \overline{\mathfrak{D}}^{N,\Delta t}$ and $\partial \mathfrak{D}^{N,\Delta t} = \overline{\mathfrak{D}}^{N,\Delta t} \setminus \mathfrak{D}^{N,\Delta t}$. Let $\mathfrak{m}^* = \max\{\mathfrak{m}_1^*, \mathfrak{m}_2^*\}$.

Lemma 6.3. *Suppose that the following conditions hold for $N \geq N_0$:*

$$2\eta_0 \mathfrak{m}^* \leq N/\ln N \quad \text{and} \quad (6.19)$$

$$\frac{\mathfrak{m}N}{2} \geq \left(\|b\| + \frac{1}{\Delta t} \right), \quad (6.20)$$

where N_0 is some positive integer. Then, if a mesh function ψ defined on $\overline{\mathfrak{D}}^{N,\Delta t}$ satisfies that $\psi \leq 0$ on $\partial \mathfrak{D}^{N,\Delta t}$ and $\mathbf{L}_{hyb}^{N,\Delta t} \psi \geq 0$ in $\mathfrak{D}^{N,\Delta t}$, then $\psi \leq 0$ on $\overline{\mathfrak{D}}^{N,\Delta t}$.

Proof: In this proof, we use [[99], Lemma 3.12] and for clarity of the presentation, we discuss the proof in

detailed below. Let $\omega_j^n \leq 0$, for all j and n . Then, following the hypothesis of the discrete maximum principle, we consider the mesh function ψ such that

$$\psi_j^0 = \omega_j^0, \quad \text{for } 0 \leq j \leq N, \quad (6.21)$$

and satisfies the following system for $n = 0, 1, \dots, M$,

$$\begin{cases} -L_{hyb}^{N,\Delta t} \psi_j^{n+1} = \omega_j^{n+1}, & \text{for } 1 \leq j \leq N-1, \\ \psi_0^{n+1} = \omega_0^{n+1}, \quad \psi_N^{n+1} = \omega_N^{n+1}. \end{cases} \quad (6.22)$$

For simplifying the proof, we set $\psi^n = (\psi_0^n, \dots, \psi_N^n)$ and $\omega^n = (\omega_0^n, \dots, \omega_N^n)$, for $n = 0, 1, \dots, M$, so that (6.22) can be rewritten as

$$\mathcal{A}\psi^{n+1} - \mathcal{B}\psi^n = \omega^{n+1}, \quad n = 0, 1, \dots, M-1, \quad (6.23)$$

where the matrices \mathcal{A} and \mathcal{B} are respectively given by

$$\begin{cases} \mathcal{A}_{j,j} = 1, & \text{for } j = 0, N, \\ \mathcal{A}_{j,j-1} = -\mu_j^-, \quad \mathcal{A}_{j,j} = -\mu_j^c, \quad \mathcal{A}_{j,j+1} = -\mu_j^+, & \text{for } 1 \leq j \leq N-1, \end{cases} \quad (6.24)$$

and

$$\begin{cases} \mathcal{B}_{j,j} = 0, & \text{for } j = 0, N, \\ \mathcal{B}_{j,j-1} = \lambda_j^-, \quad \mathcal{B}_{j,j} = \lambda_j^c, \quad \mathcal{B}_{j,j+1} = \lambda_j^+, & \text{for } 1 \leq j \leq N-1. \end{cases} \quad (6.25)$$

Now, the following two cases are considered to show that \mathcal{A} is an M-matrix.

Case 1. Let $\varepsilon > 2\|a\|N^{-1}$. Then, we have

$$\begin{cases} \mathbf{p}_j \geq (\varepsilon - \|a\|h_j/2) > 0, & \text{for } 1 \leq j < N/2, \\ \mathbf{q}_j \geq (\varepsilon - \|a\|h_{j+1}/2) > 0, & \text{for } N/2 < j \leq N-1. \end{cases}$$

Hence, for $1 \leq j < N/2$ and $N/2 < j \leq N-1$, it follows from (6.24) that

$$\begin{cases} \mathcal{A}_{j,j-1} < 0, \quad \mathcal{A}_{j,j} > 0, \quad \mathcal{A}_{j,j+1} < 0, \\ \text{and} \quad |\mathcal{A}_{j,j+1}| + |\mathcal{A}_{j,j-1}| \leq |\mathcal{A}_{j,j}|. \end{cases} \quad (6.26)$$

Now, let $j = N/2$. Under the assumption (6.20) and using $h \leq 4N^{-1}$, we have

$$\begin{aligned}\mathcal{A}_{N/2, N/2-1} &= \frac{1}{2h} \left[\frac{-2\mathbf{p}_{N/2-1} + 3a_{N/2-1}h + b_{N/2-1}^{n+1}h^2 + \frac{h^2}{\Delta t}}{\mathbf{p}_{N/2-1} - a_{N/2-1}h} \right], \\ &\leq \frac{1}{2h} \left[\frac{-2\mathbf{p}_{N/2-1} + 3a_{N/2-1}h + (||b|| + \frac{1}{\Delta t})h^2}{\mathbf{p}_{N/2-1} - a_{N/2-1}h} \right], \\ &\leq -\frac{1}{2h} \left[\frac{2\mathbf{p}_{N/2-1} + (3\mathbf{m}_1N/4 - (||b|| + \frac{1}{\Delta t}))h^2}{\mathbf{p}_{N/2-1} - a_{N/2-1}h} \right],\end{aligned}$$

and

$$\begin{aligned}\mathcal{A}_{N/2, N/2+1} &= \frac{1}{2h} \left[\frac{-2\mathbf{q}_{N/2+1} - 3a_{N/2+1}h + b_{N/2+1}^{n+1}h^2 + \frac{h^2}{\Delta t}}{\mathbf{q}_{N/2+1} + a_{N/2+1}h} \right], \\ &\leq \frac{1}{2h} \left[\frac{-2\mathbf{q}_{N/2+1} - 3a_{N/2+1}h + (||b|| + \frac{1}{\Delta t})h^2}{\mathbf{q}_{N/2+1} + a_{N/2+1}h} \right], \\ &\leq -\frac{1}{2h} \left[\frac{2\mathbf{q}_{N/2+1} + (3\mathbf{m}_2N/4 - (||b|| + \frac{1}{\Delta t}))h^2}{\mathbf{q}_{N/2+1} + a_{N/2+1}h} \right].\end{aligned}$$

Also, it clear that $\mathcal{A}_{N/2, N/2-1} < 0$, $\mathcal{A}_{N/2, N/2+1} < 0$ and

$$\mathcal{A}_{N/2, N/2} = \frac{1}{2h} \left[\frac{2\mathbf{p}_{N/2-1} - 3a_{N/2-1}h}{\mathbf{p}_{N/2-1} - a_{N/2-1}h} + \frac{2\mathbf{q}_{N/2+1} + 3a_{N/2+1}h}{\mathbf{q}_{N/2+1} + a_{N/2+1}h} \right] > 0,$$

and hence,

$$|\mathcal{A}_{N/2, N/2+1}| + |\mathcal{A}_{N/2, N/2-1}| \leq |\mathcal{A}_{N/2, N/2}|.$$

Case 2. Let $\varepsilon \leq 2||a||N^{-1}$. Under the assumption (6.19), we obtain that

$$\begin{cases} \mathbf{p}_j \geq (\mathbf{m}^* + a_j)h/2 > 0, & \text{for } N/4 < j < N/2, \\ \mathbf{q}_j \geq (\mathbf{m}^* - a_j)h/2 > 0, & \text{for } N/2 < j < 3N/4. \end{cases}$$

Likewise the previous case, (6.26) follows from (6.24) for $N/4 < j < 3N/4$. Next, we directly obtain from (6.24) that $\mathcal{A}_{j, j+1} < 0$, $\mathcal{A}_{j, j} > 0$, for $1 \leq j \leq N/4$, and $\mathcal{A}_{j, j-1} < 0$, $\mathcal{A}_{j, j} > 0$, for $3N/4 \leq j \leq N-1$. Now, under the assumption (6.20) and using the inequalities $H_l \leq 4N^{-1}$, $H_r \leq 4N^{-1}$, we obtain from (6.24) for $1 \leq j \leq N/4$ that

$$\begin{aligned}\mathcal{A}_{j, j-1} &\leq -\frac{2\varepsilon}{h_j \widehat{h_j}} + \frac{a_{j-1/2}}{h_j} + \frac{1}{2} \left(||b|| + \frac{1}{\Delta t} \right), \\ &\leq -\left[\frac{2\varepsilon}{h_j \widehat{h_j}} + \frac{1}{2} \left(\frac{\mathbf{m}_1 N}{2} - \left(||b|| + \frac{1}{\Delta t} \right) \right) \right], \\ &< 0,\end{aligned}$$

and for $3N/4 \leq j \leq N-1$,

$$\begin{aligned}\mathcal{A}_{j,j+1} &= \frac{-2\varepsilon}{h_{j+1}\hat{h}_j} - \frac{a_{j+1/2}}{h_{j+1}} + \frac{b_{j+1/2}^{n+1}}{2} + \frac{1}{2\Delta t}, \\ &\leq -\left[\frac{2\varepsilon}{h_{j+1}\hat{h}_j} + \frac{1}{2}\left(\frac{\mathfrak{m}_2 N}{2} - \left(\|b\| + \frac{1}{\Delta t}\right)\right)\right], \\ &< 0.\end{aligned}$$

Further, it straightforward to obtain that $|\mathcal{A}_{j,j+1}| + |\mathcal{A}_{j,j-1}| \leq |\mathcal{A}_{j,j}|$, for $1 \leq j \leq N/4$ and $3N/4 \leq j \leq N-1$, Thus, in both the cases it is proved that \mathcal{A} is an M-matrix and it is easy to see that \mathcal{A} is also an irreducible. Hence, $\mathcal{A}^{-1} \geq 0$.

Afterwards, in order to show that $\psi^n \leq 0$ for each n , we use induction on n . Firstly, it follows from (6.21) and (6.22) that $\psi^0 \leq 0$. Now, we assume that $\psi^n \leq 0$, for each $n \in \{0, 1, \dots, M\}$. Since, $\mathcal{A}^{-1} \geq 0$ and from (6.25) we have $\mathcal{B} \geq 0$, by applying the induction hypothesis, it follows from (6.23) that $\psi^{n+1} \leq 0$, and this complete the proof. ■

Now, consequently using Lemma 6.3, we establish the following stability result

Lemma 6.4. *Under the conditions given in (6.19) and (6.20), the solution Y of (6.15)-(6.18) satisfies the following bound*

$$\|Y\|_{\overline{\mathfrak{D}}^{N,\Delta t}} \leq \|Y\|_{\partial\mathfrak{D}^{N,\Delta t}} + \frac{1}{\gamma} \|\tilde{\mathcal{G}}\|_{\overline{\mathfrak{D}}^{N,\Delta t}},$$

where $\gamma = \min\{\mathfrak{m}_1/\mathfrak{d}, \mathfrak{m}_2/(1-\mathfrak{d})\}$.

Proof: We consider the mesh function

$$\psi_j^{\pm,n} = -\|Y\|_{\partial\mathfrak{D}^{N,\Delta t}} \pm Y_j^n - \begin{cases} \frac{x_j}{\gamma\mathfrak{d}} \|\tilde{\mathcal{G}}\|_{\overline{\mathfrak{D}}^{N,\Delta t}}, & \text{for } 0 \leq j \leq N/2, \\ \frac{1-x_j}{\gamma(1-\mathfrak{d})} \|\tilde{\mathcal{G}}\|_{\overline{\mathfrak{D}}^{N,\Delta t}}, & \text{for } N/2 \leq j \leq N. \end{cases}$$

Then, it clearly shows that $\psi_j^{\pm,n} \leq 0$ on $\partial\mathfrak{D}^{N,\Delta t}$. Now, when $\varepsilon > 2\|a\|N^{-1}$, for $1 \leq j < N/2$, we obtain that

$$\mathbf{L}_{hyb}^{N,\Delta t} \psi_j^{\pm,n+1} = \pm \mathbf{L}_{hyb}^{N,\Delta t} Y_j^{\pm,n+1} - \frac{a_j}{\gamma\mathfrak{d}} \|\tilde{\mathcal{G}}\|_{\overline{\mathfrak{D}}^{N,\Delta t}} + b_j^{n+1} \left(\frac{x_j}{\gamma\mathfrak{d}} \|\tilde{\mathcal{G}}\|_{\overline{\mathfrak{D}}^{N,\Delta t}} + \|Y\|_{\partial\mathfrak{D}^{N,\Delta t}} \right) \geq 0,$$

and when $\varepsilon \leq 2\|a\|N^{-1}$, we have

$$\mathbf{L}_{hyb}^{N,\Delta t} \psi_j^{\pm,n+1} = \begin{cases} \pm \mathbf{L}_{hyb}^{N,\Delta t} Y_j^{\pm,n+1} - \frac{a_j}{\gamma\mathfrak{d}} \|\tilde{\mathcal{G}}\|_{\overline{\mathfrak{D}}^{N,\Delta t}} + b_j^{n+1} \left(\frac{x_j}{\gamma\mathfrak{d}} \|\tilde{\mathcal{G}}\|_{\overline{\mathfrak{D}}^{N,\Delta t}} + \|Y\|_{\partial\mathfrak{D}^{N,\Delta t}} \right), & \text{for } 1 \leq j \leq N/4, \\ \pm \mathbf{L}_{hyb}^{N,\Delta t} Y_j^{\pm,n+1} - \frac{a_{j-1/2}}{\gamma\mathfrak{d}} \|\tilde{\mathcal{G}}\|_{\overline{\mathfrak{D}}^{N,\Delta t}} + b_{j-1/2}^{n+1} \left(\frac{x_{j-1/2}}{\gamma\mathfrak{d}} \|\tilde{\mathcal{G}}\|_{\overline{\mathfrak{D}}^{N,\Delta t}} + \|Y\|_{\partial\mathfrak{D}^{N,\Delta t}} \right), & \text{for } N/4 < j < N/2, \end{cases}$$

$$\geq 0.$$

Similarly, one can show that $L_{hyb}^{N,\Delta t} \psi_j^{\pm,n+1} \geq 0$, for $N/2 < j \leq N-1$. Next, at the point $x_{N/2} = \mathbf{d}$, we have

$$\begin{aligned} & L_{hyb}^{N,\Delta t} \psi_{N/2}^{\pm,n+1} \\ &= \frac{h/2}{(\mathbf{p}_{N/2-1} - a_{N/2-1}h)} L_{hyb}^{N,\Delta t} \psi_{N/2-1}^{\pm,n+1} + \frac{h/2}{(\mathbf{q}_{N/2+1} + a_{N/2+1}h)} L_{hyb}^{N,\Delta t} \psi_{N/2+1}^{\pm,n+1} + (D_x^F - D_x^B) \psi_{N/2}^{\pm,n+1}, \\ &\geq (D_x^F - D_x^B) \psi_{N/2}^{\pm,n+1} \geq 0. \end{aligned}$$

Therefore, by applying Lemma 6.3, we obtain the required stability bound. ■

6.4 Auxiliary results

On $\bar{\Omega}^N = \{x_j\}_0^N$, let us introduce two mesh functions

$$\begin{cases} \mathcal{S}_j(\theta) = \prod_{k=1}^j \left(1 + \frac{\theta h_k}{\varepsilon}\right), & \text{for } 1 \leq j \leq N/2, \\ \mathcal{R}_j(\theta) = \prod_{k=j+1}^N \left(1 + \frac{\theta h_k}{\varepsilon}\right), & \text{for } N/2 \leq j \leq N-1. \end{cases}$$

We set $\mathcal{S}_0(\theta) = 1$ and $\mathcal{R}_N(\theta) = 1$, where θ is a positive constant.

Lemma 6.5. *The mesh functions $\mathcal{S}_j(\theta)$ and $\mathcal{R}_j(\theta)$ satisfy the following bounds:*

$$\begin{cases} \exp(-\theta(\mathbf{d} - x_j)/\varepsilon) \leq \frac{\mathcal{S}_j(\theta)}{\mathcal{S}_{N/2}(\theta)}, & \text{for } 1 \leq j < N/2, \\ \exp(-\theta(x_j - \mathbf{d})/\varepsilon) \leq \frac{\mathcal{R}_j(\theta)}{\mathcal{R}_{N/2}(\theta)}, & \text{for } N/2 < j \leq N-1. \end{cases}$$

Proof: See [83, Lemma 5.10] for the proof. ■

Lemma 6.6. *Let $\theta = \mathfrak{m}/2$. Then, for some constant C , $\mathcal{S}_j(\theta)$ and $\mathcal{R}_j(\theta)$ satisfy the following bounds:*

$$\begin{cases} \frac{\mathcal{S}_j(\theta)}{\mathcal{S}_{N/2}(\theta)} \leq CN^{-4}(1 - 2j/N), & \text{for } N/4 \leq j < N/2, \\ \frac{\mathcal{R}_j(\theta)}{\mathcal{R}_{N/2}(\theta)} \leq CN^{-4}(2j/N - 1), & \text{for } N/2 < j \leq 3N/4. \end{cases}$$

Proof: See [83, Lemma 5.7] for the proof. ■

Lemma 6.7. *Let $\theta = \mathfrak{m}/2$. Then, there exist some constant C such that*

$$\begin{cases} -L_{hyb}^{N,\Delta t} \mathcal{S}_j(\theta) \geq \frac{C}{\varepsilon + \theta h} \mathcal{S}_j(\theta), & \text{for } N/4 < j < N/2, \\ -L_{hyb}^{N,\Delta t} \mathcal{R}_j(\theta) \geq \frac{C}{\varepsilon + \theta h} \mathcal{R}_j(\theta), & \text{for } N/2 < j < 3N/4. \end{cases}$$

Proof: $\mathcal{S}_{j-1}(\theta) = \left(\frac{\varepsilon}{\varepsilon + \theta h_j}\right) \mathcal{S}_j(\theta)$, for $j < N/2$ and $\mathcal{R}_{j+1}(\theta) = \left(\frac{\varepsilon}{\varepsilon + \theta h_j}\right) \mathcal{R}_j(\theta)$, for $j > N/2$. Then, a

straightforward calculation yields that for $N/4 < j < N/2$,

$$\begin{aligned} -L_{hyb}^{N,\Delta t} \mathcal{S}_j(\theta) &\geq -\frac{\theta}{h} (\mathcal{S}_j(\theta) - \mathcal{S}_{j-1}(\theta)) - a_j \frac{\theta}{2\varepsilon} (\mathcal{S}_j(\theta) + \mathcal{S}_{j-1}(\theta)) + b_j^{n+1} \mathcal{S}_j(\theta), \\ &\geq \frac{\theta}{\varepsilon} \mathcal{S}_{j-1}(\theta) (-a_j - \theta) - a_j \frac{\theta^2 h}{2\varepsilon^2} \mathcal{S}_{j-1}(\theta), \end{aligned}$$

and for $N/2 < j < 3N/4$,

$$\begin{aligned} -L_{hyb}^{N,\Delta t} \mathcal{R}_j(\theta) &\geq \frac{\theta}{h} (\mathcal{R}_{j+1}(\theta) - \mathcal{R}_j(\theta)) + a_j \frac{\theta}{\varepsilon} (\mathcal{R}_{j+1}(\theta) + \mathcal{R}_j(\theta)) + b_j^{n+1} \mathcal{R}_j(\theta), \\ &\geq \frac{\theta}{\varepsilon} \mathcal{R}_{j+1}(\theta) (a_j - \theta) + a_j \frac{\theta^2 h}{2\varepsilon^2} \mathcal{R}_{j+1}(\theta). \end{aligned}$$

Now, using $a_j < -m_1 \leq -2\theta$ and $a_j > m_2 \geq 2\theta$, respectively for $N/4 < j < N/2$ and $N/2 < j < 3N/4$, we obtain the desired result. \blacksquare

Next, we introduce two mesh functions Ψ_l and Ψ_r , respectively on $\bar{\Omega}^N \cap [0, d]$ and $\bar{\Omega}^N \cap [d, 1]$, such that they are solutions of the following discrete problems:

$$\begin{cases} \varepsilon \delta_x^2 \Psi_{l,j} - \theta D_x^- \Psi_{l,j} = 0, & \text{for } 1 \leq j < N/2, \\ \Psi_{l,0} = 0, \quad \Psi_{l,N/2} = 1, \end{cases} \quad (6.27)$$

and

$$\begin{cases} \varepsilon \delta_x^2 \Psi_{r,j} + \theta D_x^+ \Psi_{r,j} = 0, & \text{for } N/2 < j \leq N-1, \\ \Psi_{r,N/2} = 1, \quad \Psi_{r,N} = 0, \end{cases} \quad (6.28)$$

Lemma 6.8. *Let $\theta = m/2$. Then, the mesh functions Ψ_l and Ψ_r , respectively satisfy the following properties:*

$$\begin{cases} \Psi_{l,j} \geq 0, \quad \text{and} \quad D_x^- \Psi_{l,j} \geq 0, & \text{for } 1 \leq j \leq N/2, \\ \text{and} \quad \Psi_{l,N/4} \leq CN^{-2}, & \text{for some constant } C. \end{cases} \quad (6.29)$$

and

$$\begin{cases} \Psi_{r,j} \geq 0, \quad \text{and} \quad D_x^+ \Psi_{r,j} \leq 0, & \text{for } N/2 \leq j \leq N-1, \\ \text{and} \quad \Psi_{r,3N/4} \leq CN^{-2}, & \text{for some constant } C. \end{cases} \quad (6.30)$$

Proof. Here, we provide the outline of the proof with suitable modifications of the approach introduced in [32]. The solution Ψ_l of the discrete problem (6.27) can be expressed in the following form:

$$\Psi_{l,j} = \begin{cases} \Psi_{l,N/4} r_j, & \text{for } 0 \leq j \leq N/4, \\ 1 + (\Psi_{l,N/4} - 1) s_j, & \text{for } N/4 \leq j \leq N/2, \end{cases} \quad (6.31)$$

where $r_j = \frac{\sigma^j - 1}{\sigma^{N/4} - 1}$, $\sigma = 1 + \frac{\theta H_l}{\varepsilon}$; $s_j = \frac{1 - \rho^{j-N/2}}{1 - \rho^{-N/4}}$, $\rho = 1 + \frac{\theta h}{\varepsilon}$; and $\Psi_{l,N/4}$ satisfies that

$$\varepsilon \delta_x^2 \Psi_{l,N/4} - \theta D_x^- \Psi_{l,N/4} = 0. \quad (6.32)$$

From (6.31) and (6.32), we get

$$\Psi_{l,N/4} = \frac{D_x^+ \ell_{N/4}}{[D_x^+ \ell_{N/4} - (1/2)(\rho + \sigma) D_x^+ r_{N/4}]}. \quad (6.33)$$

and

$$D_x^- \Psi_{l,j} = \begin{cases} \Psi_{l,N/4} \frac{\theta \sigma^{j-1}}{\varepsilon (\sigma^{N/4} - 1)}, & \text{for } 1 \leq j \leq N/4, \\ (1 - \Psi_{l,N/4}) \frac{\theta \rho^{j-N/2-1}}{\varepsilon (\rho^{N/4} - 1)}, & \text{for } N/4 < j \leq N/2. \end{cases} \quad (6.34)$$

Now, by using the inequality $\ln(1 + \xi) > \xi(1 - \xi/2)$, for $0 < \xi < 1$, and setting $\xi = 8N^{-1} \ln N$, we obtain that

$$\rho^{-N/4} = (1 + \xi)^{-N/4} \leq CN^{-2}. \quad (6.35)$$

Hence, the desired results for Ψ_l follows from (6.33), (6.34) and (6.35); and the results for Ψ_r can be obtained analogously. ■

6.5 Error analysis

In this section, we obtain the ε -uniform error estimate *via* decomposition of the discrete solution.

6.5.1 Decomposition of the discrete solution

Here, the discrete solution Y is decomposed as

$$Y_j^{n+1} = \begin{cases} \mathcal{V}_{l,j}^{n+1} + \mathcal{Z}_{l,j}^{n+1}, & \text{for } 0 \leq j < N/2, \\ \mathcal{V}_{l,j}^{n+1} + \mathcal{Z}_{l,j}^{n+1} = \mathcal{V}_{r,j}^{n+1} + \mathcal{Z}_{r,j}^{n+1}, & \text{for } j = N/2, \\ \mathcal{V}_{r,j}^{n+1} + \mathcal{Z}_{r,j}^{n+1}, & \text{for } N/2 < j \leq N, \end{cases} \quad (6.36)$$

where the mesh functions \mathcal{V}_l and \mathcal{V}_r are considered as the smooth components for approximating v respectively to the left and the right side of the point $x_{N/2} = \mathbf{d}$, and they satisfy the following discrete problems:

$$\begin{cases} \mathcal{V}_{l,j}^0 = v(x_j, 0), & \text{for } 0 \leq j \leq N/2, \\ \begin{cases} \mathcal{L}_{hyb}^{N,\Delta t} \mathcal{V}_{l,j}^{n+1} = \tilde{\mathcal{G}}_j^{n+1}, & \text{for } 1 \leq j < N/2, \\ \mathcal{V}_{l,0}^{n+1} = v(0, t_{n+1}), & \mathcal{V}_{l,N/2}^{n+1} = v(\mathbf{d}^-, t_{n+1}), \end{cases} & n = 0, 1, \dots, M-1, \end{cases} \quad (6.37)$$

and

$$\left\{ \begin{array}{l} \mathcal{V}_{r,j}^0 = v(x_j, 0), \quad \text{for } N/2 \leq j \leq N, \\ \left\{ \begin{array}{l} L_{hyb}^{N,\Delta t} \mathcal{V}_{r,j}^{m+1} = \tilde{\mathcal{G}}_j^{n+1}, \quad \text{for } N/2 < j \leq N-1, \\ \mathcal{V}_{r,N/2}^{m+1} = v(\mathbf{d}^+, t_{n+1}), \quad \mathcal{V}_{r,N}^{m+1} = v(1, t_{n+1}), \quad n = 0, 1, \dots, M-1. \end{array} \right. \end{array} \right. \quad (6.38)$$

On the other hand, we consider the mesh functions Z_l and Z_r as the layer components for approximating z respectively to the either side of the point $x_{N/2} = \mathbf{d}$, and they must satisfy the following discrete problems:

$$\left\{ \begin{array}{l} Z_{l,j}^0 = 0, \quad \text{for } 0 \leq j \leq N/2, \quad Z_{r,j}^0 = 0, \quad \text{for } N/2 \leq j \leq N, \\ \left\{ \begin{array}{l} L_{hyb}^{N,\Delta t} Z_{l,j}^{n+1} = 0, \quad \text{for } 1 \leq j < N/2, \\ L_{hyb}^{N,\Delta t} Z_{r,j}^{n+1} = 0, \quad \text{for } N/2 < j \leq N-1, \\ Z_{l,0}^{n+1} = 0, \quad Z_{r,N}^{n+1} = 0, \\ D_x^F \mathcal{V}_{r,N/2}^{m+1} + D_x^F Z_{r,N/2}^{n+1} = D_x^B \mathcal{V}_{l,N/2}^{m+1} + D_x^B Z_{l,N/2}^{n+1}, \quad n = 0, 1, \dots, M-1. \end{array} \right. \end{array} \right. \quad (6.39)$$

In the subsequent sections, we estimate the error $(Y_j^{n+1} - y(x_j, t_{n+1}))$ in the outer regions (*i.e.*, for $1 \leq j \leq N/4$ and $3N/4 \leq j \leq N-1$) and in the interior layer regions (*i.e.*, for $N/4 < j < N/2$ and $N/2 < j < 3N/4$) separately in order to establish the main convergence result.

6.5.2 Error in the outer regions

At first, we deduce the error estimates corresponding to the smooth components in the following lemma.

Lemma 6.9. *Under the conditions given in (6.19)-(6.20), the errors corresponding to the smooth components satisfy the following estimates:*

$$|\mathcal{V}_{l,j}^{m+1} - v(x_j, t_{n+1})| \leq \begin{cases} C(N^{-1}(N^{-1} + \chi_\varepsilon) + \Delta t)x_j, & \text{for } 1 \leq j \leq N/4, \\ C(N^{-2} + \Delta t)x_j, & \text{for } N/4 < j < N/2, \end{cases}$$

and

$$|\mathcal{V}_{r,j}^{m+1} - v(x_j, t_{n+1})| \leq \begin{cases} C(N^{-1}(N^{-1} + \chi_\varepsilon) + \Delta t)(1 - x_j), & \text{for } 3N/4 \leq j \leq N-1, \\ C(N^{-2} + \Delta t)(1 - x_j), & \text{for } N/2 < j < 3N/4, \end{cases}$$

where

$$\chi_\varepsilon = \begin{cases} \varepsilon, & \text{when } \varepsilon \leq 2\|a\|N^{-1}, \\ 0, & \text{when } \varepsilon > 2\|a\|N^{-1}. \end{cases}$$

Proof: In the proof the following two cases are considered.

Case 1. Let $\varepsilon > 2\|a\|N^{-1}$. For $1 \leq j < N/2$, the truncation error is defined as

$$\begin{aligned} \mathbf{L}_{hyb}^{N,\Delta t} \left(\mathcal{V}_{l,j}^{n+1} - v(x_j, t_{n+1}) \right) &= \left(\mathcal{L}_\varepsilon - \mathbf{L}_{hyb}^{N,\Delta t} \right) v(x_j, t_{n+1}), \\ &= \left(\varepsilon \left(\frac{\partial^2}{\partial x^2} - \delta_x^2 \right) + a_j \left(\frac{\partial}{\partial x} - D_x^* \right) - \left(\frac{\partial}{\partial t} - D_t^- \right) \right) v(x_j, t_{n+1}). \end{aligned}$$

Now, the truncation error satisfies the following bound

$$\left| \mathbf{L}_{hyb}^{N,\Delta t} \left(\mathcal{V}_{l,j}^{n+1} - v(x_j, t_{n+1}) \right) \right| \leq \begin{cases} C \left[\varepsilon \hat{h}_j \left\| \frac{\partial^3 v}{\partial x^3} \right\| + h_j h_{j+1} \left\| \frac{\partial^3 v}{\partial x^3} \right\| + \Delta t \left\| \frac{\partial^2 v}{\partial t^2} \right\| \right], & \text{for } j = N/4, \\ C \left[\varepsilon h_j^2 \left\| \frac{\partial^4 v}{\partial x^4} \right\| + h_j^2 \left\| \frac{\partial^3 v}{\partial x^3} \right\| + \Delta t \left\| \frac{\partial^2 v}{\partial t^2} \right\| \right], & \text{otherwise.} \end{cases}$$

Then, using $h_j \leq CN^{-1}$ and Theorem 6.1, we obtain the following estimate

$$\left| \mathbf{L}_{hyb}^{N,\Delta t} \left(\mathcal{V}_{l,j}^{n+1} - v(x_j, t_{n+1}) \right) \right| \leq \begin{cases} C \left(N^{-1}(N^{-1} + \varepsilon) + \Delta t \right), & \text{for } j = N/4, \\ C \left(N^{-2} + \Delta t \right), & \text{otherwise.} \end{cases}$$

Afterward, we choose the discrete function

$$\Phi_{l,j}^n = -CN^{-2}\varphi_l(x_j) - C(N^{-2} + \Delta t)x_j, \quad \text{for } 0 \leq j \leq N/2,$$

where

$$\varphi_l(x_j) = \begin{cases} \frac{x_j}{\mathbf{d} - \mathbf{q}}, & \text{for } 0 \leq j < N/4, \\ 1, & \text{for } N/4 \leq j \leq N/2, \end{cases}$$

and employing Lemma 6.3 to $\Phi_{l,j}^{n+1} \pm \left(\mathcal{V}_{l,j}^{n+1} - v(x_j, t_{n+1}) \right)$, over $\overline{\mathfrak{D}}^{N,\Delta t} \cap \left([0, \mathbf{d}] \times [0, T] \right)$, we obtain that

$$\left| \mathcal{V}_{l,j}^{n+1} - v(x_j, t_{n+1}) \right| \leq -\Phi_{l,j}^{n+1} \leq C(N^{-2} + \Delta t)x_j, \quad \text{for } 1 \leq j < N/2.$$

Next, for $N/2 < j \leq N-1$, we choose the following discrete function

$$\Phi_{r,j}^n = -CN^{-2}\varphi_r(x_j) - C(N^{-2} + \Delta t)(1 - x_j), \quad \text{for } N/2 \leq j \leq N,$$

where

$$\varphi_r(x_j) = \begin{cases} 1, & \text{for } N/2 \leq j \leq 3N/4, \\ \frac{1 - x_j}{1 - (\mathbf{d} + \mathbf{q})}, & \text{for } 3N/4 < j \leq N, \end{cases}$$

and arguing similarly for $\left(\mathcal{V}_{r,j}^{n+1} - v(x_j, t_{n+1}) \right)$, over $\overline{\mathfrak{D}}^{N,\Delta t} \cap \left([\mathbf{d}, 1] \times [0, T] \right)$, one can deduce the desired result for $N/2 < j \leq N-1$.

Case 2. Let $\varepsilon \leq 2\|a\|N^{-1}$. For $1 \leq j < N/2$ and $N/2 < j \leq N-1$, the truncation errors are respectively

given by

$$\mathbb{L}_{hyb}^{N,\Delta t} \left(\mathcal{V}_{l,j}^{n+1} - v(x_j, t_{n+1}) \right) = \begin{cases} \left((\mathcal{L}_\varepsilon v)_{j-1/2} - \mathcal{L}_\varepsilon^{N,\Delta t} v(x_j, t_{n+1}) \right), & \text{for } 1 \leq j \leq N/4, \\ \left(\mathcal{L}_\varepsilon - \mathcal{L}_\varepsilon^{N,\Delta t} \right) v(x_j, t_{n+1}), & \text{for } N/4 < j < N/2, \end{cases}$$

and

$$\mathbb{L}_{hyb}^{N,\Delta t} \left(\mathcal{V}_{r,j}^{n+1} - v(x_j, t_{n+1}) \right) = \begin{cases} \left(\mathcal{L}_\varepsilon - \mathcal{L}_\varepsilon^{N,\Delta t} \right) v(x_j, t_{n+1}), & \text{for } N/2 < j < 3N/4, \\ \left((\mathcal{L}_\varepsilon v)_{j+1/2} - \mathcal{L}_\varepsilon^{N,\Delta t} v(x_j, t_{n+1}) \right), & \text{for } 3N/4 \leq j \leq N-1. \end{cases}$$

Now, for $1 \leq j < N/2$, the truncation error satisfies the following bound

$$\left| \mathbb{L}_{hyb}^{N,\Delta t} \left(\mathcal{V}_{l,j}^{n+1} - v(x_j, t_{n+1}) \right) \right| \leq \begin{cases} C \left[\varepsilon \hat{h}_j \left\| \frac{\partial^3 v}{\partial x^3} \right\| + h_j^2 \left(\left\| \frac{\partial^3 v}{\partial x^3} \right\| + \left\| \frac{\partial^2 v}{\partial x^2} \right\| + \left\| \frac{\partial v}{\partial x} \right\| \right) + \Delta t \left\| \frac{\partial^2 v}{\partial t^2} \right\| \right], & \text{for } 1 \leq j \leq N/4, \\ C \left[h_j \left(\varepsilon \hat{h}_j \left\| \frac{\partial^4 v}{\partial x^4} \right\| + \left\| \frac{\partial^3 v}{\partial x^3} \right\| \right) + \Delta t \left\| \frac{\partial^2 v}{\partial t^2} \right\| \right], & \text{for } N/4 < j < N/2, \end{cases}$$

and using $h_j \leq CN^{-1}$ and Theorem 6.1, we obtain that

$$\left| \mathbb{L}_{hyb}^{N,\Delta t} \left(\mathcal{V}_{l,j}^{n+1} - v(x_j, t_{n+1}) \right) \right| \leq \begin{cases} C \left(N^{-2} + N^{-1} \varepsilon + \Delta t \right), & \text{for } 1 \leq j \leq N/4, \\ C \left(N^{-2} + \Delta t \right), & \text{for } N/4 < j < N/2. \end{cases}$$

Afterwards, by choosing the discrete function

$$\Phi_{l,j}^n = \begin{cases} -C \left(N^{-2} + N^{-1} \varepsilon + \Delta t \right) x_j, & \text{for } 0 \leq j \leq N/4, \\ -C \left(N^{-2} + \Delta t \right) x_j, & \text{for } N/4 < j \leq N/2, \end{cases}$$

and employing Lemma 6.3 to $\Phi_{l,j}^{n+1} \pm \left(\mathcal{V}_{l,j}^{n+1} - v(x_j, t_{n+1}) \right)$, over $\overline{\mathfrak{D}}^{N,\Delta t} \cap \left([0, \mathfrak{d}] \times [0, T] \right)$, yields the following estimate

$$\left| \mathcal{V}_{l,j}^{n+1} - v(x_j, t_{n+1}) \right| \leq -\Phi_{l,j}^{n+1} \leq \begin{cases} C \left(N^{-2} + N^{-1} \varepsilon + \Delta t \right) x_j, & \text{for } 1 \leq j \leq N/4, \\ C \left(N^{-2} + \Delta t \right) x_j, & \text{for } N/4 < j < N/2. \end{cases}$$

Similarly, by considering the discrete function

$$\Phi_{r,j}^n = \begin{cases} -C(N^{-2} + \Delta t)(1 - x_j), & \text{for } N/2 < j < 3N/4, \\ -C(N^{-2} + N^{-1}\varepsilon + \Delta t)(1 - x_j), & \text{for } 3N/4 \leq j \leq N, \end{cases}$$

and employing Lemma 6.3 to $\Phi_{r,j}^{n+1} \pm (v_{r,j}^{n+1} - v(x_j, t_{n+1}))$, over $\overline{\mathfrak{D}}^{N,\Delta t} \cap ([d, 1] \times [0, T])$, we obtain the desired result for $N/2 < j \leq N - 1$. \blacksquare

Now, we deduce the error estimates corresponding to the layer components in the following lemma.

Lemma 6.10. *Let $\theta = \mathfrak{m}/2$. Under the conditions given in (6.19) and (6.20), the errors corresponding to the layer components satisfy the following estimates:*

$$\begin{cases} |Z_{l,j}^{n+1} - z(x_j, t_{n+1})| \leq CN^{-2}, & \text{for } 1 \leq j \leq N/4, \\ |Z_{r,j}^{n+1} - z(x_j, t_{n+1})| \leq CN^{-2}, & \text{for } 3N/4 \leq j \leq N - 1. \end{cases}$$

Proof: At first, we obtain the error estimate associated with Z_l , for $1 \leq j \leq N/4$. For this purpose, we consider the mesh function Ψ_l defined in (6.27). Now, when $\varepsilon > 2\|a\|N^{-1}$, for $1 \leq j < N/2$, we obtain that

$$\begin{aligned} L_{hyb}^{N,\Delta t} \Psi_{l,j} &= \varepsilon \delta_x^2 \Psi_{l,j} + a_j D_x^* \Psi_{l,j} - b_j^{n+1} \Psi_{l,j} - D_t^- \Psi_{l,j}, \\ &= (\theta + a_j) D_x^- \Psi_{l,j} + a_j (D_x^* - D_x^-) \Psi_{l,j} - b_j^{n+1} \Psi_{l,j}, \\ &= (\theta + a_j) D_x^- \Psi_{l,j} + \frac{a_j h_j}{2} \delta_x^2 \Psi_{l,j} - b_j^{n+1} \Psi_{l,j}, \\ &\leq 0, \end{aligned}$$

and when $\varepsilon \leq 2\|a\|N^{-1}$, we have

$$\begin{aligned} L_{hyb}^{N,\Delta t} \Psi_{l,j} &= \begin{cases} \varepsilon \delta_x^2 \Psi_{l,j} + a_{j-1/2} D_x^- \Psi_{l,j} - b_{j-1/2}^{n+1} \Psi_{l,j} - D_t^- \Psi_{l,j-1/2}, & \text{for } 1 \leq j \leq N/4, \\ \varepsilon \delta_x^2 \Psi_{l,j} + a_j D_x^* \Psi_{l,j} - b_j^{n+1} \Psi_{l,j} - D_t^- \Psi_{l,j}, & \text{for } N/4 < j < N/2, \end{cases} \\ &= \begin{cases} (\theta + a_{j-1/2}) D_x^- \Psi_{l,j} - b_{j-1/2}^{n+1} \Psi_{l,j} - D_t^- \Psi_{l,j-1/2}, & \text{for } 1 \leq j \leq N/4, \\ (\theta + a_j) D_x^- \Psi_{l,j} + \frac{a_j h_j}{2} \delta_x^2 \Psi_{l,j} - b_j^{n+1} \Psi_{l,j}, & \text{for } N/4 < j < N/2, \end{cases} \\ &\leq 0. \end{aligned}$$

Therefore, by employing Lemma 6.3 to $-|Z_{l,N/2}^{n+1}| \Psi_{l,j} \pm Z_{l,j}^{n+1}$, over $\overline{\mathfrak{D}}^{N,\Delta t} \cap ([0, d] \times [0, T])$ and using Lemma 6.8, we obtain that

$$|Z_{l,j}^{n+1}| \leq |Z_{l,N/2}^{n+1}| \Psi_{l,j} \leq C \Psi_{l,N/4} \leq CN^{-2}, \quad \text{for } 1 \leq j \leq N/4.$$

Thus, using Theorem 6.1, for $1 \leq j \leq N/4$, we have

$$|Z_{l,j}^{n+1} - z(x_j, t_{n+1})| \leq |Z_{l,j}^{n+1}| + |z(x_j, t_{n+1})| \leq (CN^{-2} + C \exp(-\theta\eta/\varepsilon)) \leq CN^{-2}.$$

On the other hand, by considering the mesh function Ψ_r defined in (6.28) and following the similar argument as given above for $(Z_r - z)$, over $\overline{\mathfrak{D}}^{N,\Delta t} \cap ([d, 1] \times [0, T])$, we obtain that

$$|Z_{r,j}^{n+1} - z(x_j, t_{n+1})| \leq CN^{-2}, \quad \text{for } 3N/4 \leq j \leq N-1.$$

Hence, the proof is complete. ■

Now, by considering the following decomposition

$$(Y_j^n - y(x_j, t_n)) = \begin{cases} (\mathcal{V}_{l,j}^n - v(x_j, t_n)) + (Z_{l,j}^n - z(x_j, t_n)), & \text{for } 1 \leq j \leq N/4, \\ (\mathcal{V}_{r,j}^n - v(x_j, t_n)) + (Z_{r,j}^n - z(x_j, t_n)), & \text{for } 3N/4 \leq j \leq N-1. \end{cases}$$

and using Lemma 6.9 and 6.10, we obtain the bound of $|Y_j^{n+1} - y(x_j, t_{n+1})|$ in the outer regions, as given in the following lemma.

Lemma 6.11. *Let $\theta = \mathfrak{m}/2$. Under the conditions given in (6.19) and (6.20), the error corresponding to the fully discrete scheme (6.15)-(6.18) satisfies the following estimate:*

$$|Y_j^{n+1} - y(x_j, t_{n+1})| \leq C(N^{-1}(N^{-1} + \chi_\varepsilon) + \Delta t), \quad \text{for } 1 \leq j \leq N/4 \text{ and } 3N/4 \leq j \leq N-1.$$

Corollary 6.1. *It is clear from Lemma 6.11 that one can obtain the following estimate:*

$$|Y_j^{n+1} - y(x_j, t_{n+1})| \leq C(N^{-2} + \Delta t), \quad \text{for } 1 \leq j \leq N/4 \text{ and } 3N/4 \leq j \leq N-1, \quad (6.40)$$

when $\varepsilon > 2\|a\|N^{-1}$ and (6.40) also holds if we choose $\varepsilon \leq 2\|a\|N^{-1}$.

6.5.3 Error in the interior layer region

Here, the error $|Y_j^{n+1} - y(x_j, t_{n+1})|$ is estimated for the interior layer region. At first, we derive bounds for the truncation errors. For $N/4 < j < N/2$ and $N/2 < j < 3N/4$, the truncation error takes the following form

$$\begin{aligned} L_{hyb}^{N,\Delta t}(Y_j^{n+1} - y(x_j, t_{n+1})) &= (\mathcal{L}_\varepsilon - L_{hyb}^{N,\Delta t})y(x_j, t_{n+1}), \\ &= \left(\varepsilon \left(\frac{\partial^2}{\partial x^2} - \delta_x^2 \right) + a_j \left(\frac{\partial}{\partial x} - D_x^* \right) - \left(\frac{\partial}{\partial t} - D_t^- \right) \right) y(x_j, t_{n+1}). \end{aligned}$$

Here, we use the Taylor's theorem with the remainder term in the integral form to derive the bound for the truncation error and hence, for $N/4 < j < N/2$, the truncation error satisfies the following bound

$$|L_{hyb}^{N,\Delta t}(Y_j^{n+1} - y(x_j, t_{n+1}))| \leq \left[Ch \int_{x_{j-1}}^{x_{j+1}} \left(\varepsilon \left| \frac{\partial^4 y(s, t_{n+1})}{\partial s^4} \right| + \left| \frac{\partial^3 y(s, t_{n+1})}{\partial s^3} \right| \right) ds \right] + C\Delta t \left\| \frac{\partial^2 y}{\partial t^2} \right\|.$$

Now, using Theorem 6.1, for $N/4 < j < N/2$, we obtain the following estimate

$$\begin{aligned} \left| \mathbf{L}_{hyb}^{N,\Delta t} \left(Y_j^{n+1} - y(x_j, t_{n+1}) \right) \right| &\leq C \left[\left(h^2 + h\varepsilon^{-2} \exp(-\mathbf{m}_1(\mathbf{d} - x_j)/\varepsilon) \sinh(\mathbf{m}_1 h/\varepsilon) \right) + \Delta t \right], \\ &\leq C \left[\left(h^2 + h^2\varepsilon^{-3} \exp(-\mathbf{m}_1(\mathbf{d} - x_j)/\varepsilon) \right) + \Delta t \right], \end{aligned} \quad (6.41)$$

since, $\sinh(\mathbf{m}_1 h/\varepsilon) \leq C(\mathbf{m}_1 h/\varepsilon)$, for $\mathbf{m}_1 h/\varepsilon \leq 2$, which follows from the assumption (6.19). Approaching in the similar way as discussed above, for $N/2 < j < 3N/4$, we have

$$\left| \mathbf{L}_{hyb}^{N,\Delta t} \left(Y_j^{n+1} - y(x_j, t_{n+1}) \right) \right| \leq C \left[\left(h^2 + h^2\varepsilon^{-3} \exp(-\mathbf{m}_2(x_j - \mathbf{d})/\varepsilon) \right) + \Delta t \right]. \quad (6.42)$$

At the point $x_{N/2} = \mathbf{d}$, we get the following form of the truncation error:

$$\begin{aligned} \mathbf{L}_{hyb}^{N,\Delta t} \left(Y_{N/2}^{n+1} - y(x_{N/2}, t_{n+1}) \right) &= \frac{h/2}{(\mathbf{p}_{N/2-1} - a_{N/2-1}h)} \mathbf{L}_{hyb}^{N,\Delta t} \left(Y_{N/2-1}^{n+1} - y(x_{N/2-1}, t_{n+1}) \right) \\ &+ \frac{h/2}{(\mathbf{q}_{N/2+1} + a_{N/2+1}h)} \mathbf{L}_{hyb}^{N,\Delta t} \left(Y_{N/2+1}^{n+1} - y(x_{N/2+1}, t_{n+1}) \right) + \left[\left[\frac{\partial u}{\partial x} \right] (x_{N/2}, t_{n+1}) - (D_x^F - D_x^B) y(x_{N/2}, t_{n+1}) \right], \end{aligned}$$

Then, using (6.41), (6.42) and the interface condition in (6.2), we obtain the following estimate

$$\left| \mathbf{L}_{hyb}^{N,\Delta t} \left(Y_{N/2}^{n+1} - y(x_{N/2}, t_{n+1}) \right) \right| \leq C \left(h^2\varepsilon^{-3} + \Delta t \right). \quad (6.43)$$

Further, from Corollary 6.1, we have

$$|Y_j^{n+1} - y(x_j, t_{n+1})| \leq C \left(N^{-2} + \Delta t \right), \quad \text{for } j = N/4 \text{ and } j = 3N/4. \quad (6.44)$$

Afterwards, with sufficiently large C , we consider the discrete function

$$\Upsilon_j^n = \begin{cases} -C \left(1 + \left[x_j - (\mathbf{d} - \eta) \right] \right) \left(N^{-2} + \Delta t \right) - Ch^2\varepsilon^{-2} \left(\frac{\mathcal{S}_j(\theta)}{\mathcal{S}_{N/2}(\theta)} \right), & \text{for } N/4 \leq j \leq N/2, \\ -C \left(1 + \left[(\mathbf{d} + \eta) - x_j \right] \right) \left(N^{-2} + \Delta t \right) - Ch^2\varepsilon^{-2} \left(\frac{\mathcal{R}_j(\theta)}{\mathcal{R}_{N/2}(\theta)} \right), & \text{for } N/2 < j \leq 3N/4. \end{cases}$$

Now, using the condition $\theta = \mathbf{m}/2$ and applying Lemmas 6.5 and 6.7, we have

$$\mathbf{L}_{hyb}^{N,\Delta t} \Upsilon_j^{n+1} \geq \begin{cases} C(-a_j) \left(N^{-2} + \Delta t \right) + C \frac{h^2\varepsilon^{-2}}{(\varepsilon + \theta h)} \exp(-\mathbf{m}_1(\mathbf{d} - x_j)/\varepsilon), & \text{for } N/4 < j < N/2, \\ C(a_j) \left(N^{-2} + \Delta t \right) + C \frac{h^2\varepsilon^{-2}}{(\varepsilon + \theta h)} \exp(-\mathbf{m}_2(x_j - \mathbf{d})/\varepsilon), & \text{for } N/2 < j < 3N/4, \end{cases}$$

and hence, employing the inequality $h\varepsilon^{-1} \leq 2/\mathfrak{m}^*$ implied by the assumption (6.19), we obtain that

$$\mathbf{L}_{hyb}^{N,\Delta t} \Upsilon_j^{n+1} \geq \begin{cases} C(\mathfrak{m}_1)(N^{-2} + \Delta t) + Ch^2\varepsilon^{-3} \exp(-\mathfrak{m}_1(\mathbf{d} - x_j)/\varepsilon), & \text{for } N/4 < j < N/2, \\ C(\mathfrak{m}_2)(N^{-2} + \Delta t) + Ch^2\varepsilon^{-3} \exp(-\mathfrak{m}_2(x_j - \mathbf{d})/\varepsilon), & \text{for } N/2 < j < 3N/4. \end{cases} \quad (6.45)$$

Next, for the point $x_{N/2} = \mathbf{d}$, the condition $\theta = \mathfrak{m}/2$ and the inequality $h\varepsilon^{-1} \leq 2/\mathfrak{m}^*$ are used together with (6.45) to obtain

$$\begin{aligned} & \mathbf{L}_{hyb}^{N,\Delta t} \Upsilon_{N/2}^{n+1} \\ &= \frac{h/2}{(\mathbf{p}_{N/2-1} - a_{N/2-1}h)} \mathbf{L}_{hyb}^{N,\Delta t} \Upsilon_{N/2-1}^{n+1} + \frac{h/2}{(\mathbf{q}_{N/2+1} + a_{N/2+1}h)} \mathbf{L}_{hyb}^{N,\Delta t} \Upsilon_{N/2+1}^{n+1} + (D_x^F - D_x^B) \Upsilon_{N/2}^{n+1}, \\ &\geq (D_x^F - D_x^B) \Upsilon_{N/2}^{n+1}, \\ &\geq 2C \left[(N^{-2} + \Delta t) + \frac{h^2\varepsilon^{-2}}{(\varepsilon + \theta h)} \right], \\ &\geq 2C \left[(N^{-2} + \Delta t) + h^2\varepsilon^{-3} \right]. \end{aligned} \quad (6.46)$$

Therefore, it follows from (6.44)-(6.46) that one can apply Lemma 6.3 to $\Upsilon_j^{n+1} \pm (Y_j^{n+1} - y(x_j, t_{n+1}))$, over $\overline{\mathcal{D}}^{N,\Delta t} \cap ([\mathbf{d} - \eta, \mathbf{d} + \eta] \times [0, T])$; and finally, we use Lemma 6.6 and $h = 4\eta_0\varepsilon N^{-1} \ln N$ to obtain the desired estimate in the following lemma.

Lemma 6.12. *Let $\theta = \mathfrak{m}/2$. Under the conditions given in (6.19) and (6.20), the error corresponding to the fully discrete scheme (6.15)-(6.18) satisfies the following estimate:*

$$|Y_j^{n+1} - y(x_j, t_{n+1})| \leq C(N^{-2} \ln^2 N + \Delta t), \quad \text{for } N/4 < j < 3N/4. \quad (6.47)$$

6.5.4 The main convergence result

Theorem 6.2. *Let $\theta = \mathfrak{m}/2$. Under the conditions given in (6.19) and (6.20), the error corresponding to the fully discrete scheme (6.15)-(6.18) satisfies the following estimate:*

$$|Y_j^{n+1} - y(x_j, t_{n+1})| \leq \begin{cases} C(N^{-2} + \Delta t), & \text{for } 1 \leq j \leq N/4 \text{ and } 3N/4 \leq j \leq N-1, \\ C(N^{-2} \ln^2 N + \Delta t), & \text{for } N/4 < j < 3N/4. \end{cases} \quad (6.48)$$

Proof: The estimate in (6.48) is derived using (6.40) and (6.47). ■

Remark 6.1. It is to be mentioned that the existing hybrid scheme proposed in [83] satisfies the error estimate (6.48), provided the parameter ε satisfies the condition $\varepsilon < CN^{-1}$ and is also demonstrated through the numerical experiments in Section 6.7. Further, the numerical results presented in Section 6.7 reveal that for the larger values of the parameter ε , in particular when $\varepsilon \gg N^{-1}$, the existing hybrid scheme is at worst

$O(N^{-1})$ accurate in space both outside as well as inside the interior layers; and this is in strong contrast with the numerical results produced by the newly proposed method.

6.6 Semilinear singularly perturbed parabolic problem

In this section, we consider the following class of semi-linear singularly perturbed parabolic IBVPs having discontinuous convection coefficient:

$$\begin{cases} \varepsilon \frac{\partial^2 y}{\partial x^2} + a(x) \frac{\partial y}{\partial x} - \frac{\partial y}{\partial t} = g(x, t, y), & (x, t) \in \mathfrak{D}^- \cup \mathfrak{D}^+, \\ y(x, 0) = q_0(x), & x \in \overline{\Omega}, \\ y(0, t) = s_l(t), & y(1, t) = s_r(t), \\ [y](d, t) = 0, & \left[\frac{\partial y}{\partial x} \right](d, t) = 0, \quad t \in (0, T], \end{cases} \quad (6.49)$$

where ε is a small parameter such that $\varepsilon \in (0, 1]$; $a(x)$ and $g(x, t, y)$ are supposed to be sufficiently smooth functions in their respective domains; and they satisfy the conditions given in (6.3), with the assumption that

$$\mathbb{k}_1 \leq \frac{\partial g(x, t, y)}{\partial y} \leq \mathbb{k}_2, \quad \text{for } (x, t, y) \in (\mathfrak{D}^- \cup \mathfrak{D}^+) \times \mathbb{R}; \quad \mathbb{k}_1, \mathbb{k}_2 > 0.$$

Then, the existence and the uniqueness of the solution of the IBVP (6.49) can be asserted under the sufficient smoothness and the suitable compatibility conditions imposed on the data q_0 , s_l and s_r . For further details, one can refer the book [65] and the article [97].

We now apply the Newton's linearization technique to the semi-linear parabolic IBVP (6.49). This process generates the sequence $\{y^k\}_{k=0}^\infty$, in which the starting solution y^0 satisfies the initial and boundary conditions of the IBVP (6.49). For all $k \geq 0$, y^{k+1} is defined as the solution of the following linear parabolic IBVP:

$$\begin{cases} \varepsilon \frac{\partial^2 y^{k+1}}{\partial x^2} + a(x) \frac{\partial y^{k+1}}{\partial x} - b^k(x, t) y^{k+1} - \frac{\partial y^{k+1}}{\partial t} = \mathcal{G}^k(x, t), & (x, t) \in \mathfrak{D}^- \cup \mathfrak{D}^+, \\ y^{k+1}(x, 0) = q_0(x), & x \in \overline{\Omega}, \\ y^{k+1}(0, t) = s_l(t), & y^{k+1}(1, t) = s_r(t), \\ [y^{k+1}](d, t) = 0, & \left[\frac{\partial y^{k+1}}{\partial x} \right](d, t) = 0, \quad t \in (0, T], \end{cases} \quad (6.50)$$

where

$$\begin{cases} b^k(x, t) = \frac{\partial g}{\partial y}(x, t, y^k), \\ \mathcal{G}^k(x, t) = g(x, t, y^k) - b^k(x, t) y^k. \end{cases}$$

Afterwards, for each iteration k , we solve the IBVP (6.50) numerically and use the following condition as the stopping criterion for the convergence of the numerical solution

$$\max_{0 \leq j \leq N, n=M} |Y^{k+1}(x_j, t_n) - Y^k(x_j, t_n)| \leq \text{TOL}, \quad (6.51)$$

where TOL is the prescribed error constant to be chosen later and $Y^k(x_j, t_n)$ denote the numerical solution obtained at the k^{th} iteration at the mesh point $(x_j, t_n) \in \overline{\mathfrak{D}}^{N, \Delta t}$. In this regard, one can refer the book [29]. The numerical results corresponding to the semi-linear parabolic IBVP (6.49) are presented in the subsequent section.

6.7 Numerical experiments

In this section, for verifying the theoretical result as well as the efficiency of the newly proposed numerical method, we perform the numerical experiments for the following test examples and also compare the numerical results of the proposed method with the existing hybrid scheme proposed in [83]. In all the test examples, we consider the interface conditions as stated in (6.2) for $d = 0.5$. In all the experiments, we choose the constant $\eta_0 = 2.2$.

6.7.1 Test examples

Example 6.1. Consider the following parabolic IBVP:

$$\begin{cases} \varepsilon \frac{\partial^2 y}{\partial x^2} + a(x) \frac{\partial y}{\partial x} - x(1-x)y - \frac{\partial y}{\partial t} = g(x, t), & (x, t) \in [(0, 0.5) \cup (0.5, 1)] \times (0, 1], \\ y(x, 0) = q_0(x), & x \in [0, 1], \\ y(0, t) = 0, \quad y(1, t) = 0, & t \in (0, 1], \end{cases}$$

with

$$a(x) = \begin{cases} -(1 + x(0.5 - x)), & x \in (0, 0.5), \\ (1 + x(x - 0.5)), & x \in (0.5, 1). \end{cases}$$

Here, the exact solution $y(x, t)$ is given by

$$y(x, t) = \begin{cases} \exp(-t) \left(\frac{1 - \exp(-(0.5 - x)/\varepsilon)}{1 - \exp(-0.5/\varepsilon)} - \cos(\pi x) \right), & (x, t) \in (0, 0.5) \times (0, 1], \\ \exp(-t) \left(\frac{-1 + \exp(-(x - 0.5)/\varepsilon)}{1 - \exp(-0.5/\varepsilon)} - \cos(\pi x) \right), & (x, t) \in [0.5, 1) \times (0, 1], \end{cases}$$

and accordingly, the initial data $q_0(x)$ and the term $g(x, t)$ are chosen.

For each ε , the maximum point-wise error and the corresponding order of convergence are respectively computed by

$$e_\varepsilon^{N, \Delta t} = \max_{0 \leq j \leq N, n=M} |y(x_j, t_n) - Y^{N, \Delta t}(x_j, t_n)|,$$

and

$$r_\varepsilon^{N, \Delta t} = \log_2 \left(\frac{e_\varepsilon^{N, \Delta t}}{e_\varepsilon^{2N, \Delta t/2}} \right),$$

where $y(x_j, t_n)$ and $Y^{N, \Delta t}(x_j, t_n)$, respectively denote the exact and the numerical solution computed on $\overline{\mathfrak{D}}^{N, \Delta t}$. Further, for each N and Δt , the ε -uniform maximum point-wise error and the corresponding ε -uniform

order of convergence are respectively computed by

$$e^{N,\Delta t} = \max_{\varepsilon} e_{\varepsilon}^{N,\Delta t} \quad \text{and} \quad r^{N,\Delta t} = \log_2 \left(\frac{e^{N,\Delta t}}{e^{2N,\Delta t/2}} \right).$$

Example 6.2. Consider the following parabolic IBVP:

$$\begin{cases} \varepsilon \frac{\partial^2 y}{\partial x^2} + a(x) \frac{\partial y}{\partial x} - x(1-x)y - \frac{\partial y}{\partial t} = g(x, t), & (x, t) \in [(0, 0.5) \cup (0.5, 1)] \times (0, 1], \\ y(x, 0) = 0, & x \in [0, 1], \\ y(0, t) = t^2, & y(1, t) = 0, \quad t \in (0, 1], \end{cases}$$

with

$$a(x) = \begin{cases} -(1 + x(1-x)), & x \in (0, 0.5), \\ (1 + x(1-x)), & x \in (0.5, 1), \end{cases}$$

and

$$g(x, t) = \begin{cases} 2(1+x^2)t^2, & (x, t) \in (0, 0.5) \times (0, 1], \\ 3(1+x^2)t^2, & (x, t) \in (0.5, 1) \times (0, 1]. \end{cases}$$

Since, the exact solution of Example 6.2 is not known, the following technique is used in order to demonstrate the accuracy and the ε -uniform convergence of the proposed method. We denote $\widehat{Y}^{2N,\Delta t/2}$ as the numerical solution computed on the fine mesh $\widehat{\Omega}^{2N,\Delta t/2} = \widehat{\Omega}^{2N} \times \wedge^{\Delta t/2}$, with $\Delta t/2 = T/2M$. Here, $\widehat{\Omega}^N$ denotes a piecewise-uniform Shishkin mesh as like $\bar{\Omega}^N$ with the transition parameters $\widehat{\eta}_1, \widehat{\eta}_2$ given by

$$\widehat{\eta}_1 = \min \left\{ \frac{d}{2}, \eta_0 \varepsilon \ln \left(\frac{N}{2} \right) \right\}, \quad \widehat{\eta}_2 = \min \left\{ \frac{1-d}{2}, \eta_0 \varepsilon \ln \left(\frac{N}{2} \right) \right\},$$

such that the j^{th} point of $\bar{\Omega}^N$ matches with the $2j^{\text{th}}$ point of $\widehat{\Omega}^{2N}$, for $j = 0, 1, \dots, N$. For each ε , the maximum point-wise error and the corresponding order of convergence are respectively computed by

$$\widehat{e}_{\varepsilon}^{N,\Delta t} = \max_{0 \leq j \leq N, n=M} |U^{N,\Delta t}(x_j, t_n) - \widehat{U}^{2N,\Delta t/2}(x_j, t_n)|,$$

and

$$\widehat{r}_{\varepsilon}^{N,\Delta t} = \log_2 \left(\frac{\widehat{e}_{\varepsilon}^{N,\Delta t}}{\widehat{e}_{\varepsilon}^{2N,\Delta t/2}} \right).$$

Further, for each N and Δt , the quantities $\widehat{e}^{N,\Delta t}$ and $\widehat{r}^{N,\Delta t}$ are defined analogously to $e^{N,\Delta t}$ and $r^{N,\Delta t}$ based on the error $\widehat{e}_{\varepsilon}^{N,\Delta t}$ as in the previous example.

Example 6.3. Consider the following semi-linear parabolic IBVP:

$$\begin{cases} \varepsilon \frac{\partial^2 y}{\partial x^2} + a(x) \frac{\partial y}{\partial x} + \exp(y) - \frac{\partial y}{\partial t} = g(x, t), & (x, t) \in [(0, 0.5) \cup (0.5, 1)] \times (0, 1], \\ y(x, 0) = q_0(x), & x \in [0, 1], \\ y(0, t) = 0, \quad y(1, t) = 0, & t \in [0, 1], \end{cases}$$

where $a(x)$ and the exact solution $y(x, t)$ are the same as we define previously in Example 6.1 and accordingly, the initial data q_0 and the term $g(x, t)$ are chosen.

Here, we use the linearization technique described previously in Section 6.6 for Example 6.3 and for each iteration k , we compute the numerical solution of the resulting linear IBVP of the form (6.50):

$$\begin{cases} \varepsilon \frac{\partial^2 y^{k+1}}{\partial x^2} + a(x) \frac{\partial y^{k+1}}{\partial x} + \exp(y^k) y^{k+1} - \frac{\partial y^{k+1}}{\partial x} = g(x, t) - \exp(y^k)(1 - y^k), \\ y^{k+1}(x, 0) = q_0(x), & x \in [0, 1], \\ y^{k+1}(0, t) = 0, \quad y^{k+1}(1, t) = 0, & t \in [0, 1], \end{cases} \quad (x, t) \in [(0, 0.5) \cup (0.5, 1)] \times (0, 1],$$

until the stopping criterion (6.51) is fulfilled with $\text{TOL} = 10^{-10}$.

As we know the exact solution of Example 6.3, for each ε , the maximum point-wise error $e_\varepsilon^{N, \Delta t}$ and the corresponding order of convergence $r_\varepsilon^{N, \Delta t}$ for Example 6.3 are computed by following the definitions given in Example 6.1; and the quantities $e^{N, \Delta t}$ and $r^{N, \Delta t}$ are defined analogously, for each N and Δt .

6.7.2 Numerical results and observations

From Fig 6.2, one can observe the presence of interior layers closest to the point of discontinuity $x = 0.5$ in the respective numerical solutions of Examples 6.1, 6.2 and 6.3. Moreover, from the surface plots displayed in Figs ??, 6.4 and 6.5, one can completely visualize the numerical solutions. The above figures are drawn using the newly proposed method by choosing $\Delta t = 0.8/N$.

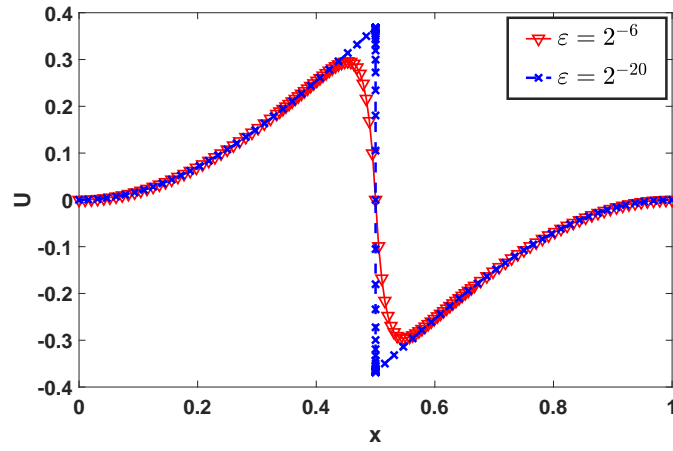
For various values of ε , N and Δt , we display the maximum point-wise errors and the ε -uniform errors together with the corresponding order of convergence produced by the proposed method in Tables 6.1, 6.2 and 6.3, respectively for Examples 6.1, 6.2 and 6.3, taking $\Delta t = 1.6/N$ and choosing $\mathbb{S}_\varepsilon = \{2^0, 2^{-2}, \dots, 2^{-20}\}$ as the set of values of the parameter ε .

From Tables 6.1-6.3, we observe that the ε -uniform errors are decreasing monotonically as N increases and it ensures that the proposed method is ε -uniformly convergent. However, the order of convergence displayed in Tables 6.1-6.3 does not truly represent the spatial order of convergence of the proposed method. It is because of the dominance of the temporal error over the spatial error according to the estimate of Theorem 6.2 and as a result, we notice that with the reduction (or increment) of the time step Δt , the rate of convergence of the ε -uniform errors is increasing (or decreasing) and it is straightway visible from Fig 6.6.

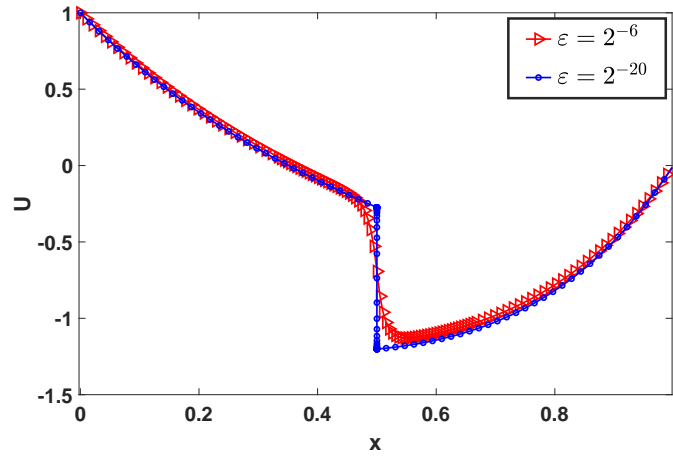
Next, for verifying the spatial order of convergence of the present method, we compute the maximum point-wise errors together with the corresponding order of convergence for the different regions of $\bar{\Omega}$ by choosing $\Delta t = 1/N^2$. Those computational results are presented in Tables 6.4, 6.5 and 6.6, respectively for Examples 6.1, 6.2

and 6.3, and also compared with the existing hybrid scheme by choosing the same discretization parameter Δt . Tables 6.4- 6.6 provide a clear evidence that irrespective of the smaller as well the larger values of the parameter ε , the proposed method is at least second-order spatially accurate in the outer regions and almost second-order spatially accurate (up to the logarithmic factor) in the interior layer regions; and it very well supports the theoretical result established in Theorem 6.2. On the other hand, from Tables 6.4- 6.6, we observe that when $\varepsilon = 2^{-6}$ the spatial error due to the existing hybrid scheme is $O(N^{-1})$ in the outer regions and is $O(N^{-2} \ln^2 N)$ in the interior layer regions. Apart from this, we notice that when $\varepsilon = 2^{-4}$ the existing method is $O(N^{-1})$ accurate in space, whereas the present method is $O(N^{-2})$ accurate in space, both outside as well as inside the interior layers. It is to be noted that the mesh $\bar{\Omega}^N$ becomes the equidistant mesh whenever $\varepsilon = 2^{-4}$. The above observations show that the newly proposed method yields comparatively higher-order accurate numerical results than the existing hybrid scheme whenever $\varepsilon \gg N^{-1}$ (e.g., $\varepsilon = 2^{-4}, 2^{-6}$). As a compliment of this observation, for $\varepsilon = 2^{-4}, 2^{-6}$, the maximum point-wise errors displayed in Tables 6.4, 6.5 and 6.6 are graphically represented in Figs 6.7, 6.8 and 6.9, respectively. Nevertheless, it is observed that both the methods converge with the same order of accuracy inside and outside the interior layers whenever $\varepsilon \ll N^{-1}$ (e.g., $\varepsilon = 2^{-14}$).

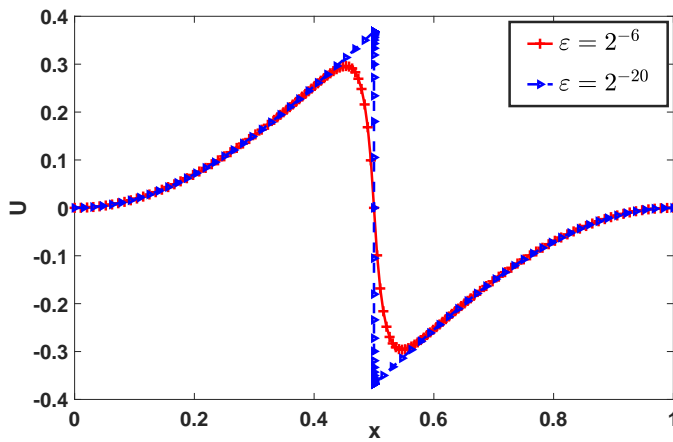
Finally, to show that the present method performs more efficiently than the existing hybrid scheme, we compare the computational time of both the methods in Tables 6.7, 6.8 and 6.9, respectively for Examples 6.1, 6.2 and 6.3. More specifically, for the larger values of ε (e.g., $\varepsilon = 2^{-4}, 2^{-6}$), we notice that the present method takes comparatively less computational time than the existing method as N increases; although for the smaller values of ε (e.g., $\varepsilon = 2^{-20}$) both the methods take approximately same computational time.



(a) Example 6.1.

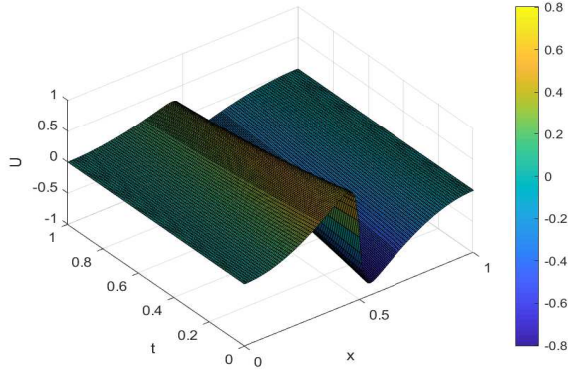


(b) Example 6.2.

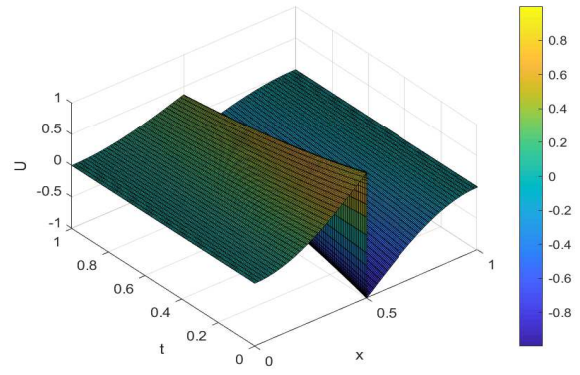


(c) Example 6.3.

Figure 6.2: Numerical solutions computed at $t = 1$ for $N = 128$

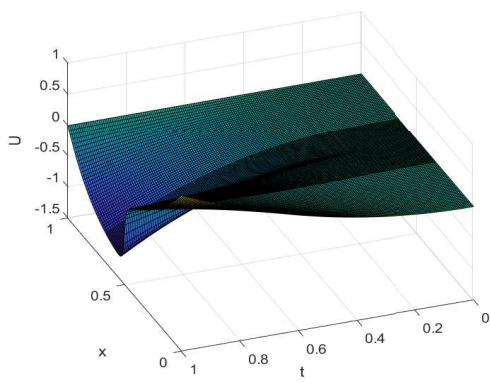


(a) for $\varepsilon = 2^{-6}$, $N = 128$

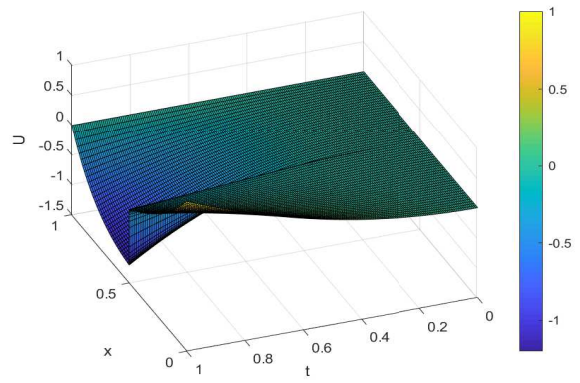


(b) for $\varepsilon = 2^{-20}$, $N = 128$

Figure 6.3: Surface plots of the numerical solutions of Example 6.1

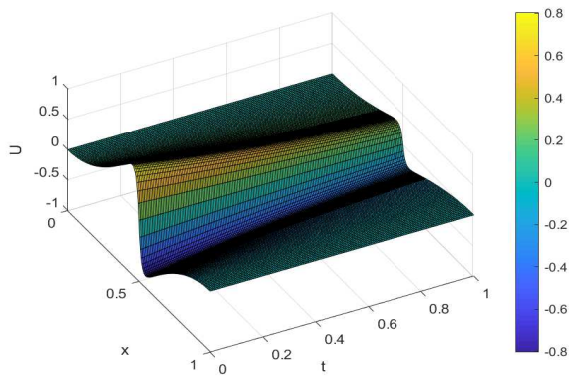


(a) for $\varepsilon = 2^{-6}$, $N = 128$

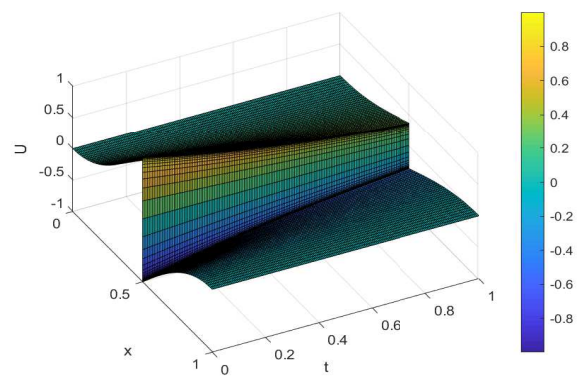


(b) for $\varepsilon = 2^{-20}$, $N = 128$

Figure 6.4: Surface plots of the numerical solutions of Example 6.2



(a) for $\varepsilon = 2^{-6}$, $N = 128$



(b) for $\varepsilon = 2^{-20}$, $N = 128$

Figure 6.5: Surface plots of the numerical solutions of Example 6.3

Table 6.1: ε -uniform maximum point-wise errors and order of convergence for Example 6.1

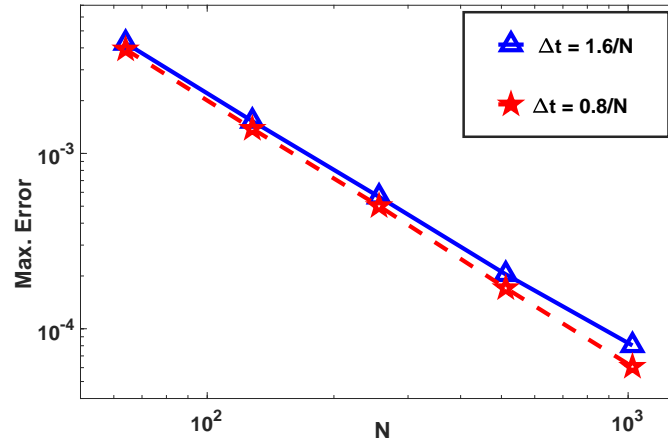
$\varepsilon \in \mathbb{S}_\varepsilon$	Number of mesh-intervals N / time step-size Δt ($\Delta t = 1.6/N$)				
	$64 / \frac{1}{40}$	$128 / \frac{1}{80}$	$256 / \frac{1}{160}$	$512 / \frac{1}{320}$	$1024 / \frac{1}{640}$
$e^{N,\Delta t}$	4.2584e-03	1.5292e-03	5.6558e-04	2.0435e-04	8.0317e-05
$r^{N,\Delta t}$	1.4775	1.4350	1.4687	1.3473	
$\varepsilon \in \mathbb{S}_\varepsilon$	Number of mesh-intervals N / time step-size Δt ($\Delta t = 0.8/N$)				
	$64 / \frac{1}{80}$	$128 / \frac{1}{160}$	$256 / \frac{1}{320}$	$512 / \frac{1}{640}$	$1024 / \frac{1}{1280}$
$e^{N,\Delta t}$	3.9224e-03	1.3828e-03	5.0114e-04	1.7059e-04	6.0758e-05
$r^{N,\Delta t}$	1.5042	1.4643	1.5547	1.4893	

Table 6.2: ε -uniform maximum point-wise errors and order of convergence for Example 6.2

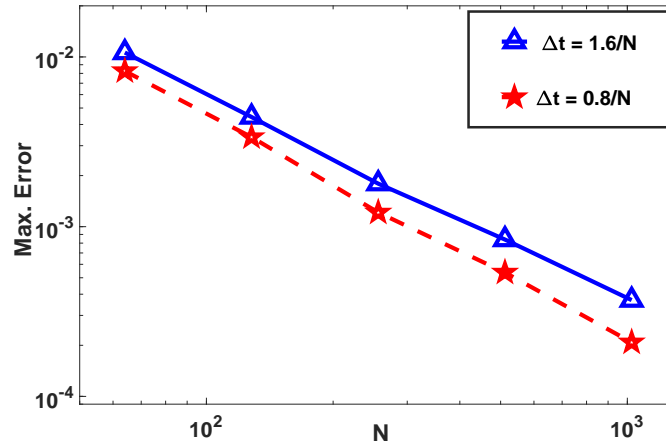
$\varepsilon \in \mathbb{S}_\varepsilon$	Number of mesh-intervals N / time step-size Δt ($\Delta t = 1.6/N$)				
	$64 / \frac{1}{40}$	$128 / \frac{1}{80}$	$256 / \frac{1}{160}$	$512 / \frac{1}{320}$	$1024 / \frac{1}{640}$
$\hat{e}^{N,\Delta t}$	1.0616e-02	4.4259e-03	1.7923e-03	8.3973e-04	3.6933e-04
$\hat{r}^{N,\Delta t}$	1.2622	1.3042	1.0938	1.1850	
$\varepsilon \in \mathbb{S}_\varepsilon$	Number of mesh-intervals N / time step-size Δt ($\Delta t = 0.8/N$)				
	$64 / \frac{1}{80}$	$128 / \frac{1}{160}$	$256 / \frac{1}{320}$	$512 / \frac{1}{640}$	$1024 / \frac{1}{1280}$
$\hat{e}^{N,\Delta t}$	8.2544e-03	3.3693e-03	1.2124e-03	5.3692e-04	2.0824e-04
$\hat{r}^{N,\Delta t}$	1.2927	1.4746	1.1751	1.3664	

Table 6.3: ε -uniform maximum point-wise errors and order of convergence for Example 6.3

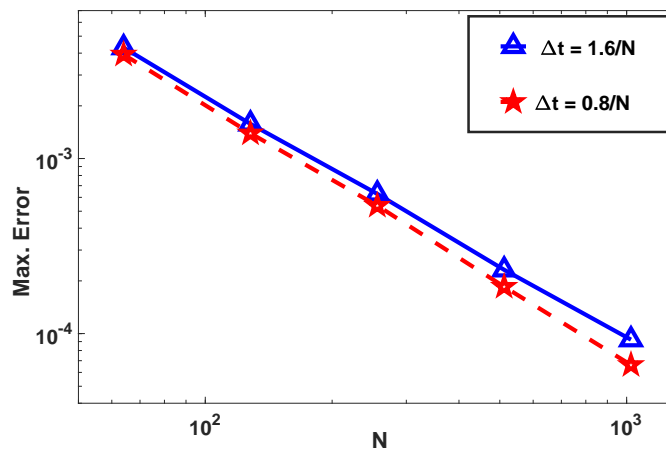
$\varepsilon \in \mathbb{S}_\varepsilon$	Number of mesh-intervals N / time step-size Δt ($\Delta t = 1.6/N$)				
	$64 / \frac{1}{40}$	$128 / \frac{1}{80}$	$256 / \frac{1}{160}$	$512 / \frac{1}{320}$	$1024 / \frac{1}{640}$
$e^{N,\Delta t}$	4.3011e-03	1.5764e-03	6.2794e-04	2.3139e-04	9.2303e-05
$r^{N,\Delta t}$	1.4480	1.3280	1.4403	1.3259	
$\varepsilon \in \mathbb{S}_\varepsilon$	Number of mesh-intervals N / time step-size Δt ($\Delta t = 0.8/N$)				
	$64 / \frac{1}{80}$	$128 / \frac{1}{160}$	$256 / \frac{1}{320}$	$512 / \frac{1}{640}$	$1024 / \frac{1}{1280}$
$e^{N,\Delta t}$	3.9284e-03	1.3933e-03	5.3807e-04	1.8526e-04	6.6182e-05
$r^{N,\Delta t}$	1.4955	1.3726	1.5383	1.4850	



(a) Example 6.1.



(b) Example 6.2.

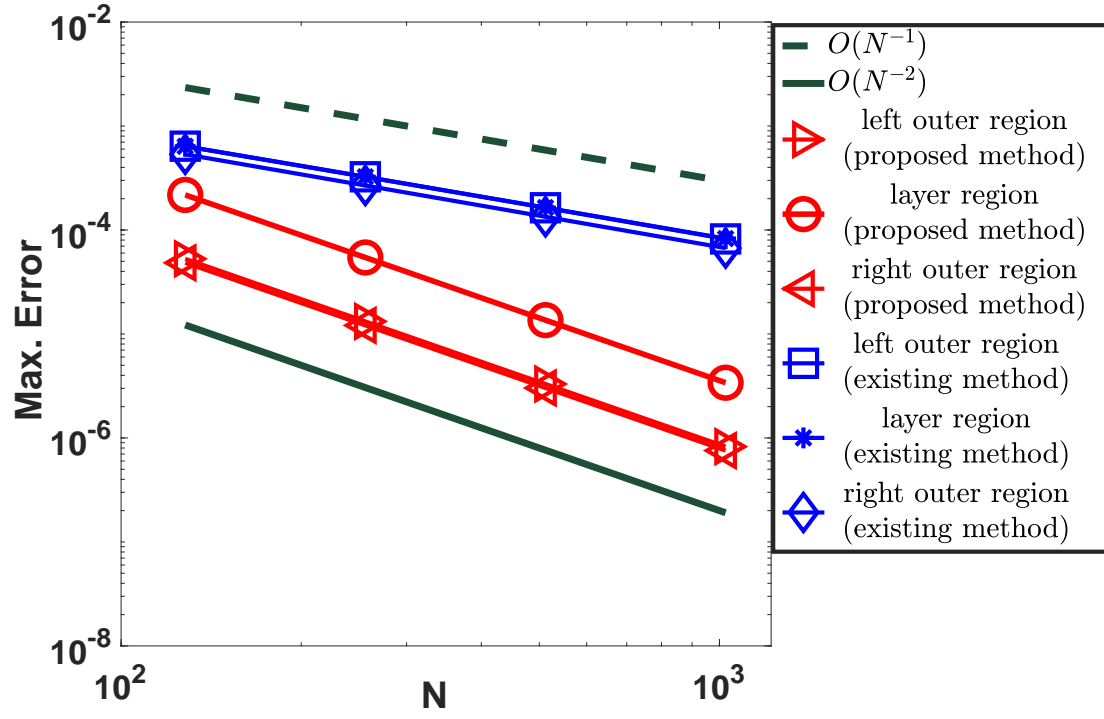


(c) Example 6.3.

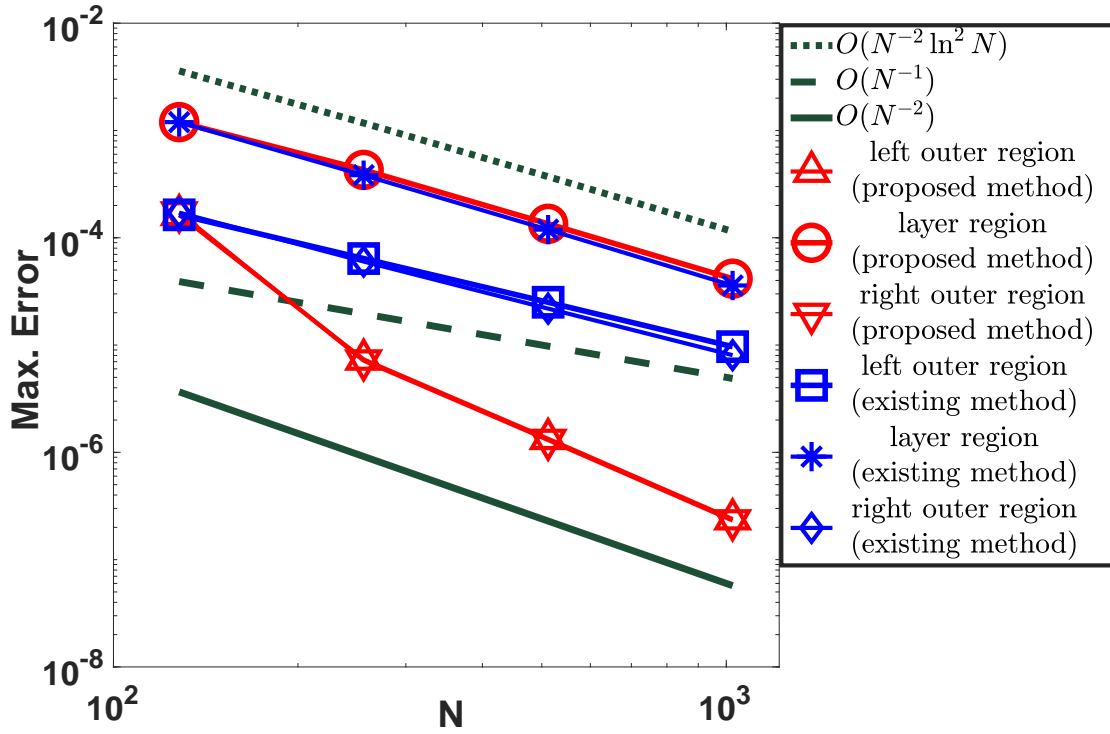
Figure 6.6: Loglog plot of ε —uniform maximum point-wise errors computed with $\Delta t = 0.8/N$ and $1.6/N$

Table 6.4: Comparison (regionwise) of maximum point-wise errors and order of convergence for Example 6.1, taking $\Delta t = \frac{1}{N^2}$.

N	proposed method			existing method		
	left outer region	interior layer region	right outer region	left outer region	interior layer region	right outer region
	$[0, d - \eta_1]$	$(d - \eta_1, d + \eta_2)$	$[d + \eta_2, 1]$	$[0, d - \eta_1]$	$(d - \eta_1, d + \eta_2)$	$[d + \eta_2, 1]$
$\varepsilon = 2^{-4} \approx 10^{-1}$						
128	5.2842e-05 1.9999	2.1747e-04 1.9996	4.8370e-05 1.9997	6.4002e-04 0.97855	6.3767e-04 0.97322	5.3445e-04 0.99680
256	1.3211e-05 2.0000	5.4383e-05 2.0005	1.2095e-05 1.9999	3.2481e-04 0.98971	3.2481e-04 0.98499	2.6782e-04 0.99876
512	3.3029e-06 2.0000	1.3591e-05 2.0001	3.0239e-06 2.0000	1.6356e-04 0.99496	1.6410e-04 0.98903	1.3402e-04 0.99947
1024	8.2573e-07	3.3975e-06	7.5600e-07	8.2069e-05	8.2677e-05	6.7037e-05
$\varepsilon = 2^{-6} \approx 10^{-2}$						
128	1.6355e-04 4.4763	1.1960e-03 1.4790	1.7158e-04 4.5836	1.6355e-04 1.3531	1.1960e-03 1.6430	1.7158e-04 1.5147
256	7.3477e-06 2.4563	4.2904e-04 1.6697	7.1560e-06 2.4588	6.4021e-05 1.3536	3.8295e-04 1.6858	6.0046e-05 1.4576
512	1.3388e-06 2.4882	1.3486e-04 1.6993	1.3017e-06 2.4915	2.5053e-05 1.3745	1.1903e-04 1.7294	2.1863e-05 1.4421
1024	2.3861e-07	4.1527e-05	2.3145e-07	9.6625e-06	3.5898e-05	8.0463e-06
$\varepsilon = 2^{-14} \approx 10^{-4}$						
128	7.1015e-05 1.9993	1.2417e-03 1.6182	1.6415e-04 2.0014	7.1015e-05 1.9993	1.2417e-03 1.6182	1.6415e-04 2.0014
256	1.7762e-05 1.9558	4.0449e-04 1.6598	4.0998e-05 1.9839	1.7762e-05 1.9558	4.0449e-04 1.6598	4.0998e-05 1.9839
512	4.5785e-06 1.8815	1.2801e-04 1.6962	1.0364e-05 1.9524	4.5785e-06 1.8815	1.2801e-04 1.6962	1.0364e-05 1.9524
1024	1.2426e-06	3.9504e-05	2.6779e-06	1.2426e-06	3.9504e-05	2.6779e-06
$\varepsilon = 2^{-20} \approx 10^{-6}$						
128	6.9611e-05 2.0365	1.2426e-03 1.6174	1.6322e-04 2.0153	6.9611e-05 2.0365	1.2426e-03 1.6174	1.6322e-04 2.0153
256	1.6967e-05 2.0301	4.0497e-04 1.6586	4.0374e-05 2.0126	1.6967e-05 2.0301	4.0497e-04 1.6586	4.0374e-05 2.0126
512	4.1542e-06 2.0224	1.2828e-04 1.6941	1.0006e-05 2.0093	4.1542e-06 2.0224	1.2828e-04 1.6941	1.0006e-05 2.0093
1024	1.0226e-06	3.9643e-05	2.4853e-06	1.0226e-06	3.9643e-05	2.4853e-06



(a) $\varepsilon = 2^{-4}$.



(b) $\varepsilon = 2^{-6}$.

Figure 6.7: Loglog plot for comparison of the spatial order of convergence for Example 6.1

Table 6.5: Comparison (regionwise) of maximum point-wise errors and order of convergence for Example 6.2, taking $\Delta t = \frac{1}{N^2}$.

N	proposed method			existing method		
	left outer region	interior layer region	right outer region	left outer region	interior layer region	right outer region
	$[0, d - \eta_1]$	$(d - \eta_1, d + \eta_2)$	$[d + \eta_2, 1]$	$[0, d - \eta_1]$	$(d - \eta_1, d + \eta_2)$	$[d + \eta_2, 1]$
$\varepsilon = 2^{-4} \approx 10^{-1}$						
128	3.6741e-05 1.9956	3.4463e-04 1.9482	3.7954e-05 1.9988	2.7689e-04 0.98082	5.4828e-04 1.0614	5.4502e-04 1.0176
256	9.2131e-06 1.9978	8.9303e-05 1.9690	9.4967e-06 1.9993	1.4030e-04 0.99060	2.6271e-04 1.0087	2.6922e-04 1.0083
512	2.3068e-06 1.9989	2.2811e-05 1.9836	2.3753e-06 1.9996	7.0609e-05 0.99530	1.3057e-04 1.0042	1.3384e-04 1.0041
1024	5.7714e-07	5.7679e-06	5.9400e-07	3.5420e-05	6.5095e-05	6.6730e-05
$\varepsilon = 2^{-6} \approx 10^{-2}$						
128	3.2120e-04 4.6043	2.3229e-03 1.9117	8.5687e-04 4.8579	1.5323e-04 1.2016	2.0015e-03 1.5733	4.1927e-04 1.2134
256	1.3205e-05 2.2595	6.1737e-04 1.6654	2.9550e-05 2.2705	6.6626e-05 1.1888	6.7257e-04 1.5793	1.8080e-04 1.1881
512	2.7577e-06 2.2826	1.9463e-04 1.6951	6.1242e-06 2.3017	2.9227e-05 1.1959	2.2507e-04 1.5804	7.9352e-05 1.1875
1024	5.6679e-07	6.0108e-05	1.2421e-06	1.2757e-05	7.5262e-05	3.4840e-05
$\varepsilon = 2^{-14} \approx 10^{-4}$						
128	4.8928e-05 1.9671	1.9899e-03 1.6382	1.4797e-04 1.9752	4.8928e-05 1.9671	1.9899e-03 1.6382	1.4797e-04 1.9752
256	1.2514e-05 1.9387	6.3924e-04 1.6821	3.7633e-05 1.9499	1.2514e-05 1.9387	6.3924e-04 1.6821	3.7633e-05 1.9499
512	3.2644e-06 1.8843	1.9920e-04 1.7046	9.7406e-06 1.9042	3.2644e-06 1.8843	1.9920e-04 1.7046	9.7406e-06 1.9042
1024	8.8425e-07	6.1113e-05	2.6024e-06	8.8425e-07	6.1113e-05	2.6024e-06
$\varepsilon = 2^{-20} \approx 10^{-6}$						
128	4.8074e-05 1.9978	1.9887e-03 1.6392	1.4592e-04 2.0003	4.8074e-05 1.9978	1.9887e-03 1.6392	1.4592e-04 2.0003
256	1.2036e-05 1.9990	6.3844e-04 1.6838	3.6473e-05 1.9992	1.2036e-05 1.9989	6.3844e-04 1.6838	3.6473e-05 1.9992
512	3.0113e-06 1.9980	1.9872e-04 1.7073	9.1231e-06 1.9983	3.0113e-06 1.9980	1.9872e-04 1.7073	9.1231e-06 1.9983
1024	7.5384e-07	6.0854e-05	2.2835e-06	7.5385e-07	6.0854e-05	2.2835e-06

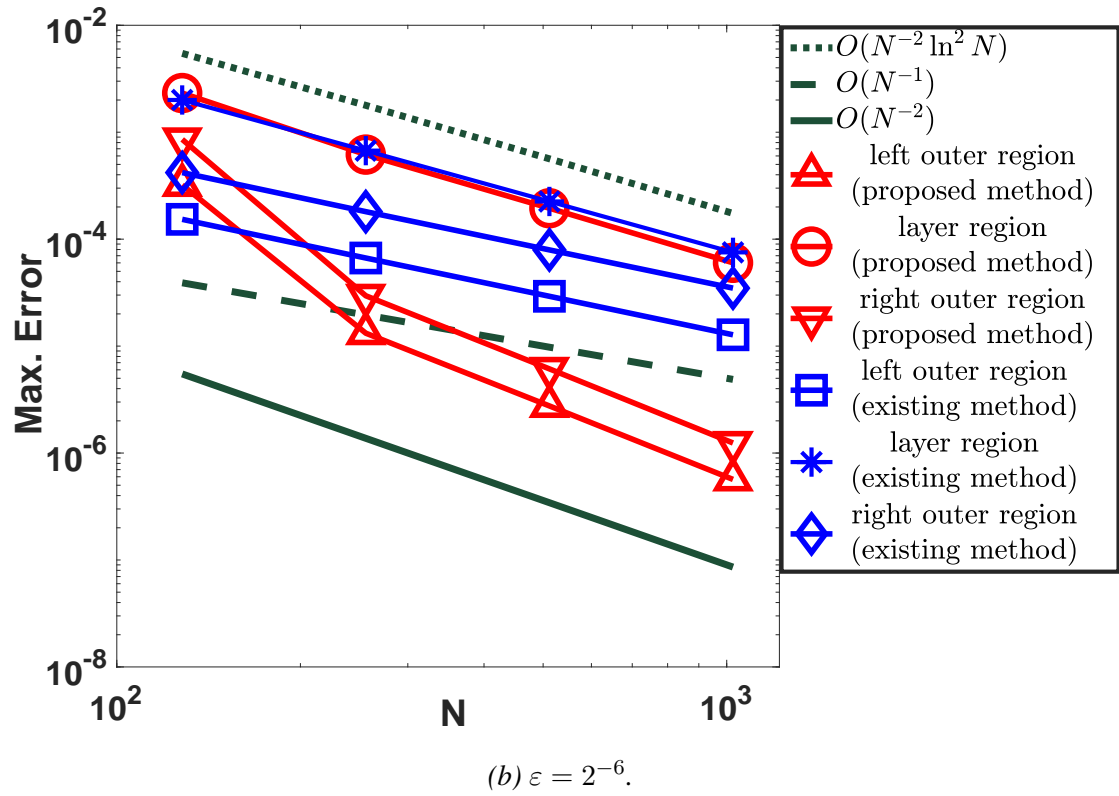
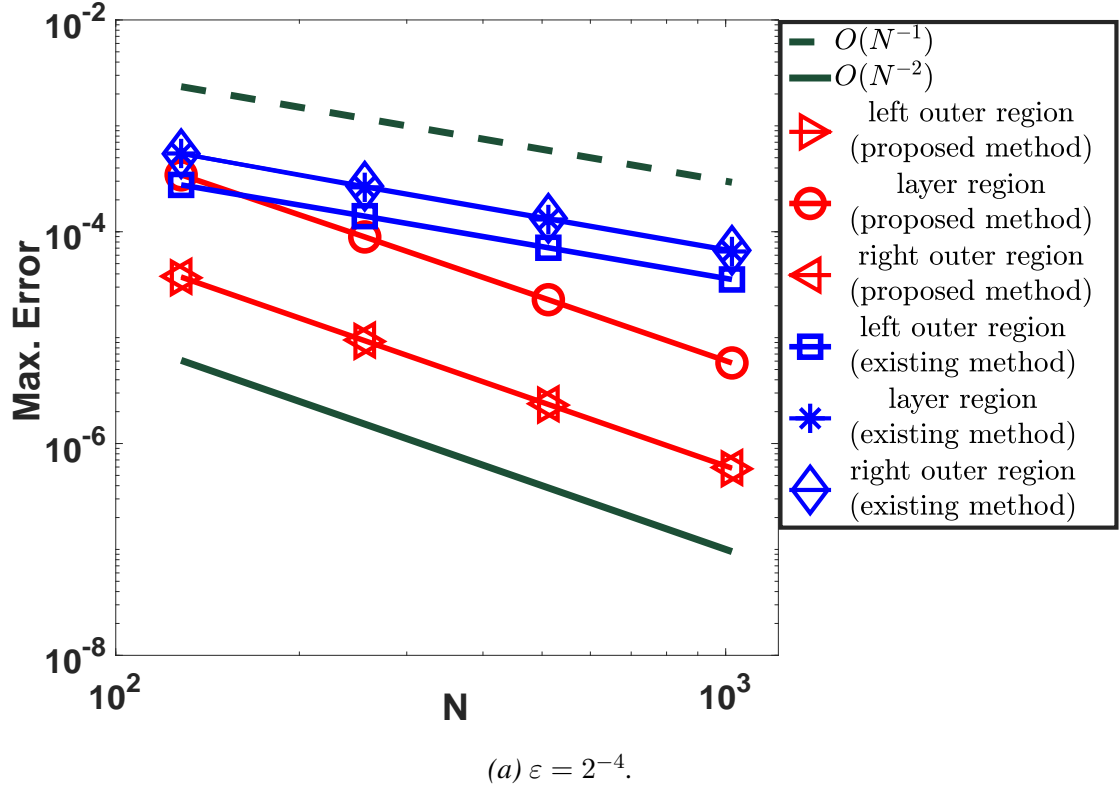
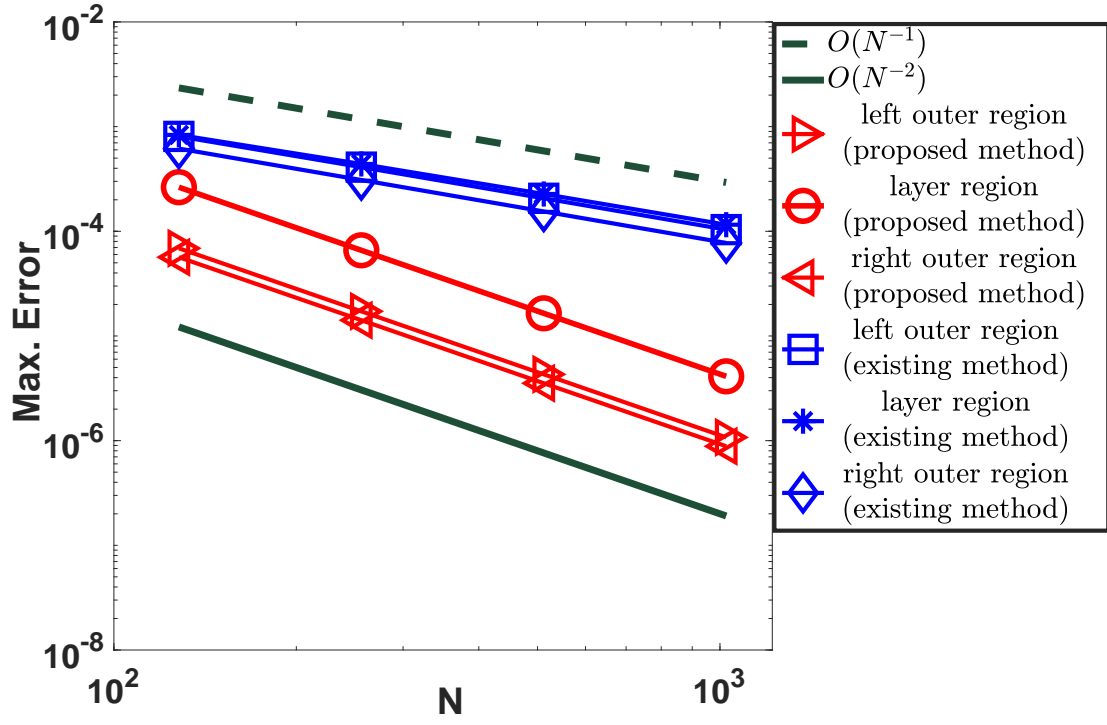


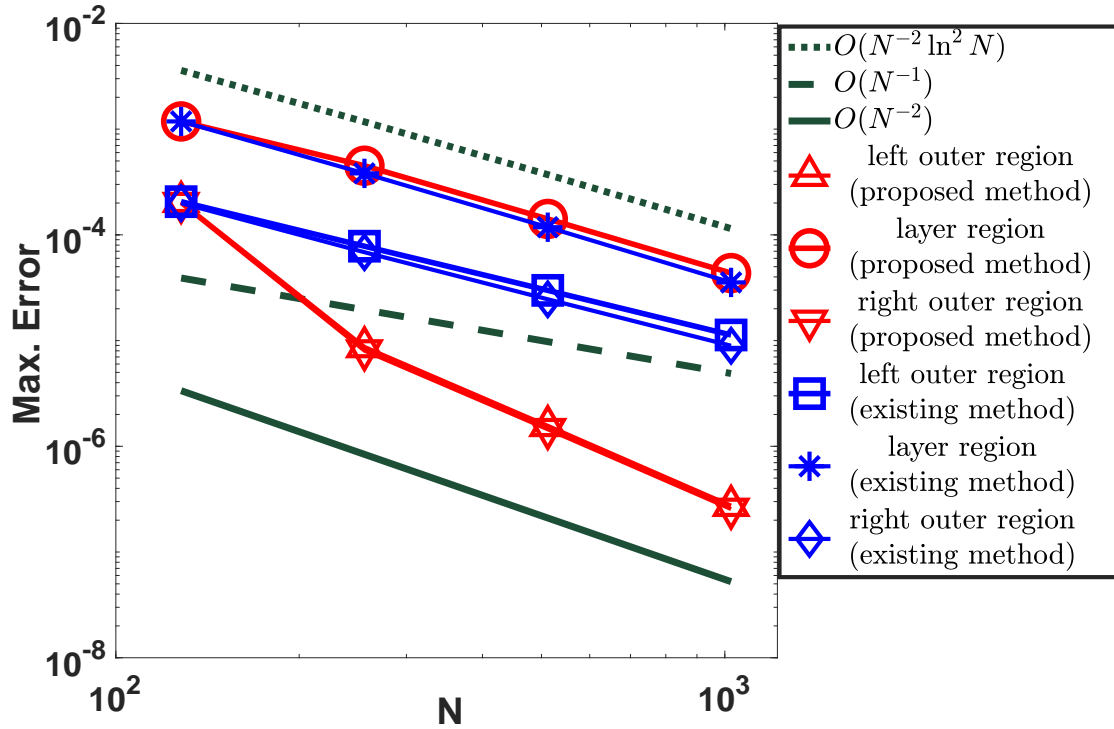
Figure 6.8: Loglog plot for comparison of the spatial order of convergence for Example 6.2

Table 6.6: Comparison (region wise) of maximum point-wise errors and order of convergence for Example 6.3, taking $\Delta t = \frac{1}{N^2}$.

N	proposed method			existing method		
	left outer region	interior layer region	right outer region	left outer region	interior layer region	right outer region
	$[0, d - \eta_1]$	$(d - \eta_1, d + \eta_2)$	$[d + \eta_2, 1]$	$[0, d - \eta_1]$	$(d - \eta_1, d + \eta_2)$	$[d + \eta_2, 1]$
$\varepsilon = 2^{-4} \approx 10^{-1}$						
128	6.8810e-05 1.9999	2.6375e-04 2.0019	5.6555e-05 1.9997	8.0664e-04 0.97580	8.3314e-04 0.92164	6.1630e-04 0.99566
256	1.7204e-05 2.0000	6.5853e-05 2.0000	1.4142e-05 1.9999	4.1014e-04 0.98848	4.3982e-04 0.95270	3.0908e-04 0.99828
512	4.3009e-06 2.0000	1.6463e-05 2.0001	3.5357e-06 2.0000	2.0672e-04 0.99438	2.2724e-04 0.97453	1.5472e-04 0.99925
1024	1.0752e-06	4.1154e-06	8.8394e-07	1.0376e-04	1.1564e-04	7.7402e-05
$\varepsilon = 2^{-6} \approx 10^{-2}$						
128	2.0601e-04 4.5644	1.1826e-03 1.3920	1.9930e-04 4.6310	2.0601e-04 1.3993	1.1826e-03 1.6325	1.9930e-04 1.5404
256	8.7068e-06 2.4779	4.5061e-04 1.6721	8.0435e-06 2.4726	7.8101e-05 1.3877	3.8143e-04 1.6913	6.8517e-05 1.4787
512	1.5629e-06 2.5088	1.4140e-04 1.7011	1.4491e-06 2.5054	2.9848e-05 1.4017	1.1811e-04 1.7347	2.4584e-05 1.4599
1024	2.7460e-07	4.3489e-05	2.5521e-07	1.1297e-05	3.5486e-05	8.9370e-06
$\varepsilon = 2^{-14} \approx 10^{-4}$						
128	1.1722e-04 1.9937	1.2118e-03 1.6093	2.0673e-04 1.9994	1.1722e-04 1.9937	1.2118e-03 1.6093	2.0673e-04 1.9994
256	2.9434e-05 1.9589	3.9716e-04 1.6549	5.1704e-05 1.9831	2.9434e-05 1.9589	3.9716e-04 1.6549	5.1704e-05 1.9831
512	7.5713e-06 1.8991	1.2612e-04 1.6930	1.3078e-05 1.9538	7.5713e-06 1.8991	1.2612e-04 1.6930	1.3078e-05 1.9538
1024	2.0299e-06	3.9007e-05	3.3761e-06	2.0299e-06	3.9007e-05	3.3761e-06
$\varepsilon = 2^{-20} \approx 10^{-6}$						
128	1.1545e-04 2.0233	1.2128e-03 1.6083	2.0567e-04 2.0125	1.1545e-04 2.0233	1.2128e-03 1.6083	2.0567e-04 2.0125
256	2.8400e-05 2.0182	3.9778e-04 1.6532	5.0976e-05 2.0100	2.8400e-05 2.0182	3.9778e-04 1.6532	5.0976e-05 2.0100
512	7.0109e-06 2.0129	1.2647e-04 1.6902	1.2656e-05 2.0073	7.0109e-06 2.0129	1.2647e-04 1.6902	1.2656e-05 2.0073
1024	1.7371e-06	3.9191e-05	3.1480e-06	1.7371e-06	3.9191e-05	3.1480e-06



(a) $\varepsilon = 2^{-4}$.



(b) $\varepsilon = 2^{-6}$.

Figure 6.9: Loglog plot for comparison of the spatial order of convergence for Example 6.3

Table 6.7: Comparison of computational time (in seconds) for Example 6.1, taking $\Delta t = \frac{1}{N^2}$.

	$\varepsilon = 2^{-4} \approx 10^{-1}$			
N	128	256	512	1024
proposed method	1.4793	31.4178	410.0085	6546.2610
existing method	2.4221	39.0740	454.6845	6982.3169
	$\varepsilon = 2^{-6} \approx 10^{-2}$			
N	128	256	512	1024
proposed method	2.4758	31.5279	410.1390	6544.0744
existing method	2.3914	39.3110	454.9408	6998.2790
	$\varepsilon = 2^{-20} \approx 10^{-6}$			
N	128	256	512	1024
proposed method	2.4726	39.5603	459.8931	7020.4788
existing method	2.3305	38.7301	452.1004	6947.0626

Table 6.8: Comparison of computational time (in seconds) for Example 6.2, taking $\Delta t = \frac{1}{N^2}$.

	$\varepsilon = 2^{-4} \approx 10^{-1}$			
N	128	256	512	1024
proposed method	15.4459	219.7051	3477.7996	54903.7533
existing method	18.6910	241.3062	3699.1750	56417.5973
	$\varepsilon = 2^{-6} \approx 10^{-2}$			
N	128	256	512	1024
proposed method	16.5324	221.4601	3481.3048	54854.0630
existing method	19.2644	246.1654	3734.7835	56694.4203
	$\varepsilon = 2^{-20} \approx 10^{-6}$			
N	128	256	512	1024
proposed method	20.0139	248.0453	3728.9498	56949.5886
existing method	19.2974	247.4739	3723.3609	56597.2608

Table 6.9: Comparison of computational time (in seconds) for Example 6.3, taking $\Delta t = \frac{1}{N^2}$.

	$\varepsilon = 2^{-4} \approx 10^{-1}$			
N	128	256	512	1024
proposed method	4.6762	94.7763	1221.8305	19466.2941
existing method	6.4231	110.0671	1314.4793	20379.2004
	$\varepsilon = 2^{-6} \approx 10^{-2}$			
N	128	256	512	1024
proposed method	6.7264	93.4455	1225.2659	19284.9816
existing method	6.3972	108.9556	1314.8121	20329.9364
	$\varepsilon = 2^{-20} \approx 10^{-6}$			
N	128	256	512	1024
proposed method	6.6576	111.1485	1332.6940	20366.3504
existing method	6.4316	108.9218	1311.2975	20343.9922

Efficient Numerical Method for Model problem-II

This type of model problems appear in the semiconductor device modeling (see, e.g., [73]). The content of this part are given here: In Section 6.8, we discuss properties of the analytical solution which includes the stability of the analytical solution as well as the asymptotic behavior of the smooth and layer components. Section 6.9 introduces the suitable mesh for discretizing the domain $\overline{\mathcal{D}}$ and provides description of the newly proposed numerical method. Further, the stability of the proposed method is also discussed here. The ε -uniform convergence result of the proposed method has been established in 6.10. Finally, numerical experiments are carried out in Section 6.11. Here, we also compare the numerical results of the present method with the implicit upwind finite difference scheme.

6.8 The analytical solution of model-II

This section addresses the stability of the analytical solution of the IBVP (6.1)-(6.3) with (6.5) together with the bounds of the derivatives of the smooth and layer component. These properties are important for the convergence analysis of the numerical approximation of the IBVP (6.1)-(6.3) with (6.5). we assume that the data associated with the boundary and the initial conditions, *i.e.*, q_0 , s_l and s_r are sufficiently piecewise smooth functions and satisfy the following compatibility conditions at the corner points $(0, 0)$ and $(1, 0)$:

$$q_0(0) = s_l(0), \quad q_0(1) = s_r(0), \quad (6.52)$$

$$\begin{cases} -\frac{ds_l(0)}{dt} = g(0, 0) - \varepsilon \frac{d^2 q_0(0)}{dx^2} - a(0) \frac{dq_0(0)}{dx} + b(0, 0)q_0(0), \\ -\frac{ds_r(0)}{dt} = g(1, 0) - \varepsilon \frac{d^2 q_0(1)}{dx^2} - a(1) \frac{dq_0(1)}{dx} + b(1, 0)q_0(1), \end{cases} \quad (6.53)$$

and

$$\begin{cases} \frac{d^2 s_l(0)}{dt^2} = \mathcal{L}_{x,\varepsilon}(\mathcal{L}_{x,\varepsilon} q_0 - g)(0, 0) - q_0(0) \frac{\partial b(0, 0)}{\partial t} - \frac{\partial g(0, 0)}{\partial t}, \\ \frac{d^2 s_r(1)}{dt^2} = \mathcal{L}_{x,\varepsilon}(\mathcal{L}_{x,\varepsilon} s_0 - g)(1, 0) - q_0(1) \frac{\partial b(1, 0)}{\partial t} - \frac{\partial g(1, 0)}{\partial t}. \end{cases} \quad (6.54)$$

We also assume the necessary compatibility conditions at the point $(d, 0)$. Then, under these hypothesis the IBVP (6.1)-(6.3) with (6.5) possesses a unique solution $y \in \mathcal{C}^{1+\gamma}(\mathcal{D}) \cap \mathcal{C}^{4+\gamma}(\mathcal{D}^- \cup \mathcal{D}^+)$. At first, we prove the maximum principle for the differential operator $\mathcal{L}_\varepsilon \equiv \mathcal{L}_{x,\varepsilon} - \frac{\partial}{\partial t}$ in the following lemma. The outline of the proof of Lemma 6.13 is given below for clarity of presentation. Let $\partial\mathcal{D} = \overline{\mathcal{D}} \setminus \mathcal{D}$.

Lemma 6.13 (Maximum principle). *Suppose that a function $\psi \in \mathcal{C}^0(\overline{\mathcal{D}}) \cap \mathcal{C}^2(\mathcal{D}^- \cup \mathcal{D}^+)$ satisfies that $\psi(x, t) \leq 0$, $(x, t) \in \partial\mathcal{D}$, $[\frac{\partial\psi}{\partial x}](d, t) \geq 0$, $t > 0$; and $\mathbb{L}_\varepsilon\psi(x, t) \geq 0$, for all $(x, t) \in \mathcal{D}^- \cup \mathcal{D}^+$, then $\psi(x, t) \leq 0$, for all $(x, t) \in \overline{\mathcal{D}}$.*

Proof. Let us introduce a function w on $\overline{\mathcal{D}}$ satisfying

$$\psi(x, t) = \exp(-m_1(x - d)/2\varepsilon)w(x, t), \quad x < d,$$

and

$$\psi(x, t) = \exp(-\mathfrak{m}_2(x - \mathfrak{d})/2\varepsilon)w(x, t), \quad x \geq \mathfrak{d}.$$

We select $\mathfrak{m}_1 < \mathfrak{m}_2$. We assume that the maximum value of w is achieved at (q, t) in $\overline{\mathfrak{D}}$ and $w(q, t) > 0$. If $(q, t) \in \mathfrak{D}^- \cup \mathfrak{D}^+$, then

$$\begin{aligned} \mathbb{L}_\varepsilon \psi(q, t) &= \exp(-\mathfrak{m}_1(q - \mathfrak{d})/2\varepsilon) \left[\varepsilon \left(\frac{\partial^2 w(q, t)}{\partial x^2} - \frac{\mathfrak{m}_1}{\varepsilon} \frac{\partial w(q, t)}{\partial x} + \frac{\mathfrak{m}_1^2}{4\varepsilon^2} w(q, t) \right) \right. \\ &\quad \left. + a(x) \left(\frac{\partial w(q, t)}{\partial x} - \frac{\mathfrak{m}_1}{2\varepsilon} w(q, t) \right) - b(x, t)w(q, t) - \frac{\partial w(q, t)}{\partial t} \right] < 0, \end{aligned}$$

which is a contradiction. The only possibility is $(q, t) = (\mathfrak{d}, t)$. Note that

$$\left[\frac{\partial \psi(\mathfrak{d}, t)}{\partial x} \right] = \left[\frac{\partial w}{\partial x} \right](\mathfrak{d}, t) + [(\mathfrak{m}_1 - \mathfrak{m}_2)/2\varepsilon]w(\mathfrak{d}, t).$$

Since $\frac{\partial w(\mathfrak{d}^+, t)}{\partial x} < 0$, $\frac{\partial w(\mathfrak{d}^-, t)}{\partial x} > 0$, $\left[\frac{\partial w}{\partial x} \right](\mathfrak{d}, t) \leq 0$ and $\mathfrak{m}_1 < \mathfrak{m}_2$. Therefore, $\left[\frac{\partial \psi(\mathfrak{d}, t)}{\partial x} \right] < 0$, which is also a contradiction. Hence, the proof is complete. \blacksquare

Now from Lemma 6.13, the following stability result can be deduced.

Lemma 6.14. *The solution $y(x, t)$ of the IBVP (6.1)-(6.3) with (6.5) satisfies that*

$$\|y\|_{\overline{\mathfrak{D}}} \leq \|y\|_\infty + \frac{1}{\mathfrak{m}_0} \|g\|_{\overline{\mathfrak{D}}}. \quad (6.55)$$

Proof. Consider the two functions $\Psi_\pm(x, t) = -\|y\|_\infty - \frac{(1-x)}{\mathfrak{m}_0} \|g\| \pm y(x, t)$. Clearly, $\Psi_\pm(0, t) \leq 0$, $\Psi_\pm(1, t) \leq 0$, $\Psi_\pm(x, 0) \leq 0$ and for each $(x, t) \in \mathfrak{D}^- \cup \mathfrak{D}^+$

$$\mathcal{L}_\varepsilon \Psi_\pm(x, t) \geq \frac{a(x)}{\mathfrak{m}_0} \|g\| \pm g(x, t) \geq 0.$$

It is also clear that $\left[\frac{\partial \Psi_\pm(\mathfrak{d}, t)}{\partial x} \right] \geq 0$. It follows from the maximum principle that $\Psi_\pm(x, t) \leq 0$ for all $(x, t) \in \overline{\mathfrak{D}}$ which yields the desired bound of y . \blacksquare

The solution y is now decomposed into the smooth component v and the layer component z such that $y = v + z$. To define v and z , we extended the approach given in [33]. Here, we define the smooth component v as $v(x, t) = v_0(x, t) + \varepsilon v_1(x, t) + \varepsilon^2 v_2(x, t) + \varepsilon^3 v_3(x, t)$, where $v_0, v_1, v_2, v_3 \in \mathcal{C}^0(\overline{\mathfrak{D}})$ satisfies the following problems:

$$\begin{cases} a(x) \frac{\partial v_0}{\partial x} - b(x, t)v_0 - \frac{\partial v_0}{\partial t} = g(x, t), & (x, t) \in \mathfrak{D}^- \cup \mathfrak{D}^+, \\ v_0(x, 0) = q_0(x), \quad x \in \overline{\Omega}, \quad v_0(1, t) = y(1, t), \end{cases} \quad (6.56)$$

$$\begin{cases} a(x) \frac{\partial v_l}{\partial x} - b(x, t)v_l - \frac{\partial v_l}{\partial t} = -\frac{\partial^2 v_{l-1}}{\partial x^2}, & (x, t) \in \mathfrak{D}^- \cup \mathfrak{D}^+, \\ v_l(x, 0) = 0, \quad x \in \overline{\Omega}, \quad v_l(1, t) = 0, \quad l = 1, 2, \end{cases} \quad (6.57)$$

and

$$\begin{cases} \mathcal{L}_\varepsilon v_3(x, t) = -\frac{\partial^2 v_2}{\partial x^2}, & (x, t) \in \mathfrak{D}^- \cup \mathfrak{D}^+, \\ v_3(x, 0) = 0, & \bar{\Omega}, \\ v_3(0, t) = 0, & v_3(\mathbf{d}, t) = 0, \quad v_3(1, t) = 0, \quad t \in (0, T]. \end{cases} \quad (6.58)$$

Thus, the smooth component v satisfies that

$$\begin{cases} \mathcal{L}_\varepsilon v(x, t) = g(x, t), & (x, t) \in \mathfrak{D}^- \cup \mathfrak{D}^+, \\ v(x, 0) = y(x, 0), \\ v(0, t) = v_0(0, t) + \varepsilon v_1(0, t) + \varepsilon^2 v_2(0, t), \\ v(\mathbf{d}, t) = v_0(\mathbf{d}, t) + \varepsilon v_1(\mathbf{d}, t) + \varepsilon^2 v_2(\mathbf{d}, t), \quad v(1, t) = y(1, t), \quad t \in (0, T]. \end{cases} \quad (6.59)$$

We note that

$$|[v](\mathbf{d}, t)|, \left| \left[\frac{\partial v}{\partial x} \right](\mathbf{d}, t) \right|, \left| \left[\frac{\partial^2 v}{\partial x^2} \right](\mathbf{d}, t) \right|, \left| \left[\frac{\partial^3 v}{\partial x^3} \right](\mathbf{d}, t) \right| \leq C. \quad (6.60)$$

Theorem 6.3. $\forall j, k \in \mathbb{N} \cup \{0\}$ satisfying $0 \leq j \leq 3$ and $0 \leq j + 2k \leq 4$, the smooth component v defined in (6.59) satisfies the following bounds

$$\left| \frac{\partial^{j+k} v}{\partial x^j \partial t^k} \right|_{\mathfrak{D}^- \cup \mathfrak{D}^+} \leq C, \quad \left| \frac{\partial^4 v}{\partial x^4} \right|_{\mathfrak{D}^- \cup \mathfrak{D}^+} \leq C\varepsilon^{-1}, \quad (6.61)$$

Proof. We derive the bounds (6.61) for the smooth component v in the sub-region $\bar{\mathfrak{D}}^-$ and $\bar{\mathfrak{D}}^+$ separately. At first, we consider the analysis on the sub-region $\bar{\mathfrak{D}}^+$. We extend the domain \mathfrak{D}^+ to the domain $\mathfrak{D}^{e+} = \Omega^{e+} \times (0, T] = (-1, 1) \times (0, T]$ such that $\bar{\mathfrak{D}}^{e+} = \bar{\Omega}^{e+} \times (0, T] = [-1, 1] \times [0, T] \supset \bar{\mathfrak{D}}^+$.

The function $v(x, t)$, $(x, t) \in \bar{\mathfrak{D}}^+$ is the restrictions to $\bar{\mathfrak{D}}^+$ of the function $v^e(x, t)$, $(x, t) \in \bar{\mathfrak{D}}^{e+}$, i.e., $v(x, t) = v^e(x, t)$, $(x, t) \in \bar{\mathfrak{D}}^+$, such that

$$v^e(x, t) = v_0^e(x, t) + \varepsilon v_1^e(x, t) + \varepsilon^2 v_2^e(x, t) + \varepsilon^3 v_3^e(x, t),$$

where the functions v_0^e , v_1^e , v_2^e , v_3^e are respective solutions of the following problems:

$$\begin{cases} a^e(x) \frac{\partial v_0^e}{\partial x} - b^e(x, t) v_0^e - \frac{\partial v_0^e}{\partial t} = g^e(x, t), & (x, t) \in \mathfrak{D}^{e+}, \\ v_0^e(x, 0) = \mathbf{q}_0^e(x), \quad x \in \bar{\Omega}^{e+}, \quad v_0^e(1, t) = \mathbf{s}_r(t), \quad t \in (0, T], \end{cases} \quad (6.62)$$

$$\begin{cases} a^e(x) \frac{\partial v_l^e}{\partial x} - b^e(x, t) v_l^e - \frac{\partial v_l^e}{\partial t} = -\frac{\partial^2 v_{l-1}^e}{\partial x^2}, & (x, t) \in \mathfrak{D}^{e+}, \\ v_l^e(x, 0) = 0, \quad x \in \bar{\Omega}^{e+}, \quad v_l^e(1, t) = 0, \quad l = 1, 2, \quad t \in (0, T], \end{cases} \quad (6.63)$$

and

$$\begin{cases} \mathcal{L}_\varepsilon v_3^e(x, t) = -\frac{\partial^2 v_2^e}{\partial x^2}, & (x, t) \in \mathfrak{D}^{e+}, \\ v_3^e(x, 0) = 0 & x \in \bar{\Omega}^{e+}, \\ v_3^e(-1, t) = 0, \quad v_3^e(\mathbf{d}, t) = 0, \quad v_3^e(1, t) = 0, \quad t \in (0, T]. \end{cases} \quad (6.64)$$

where

$$\mathcal{L}_\varepsilon v_3^e(x, t) = \varepsilon \frac{\partial^2 v_3^e(x, t)}{\partial x^2} + a^e(x) \frac{\partial v_3^e(x, t)}{\partial x} - b^e(x, t) v_3^e(x, t) - \frac{\partial v_3^e(x, t)}{\partial t}.$$

The functions $a^e(x)$, $x \in \bar{\Omega}^{e+}$; $b^e(x, t)$, $(x, t) \in \bar{\mathfrak{D}}^{e+}$; $g(x, t)$, $(x, t) \in \bar{\mathfrak{D}}^{e+}$; q_0^e , $x \in \bar{\Omega}^{e+}$ are defined respectively. Then, using the arguments of [83], one can obtain that the smooth component $v(x, t)$, $(x, t) \in \bar{\mathfrak{D}}^+$ satisfies the following bound:

$$\left| \frac{\partial^{j+k} v(x, t)}{\partial x^j \partial t^k} \right| \leq C(1 + \varepsilon^{3-j}), \quad \text{for } 0 \leq j + 2k \leq 4. \quad (6.65)$$

In the same way, we obtain the bound for the smooth component $v(x, t)$, $(x, t) \in \bar{\mathfrak{D}}^-$. ■

Next, we define the layer component z of the solution y in the following way: Find $z \in \mathcal{C}^0(\bar{\mathfrak{D}})$ such that

$$\begin{cases} \mathcal{L}_\varepsilon z = 0, & (x, t) \in \mathfrak{D}^- \cup \mathfrak{D}^+, \\ z(x, 0) = 0, & x \in \bar{\Omega}, \\ z(0, t) = y(0, t) - v(0, t), & z(1, t) = 0, \\ \left[\frac{\partial z}{\partial x} \right](\mathbf{d}, t) = - \left[\frac{\partial v}{\partial x} \right](\mathbf{d}, t), & t \in (0, T]. \end{cases} \quad (6.66)$$

We can further decompose z as

$$z(x, t) = z_1(x, t) + z_2(x, t),$$

where $z_1 \in \mathcal{C}^{2+\gamma}(\bar{\mathfrak{D}})$ is the boundary layer function satisfying

$$\begin{cases} \mathcal{L}_\varepsilon z_1 = 0, & (x, t) \in \mathfrak{D}^-, \\ z_1(x, 0) = 0, & x \in \bar{\Omega}^-, \\ z_1(0, t) = y(0, t) - v(0, t), & z_1(\mathbf{d}, t) = 0, \quad t \in (0, T], \end{cases} \quad (6.67)$$

with $z_1(x, t) = 0$, $(x, t) \in \bar{\mathfrak{D}}^+$, and $z_2 \in \mathcal{C}^\gamma(\mathfrak{D})$ is the interior layer function satisfying

$$\begin{cases} \mathcal{L}_\varepsilon z_2 = 0, & (x, t) \in \mathfrak{D}^- \cup \mathfrak{D}^+, \\ z_2(x, 0) = 0, & x \in \bar{\Omega}, \\ z_2(0, t) = 0, & z_2(1, t) = 0, \\ \left[\frac{\partial z_2}{\partial x} \right](\mathbf{d}, t) = - \left[\frac{\partial v}{\partial x} \right](\mathbf{d}, t), & t \in (0, T]. \end{cases} \quad (6.68)$$

Theorem 6.4. $\forall j, k \in \mathbb{N} \cup \{0\}$ satisfying $0 \leq j \leq 3$ and $0 \leq j + 2k \leq 4$, the boundary layer component z_1 and the interior layer component z_2 define in (6.67) and (6.68) respectively satisfy the following bounds:

$$\begin{cases} \left| \frac{\partial^{j+k} z_1}{\partial x^j \partial t^k} \right| \leq C \left(\varepsilon^{-j} \exp(-\mathfrak{m}_0 x / \varepsilon) \right), & (x, t) \in \bar{\mathfrak{D}}^-, \\ \left| \frac{\partial^4 z_2}{\partial x^4} \right| \leq C \left(\varepsilon^{-4} \exp(-\mathfrak{m}_0 x / \varepsilon) \right), & (x, t) \in \bar{\mathfrak{D}}^-, \end{cases} \quad (6.69)$$

and

$$\left\{ \begin{array}{l} |z_2(x, t)| \leq C\varepsilon, (x, t) \in \overline{\mathfrak{D}}^- \cup \overline{\mathfrak{D}}^+, \\ \left| \frac{\partial^{j+k} z_2}{\partial x^j \partial t^k} \right| \leq C \left(\varepsilon^{1-k} \exp(-\mathfrak{m}_0 x / \varepsilon) \right), (x, t) \in \overline{\mathfrak{D}}^-, \\ \left| \frac{\partial^4 z_2}{\partial x^4} \right| \leq C \left(\varepsilon^{-3} \exp(-\mathfrak{m}_0 x / \varepsilon) \right), (x, t) \in \overline{\mathfrak{D}}^-, \\ \left| \frac{\partial^{j+k} z_2}{\partial x^j \partial t^k} \right| \leq C \left(\varepsilon^{1-k} \exp(-\mathfrak{m}_0 (x - \mathfrak{d}) / \varepsilon) \right), (x, t) \in \overline{\mathfrak{D}}^+, \\ \left| \frac{\partial^4 z_2}{\partial x^4} \right| \leq C \left(\varepsilon^{-3} \exp(-\mathfrak{m}_0 (x - \mathfrak{d}) / \varepsilon) \right), (x, t) \in \overline{\mathfrak{D}}^+. \end{array} \right. \quad (6.70)$$

Proof. The bounds (6.69) for the component z_1 and its derivatives follows from the arguments of [90, Lemmas 2.6 and 2.7].

To find the bound for z_2 in (6.70), we use the barrier functions $\Phi(x, t) = -\Psi(x, t) \pm z_2(x, t)$, where

$$\Psi(x, t) = \begin{cases} \frac{C\varepsilon}{\mathfrak{m}_0} e^{-\mathfrak{m}_0 x / \varepsilon}, & (x, t) \in \overline{\mathfrak{D}}^-, \\ \frac{C\varepsilon}{\mathfrak{m}_0} e^{-\mathfrak{m}_0 (x - \mathfrak{d}) / \varepsilon}, & (x, t) \in \overline{\mathfrak{D}}^+. \end{cases} \quad (6.71)$$

Note that $\Phi(x, 0) = -\Psi(x, 0) \leq 0$, $\Phi(0, t) = -\Psi(0, t) \leq 0$ and $\Phi(1, t) = -\Psi(1, t) \leq 0$. Next, we have

$$\mathcal{L}_\varepsilon \Phi(x, t) \geq \begin{cases} C \exp(-\mathfrak{m}_0 x / \varepsilon) \left[-\mathfrak{m}_0 + a(x) + \frac{b\varepsilon}{\mathfrak{m}_0} \right] \geq 0, & (x, t) \in \overline{\mathfrak{D}}^-, \\ C \exp(-\mathfrak{m}_0 (x - \mathfrak{d}) / \varepsilon) \left[-\mathfrak{m}_0 + a(x) + \frac{b\varepsilon}{\mathfrak{m}_0} \right] \geq 0, & (x, t) \in \overline{\mathfrak{D}}^+, \end{cases} \quad (6.72)$$

and $\left[\frac{\partial \Phi}{\partial x} \right](\mathfrak{d}, t) = \left[\frac{\partial \Psi}{\partial x} \right](\mathfrak{d}, t) \pm \left[\frac{\partial z_2}{\partial x} \right](\mathfrak{d}, t) \geq 0$. We use Lemma 6.13 for obtaining the required bound of z_2 . As in [90, Lemma 2.7], the desired bounds on the derivatives of $z_2(x, t)$ in (6.70) can be obtained over the domain $\overline{\mathfrak{D}}^-$ and $\overline{\mathfrak{D}}^+$ separately. \blacksquare

6.9 The discrete solution and stability analysis of the model problem-II

In this section, we introduce the modified layer adapted mesh to discretize the domain $\overline{\mathfrak{D}}$ and provide the description of the proposed numerical method for discretizing the IBVP (6.1)–(6.3) with (6.5). The stability of the proposed method is also discussed here.

6.9.1 Modified layer-adapted mesh

We choose $N (\geq 8)$ as even positive integer. Now, to discretize the domain $\overline{\mathfrak{D}} = \overline{\Omega} \times [0, T]$, we construct a mesh $\overline{\mathfrak{D}}^{N,M} = \overline{\Omega}^N \times \Lambda^M$, where $\overline{\Omega}^N = \{x_j\}_{j=0}^N$, denotes the modified layer-adapted mesh on the spatial domain $\overline{\Omega}$ and Λ^M denotes the equidistant mesh on the temporal domain $[0, T]$. To construct $\overline{\Omega}^N$, we divide $\overline{\Omega}$ into five sub-interval as

$$\overline{\Omega} = [0, \eta_1] \cup [\eta_1, \mathfrak{d} - \mathfrak{p}^*] \cup [\mathfrak{d} - \mathfrak{p}^*, \mathfrak{d}] \cup [\mathfrak{d}, \mathfrak{d} + \eta_2] \cup [\mathfrak{d} + \eta_2, 1]. \quad (6.73)$$

where

$$\eta_1 = \min \left\{ \frac{\mathfrak{d}}{2}, \eta_0 \varepsilon \ln N \right\}, \quad \eta_2 = \min \left\{ \frac{1 - \mathfrak{d}}{2}, \eta_0 \varepsilon \ln N \right\},$$

and $p^* = \frac{8\eta_2}{N}$, η_0 is a positive constant; and we place equidistant mesh on each sub-interval as depicted in Fig 6.10.

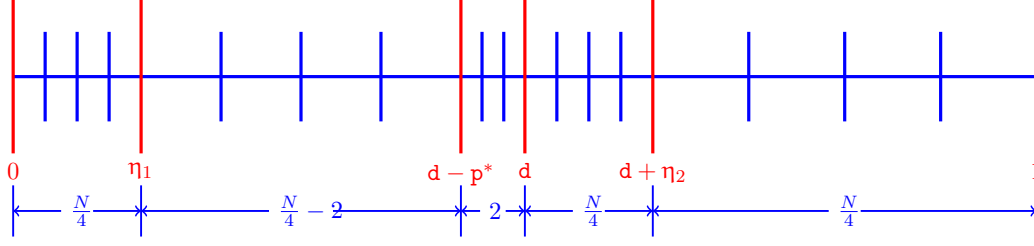


Figure 6.10: Modified layer-adapted mesh in the spatial direction

We denote the step size in the temporal direction by $\Delta t = t_n - t_{n-1} = T/M$, $1 \leq n \leq M$ and the mesh width in the spatial direction by $h_j = x_j - x_{j-1}$, $1 \leq j \leq N$, with $\hat{h}_j = h_j + h_{j+1}$, $1 \leq j \leq N - 1$. We further denote h_j as follows:

$$h_j = \begin{cases} h_1 = \frac{4\eta_1}{N}, & \text{for } 1 \leq j \leq N/4, \\ H_1 = \frac{4(d - p^* - \eta_1)}{N}, & \text{for } N/4 + 1 \leq j \leq N/2 - 2, \\ h_2 = \frac{4\eta_2}{N}, & \text{for } N/2 + 1 \leq j \leq 3N/4, \\ H_2 = \frac{4(1 - d - \eta_2)}{N}, & \text{for } 3N/4 + 1 \leq j \leq N. \end{cases}$$

Remark 6.2. It shown in [Appendix A] that the discrete maximum principle for the proposed finite difference operator can not be proved on the standard Shishkin mesh as depicted in Fig 6.11, by converting the system (6.77) into a new system (6.86). To overcome this difficulty, we construct the modified layer adapted mesh.

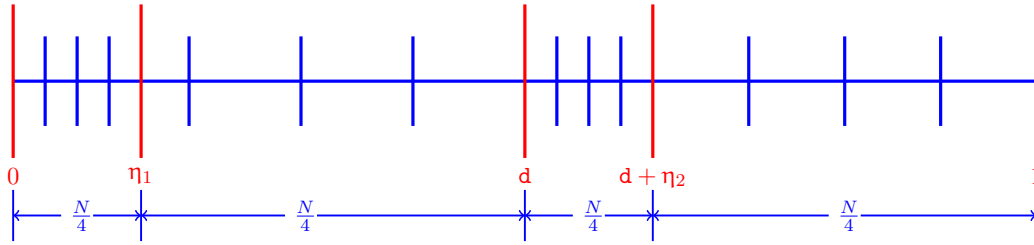


Figure 6.11: Standard Shishkin mesh in the spatial direction

6.9.2 Proposed numerical method

In order to constitute the numerical method for approximation of the IBVP (6.1)-(6.3) with (6.5), we utilize the implicit midpoint operator $\mathcal{L}_{mup}^{N,M}$, and the implicit modified central difference operator $\mathcal{L}_{mcd}^{N,M}$ which are respectively defined as

$$\begin{cases} \mathcal{L}_{mcd}^{N,M} Y_j^{n+1} = \varepsilon D_x^+ D_x^- Y_j^{n+1} + a_j D_x^* Y_j^{n+1} - b_j^{n+1} Y_j^{n+1} - D_t^- Y_j^{n+1}, \\ \mathcal{L}_{mup}^{N,M} Y_j^{n+1} = \varepsilon D_x^+ D_x^- Y_j^{n+1} + a_{j+1/2} D_x^+ Y_j^{n+1} - b_{j+1/2}^{n+1} Y_{j+1/2}^{n+1} - D_t^- Y_{j+1/2}^{n+1}, \end{cases} \quad (6.74)$$

and at the point of discontinuity, we utilize the following one-sided second-order difference operators

$$\begin{cases} D_x^F Y_{N/2}^{n+1} = (-Y_{N/2+2}^{n+1} + 4Y_{N/2+1}^{n+1} - 3Y_{N/2}^{n+1})/2h_{j+1}, \\ D_x^B Y_{N/2}^{n+1} = (Y_{N/2-2}^{n+1} - 4Y_{N/2-1}^{n+1} + 3Y_{N/2}^{n+1})/2h_{j-1}. \end{cases} \quad (6.75)$$

The proposed numerical method is now described in the following form on the mesh $\mathfrak{D}^{N,M}$:

$$\left\{ \begin{array}{l} Y_j^0 = q_0(x_j), \quad \text{for } 0 \leq j \leq N, \\ \mathcal{L}_{mcd}^{N,M} Y_j^{n+1} = g_j^{n+1}, \quad \text{for } 1 \leq j \leq N/4 - 1 \text{ and } N/2 + 1 \leq j \leq 3N/4 - 1, \\ \mathcal{L}_{mcd}^{N,M} Y_j^{n+1} = g_j^{n+1}, \quad \text{for } N/4 \leq j \leq N/2 - 1 \text{ and } 3N/4 \leq j \leq N - 1, \\ \quad \text{and when } \varepsilon > 2||a||N^{-1}, \\ \mathcal{L}_{mup}^{N,M} Y_j^{n+1} = g_{j+1/2}^{n+1}, \quad \text{for } N/4 \leq j \leq N/2 - 1, \\ \quad \text{and when } \varepsilon \leq 2||a||N^{-1}, \\ \mathcal{L}_{mup}^{N,M} Y_j^{n+1} = g_{j+1/2}^{n+1}, \quad \text{for } 3N/4 \leq j \leq N - 1, \\ \quad \text{and when } \varepsilon \leq 2||a||N^{-1}, \\ D_x^F Y_j^{n+1} - D_x^B Y_j^{n+1} = 0, \quad \text{for } j = N/2, \\ Y_0^{n+1} = s_l(t_{n+1}), \quad Y_N^{n+1} = s_r(t_{n+1}), \quad \text{for } n = 0, \dots, M - 1. \end{array} \right. \quad (6.76)$$

Now, we rewrite (6.76) in the following form:

$$\left\{ \begin{array}{l} Y_j^0 = q_0(x_j), \quad \text{for } 0 \leq j \leq N, \\ \left\{ \begin{array}{l} \mathcal{L}_\varepsilon^{N,M} Y_j^{n+1} = \mathcal{F}_j^{n+1}, \quad \text{for } 1 \leq j \leq N - 1, \\ Y_0^{n+1} = s_l(t_{n+1}), \quad Y_N^{n+1} = s_r(t_{n+1}), \quad \text{for } n = 0, \dots, M - 1, \end{array} \right. \end{array} \right. \quad (6.77)$$

where the difference operator $\mathcal{L}_\varepsilon^{N,M}$ is defined as

$$\mathcal{L}_\varepsilon^{N,M} Y_j^{n+1} = \begin{cases} [\mu_j^- Y_{j-1}^{n+1} + \mu_j^c Y_j^{n+1} + \mu_j^+ Y_{j+1}^{n+1}] + [\lambda_j^- Y_{j-1}^n + \lambda_j^c Y_j^n + \lambda_j^+ Y_{j+1}^n], \\ \quad \text{for } 1 \leq j \leq N/2 - 1 \text{ and } N/2 + 1 \leq j \leq N - 1, \\ [\nu_j^{-,2} Y_{j-2}^{n+1} + \nu_j^{-,1} Y_{j-1}^{n+1} + \nu_j^c Y_j^{n+1} + \nu_j^{+,1} Y_{j+1}^{n+1} + \nu_j^{+,2} Y_{j+2}^{n+1}], \\ \quad \text{for } j = N/2, \end{cases} \quad (6.78)$$

and the term \mathcal{F}_j^{n+1} as

$$\mathcal{F}_j^{n+1} \equiv \begin{cases} g_j^{n+1}, & \text{for } 1 \leq j \leq N/4 - 1 \text{ and } N/2 + 1 \leq j \leq 3N/4 - 1, \\ g_{j+1/2}^{n+1}, & \text{for } N/4 \leq j \leq N/2 - 1, \text{ and when } \varepsilon \leq 2\|a\|N^{-1}, \\ g_{j+1/2}^{n+1}, & \text{for } 3N/4 \leq j \leq N - 1, \text{ and when } \varepsilon \leq 2\|a\|N^{-1}, \\ g_j^{n+1}, & \text{for } N/4 \leq j \leq N/2 - 1 \text{ and } 3N/4 \leq j \leq N - 1, \text{ and when } \varepsilon > 2\|a\|N^{-1}, \\ 0, & \text{for } j = N/2. \end{cases} \quad (6.79)$$

Let us denote $\mathbf{p}_j = \varepsilon - \frac{1}{2}a_j h_{j+1}$, for $1 \leq j \leq N/2 - 1$ and $N/2 + 1 \leq j \leq N - 1$. When $\varepsilon > 2\|a\|N^{-1}$, for $1 \leq j \leq N/2 - 1$ and $N/2 + 1 \leq j \leq N - 1$, the coefficients in (6.78) are given by

$$\begin{cases} \mu_j^- = \frac{2\mathbf{p}_j}{h_j \widehat{h_j}}, \\ \mu_j^c = \frac{-2\mathbf{p}_j}{h_j h_{j+1}} - \frac{a_j}{h_{j+1}} - b_j^{n+1} - \frac{1}{\Delta t}, \\ \mu_j^+ = \frac{2\mathbf{p}_j}{h_{j+1} \widehat{h_j}} + \frac{a_j}{h_{j+1}}, \\ \lambda_j^- = 0, \quad \lambda_j^c = \frac{1}{\Delta t}, \quad \lambda_j^+ = 0. \end{cases} \quad (6.80)$$

Next, when $\varepsilon \leq 2\|a\|N^{-1}$, for $N/4 \leq j \leq N/2 - 1$ and $3N/4 \leq j \leq N - 1$, the coefficients in (6.78) are given by

$$\begin{cases} \mu_j^- = \frac{2\varepsilon}{h_j \widehat{h_j}}, \\ \mu_j^c = \frac{-2\varepsilon}{h_j h_{j+1}} - \frac{a_{j+1/2}}{h_{j+1}} - \frac{b_{j+1/2}^{n+1}}{2} - \frac{1}{2\Delta t}, \\ \mu_j^+ = \frac{2\varepsilon}{h_{j+1} \widehat{h_j}} + \frac{a_{j+1/2}}{h_{j+1}} - \frac{b_{j+1/2}^{n+1}}{2} - \frac{1}{2\Delta t}, \\ \lambda_j^- = 0, \quad \lambda_j^c = \frac{1}{2\Delta t}, \quad \lambda_j^+ = \frac{1}{2\Delta t}, \end{cases} \quad (6.81)$$

and for $1 \leq j \leq N/4 - 1$ and $N/2 + 1 \leq j \leq 3N/4 - 1$,

$$\begin{cases} \mu_j^- = \frac{2\mathbf{p}_j}{h_j \widehat{h_j}}, \\ \mu_j^c = \frac{-2\mathbf{p}_j}{h_j h_{j+1}} - \frac{a_j}{h_{j+1}} - b_j^{n+1} - \frac{1}{\Delta t}, \\ \mu_j^+ = \frac{2\mathbf{p}_j}{h_{j+1} \widehat{h_i}} + \frac{a_j}{h_{j+1}}, \\ \lambda_j^- = 0, \quad \lambda_j^c = \frac{1}{\Delta t}, \quad \lambda_j^+ = 0. \end{cases} \quad (6.82)$$

Finally, the coefficients in (6.78) for $j = N/2$, are given by

$$\begin{cases} \nu_{N/2}^{-,2} = \frac{-1}{2h_{j-1}}, & \nu_{N/2}^{-,1} = \frac{2}{h_{j-1}}, \\ \nu_{N/2}^c = \frac{-3}{2} \left(\frac{1}{h_{j-1}} + \frac{1}{h_{j+1}} \right), \\ \nu_{N/2}^{+,1} = \frac{2}{h_{j+1}}, & \nu_{N/2}^{+,2} = \frac{-1}{2h_{j+1}}. \end{cases} \quad (6.83)$$

6.9.3 Inverse monotonicity of the proposed numerical method

It is easy to check that the difference operator defined in (6.78) does not satisfy the discrete maximum principle. We overcome this difficulty by replacing $Y_{N/2-2}^{n+1}$ and $Y_{N/2+2}^{n+1}$ in (6.78) corresponding to $x_{N/2} = d$ with the following expressions:

$$\begin{cases} Y_{N/2+2}^{n+1} = \frac{1}{\mu_{N/2+1}^+} \left[g_{N/2+1}^{n+1} - \mu_{N/2+1}^c Y_{N/2+1}^{n+1} - \mu_{N/2+1}^- Y_{N/2}^{n+1} - \frac{1}{\Delta t} Y_{N/2+1}^n \right], \\ Y_{N/2-2}^{n+1} = \frac{1}{\mu_{N/2-1}^-} \left[g_{N/2-1}^{n+1} - \mu_{N/2-1}^c Y_{N/2-1}^{n+1} - \mu_{N/2-1}^+ Y_{N/2}^{n+1} - \frac{1}{\Delta t} Y_{N/2-1}^n \right]. \end{cases} \quad (6.84)$$

when $\varepsilon > 2\|a\|N^{-1}$, and

$$\begin{cases} Y_{N/2+2}^{n+1} = \frac{1}{\mu_{N/2+1}^+} \left[g_{N/2+1}^{n+1} - \mu_{N/2+1}^c Y_{N/2+1}^{n+1} - \mu_{N/2+1}^- Y_{N/2}^{n+1} - \frac{1}{\Delta t} Y_{N/2+1}^n \right], \\ Y_{N/2-2}^{n+1} = \frac{1}{\mu_{N/2-1}^-} \left[g_{(N/2-1)+1/2}^{n+1} - \mu_{N/2-1}^c Y_{N/2-1}^{n+1} - \mu_{N/2-1}^+ Y_{N/2}^{n+1} - \frac{1}{\Delta t} Y_{(N/2-1)+1/2}^n \right]. \end{cases} \quad (6.85)$$

when $\varepsilon \leq 2\|a\|N^{-1}$. We thus convert the system of equations in (6.77) to the following form:

$$\begin{cases} Y_j^0 = q_0(x_j), & \text{for } 0 \leq j \leq N, \\ \mathbb{L}_{\mathbb{H}}^{N,M} Y_j^{n+1} = \mathbb{F}_j^{n+1}, & \text{for } 1 \leq j \leq N-1, \\ Y_0^{n+1} = s_l(t_{n+1}), \quad Y_N^{n+1} = s_r(t_{n+1}), & \text{for } n = 0, 1, \dots, M-1. \end{cases} \quad (6.86)$$

Here, the difference operator $\mathbb{L}_{\mathbb{H}}^{N,M}$ is defined as

$$\mathbb{L}_{\mathbb{H}}^{N,M} Y_j^{n+1} = \begin{cases} [\hat{\mu}_j^- Y_{j-1}^{n+1} + \hat{\mu}_j^c Y_j^{n+1} + \hat{\mu}_j^+ Y_{j+1}^{n+1}] + [\hat{\lambda}_j^- Y_{j-1}^n + \hat{\lambda}_j^c Y_j^n + \hat{\lambda}_j^+ Y_{j+1}^n], & \text{for } j = N/2, \\ \mathcal{L}_{\varepsilon}^{N,M} Y_j^{n+1}, & \text{for } j \neq N/2, \end{cases} \quad (6.87)$$

where

$$\left\{ \begin{array}{l} \hat{\mu}_{N/2}^- = \frac{1}{2h_2} \frac{\mu_{N/2-1}^c}{\mu_{N/2-1}^-} + \frac{2}{h_2}, \\ \hat{\mu}_{N/2}^c = \frac{1}{2h_2} \frac{\mu_{N/2+1}^-}{\mu_{N/2+1}^+} - \left(\frac{3}{2h_2} + \frac{3}{2h_2} \right) + \frac{1}{2h_2} \frac{\mu_{N/2-1}^+}{\mu_{N/2-1}^-}, \\ \hat{\mu}_{N/2}^+ = \frac{1}{2h_2} \frac{\mu_{N/2+1}^c}{\mu_{N/2+1}^+} + \frac{2}{h_2}, \\ \hat{\lambda}_{N/2}^- = \frac{1}{2h_2 \Delta t \mu_{N/2-1}^-}, \\ \hat{\lambda}_{N/2}^c = 0, \\ \hat{\lambda}_{N/2}^+ = \frac{1}{2h_2 \Delta t \mu_{N/2+1}^+}. \end{array} \right. \quad (6.88)$$

when $\varepsilon > 2\|a\|N^{-1}$ and

$$\left\{ \begin{array}{l} \hat{\mu}_{N/2}^- = \frac{1}{2h_2} \frac{\mu_{N/2-1}^c}{\mu_{N/2-1}^-} + \frac{2}{h_2}, \\ \hat{\mu}_{N/2}^c = \frac{1}{2h_2} \frac{\mu_{N/2+1}^-}{\mu_{N/2+1}^+} - \left(\frac{3}{2h_2} + \frac{3}{2h_2} \right) + \frac{1}{2h_2} \frac{\mu_{N/2-1}^+}{\mu_{N/2-1}^-}, \\ \hat{\mu}_{N/2}^+ = \frac{1}{2h_2} \frac{\mu_{N/2+1}^c}{\mu_{N/2+1}^+} + \frac{2}{h_2}, \\ \hat{\lambda}_{N/2}^- = \frac{1}{4h_2 \Delta t \mu_{N/2-1}^-}, \\ \hat{\lambda}_{N/2}^c = \frac{1}{4h_2 \Delta t \mu_{N/2-1}^-}, \\ \hat{\lambda}_{N/2}^+ = \frac{1}{2h_2 \Delta t \mu_{N/2+1}^+}. \end{array} \right. \quad (6.89)$$

When $\varepsilon \leq 2\|a\|N^{-1}$; and the right-hand side term \mathbb{F}_j^{n+1} is defined as

$$\mathbb{F}_j^{n+1} = \left\{ \begin{array}{ll} \frac{\mathcal{G}_{N/2+1}^{n+1}}{2h_2 \mu_{N/2+1}^+} + \frac{\mathcal{G}_{N/2-1}^{n+1}}{2h_2 \mu_{N/2-1}^-}, & \text{for } j = N/2 \text{ and when } \varepsilon > 2\|a\|N^{-1}, \\ \frac{\mathcal{G}_{N/2+1}^{n+1}}{2h_2 \mu_{N/2+1}^+} + \frac{\mathcal{G}_{(N/2-1)+1/2}^{n+1}}{2h_2 \mu_{N/2-1}^-}, & \text{for } j = N/2 \text{ and when } \varepsilon \leq 2\|a\|N^{-1}, \\ \mathcal{F}_j^{n+1}, & \text{for } j \neq N/2. \end{array} \right. \quad (6.90)$$

Let $\mathfrak{D}^{N,M} = \mathfrak{D} \cap \overline{\mathfrak{D}}^{N,M}$ and $\partial \mathfrak{D}^{N,M} = \overline{\mathfrak{D}}^{N,M} \setminus \mathfrak{D}^{N,M}$. The difference operator $\mathbb{L}_{\mathfrak{H}}^{N,M}$ defined by (6.87) satisfies the following discrete maximum principle.

Lemma 6.15 (Discrete maximum principle). *Assume that there exists a positive integer N_0 such that for $N \geq N_0$ the following conditions hold:*

$$\frac{N}{\ln N} > 6\eta_0 \|a\|_{\infty} \quad \text{and} \quad (6.91)$$

$$(\|b\|_\infty + \frac{1}{\Delta t}) \leq \frac{m_0 N}{4}. \quad (6.92)$$

Then, if any mesh function Ψ satisfies that $\Psi \leq 0$ on $\partial\mathfrak{D}^{N,M}$ and $\mathbb{L}_H^{N,M}\Psi \geq 0$ in $\mathfrak{D}^{N,M}$, then it implies that $\Psi \leq 0$ at each point of $\overline{\mathfrak{D}}^{N,M}$.

Proof. According to the hypothesis of the discrete maximum principle, we assume that the mesh function Ψ satisfies the following:

$$\Psi_j^0 = \rho_j^0, \quad \text{for } 0 \leq j \leq N, \quad (6.93)$$

and

$$\begin{cases} -\mathbb{L}_H^{N,M}\Psi_j^{n+1} = \rho_j^{n+1}, & \text{for } 1 \leq j \leq N-1, \\ \Psi_0^{n+1} = \rho_0^{n+1}, \quad \Psi_N^{n+1} = \rho_N^{n+1}, & \text{for } n = 0, 1, \dots, M-1, \end{cases} \quad (6.94)$$

where $\rho_j^n \leq 0$, for all j and n . Now, we set

$$\begin{aligned} -\mathbb{L}_H^{N,M}\Psi_j^{n+1} &= [\mathbf{A}(j, j-1)\Psi_{j-1}^{n+1} + \mathbf{A}(j, j)\Psi_j^{n+1} + \mathbf{A}(j, j+1)\Psi_{j+1}^{n+1}] - \\ &\quad [\mathbf{B}(j, j-1)\Psi_{j-1}^n + \mathbf{B}(j, j)\Psi_j^n + \mathbf{B}(j, j+1)\Psi_{j+1}^n], \end{aligned} \quad (6.95)$$

for $1 \leq j \leq N-1$, together with

$$\mathbf{A}(j, j) = 1, \quad \text{for } j = 0, N \text{ and } \mathbf{B}(j, j) = 1, \quad \text{for } j = 0, N.$$

Therefore, (6.94) can be rewritten as

$$\mathbf{A}\Psi^{n+1} - \mathbf{B}\Psi^n = \rho^{n+1}, \quad \text{for } n = 0, 1, \dots, M-1, \quad (6.96)$$

where $\mathbf{A} := \mathbf{A}(j, j)$, $\mathbf{B} := \mathbf{B}(j, j)$ and $\Psi^n = (\Psi_0^n, \dots, \Psi_N^n)$, $\rho^n = (\rho_0^n, \dots, \rho_N^n)$, for $n \in \{0, 1, \dots, M\}$. It is obvious that the matrix $\mathbf{B} \geq 0$, and below we prove that the matrix \mathbf{A} is an M-matrix. Then, according to [Lemma 3.12, Part II] given in the book of Roos et al. [99], the desired result follows from (6.96). Now, to prove that the M-matrix criterion of \mathbf{A} , we consider the following two cases.

Case 1. Let $\varepsilon > 2\|a\|N^{-1}$. For $1 \leq j \leq N/4 - 1$, $N/2 + 1 \leq j \leq 3N/4 - 1$ and $j = N/2 - 1$, $N/2 - 2$, we have

$$\mathbf{p}_j = \varepsilon - a_j h_{j+1}/2 \geq \varepsilon - \frac{\|a\|h_1}{2}. \quad (6.97)$$

Again, for $N/4 \leq j \leq N/2 - 3$,

$$\mathbf{p}_j = \varepsilon - a_j h_{j+1}/2 \geq \varepsilon - \frac{\|a\|H_1}{2}. \quad (6.98)$$

and for $3N/4 \leq j \leq N-1$,

$$\mathbf{p}_j = \varepsilon - a_j h_{j+1}/2 \geq \varepsilon - \frac{\|a\|H_2}{2}. \quad (6.99)$$

Since, $h_1, H_1, H_2 \leq 4N^{-1}$; (6.24), (6.98) and (6.40) imply that for $1 \leq j \leq N/2 - 1$ and $N/2 + 1 \leq j \leq N-1$, $\mathbf{p}_j \geq \varepsilon - 2\|a\|N^{-1} > 0$. Now, for $1 \leq j \leq N/2 - 1$ and $N/2 + 1 \leq j \leq N-1$, it is straightforward from

(6.80) that $\mathbf{A}(j, j) = -\mu_j^c > 0$, $\mathbf{A}(j, j-1) = -\mu_j^- < 0$, $\mathbf{A}(j, j+1) = -\mu_j^+ < 0$ and hence,

$$\begin{aligned}
& |\mathbf{A}(j, j)| - |\mathbf{A}(j, j+1)| - |\mathbf{A}(j, j-1)| \\
&= \frac{2\mathbf{p}_j}{h_j h_{j+1}} + \frac{a_j}{h_{j+1}} + b_j^{n+1} + \frac{1}{\Delta t} - \frac{2\mathbf{p}_j}{h_j \widehat{h}_j} - \frac{2\mathbf{p}_j}{h_{j+1} \widehat{h}_j} - \frac{a_j}{h_{j+1}}, \\
&= b_j^{n+1} + \frac{1}{\Delta t} > 0.
\end{aligned} \tag{6.100}$$

Next, we consider $j = N/2$. Here, using (6.92) and $h_2 \leq 4N^{-1}$, we obtain from (6.88) that

$$\begin{aligned}
\mathbf{A}(N/2, N/2+1) &= -\widehat{\mu}_{N/2}^+ \\
&= \frac{1}{2h_2} \left[-4 + \frac{2\mathbf{p}_{N/2+1} + a_{N/2+1}h_2 + b_{N/2+1}^{n+1}h_2^2 + \frac{h_2^2}{\Delta t}}{\mathbf{p}_{N/2+1} + a_{N/2+1}h_2} \right], \\
&\leq \frac{1}{2h_2} \left[\frac{-2\mathbf{p}_{N/2+1} - 3a_{N/2+1}h_2 + h_2^2(b_{N/2+1}^{n+1} + \frac{1}{\Delta t})}{\mathbf{p}_{N/2+1} + a_{N/2+1}h_2} \right], \\
&\leq \frac{1}{2h_2} \left[\frac{-2\mathbf{p}_{N/2+1} - 3\mathfrak{m}_0h_2 + h_2^2\frac{\mathfrak{m}_0N}{4}}{\mathbf{p}_{N/2+1} + a_{N/2+1}h_2} \right], \\
&\leq \frac{1}{2h_2} \left[\frac{-2\mathbf{p}_{N/2+1} - 3\mathfrak{m}_0h_2 + \mathfrak{m}_0h_2}{\mathbf{p}_{N/2+1} + a_{N/2+1}h_2} \right] \leq 0.
\end{aligned} \tag{6.101}$$

Again, using (6.92) and $h_2 \leq 4N^{-1}$, from (6.88) we have

$$\begin{aligned}
\mathbf{A}(N/2, N/2) &= -\widehat{\mu}_{N/2}^c \\
&= -\frac{1}{2h_2} \left[\frac{\mathbf{p}_{N/2+1}}{\mathbf{p}_{N/2+1} + a_{N/2+1}h_2} \right] + \frac{3}{h_2} - \frac{1}{2h_2} \left[\left(\frac{\mathbf{p}_{N/2-1} + a_{N/2-1}h_2}{\mathbf{p}_{N/2-1}} \right) \right], \\
&= \frac{1}{2h_2} \left[\frac{2\mathbf{p}_{N/2-1} - a_{N/2+1}h_2}{\mathbf{p}_{N/2-1}} \right] + \frac{1}{2h_2} \left[\left(\frac{2\mathbf{p}_{N/2+1} + 3a_{N/2+1}h_2}{\mathbf{p}_{N/2+1} + a_{N/2+1}h_2} \right) \right], \\
&\geq \frac{1}{h_2\mathbf{p}_{N/2-1}} \left[\varepsilon - \|a\|h_2 \right],
\end{aligned} \tag{6.102}$$

and

$$\begin{aligned}
\mathbf{A}(N/2, N/2 - 1) &= -\widehat{\mu}_{N/2}^-, \\
&= \frac{1}{2h_2} \left[-4 + \frac{2\mathbf{p}_{N/2-1} + a_{N/2-1}h_2 + b_{N/2-1}^{n+1}h_2^2 + \frac{h_2^2}{\Delta t}}{\mathbf{p}_{N/2-1}} \right], \\
&= \frac{1}{2h_2} \left[\frac{-2\mathbf{p}_{N/2-1} + a_{N/2-1}h_2 + h_2^2(b_{N/2-1}^{n+1} + \frac{1}{\Delta t})}{\mathbf{p}_{N/2-1}} \right], \\
&= \frac{1}{2h_2} \left[\frac{-2\varepsilon + 3a_{N/2-1}h_2 - \mathbf{m}_0h_2 + h_2^2\frac{\mathbf{m}_0N}{4}}{\mathbf{p}_{N/2-1}} \right], \\
&\leq \frac{1}{h_2\mathbf{p}_{N/2-1}} \left[-\varepsilon + \frac{3}{2}\|a\|h_2 \right],
\end{aligned} \tag{6.103}$$

since $h_2 = \frac{4\eta_2}{N} = \frac{4\eta_0\varepsilon \ln N}{N}$, using the condition (6.91), we have $\mathbf{A}(N/2, N/2) > 0$ and $\mathbf{A}(N/2, N/2 - 1) < 0$. Further, we have

$$|\mathbf{A}(N/2, N/2)| - |\mathbf{A}(N/2, N/2 + 1)| - |\mathbf{A}(N/2, N/2 - 1)| > 0. \tag{6.104}$$

Case 2. Let $\varepsilon \leq 2\|a\|N^{-1}$. For $1 \leq j \leq N/4 - 1$, under the condition (6.91), we obtain that

$$\begin{aligned}
\mathbf{P}_j &= \varepsilon - \frac{a_j h_1}{2}, \\
&\geq \frac{h_1}{2} \left(3\|a\| - a_j \right) > 0.
\end{aligned}$$

and similarly for $N/2 + 1 \leq j \leq 3N/4 - 1$, we have $\mathbf{P}_j = \varepsilon - \frac{a_j h_{j+1}}{2} = \varepsilon - \frac{a_j h_2}{2} > 0$. Likewise the previous case one can obtain from (6.82) that

$$\begin{cases} \mathbf{A}(j, j) = -\mu_j^c > 0, \mathbf{A}(j, j - 1) = -\mu_j^- < 0, \mathbf{A}(j, j + 1) = \mu_j^+ < 0, \\ \text{and } |\mathbf{A}(j, j)| - |\mathbf{A}(j, j + 1)| - |\mathbf{A}(j, j - 1)| > 0. \end{cases}$$

Now, for $N/4 \leq j \leq N/2 - 1$ and $3N/4 \leq j \leq N - 1$, it is straightforward from (6.81) that

$$\mathbf{A}(j, j) = -\mu_j^c > 0, \mathbf{A}(j, j - 1) = -\mu_j^- < 0.$$

Under the assumption (6.92) and using inequalities $h_2, H_1, H_2 \leq 4N^{-1}$, we obtain from (6.81) that

$$\begin{aligned}
\mathbf{A}(j, j + 1) &= -\mu_j^+ = -\frac{2\varepsilon}{h_{j+1}\hat{h}_j} - \frac{a_{j+1/2}}{h_{j+1}} + \frac{b_{j+1/2}^{n+1}}{2} + \frac{1}{2\Delta t}, \\
&\leq -\frac{a_{j+1/2}}{h_{j+1}} + \frac{b_{j+1/2}^{n+1}}{2} + \frac{1}{2\Delta t}, \\
&= \frac{1}{2} \left[-\frac{\mathbf{m}_0 N}{2} + \|b\| + \frac{1}{\Delta t} \right] < 0.
\end{aligned}$$

Further, we have

$$\begin{aligned}
& |\mathbf{A}(j, j)| - |\mathbf{A}(j, j+1)| - |\mathbf{A}(j, j-1)| \\
&= \frac{2\varepsilon}{h_j h_{j+1}} + \frac{a_{j+1/2}}{h_{j+1}} + \frac{b_{j+1/2}^{n+1}}{2} + \frac{1}{2\Delta t} - \frac{2\varepsilon}{h_{j+1} \hat{h}_j} - \frac{a_{j+1/2}}{h_{j+1}} + \frac{b_{j+1/2}^{n+1}}{2} + \frac{1}{2\Delta t} - \frac{2\varepsilon}{h_j \hat{h}_j}, \\
&= b_{j+1/2}^{n+1} + \frac{1}{\Delta t} > 0.
\end{aligned} \tag{6.105}$$

Next, we consider $j = N/2$. Likewise the previous case, from (6.89) we have

$$\mathbf{A}(N/2, N/2+1) = -\hat{\mu}_{N/2}^+ \leq \frac{1}{2h_2} \left[\frac{-2\mathbf{p}_{N/2+1} - 3\mathbf{m}_0 h_2 + \mathbf{m}_0 h_2}{\mathbf{p}_{N/2+1} + a_{N/2+1} h_2} \right] < 0.$$

Again, using the condition (6.92) and $h_2 \leq 4N^{-1}$, from (6.89) we have

$$\begin{aligned}
\mathbf{A}_{(N/2, N/2-1)} &= -\hat{\mu}_{N/2}^- \\
&= \frac{1}{2h_2} \left[-4 + \frac{2\varepsilon + a_{(N/2-1)+\frac{1}{2}} h_2 + \frac{h_2^2}{2} (b_{(N/2-1)+\frac{1}{2}}^{n+1} + \frac{1}{\Delta t})}{\varepsilon} \right], \\
&= \frac{1}{2h_2} \left[\frac{-2\varepsilon + a_{(N/2-1)+\frac{1}{2}} h_2 + h_2^2 \frac{\mathbf{m}_0 N}{8}}{\varepsilon} \right], \\
&\leq \frac{1}{2h_2} \left[\frac{-2\varepsilon + \|a\| h_2 + \frac{\mathbf{m}_0 h_2}{2}}{\varepsilon} \right], \\
&\leq \frac{1}{\varepsilon h_2} \left[-\varepsilon + \frac{3}{4} \|a\| h_2 \right],
\end{aligned} \tag{6.106}$$

and

$$\begin{aligned}
\mathbf{A}(N/2, N/2) &= -\hat{\mu}_{N/2}^c \\
&= -\frac{1}{2h_2} \left[\frac{\mathbf{p}_{N/2+1}}{(\mathbf{p}_{N/2+1} + a_{N/2+1} h_2)} \right] + \frac{3}{h_2} \\
&\quad + \frac{h_2}{2\varepsilon} \left(\frac{1}{2\Delta t} + \frac{b_{(N/2-1)+\frac{1}{2}}^{n+1}}{2} - \frac{a_{(N/2-1)+\frac{1}{2}}}{h_2} - \frac{\varepsilon}{h_2^2} \right), \\
&\geq \frac{1}{2h_2} \left[\frac{2\mathbf{p}_{N/2+1} + 3a_{(N/2-1)+\frac{1}{2}}}{(\mathbf{p}_{N/2+1} + a_{N/2+1} h_2)} \right] + \frac{1}{h_2} + \frac{a_{N/2+1} h_2}{2\varepsilon}, \\
&> \frac{1}{h_2 \varepsilon} \left[\varepsilon - \frac{\|a\| h_2}{2} \right],
\end{aligned} \tag{6.107}$$

since $h_2 = \frac{4\eta_2}{N} = \frac{4\eta_0 \varepsilon \ln N}{N}$, using the condition (6.91), we have $\mathbf{A}(N/2, N/2) > 0$ and $\mathbf{A}(N/2, N/2-1) <$

0. Further, we have

$$|\mathbf{A}(N/2, N/2)| - |\mathbf{A}(N/2, N/2 + 1)| - |\mathbf{A}(N/2, N/2 - 1)| > 0. \quad (6.108)$$

Hence, the matrix \mathbf{A} is an M-matrix. ■

By using the discrete maximum principle with a suitable barrier function, we can obtain the following stability result.

Lemma 6.16. *Assume that the conditions (6.91) and (6.92) hold. Then, the solution Y of the discrete problem (6.86)-(6.90) satisfies that*

$$\|Y\|_{\overline{\mathfrak{D}}^{N,M}} \leq \|Y\|_{\partial\mathfrak{D}^{N,M}} + \frac{1}{\mathfrak{m}_0} \|\mathbb{F}\|_{\overline{\mathfrak{D}}^{N,M}}.$$

Proof. We introduce the mesh functions

$$\Psi_{\pm}(x_j, t_{n+1}) = -\|Y\|_{\partial\mathfrak{D}^{N,M}} - \frac{(1-x_j)}{\mathfrak{m}_0} \|\mathbb{F}\|_{\overline{\mathfrak{D}}^{N,M}} \pm Y_j^{n+1}. \quad (6.109)$$

Note that $\Psi_{\pm}(0, t_{n+1}), \Psi_{\pm}(1, t_{n+1}) \leq 0$ and $\Psi_{\pm}(x_j, 0) \leq 0$. When $\varepsilon > 2\|a\|N^{-1}$ for $1 \leq j \leq N/2 - 1, N/2 + 1 \leq j \leq N - 1$,

$$\begin{aligned} \mathbb{L}_{\mathbf{H}}^{N,M} \Psi_{\pm}(x_j, t_{n+1}) &= \varepsilon D_x^+ D_x^- \left(-\|Y\|_{\partial\mathfrak{D}^{N,M}} - \frac{(1-x_j)}{\mathfrak{m}_0} \|\mathbb{F}\| \right) \\ &\quad + a(x_j) D_x^* \left(-\|Y\|_{\partial\mathfrak{D}^{N,M}} - \frac{(1-x_j)}{\mathfrak{m}_0} \|\mathbb{F}\| \right) \\ &\quad - b_j^{n+1} \left(-\|Y\|_{\partial\mathfrak{D}^{N,M}} - \frac{(1-x_j)}{\mathfrak{m}_0} \|\mathbb{F}\| \right) \\ &\quad - D_t^- \left(-\|Y\|_{\partial\mathfrak{D}^{N,M}} - \frac{(1-x_j)}{\mathfrak{m}_0} \|\mathbb{F}\| \right) \pm \mathbb{L}_{\mathbf{H}}^{N,M} Y_j^{n+1}, \\ &\geq \frac{a_j}{\mathfrak{m}_0} \|\mathbb{F}\| \pm \mathbb{L}_{\mathbf{H}}^{N,M} Y_j^{n+1} \geq \|\mathbb{F}\| \pm \mathbb{F}_j^{n+1} \geq 0. \end{aligned}$$

Next, when $\varepsilon \leq 2\|a\|N^{-1}$, $N/4 \leq j \leq N/2 - 1, 3N/4 \leq j \leq N - 1$,

$$\begin{aligned} \mathbb{L}_{\mathbf{H}}^{N,M} \Psi_{\pm}(x_j, t_{n+1}) &= \varepsilon D_x^+ D_x^- \left(-\|Y\|_{\partial\mathfrak{D}^{N,M}} - \frac{(1-x_j)}{\mathfrak{m}_0} \|\mathbb{F}\| \right) \\ &\quad + a_{j+1/2} D_x^* \left(-\|Y\|_{\partial\mathfrak{D}^{N,M}} - \frac{(1-x_j)}{\mathfrak{m}_0} \|\mathbb{F}\| \right) \\ &\quad - b_{j+1/2}^{n+1} \left(-\|Y\|_{\partial\mathfrak{D}^{N,M}} - \frac{(1-x_{j+1/2})}{\mathfrak{m}_0} \|\mathbb{F}\| \right) \\ &\quad - D_t^- \left(-\|Y\|_{\partial\mathfrak{D}^{N,M}} - \frac{(1-x_{j+1/2})}{\mathfrak{m}_0} \|\mathbb{F}\| \right) \pm \mathbb{L}_{\mathbf{H}}^{N,M} Y_j^{n+1}, \\ &\geq \frac{a_{j+1/2}}{\mathfrak{m}_0} \|\mathbb{F}\| \pm \mathbb{L}_{\mathbf{H}}^{N,M} Y_j^{n+1} \geq \|\mathbb{F}\| \pm \mathbb{F}_{j+1/2}^{n+1} \geq 0. \end{aligned}$$

Similarly, for $j = N/2$, we have

$$\mathbb{L}_{\mathbf{H}}^{N,M} \Psi_{\pm}(x_{N/2}, t_{n+1}) \geq D_x^F \Psi_{\pm}(x_{N/2}, t_{n+1}) - D_x^B \Psi_{\pm}(x_{N/2}, t_{n+1}) \geq 0. \quad (6.110)$$

Lemma 6.15 implies that $\Psi_{\pm}(x_j, t_{n+1}) \leq 0$ for all $0 \leq j \leq N$, which yields the desired bound on Y .

6.10 Error analysis

Now, we decompose numerical solution $Y = \mathcal{V} + \mathcal{Z}$ where \mathcal{V} , \mathcal{Z} are smooth and layer component of Y , respectively. Define the function \mathcal{V} to be the solution of

$$\begin{cases} \mathbb{L}_{\mathbf{H}}^{N,M} \mathcal{V}_j^{m+1} = \mathbb{F}_j^{m+1}, \text{ for all } (x_j, t_n) \in \mathfrak{D}^{N,M} \setminus (\mathbf{d}, t_{n+1}), \\ \mathcal{V}_j^0 = v(x_j, 0), \quad \mathcal{V}_0^{m+1} = v(0, t_{n+1}), \\ \mathcal{V}_{N/2}^{m+1} = v(\mathbf{d}, t_{n+1}), \quad \mathcal{V}_N^{m+1} = v(1, t_{n+1}), \quad \text{for } n = 0, 1, \dots, M-1. \end{cases} \quad (6.111)$$

In the following lemma, we obtain the error bounds associated with the smooth component.

Lemma 6.17. *Under the assumption (6.91) and (6.92) of Lemma 6.15, the errors associated with smooth component satisfy the following estimates:*

$$\left| \mathcal{V}_j^{m+1} - v(x_j, t_{n+1}) \right| \leq \begin{cases} C(N^{-2} + \Delta t)t_{n+1}(\mathbf{d} - x_j), & \text{for } x_j \leq \mathbf{d}, \\ C(N^{-2} + \Delta t)t_{n+1}(1 - x_j), & \text{for } x_j \geq \mathbf{d}. \end{cases} \quad (6.112)$$

Proof. In this proof we consider following two cases.

Case 1. When $\varepsilon > 2\|a\|N^{-1}$. For $1 \leq j \leq N/2 - 1$, we define the truncation error as

$$\begin{aligned} \mathbb{L}_{\mathbf{H}}^{N,M}(\mathcal{V}_j^{m+1} - v(x_j, t_{n+1})) &= (\mathcal{L}_{\varepsilon} - \mathbb{L}_{\mathbf{H}}^{N,M})v(x_j, t_{n+1}), \\ &= \left(\varepsilon \left(\frac{\partial^2}{\partial x^2} - \delta_x^2 \right) + a_j \left(\frac{\partial}{\partial x} - D_x^* \right) - \left(\frac{\partial}{\partial t} - D_t^- \right) \right) v(x_j, t_{n+1}). \end{aligned}$$

Then, the truncation error satisfies the satisfies that

$$\left| \mathbb{L}_{\mathbf{H}}^{N,M}(\mathcal{V}_j^{m+1} - v(x_j, t_{n+1})) \right| \leq \begin{cases} C \left[\varepsilon \hat{h}_j \left\| \frac{\partial^3 v}{\partial x^3} \right\| + h_j h_{j+1} \left\| \frac{\partial^3 v}{\partial x^3} \right\| + \Delta t \left\| \frac{\partial^2 v}{\partial t^2} \right\| \right], & \text{for } j = N/4, \\ C \left[\varepsilon h_j^2 \left\| \frac{\partial^4 v}{\partial x^4} \right\| + h_j^2 \left\| \frac{\partial^3 v}{\partial x^3} \right\| + \Delta t \left\| \frac{\partial^2 v}{\partial t^2} \right\| \right], & \text{otherwise.} \end{cases} \quad (6.113)$$

Now, using $h_j \leq CN^{-1}$ and the bounds on the derivative of v from equation (6.61), we obtain the that

$$\left| \mathbb{L}_{\mathbf{H}}^{N,M}(\mathcal{V}_j^{m+1} - v(x_j, t_{n+1})) \right| \leq \begin{cases} C \left[\varepsilon N^{-1} + N^{-2} + \Delta t \right], & \text{for } j = N/4, \\ C \left[N^{-2} + \Delta t \right], & \text{otherwise.} \end{cases}$$

We choose the barrier function

$$\Phi_j^{n+1} = C(N^{-2} + \Delta t)t_{n+1}\gamma(x_j) + C(N^{-2} + \Delta t)t_{n+1}(\mathbf{d} - x_j),$$

where

$$\gamma(x_j) = \begin{cases} 1, & \text{for } 0 \leq x_j \leq \eta_1, \\ \frac{\mathbf{d}-x_j}{\mathbf{d}-\eta_1}, & \text{for } \eta_1 \leq x_j \leq \mathbf{d}. \end{cases}$$

Here, we have

$$\begin{aligned} D_x^+ \gamma(x_j) &= \begin{cases} 0, & 0 \leq j < N/4, \\ \frac{-1}{\mathbf{d}-\eta_1}, & N/4 \leq j < N/2, \end{cases} \quad \text{and} \quad D_x^- \gamma(x_j) = \begin{cases} 0, & 0 < j \leq N/4, \\ \frac{-1}{\mathbf{d}-\eta_1}, & N/4 < j \leq N/2, \end{cases} \\ D_x^* \gamma(x_j) &= \begin{cases} 0, & 0 \leq j < N/4, \\ \frac{-h_1 N}{4\mathbf{d}(\mathbf{d}-\eta_1)}, & j = N/4, \\ \frac{-1}{(\mathbf{d}-\eta_1)}, & N/4 < j < N/2, \end{cases} \quad \text{and} \quad \delta_x^2 \gamma(x_j) = \begin{cases} 0, & 0 \leq j < N/4, \\ \frac{-2N}{4\mathbf{d}(\mathbf{d}-\eta_1)}, & j = N/4, \\ 0, & N/4 < j < N/2. \end{cases} \end{aligned}$$

Now, using the above expressions, one can get

$$\begin{aligned} \mathbb{L}_{\mathbf{H}}^{N,M} \Phi_j^{n+1} &= \varepsilon \delta_x^2 \Phi_j^{n+1} + a_j D_x^* \Phi_j^{n+1} - b_j^{n+1} \Phi_j^{n+1} - D_t^- \Phi_j^{n+1}, \\ &\leq \varepsilon \delta_x^2 \Phi_j^{n+1} + a_j D_x^* \Phi_j^{n+1}, \\ &= \varepsilon \delta_x^2 (C(N^{-2} + \Delta t) t_{n+1} \gamma(x_j) + C(N^{-2} + \Delta t) t_{n+1} (\mathbf{d} - x_j)) \\ &\quad + a_j D_x^* (C(N^{-2} + \Delta t) t_{n+1} \gamma(x_j) + C(N^{-2} + \Delta t) t_{n+1} (\mathbf{d} - x_j)), \\ &= \varepsilon C(N^{-2} + \Delta t) t_{n+1} \delta_x^2 \gamma(x_j) + C(N^{-2} + \Delta t) t_{n+1} \delta_x^2 (\mathbf{d} - x_j) \\ &\quad + a_j C(N^{-2} + \Delta t) t_{n+1} D_x^* \gamma(x_j) + a_j C(N^{-2} + \Delta t) t_{n+1} D_x^* (\mathbf{d} - x_j). \end{aligned} \tag{6.114}$$

The equation (6.114) implies that

$$\mathbb{L}_{\mathbf{H}}^{N,M} \Phi_j^{n+1} \leq \begin{cases} -C(N^{-2} + \Delta t), & \text{for } 0 < j < N/4, \\ -C(\varepsilon N^{-1} + N^{-2} + \Delta t), & \text{for } j = N/4, \\ -C(N^{-2} + \Delta t), & \text{for } N/4 < j < N/2. \end{cases}$$

Therefore, we have

$$|\mathbb{L}_{\mathbf{H}}^{N,M} (\mathcal{V}_j^{n+1} - v(x_j, t_{n+1}))| \leq -\mathbb{L}_{\mathbf{H}}^{N,M} \Phi_j^{n+1},$$

and applying Lemma 6.15 to $-\Phi_j^{n+1} \pm (\mathcal{V}_j^{n+1} - v(x_j, t_{n+1}))$, over $\overline{\mathfrak{D}}^{N,M} \cap \overline{\mathfrak{D}}^-$ yields that

$$\begin{aligned} |(\mathcal{V}_j^{n+1} - v(x_j, t_{n+1}))| &\leq \Phi_j^{n+1} \\ &\leq C(N^{-2} + \Delta t) t_{n+1} (\mathbf{d} - x_j), \quad \text{for } x_j \leq \mathbf{d}. \end{aligned}$$

Now, for $N/2 + 1 \leq j \leq N - 1$, the truncation error satisfies that

$$|\mathbb{L}_{\mathbb{H}}^{N,M}(\mathcal{V}_j^{n+1} - v(x_j, t_{n+1}))| \leq \begin{cases} C \left[\varepsilon \hat{h}_j \left\| \frac{\partial^3 v}{\partial x^3} \right\| + h_j h_{j+1} \left\| \frac{\partial^3 v}{\partial x^3} \right\| + \Delta t \left\| \frac{\partial^2 v}{\partial t^2} \right\| \right], & \text{for } j = 3N/4, \\ C \left[\varepsilon h_j^2 \left\| \frac{\partial^4 v}{\partial x^4} \right\| + h_j^2 \left\| \frac{\partial^3 v}{\partial x^3} \right\| + \Delta t \left\| \frac{\partial^2 v}{\partial t^2} \right\| \right], & \text{otherwise.} \end{cases} \quad (6.115)$$

Now, using $h_j \leq CN^{-1}$ and the bounds on the derivative of v , we obtain that

$$\mathbb{L}_{\mathbb{H}}^{N,M}(\mathcal{V}_j^{n+1} - v(x_j, t_{n+1})) \leq \begin{cases} C[\varepsilon N^{-1} + N^{-2} + \Delta t], & \text{for } j = 3N/4, \\ C[N^{-2} + \Delta t], & \text{otherwise.} \end{cases}$$

We consider the following barrier function for $N/2 + 1 \leq j \leq N - 1$,

$$\Phi_j^{n+1} = C(N^{-2} + \Delta t)t_{n+1}\gamma(x_j) + C(N^{-2} + \Delta t)t_{n+1}(1 - x_j),$$

where

$$\gamma(x_j) = \begin{cases} 1, & \text{for } \mathbf{d} \leq x_j \leq \mathbf{d} + \eta_2, \\ \frac{1-x_j}{1-\mathbf{d}-\eta_2}, & \text{for } \mathbf{d} + \eta_2 \leq x_j \leq 1. \end{cases}$$

Here, we have

$$D_x^+ \gamma(x_j) = \begin{cases} 0, & N/2 \leq j < 3N/4, \\ \frac{-1}{1-\mathbf{d}-\eta_2}, & 3N/4 \leq j < N-1, \end{cases} \quad D_x^- \gamma(x_j) = \begin{cases} 0, & N/2 < j \leq 3N/4, \\ \frac{-1}{1-\mathbf{d}-\eta_2}, & 3N/4 < j \leq N-1, \end{cases}$$

$$D_x^* \gamma(x_j) = \begin{cases} 0, & N/2 \leq j < 3N/4, \\ \frac{-h_2 N}{4(1-\mathbf{d})(1-\mathbf{d}-\eta_2)}, & j = 3N/4, \\ \frac{-1}{(1-\mathbf{d}-\eta_2)}, & N/4 < j < N/2, \end{cases} \quad \text{and } \delta_x^2 \gamma(x_j) = \begin{cases} 0, & N/2 \leq j < 3N/4, \\ \frac{-2N}{4(1-\mathbf{d})(1-\mathbf{d}-\eta_2)}, & j = 3N/4, \\ 0, & 3N/4 < j < N. \end{cases}$$

Now, using the above expressions, we get

$$\mathbb{L}_{\mathbb{H}}^{N,M} \Phi_j^{n+1} \leq \begin{cases} -C(N^{-2} + \Delta t), & \text{for } N/2 < j < 3N/4, \\ -C(\varepsilon N^{-1} + N^{-2} + \Delta t), & \text{for } j = 3N/4, \\ -C(N^{-2} + \Delta t), & \text{for } 3N/4 < j < N. \end{cases}$$

Therefore, we have

$$|\mathbb{L}_{\mathbb{H}}^{N,M}(\mathcal{V}_j^{n+1} - v(x_j, t_{n+1}))| \leq -\mathbb{L}_{\mathbb{H}}^{N,M} \Phi_j^{n+1},$$

and applying Lemma 6.15 to $-\Phi_j^{n+1} \pm (\mathcal{V}_j^{n+1} - v(x_j, t_{n+1}))$, over the region $\overline{\mathfrak{D}}^{N,M} \cap \overline{\mathfrak{D}}^+$ yields that

$$\begin{aligned} |(\mathcal{V}_j^{n+1} - v(x_j, t_{n+1}))| &\leq \Phi_j^{n+1} \\ &\leq C(N^{-2} + \Delta t)t_{n+1}(1 - x_j), \quad \text{for } x_j \geq \mathbf{d}. \end{aligned}$$

Case 2. When $\varepsilon \leq 2\|a\|N^{-1}$. For $N/4 \leq j \leq N/2 - 1$ and $3N/4 \leq j \leq N - 1$, we obtain that

$$\begin{aligned} \left| \mathbb{L}_{\mathbf{H}}^{N,M}(\mathcal{V}_j^{n+1} - v(x_j, t_{n+1})) \right| &= \left| ((\mathcal{L}_\varepsilon v)_{j+1/2} - \mathbb{L}_{\mathbf{H}}^{N,M} v(x_j, t_{n+1})) \right|, \\ &\leq \left[C\varepsilon \hat{h}_j \left\| \frac{\partial v^3}{\partial x^3} \right\| + Ch_{j+1}^2 \left\| \frac{\partial^3 v}{\partial x^3} \right\| + C\Delta t \left\| \frac{\partial^2 v}{\partial t^2} \right\| \right], \\ &\leq C(N^{-2} + \Delta t). \end{aligned}$$

For $1 \leq j < N/4$ and $N/2 < j \leq 3N/4$, from (6.113) and (6.115), we get

$$\left| \mathbb{L}_{\mathbf{H}}^{N,M}(\mathcal{V}_j^{n+1} - v(x_j, t_{n+1})) \right| \leq C(N^{-2} + \Delta t), \quad \text{for } 1 \leq j < N/4, \quad N/2 < j < 3N/4.$$

Now, applying Lemma 6.15 separately to the discrete functions $C(N^{-2} + \Delta t)t_{n+1}(\mathbf{d} - x_j) \pm (\mathcal{V}_j^{n+1} - v(x_j, t_{n+1}))$, over $\overline{\mathfrak{D}}^{N,M} \cap \overline{\mathfrak{D}}^-$ and to the discrete functions $C(N^{-2} + \Delta t)t_{n+1}(1 - x_j) \pm (\mathcal{V}_j^{n+1} - v(x_j, t_{n+1}))$ over $\overline{\mathfrak{D}}^{N,M} \cap \overline{\mathfrak{D}}^+$, we obtain the desired estimate in (6.112). \blacksquare

Next, we define the function Z to be the solution of

$$\begin{cases} \mathbb{L}_{\mathbf{H}}^{N,M} Z_j^{n+1} = 0, & \text{for } (x_j, t_{n+1}) \in \mathfrak{D}^{N,M} \setminus (\mathbf{d}, t_{n+1}), \\ Z_j^0 = z(x_j, 0), \quad Z_0^{n+1} = z(0, t_{n+1}), \\ Z_N^{n+1} = z(1, t_{n+1}), \quad [DZ(\mathbf{d}, t_{n+1})] = -[D\mathcal{V}(\mathbf{d}, t_{n+1})]. \end{cases} \quad (6.116)$$

We define the jump in the discrete derivative of the mesh function Z at the point (\mathbf{d}, t_{n+1}) by

$$[D\Psi(\mathbf{d}, t_{n+1})] = D_x^F \Psi(\mathbf{d}, t_{n+1}) - D_x^B \Psi(\mathbf{d}, t_{n+1}).$$

Similarly to the continuous case we can further decompose Z as

$$Z = Z_1 + Z_2$$

where Z_1 (the discrete analogue of the boundary function z_1) is defined as the solution of

$$\begin{cases} \mathbb{L}_{\mathbf{H}}^{N,M} Z_{1,j}^{n+1} = 0, & \text{in } \mathfrak{D}^{N,M} \cap \mathfrak{D}^-, \\ Z_{1,j}^0 = z_1(x_j, 0), \quad 0 \leq j < N/2, \\ Z_{1,0}^{n+1} = z_1(0, t_{n+1}), \quad Z_{1,N/2}^{n+1} = 0, & \text{for } n = 0, 1, \dots, M-1, \end{cases} \quad (6.117)$$

with $Z_{1,j}^{n+1} = 0$, in $\overline{\mathfrak{D}}^{N,M} \cap \overline{\mathfrak{D}}^+$, and Z_2 (the discrete analogue of the interior layer function z_2) is defined as

the solution of

$$\begin{cases} \mathbb{L}_{\mathbf{H}}^{N,M} Z_{2,j}^{n+1} = 0, & \text{in } \mathfrak{D}^{N,M} \setminus (\mathbf{d}, t_{n+1}), \\ Z_{2,j}^0 = 0, \quad Z_{2,0}^{n+1} = 0, \quad Z_{2,N}^{n+1} = 0, \\ [DZ_2(\mathbf{d}, t_{n+1})] = -[D\mathcal{V}(\mathbf{d}, t_{n+1})] - [DZ_1(\mathbf{d}, t_{n+1})], & \text{for } n = 0, 1, \dots, M-1. \end{cases} \quad (6.118)$$

Lemma 6.18. *Under the assumptions (6.91) and (6.92) of Lemma 6.15, the errors associated with the boundary layer component satisfy the following estimates:*

$$\left| Z_{1,j}^{n+1} - z_1(x_j, t_{n+1}) \right| \leq \begin{cases} C(N^{-2} \ln^2 N + \Delta t) t_{n+1} (\mathbf{d} + x_j), & \text{for } 1 \leq j < N/4, \\ CN^{-2} t_{n+1}, & \text{for } N/4 \leq j \leq N/2 - 1. \end{cases} \quad (6.119)$$

Proof. The proof follows from [118, lemma 10] for the region $N/4 \leq j \leq N/2 - 1$. Next, we obtain an estimate (6.119) for the boundary layer region $1 \leq j < N/4$ by using the truncation error approach and constructing suitable barrier functions. \blacksquare

Lemma 6.19. *Under the assumptions (6.91) and (6.92) of Lemma 6.15, the errors associated with interior layer component satisfy the following estimate:*

$$\left| Z_{2,j}^{n+1} - z_2(x_j, t_{n+1}) \right| \leq CN^{-2}, \quad \text{for } 3N/4 \leq j \leq N-1, \quad (6.120)$$

and

$$\left| Z_{2,j}^{n+1} - z_2(x_j, t_{n+1}) \right| \leq C(N^{-2} \ln^2 N + \Delta t), \quad \text{for } 1 \leq j \leq 3N/4 - 1. \quad (6.121)$$

Proof. The proof of the estimate in (6.120) for the region $3N/4 \leq j \leq N-1$, follows from [118, Lemma 10]. Next, we proceed to derive the estimate in (6.121). When $\varepsilon > 2\|a\|N^{-1}$ and $N/4 \leq j \leq N/2 - 1$, the truncation error satisfies that

$$\left| \mathbb{L}_{\mathbf{H}}^{N,M} (Z_{2,j}^{n+1} - z_2(x_j, t_{n+1})) \right| \leq \begin{cases} C \left[\varepsilon \left\| \frac{\partial^2 z_2}{\partial x^2} \right\| + h_{j+1} \left\| \frac{\partial^2 z_2}{\partial x^2} \right\| + \Delta t \left\| \frac{\partial^2 z_2}{\partial t^2} \right\| \right], & \text{for } j = N/4, \\ C \left[\varepsilon h_{j+1} \left\| \frac{\partial^3 z_2}{\partial x^3} \right\| + h_{j+1} \left\| \frac{\partial^2 z_2}{\partial x^2} \right\| + \Delta t \left\| \frac{\partial^2 z_2}{\partial t^2} \right\| \right], & \text{otherwise,} \end{cases}$$

Further, from the derivatives bounds on z_2 in Theorem 6.4, we obtain that

$$\left| \mathbb{L}_{\mathbf{H}}^{N,M} (Z_{2,j}^{n+1} - z_2(x_j, t_{n+1})) \right| \leq \begin{cases} C \left(\exp(-\mathfrak{m}_0 x_j / \varepsilon) + h_{j+1} \varepsilon^{-1} \exp(-\mathfrak{m}_0 x_j / \varepsilon) + \Delta t \right), & \text{for } j = N/4, \\ C \left(h_{j+1} \varepsilon^{-1} \exp(-\mathfrak{m}_0 x_j / \varepsilon) + \Delta t \right), & \text{otherwise.} \end{cases}$$

The relation $\varepsilon > 2\|a\|N^{-1}$ implies that $\frac{h_{j+1}}{\varepsilon} \leq \frac{2}{\|a\|}$. We have the transition parameter $\eta_1 = \eta_0 \varepsilon \ln N$ and let $\eta_0 = \frac{2}{\mathfrak{m}_0}$, so one can get $\exp(-\mathfrak{m}_0 x_j / \varepsilon) \leq N^{-2}$, $N/4 \leq j \leq N/2 - 1$. After that, we have

$$\left| \mathbb{L}_{\mathbf{H}}^{N,M} (Z_{2,j}^{n+1} - z_2(x_j, t_{n+1})) \right| \leq C(N^{-2} + \Delta t), \quad \text{for } N/4 \leq j \leq N/2 - 1. \quad (6.122)$$

When $\varepsilon \leq 2||a||N^{-1}$, for $N/4 \leq j \leq N/2 - 1$, we have

$$\begin{aligned} |\mathbb{L}_{\mathbf{H}}^{N,M}(Z_{2,j}^{n+1} - z_2(x_j, t_{n+1}))| &= ((\mathcal{L}_{\varepsilon} z_2)_{j+1/2} - \mathbb{L}_{\mathbf{H}}^{N,M} z_2(x_j, t_{n+1})), \\ &\leq \left[C\varepsilon \left\| \frac{\partial^2 z_2}{\partial x^2} \right\| + C \left\| \frac{\partial z_2}{\partial x} \right\| + C\Delta t \left\| \frac{\partial^2 z_2}{\partial t^2} \right\| \right]. \end{aligned}$$

Further, from the derivatives bounds on z_2 in Theorem 6.4, we obtain that

$$|\mathbb{L}_{\mathbf{H}}^{N,M}(Z_{2,j}^{n+1} - z_2(x_j, t_{n+1}))| \leq C(\exp(-\mathfrak{m}_0 x_j / \varepsilon) + \Delta t), \quad N/4 \leq j \leq N/2 - 1. \quad (6.123)$$

The inequalities $\exp(-\mathfrak{m}_0 x_j / \varepsilon) \leq N^{-2}$, for $N/4 \leq j \leq N/2 - 1$, imply that

$$|\mathbb{L}_{\mathbf{H}}^{N,M}(Z_{2,j}^{n+1} - z_2(x_j, t_{n+1}))| \leq C(N^{-2} + \Delta t), \quad \text{for } N/4 \leq j \leq N/2 - 1. \quad (6.124)$$

Finally, for $1 \leq j < N/4$ and $N/2 < j < 3N/4$, we have

$$\begin{aligned} |\mathbb{L}_{\mathbf{H}}^{N,M}(Z_{2,j}^{n+1} - z_2(x_j, t_{n+1}))| &\leq C \left[\varepsilon h_j^2 \left\| \frac{\partial^4 z_2}{\partial x^4} \right\| + h_j^2 \left\| \frac{\partial^3 z_2}{\partial x^3} \right\| + \Delta t \left\| \frac{\partial^2 z_2}{\partial t^2} \right\| \right], \\ &\leq C(N^{-2} \ln^2 N + \Delta t). \end{aligned} \quad (6.125)$$

Now, we derive truncation error at the point of discontinuity. From the proposed scheme (6.76), we have

$$[D(Y_{N/2}^{n+1} - y(\mathfrak{d}, t_{n+1}))] = -[Dy(\mathfrak{d}, t_{n+1})],$$

The preceding equation, as well as the equations (6.111) and (6.117), imply that

$$\begin{aligned} [D(Z_{2,N/2}^{n+1} - z_2(\mathfrak{d}, t_{n+1}))] &= -[Dy(\mathfrak{d}, t_{n+1})] - [D(Z_{1,N/2}^{n+1} - z_1(\mathfrak{d}, t_{n+1}))] - [D(\mathcal{V}_{N/2}^{n+1} - v(\mathfrak{d}, t_{n+1}))], \\ &= -[Dy(\mathfrak{d}, t_{n+1})] + [Dz_1(\mathfrak{d}, t_{n+1})] + [Dv(\mathfrak{d}, t_{n+1})]. \end{aligned}$$

Here, we get

$$\begin{aligned} &|[D(Z_{2,N/2}^{n+1} - z_2(\mathfrak{d}, t_{n+1}))]| \\ &\leq |D_x^F y(\mathfrak{d}, t_{n+1}) - y_x(\mathfrak{d}, t_{n+1})| + |D_x^B y(\mathfrak{d}, t_{n+1}) - y_x(\mathfrak{d}, t_{n+1})| + |D_x^B z_1(\mathfrak{d}, t_{n+1}) - z_{1,x}(\mathfrak{d}, t_{n+1})| \\ &\quad + |D_x^F v(\mathfrak{d}, t_{n+1}) - v_x(\mathfrak{d}, t_{n+1})| + |D_x^B v(\mathfrak{d}, t_{n+1}) - v_x(\mathfrak{d}, t_{n+1})|, \\ &\leq Ch_2^2 \left| \frac{\partial^3 y}{\partial x^3} \right| + Ch_2^2 \left| \frac{\partial^3 z_1}{\partial x^3} \right| + Ch_2^2 \left| \frac{\partial^3 v}{\partial x^3} \right|. \end{aligned}$$

From the previous expression and by using the Theorem 6.3 and 6.4, we get

$$|[D(Z_{2,N/2}^{n+1} - z_2(\mathfrak{d}, t_{n+1}))]| \leq Ch_2^2 \varepsilon^{-2} + Ch_2^2 + Ch_2^2 \leq CN^{-2} \ln^2 N. \quad (6.126)$$

Now, for sufficiently large C , we consider the following discrete functions

$$\Phi^{\pm}(x_j, t_{n+1}) = -C(N^{-2} \ln^2 N + \Delta t)(1 - x_j) \pm (Z_{2,j}^{n+1} - z_2(x_j, t_{n+1})), \quad 0 \leq j \leq 3N/4.$$

From (6.122), (6.124) and (6.125) we have for $j \neq N/2$, $1 \leq j \leq 3N/4 - 1$,

$$\begin{aligned} \mathbb{L}_H^{N,M} \Phi^\pm(x_j, t_{n+1}) &= \mathbb{L}_H^{N,M} (-C(N^{-2} \ln^2 N + \Delta t)(1 - x_j)) \pm \mathbb{L}_H^{N,M} (Z_{2,j}^{n+1} - z_2(x_j, t_{n+1})), \\ &\geq 0. \end{aligned}$$

From (6.126), we have for $j = N/2$,

$$\mathbb{L}_H^{N,M} \Phi^\pm(x_j, t_{n+1}) \geq D_x^F \Phi^\pm(x_j, t_{n+1}) - D_x^B \Phi^\pm(x_j, t_{n+1}) \geq 0.$$

Now, applying Lemma 6.15 for the region $0 \leq j \leq 3N/4$, we obtain the desired estimate in (6.121). ■

6.10.1 Main convergence result

The error associated with the numerical solution can be decomposed as

$$Y_j^{n+1} - y(x_j, t_{n+1}) = \begin{cases} \mathcal{V}_j^{n+1} - v(x_j, t_{n+1}) + Z_{1,j}^{n+1} - z_1(x_j, t_{n+1}) + Z_{2,j}^{n+1} - z_2(x_j, t_{n+1}), & 0 \leq j < N/2, \\ \mathcal{V}_j^{n+1} - v(x_{N/2}, t_{n+1}) + Z_{1,j}^{n+1} - z_1(x_{N/2}, t_{n+1}) + Z_{2,j}^{n+1} - z_2(x_{N/2}, t_{n+1}), & j = N/2, \\ \mathcal{V}_j^{n+1} - v(x_j, t_{n+1}) + Z_{2,j}^{n+1} - z_2(x_j, t_{n+1}), & N/2 < j \leq N. \end{cases}$$

Theorem 6.5 (Global error). *Under the assumptions (6.91) and (6.92) of Lemma 6.15, the error corresponding to the discrete problem (6.86)-(6.90) satisfies the following estimates:*

$$|Y_j^{n+1} - y(x_j, t_{n+1})| \leq \begin{cases} C(N^{-2} \ln^2 N + \Delta t), & 1 \leq j < 3N/4, \\ C(N^{-2} + \Delta t), & 3N/4 \leq j \leq N - 1. \end{cases}$$

Proof. The Proof follows from Lemma 6.17, 6.18 and 6.19. ■

6.11 Numerical experiments

In this section, in order to verify the theoretical result as well as the efficiency of the proposed numerical method, we carryout numerical experiments on the following test examples and also compare the numerical results of the proposed method with the classical implicit upwind scheme (6.127)-(6.128). In all of the evaluations, we select the constant $\eta_0 = 2.2$ and $d = 1/2$.

6.11.1 The classical implicit upwind scheme

We introduce the classical implicit upwind scheme for the problem (6.1)-(6.3) with (6.5), which takes the following form:

$$\begin{cases} Y_j^0 = q_0(x_j), & \text{for } j = 0, \dots, N, \\ \begin{cases} \mathcal{L}_{up}^{N,M} Y_j^{n+1} = g_j^{n+1}, & \text{for } j = 1, \dots, N/2 - 1, \text{ and } j = N/2 + 1, \dots, N - 1, \\ D_x^+ Y_j^{n+1} - D_x^- Y_j^{n+1} = 0, & \text{for } j = N/2, \\ Y_0^{n+1} = s_l(t_{n+1}), Y_N^{n+1} = s_r(t_{n+1}), & \text{for } n = 0, \dots, M - 1, \end{cases} \end{cases} \quad (6.127)$$

where the difference operator $\mathcal{L}_{up}^{N,M}$ is defined as

$$\mathcal{L}_{up}^{N,M} Y_j^{n+1} = \varepsilon D_x^+ D_x^- Y_j^{n+1} + a_j D_x^+ Y_j^{n+1} - b_j^{n+1} Y_j^{n+1} - D_t^- Y_j^{n+1}, \quad (6.128)$$

and for $j = N/2$,

$$D_x^+ Y_j^{n+1} = (Y_{j+1}^{n+1} - Y_j^{n+1})/h_{j+1}, \quad D_x^- Y_j^{n+1} = (Y_j^{n+1} - Y_{j-1}^{n+1})/h_j. \quad (6.129)$$

6.11.2 Test examples

Example 6.4. Consider the parabolic IBVP of the form (6.1)-(6.3) with (6.5), where $a(x) = 1$, $b(x, t) = 0$,

$$g(x, t) = \begin{cases} -9, & \text{for } (x, t) \in (0, 1/2) \times (0, 1], \\ 9(x-1)^2, & \text{for } (x, t) \in (1/2, 1) \times (0, 1]. \end{cases}$$

Here, the exact solution is given by

$$y(x, t) = \begin{cases} \exp(-t) \left(-9(x + \varepsilon e^{\frac{-x}{\varepsilon}} + C_1 \varepsilon (1 - e^{\frac{-x}{\varepsilon}})) + 9\varepsilon - 1 \right), & (x, t) \in (0, d) \times (0, 1], \\ \exp(-t) \left(-9(\varepsilon e^{\frac{-1}{2\varepsilon}} + \frac{1}{2} - \varepsilon) - C_1 \varepsilon (e^{\frac{-1}{2\varepsilon}} - 1) + \left(\frac{45\varepsilon}{4} + 9\varepsilon^2 + 18\varepsilon^3 \right) e^{-(x-\frac{1}{2})/\varepsilon} \right. \\ \left. - \frac{45\varepsilon}{4} - 9\varepsilon^2 - 18\varepsilon^3 - 9\varepsilon e^{\frac{-x}{\varepsilon}} + 9\varepsilon e^{\frac{-1}{2\varepsilon}} + 3[(x-1)^3 + \frac{1}{8}] - 9\varepsilon[(x-1)^2 - \frac{1}{4}] + \right. \\ \left. 18\varepsilon^2(x - \frac{1}{2}) - 1 - C_3 \varepsilon (e^{\frac{-x}{\varepsilon}} - e^{\frac{-1}{2\varepsilon}}) \right), & (x, t) \in [d, 1) \times (0, 1], \end{cases}$$

with $C_3 = C_1 = \frac{41}{8} + 18\varepsilon^3 + 9\varepsilon e^{\frac{-1}{\varepsilon}} - \frac{45\varepsilon/4 + 9\varepsilon^2 + 18\varepsilon^3}{\varepsilon(1 - e^{-\frac{1}{\varepsilon}})} e^{\frac{-1}{2\varepsilon}}$, and accordingly, the data $q_0(x)$, $s_l(t)$ and $s_r(t)$ are chosen.

Since, the exact solution is known, for each ε , we compute maximum point-wise errors by

$$e_\varepsilon^{N,M} = \max_{0 \leq j \leq N} \max_{0 \leq n \leq M} |Y^{N,M}(x_j, t_n) - y(x_j, t_n)|,$$

and the corresponding order of convergence by $r_\varepsilon^{N,M} = \log_2 \left(\frac{e_\varepsilon^{N,M}}{e_\varepsilon^{2N,2M}} \right)$, where $y(x_j, t_n)$ and $Y^{N,M}(x_j, t_n)$, respectively denote the exact and the numerical solution computed on $\overline{\mathcal{D}}^{N,M}$. Further, for each N and M , we calculate the ε -uniform maximum point-wise errors by $e^{N,M} = \max_\varepsilon e_\varepsilon^{N,M}$ and the corresponding order of convergence by $r^{N,M} = \log_2 \left(\frac{e^{N,M}}{e^{2N,2M}} \right)$.

Example 6.5. Consider the parabolic IBVP of the form (6.8)-(6.3) with (6.5), where $b(x, t) = 1 - xt$,

$$a(x) = \begin{cases} 1 + x(1 - x), & x \in [0, d], \\ 1.5 + x(1 - x), & x \in [d, 1], \end{cases}$$

and

$$g(x, t) = \begin{cases} 2(1 + x^2)t^2, & (x, t) \in [0, \mathfrak{d}) \times (0, 1], \\ -3(1 - x^2)t^2, & (x, t) \in [\mathfrak{d}, 1] \times (0, 1]. \end{cases}$$

Here, we set $q_0(x) = 0$, $x \in [0, 1]$ and $s_l(t) = \frac{2}{3}t^3$, $s_r(t) = 0$, $t \in [0, 1]$.

Since the exact solution of Example 6.5 is not known, the following technique is used to illustrate the accuracy and ε -uniform convergence of the proposed method. We denote $\hat{Y}^{2N, 2M}$ as the numerical solution computed on the fine mesh $\hat{\mathfrak{D}}^{2N, 2M}$ with $2N$ mesh-intervals in the spatial direction and $2M$ mesh-intervals in the temporal direction, such that the transition parameters η_1 , η_2 and the point p^* remain unaltered after doubling the mesh-intervals. For each ε , we compute the maximum point-wise errors by

$$\hat{e}_\varepsilon^{N, M} = \max_{0 \leq j \leq N, 0 \leq n \leq M} |Y^{N, M}(x_j, t_n) - \hat{Y}^{2N, 2M}(x_j, t_n)|,$$

and the corresponding order of convergence by $\hat{r}_\varepsilon^{N, M} = \log_2 \left(\frac{\hat{e}_\varepsilon^{N, M}}{\hat{e}_\varepsilon^{2N, 2M}} \right)$. Further, for each N and M , the quantities $\hat{e}^{N, M}$ and $\hat{r}^{N, M}$ are defined analogously to $e^{N, M}$ and $r^{N, M}$.

Example 6.6. Consider the following semi-linear parabolic IBVP:

$$\begin{cases} \varepsilon \frac{\partial^2 y}{\partial x^2} + \frac{\partial y}{\partial x} - \exp(y) - \frac{\partial y}{\partial t} = g(x, t), & (x, t) \in [(0, \mathfrak{d}) \cup (\mathfrak{d}, 1)] \times (0, 1], \\ y(x, 0) = q_0(x), & x \in [0, 1], \\ y(0, t) = s_l(t), \quad y(1, t) = s_r(t), & t \in [0, 1], \end{cases}$$

where the exact solution $y(x, t)$ are the same as we define previously in Example 6.4 and accordingly, the data $q_0(x)$, $s_l(t)$, $s_r(t)$ and the term $g(x, t)$ are chosen.

To compute the numerical solution of the proposed methods in (6.77) and (6.127) for Example 6.6, a nonlinear system needs to be solved at each time step. For that, we use the Newton's iterative method as we define in Chapter 4.

6.11.3 Numerical findings and observations

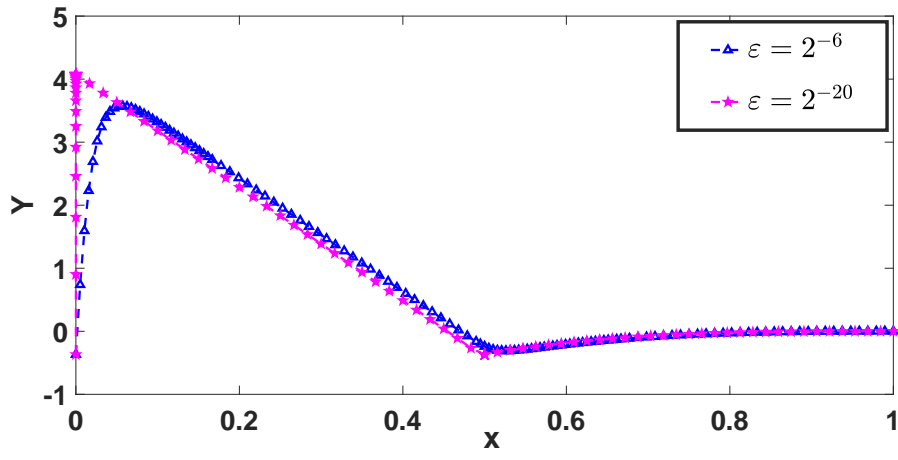
The numerical solutions of Examples 6.4, 6.5 and 6.6, consist of boundary layer at $x = 0$ and an interior layer right side of point of discontinuity at $x = 1/2$. This can be observe from Fig 6.12. In addition, from the surface plots displayed in Figs 6.13, one can fully visualize the numerical solutions.

For different values of ε , N and Δt , the ε -uniform errors are shown in tables 6.10, 6.12, and 6.14, respectively for Examples 6.4, 6.5 and 6.6, with $\Delta t = 1.6/N$. In comparison, to view the effect of a temporal error, we show the ε -uniform error along with the respective order of convergence determined using the proposed method in Tables 6.10, 6.12 and 6.14, respectively for Examples 6.4, 6.5 and 6.6, with $\Delta t = 0.8/N$ and choosing $\mathbb{S}_\varepsilon = \{2^0, 2^{-2}, \dots, 2^{-20}\}$ as the set of values of the parameter ε . In order to highlight the robustness of the proposed method, we provide the computational results of the classical implicit upwind scheme in Tables 6.11, 6.13 and 6.15, respectively for Examples 6.4, 6.5 and 6.6. This represents the ε -uniform convergence of

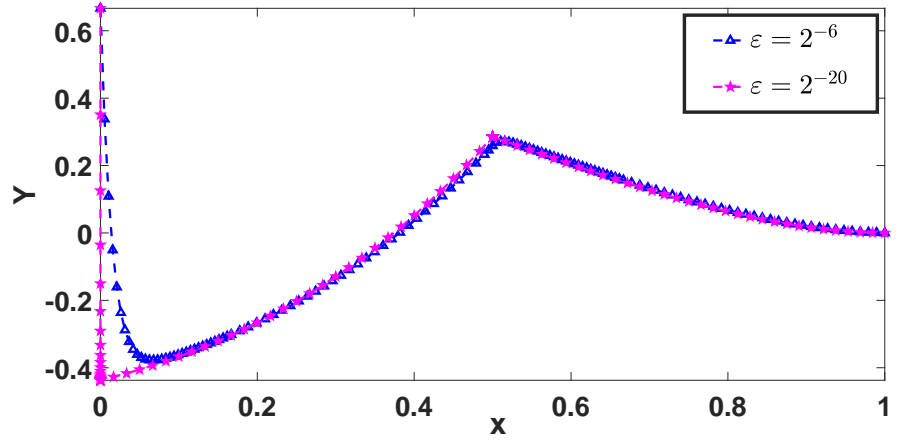
the proposed method as well as the classical implicit upwind scheme. In support of this observation, the calculated ε -uniform errors in Tables 6.10-6.15 are depicted in Figs 6.14, 6.15 and 6.14; and this clearly illustrates robustness of the proposed method in comparison with classical upwind scheme.

The order of convergence shown in Tables 6.10-6.15, however, does not really reflect the spatial order of convergence of the method proposed. According to the estimation of Theorem 6.5, it is because of the influence of the temporal error over the spatial error.

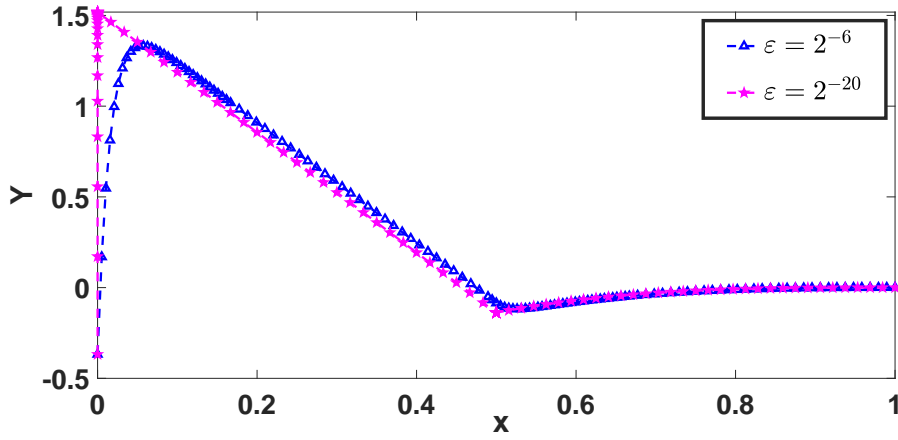
We take $\Delta t = 1/N^2$ for verifying the spatial order of convergence of the present method. We compare region-wise errors and the order of convergence the proposed method with the implicit upwind scheme in Tables 6.16-6.21. It confirms that the proposed method is almost second-order accurate in space, whereas the implicit upwind scheme is almost first-order accurate in space.



(a) Example 6.4.

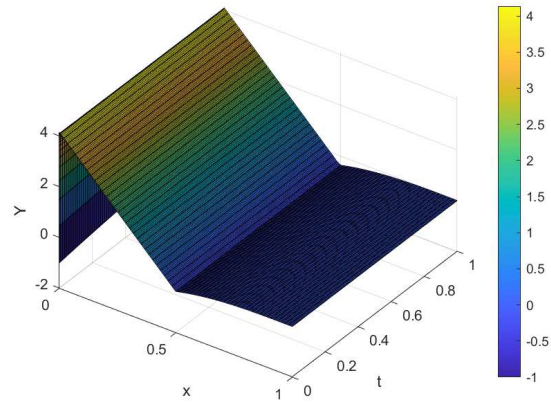


(b) Example 6.5.

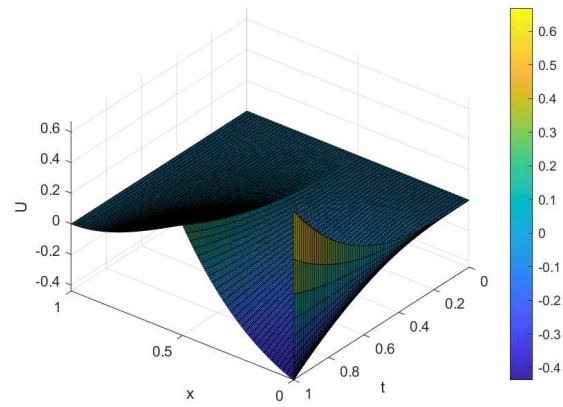


(c) Example 6.6

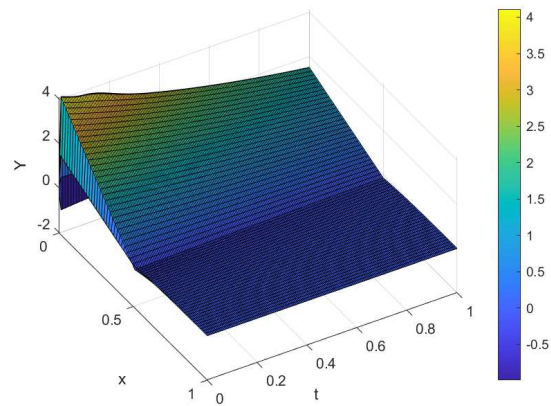
Figure 6.12: Numerical solutions obtain using the proposed method at $t = 1$ for $N = 128$



(a) Example 6.4.



(b) Example 6.5.



(c) Example 6.6

Figure 6.13: Surface plot of the numerical solutions obtained using the proposed method

Table 6.10: ε -uniform maximum point-wise errors and order of convergence for Example 6.4 .

$\varepsilon \in \mathbb{S}_\varepsilon$	Number of mesh intervals N / time step size Δt ($\Delta t = 1.6/N$)				
	$64 / \frac{1}{40}$	$128 / \frac{1}{80}$	$256 / \frac{1}{160}$	$512 / \frac{1}{320}$	$1024 / \frac{1}{640}$
$e^{N,M}$	5.1873e-02	1.7613e-02	6.0240e-03	2.1204e-03	8.0021e-04
$r^{N,M}$	1.5583	1.5479	1.5064	1.4058	
$\varepsilon \in \mathbb{S}_\varepsilon$	Number of mesh intervals N / time step size Δt ($\Delta t = 0.8/N$)				
	$64 / \frac{1}{80}$	$128 / \frac{1}{160}$	$256 / \frac{1}{320}$	$512 / \frac{1}{640}$	$1024 / \frac{1}{1280}$
$e^{N,M}$	5.1971e-02	1.7588e-02	5.7087e-03	1.8428e-03	6.1854e-04
$r^{N,M}$	1.5631	1.6234	1.6313	1.5750	

Table 6.11: ε -uniform maximum point-wise errors and order of convergence for Example 6.4 computed with $\Delta t = 0.8/N$ using classical upwind scheme.

$\varepsilon \in \mathbb{S}_\varepsilon$	Number of mesh-intervals N / time step-size Δt				
	$64 / \frac{1}{80}$	$128 / \frac{1}{160}$	$256 / \frac{1}{320}$	$512 / \frac{1}{640}$	$1024 / \frac{1}{1280}$
$e^{N,M}$	4.3475e-01	2.7500e-01	1.6551e-01	9.6480e-02	5.4719e-02
$r^{N,M}$	0.66075	0.73250	0.77865	0.881819	

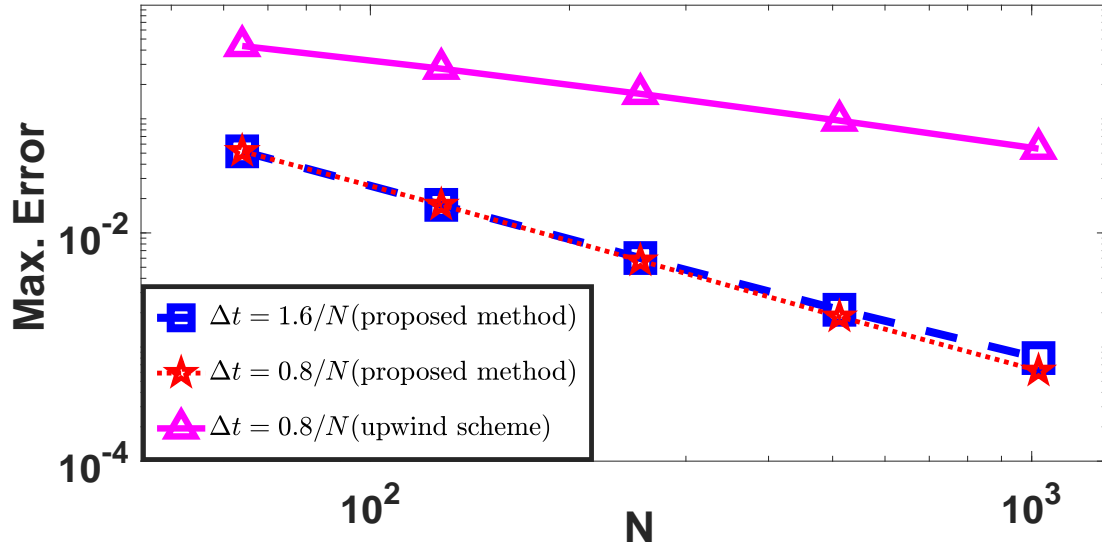


Figure 6.14: Loglog plot for comparison of ε -uniform maximum point-wise errors of Example 6.4

Table 6.12: ε -uniform maximum point-wise errors and order of convergence for Example 6.5 .

$\varepsilon \in \mathbb{S}_\varepsilon$	Number of mesh intervals N / time step size Δt ($\Delta t = 1.6/N$)				
	$64 / \frac{1}{40}$	$128 / \frac{1}{80}$	$256 / \frac{1}{160}$	$512 / \frac{1}{320}$	$1024 / \frac{1}{640}$
$e^{N,M}$	8.8576e-03	3.0491e-03	9.5133e-04	3.1235e-04	1.1098e-04
$r^{N,M}$	1.5385	1.6804	1.6068	1.4929	
$\varepsilon \in \mathbb{S}_\varepsilon$	Number of mesh intervals N / time step size Δt ($\Delta t = 0.8/N$)				
	$64 / \frac{1}{80}$	$128 / \frac{1}{160}$	$256 / \frac{1}{320}$	$512 / \frac{1}{640}$	$1024 / \frac{1}{1280}$
$e^{N,M}$	9.0961e-03	3.1439e-03	9.9233e-04	3.2219e-04	9.9738e-05
$r^{N,M}$	1.5327	1.6637	1.6229	1.6917	

Table 6.13: ε -uniform maximum point-wise errors and order of convergence for Example 6.5 computed with $\Delta t = 0.8/N$ using classical upwind scheme.

$\varepsilon \in \mathbb{S}_\varepsilon$	Number of mesh-intervals N / time step-size Δt				
	$64 / \frac{1}{80}$	$128 / \frac{1}{160}$	$256 / \frac{1}{320}$	$512 / \frac{1}{640}$	$1024 / \frac{1}{1280}$
$e^{N,M}$	4.8664e-02	3.0798e-02	1.8744e-02	1.0924e-02	6.1905e-03
$r^{N,M}$	0.66000	0.71644	0.77897	0.81931	

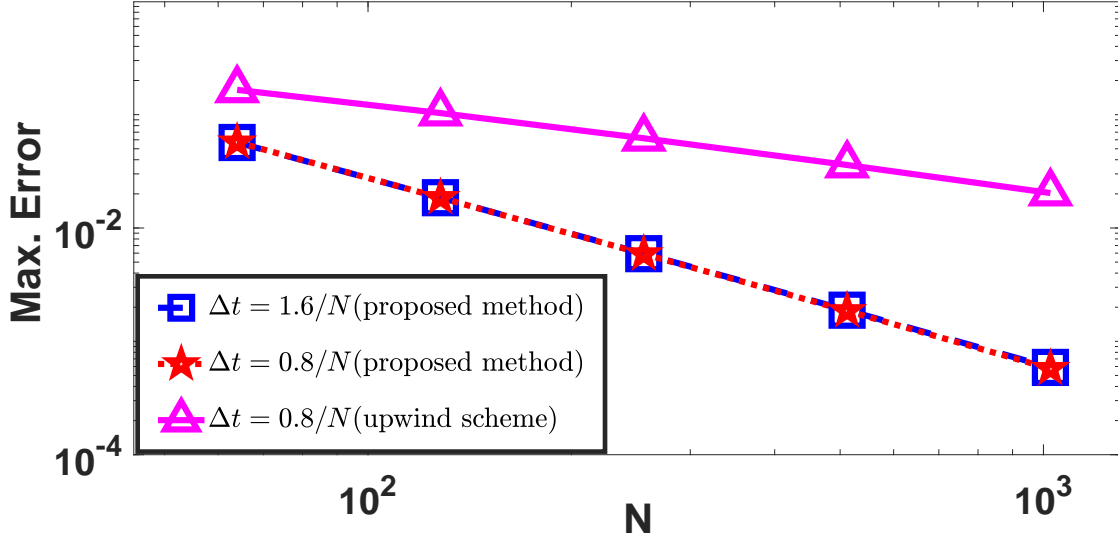


Figure 6.15: Loglog plot for comparison of ε -uniform maximum point-wise errors of Example 6.5

Table 6.14: ε -uniform maximum point-wise errors and order of convergence for Example 6.6 .

$\varepsilon \in \mathbb{S}_\varepsilon$	Number of mesh intervals N / time step size Δt ($\Delta t = 1.6/N$)				
	$64 / \frac{1}{40}$	$128 / \frac{1}{80}$	$256 / \frac{1}{160}$	$512 / \frac{1}{320}$	$1024 / \frac{1}{640}$
$e^{N,M}$	5.6779e-02	1.8501e-02	5.9339e-03	1.8830e-03	5.8876e-04
$r^{N,M}$	1.6178	1.6405	1.6560	1.6772	
$\varepsilon \in \mathbb{S}_\varepsilon$	Number of mesh intervals N / time step size Δt ($\Delta t = 0.8/N$)				
	$64 / \frac{1}{80}$	$128 / \frac{1}{160}$	$256 / \frac{1}{320}$	$512 / \frac{1}{640}$	$1024 / \frac{1}{1280}$
$e^{N,M}$	5.7096e-02	1.8476e-02	5.8949e-03	1.8562e-03	5.7408e-04
$r^{N,M}$	1.6277	1.6481	1.6672	1.6930	

Table 6.15: ε -uniform maximum point-wise errors and order of convergence for Example 6.6 computed with $\Delta t = 0.8/N$ using classical upwind scheme.

$\varepsilon \in \mathbb{S}_\varepsilon$	Number of mesh-intervals N / time step-size Δt				
	$64 / \frac{1}{80}$	$128 / \frac{1}{160}$	$256 / \frac{1}{320}$	$512 / \frac{1}{640}$	$1024 / \frac{1}{1280}$
$e^{N,M}$	1.6542e-01	1.0325e-01	6.1866e-02	3.5957e-02	2.0346e-02
$r^{N,M}$	0.68002	0.73887	0.78286	0.82153	

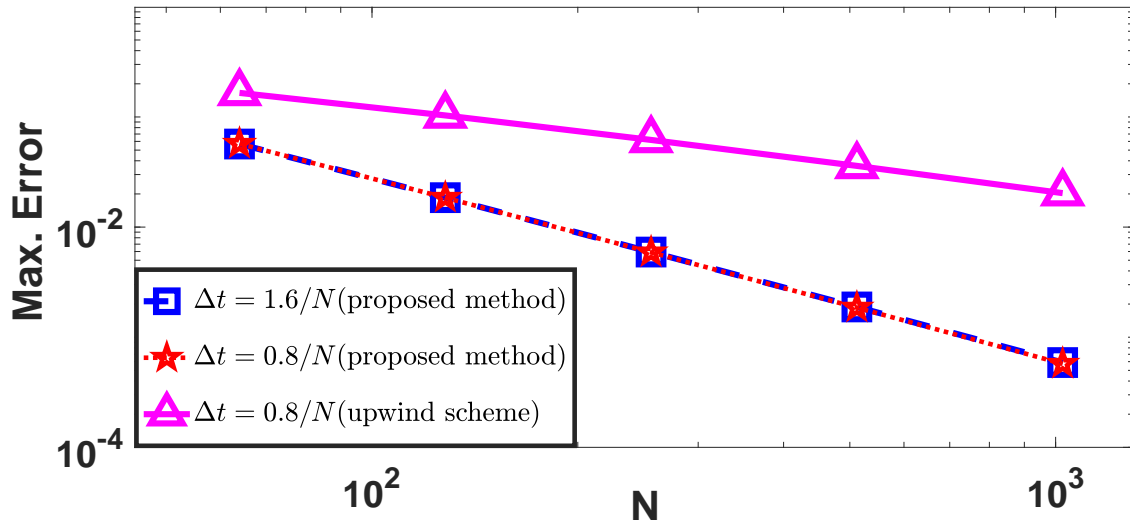


Figure 6.16: Loglog plot for comparison of ε -uniform maximum point-wise errors of Example 6.6

Table 6.16: Comparison of spatial errors for Example 6.4 computed in the region i.e., in $[0, d + \eta]$, using $\Delta t = 1/N^2$.

N	proposed method		implicit upwind scheme	
	error	order of convergence	error	order of convergence
$\varepsilon = 2^{-4} \approx 10^{-1}$				
128	2.1775e-03	1.9579	3.5197e-02	0.99215
256	5.6049e-04	1.9770	1.7695e-02	0.99623
512	1.4237e-04	1.9881	8.8704e-03	0.99816
$\varepsilon = 2^{-6} \approx 10^{-2}$				
128	8.0639e-03	1.5396	8.8974e-02	0.73215
256	2.7738e-03	1.6437	5.3563e-02	0.78425
512	8.8771e-04	1.6843	3.1101e-02	0.81937
$\varepsilon = 2^{-14} \approx 10^{-4}$				
128	6.3986e-03	1.6206	1.0803e-01	0.74148
256	2.0809e-03	1.6593	6.4617e-02	0.79174
512	6.5880e-04	1.6943	3.7326e-02	0.82847
$\varepsilon = 2^{-20} \approx 10^{-6}$				
128	6.3931e-03	1.6204	1.0812e-01	0.74140
256	2.0793e-03	1.6590	6.4673e-02	0.79180
512	6.5842e-04	1.6940	3.7356e-02	0.82852

Table 6.17: Comparison of spatial errors for Example 6.4 computed in the region i.e., in $(d + \eta, 1]$, using $\Delta t = 1/N^2$.

N	proposed method		implicit upwind scheme	
	errors	order of convergence	errors	order of convergence
$\varepsilon = 2^{-4} \approx 10^{-1}$				
128	1.3643e-05	1.8497	5.9151e-04	1.3371
256	3.7854e-06	1.9264	2.3414e-04	1.2036
512	9.9585e-07	1.9635	1.0166e-04	1.1136
$\varepsilon = 2^{-6} \approx 10^{-2}$				
128	2.2784e-04	4.5876	2.5592e-03	1.3102
256	9.4758e-06	2.3633	1.0321e-03	1.3284
512	1.8416e-06	2.3944	4.1097e-04	1.3483
$\varepsilon = 2^{-14} \approx 10^{-4}$				
128	8.9602e-05	1.9684	7.9095e-03	1.0167
256	2.2897e-05	1.9379	3.9091e-03	1.0088
512	5.9759e-06	1.8826	1.9427e-03	1.0048
$\varepsilon = 2^{-20} \approx 10^{-6}$				
128	8.8009e-05	1.9995	7.9406e-03	1.0159
256	2.2009e-05	1.9990	3.9267e-03	1.0079
512	5.5063e-06	1.9999	1.9526e-03	1.0040

Table 6.18: Comparison of spatial errors for Example 6.5 computed in the region i.e., in $[0, d + \eta]$, using $\Delta t = 1/N^2$.

N	proposed method		implicit upwind scheme	
	error	order of convergence	error	order of convergence
$\varepsilon = 2^{-4} \approx 10^{-1}$				
128	7.6853e-04	1.8379	9.3857e-03	0.94027
256	2.1499e-04	1.9129	4.8912e-03	0.96866
512	5.7093e-05	1.9547	2.4993e-03	0.98444
$\varepsilon = 2^{-6} \approx 10^{-2}$				
128	3.1262e-03	1.6660	2.6755e-02	0.70905
256	9.8514e-04	1.6465	1.6366e-02	0.76724
512	3.1467e-04	1.6844	9.6159e-03	0.81193
$\varepsilon = 2^{-14} \approx 10^{-4}$				
128	2.9237e-03	1.6390	3.0797e-02	0.71652
256	9.3878e-04	1.6686	1.8742e-02	0.77903
512	2.9531e-04	1.6992	1.0922e-02	0.81937
$\varepsilon = 2^{-20} \approx 10^{-6}$				
128	2.9233e-03	1.6392	3.0821e-02	0.71667
256	9.3851e-04	1.6687	1.8754e-02	0.77909
512	2.9519e-04	1.6995	1.0929e-02	0.81938

Table 6.19: Comparison of spatial errors for Example 6.5 computed in the region i.e., in $(d + \eta, 1]$, using $\Delta t = 1/N^2$.

N	proposed method		implicit upwind scheme	
	errors	order of convergence	errors	order of convergence
$\varepsilon = 2^{-4} \approx 10^{-1}$				
128	1.3229e-05	2.0076	6.3594e-04	0.97485
256	3.2898e-06	2.0044	3.2356e-04	0.98771
512	8.1996e-07	2.0023	1.6316e-04	0.99393
$\varepsilon = 2^{-6} \approx 10^{-2}$				
128	1.2775e-04	4.3162	1.2609e-03	1.1011
256	6.4128e-06	2.2778	5.8777e-04	1.1237
512	1.3224e-06	2.3079	2.6973e-04	1.1474
$\varepsilon = 2^{-14} \approx 10^{-4}$				
128	2.4925e-05	1.9791	2.0794e-03	0.97766
256	6.3224e-06	1.9582	1.0559e-03	0.98881
512	1.6270e-06	1.9200	5.3207e-04	0.99457
$\varepsilon = 2^{-20} \approx 10^{-6}$				
128	2.4650e-05	1.9997	2.0828e-03	0.97736
256	6.1636e-06	1.9993	1.0579e-03	0.98849
512	1.5416e-06	1.9986	5.3317e-04	0.99429

Table 6.20: Comparison of spatial errors for Example 6.6 computed in the region i.e., in $[0, d + \eta]$, using $\Delta t = 1/N^2$.

N	proposed method		implicit upwind scheme	
	error	order of convergence	error	order of convergence
$\varepsilon = 2^{-4} \approx 10^{-1}$				
128	1.2432e-03	1.9740	3.0100e-02	0.95494
256	3.1644e-04	1.9864	1.5527e-02	0.97906
512	7.9862e-05	1.9928	7.8772e-03	0.98914
$\varepsilon = 2^{-6} \approx 10^{-2}$				
128	6.8041e-03	1.6140	9.4060e-02	0.73351
256	2.2229e-03	1.6548	5.6571e-02	0.78255
512	7.0598e-04	1.6912	3.2887e-02	0.81998
$\varepsilon = 2^{-14} \approx 10^{-4}$				
128	6.6977e-03	1.6397	1.0321e-01	0.73892
256	2.1494e-03	1.6696	6.1840e-02	0.78283
512	6.7565e-04	1.7004	3.5943e-02	0.82151
$\varepsilon = 2^{-20} \approx 10^{-6}$				
128	6.6982e-03	1.6398	1.0325e-01	0.73887
256	2.1495e-03	1.6696	6.1866e-02	0.78286
512	6.7568e-04	1.7003	3.5957e-02	0.821536

Table 6.21: Comparison of errors for Example 6.6 computed in the region i.e., in $(d + \eta, 1]$, using $\Delta t = 1/N^2$.

N	proposed method		implicit upwind scheme	
	errors	order of convergence	errors	order of convergence
$\varepsilon = 2^{-4} \approx 10^{-1}$				
128	7.8026e-06	1.8230	3.3433e-04	0.98417
256	2.2052e-06	1.9143	1.6901e-04	0.93772
512	5.8504e-07	1.9577	8.8234e-05	0.96944
$\varepsilon = 2^{-6} \approx 10^{-2}$				
128	1.8747e-04	4.5573	2.1999e-03	1.2921
256	7.9627e-06	2.3460	8.9836e-04	1.3129
512	1.5661e-06	2.3773	3.6160e-04	1.3338
$\varepsilon = 2^{-14} \approx 10^{-4}$				
128	6.8055e-05	1.9673	6.6577e-03	1.0102
256	1.7403e-05	1.9361	3.3054e-03	1.0055
512	4.5480e-06	1.8794	1.6464e-03	1.0031
$\varepsilon = 2^{-20} \approx 10^{-6}$				
128	6.6789e-05	1.9995	6.6838e-03	1.0094
256	1.6703e-05	1.9989	3.3202e-03	1.0047
512	4.1787e-06	1.9979	1.6547e-03	1.0024

6.12 Conclusion

Analyzing theoretical and numerical aspects of FMMs for finding efficient numerical solutions to singularly perturbed problems with nonsmooth data has received significant attention in recent years. In connection with this, it is to be noted that not much work is available in the literature dealing with higher-order accurate FMMs. In this chapter, we consider two different classes of model problems with nonsmooth data. The model problem-I contains the singularly perturbed PDEs with nonsmooth data of case-I, exhibiting strong interior layers, and the model problem-II contains the singularly perturbed PDEs with the nonsmooth data of case-II, exhibiting both boundary and weak interior layers. Higher-order spatially accurate FMMs are devised and analyzed to achieve better numerical approximations of those types of problems than the existing FMMs. In this regard, the following observations are made, and theoretical challenges are resolved.

For singularly perturbed interface problems, proving ε -uniform stability of the fully discrete solution is a challenging task and the central part of the convergence analysis of the numerical method. Here, we transform the system of equations corresponding to the finite difference operator into a new system of equations which enables us to establish the discrete maximum principle and, consequently, to deduce the stability result of the proposed finite difference methods. However, to accomplish this purpose, we utilize a suitable layer-resolving Shishkin mesh in the case of the model problem-I and a modified layer-adapted mesh in the case of the model problem-II. In fact, it is shown that it is difficult to establish the monotonicity of the newly developed FMM for model problem-II on the standard layer-resolving Shishkin mesh. It is important to note that by introducing the modified layer-adapted mesh, and we overcome this theoretical challenge.

In both cases, the newly proposed methods are proven to be ε -uniformly convergent in the discrete supremum norm; and almost second-order accurate in space, not only for $\varepsilon \ll N^{-1}$, but also for $\varepsilon \gg N^{-1}$. These theoretical findings are verified by the numerous numerical experiments and are observed while solving the semi-linear singularly perturbed parabolic IBVPs by using Newton's linearization technique. In addition to the above, the numerical experiments reveal that the newly proposed methods exhibit notable improvement over the existing numerical methods in terms of the spatial order of convergence; hence, one can conclude that the current numerical algorithms devised for both the model problems are robust in comparison with the existing methods.

Chapter 7

Parameter-Uniform Higher-Order Time-Accurate Numerical Method for Singularly Perturbed Semilinear Parabolic PDEs with Nonsmooth Data

Developing a parameter-robust higher-order accurate numerical approximation of singularly perturbed nonlinear PDEs with nonsmooth data is a desirable and challenging task to better understand the complex phenomena. In this chapter, a class of singularly perturbed semilinear parabolic convection-diffusion problems with discontinuous data is dealt with. The considered nonlinear problem is approximated by utilizing the Crank-Nicolson method for the temporal discretization on an equidistant mesh and the standard finite difference scheme for the spatial discretization on a suitable layer-resolving Shishkin mesh. The existence and stability of the solution are discussed for both the continuous and discrete problems. The numerical approximation is proved to be uniformly convergent and high-order time accurate in the discrete supremum norm. The theoretical error estimates are finally verified by numerical experiments, which also include a comparison of the proposed numerical method with the implicit upwind method in terms of order of accuracy.

7.1 Introduction

We consider the following class of singularly perturbed semilinear parabolic convection-diffusion IBVPs with discontinuous data:

$$\begin{cases} \mathbb{L}_{x,\varepsilon} y(x, t) - \frac{\partial y(x, t)}{\partial t} - b(x, t, y(x, t)) = g(x, t), & (x, t) \in \mathfrak{D}^- \cup \mathfrak{D}^+, \\ y(x, 0) = \mathbf{q}_0(x), & x \in \bar{\Omega}, \\ y(0, t) = \mathbf{s}_l(t), \quad y(1, t) = \mathbf{s}_r(t), & t \in (0, T], \end{cases} \quad (7.1)$$

where

$$\mathbb{L}_{x,\varepsilon} y = \varepsilon \frac{\partial^2 y}{\partial x^2} + a(x) \frac{\partial y}{\partial x},$$

and together with the interface conditions

$$[y](\mathbf{d}, t) = 0, \quad \left[\frac{\partial y}{\partial x} \right](\mathbf{d}, t) = 0, \quad t \in (0, T]. \quad (7.2)$$

Here, ε is a small parameter such that $\varepsilon \in (0, 1]$. It is assumed that the convection coefficient $a(x)$ is smooth on $\bar{\Omega}^-$ and $\bar{\Omega}^+$, and the source term $g(x, t)$ is smooth enough on $\bar{\mathcal{D}}^-$ and $\bar{\mathcal{D}}^+$ such that

$$\begin{cases} a(x) \geq m > 0, & \text{on } \Omega^- \cup \Omega^+, \\ |[a](d)| \leq C, \quad |[g](d, t)| \leq C. \end{cases} \quad (7.3)$$

Further, it is assumed that the nonlinear term $b(x, t, y)$ is sufficiently smooth on $\bar{\mathcal{D}} \times \mathbb{R}$, and satisfies the condition

$$\frac{\partial b(x, t, y)}{\partial y} \geq \beta > 0, \quad (x, t, y) \in \bar{\mathcal{D}} \times \mathbb{R}. \quad (7.4)$$

The solution $y(x, t)$ of the nonlinear IBVP (7.1)-(7.4), generally, possesses an interior layer arises to the right side of $x = d$, in addition to the boundary layer at $x = 0$ as $\varepsilon \rightarrow 0$. Since g is discontinuous at (d, t) , the solution $y \notin \mathcal{C}^2(\bar{\mathcal{D}})$, but the first derivative of the solution exists in the space variable x and is continuous. In the model problem, apart from imposing the smoothness criterion on a, b and g , the boundary and the initial data, *i.e.*, s_l, s_r and q_0 are assumed to be sufficiently smooth. Besides this, the following compatibility conditions are imposed at the corner points $(0, 0)$ and $(1, 0)$:

$$q_0(0) = s_l(0), \quad q_0(1) = s_r(0), \quad (7.5)$$

and

$$\begin{cases} \frac{ds_l(0)}{dt} = -g(0, 0) + \varepsilon \frac{d^2 q_0(0)}{dx^2} + a(0) \frac{dq_0(0)}{dx} - b(0, 0, q_0(0)), \\ \frac{ds_r(0)}{dt} = -g(1, 0) + \varepsilon \frac{d^2 q_0(1)}{dx^2} + a(1) \frac{dq_0(1)}{dx} - b(1, 0, q_0(1)). \end{cases} \quad (7.6)$$

Further, in order to derive the bounds of the derivatives up to third-order in space and third-order in time, we require the solution $y(x, t) \in \mathcal{C}^{1+\gamma}(\bar{\mathcal{D}}) \cap \mathcal{C}^{4+\gamma}(\mathcal{D}^- \cup \mathcal{D}^+)$, which is ensured by the assumption of the compatibility conditions in (7.5)-(7.6) together with the following compatibility conditions at the corner points $(0, 0)$ and $(1, 0)$:

$$\begin{cases} \frac{d^2 s_l(0)}{dt^2} = -\frac{\partial g(0, 0)}{\partial t} - \frac{\partial b(0, 0, q_0(0))}{\partial t} + \left(\mathbb{L}_{x, \varepsilon} - \frac{\partial b(x, t, q_0)}{\partial y} \right) \left(-g + \mathbb{L}_{x, \varepsilon} q_0 - b(x, t, q_0) \right) (0, 0), \\ \frac{d^2 s_r(0)}{dt^2} = -\frac{\partial g(1, 0)}{\partial t} - \frac{\partial b(1, 0, q_0(1))}{\partial t} + \left(\mathbb{L}_{x, \varepsilon} - \frac{\partial b(x, t, q_0)}{\partial y} \right) \left(-g + \mathbb{L}_{x, \varepsilon} q_0 - b(x, t, q_0) \right) (1, 0). \end{cases} \quad (7.7)$$

The above compatibility conditions are derived from [Chapter 5, §6] of the book [65] by Ladyzenskaja et al. The compatibility conditions at the transition point $(d, 0)$ follows similarly. We set $\mathbb{T}_\varepsilon y(x, t) = \mathbb{L}_{x, \varepsilon} y(x, t) - \frac{\partial y(x, t)}{\partial t} - b(x, t, y(x, t))$.

The layout of the rest of this chapter is given as follows. In Section 7.2, a comparison principle as well as some a-priori bounds of the analytical solution and its derivatives are presented via decomposition of the solution (into the smooth and the layer components) and their derivatives are also derived. In Section 7.3, we construct the fully-implicit FMM given in (7.29) and establish ε -uniform convergence of the proposed method (7.29). Error analysis of the proposed method is provided in Section 7.4. Finally, numerical experiments are carried out in Section 7.5, to demonstrate the accuracy and the efficiency of the proposed FMM, which also include

comparison of the proposed numerical method along with the fully-implicit upwind method. The conclusion of this chapter is provided in Section 7.6.

7.2 The analytical solution of continuous problem

To discuss about existence of the solution $y(x, t)$ of the nonlinear IBVP (7.1)-(7.4), we use the method of upper and lower solutions.

Definition 7.1. A function $u \in \mathcal{C}^0(\overline{\mathfrak{D}}) \cap \mathcal{C}^2(\mathfrak{D}^- \cup \mathfrak{D}^+)$ is called a lower solution of the IBVP (7.1)-(7.4) if

$$\begin{cases} u(x, 0) \leq y(x, 0), & x \in \overline{\Omega}, \\ \mathbb{L}_{x,\varepsilon} u(x, t) - \frac{\partial u(x, t)}{\partial t} - b(x, t, u(x, t)) \geq g(x, t), & (x, t) \in \mathfrak{D}^- \cup \mathfrak{D}^+, \\ \frac{\partial u(\mathfrak{d}^+, t)}{\partial x} \geq \frac{\partial u(\mathfrak{d}^-, t)}{\partial x}, \\ u(0, t) \leq y(0, t), \quad u(1, t) \leq y(1, t), & t \in (0, T]. \end{cases} \quad (7.8)$$

Similarly, $v \in \mathcal{C}^0(\overline{\mathfrak{D}}) \cap \mathcal{C}^2(\mathfrak{D}^- \cup \mathfrak{D}^+)$ is called an upper solution of the IBVP (7.1)-(7.4) if

$$\begin{cases} v(x, 0) \geq y(x, 0), & x \in \overline{\Omega}, \\ \mathbb{L}_{x,\varepsilon} v(x, t) - \frac{\partial v(x, t)}{\partial t} - b(x, t, v(x, t)) \leq g(x, t), & (x, t) \in \mathfrak{D}^- \cup \mathfrak{D}^+, \\ \frac{\partial v(\mathfrak{d}^+, t)}{\partial x} \leq \frac{\partial v(\mathfrak{d}^-, t)}{\partial x}, \\ v(0, t) \geq y(0, t), \quad v(1, t) \geq y(1, t), & t \in (0, T]. \end{cases} \quad (7.9)$$

Lemma 7.1 ([92]). *Let there exist two functions $u, v \in \mathcal{C}^0(\overline{\mathfrak{D}}) \cap \mathcal{C}^2(\mathfrak{D}^- \cup \mathfrak{D}^+)$ such that $v(x, t) \geq u(x, t)$, $\forall (x, t) \in \overline{\mathfrak{D}}$, which are lower and upper solutions for the IBVP (7.1)-(7.4), respectively. Then there exist a solution y of the IBVP (7.1)-(7.4) such that*

$$u(x, t) \leq y(x, t) \leq v(x, t), \quad \forall (x, t) \in \overline{\mathfrak{D}}.$$

Hence, to prove existence of the analytical solution, we need to construct a lower and an upper solutions.

Theorem 7.1. *Assume that function b satisfies (7.4). Then, the nonlinear IBVP (7.1)-(7.4) has a solution $y(x, t)$ in $\overline{\mathfrak{D}}$ satisfying*

$$\|y\|_{\overline{\mathfrak{D}}} \leq \frac{K}{\beta},$$

where $K = \max_{(x,t) \in \overline{\mathfrak{D}}} \{|g(x, t) + b(x, t, 0)|, \beta \|y\|_{\partial \mathfrak{D}}\}$.

Proof. Define $(x, t) \in \overline{\mathfrak{D}}$, let $u(x, t) = -K/\beta$ and $v(x, t) = K/\beta$. Then $u(x, 0) \leq y(x, 0) \leq v(x, 0)$ and $u(x, t) \leq y(x, t) \leq v(x, t)$ on $\partial \mathfrak{D}$. We obtain

$$\mathbb{L}_{x,\varepsilon}(-K/\beta) - \frac{\partial(-K/\beta)}{\partial t} - b(x, t, (-K/\beta)) + b(x, t, 0) \geq K \geq g(x, t) + b(x, t, 0), \quad (x, t) \in \mathfrak{D}^- \cup \mathfrak{D}^+,$$

and similarly we obtain

$$\mathbb{L}_{x,\varepsilon}(K/\beta) - \frac{\partial(K/\beta)}{\partial t} - b(x, t, (K/\beta)) + b(x, t, 0) \leq -K \leq g(x, t) + b(x, t, 0), \quad (x, t) \in \mathfrak{D}^- \cup \mathfrak{D}^+,$$

further, we have at the point of discontinuity (d, t) :

$$\left[\frac{\partial}{\partial x}(-K/\beta) \right](d, t) = 0, \quad \left[\frac{\partial}{\partial x}(K/\beta) \right](d, t) = 0.$$

Hence, u and v are lower and upper solution with $u(x, t) \leq v(x, t), \forall (x, t) \in \overline{\mathfrak{D}}$. By the previous theorem there exist a solution to the IBVP (7.1)-(7.4) and

$$u(x, t) \leq y(x, t) \leq v(x, t), \forall (x, t) \in \overline{\mathfrak{D}}.$$

■

Lemma 7.2 (Comparison Principle). *Let the functions $v, w \in \mathcal{C}^0(\overline{\mathfrak{D}}) \cap \mathcal{C}^2(\mathfrak{D}^- \cup \mathfrak{D}^+)$ be such that $v \leq w$ on $\partial\mathfrak{D}$, $\left[\frac{\partial v}{\partial t} \right](d, t) \geq \left[\frac{\partial w}{\partial t} \right](d, t)$ and $\mathbb{T}_\varepsilon v \geq \mathbb{T}_\varepsilon w$ in $\mathfrak{D}^- \cup \mathfrak{D}^+$. Then, it implies that $v \leq w$ on $\overline{\mathfrak{D}}$.*

Proof: Here, we use method of contradiction. Firstly, we suppose that there exists (x^*, t^*) in $\overline{\mathfrak{D}}$ such that $v(x^*, t^*) > w(x^*, t^*)$. Since, $v - w \in \mathcal{C}^0(\overline{\mathfrak{D}})$, without loss of generality, we assume that $v - w$ takes it positive maximum at (x^*, t^*) . Now, in conformity with the hypothesis of the comparison principle, $v - w \leq 0$ on $\partial\mathfrak{D} \implies (x^*, t^*) \notin \partial\mathfrak{D}$. Therefore, we derive

$$\begin{aligned} (\mathbb{T}_\varepsilon v - \mathbb{T}_\varepsilon w)(x^*, t^*) &= \frac{\partial(v - w)(x^*, t^*)}{\partial t} + \mathbb{L}_{x,\varepsilon}(v - w)(x^*, t^*) - b(x^*, t^*, v) + b(x^*, t^*, w), \\ &\leq - \left(\int_0^1 \frac{b(x^*, t^*, w + \xi(v - w))}{\partial y} d\xi \right) (v - w)(x^*, t^*). \end{aligned} \quad (7.10)$$

Thus, from the assumption (7.4), we have $\mathbb{T}_\varepsilon v(x^*, t^*) < \mathbb{T}_\varepsilon w(x^*, t^*)$ and this contradicts the hypothesis that $\mathbb{T}_\varepsilon v(x, t) \geq \mathbb{T}_\varepsilon w(x, t)$, for all $(x, t) \in \mathfrak{D}^- \cup \mathfrak{D}^+$. Next, the only remaining possibility is that $(x^*, t^*) = (d, t^*)$. Since, at the point (d, t^*) the function $v - w$ takes its maximum value, then $\frac{\partial(v-w)(d^-, t^*)}{\partial x} \geq 0$ and $\frac{\partial(v-w)(d^+, t^*)}{\partial x} \leq 0$, which implies that $\left[\frac{\partial(v-w)}{\partial x} \right](d, t^*) \geq 0$. This completes the proof. ■

The following result follows from Theorem 7.2.

Corollary 7.1. *Let the function $\Phi \in \mathcal{C}^0(\overline{\mathfrak{D}}) \cap \mathcal{C}^2(\mathfrak{D}^- \cup \mathfrak{D}^+)$. For any given functions $v, w \in \mathcal{C}^0(\overline{\mathfrak{D}})$, the differential operator $\tilde{\mathbb{T}}_{\varepsilon, (v, w)}$ defined by*

$$\tilde{\mathbb{T}}_{\varepsilon, (v, w)}\Phi = \mathbb{L}_{x,\varepsilon}\Phi - \left(\int_0^1 \frac{\partial b(x, t, w(x, t) + \xi(v - w)(x, t))}{\partial y} d\xi \right) \Phi - \frac{\partial \Phi}{\partial t},$$

satisfies the maximum principle, i.e., if $\Phi \leq 0$ on $\partial\mathfrak{D}$, $\left[\frac{\partial \Phi}{\partial x} \right](d, t) \geq 0$ and $\tilde{\mathbb{T}}_{\varepsilon, (v, w)}\Phi \geq 0$ in $\mathfrak{D}^- \cup \mathfrak{D}^+$, then it implies that $\Phi \leq 0$ on $\overline{\mathfrak{D}}$.

Corollary 7.1 is used to deduce the following ε -uniform stability result.

Lemma 7.3 (Stability). *Let the functions $v, w \in \mathcal{C}^0(\overline{\mathfrak{D}}) \cap \mathcal{C}^2(\mathfrak{D}^- \cup \mathfrak{D}^+)$, then it satisfies*

$$\|v - w\|_{\overline{\mathfrak{D}}} \leq \|v - w\|_{\partial\mathfrak{D}} + \frac{1}{\beta} \|\mathbb{T}_\varepsilon v - \mathbb{T}_\varepsilon w\|_{\overline{\mathfrak{D}^- \cup \mathfrak{D}^+}}. \quad (7.11)$$

Proof. Consider the following functions

$$\Phi^\pm(x, t) = -\|v - w\|_{\partial\mathfrak{D}} - \frac{1}{\beta} \|\mathbb{T}_\varepsilon v - \mathbb{T}_\varepsilon w\|_{\mathfrak{D}} \pm (v - w)(x, t), \text{ in } \overline{\mathfrak{D}}.$$

Note that $\Phi^\pm(x, t) \leq 0$, $(x, t) \in \partial\mathfrak{D}$, and

$$\begin{aligned} \tilde{\mathbb{T}}_{\varepsilon, (v, w)} \Phi^\pm(x, t) &\geq \left(\int_0^1 \frac{\partial b(x, t, w + \xi(v - w))}{\partial y} d\xi \right) \left(\frac{1}{\beta} \|\mathbb{T}_\varepsilon v - \mathbb{T}_\varepsilon w\|_{\mathfrak{D}} \right) \pm (\mathbb{T}_\varepsilon v - \mathbb{T}_\varepsilon w)(x, t), \\ &\geq 0, \end{aligned}$$

and $[\frac{\partial \Phi^\pm}{\partial x}](\mathfrak{d}, t) = \pm [\frac{\partial (v-w)}{\partial x}](\mathfrak{d}, t) \geq 0$. The maximum principle in Corollary 7.1 implies that $\Phi^\pm(x, t) \leq 0$ for all $(x, t) \in \overline{\mathfrak{D}}$, from which the result follows immediately. \blacksquare

We now consider the decomposition of the solution $y = p + q$ into the smooth component p and the layer component q . Here, the smooth component p is decomposed in the following form

$$p = p_0 + \varepsilon p_1 + \varepsilon^2 p_2, \text{ in } \mathfrak{D}, \quad (7.12)$$

where the functions p_0, p_1 and p_2 , receptively, satisfy the following problems:

$$\begin{cases} a(x) \frac{\partial p_0}{\partial x} - b(x, t, p_0) - \frac{\partial p_0}{\partial t} = g, & \text{in } \mathfrak{D}^- \cup \mathfrak{D}^+, \\ p_0(x, 0) = q_0(x), \quad x \in \overline{\Omega}, \quad p_0(1, t) = p(1, t), \quad t \in (0, T], \end{cases} \quad (7.13)$$

$$\begin{cases} a(x) \frac{\partial p_1}{\partial x} - \frac{1}{\varepsilon} [b(x, t, p_0 + \varepsilon p_1) - b(x, t, p_0)] - \frac{\partial p_1}{\partial t} = -\frac{\partial^2 p_0}{\partial x^2}, & \text{in } \mathfrak{D}^- \cup \mathfrak{D}^+, \\ p_1(x, 0) = 0, \quad x \in \overline{\Omega}, \quad p_1(1, t) = 0, \quad t \in (0, T], \end{cases} \quad (7.14)$$

and

$$\begin{cases} \mathbb{L}_{x, \varepsilon} p_2 - \frac{1}{\varepsilon^2} [b(x, t, p) - b(x, t, p_0 + \varepsilon p_1)] - \frac{\partial p_2}{\partial t} = -\frac{\partial^2 p_1}{\partial x^2}, & \text{in } \mathfrak{D}^- \cup \mathfrak{D}^+, \\ p_2(x, 0) = 0, \quad x \in \overline{\Omega}, \quad p_2(0, t) = 0, \quad p_2(1, t) = 0, \quad p_2(\mathfrak{d}, t) = 0, \quad t \in (0, T]. \end{cases} \quad (7.15)$$

Thus, the smooth component p satisfies that

$$\begin{cases} \mathbb{T}_\varepsilon p = g, & \text{in } \mathfrak{D}^- \cup \mathfrak{D}^+, \\ p(x, 0) = q_0(x), \quad x \in \overline{\Omega}, \\ p(0, t) = p_0(0, t) + \varepsilon p_1(0, t), \quad t \in (0, T], \\ p(\mathfrak{d}, t) = p_0(\mathfrak{d}, t) + \varepsilon p_1(\mathfrak{d}, t), \quad p(1, t) = s_r(t), \quad t \in (0, T]. \end{cases} \quad (7.16)$$

Theorem 7.2. *The smooth component p and its derivatives satisfy that*

$$\left| \frac{\partial^{l+k} p(x, t)}{\partial x^l \partial t^k} \right| \leq C \left(1 + \varepsilon^{2-l} \right), \quad (x, t) \in \overline{\mathfrak{D}}^- \cup \overline{\mathfrak{D}}^+, \quad (7.17)$$

$\forall l, k \in \mathbb{N} \cup \{0\}$, satisfying $0 \leq l + k \leq 3$.

Proof: We obtain the bounds (7.17) for the smooth component p , by deriving the corresponding bounds for the functions p_i , $i = 0, 1, 2$. At first, we consider the sub-region $\overline{\mathfrak{D}}^+$ and we define the functions $p_i(x, t)$, $(x, t) \in \overline{\mathfrak{D}}^+$ as the restriction to $\overline{\mathfrak{D}}^+$ of the function $p_i^e(x, t)$, $(x, t) \in \overline{\mathfrak{D}}^{e+}$, i.e., $p_i(x, t) = p_i^e(x, t)$, $(x, t) \in \overline{\mathfrak{D}}^+$. Here, we choose the extended domain $\mathfrak{D}^{e+} = \Omega^{e+} \times (0, T]$, where $\Omega^{e+} = (-1, 1)$ such that $\overline{\mathfrak{D}}^{e+} = [-1, 1] \times [0, T] \supset \overline{\mathfrak{D}}^+$. Here, we consider a^e , b^e , g^e , q_0^e as the smooth extension of the functions a , b , g , q_0 on their respective extended domains.

The function p_0^e is the solution of the following problem:

$$\begin{cases} a^e(x) \frac{\partial p_0^e}{\partial x} - b^e(x, t, p_0^e(x, t)) - \frac{\partial p_0^e}{\partial t} = g^e(x, t), & (x, t) \in \mathfrak{D}^{e+}, \\ p_0^e(x, 0) = q_0^e(x), & x \in \overline{\Omega}^{e+} = [-1, 1], \quad p_0^e(1, t) = s_r(t), \quad t \in (0, T]. \end{cases} \quad (7.18)$$

The function p_0^e is independent of ε . Henceforth, assuming sufficient smoothness on the data associated with the IVP (7.18) and imposing necessary compatibility conditions at $(-1, 0)$, which can be obtained by extending the result of Bobisud [4] for the existence of higher order derivatives of p_0^e , one can obtain that

$$\left| \frac{\partial^{l+k} p_0^e(x, t)}{\partial x^l \partial t^k} \right| \leq C, \quad (x, t) \in \overline{\mathfrak{D}}^{e+}, \text{ for } 0 \leq l + k \leq 3. \quad (7.19)$$

Again, the IVP (7.14) can be rewritten in the following form:

$$\begin{cases} a^e(x) \frac{\partial p_1^e}{\partial x} - \int_0^1 \frac{\partial b^e(x, t, p_0^e + \xi \varepsilon p_1^e)}{\partial y} d\xi p_1^e - \frac{\partial p_1^e}{\partial t} = -\frac{\partial^2 p_0^e}{\partial x^2}, & \text{in } \mathfrak{D}^{e+}, \\ p_1^e(x, 0) = 0, & x \in \overline{\Omega}^{e+}, \quad p_1^e(1, t) = 0, \quad t \in (0, T]. \end{cases} \quad (7.20)$$

Henceforth, applying the above arguments to (7.20), one can get

$$\left| \frac{\partial^{l+k} p_1^e(x, t)}{\partial x^l \partial t^k} \right| \leq C, \quad (x, t) \in \overline{\mathfrak{D}}^{e+}, \text{ for } 0 \leq l + k \leq 3. \quad (7.21)$$

Further, the IBVP (7.15) can be rewritten in the following form:

$$\begin{cases} \mathbb{L}_{x, \varepsilon} p_2^e - \left[\int_0^1 \frac{\partial b^e(x, t, p_0^e + \varepsilon p_1^e + \varepsilon^2 \xi p_2^e)}{\partial y} d\xi \right] - \frac{\partial p_2^e}{\partial t} = -\frac{\partial^2 p_1^e}{\partial x^2}, & \text{in } \mathfrak{D}^{e+}, \\ p_2^e(x, 0) = 0, & x \in \overline{\Omega}^{e+}, \quad p_2^e(-1, t) = 0, \quad p_2^e(1, t) = 0, \quad t \in (0, T], \end{cases} \quad (7.22)$$

where $\mathbb{L}_{x, \varepsilon} \equiv \varepsilon \frac{\partial^2}{\partial x^2} + a^e(x) \frac{\partial}{\partial x}$. The IBVP (7.22) is similar to the linearized form of the IBVP (4.1) and

henceforth, applying the approach of [Chapter 4, Theorem 4.1] analogously to the function p_2^ε , one can have

$$\left| \frac{\partial^{j+k} p_2^\varepsilon(x, t)}{\partial x^j \partial t^k} \right| \leq C\varepsilon^{-l}, \quad (x, t) \in \overline{\mathfrak{D}}^{e+}, \text{ for } 0 \leq l + k \leq 3.$$

Next, the desired result (7.17) is obtained on the domain $\overline{\mathfrak{D}}^{e+}$ by invoking the bounds on p_i^ε , $i = 0, 1, 2$ to the decomposition $p^\varepsilon = p_0^\varepsilon + \varepsilon p_1^\varepsilon + \varepsilon^2 p_2^\varepsilon$. In the same way, the desired result (7.17) is obtained on the domain $\overline{\mathfrak{D}}^{e-}$. ■

We now define the layer component q as the solution of the following nonlinear IBVP:

$$\begin{cases} \mathbb{L}_{x,\varepsilon} q(x, t) - [b(x, t, y(x, t)) - b(x, t, p(x, t))] - \frac{\partial q(x, t)}{\partial t} = 0, & \text{in } \mathfrak{D}^- \cup \mathfrak{D}^+, \\ q(x, 0) = 0, & x \in \overline{\Omega}, \\ q(0, t) = y(0, t) - p(0, t), \quad q(1, t) = 0, & t \in (0, T], \\ \left[\frac{\partial q}{\partial x} \right](\mathfrak{d}, t) = - \left[\frac{\partial p}{\partial x} \right](\mathfrak{d}, t), & t \in (0, T]. \end{cases} \quad (7.23)$$

We can further decompose q as

$$q = q_1 + q_2,$$

where $q_1 \in \mathcal{C}^{2+\gamma}(\overline{\mathfrak{D}})$ is the boundary layer function satisfying $q_1(x, t) = 0$, $(x, t) \in \overline{\mathfrak{D}}^+$ and

$$\begin{cases} \mathbb{L}_{x,\varepsilon} q_1(x, t) - [b(x, t, p(x, t) + q_1(x, t)) - b(x, t, p(x, t))] - \frac{\partial q_1(x, t)}{\partial t} = 0, & \text{in } \mathfrak{D}^-, \\ q_1(x, 0) = 0, & x \in \overline{\Omega}^-, \\ q_1(0, t) = y(0, t) - p(0, t), \quad q_1(\mathfrak{d}, t) = 0, & t \in (0, T], \end{cases} \quad (7.24)$$

and hence $q_2 \in \mathcal{C}^0(\overline{\mathfrak{D}})$ is the interior layer function satisfying

$$\begin{cases} \mathbb{L}_{x,\varepsilon} q_2(x, t) - [b(x, t, y(x, t)) - b(x, t, p(x, t) + q_1(x, t))] - \frac{\partial q_2(x, t)}{\partial t} = 0, & \text{in } \mathfrak{D}^-, \\ \mathbb{L}_{x,\varepsilon} q_2(x, t) - [b(x, t, p(x, t) + q_2(x, t)) - b(x, t, p(x, t))] - \frac{\partial q_2(x, t)}{\partial t} = 0, & \text{in } \mathfrak{D}^+, \\ q_2(x, 0) = 0, & x \in \overline{\Omega}, \\ q_2(0, t) = 0, \quad q_2(1, t) = 0, & t \in (0, T], \\ \left[\frac{\partial q_2}{\partial x} \right](\mathfrak{d}, t) = - \left[\frac{\partial p}{\partial x} \right](\mathfrak{d}, t), & t \in (0, T]. \end{cases} \quad (7.25)$$

Theorem 7.3. $\forall l, k \in \mathbb{N} \cup \{0\}$ satisfying $0 \leq l + k \leq 3$, the boundary layer component q_1 defined in (7.24)

and the interior layer component q_2 defined in (7.25), respectively satisfy the following bounds:

$$\begin{cases} \left| \frac{\partial^{l+k} q_1}{\partial x^l \partial t^k} \right| \leq C \left(\varepsilon^{-l} \exp \left(-\frac{\mathfrak{m}x}{\varepsilon} \right) \right), & (x, t) \in \overline{\mathfrak{D}}^-, \\ \left| \frac{\partial^{l+k} q_2}{\partial x^l \partial t^k} \right| \leq C \left(\varepsilon^{1-l} \exp \left(-\frac{\mathfrak{m}x}{\varepsilon} \right) \right), & (x, t) \in \overline{\mathfrak{D}}^-, \\ \left| \frac{\partial^{l+k} q_2}{\partial x^l \partial t^k} \right| \leq C \left(\varepsilon^{1-l} \exp \left(-\frac{\mathfrak{m}(x-\mathfrak{d})}{\varepsilon} \right) \right), & (x, t) \in \overline{\mathfrak{D}}^+. \end{cases} \quad (7.26)$$

Proof: The IBVP (7.24) can be rewritten in the following form:

$$\begin{cases} \mathbb{L}_{x,\varepsilon} q_1 - \left[\int_0^1 \frac{\partial b(x, t, p + \xi((p + q_1) - p))}{\partial y} d\xi \right] q_1 - \frac{\partial q_1}{\partial t} = 0, & (x, t) \in \mathfrak{D}^-, \\ q_1(x, 0) = 0, & x \in \overline{\Omega}^-, \\ q_1(0, t) = y(0, t) - p(0, t), & q_1(\mathfrak{d}, t) = 0, \quad t \in (0, T]. \end{cases} \quad (7.27)$$

Here, we introduce a differential operator $\widetilde{\mathbb{T}}_{\varepsilon, (p+q_1, p)}$ such that

$$\widetilde{\mathbb{T}}_{\varepsilon, (p+q_1, p)} q_1 = \mathbb{L}_{x,\varepsilon} q_1 - \left[\int_0^1 \frac{\partial b(x, t, p + \xi q_1)}{\partial y} d\xi \right] q_1 - \frac{\partial q_1}{\partial t}.$$

Now, we choose the functions

$$\Psi^\pm(x, t) = -C \exp(-\mathfrak{m}x/\varepsilon) \pm q_1(x, t), \quad (x, t) \in \overline{\mathfrak{D}}^-,$$

for sufficiently large C . Note that

$$\Psi^\pm(x, t) \leq 0, \quad (x, t) \in \partial \mathfrak{D}^-,$$

and

$$\widetilde{\mathbb{T}}_{\varepsilon, (p+q_1, p)} \Psi^\pm(x, t) \geq 0, \quad (x, t) \in \mathfrak{D}^-.$$

Since $\widetilde{\mathbb{T}}_{\varepsilon, (p+q_1, p)}$ satisfies the maximum principle, we have

$$\Psi^\pm(x, t) \leq 0 \implies |q_1(x, t)| \leq C \exp \left(-\frac{\mathfrak{m}x}{\varepsilon} \right), \quad (x, t) \in \overline{\mathfrak{D}}^-.$$

The bounds on the derivatives of q_1 are derived from the argument presented in [99, Chapter 2]. Next, we write

the IBVP (7.25), in the following form

$$\left\{ \begin{array}{l} \mathbb{L}_{x,\varepsilon} q_2 - \left[\int_0^1 \frac{\partial b(x, t, p + q_1 + \xi(y - (p + q_1)))}{\partial y} d\xi \right] q_2 - \frac{\partial q_2}{\partial t} = 0, \quad (x, t) \in \mathfrak{D}^-, \\ \mathbb{L}_{x,\varepsilon} q_2 - \left[\int_0^1 \frac{\partial b(x, t, p + \xi q_2)}{\partial y} d\xi \right] q_2 - \frac{\partial q_2}{\partial t} = 0, \quad (x, t) \in \mathfrak{D}^+, \\ q_2(x, 0) = 0, \quad x \in \bar{\Omega}, \\ q_2(0, t) = 0, \quad q_2(1, t) = 0, \quad t \in (0, T], \\ \left[\frac{\partial q_2}{\partial x} \right](0, t) = - \left[\frac{\partial p}{\partial x} \right](d, t), \quad t \in (0, T]. \end{array} \right. \quad (7.28)$$

The bounds on q_2 and its derivatives can be derived from the arguments presented in [Chapter 6, Theorem 6.4], and thus the proof is complete. \blacksquare

7.3 The discrete solution of continuous problem

The goal of this section is to introduce the layer-adapted mesh and to provide description of the numerical method investigated in this chapter.

Here, we choose $N(\geq 8)$ as an even positive integer. Now, to discretize the domain $\bar{\mathfrak{D}} = \bar{\Omega} \times [0, T]$, we construct a rectangular mesh $\bar{\mathfrak{D}}^{N, \Delta t} = \bar{\Omega}^N \times \Lambda^{\Delta t}$, where $\Lambda^{\Delta t}$ denotes the equidistant mesh on the temporal domain $[0, T]$ such that $\Lambda^{\Delta t} = \{t_n = n\Delta t, n = 0, \dots, M, \Delta t = T/M\}$, whereas $\bar{\Omega}^N = \{x_j\}_{j=0}^N$ denotes the piecewise-uniform Shishkin mesh on the spatial domain $\bar{\Omega}$ as depicted in Fig 7.1. The Shishkin mesh is condensed near $x = 0$ and in the vicinity of the right side of $x = d$. To construct $\bar{\Omega}^N$, $\bar{\Omega}$ is divided into four sub-intervals as

$$\bar{\Omega} = [0, \eta_1] \cup [\eta_1, d] \cup [d, d + \eta_2] \cup [d + \eta_2, 1],$$

$$\text{where } \eta_1 = \min \left\{ \frac{d}{2}, \eta_0 \varepsilon \ln N \right\}, \quad \eta_2 = \min \left\{ \frac{1-d}{2}, \eta_0 \varepsilon \ln N \right\}, \quad \eta_0 \text{ is a positive constant,}$$

and in each sub-interval an equidistant mesh with $N/4$ mesh intervals are placed. Let $h_j = x_j - x_{j-1}$, $j = 1, \dots, N$, with $\hat{h}_j = h_j + h_{j+1}$, $j = 1, \dots, N-1$.

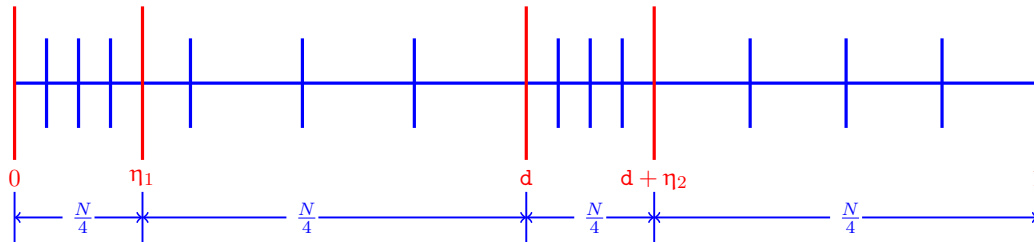


Figure 7.1: Standard Shishkin mesh in the spatial direction

We further denote the mesh width h_j as follows: $h_j = h_1 = \frac{4\eta_1}{N}$, for $j = 1, \dots, N/4$; $h_j = H_1 = \frac{4(d - \eta_1)}{N}$,

for $j = N/4 + 1, \dots, N/2$; $h_j = h_2 = \frac{4\eta_2}{N}$, for $j = N/2 + 1, \dots, 3N/4$; and $h_j = H_2 = \frac{4(1-d-\eta_2)}{N}$, for $j = 3N/4 + 1, \dots, N$.

Here, we proposed to approximate the nonlinear IBVP (7.1)-(7.4) by utilizing the Crank-Nicolson method to discretize in time and the standard upwind finite difference scheme to discretize in space. The nonlinear finite difference scheme takes the following form:

$$\left\{ \begin{array}{l} Y_j^0 = q_0(x_j), \quad 0 \leq j \leq N, \\ \mathbb{L}_{x,\varepsilon}^N \frac{Y_j^{n+1} + Y_j^n}{2} - b\left(x_j, t_{n+1/2}, \frac{Y_j^{n+1} + Y_j^n}{2}\right) - D_t^- Y_j^{n+1} = \frac{g(x_j, t_{n+1}) + g(x_j, t_n)}{2}, \\ \hspace{15em} \text{for } j \neq N/2, \quad 1 \leq j \leq N-1, \\ D_x^- Y_j^{n+1} - D_x^+ Y_j^{n+1} = 0, \quad \text{for } j = N/2, \\ Y_0^{n+1} = y(0, t_{n+1}), \quad Y_N^{n+1} = y(1, t_{n+1}), \quad \text{for } n = 0, 1, \dots, M-1, \end{array} \right. \quad (7.29)$$

where $\mathbb{L}_{x,\varepsilon}^N \frac{Y_j^{n+1} + Y_j^n}{2} = \left(\varepsilon D_x^+ D_x^- + a(x_j) D_x^+ \right) \frac{Y_j^{n+1} + Y_j^n}{2}$. To discuss the stability of the proposed nonlinear scheme (7.29), we rewrite the nonlinear scheme (7.29) in the following form:

$$\left\{ \begin{array}{l} Y_j^0 = q_0(x_j), \quad 0 \leq j \leq N, \\ \mathbb{T}_\varepsilon^{N,\Delta t} Y_j^{n+1} = \mathbb{G}_j^{n+1}, \quad (x_j, t_n) \in \mathfrak{D}^{N,\Delta t}, \\ Y_0^{n+1} = y(0, t_{n+1}), \quad Y_N^{n+1} = y(1, t_{n+1}), \quad \text{for } n = 0, 1, \dots, M-1, \end{array} \right. \quad (7.30)$$

where

$$\mathbb{T}_\varepsilon^{N,\Delta t} Y_j^{n+1} = \left\{ \begin{array}{l} \mathbb{L}_{x,\varepsilon}^N \frac{Y_j^{n+1} + Y_j^n}{2} - b\left(x_j, t_{n+1/2}, \frac{Y_j^{n+1} + Y_j^n}{2}\right) - D_t^- Y_j^{n+1}, \\ \hspace{15em} \text{for } j \neq N/2, \quad 1 \leq j \leq N-1, \\ D_x^- Y_j^{n+1} - D_x^+ Y_j^{n+1}, \quad \text{for } j = N/2, \end{array} \right.$$

and the right-side vector \mathbb{G}^{n+1} is given by

$$\mathbb{G}_j^{n+1} = \left\{ \begin{array}{l} \frac{g(x_j, t_{n+1}) + g(x_j, t_n)}{2}, \quad \text{for } j \neq N/2, \quad 1 \leq j \leq N-1, \\ 0, \quad \text{for } j = N/2. \end{array} \right.$$

Lemma 7.4 (Discrete comparison principle). *Assume that the following condition holds:*

$$\frac{2}{\Delta t} \geq \left[\frac{2\varepsilon}{h_j h_{j+1}} + \frac{a(x_j)}{h_{j+1}} + \int_0^1 \frac{\partial b\left(x_j, t_{n+1/2}, Z_j^{*,n+1/2}(\xi)\right)}{\partial y} d\xi \right]. \quad (7.31)$$

Then, if two arbitrary mesh functions V and W defined on $\overline{\mathfrak{D}}^{N,\Delta t}$ satisfy that $V \leq W$ on $\partial \mathfrak{D}^{N,\Delta t}$, and $\mathbb{T}_\varepsilon^{N,\Delta t} V \geq \mathbb{T}_\varepsilon^{N,\Delta t} W$ in $\mathfrak{D}^{N,\Delta t}$, it implies that $V \leq W$ on $\overline{\mathfrak{D}}^{N,\Delta t}$.

Proof: Let $\omega_j^n \leq 0$, for all j and n . Then, inconformity with the hypothesis of the discrete comparison principle,

we assume that $V_j^0 - W_j^0 = \omega_j^0$ for $0 \leq j \leq N$ and consider the following system

$$\begin{cases} -[\mathbb{T}_\varepsilon^{N,\Delta t} V_j^{n+1} - \mathbb{T}_\varepsilon^{N,\Delta t} W_j^{n+1}] = \omega_j^{n+1}, & \text{for } 1 \leq j \leq N-1, \\ V_0^{n+1} - W_0^{n+1} = \omega_0^{n+1}, \quad V_N^{n+1} - W_N^{n+1} = \omega_N^{n+1}, & \text{for } n = 0, 1, \dots, M-1. \end{cases} \quad (7.32)$$

Now, let $Z_j^n = V_j^n - W_j^n$ for all n . Then, we have

$$\begin{aligned} & \mathbb{T}_\varepsilon^{N,\Delta t} V_j^{n+1} - \mathbb{T}_\varepsilon^{N,\Delta t} W_j^{n+1} \\ &= \begin{cases} \mathbb{L}_{x,\varepsilon}^N \frac{Z_j^{n+1} + Z_j^n}{2} - \left[\int_0^1 \frac{\partial b(x_j, t_{n+1/2}, Z_j^{*,n+1/2}(\xi))}{\partial y} d\xi \right] \frac{Z_j^{n+1} + Z_j^n}{2} - D_t^- Z_j^{n+1}, & \text{for } j \neq N/2, 1 \leq j \leq N-1, \\ D_x^- Z_j^{n+1} - D_x^+ Z_j^{n+1}, & \text{for } j = N/2, \end{cases} \end{aligned} \quad (7.33)$$

where $Z_j^{*,n+1/2}(\xi) = \frac{W_j^{n+1} + W_j^n}{2} + \xi \left(\frac{Z_j^{n+1} + Z_j^n}{2} \right)$. For simplifying the proof, we set $Z^n = (Z_0^n, Z_1^n, \dots, Z_N^n)$ and $\omega^n = (\omega_0^n, \omega_1^n, \dots, \omega_N^n)$, for $n = 0, 1, \dots, M$. Here, we can rewrite equation (7.32) in the following form:

$$\mathbf{A}Z^{n+1} - \mathbf{B}Z^n = \omega^{n+1}, \text{ for } n = 0, 1, \dots, M-1. \quad (7.34)$$

Here, the matrix \mathbf{A} is given by $\mathbf{A}_{j,j} = 1$, for $j = 0, N$, and

$$\begin{cases} \mathbf{A}_{j,j-1} = -\frac{1}{2} \frac{2\varepsilon}{h_j(h_j + h_{j-1})}, & \text{for } j \neq N/2, 1 \leq j \leq N-1, \\ \mathbf{A}_{j,j} = \frac{1}{2} \left[+\frac{2\varepsilon}{h_j h_{j+1}} + \frac{a(x_j)}{h_{j+1}} + \int_0^1 \frac{\partial b(x_j, t_{n+1/2}, Z_j^{*,n+1/2}(\xi))}{\partial y} d\xi \right] + \frac{1}{\Delta t}, & \text{for } j \neq N/2, 1 \leq j \leq N-1, \\ \mathbf{A}_{j,j+1} = \frac{-1}{2} \left[\frac{2\varepsilon}{h_{j+1}(h_j + h_{j+1})} + \frac{a(x_j)}{h_{j+1}} \right], & \text{for } j \neq N/2, 1 \leq j \leq N-1, \\ \mathbf{A}_{j,j-1} = -\frac{1}{h_j}, \quad \mathbf{A}_{j,j} = \frac{1}{h_j} + \frac{1}{h_{j+1}}, \quad \mathbf{A}_{j,j+1} = -\frac{1}{h_{j+1}}, & \text{for } j = N/2, \end{cases}$$

and the matrix \mathbf{B} is given by

$$\begin{cases} \mathbf{B}_{j,j-1} = \frac{1}{2} \frac{2\varepsilon}{h_j(h_j + h_{j-1})}, & \text{for } j \neq N/2, 1 \leq j \leq N-1, \\ \mathbf{B}_{j,j} = \frac{1}{2} \left[-\frac{2\varepsilon}{h_j h_{j+1}} - \frac{a(x_j)}{h_{j+1}} - \int_0^1 \frac{\partial b(x_j, t_{n+1/2}, Z_j^{*,n+1/2}(\xi))}{\partial y} d\xi \right] + \frac{1}{\Delta t}, & \text{for } j \neq N/2, 1 \leq j \leq N-1, \\ \mathbf{B}_{j,j+1} = \frac{1}{2} \left[\frac{2\varepsilon}{h_{j+1}(h_j + h_{j+1})} + \frac{a(x_j)}{h_{j+1}} \right], & \text{and } j \neq N/2, 1 \leq j \leq N-1, \\ \mathbf{B}_{j,j-1} = 0, \quad \mathbf{B}_{j,j} = 0, \quad \mathbf{B}_{j,j+1} = 0, & \text{for } j = N/2. \end{cases}$$

One can show that, the matrix \mathbf{A} is an M-matrix and it is straightforward that the matrix $\mathbf{B} \geq 0$ under the assumption (7.31). Therefore, the desire result follows from [99, Lemma 3.12]. \blacksquare

As a consequence of Lemma 7.4, we get

Corollary 7.2. *Let Ψ^{n+1} be any mesh function defined on $\overline{\mathfrak{D}}^{N,\Delta t}$. Then, for any given mesh functions V and W defined on $\overline{\mathfrak{D}}^{N,\Delta t}$ such that $Z = V - W$, the difference operator $\tilde{\mathbb{T}}_{\varepsilon,(V,W)}^{N,\Delta t}$ defined by*

$$\begin{aligned} & \tilde{\mathbb{T}}_{\varepsilon,(V,W)}^{N,\Delta t} \Psi_j^{n+1} \\ &= \begin{cases} \mathbb{L}_{x,\varepsilon}^N \frac{\Psi_j^{n+1} + \Psi_j^n}{2} - \left[\int_0^1 \frac{\partial b(x_j, t_{n+1/2}, Z_j^{*,n+1/2}(\xi))}{\partial y} d\xi \right] \frac{\Psi_j^{n+1} + \Psi_j^n}{2} - D_t^- \Psi_j^{n+1}, \\ \quad \text{for } j \neq N/2, 1 \leq j \leq N-1, \\ D_x^- \Psi_j^{n+1} - D_x^+ \Psi_j^{n+1}, \quad \text{for } j = N/2, \end{cases} \end{aligned} \quad (7.35)$$

satisfies the discrete maximum principle, i.e., if $\Psi \leq 0$ on $\partial \mathfrak{D}^{N,\Delta t}$ and $\tilde{\mathbb{T}}_{\varepsilon,(V,W)}^{N,\Delta t} \Psi_j^{n+1} \geq 0$ in $\mathfrak{D}^{N,\Delta t}$, then it implies that $\Psi \leq 0$ on $\overline{\mathfrak{D}}^{N,\Delta t}$.

Lemma 7.5 (Stability). *Let V and W be two arbitrary mesh functions defined on $\overline{\mathfrak{D}}^{N,\Delta t}$. Then, under the condition (7.31), we have*

$$\|V - W\|_{\overline{\mathfrak{D}}^{N,\Delta t}} \leq \|V - W\|_{\partial \mathfrak{D}^{N,\Delta t}} + \frac{1}{\beta} \|\mathbb{T}_{\varepsilon}^{N,\Delta t} V - \mathbb{T}_{\varepsilon}^{N,\Delta t} W\|_{\overline{\mathfrak{D}}^{N,\Delta t}}. \quad (7.36)$$

Proof. We consider the mesh functions

$$\Psi^{\pm}(x_j, t_{n+1}) = -\|V - W\|_{\partial \mathfrak{D}^{N,\Delta t}} - \frac{1}{\beta} \|\mathbb{T}_{\varepsilon}^{N,\Delta t} V - \mathbb{T}_{\varepsilon}^{N,\Delta t} W\| \pm (V - W).$$

Note that $\Psi^{\pm}(x_j, t_{n+1}) \leq 0$, on $\partial \mathfrak{D}^{N,\Delta t}$ and we have

$$\tilde{\mathbb{T}}_{\varepsilon,(V,W)}^{N,\Delta t} \Psi^{\pm}(x_j, t_{n+1}) \geq 0, \quad \text{in } \mathfrak{D}^{N,\Delta t} \setminus (\mathbf{d}, t_{n+1}),$$

and $D_x^+ \Psi^{\pm}(x_{N/2}, t_{n+1}) - D_x^- \Psi^{\pm}(x_{N/2}, t_{n+1}) = \pm (D_x^+ - D_x^-)(V - W)(x_{N/2}, t_{n+1}) \geq 0$. The discrete maximum principle in Corollary 7.2 implies that $\Psi^{\pm}(x_j, t_{n+1}) \leq 0$, for all $(x_j, t_{n+1}) \in \overline{\mathfrak{D}}^{N,\Delta t}$. The result of which follows immediately. \blacksquare

Remark 7.1. From the discrete comparison principle, one can obtain the existence and uniqueness of the solution to the discrete problem (7.29)(see the Hadamard's Theorem 5.3.10 in [91]).

7.4 Error analysis

We decompose the numerical solution Y into $Y = \mathcal{P} + Q$ where \mathcal{P} and Q are the smooth and layer components of Y , respectively. The function \mathcal{P} is defined to be the solution of

$$\begin{cases} \mathbb{T}_{\varepsilon}^{N,\Delta t} \mathcal{P}_j^{n+1} = \mathbb{G}_j^{n+1}, & \text{in } \mathfrak{D}^{N,\Delta t} \setminus (\mathbf{d}, t), \\ \mathcal{P}_j^0 = p(x_j, 0), \quad \mathcal{P}_0^{n+1} = p(0, t_{n+1}), \\ \mathcal{P}_{N/2}^{n+1} = p(\mathbf{d}, t_{n+1}), \quad \mathcal{P}_N^{n+1} = p(1, t_{n+1}), \quad n = 0, 1, \dots, M-1. \end{cases} \quad (7.37)$$

In the following lemma, we establish the error estimate associated with the smooth component.

Lemma 7.6. *Under the assumption (7.31) of Lemma 7.4, the error associated with smooth component satisfies the following estimate:*

$$|\mathcal{P}_j^{n+1} - p(x_j, t_{n+1})| \leq \begin{cases} C(N^{-1} + (\Delta t)^2)(\mathbf{d} - x_j), & x_j \leq \mathbf{d}, \\ C(N^{-1} + (\Delta t)^2)(1 - x_j), & x_j \geq \mathbf{d}. \end{cases} \quad (7.38)$$

Proof. From the equation (7.9) and (7.37), we have

$$\begin{aligned} \mathbb{L}_{x,\varepsilon}^N \frac{\mathcal{P}_j^{n+1} + \mathcal{P}_j^n}{2} - b\left(x_j, t_{n+1/2}, \frac{\mathcal{P}_j^{n+1} + \mathcal{P}_j^n}{2}\right) - D_t^- \mathcal{P}_j^{n+1} &= \mathbb{L}_{x,\varepsilon} \frac{p(x_j, t_{n+1}) + p(x_j, t_n)}{2} - \\ &b\left(x_j, t_{n+1/2}, p(x_j, t_{n+1/2})\right) - \frac{\partial p(x_j, t_{n+1/2})}{\partial t}, \quad \text{in } \mathfrak{D}^{N,\Delta t} \setminus (\mathbf{d}, t). \end{aligned}$$

Utilizing the derivative bound of p from Theorem 7.2 and the relation

$$b\left(x_j, t_{n+1/2}, p(x_j, t_{n+1/2})\right) = b\left(x_j, t_{n+1/2}, \frac{p(x_j, t_n) + p(x_j, t_{n+1})}{2}\right) + O(\Delta t)^2,$$

the preceding equation can be written as follows:

$$\begin{aligned} \mathbb{L}_{x,\varepsilon}^N \left(\frac{\mathcal{P}_j^{n+1} + \mathcal{P}_j^n}{2} - \frac{p(x_j, t_{n+1}) + p(x_j, t_n)}{2} \right) &- \left[\int_0^1 \frac{\partial b(x_j, t_{n+1/2}, \mathcal{P}_j^{*,n+1/2}(\xi))}{\partial y} d\xi \right] \times \\ &\left(\frac{\mathcal{P}_j^{n+1} + \mathcal{P}_j^n}{2} - \frac{p(x_j, t_{n+1}) + p(x_j, t_n)}{2} \right) - D_t^- (\mathcal{P}_j^{n+1} - p(x_j, t_{n+1})) \\ &= \varepsilon \left(\frac{\partial^2}{\partial x^2} - D_x^+ D_x^- \right) \frac{p(x_j, t_{n+1}) + p(x_j, t_n)}{2} + a(x_j) \left(\frac{\partial}{\partial x} - D_x^+ \right) \frac{p(x_j, t_{n+1}) + p(x_j, t_n)}{2} \\ &- \left(\frac{\partial p(x_j, t_{n+1/2})}{\partial t} - D_t^- p(x_j, t_{n+1}) \right) + O(\Delta t)^2, \end{aligned} \quad (7.39)$$

where $\mathcal{P}_j^{*,n+1/2}(\xi) = \frac{p(x_j, t_{n+1}) + p(x_j, t_n)}{2} + \xi \left(\frac{\mathcal{P}_j^{n+1} + \mathcal{P}_j^n}{2} - \frac{p(x_j, t_{n+1}) + p(x_j, t_n)}{2} \right)$. Now, for any mesh function Ψ we introduce a discrete operator $\mathbb{L}_{\varepsilon, \mathcal{P}^*}^{N,\Delta t}$ given by

$$\mathbb{L}_{\varepsilon, \mathcal{P}^*}^{N,\Delta t} \Psi = \tilde{\mathbb{T}}_{\varepsilon, (p, \mathcal{P})}^{N,\Delta t} \Psi.$$

Afterwards, from (7.39) by using the derivative bounds of $p(x, t)$ given in Theorem 7.2, we obtain bounds of the truncation errors:

$$|\mathbb{L}_{\varepsilon, \mathcal{P}^*}^{N,\Delta t} (\mathcal{P}_j^{n+1} - p(x_j, t_{n+1}))| \leq C[N^{-1} + (\Delta t)^2], \quad \text{in } \mathfrak{D}^{N,\Delta t} \setminus (\mathbf{d}, t). \quad (7.40)$$

Consider the following discrete functions separately:

$$\begin{cases} \Psi^\pm(x_j, t_{n+1}) = -C(N^{-1} + (\Delta t)^2)(\mathbf{d} - x_j) \pm (\mathcal{P}_j^{n+1} - p(x_j, t_{n+1})), & \text{in } [0, \mathbf{d}] \times [0, T], \\ \Psi^\pm(x_j, t_{n+1}) = -C(N^{-1} + (\Delta t)^2)(1 - x_j) \pm (\mathcal{P}_j^{n+1} - p(x_j, t_{n+1})), & \text{in } [\mathbf{d}, 1] \times [0, T], \end{cases} \quad (7.41)$$

and apply Corollary 7.2 for the operator $\mathbb{L}_{\varepsilon, \mathcal{P}^*}^{N, \Delta t}$ together with the truncation error bounds in (7.40), to obtain required estimate (7.38). ■

Now, we define the layer component Q to be the solution of

$$\begin{cases} \mathbb{L}_{x, \varepsilon}^N \frac{Q_j^{n+1} + Q_j^n}{2} - \left[b\left(x_j, t_{n+1/2}, \frac{Y_j^{n+1} + Y_j^n}{2}\right) - b\left(x_j, t_{n+1/2}, \frac{\mathcal{P}_j^{n+1} + \mathcal{P}_j^n}{2}\right) \right] - D_t^- Q_j^{n+1} = 0, \\ \quad \text{in } \mathfrak{D}^{N, \Delta t} \setminus (\mathbf{d}, t_{n+1}), \\ Q_j^0 = q(x_j, 0), \quad Q_0^{n+1} = q(0, t_{n+1}), \\ Q_N^{n+1} = q(1, t_{n+1}), \quad [DQ(\mathbf{d}, t_{n+1})] = -[D\mathcal{P}(\mathbf{d}, t_{n+1})] \quad n = 0, 1, \dots, M-1. \end{cases} \quad (7.42)$$

We define the jump in the discrete derivative of the mesh function Z at the point (\mathbf{d}, t_{n+1}) by

$$[DZ(\mathbf{d}, t_{n+1})] = D_x^+ Z(\mathbf{d}, t_{n+1}) - D_x^- Z(\mathbf{d}, t_{n+1}).$$

Similar to the continuous case, we can further decompose Q as

$$Q = Q_1 + Q_2,$$

where Q_1 (the discrete analogue of the boundary layer function q_1) is defined as the solution of

$$\begin{cases} \mathbb{L}_{x, \varepsilon}^N \frac{Q_{1,j}^{n+1} + Q_{1,j}^n}{2} - \left[b\left(x_j, t_{n+1/2}, \frac{\mathcal{P}_j^{n+1} + \mathcal{P}_j^n}{2} + \frac{Q_{1,j}^{n+1} + Q_{1,j}^n}{2}\right) - b\left(x_j, t_{n+1/2}, \frac{\mathcal{P}_j^{n+1} + \mathcal{P}_j^n}{2}\right) \right] - D_t^- Q_{1,j}^{n+1} = 0, \quad \text{in } \mathfrak{D}^{N, \Delta t} \cap \mathfrak{D}^-, \\ Q_{1,j}^0 = q_1(x_j, 0), \quad 0 \leq j \leq N/2, \\ Q_{1,0}^{n+1} = q_1(0, t_{n+1}), \quad Q_{1,N/2}^{n+1} = q_1(\mathbf{d}, t_{n+1}), \quad n = 0, 1, \dots, M-1, \end{cases} \quad (7.43)$$

with $Q_{1,j}^{n+1} \equiv 0$ on $\overline{\mathfrak{D}^{N, \Delta t}} \cap \overline{\mathfrak{D}^+}$. Here, Q_2 (the discrete analogue of the interior layer function Q_2) satisfies that

$$\begin{cases} \mathbb{L}_{x, \varepsilon}^N \frac{Q_{2,j}^{n+1} + Q_{2,j}^n}{2} - \left[b\left(x_j, t_{n+1/2}, \frac{Y_j^{n+1} + Y_j^n}{2}\right) - b\left(x_j, t_{n+1/2}, \frac{\mathcal{P}_j^{n+1} + \mathcal{P}_j^n}{2} + \frac{Q_{1,j}^{n+1} + Q_{1,j}^n}{2}\right) \right] - D_t^- Q_{2,j}^{n+1} = 0, \quad \text{in } \mathfrak{D}^{N, \Delta t} \cap \mathfrak{D}^-, \\ \mathbb{L}_{x, \varepsilon}^N \frac{Q_{2,j}^{n+1} + Q_{2,j}^n}{2} - \left[b\left(x_j, t_{n+1/2}, \frac{\mathcal{P}_j^{n+1} + \mathcal{P}_j^n}{2} + \frac{Q_{2,j}^{n+1} + Q_{2,j}^n}{2}\right) - b\left(x_j, t_{n+1/2}, \frac{\mathcal{P}_j^{n+1} + \mathcal{P}_j^n}{2}\right) \right] - D_t^- Q_{2,j}^{n+1} = 0, \quad \text{in } \mathfrak{D}^{N, \Delta t} \cap \mathfrak{D}^+, \\ Q_{2,j}^0 = 0, \quad 0 \leq j \leq N, \\ Q_{2,0}^{n+1} = 0, \quad Q_{2,N}^{n+1} = 0, \\ [DQ_2(\mathbf{d}, t_{n+1})] = -[D\mathcal{P}(\mathbf{d}, t_{n+1})] - [DQ_1(\mathbf{d}, t_{n+1})] \quad n = 0, 1, \dots, M-1. \end{cases} \quad (7.44)$$

Lemma 7.7. *Under the assumption (7.31) of Lemma 7.4, the error associated with boundary layer component*

satisfy the following estimate:

$$|Q_{1,j}^{n+1} - q_1(x_j, t_{n+1})| \leq \begin{cases} C(N^{-1} \ln N + (\Delta t)^2), & \text{for } 1 \leq j < N/4, \\ CN^{-1}, & \text{for } N/4 \leq j < N/2. \end{cases} \quad (7.45)$$

Proof. We now consider $\eta = \frac{\varepsilon}{\alpha} \ln N$. At first, consider $N/4 \leq j \leq N/2 - 1$. From the triangle inequality, we have

$$|Q_{1,j}^{n+1} - q_1(x_j, t_{n+1})| \leq |Q_{1,j}^{n+1}| + |q_1(x_j, t_{n+1})|.$$

Using Theorem 7.3 for $N/4 \leq j \leq N/2 - 1$, we have

$$|q_1(x_j, t_{n+1})| \leq C \exp(-\mathfrak{m}x_j/\varepsilon) \leq C \exp(-\mathfrak{m}\eta/\varepsilon) = CN^{-1}.$$

Now, for deriving bound for $Q_{1,j}^{n+1}$, we introduce the mesh function Φ_j^{n+1} , which is the solution of the following discrete problem:

$$\begin{cases} \varepsilon D_x^+ D_x^- \Phi_j^{n+1} + \mathfrak{m} D_x^+ \Phi_j^{n+1} = 0, & \text{for } 1 \leq j \leq N/2 - 1, \\ \Phi_0^{n+1} = 1, \quad \Phi_{N/2}^{n+1} = 0, \end{cases} \quad (7.46)$$

where

$$\begin{cases} \Phi_j^{n+1} \geq 0 \quad \text{and} \quad D_x^+ \Phi_j^{n+1} \leq 0, & \text{for } 1 \leq j \leq N/2 - 1, \\ \Phi_{N/4}^{n+1} \leq CN^{-1}, & \text{for some } C. \end{cases}$$

Here, for any mesh function Ψ , we introduce a discrete operator $\mathbb{L}_{\varepsilon, Q_1^*}^{N, \Delta t}$ defined by

$$\mathbb{L}_{\varepsilon, Q_1^*}^{N, \Delta t} \Psi = \tilde{\mathbb{T}}_{\varepsilon, (P+Q_1, P)}^{N, \Delta t} \Psi,$$

where $Q_{1,j}^{*,n+1/2}(\xi) = \frac{P_j^{n+1} + P_j^n}{2} + \xi \left(\frac{Q_{1,j}^{n+1} + Q_{1,j}^n}{2} \right)$. Then, we rewrite the discrete problem (7.43) in the following form:

$$\begin{cases} \mathbb{L}_{\varepsilon, Q_1^*}^{N, \Delta t} Q_{1,j}^{n+1} = 0, & \text{for } 1 \leq j \leq N/2 - 1, \\ Q_{1,j}^0 = q_1(x_j, 0), & \text{for } 1 \leq j \leq N/2 - 1, \quad Q_{1,0}^{n+1} = q_1(0, t_{n+1}), \\ Q_{1,N/2}^{n+1} = q_1(\mathfrak{d}, t_{n+1}), & n = 0, 1, \dots, M-1. \end{cases}$$

Further, we obtain that

$$\mathbb{L}_{\varepsilon, Q_1^*}^{N, \Delta t} \Phi_j^{n+1} \leq 0, \quad \text{for } 1 \leq j \leq N/2 - 1.$$

We choose the discrete functions

$$\Psi^\pm(x_j, t_{n+1}) = -|Q_{1,0}^{n+1}| \Phi_j^{n+1} \pm Q_{1,j}^{n+1}, \quad \text{for } 0 \leq j \leq N/2,$$

for sufficiently large C . Then, $\Psi^\pm(x_0, t_{n+1}) \leq 0$, $\Psi^\pm(x_{N/2}, t_{n+1}) = 0$ and

$$\mathbb{L}_{\varepsilon, Q_1^*}^{N, \Delta t} \Psi_j^\pm \geq 0, \quad \text{for } 1 \leq j \leq N/2 - 1.$$

Applying Corollary 7.2 to the operator $\mathbb{L}_{\varepsilon, Q_1^*}^{N, \Delta t}$, we obtain that

$$|Q_{1,j}^{n+1}| \leq |Q_{1,0}^{n+1}| \Phi_j^{n+1} \leq |Q_{1,0}^{n+1}| \Phi_{N/4}^{n+1} \leq CN^{-1}, \quad \text{for } N/4 \leq j \leq N/2 - 1.$$

Therefore, we get

$$|Q_{1,j}^{n+1} - q_1(x_j, t_{n+1})| \leq CN^{-1}, \quad \text{for } N/4 \leq j \leq N/2 - 1.$$

Next, consider $x_j \in [0, \eta]$. Here, $|Q_{1,N/4}^{n+1}| \leq CN^{-1}$. From the equations (7.24) and (7.43), we have

$$\begin{aligned} & \mathbb{L}_{x,\varepsilon}^N \frac{Q_{1,j}^{n+1} + Q_{1,j}^n}{2} - \left[b\left(x_j, t_{n+1/2}, \frac{p_j^{n+1} + p_j^n}{2} + \frac{Q_{1,j}^{n+1} + Q_{1,j}^n}{2}\right) - b\left(x_j, t_{n+1/2}, \frac{p_j^{n+1} + p_j^n}{2}\right) \right] - \\ & D_t^- Q_{1,j}^{n+1} = \mathbb{L}_{x,\varepsilon} \frac{q(x_j, t_{n+1}) + q(x_j, t_n)}{2} - \left[b\left(x_j, t_{n+1/2}, p(x_j, t_{n+1/2}) + q_1(x_j, t_{n+1/2})\right) - \right. \\ & \left. b\left(x_j, t_{n+1/2}, p(x_j, t_{n+1/2})\right) \right] - \frac{\partial q(x_j, t_{n+1/2})}{\partial t}, \quad \text{in } \mathfrak{D}^{N, \Delta t} \cap \mathfrak{D}^-. \end{aligned}$$

The preceding equation can be written as follows:

$$\begin{aligned} & \mathbb{L}_{x,\varepsilon}^N \left(\frac{Q_{1,j}^{n+1} + Q_{1,j}^n}{2} - \frac{q_1(x_j, t_{n+1}) + q_1(x_j, t_n)}{2} \right) - \left[\int_0^1 \frac{\partial b(x_j, t_{n+1/2}, [p^* + Q_1^*]_j^{n+1/2}(\xi))}{\partial y} d\xi \right] \times \\ & \left(\frac{Q_{1,j}^{n+1} + Q_{1,j}^n}{2} - \frac{q_1(x_j, t_{n+1}) + q_1(x_j, t_n)}{2} \right) - D_t^- (Q_{1,j}^{n+1} - q_1(x_j, t_{n+1})) \\ & = \varepsilon \left(\frac{\partial^2}{\partial x^2} - D_x^+ D_x^- \right) \frac{q_1(x_j, t_{n+1}) + q_1(x_j, t_n)}{2} + a(x_j) \left(\frac{\partial}{\partial x} - D_x^+ \right) \frac{q_1(x_j, t_{n+1}) + q_1(x_j, t_n)}{2} \\ & + \frac{\partial q_1(x_j, t_{n+1/2})}{\partial t} - D_t^- q_1(x_j, t_{n+1}) + \left[\int_0^1 \frac{\partial b(x_j, t_{n+1/2}, [p^* + Q_1^*]_j^{n+1/2}(\xi))}{\partial y} d\xi - \right. \\ & \left. \int_0^1 \frac{\partial b(x_j, t_{n+1/2}, p_j^{*,n+1/2}(\xi))}{\partial y} d\xi \right] \times \left(\frac{p_j^{n+1} + p_j^n}{2} - \frac{p(x_j, t_{n+1}) + p(x_j, t_n)}{2} \right) + O(\Delta t)^2, \end{aligned} \quad (7.47)$$

where $[p^* + Q_1^*]_j^{n+1/2}(\xi) = \frac{p_j^{n+1} + p_j^n}{2} + \frac{q_{1,j}^{n+1} + q_{1,j}^n}{2} + \xi \left(\frac{p_j^{n+1} + p_j^n}{2} + \frac{Q_{1,j}^{n+1} + Q_{1,j}^n}{2} - \frac{p_j^{n+1} + p_j^n}{2} - \frac{q_{1,j}^{n+1} + q_{1,j}^n}{2} \right)$ and $p_j^{*,n+1/2}(\xi) = \frac{p_j^{n+1} + p_j^n}{2} + \xi \left(\frac{p_j^{n+1} + p_j^n}{2} - \frac{p_j^{n+1} + p_j^n}{2} \right)$. Now, for any mesh function Ψ we introduce a discrete operator $\mathbb{L}_{\varepsilon, p^* + Q_1^*}^{N, \Delta t}$ given by

$$\mathbb{L}_{\varepsilon, p^* + Q_1^*}^{N, \Delta t} \Psi = \tilde{\mathbb{T}}_{\varepsilon, (p + Q_1, p + q_1)}^{N, \Delta t} \Psi.$$

Afterwards, from (7.47) by using the derivative bound of $q_1(x, t)$ given in Theorem 7.3, we obtain bounds of

the truncation error for the region $1 \leq j \leq N/4 - 1$,

$$|\mathbb{L}_{\varepsilon, \mathcal{P}^* + Q_1^*}^{N, \Delta t} (Q_{1,j}^{n+1} - q_1(x_j, t_{n+1}))| \leq C\eta\varepsilon^{-2}N^{-1} \exp(-\mathfrak{m}x_{j-1}/\varepsilon) + C[N^{-1} + (\Delta t)^2]. \quad (7.48)$$

We choose the discrete functions for $0 \leq j \leq N/4$,

$$\Psi^\pm(x_j, t_{n+1}) = -C(N^{-1} + \Delta t^2) - C(N^{-1} + \Delta t^2)(\eta - x_j) - C\frac{h}{\varepsilon} \left(\frac{\Theta_j(\lambda)}{\Theta_0(\lambda)} \right) \pm (Q_{1,j}^{n+1} - q_1(x_j, t_{n+1}))$$

where

$$\begin{cases} \Theta_j(\lambda) = \prod_{k=j+1}^N \left(1 + \frac{\lambda h_k}{\varepsilon} \right), & \text{for } 0 \leq j \leq N-1, \\ \Theta_N(\lambda) = 1, \end{cases}$$

and λ is a positive constant. We have $-\mathbb{L}_{\varepsilon, \mathcal{P}^* + Q_1^*}^{N, \Delta t} \Theta_j(\lambda) \geq \frac{C}{\varepsilon} \Theta_j(\lambda)$, for $1 \leq j \leq N/4$, and hence, use of (7.48) for $\lambda < \mathfrak{m}/2$ yields that

$$\mathbb{L}_{\varepsilon, \mathcal{P}^* + Q_1^*}^{N, \Delta t} \Psi^\pm(x_j, t_{n+1}) \geq 0.$$

Now, apply Corollary 7.2 for the operator $\mathbb{L}_{\varepsilon, \mathcal{P}^* + Q_1^*}^{N, \Delta t}$ to get $\Psi^\pm(x_j, t_{n+1}) \leq 0$, for all $0 \leq j \leq N/4$. Hence, we get

$$|Q_{1,j}^{n+1} - q_1(x_j, t_{n+1})| \leq C(N^{-1} \ln N + (\Delta t)^2), \quad \text{for } 0 \leq j < N/4.$$

Thus, we obtain the desired result (7.45). ■

Lemma 7.8. *Under the assumption (7.31) of Lemma 7.4, the error associated with interior layer component satisfy the following estimates:*

$$|Q_{2,j}^{n+1} - q_2(x_j, t_{n+1})| \leq CN^{-1}, \quad \text{for } N/4 \leq j \leq N/2 - 1, \text{ and } 3N/4 \leq j \leq N-1, \quad (7.49)$$

and

$$|Q_{2,j}^{n+1} - q_2(x_j, t_{n+1})| \leq C(N^{-1} \ln N + (\Delta t)^2), \quad \text{for } 1 \leq j \leq N/4 - 1. \quad (7.50)$$

Proof. Let $3N/4 \leq j \leq N-1$. From the triangle inequality, we have

$$|Q_{2,j}^{n+1} - q_2(x_j, t_{n+1})| \leq |Q_{2,j}^{n+1}| + |q_2(x_j, t_{n+1})|. \quad (7.51)$$

Using Theorem 7.3 for $3N/4 \leq j \leq N-1$, we have

$$|q_2(x_j, t_{n+1})| \leq C\varepsilon \exp(-\mathfrak{m}(x_j - \mathfrak{d})/\varepsilon) \leq C \exp(-\mathfrak{m}(\mathfrak{d} + \eta)/\varepsilon) = CN^{-1}, \quad \text{for } 3N/4 \leq j \leq N-1. \quad (7.52)$$

Now, for deriving bound for $Q_{2,j}^{n+1}$, we introduce the mesh function Φ_j^{n+1} , which is the solution of the following discrete problem:

$$\begin{cases} \varepsilon D_x^+ D_x^- \Phi_j^{n+1} + \mathfrak{m} D_x^+ \Phi_j^{n+1} = 0, & \text{for } N/2 < j \leq N-1, \\ \Phi_{N/2}^{n+1} = 1, \quad \Phi_N^{n+1} = 0, \end{cases} \quad (7.53)$$

where

$$\begin{cases} \Phi_j^{n+1} \geq 0 \quad \text{and} \quad D_x^+ \Phi_j^{n+1} \leq 0, & \text{for } N/2 < j \leq N-1, \\ \Phi_{3N/4}^{n+1} \leq CN^{-1}, & \text{for some } C. \end{cases}$$

Here, for any mesh function Ψ , we introduce a linear discrete operator $\mathbb{L}_{\varepsilon, Q_2^*}^{N, \Delta t}$ defined by

$$\mathbb{L}_{\varepsilon, Q_2^*}^{N, \Delta t} \Psi = \tilde{\mathbb{T}}_{\varepsilon, (P+Q_2, P)}^{N, \Delta t} \Psi,$$

where $Q_{2,j}^{*,n+1/2}(\xi) = \frac{\mathcal{P}_j^{n+1} + \mathcal{P}_j^n}{2} + \xi \left(\frac{Q_{2,j}^{n+1} + Q_{2,j}^n}{2} \right)$. Then, we rewrite the discrete problem (7.44) in the following form:

$$\begin{cases} \mathbb{L}_{\varepsilon, Q_2^*}^{N, \Delta t} Q_{2,j}^{n+1} = 0, & \text{for } N/2 < j \leq N-1, \\ Q_{2,j}^0 = 0, & N/2 \leq j \leq N, \quad Q_{2,0}^{n+1} = 0, \quad n = 0, 1, \dots, M-1, \\ Q_{2,N}^{n+1} = 0, & [DQ_2(\mathbf{d}, t_{n+1})] = -[D\mathcal{P}(\mathbf{d}, t_{n+1})] - [DQ_1(\mathbf{d}, t_{n+1})]. \end{cases}$$

Further, we obtain that

$$\mathbb{L}_{\varepsilon, Q_2^*}^{N, \Delta t} \Phi_j^{n+1} \leq 0, \quad \text{for } N/2 < j \leq N-1.$$

We choose the discrete function for $N/2 \leq j \leq N$,

$$\Psi^\pm(x_j, t_{n+1}) = -|Q_{2,N/2}^{n+1}| \Phi_j^{n+1} \pm Q_{2,j}^{n+1},$$

for sufficiently large C . Then $\Psi^\pm(x_{N/2}, t_{n+1}) = 0$, $\Psi^\pm(x_N, t_{n+1}) = 0$ and

$$\mathbb{L}_{\varepsilon, Q_2^*}^{N, \Delta t} \Psi_j^\pm \geq 0, \quad \text{for } N/2 < j < N.$$

Applying Corollary 7.2 to the operator $\mathbb{L}_{\varepsilon, Q_2^*}^{N, \Delta t}$, we obtain that

$$|Q_{2,j}^{n+1}| \leq |Q_{2,N/2}^{n+1}| \Phi_j^{n+1} \leq |Q_{2,N/2}^{n+1}| \Phi_{3N/4}^{n+1} \leq CN^{-1}, \quad \text{for } 3N/4 \leq j \leq N-1. \quad (7.54)$$

Therefore, we obtain the desired estimate (7.49) from (7.51), (7.52) and (7.54).

The estimate (7.50) for $N/4 \leq j \leq N/2 - 1$ and $1 \leq j \leq N/4 - 1$, can be obtained by using the approach given in Lemma 7.7 and constructing suitable barrier functions for both regions. ■

The error associated with the numerical solution can be decomposed as

$$Y_j^{n+1} - y(x_j, t_{n+1}) = \begin{cases} \mathcal{P}_j^{n+1} - p(x_j, t_{n+1}) + Q_{1,j}^{n+1} - q_1(x_j, t_{n+1}) + Q_{2,j}^{n+1} - q_2(x_j, t_{n+1}), & 0 \leq j < N/2, \\ \mathcal{P}_j^{n+1} - p(x_j, t_{n+1}) + Q_{1,j}^{n+1} - q_1(x_j, t_{n+1}) + Q_2^{n+1} - q_2(x_j, t_{n+1}), & j = N/2, \\ \mathcal{P}_j^{n+1} - p(x_j, t_{n+1}) + Q_{2,j}^{n+1} - q_2(x_j, t_{n+1}), & N/2 < j \leq N. \end{cases}$$

Theorem 7.4 (Global error). *Under the assumption (7.31) of Lemma 7.4, the error associated with the discrete*

problem (7.29) satisfies the following estimates:

$$|Y_j^{n+1} - y(x_j, t_{n+1})| \leq \begin{cases} C(N^{-1} \ln N + (\Delta t)^2), & \text{for } 1 \leq j < N/4, \text{ and } N/2 \leq j < 3N/4, \\ C(N^{-1} + (\Delta t)^2), & \text{for } N/4 \leq j < N/2, \text{ and } 3N/4 \leq j \leq N-1. \end{cases} \quad (7.55)$$

Proof. At first, we derive the estimate (7.55) for $N/2 \leq j < 3N/4$. From Lemmas 7.6, 7.7 and 7.8, we have $|Y_{N/2-1}^{n+1} - y(x_{N/2-1}, t_{n+1})| \leq C(N^{-1} + (\Delta t)^2)$ and $|Y_{3N/4}^{n+1} - y(x_{3N/4}, t_{n+1})| \leq C(N^{-1} + (\Delta t)^2)$. The truncation error at the point of discontinuity is given by,

$$\begin{aligned} |(D_x^+ - D_x^-)(Y_{N/2}^{n+1} - y(\mathbf{d}, t_{n+1}))| &= |(D_x^- - D_x^+)y(\mathbf{d}, t_{n+1}) + \left[\frac{\partial y}{\partial x}\right](\mathbf{d}, t_{n+1})| \\ &\leq \left|\frac{\partial y(\mathbf{d}^+, t_{n+1})}{\partial x} - D_x^+ y(\mathbf{d}, t_{n+1})\right| + \left|\frac{\partial y(\mathbf{d}^-, t_{n+1})}{\partial x} - D_x^- y(\mathbf{d}, t_{n+1})\right|, \\ &\leq \frac{1}{2}h_2 \left|\frac{\partial^2 y}{\partial x^2}\right|_{[\mathbf{d}, \mathbf{d}+h_2]} + \frac{1}{2}H_1 \left|\frac{\partial^2 y}{\partial x^2}\right|_{[\mathbf{d}-H_1, \mathbf{d}]} \\ &\leq CN^{-1} \ln N + CN^{-1} \leq CN^{-1} \ln N. \end{aligned}$$

Now, for the region $N/2 < j < 3N/4$, from the equations (7.1) and (7.30), we have

$$\begin{aligned} \mathbb{L}_{x,\varepsilon}^N \frac{Y_j^{n+1} + Y_j^n}{2} - b\left(x_j, t_{n+1/2}, \frac{Y_j^{n+1} + Y_j^n}{2}\right) - D_t^- Y_j^{n+1} \\ = \mathbb{L}_{x,\varepsilon} \frac{y(x_j, t_{n+1}) + y(x_j, t_n)}{2} - b\left(x_j, t_{n+1/2}, y(x_j, t_{n+1/2})\right) - \frac{\partial y(x_j, t_{n+1/2})}{\partial t}. \end{aligned}$$

The preceding equation can be written as follows:

$$\begin{aligned} \mathbb{L}_{x,\varepsilon}^N \left(\frac{Y_j^{n+1} + Y_j^n}{2} - \frac{y(x_j, t_{n+1}) + y(x_j, t_n)}{2} \right) - \left[\int_0^1 \frac{\partial b(x_j, t_{n+1/2}, Y_j^{*,n+1/2}(\xi))}{\partial y} d\xi \right] \times \\ \left(\frac{Y_j^{n+1} + Y_j^n}{2} - \frac{y(x_j, t_{n+1}) + y(x_j, t_n)}{2} \right) - D_t^- (Y_j^{n+1} - y(x_j, t_{n+1})) \\ = \varepsilon \left(\frac{\partial^2}{\partial x^2} - D_x^+ D_x^- \right) \frac{y(x_j, t_{n+1}) + y(x_j, t_n)}{2} + a(x_j) \left(\frac{\partial}{\partial x} - D_x^+ \right) \frac{y(x_j, t_{n+1}) + y(x_j, t_n)}{2} - \\ \left(\frac{\partial y(x_j, t_{n+1/2})}{\partial t} - D_t^- y(x_j, t_{n+1}) \right) + O(\Delta t)^2, \quad \text{for } N/2 < j < 3N/4, \end{aligned} \quad (7.56)$$

where $Y_j^{*,n+1/2}(\xi) = y(x_j, t_{n+1/2}) + \xi(Y_j^{n+1/2} - y(x_j, t_{n+1/2}))$. Now, for any mesh function Ψ we introduce a discrete operator $\mathbb{L}_{\varepsilon, Y^*}^{N, \Delta t}$ given by

$$\mathbb{L}_{\varepsilon, Y^*}^{N, \Delta t} \Psi = \tilde{\mathbb{T}}_{\varepsilon, (Y, y)}^{N, \Delta t} \Psi.$$

Afterwards, from (7.56) by using the derivative bounds of $y(x, t)$ obtain from the Theorem 7.2 and 7.3, we obtain bounds of the truncation errors:

$$|\mathbb{L}_{\varepsilon, Y^*}^{N, \Delta t} (Y_j^{n+1} - y(x_j, t_{n+1}))| \leq C[N^{-1} \ln N + (\Delta t)^2], \quad \text{for } 3N/4 < j < N. \quad (7.57)$$

Consider the discrete functions

$$\Psi^\pm(x_j, t_{n+1}) = -C(N^{-1} \ln N + (\Delta t)^2)(1-x_j) \pm (Y_j^{n+1} - y(x_j, t_{n+1})), \quad \text{for } N/2 - 1 \leq j \leq 3N/4, \quad (7.58)$$

and apply Corollary 7.2 for the operator $\mathbb{L}_{\varepsilon, Y^*}^{N, \Delta t}$ together with the truncation error bounds in (7.57), to obtain that

$$|Y_j^{n+1} - y(x_j, t_{n+1})| \leq C(N^{-1} \ln N + (\Delta t)^2), \quad \text{for } N/2 \leq j < 3N/4.$$

Finally, we obtain the required estimate (7.55) for the remaining regions by invoking Lemmas 7.6, 7.7 and 7.8. ■

7.5 Numerical experiment

In this section, we present the numerical results for one test problems of the form (7.1)-(7.4), utilizing the proposed FMMs in (7.29). For this test example, we select the constant $\eta_0 = 1$, $d = 1/2$ and implement the Thomas algorithm to solve the tridiagonal linear systems involved in our methods. The numerical results are also compared with the fully-implicit upwind FMM, which is mentioned below as well.

7.5.1 The fully-implicit upwind FMM

In this section, we approximate the problem (7.1)-(7.4) by a fully implicit numerical method that combines an implicit Euler method to discretize in the temporal direction and a classical upwind scheme to discretize in the spatial direction.

Find a mesh function Y such that

$$\begin{cases} Y_j^0 = q_0(x_j), & 0 \leq j \leq N, \\ \mathbb{L}_{x, \varepsilon}^N Y_j^{n+1} - b(x_j, t_{n+1}, Y_j^{n+1}) - D_t^- Y_j^{n+1} = g(x_j, t_{n+1}), \\ Y_0^{n+1} = y(0, t_{n+1}), \quad Y_N^{n+1} = y(1, t_{n+1}), & \text{for } n = 0, 1, \dots, M-1, \\ D_x^- Y_{N/2}^{n+1} - D_x^+ Y_{N/2}^{n+1} = 0, \end{cases} \quad (7.59)$$

where $\mathbb{L}_{x, \varepsilon}^N Y_j^{n+1} = (\varepsilon D_x^+ D_x^- + a(x_j) D_x^+) Y_j^{n+1}$. The existence and stability of the solution Y_j^{n+1} of the nonlinear discrete problem (7.59) can be obtained in the same way as in Section 7.3. Furthermore, following the error analysis given in Section 7.4, one can prove ε -uniform error estimate for the FMM (7.59).

Theorem 7.5 (Global error). *The errors in the numerical solution satisfy the following estimates*

$$|Y_j^{n+1} - y(x_j, t_{n+1})| \leq \begin{cases} C(N^{-1} \ln N + \Delta t), & \text{for } 0 \leq j < N/4, \text{ and } N/2 \leq j < 3N/4, \\ C(N^{-1} + \Delta t), & \text{for } N/4 \leq j < N/2, \text{ and } 3N/4 \leq j \leq N. \end{cases}$$

where Y_j^{n+1} is the solution of nonlinear discrete problem (7.59) and y is the solution of the continuous problem (7.1)-(7.4).

7.5.2 Test Example

Example 7.1. Consider the following semi-linear parabolic IBVP:

$$\begin{cases} \varepsilon \frac{\partial^2 y}{\partial x^2} + a(x) \frac{\partial y}{\partial x} - y \exp(y^2) - \frac{\partial y}{\partial t} = g(x, t), & (x, t) \in [(0, d) \cup (d, 1)] \times (0, 1], \\ y(x, 0) = 0, & x \in [0, 1], \\ y(0, t) = -\frac{2}{3}t^3, & y(1, t) = 0, \quad t \in [0, 1], \end{cases}$$

where

$$a(x) = \begin{cases} 1 + x - x^2, & x \in [0, d], \\ 2 - x + x^2, & x \in [d, 1], \end{cases} \quad \text{and } g(x, t) = \begin{cases} -2 \sin(\pi x)(1 + x^2)t^2, & (x, t) \in [0, d] \times (0, 1], \\ 3 \cos(\pi x)(1 - x^2)t^2, & (x, t) \in [d, 1] \times (0, 1]. \end{cases}$$

Because the exact solution for this example is unknown, the computational results are investigated using the double mesh method. In the same way as we have done in Chapter 4, we determine the maximum nodal error and the related order of convergence for each ε .

To compute the numerical solution of the FMMs in (7.29) and (7.59) for Example 7.1, a nonlinear system needs to be solved at each time step. For that, we use the Newton's iterative method as we define in Chapter 4.

7.5.3 Numerical results and observations

In Fig 7.2, we draw surface plot of numerical solution for Example 7.1 and it shows that the numerical solution generates boundary layer closer to $x = 0$ and interior layer at the right side of point of discontinuity $x = 1/2$. For different values of ε , N and Δt , the computed ε -uniform errors and order of convergence are displayed in Tables 7.1 for Example 7.1. This shows the monotonically decreasing behavior of the ε -uniform errors with increasing N , and it definitely represents the ε -uniform convergence of the FMMs given in (7.29). Next, in order to visualize the effect of the temporal accuracy, we choose a suitably large $N = 2048$ to reduce the influence of the spatial error. In Tables 7.2, we display the numerical results for Example 7.1, of the proposed FMMs in (7.29) and (7.59), respectively.

7.6 Conclusion

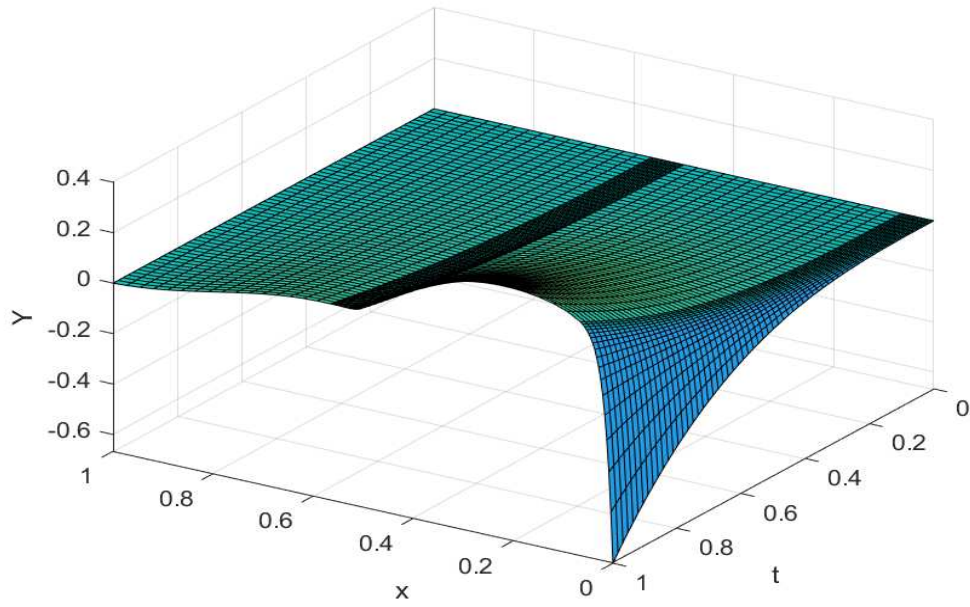
In this chapter, we consider a class of singularly perturbed semilinear parabolic convection-diffusion IBVPs with a jump discontinuity in the source term and in the convection term. Here, the convection coefficient has the same sign pattern throughout the domain. Due to the discontinuity in the data of this type, a weak interior layer and a boundary layer appear in the solution. In this regard, the following results are derived.

At first, the lower and upper solutions approach is used to study the existence of the analytical solution of the nonlinear problem. The ε -uniform stability result of the analytical is obtained by establishing the comparison principle for the continuous nonlinear operator; and we derive a-priori bounds of the derivatives of the analytical solution via decomposition of the solution.

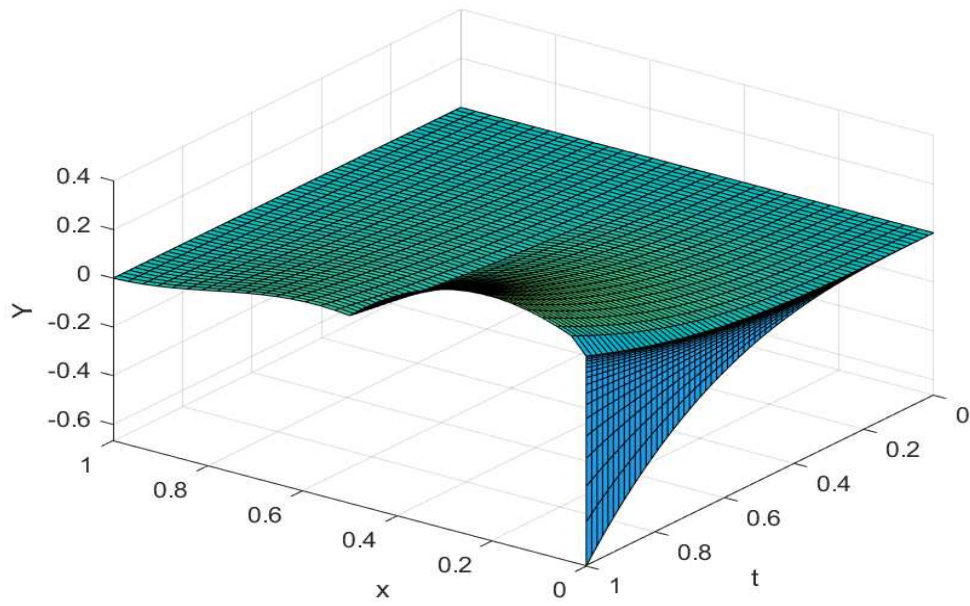
Further, we establish the comparison principle for the nonlinear discrete problem to obtain the ε -uniform stability result of the discrete solution and provide a decomposition of the discrete solution, which enables us to prove the ε -uniform convergence of the proposed finite difference approximation in the discrete supremum

norm. It is proved that the proposed method is second-order accurate in time and almost first-order accurate in space, irrespective of the parameter- ϵ .

The above theoretical findings are verified by the numerical experiments and moreover, it is shown that the current numerical method is robust in comparison with the implicit upwind method. In this context, it is worthy to the mention that to the best of our knowledge, there are hardly any research work related to the Crank-Nicolson based numerical approximation of singularly perturbed nonlinear parabolic PDEs with nonsmooth data arising in the semiconductor device modeling; and in that case, this is first such attempt made in the literature.



(a) for $\varepsilon = 2^{-6}$



(b) for $\varepsilon = 2^{-20}$

Figure 7.2: Surface plots of numerical solution for Example 7.1

Table 7.1: ε -uniform maximum point-wise errors and order of convergence for Example 7.1 computed with $\Delta t = 1/N$ using the proposed nonlinear scheme (7.29)

ε	Number of mesh-intervals N / time step-size Δt					
	$32/\frac{1}{32}$	$64/\frac{1}{64}$	$128/\frac{1}{128}$	$256/\frac{1}{256}$	$512/\frac{1}{512}$	$1024/\frac{1}{1024}$
2^0	7.7706e-03	3.8090e-03	1.8849e-03	9.3746e-04	4.6748e-04	2.3343e-04
	1.0286	1.0149	1.0076	1.0039	1.0019	
2^{-2}	9.2773e-03	4.6100e-03	2.2999e-03	1.1488e-03	5.7424e-04	2.8708e-04
	1.0089	1.0032	1.0014	1.0004	1.0002	
2^{-4}	2.6663e-02	1.6198e-02	8.7194e-03	4.5185e-03	2.3039e-03	1.1632e-03
	0.71900	0.89354	0.94839	0.97178	0.98599	
2^{-6}	3.7572e-02	2.2843e-02	1.3290e-02	7.5496e-03	4.2191e-03	2.3276e-03
	0.71790	0.78138	0.81590	0.83946	0.85812	
2^{-8}	4.0466e-02	2.6147e-02	1.5448e-02	8.7225e-03	4.8127e-03	2.6224e-03
	0.63008	0.75919	0.82463	0.85791	0.87595	
2^{-10}	4.0162e-02	2.6363e-02	1.5806e-02	9.0796e-03	5.0706e-03	2.7724e-03
	0.60734	0.73805	0.79976	0.84047	0.87100	
2^{-12}	3.9914e-02	2.6201e-02	1.5677e-02	8.9947e-03	5.0459e-03	2.7904e-03
	0.60726	0.74101	0.80146	0.83396	0.85465	
2^{-14}	3.9837e-02	2.6137e-02	1.5610e-02	8.9259e-03	4.9870e-03	2.7507e-03
	0.60801	0.74367	0.80636	0.83983	0.85839	
2^{-16}	3.9817e-02	2.6119e-02	1.5590e-02	8.9038e-03	4.9645e-03	2.7298e-03
	0.60826	0.74451	0.80813	0.84277	0.86283	
2^{-18}	3.9812e-02	2.6115e-02	1.5585e-02	8.8979e-03	4.9582e-03	2.7235e-03
	0.60832	0.74474	0.80861	0.84364	0.86435	
2^{-20}	3.9811e-02	2.6114e-02	1.5583e-02	8.8964e-03	4.9566e-03	2.7218e-03
	0.60834	0.74479	0.80873	0.84386	0.86476	
2^{-22}	3.9810e-02	2.6113e-02	1.5583e-02	8.8960e-03	4.9562e-03	2.7214e-03
	0.60834	0.74481	0.80876	0.84392	0.86487	
2^{-24}	3.9810e-02	2.6113e-02	1.5583e-02	8.8959e-03	4.9561e-03	2.7213e-03
	0.60835	0.74481	0.80877	0.84394	0.86489	
$e^{N,\Delta t}$	4.0466e-02	2.6363e-02	1.5806e-02	9.0796e-03	5.0706e-03	2.7904e-03
$r^{N,\Delta t}$	0.61822	0.73805	0.79976	0.84047	0.86168	

Table 7.2: Comparison of the temporal accuracy for Example 7.1 computed using the FMMs (7.29) and (7.59)

ε	Number of space intervals $N = 2048$				
	$\Delta t = \frac{1}{16}$	$\Delta t = \frac{1}{32}$	$\Delta t = \frac{1}{64}$	$\Delta t = \frac{1}{128}$	$\Delta t = \frac{1}{256}$
2^{-4}	implicit-Euler method (7.59)				
	2.9909e-03	1.5046e-03	7.5416e-04	3.7748e-04	1.8883e-04
	0.99114	0.99647	0.99849	0.99931	
	Crank-Nicolson scheme (7.29)				
	2.5545e-05	6.3642e-06	1.5896e-06	3.9731e-07	9.9321e-08
	2.0050	2.0013	2.0003	2.0001	
2^{-8}	implicit-Euler method (7.59)				
	4.6306e-03	2.3283e-03	1.1654e-03	5.8278e-04	2.9140e-04
	0.99192	0.99848	0.99978	0.99995	
	Crank-Nicolson scheme (7.29)				
	3.5889e-05	9.9039e-06	2.4770e-06	6.1946e-07	1.5488e-07
	1.8575	1.9994	1.9995	1.9999	
2^{-16}	implicit-Euler method (7.59)				
	4.8395e-03	2.4338e-03	1.2181e-03	6.0911e-04	3.0457e-04
	0.99162	0.99866	0.99980	0.99992	
	Crank-Nicolson scheme (7.29)				
	4.1919e-05	1.0307e-05	2.6340e-06	6.5945e-07	1.6488e-07
	2.0240	1.9683	1.9979	1.9999	
2^{-24}	implicit-Euler method (7.59)				
	4.8405e-03	2.4344e-03	1.2183e-03	6.0924e-04	3.0464e-04
	0.99161	0.99866	0.99980	0.99992	
	Crank-Nicolson scheme (7.29)				
	4.1974e-05	1.0301e-05	2.6346e-06	6.5964e-07	1.6492e-07
	2.0267	1.9671	1.9979	1.9999	

Chapter 8

Conclusions

This chapter is dedicated to a brief review of the outcomes of the research work that contributed to the thesis, emphasizing their relevance and significance in the context of parameter-robust numerical solutions of singularly perturbed linear and nonlinear parabolic PDEs with smooth and nonsmooth data. It further highlights a variety of future scopes for possible extensions of the current work.

8.1 Outcomes of the research works

The following is the summary of the research findings made in the thesis, along with some key observations:

- An ε -uniformly convergent robust numerical algorithm is developed and analyzed for a class of singularly perturbed one-dimensional linear parabolic convection-diffusion IBVPs with time-dependent convection coefficient and possessing a regular boundary layer. The current numerical algorithm consists of two parts. The first one is the development of a new hybrid FMM, which produces at least a second-order accurate numerical solution with respect to the spatial variable both in the outer region (outside the boundary layer) as well as in the boundary layer region (inside the boundary layer), regardless of the cases $\varepsilon \gg N^{-1}$ and $\varepsilon \ll N^{-1}$. This reflects that there is an improvement in the region-wise accuracy of the newly developed method in comparison with the existing numerical method. The other one is the implementation of the Richardson extrapolation technique solely in the temporal direction (called temporal Richardson extrapolation) for enhancing the temporal accuracy from first-order to second-order.

As a result, the resulting numerical solution is proven to be second-order ε -uniformly convergent not only in the spatial variable but also in the temporal variable. Moreover, a significant reduction in the computational time is noticed corresponding to the newly developed FMM along with the temporal Richardson extrapolation, regardless of the smaller and larger values of ε . The above findings indeed overshadow the drawbacks of the existing hybrid scheme.

- The idea behind the newly developed algorithm is further extended for the cost-effective higher-order numerical approximation of two-dimensional singularly perturbed linear parabolic problems with time-dependent boundary conditions by proposing a new FSFMM and, later, by the extrapolation technique. It is proved that the corresponding fully discrete scheme is ε -uniformly convergent in the discrete supremum norm; and the spatial accuracy of the scheme is at least two in the outer region and is almost two in the boundary layer region, regardless of the larger and smaller values of ε . Afterwards, the method is proven to be second-order accurate in time by means of the temporal Richardson extrapolation.

Here, we perform the error analysis for the newly designed fractional-step method in two-steps, which discretizes first in time and then in space. It is important to note that in [22] the two-step analysis is carried out in the reverse order which firstly converts the IBVP into the semidiscrete IVP via spatial discretization and later into the fully-discrete problem via temporal discretization. For the spatial discretization of the IVP, it utilizes the convergence result of the upwind finite difference scheme proved in [20], because the pentadiagonal structure of the upwind scheme can be further decomposed into the tridiagonal structure in the x and y -direction. However, such technique can not be extended to achieve higher-order spatial accuracy using the newly proposed finite difference scheme because of the design of the scheme; and in that case the present error analysis plays a significant role for analyzing the spatial accuracy.

It is important to note that the newly developed FSFMM utilizes an alternative evaluation of the boundary data in order to eliminate the order reduction caused by the natural evaluation of the time-dependent boundary conditions and thus produces a cost-effective, globally second-order accurate (in both space and time) numerical solution by solving the tridiagonal linear systems at each half instead of the tridiagonal block system. Moreover, the current fraction-steps method is shown to be robust in comparison with the fractional implicit upwind method.

- Further, analyzing parameter-robust numerical approximation of higher-order accuracy for singularly perturbed parabolic PDEs with nonlinearity is considered to be a desirable task due to the wide range of real-life applications and the computational challenges in tackling the nonlinearity. In this regard, a complete convergence analysis is provided for higher-order numerical approximations for a class of singularly perturbed one-dimensional linear parabolic convection-diffusion IBVPs exhibiting a regular boundary layer by proposing two novel FMMs (the fully-implicit FMM and the IMEX-FMM) followed by the extrapolation technique. It is proved that both the newly proposed methods are ε -uniformly convergent in the discrete supremum norm and achieve at least second-order accuracy in the outer region and almost second-order accuracy in the boundary layer region regardless of the larger and smaller values of ε . Thereafter, by implementing the extrapolation technique solely for the time variable, we achieve globally (in both space and time) second-order accurate numerical solutions.

It is worthy of mentioning that our error estimates justify that although the IMEX method leads to a linearized system at each time step, it does not cause a reduction in the order of convergence corresponding to the present fully-implicit method, which indeed leads to a nonlinear system at each time step. Moreover, it is shown that the IMEX-FMM produces a more cost-effective numerical solution than the fully-implicit FMM, and the newly developed FMMs are robust in comparison with the upwind FMM.

- Further investigation is carried out for cost-effective higher-order numerical approximations of two-dimensional semilinear singularly perturbed parabolic convection-diffusion problems with non-homogeneous boundary data by developing two new FSFMMs (the fully-implicit FSFMM and the IMEX-FSFMM) and later, by the extrapolation technique. It is proved that the proposed methods are ε -uniformly convergent with second-order spatial accuracy in the discrete supremum norm, irrespective of the larger and smaller values of ε . After implementing the extrapolation technique, the resulting numerical solutions are also proven to be second-order accurate in time.

Our error analysis reveals that the proposed IMEX-FSFMM (a linearized scheme) is still able to retain the

same order of accuracy as that of the fully-implicit FSFMM (a nonlinear scheme). In addition, an appropriate evaluation of the boundary data is proposed for both cases to avoid the order reduction phenomena due to the time-dependent boundary conditions. Moreover, both the newly developed fractional-step methods are robust compared to the fractional implicit upwind method.

- Next, we point out the other research findings in connection with singularly perturbed PDEs with non-smooth data. In this regard, efficient numerical approximations of two different classes of singularly perturbed parabolic PDEs with nonsmooth data are proposed and investigated. In both cases, the proposed numerical methods are proven to be ε -uniformly convergent in the discrete supremum norm and almost second-order accurate in space, not only for $\varepsilon \gg N^{-1}$, but also for $\varepsilon \ll N^{-1}$.

However, to establish the ε -stability and ε -uniform error estimates, we utilize a suitable layer-resolving Shishkin mesh in the case of PDEs having strong interior layers and a modified layer-adapted mesh in the case of PDEs having both boundary and weak interior layers. Note that by introducing the modified layer-adapted mesh, we overcome the theoretical challenge of establishing the monotonicity of the newly developed FMM on the standard layer-resolving Shishkin mesh. Moreover, a significant improvement in terms of the spatial order of convergence is observed for both the current methods compared to the existing numerical methods.

- Again, developing a parameter-robust higher-order accurate numerical approximation of singularly perturbed nonlinear PDEs with nonsmooth data is a desirable and challenging task for a better understanding of the complex phenomena. In this regard, a higher-order time accurate FMM is proposed and investigated for a class of singularly perturbed semilinear parabolic convection-diffusion IBVPs exhibiting both boundary and weak interior layers. Apart from this, we also study the existence and stability of the solution of the continuous nonlinear problem and that of the discrete nonlinear problem. The numerical approximation is proven to be uniformly convergent and second-order time accurate in the discrete supremum norm. Moreover, it is shown that the current numerical method is robust in comparison with the implicit upwind method.

8.2 Future scopes

There are plenty of opportunities to examine the potential of the higher-order methods analyzed in this thesis to study the numerical aspects of several complex PDEs. A concise description of the possible future extensions of the present work is furnished below:

The higher-order robust numerical algorithm proposed in **Chapter 2** can be further extended and analyzed for higher-order numerical approximation of the following class of singularly perturbed quasilinear problems posed on the domain $\mathfrak{D} = \Omega \times (0, T] = (0, 1) \times (0, T]$:

$$\begin{cases} \frac{\partial y(x, t)}{\partial t} - \varepsilon \frac{\partial^2 y(x, t)}{\partial x^2} + a(x, t, y(x, t)) \frac{\partial y(x, t)}{\partial x} + b(x, t, y(x, t)) = g(x, t), & (x, t) \in \mathfrak{D}, \\ y(x, 0) = q_0(x), & \text{in } \bar{\Omega}, \\ y(0, t) = s_l(t), \quad y(1, t) = s_r(t), & t \in (0, T], \end{cases} \quad (8.1)$$

where ε is a small parameter such that $(0, 1]$ and the functions a , b , g , q_0 , s_l , s_r are sufficiently smooth. It is

to be noted that the parameter-robust numerical method is analyzed for singularly perturbed quasilinear BVPs in [70] with smooth data.

A cost-effective parameter-robust FSFMM is proposed in **Chapter 3** for solving two-dimensional singularly perturbed linear parabolic convection-diffusion IBVPs with non-homogeneous Dirichlet type boundary conditions. It would be an interesting and challenging task to extend the similar method with suitable evaluation of the boundary data other than the natural choice for the following class of singularly perturbed two-dimensional linear parabolic convection-diffusion problems subject to the non-homogeneous Robin type boundary conditions posed on the domain $D = G \times (0, T] = (0, 1)^2 \times (0, T]$:

$$\begin{cases} \left(\frac{\partial}{\partial t} + L_\varepsilon \right) u(x, y, t) = g(x, y, t), & (x, y, t) \in D, \\ u(x, y, 0) = q_0(x, y), & \text{in } \bar{G}, \\ \alpha(x, y, t)u(x, y, t) + \varepsilon\mu(x, y, t)\frac{\partial u(x, y, t)}{\partial n} = s(x, y, t), & (x, y, t) \in \partial G \times (0, T], \end{cases} \quad (8.2)$$

where $L_\varepsilon u = -\varepsilon\Delta u + \vec{v}(x, y, t) \cdot \vec{\nabla} u + b(x, y, t)u$, and $\vec{v}(x, y, t) = (v_1(x, y, t), v_2(x, y, t))$, and ε is a small parameter such that $\varepsilon \in (0, 1]$. The coefficients $\vec{v}(x, y, t)$, $b(x, y, t)$, $\alpha(x, y, t)$, $\mu(x, y, t)$ and the source term $g(x, y, t)$ are considered to be sufficiently smooth with

$$\begin{cases} v_l(x, y, t) \geq m_l > 0, \quad l = 1, 2; \quad b(x, y, t) \geq \beta \geq 0, & (x, y, t) \in \bar{D}, \\ \alpha(x, y, t) + \mu(x, y, t) > 0, \quad \alpha(x, y, t), \quad \mu(x, y, t) \geq 0, & (x, y, t) \in \partial G \times (0, T]. \end{cases} \quad (8.3)$$

Recently, parameter-robust numerical methods are investigated in [101, 55] for solving singularly perturbed one dimensional parabolic PDEs with Robin type boundary conditions.

Next, one can further extend the convergence analysis of both the higher-order fully-implicit method and the higher-order IMEX method examined in **Chapter 4** for one dimensional semilinear parabolic PDEs and in **Chapter 5** for two dimensional semilinear parabolic PDEs to the coupled system of singularly perturbed semilinear parabolic convection-diffusion problems with non-homogeneous Dirichlet boundary data in one and two dimensions. Note that Clavero and Jorge in [19], and Rao and Chaturvedi in [95] recently analyze a parameter-robust numerical scheme for coupled system of singularly perturbed semilinear parabolic reaction-diffusion problems with non-homogeneous Dirichlet boundary data in one-dimension.

Again, it would be an interesting and challenging task to extend the two novel fractional-step numerical algorithms proposed in **Chapter 4** and the corresponding order reduction analysis for the following class of singularly perturbed two-dimensional nonlinear parabolic convection-diffusion problems subject to the non-homogeneous Robin type boundary conditions as shown below:

$$\begin{cases} \frac{\partial u(x, y, t)}{\partial t} + \mathbb{L}_\varepsilon u(x, y, t) + b(x, y, t, u(x, y, t)) = g(x, y, t), & \text{in } D, \\ u(x, y, 0) = q_0(x, y), & \text{in } \bar{G}, \\ \alpha(x, y, t)u(x, y, t) + \varepsilon\mu(x, y, t)\frac{\partial u(x, y, t)}{\partial n} = s(x, y, t), & (x, y, t) \in \partial G \times (0, T], \end{cases} \quad (8.4)$$

where $L_\varepsilon u = -\varepsilon \Delta u + \vec{v}(x, y, t) \cdot \vec{\nabla} u$, and $\vec{v}(x, y, t) = (v_1(x, y, t), v_2(x, y, t))$, and ε is a small parameter such that $\varepsilon \in (0, 1]$. The coefficients $\vec{v}(x, y, t)$, $b(x, y, t, u)$, $\alpha(x, y, t)$, $\mu(x, y, t)$ and the source term $g(x, y, t)$ are considered to be sufficiently smooth satisfying (8.3) and the condition

$$\frac{\partial b(x, y, t, u)}{\partial u} \geq \beta > 0, \quad (x, y, t, u) \in \bar{D} \times \mathbb{R}. \quad (8.5)$$

In **Chapter 6**, efficient numerical methods are proposed and analyzed so far for solving two different class singularly perturbed linear parabolic convection-diffusion problems with nonsmooth data in one-dimension. One can further analyze the similar second-order spatially accurate numerical methods together with the fractional-step approximation of the time derivative for solving two dimensional singularly perturbed linear parabolic convection-diffusion problems with nonsmooth data. Recently, Majumdar and Natesan in [71] devise a parameter-robust numerical scheme for solving singularly perturbed two-dimensional linear parabolic convection-diffusion problem with nonsmooth data.

Chapter 7 analyzes high-order time-accurate numerical method for singularly perturbed one-dimensional semilinear parabolic convection diffusion problems with nonsmooth data. One can develop high-order space-time accurate numerical scheme for singularly perturbed quasilinear parabolic convection diffusion problems with nonsmooth data. Note that Farrell et al. in [37] develop a parameter-robust finite difference scheme for one-dimensional singularly perturbed quasilinear convection-diffusion problems with discontinuous data.

Apart from above, we want to mention that the convergence analysis carried out in this thesis is mostly based on the layer-resolving piecewise-uniform Shishkin meshes. It would be more interesting to establish those results using the adaptive grid based on the equidistribution principle.

Bibliography

- [1] E.O. Asante-Asamani, A. Kleefeld, and B.A. Wade. A second-order exponential time differencing scheme for non-linear reaction-diffusion systems with dimensional splitting. *J. Comput. Phys.*, **415**, 2020.
- [2] D. Avijit and S. Natesan. SDFEM for singularly perturbed parabolic initial-boundary-value problems on equidistributed grids. *Calcolo*, **57**:Paper No. 23, 25, 2020.
- [3] M.G. Beckett. *The robust and efficient numerical solution of singularly perturbed boundary value problem using grid adaptivity*. PhD thesis. Department of Mathematics, University of Strathclyde, UK, 1998.
- [4] L. Bobisud. Second-order linear parabolic equations with a small parameter. *Arch. Rational Mech. Anal.*, **27**:385–397, 1967.
- [5] I. Boglaev. Monotone Schwarz iterates for a semilinear parabolic convection-diffusion problem. *J. Comput. Appl. Math.*, **183**(1):191–209, 2005.
- [6] I. Boglaev. Uniform convergence of monotone iterative methods for semilinear singularly perturbed problems of elliptic and parabolic types. *Electron. Trans. Numer. Anal.*, **20**(1):86–103, 2005.
- [7] I. Boglaev. Uniform convergent monotone iterates for semilinear singularly perturbed parabolic problems. *J. Comput. Appl. Math.*, **235**(12):3541–3553, 2011.
- [8] J.P. Boon and B. Herpigny. Model for chemotactic bacterial bands. *Bulletin of mathematical biology*, **48**(1):1–19, 1986.
- [9] B. Bujanda, C. Clavero, J.L. Gracia, and J.C. Jorge. A high order uniformly convergent alternating direction scheme for time dependent reaction-diffusion singularly perturbed problems. *Numer. Math.*, **107**(1):1–25, 2007.
- [10] A.W. Bush. *Perturbation Methods for Engineers and Scientists*. CRC Press, London, 1992.
- [11] Z. Cen. A hybrid difference scheme for a singularly perturbed convection-diffusion problem with discontinuous convection coefficient. *Appl. Math. Comput.*, **169**:689–699, 2005.
- [12] K.W. Chang and F.A. Howes. *Nonlinear singular perturbation phenomena: theory and applications*. Springer Science, 2012.
- [13] M.A.J. Chaplain and A.M. Stuart. A model mechanism for the chemotactic response of endothelial cells to tumour angiogenesis factor. *Mathematical Medicine and Biology: A Journal of the IMA*, **10**(3):149–168, 1993.
- [14] P.G. Ciarlet and J.L. Lions, editors. *Handbook of Numerical Analysis*, volume 1. North-Holland, Amsterdam, 1990.
- [15] C. Clavero and J.L. Gracia. A higher-order HODIE finite difference scheme for 1d parabolic singularly perturbed reaction-diffusion problems. *Appl. Math. Comput.*, **218**:5067–5080, 2012.
- [16] C. Clavero, J.L. Gracia, and J.C. Jorge. High-order numerical methods for one-dimensional parabolic singularly perturbed problems with regular layers. *Numer. Methods Partial Differential Equations*, **21**(1):148–169, 2005.

- [17] C. Clavero, J.L. Gracia, and J.C. Jorge. A uniformly convergent alternating direction hodie finite difference scheme for 2d time-dependent convection-diffusion problems. *IMA J. Numer. Anal.*, **26**:155–172, 2006.
- [18] C. Clavero, J.L. Gracia, and F. Lisbona. Higher-order numerical methods for one-dimensional parabolic singularly perturbed problems with regular layers. *Numer. Methods Partial Differential Equations*, **21**:149–169, 2005.
- [19] C. Clavero and J. C. Jorge. An efficient and uniformly convergent scheme for one-dimensional parabolic singularly perturbed semilinear systems of reaction-diffusion type. *Numer. Algorithms*, **85**:1005–1027, 2020.
- [20] C. Clavero and J.C. Jorge. Another uniform convergence analysis technique of some numerical methods for parabolic singularly perturbed problems. *Comput. Math. Appl.*, **70**:222–235, 2015.
- [21] C. Clavero and J.C. Jorge. Uniform convergence and order reduction of the fractional implicit Euler method to solve singularly perturbed 2D reaction-diffusion problems. *Appl. Math. Comput.*, **287/288**:12–27, 2016.
- [22] C. Clavero and J.C. Jorge. A fractional step method for 2D parabolic convection-diffusion singularly perturbed problems: uniform convergence and order reduction. *Numer. Algorithms*, **75**:809–826, 2017.
- [23] C. Clavero, J.C. Jorge, and F. Lisbona. A uniformly convergent scheme on a nonuniform mesh for convection-diffusion parabolic problems. *J. Comput. Appl. Math.*, **154**:415–429, 2003.
- [24] C. Clavero, J.C. Jorge, F. Lisbona, and G.I. Shishkin. A fractional step method on a special mesh for the resolution of multidimensional evolutionary convection-diffusion problems. *Appl. Numer. Math.*, **27**:211–231, 1998.
- [25] C. Clavero, J.C. Jorge, F. Lisbona, and G.I. Shishkin. An alternating direction scheme on a nonuniform mesh for reaction-diffusion parabolic problem. *IMA J. Numer. Anal.*, **20**:263–280, 2000.
- [26] A. Das and S. Natesan. Uniformly convergent hybrid numerical scheme for singularly perturbed delay parabolic convection-diffusion problems on shishkin mesh. *Appl. Math. Comput.*, **271**:168–186, 2015.
- [27] A. Das and S. Natesan. Second-order uniformly convergent numerical method for singularly perturbed delay parabolic partial differential equations. *Int. J. Comput. Math.*, **95**(3):490–510, 2018.
- [28] P. Das and S. Natesan. Numerical solution of a system of singularly perturbed convection-diffusion boundary-value problems using mesh equidistribution technique. *Aust. J. Math. Anal. Appl.*, **10**(1):Art. 14, 17, 2013.
- [29] E.P. Doolan, J.J.H. Miller, and W.H.A. Schildres. *Uniform Numerical Methods for Problems with Initial and Boundary Layers*. Boole Press, Dublin, 1980.
- [30] M. Van Dyke. *Perturbation Methods in Fluid Mechanics*. Academic Press, New York, 1964.
- [31] W. Eckhaus. *Mateched Asymptotic Expansions and Singular Perturbations*. North-Holland, Amsterdam, 1973.
- [32] P.A. Farrell, A.F. Hegarty, J.J.H. Miller, E. O’Riordan, and G.I. Shishkin. *Robust Computational Techniques for Boundary Layers*. Chapman & Hall/CRC Press, 2000.
- [33] P.A. Farrell, A.F. Hegarty, J.J.H. Miller, E. O’Riordan, and G.I. Shishkin. Singularly perturbed convection diffusion problems with boundary and weak interior layers. *J. Comput. Appl. Math.*, **166**(1):133–151, 2004.
- [34] P.A. Farrell, J.J.H. Miller, E. O’Riordan, and G.I. Shishkin. A uniformly convergent finite difference scheme for a singularly perturbed semilinear equation. *SIAM J. Numer. Anal.*, **33**(3):1135–1149, 1996.
- [35] P.A. Farrell, J.J.H. Miller, E. O’Riordan, and G.I. Shishkin. On the non-existence of ϵ -uniform finite difference methods on uniform meshes for semilinear two-point boundary value problems. *Math. Comp.*, **67**(222):603–617, 1998.

- [36] P.A. Farrell, E. O’Riordan, J.J.H. Miller, and G.I. Shishkin. A class of singularly perturbed semilinear differential equations with interior layers. *Math. Comp.*, **74**(252):1759–1776, 2005.
- [37] P.A. Farrell, E. O’Riordan, and G.I. Shishkin. A class of singularly perturbed quasilinear differential equations with interior layers. *Math. Comp.*, **78**(265):103–127, 2009.
- [38] J. Folkman. Tumor angiogenesis. *Adv Cancer Res*, **43**:175–203, 1985.
- [39] S. Franz and H.G. Roos. The capriciousness of numerical methods for singular perturbations. *SIAM Rev.*, **53**(1):157–173, 2011.
- [40] J.I. Freijer, T.M. Post, B.A. Ploeger, J. DeJongh, and M. Danhof. Application of the convection–dispersion equation to modelling oral drug absorption. *Bulletin of mathematical biology*, **69**(1):181–195, 2007.
- [41] A. Friedman. *Partial differential equations of parabolic type*. Courier Dover Publications, 1st edition, 2008.
- [42] K.O Friedrichs and W.R. Wasow. Singular perturbations of non-linear oscillations. *Duke Math. J.*, bf 13:367–381, 1946.
- [43] S. Gowrisankar and S. Natesan. Robust numerical scheme for singularly perturbed convection-diffusion parabolic initial-boundary-value problems on equidistributed grids. *Comput. Phys. Commun.*, **185**:2008–2019, 2014.
- [44] S. Gowrisankar and S. Natesan. An efficient robust numerical method for singularly perturbed Burgers’ equation. *Appl. Math. Comput.*, **346**:385–394, 2019.
- [45] J.L. Gracia, F.J. Lisbona, M. Madaune-Tort, and E. O’Riordan. A system of singularly perturbed semilinear equations. In *BAIL 2008-Boundary and Interior Layers*, volume **69**, pages 163–172. Springer, 2009.
- [46] J.L. Gracia and E. O’Riordan. Singularly perturbed reaction-diffusion problems with discontinuities in the initial and/or the boundary data. *J. Comput. Appl. Math.*, **370**:112638, 17, 2020.
- [47] J.L. Gracia and E. O’Riordan. Parameter-uniform approximations for a singularly perturbed convection-diffusion problem with a discontinuous initial condition. *Appl. Numer. Math.*, **162**:106–123, 2021.
- [48] J.L. Gracia, E. O’Riordan, and M. Stynes. Convergence in positive time for a finite difference method applied to a fractional convection-diffusion problem. *Comput. Methods Appl. Math.*, **18**:33–42, 2018.
- [49] V. Gupta and M.K. Kadalbajoo. Numerical approximation of modified Burgers’ equation via hybrid finite difference scheme on layer-adaptive mesh. *Neural Parallel Sci. Comput.*, **18**:167–193, 2010.
- [50] V. Gupta and M.K. Kadalbajoo. Qualitative analysis and numerical solution of Burgers’ equation via B-spline collocation with implicit Euler method on piecewise uniform mesh. *J. Numer. Math.*, **24**:797–814, 2016.
- [51] P.W. Hemker and G.I. Shishkin. Discrete approximation of singularly perturbed parabolic pdes with a discontinuous initial condition. *Comp. Fluid Dynamics*, **2**:375–392, 1994.
- [52] P.W. Hemker, G.I. Shishkin, and L.P. Shishkina. ϵ -uniform schemes with high-order time-accuracy for parabolic singular perturbation problems. *IMA J. Numer. Anal.*, **20**(1):99–121, 2000.
- [53] Joe D. Hoffman. *Numerical Methods for Engineers and Scientists*. McGraw-Hill, Inc., New York, first edition, 1992.
- [54] W. Hundsdorfer and J.G. Verwer. *Numerical Solution of Time-Dependent Advection-Diffusion-Reaction Equations*. Springer-Verlag, 2003.
- [55] G.J. Jayalakshmi and A. Tamilselvan. An ε -uniform numerical method for a class of singularly perturbed parabolic problems with robin boundary conditions having boundary turning point. *Asian-Eur. J. Math.*, **13**(1):2050025 (15 pages), 2020.

- [56] M.K. Kadalbajoo and V. Gupta. A brief survey on numerical methods for solving singularly perturbed problems. *Appl. Math. Comput.*, **217**:3641–3716, 2010.
- [57] M.K. Kadalbajoo and K.C. Patidar. A survey of numerical techniques for solving singularly perturbed ordinary differential equations. *App. Math. Comput.*, **130**:457–510, 2002.
- [58] M.K. Kadalbajoo and V.P. Ramesh. Hybrid method for numerical solution of singularly perturbed delay differential equations. *Appl. Math. Comput.*, **187**:797–814, 2007.
- [59] M.K. Kadalbajoo, K.K. Sharma, and A. Awasthi. A parameter-uniform implicit difference scheme for solving time-dependent Burgers’ equations. *Appl. Math. Comput.*, **170**:1365–1393, 2005.
- [60] H.B. Keller. *Numerical Methods for Two-Point Boundary Value Problems*. Dover, New York, 1992.
- [61] R.B. Kellogg and A. Tsan. Analysis of some differences approximations for a singular perturbation problem without turning point. *Math. Comp.*, **32**(144):1025–1039, 1978.
- [62] J. Kevorkian and J.D. Cole. *Multiple Scale and Singular Perturbation Methods*. Springer-Verlag, New York, 1996.
- [63] A. Q. M. Khaliq, B.A. Wade, M. Yousuf, and J. Vigo-Aguiar. High order smoothing schemes for inhomogeneous parabolic problems with applications to nonsmooth payoff in option pricing. *Numer. Meth. Par. Diff. Eqn.*, **23**(5):1249–1276, 2007.
- [64] A. Kreft and A. Zuber. On the physical meaning of the dispersion equation and its solutions for different initial and boundary conditions. *Chemical Engineering Science*, **33**(11):1471–1480, 1978.
- [65] O.A. Ladyzenskaja, V.A. Solonnikov, and N.N. Ural’ceva. *Linear and Quasi-Linear Equations of Parabolic Type*, volume 23 of *Translations of Mathematical Monographs*. American Mathematical Society, 1968.
- [66] P.A. Lagerstrom. *Matched Asymptotic Expansions*. Springer-Verlag, New York, 1988.
- [67] P.A. Lagerstrom and R.G. Casten. Basic concepts underlying singular perturbation techniques. *SIAM Rev.*, **14**(3):63–120, 1972.
- [68] T. Linß. *Layer-adapted meshes for reaction-convection-diffusion problems*. Springer-Verlag, Berlin, 2010.
- [69] T. Linss and N. Madden. Analysis of an alternating direction method applied to singularly perturbed reaction-diffusion problems. *Int. J. Numer. Anal. Model.*, **7**(3):507–519, 2010.
- [70] T. Linss, H.G. Roos, and R. Vulanović. Uniform pointwise convergence on Shishkin-type meshes for quasi-linear convection-diffusion problems. *SIAM J. Numer. Anal.*, **38**:897–912, 2000.
- [71] A. Majumdar and S. Natesan. Parameter-uniform numerical method for singularly perturbed 2-d parabolic convection–diffusion problem with interior layers. *Math. Methods Appl. Sci.*, :in press, 2021.
- [72] M. Mariappan and A. Tamilselvan. Higher order numerical method for a semilinear system of singularly perturbed differential equations. *Math. Commun.*, **26**(1):41–52, 2021.
- [73] P.A. Markowich, C.A. Ringhofer, and C. Schmeiser, editors. *Semiconductor equations*. Springer Science & Business Media, 1990.
- [74] P.A. Markowich and P. Szmolyan. A system of convection—diffusion equations with small diffusion coefficient arising in semiconductor physics. *J. Differ. Equ.*, **81**(2):234–254, 1989.
- [75] J. J. H. Miller, E. O’Riordan, G.I. Shishkin, and L.P. Shishkina. Fitted mesh methods for problems with parabolic boundary layers. *Math. Proc. R. Ir. Acad.*, **98 A**(2):173–190, 1998.

- [76] J.J.H. Miller, E. O’Riordan, and G.I. Shishkin. On piecewise uniform meshes for upwind and central difference operators for solving singularly perturbed problems. *IMA J. Numer. Anal.*, **15**:89–99, 1995.
- [77] J.J.H. Miller, E. O’Riordan, and G.I. Shishkin. *Fitted Numerical Methods for Singular Perturbation Problems*. World Scientific, Singapore, 1996.
- [78] J. Mohapatra and S. Natesan. Parameter-uniform numerical methods for singularly perturbed mixed boundary value problems using grid equidistribution. *J. Appl. Math. Comput.*, **37**(1-2):247–265, 2011.
- [79] K.W. Morton and D.F. Mayers. *Numerical Solution of Partial differential Equations: An Introduction*. Cambridge University Press, Cambridge, 1994.
- [80] K. Mukherjee and S. Natesan. An efficient numerical scheme for singularly perturbed parabolic problems with interior layers. *Neural Parallel Sci. Comput.*, **16**:405–418, 2008.
- [81] K. Mukherjee and S. Natesan. Parameter-uniform hybrid numerical scheme for time-dependent convection-dominated initial-boundary-value problems. *Computing*, **84**(3-4):209–230, 2009.
- [82] K. Mukherjee and S. Natesan. Richardson extrapolation technique for singularly perturbed parabolic convection-diffusion problems. *Computing*, **92**(1):1–32, 2011.
- [83] K. Mukherjee and S. Natesan. ε -Uniform error estimate of hybrid numerical scheme for singularly perturbed parabolic problems with interior layers. *Numer. Algorithms*, **58**(1):103–141, 2011.
- [84] K. Mukherjee and S. Natesan. Parameter-uniform fractional step hybrid numerical scheme for 2d singularly perturbed parabolic convection-diffusion problems. *J. Appl. Math. Comput.*, **60**(1-2):51–86, 2019.
- [85] A.H. Nayfeh. *Perturbation Methods*. John Wiley & Sons, New York, 1973.
- [86] M.J. Ng-Stynes, E. O’Riordan, and M. Stynes. Numerical methods for time-dependent convection-diffusion equations. *J. Comput. Appl. Math.*, **21**:289–310, 1988.
- [87] R.E. O’Malley. *Singular Perturbation Methods for Ordinary Differential Equations*. Springer, New York, 1991.
- [88] E. O’Riordan and J. Quinn. A linearised singularly perturbed convection-diffusion problem with an interior layer. *Appl. Numer. Math.*, **98**(C):1–17, 2015.
- [89] E. O’Riordan and G.I. Shishkin. Singularly perturbed parabolic problems with non-smooth data. *J. Comput. Appl. Math.*, **166**:233–245, 2004.
- [90] E. O’Riordan and M. Stynes. Uniformly convergent difference schemes for singularly perturbed parabolic diffusion-convection problems without turning points. *Numer. Math.*, **55**:521–544, 1989.
- [91] J.M. Ortega and W.C. Rheinboldt. *Iterative solution of nonlinear equations in several variables*. SIAM, 2000.
- [92] C.V. Pao. *Nonlinear parabolic and elliptic equations*. Plenum Press, New York, New York, 1992.
- [93] L. Prandtl. Über flüssigkeitsbewegung bei sehr kleiner reibung. In *Verhandlungen, III Inter. Math. Kongresses, Tuebner, Leipzig*, pages 485–491, 1904.
- [94] R.M. Priyadharshini, N. Ramanujam, and A. Tamilselvan. Hybrid difference schemes for a system of singularly perturbed convection-diffusion equations. *J. Appl. Math. & Informatics*, **27**(5-6):1001–1015, 2009.
- [95] S.C.S Rao and A.K. Chaturvedi. Pointwise error estimates for a system of two singularly perturbed time-dependent semilinear reaction-diffusion equations. *Math. Methods Appl. Sci.*, **44**(17):13287–13325, 2021.

- [96] S.C.S Rao and S. Chawla. Parameter-uniform convergence of a numerical method for a coupled system of singularly perturbed semilinear reaction-diffusion equations with boundary and interior layers. *J. Comput. Appl. Math.*, **352**:223–239, 2019.
- [97] V.Ya. Rivkind and N.N. Ural'tseva. Classical solvability and linear schemes for the approximate solution of the diffraction problem for quasilinear equations of parabolic and elliptic type. *J. Math. Sci.*, 1:235–264, 1973.
- [98] H.G. Roos. Layer-adapted meshes: Milestones in 50 years of history. *arXiv preprint arXiv:1909.08273*, 2019.
- [99] H.G. Roos, M. Stynes, and L. Tobiska. *Robust Numerical Methods for Singularly Perturbed Differential Equations*. Springer-Verlag, Berlin, 2nd edition, 2008.
- [100] A.A. Samarskii. *The theory of difference schemes*. CRC Press, 2001.
- [101] P.A. Selvi and N. Ramanujam. A parameter uniform difference scheme for singularly perturbed parabolic delay differential equation with robin type boundary condition. *Appl. Math. Comput.*, **296**:101–115, 2017.
- [102] G.I. Shishkin. A difference scheme on a non-uniform mesh for a differential equation with a small parameter in the highest derivative. *USSR Computational Mathematics and Mathematical Physics*, **23**(3):59–66, 1983.
- [103] G.I. Shishkin. Grid approximation of singularly perturbed parabolic equations in the presence of weak and strong transition layers generated by a discontinuous right-hand side. *Zh. Vychisl. Mat. Mat. Fiz.*, **46**(3):407–420, 2006.
- [104] G.I. Shishkin and L.P. Shishkina. The richardson extrapolation technique for quasilinear parabolic singularly perturbed convection-diffusion equations. In *Journal of Physics: Conference Series*, volume **5**, page 019. IOP Publishing, 2006.
- [105] G.I. Shishkin and L.P. Shishkina. *Difference Methods For Singular Perturbation Problems*. Chapman & Hall/CRC Press, Boca Raton, FL, 2009.
- [106] L. Shishkina and G.I. Shishkin. Conservative numerical method for a system of semilinear singularly perturbed parabolic reaction-diffusion equations. *Math. Model. Anal.*, **14**(2):211–228, 2009.
- [107] D.R. Smith. *Singular Perturbation Theory*. Cambridge University Press, Cambridge, 1985.
- [108] M. Stynes, E. O’Riordan, and J.L. Gracia. Error analysis of a finite difference method on graded meshes for a time-fractional diffusion equation. *SIAM J. Numer. Anal.*, **55**:1057–1079, 2017.
- [109] M. Stynes and H.G. Roos. The midpoint upwind scheme. *Appl. Numer. Math.*, **23**:361–374, 1997.
- [110] M. Stynes and D. Stynes. *Convection-diffusion problems*. American Mathematical Society, Providence, RI; Atlantic Association for Research in the Mathematical Sciences (AARMS), Halifax, NS, 2018.
- [111] M. Stynes and L. Tobiska. A finite difference analysis of a streamline diffusion method on a shishkin mesh. *Numer. Algorithms*, **18**:337–360, 1998.
- [112] V. Thomée. *Galerkin Finite Element Methods for Parabolic Problems*. Springer-Verlag, 1997.
- [113] L.G. Vulkov, J.J.H. Miller, and G.I. Shishkin, editors. *Analytical and Numerical Methods for Convection-Dominated and Singularly Perturbed Problems*. Nova Science Publishers, New York, USA, 2000.
- [114] B.A. Wade and Kumara Jayasuriya. Convergence of semidiscrete galerkin finite element schemes for nonhomogeneous parabolic evolution problems. *J. Math. Anal. Appl.*, **195**(3):645–657, 1995.
- [115] B.A. Wade, A. Q. M. Khaliq, M. Siddique, and M. Yousuf. Smoothing with positivity-preserving pade schemes for parabolic problems with nonsmooth data. *Numer. Methods Partial Differential Equations*, **21**(3):553–573, 2005.

- [116] B.A. Wade and A.Q.M. Khaliq. On smoothing of the Crank-Nicolson scheme for nonhomogeneous parabolic problems. *J. Comput. Meth. Sci. Eng.*, **1**(1):107–124, 2001.
- [117] W.R. Wasow. *On boundary layer problems in the theory of ordinary differential equations*. Doctoral dissertation, New York University, 1942.
- [118] N.S. Yadav and K. Mukherjee. Uniformly convergent new hybrid numerical method for singularly perturbed parabolic problems with interior layers. *Int. J. Appl. Comput. Math.*, **6**(53), 2020.
- [119] N.S. Yadav and K. Mukherjee. An efficient numerical method for singularly perturbed parabolic problems with non-smooth data. In *Computational Sciences - Modelling, Computing and Soft Computing*, Communications in Computer and Information Science, pages 159–171, 2021.

List of Publications

Papers in Journals

1. Yadav, N.S., Mukherjee, K. On ε -Uniform Higher Order Accuracy of New Efficient Numerical Method and Its Extrapolation for Singularly Perturbed Parabolic Problems with Boundary Layer. **Int. J. Appl. Comput. Math** 7, 72 (2021). <https://doi.org/10.1007/s40819-021-00979-7>.
2. Yadav, N.S., Mukherjee, K. Uniformly Convergent New Hybrid Numerical Method for Singularly Perturbed Parabolic Problems with Interior Layers. **Int. J. Appl. Comput. Math** 6, 53 (2020). <https://doi.org/10.1007/s40819-020-00804-7>.

Paper in Conference Proceeding

1. Yadav N.S., Mukherjee K. An Efficient Numerical Method for Singularly Perturbed Parabolic Problems with Non-smooth Data. In: Awasthi A., John S.J., Panda S. (eds) Computational Sciences - Modelling, Computing and Soft Computing. CSMCS 2020. **Communications in Computer and Information Science**, vol 1345. Springer, Singapore (2021). https://doi.org/10.1007/978-981-16-4772-7_12

Papers under review/submission

1. Yadav, N.S., Mukherjee, K. Convergence Analysis of Two Parameter-Robust Numerical Methods for Singularly Perturbed Time-Dependent Semilinear PDEs of Convection-Diffusion Type.
2. Yadav, N.S., Mukherjee, K. A Parameter-Robust Fractional-Step FMM for Singularly Perturbed 2D Parabolic Convection-Diffusion PDEs with Nonhomogeneous Boundary Data : Order Reduction Analysis and Higher-Order Convergence.
3. Yadav, N.S., Mukherjee, K. Stability and Error Analysis of an Efficient Parameter-Robust Numerical Method for Singularly Perturbed Parabolic PDEs with Discontinuous Source Function : A New Paradigm Using Modified Layer-Adapted Mesh.
4. Yadav, N.S., Mukherjee, K. Higher-Order Fully-Implicit Fractional-Step Numerical Method for 2D Semilinear Singularly Perturbed Parabolic PDEs with non-homogeneous boundary data: Parameter-Uniform Error Estimate and Order Reduction Analysis.
5. Yadav, N.S., Mukherjee, K. ε -Uniform Convergence Analysis of Higher-Order Implicit-Explicit Fractional-Step Numerical Method for 2D Semilinear Singularly Perturbed Parabolic PDEs with non-homogeneous boundary data.
6. Yadav, N.S., Mukherjee, K. Parameter-Uniform Higher-Order Time-Accurate Numerical Approximation for Semilinear Singularly Perturbed Parabolic Problems with Nonsmooth Data.

List of Papers Presented

1. Paper entitled "An Efficient Hybrid Numerical Scheme for Singularly Perturbed Parabolic Convection-Diffusion Problems", **International Conference on Analysis and Applied Mathematics (ICAAM2018)**, July 02-04, 2018, Department of Mathematics, NIT, Tiruchirappalli.
2. Paper entitled "Convergence analysis of new hybrid scheme for singularly perturbed parabolic problems with interior layers", **International Conference on differential equations and control problems: modeling, analysis and computations (ICDECP19)**, June 17-19, 2019, IIT, Mandi, Himachal Pradesh.
3. Paper entitled "An efficient numerical method for singularly perturbed parabolic problems with non-smooth data", **International Conference on Computational Sciences-Modelling, Computing and Soft Computing (CSMCS-2020)**, September 10-12, 2020 organized by the Department of Mathematics of National Institute of Technology Calicut, Kerala.
4. Paper entitled "An efficient numerical method for a class of singularly perturbed time-dependent convection diffusion problems with non-smooth data", **International Conference on Advances in Differential Equations and Numerical Analysis (ADENA-2020)**, 12-14, October 2020, IIT Guwahati, India.

Doctoral Committee

Chairman:

Dr. N. Sabu
Professor
Department of Mathematics, IIST,
Thiruvananthapuram, Kerala,
INDIA

External member:

Dr. Natesan Srinivasan
Professor
Department of Mathematics, IIT Guwahati,
Guwahati, Assam,
INDIA

Internal member:

Dr. Prosenjit Das
Associate Professor
Department of Mathematics, IIST
Thiruvananthapuram, Kerala,
INDIA

Ph.D Advisor:

Dr. Kaushik Mukherjee
Associate Professor
Department of Mathematics, IIST,
Thiruvananthapuram, Kerala,
INDIA

External member:

Dr. Jugal Mohapatra
Associate Professor
Department of Mathematics, NIT Rourkela,
Rourkela, Odisha,
INDIA

Internal member:

Dr. Basudeb Ghosh
Associate Professor
Department of Avionics, IIST,
Thiruvananthapuram, Kerala,
INDIA

Appendix A

Monotonicity of the proposed FMM on the standard Shishkin mesh for singularly perturbed linear parabolic PDEs exhibiting both boundary and weak interior layers

Here, we discuss about the monotonicity property of the proposed finite difference operator in [Chapter 6, Section 6.9.2] on the standard Shishkin mesh as depicted in Fig 6.11. Note that on the standard Shishkin mesh the mesh-width h_j is given as follows:

$$h_j = \begin{cases} h_1 = \frac{4\eta_1}{N}, & \text{for } 1 \leq j \leq N/4, \\ H_1 = \frac{4(d - \eta_1)}{N}, & \text{for } N/4 + 1 \leq j \leq N/2, \\ h_2 = \frac{4\eta_2}{N}, & \text{for } N/2 + 1 \leq j \leq 3N/4, \\ H_2 = \frac{4(1 - d - \eta_2)}{N}, & \text{for } 3N/4 + 1 \leq j \leq N. \end{cases} \quad (\text{A.1})$$

By following the approach considered in [Chapter 6, Section 6.9.3], we convert the system of equations in (6.77) into a new system of the following form:

$$\begin{cases} Y_j^0 = q_0(x_j), & \text{for } 0 \leq j \leq N, \\ \mathbb{L}_H^{N,M} Y_j^{n+1} = \mathbb{F}_j^{n+1}, & \text{for } 1 \leq j \leq N-1, \\ Y_0^{n+1} = s_l(t_{n+1}), \quad Y_N^{n+1} = s_r(t_{n+1}), & \text{for } n = 0, \dots, M-1. \end{cases} \quad (\text{A.2})$$

where the difference operator $\mathbb{L}_H^{N,M}$ and the term \mathbb{F}_j^{n+1} are respectively defined as

$$\mathbb{L}_H^{N,M} Y_j^{n+1} = \begin{cases} [\tilde{\mu}_j^- Y_{j-1}^{n+1} + \tilde{\mu}_j^c Y_j^{n+1} + \tilde{\mu}_j^+ Y_{j+1}^{n+1}] + [\tilde{\lambda}_j^- Y_{j-1}^n + \tilde{\lambda}_j^c Y_j^n + \tilde{\lambda}_j^+ Y_{j+1}^n], & \text{for } j = N/2, \\ \mathcal{L}_\varepsilon^{N,M} Y_j^{n+1}, & \text{for } j \neq N/2, \end{cases} \quad (\text{A.3})$$

and

$$\mathbb{F}_j^{n+1} = \begin{cases} \tilde{\gamma}_j^- g_{j-1}^{n+1} + \tilde{\gamma}_j^c g_j^{n+1} + \tilde{\gamma}_j^+ g_{j+1}^{n+1}, & \text{for } j = N/2, \\ \mathcal{F}_j^{n+1}, & \text{for } j \neq N/2. \end{cases} \quad (\text{A.4})$$

Here, one can derive the coefficients $\tilde{\mu}_j^-, \tilde{\mu}_j^c, \tilde{\mu}_j^+; \tilde{\lambda}_j^-, \tilde{\lambda}_j^c, \tilde{\lambda}_j^+; \tilde{\gamma}_j^-, \tilde{\gamma}_j^c, \tilde{\gamma}_j^+$, from the proposed scheme by considering the mesh-widths given in (A.1). Now, we set

$$-\mathbb{L}_H^{N,M} Y_j^{n+1} = \left[A_{j,j-1} Y_{j-1}^{n+1} + A_{j,j} Y_j^{n+1} + A_{j,j+1} Y_{j+1}^{n+1} \right] - \left[B_{j,j-1} Y_{j-1}^n + B_{j,j} Y_j^n + B_{j,j+1} Y_{j+1}^n \right],$$

where for $j \neq N/2$,

$$\begin{cases} A_{j,j} = -\mu_j^c, & A_{j,j+1} = -\mu_j^+, & A_{j,j-1} = -\mu_j^-, \\ B_{j,j} = \lambda_j^c, & B_{j,j+1} = \lambda_j^+, & B_{j,j-1} = \lambda_j^-, \end{cases}$$

and for $j = N/2$,

$$\begin{cases} A_{j,j} = -\tilde{\mu}_j^c, & A_{j,j+1} = -\tilde{\mu}_j^+, & A_{j,j-1} = -\tilde{\mu}_j^-, \\ B_{j,j} = \tilde{\lambda}_j^c, & B_{j,j+1} = \tilde{\lambda}_j^+, & B_{j,j-1} = \tilde{\lambda}_j^-. \end{cases}$$

It is obvious that the matrix $B = (B_{j,k}) \geq 0$. Now, by considering the case $\varepsilon \leq 2\|a\|N^{-1}$, one can derive that

$$\begin{cases} A_{N/2,N/2} = -\left[\frac{2\varepsilon - a_{N/2+1}h_2}{2h_2(2\varepsilon + a_{N/2+1}h_2)} - \frac{3}{2h_2} - \frac{3}{2H_1} - \frac{H_1}{2\varepsilon} \left(\frac{1}{2\Delta t} + \frac{b_{(N/2-1)+\frac{1}{2}}}{2} - \frac{a_{(N/2-1)+\frac{1}{2}}}{H_1} - \frac{\varepsilon}{H_1^2} \right) \right] > 0, \\ A_{N/2,N/2+1} = -\frac{1}{2h_2} \left[4 - \frac{4\varepsilon + 2h_2^2(b_{N/2+1} + \frac{1}{\Delta t})}{2\varepsilon + a_{N/2+1}h_2} \right] \leq 0, \end{cases}$$

under the assumptions $N/\ln N > 2\eta_0\|a\|$ and $\left(\frac{1}{\Delta t} + \|b\|\right) \leq m_0 N/2$. Also, we have

$$\begin{aligned} A_{N/2,N/2-1} &= -\frac{1}{2H_1} \left[4 - \frac{2\varepsilon + a_{(N/2-1)+\frac{1}{2}}H_1 + H_1^2(b_{(N/2-1)+\frac{1}{2}} + \frac{1}{\Delta t})/2}{\varepsilon} \right], \\ &= \frac{1}{2H_1} \left[-4 + \frac{2\varepsilon + a_{(N/2-1)+\frac{1}{2}}H_1 + H_1^2(b_{(N/2-1)+\frac{1}{2}} + \frac{1}{\Delta t})/2}{\varepsilon} \right], \\ &\leq \frac{1}{2H_1} \left[-2 + \frac{\|a\|H_1}{\varepsilon} + \frac{H_1^2(\|b\| + \frac{1}{\Delta t})}{2\varepsilon} \right]. \end{aligned}$$

Now, using $H_1 \leq 4N^{-1}$ and $\left(\frac{1}{\Delta t} + \|b\|\right) \leq m_0 N/2$, we have

$$A_{N/2,N/2-1} \leq \frac{1}{\varepsilon H_1} \left[-\varepsilon + 4\|a\|N^{-1} \right] \not\leq 0,$$

since $\varepsilon \leq 2\|a\|N^{-1} \leq 4\|a\|N^{-1}$. This shows that the matrix $A := (A_{j,k})$ does not satisfy the M-matrix criterion. As a result of this, one can not apply [Lemma 3.12, Part II] given in the book Roos et al. [99] to prove that $\mathbb{L}_H^{N,M}$ satisfies the discrete maximum principle.

Appendix B

Verification of compatibility conditions: test examples for 2D liner and semilinear parabolic PDEs

At first, we show that examples of Chapter 3 (for 2D linear parabolic PDE) satisfy the compatibility conditions as mentioned in the equation (3.3). According to the book [99, Section 2.2], in order to avoid any additional layer, the boundary and initial data must satisfy the compatibility conditions at the corners.

Example B.1. Consider the following parabolic IBVP:

$$\begin{cases} \frac{\partial u}{\partial t} - \varepsilon \Delta u + (1 + x(1 - x)) \frac{\partial u}{\partial x} + (1 + y(1 - y)) \frac{\partial u}{\partial y} = g(x, y, t), & \text{in } \mathbf{G} \times (0, 1], \\ u(x, y, 0) = q_0(x, y), & \text{in } \bar{\mathbf{G}}, \\ u(x, y, t) = s(x, y, t), & \text{in } \partial \mathbf{G} \times (0, T]. \end{cases}$$

Here, the exact solution is given by

$$u(x, y, t) = \exp(-t) \left[\left(\frac{1 - \exp(-(1 - x)/\varepsilon)}{1 - \exp(-1/\varepsilon)} - \cos\left(\frac{\pi x}{2}\right) \right) \left(\frac{1 - \exp(-(1 - y)/\varepsilon)}{1 - \exp(-1/\varepsilon)} - \cos\left(\frac{\pi y}{2}\right) \right) - xy \right].$$

It is obvious that

$$\begin{aligned} q_0(1, 0, 0) = s(1, 0, 0) = 0, \quad q_0(0, 0, 0) = s(0, 0, 0) = 0, \\ q_0(1, 1, 0) = s(1, 1, 0) = -1, \quad q_0(0, 1, 0) = s(0, 1, 0) = 0. \end{aligned}$$

Since g , q_0 , and s are obtained from the exact solution, one can easily check that the remaining compatibility conditions of the equation (3.3) are also satisfied by the Example B.1.

Example B.2. Consider the following parabolic IBVP:

$$\begin{cases} \frac{\partial u}{\partial t} - \varepsilon \Delta u + \frac{\partial u}{\partial x} + \frac{\partial u}{\partial y} + (1 + t^2 xy)u = g(x, y, t), & \text{in } \mathbf{G} \times (0, 1], \\ u(x, y, 0) = 0, & \text{in } \bar{\mathbf{G}}, \\ u(x, y, t) = (e^{-t} - 1)(1 + x)y, & (x, y, t) \in \partial \mathbf{G} \times (0, 1], \end{cases}$$

where $g(x, y, t) = [1 + rt^2 xy][\Phi(x)\Phi(y) - (1 + x)y] + rm_2[\Phi(x) + \Phi(y)] - r(1 + x + y)$ and $\Phi(z) =$

$m_1 + m_2 z + \exp(-(1 - z)/\varepsilon)$, $m_1 = -\exp(-1/\varepsilon)$, $m_2 = -1 - m_1$ and $r = 1 - e^{-t}$.

Here, we are not acquainted with the exact solution of Example B.2. One can check that

$$\begin{aligned} q_0(1, 0, 0) &= s(1, 0, 0) = 0, & q_0(0, 0, 0) &= s(0, 0, 0) = 0, \\ q_0(1, 1, 0) &= s(1, 1, 0) = 0, & q_0(0, 1, 0) &= s(0, 1, 0) = 0. \end{aligned}$$

Next, one can also check that

$$\frac{\partial s(x, y, 0)}{\partial t} = -L_\varepsilon(0)q_0(x, y) + g(x, y, 0), \quad \text{on } \partial G, \quad (\text{B.1})$$

where $L_\varepsilon(0)q_0 = \varepsilon \Delta q_0 + \frac{\partial q_0}{\partial x} + \frac{\partial q_0}{\partial y} + q_0$. Since $q_0(x, y) = 0$, it implies that $L_\varepsilon(0)q_0 = 0$, and from the boundary data, we obtain that $\frac{\partial s(x, y, t)}{\partial t} = -e^{-t}(1+x)y$ and $\frac{\partial s(x, y, 0)}{\partial t} = -(1+x)y$. Next, we have

$$g(x, y, 0) = [\Phi(x)\Phi(y) - (1+x)y].$$

Since $\Phi(0) = 0$ and $\Phi(1) = 0$, it gives that

$$\begin{aligned} \frac{\partial s(1, 1, 0)}{\partial t} &= g(1, 1, 0) = -2, & \frac{\partial s(0, 1, 0)}{\partial t} &= g(0, 1, 0) = -1, \\ \frac{\partial s(0, 0, 0)}{\partial t} &= g(0, 0, 0) = 0, & \frac{\partial s(1, 0, 0)}{\partial t} &= g(1, 0, 0) = 0. \end{aligned}$$

Hence, the equation (B.1) is also satisfied. Similarly, the remaining compatibility conditions of the equation (3.3) are also met.

In the same way, one can show that example of Chapter 5 (for 2D semilinear parabolic PDEs) satisfies the required compatibility conditions mentioned in the equation (5.4).